LEABHARLANN CHOLÁISTE NA TRÍONÓIDE, BAILE ÁTHA CLIATH | TRINITY COLLEGE LIBRARY DUBLIN
Ollscoil Átha Cliath | The University of Dublin

Terms and Conditions of Use of Digitised Theses from Trinity College Library Dublin

Copyright statement

All material supplied by Trinity College Library is protected by copyright (under the Copyright and Related Rights Act, 2000 as amended) and other relevant Intellectual Property Rights. By accessing and using a Digitised Thesis from Trinity College Library you acknowledge that all Intellectual Property Rights in any Works supplied are the sole and exclusive property of the copyright and/or other IPR holder. Specific copyright holders may not be explicitly identified. Use of materials from other sources within a thesis should not be construed as a claim over them.

A non-exclusive, non-transferable licence is hereby granted to those using or reproducing, in whole or in part, the material for valid purposes, providing the copyright owners are acknowledged using the normal conventions. Where specific permission to use material is required, this is identified and such permission must be sought from the copyright holder or agency cited.

Liability statement

By using a Digitised Thesis, I accept that Trinity College Dublin bears no legal responsibility for the accuracy, legality or comprehensiveness of materials contained within the thesis, and that Trinity College Dublin accepts no liability for indirect, consequential, or incidental, damages or losses arising from use of the thesis for whatever reason. Information located in a thesis may be subject to specific use constraints, details of which may not be explicitly described. It is the responsibility of potential and actual users to be aware of such constraints and to abide by them. By making use of material from a digitised thesis, you accept these copyright and disclaimer provisions. Where it is brought to the attention of Trinity College Library that there may be a breach of copyright or other restraint, it is the policy to withdraw or take down access to a thesis while the issue is being resolved.

Access Agreement

By using a Digitised Thesis from Trinity College Library you are bound by the following Terms & Conditions. Please read them carefully.

I have read and I understand the following statement: All material supplied via a Digitised Thesis from Trinity College Library is protected by copyright and other intellectual property rights, and duplication or sale of all or part of any of a thesis is not permitted, except that material may be duplicated by you for your research use or for educational purposes in electronic or print form providing the copyright owners are acknowledged using the normal conventions. You must obtain permission for any other use. Electronic or print copies may not be offered, whether for sale or otherwise to anyone. This copy has been supplied on the understanding that it is copyright material and that no quotation from the thesis may be published without proper acknowledgement.

An investigation of the effect of Δ^9-Tetrahydrocannabinol on the viability of cortical neurons

by

Eric J. Downer

Thesis submitted for the degree of Doctor of Philosophy at the University of Dublin, Trinity College

Thesis submitted October 2004

Department of Physiology
Trinity College Institute of Neuroscience
Trinity College
Dublin 2

TRINITY COLLEGE
2 6 AUG 2008
LIBRARY DUBLIN
THESIS
8549.

I Table of Contents

		Page
I	Table of contents	i
II	List of Figures	xi
III	List of Tables	xvi
IV	Acknowledgements	xvii
V	Declaration	xix
VI	Abstract	xx
VII	List of Abbreviations	xxii

Chapter 1 General Introduction

1.1	Marijuana	1
1.2	Δ^9-Tetrahydrocannabinol	3
1.3	Cannabinoid receptor	5
	1.3.1 Cannabinoid receptor subtypes	5
	1.3.2 Cannabinoid receptor distribution	7
	1.3.3 Cannabinoid receptor signal transduction	8
1.4	Endogenous cannabinoids	11
1.5	Cannabinoids and cell viability	13
	1.5.1 Neuronal toxicity/regression	13
	1.5.2 Non-neuronal cell toxicity/regression	16
	1.5.3 Neuroprotection	17
1.6	Cannabinoids and development	19
1.7	Apoptosis	23
1.8	The apoptotic pathway	25
	1.8.1 Cytochrome *c*	25
	1.8.2 Bcl-2 protein family	26
	1.8.3 Caspase-3	29
	1.8.4 Poly(ADP-ribose) polymerase	31

1.9 Mitogen-activated protein kinases 33
1.9.1 c-Jun N-terminal kinase 34
1.10 p53 37
1.11 Antisense technology 39
1.12 Objectives 42

Chapter 2 Methods

2.1 Cell culture 44
2.1.1 Aseptic technique 44
2.1.2 Sterilisation of glassware, plastics and dissection instruments 44
2.1.3 Sterility of work environment 44
2.1.4 Reagents and medium formulation 45
2.1.5 Disposal 45
2.2 Primary culture of cortical neurons 46
2.2.1 Preparation of sterile coverslips 46
2.2.2 Animals 46
2.2.3 Dissection 46
2.2.4 Dissociation procedure 47
2.2.5 Plating of resuspended neurons 47
2.3 Cell treatments 49
2.3.1 THC 49
2.3.2 CB_1 cannabinoid receptor inhibitor 49
2.3.3 p53 inhibitor 49
2.3.4 Pertussis toxin 50
2.3.5 Etoposide 50
2.4 *Ex vivo* studies 50
2.4.1 Animals 50
2.4.2 Cortical slice preparation 50
2.4.3 Drug treatment of cortical slices 51
2.5 *In vivo* studies 51
2.5.1 Animals 51

2.5.2 THC administration 51
2.5.3 AM 251 administration 52
2.5.4 Dissection 52
2.5.5 Preparation of slices for freezing 52
2.5.6 Preparation of cryostat sections 53
2.6 Protein quantification using the Bradford assay 53
2.7 Sodium Dodecyl Sulphate-Polyacrylamide Gel Electrophoresis (SDS-PAGE) 54
2.7.1 (i) preparation of cell culture protein 54
(ii) preparation of cytosolic and mitochondrial fraction 54
2.7.2 Preparation of cortical slice protein 55
2.7.3 Preparation of polyacrylamide gels 55
2.7.4 Semi-dry electrophoretic blotting of proteins 56
2.8 Western Immunoblotting 56
2.8.1 Bax expression 57
2.8.2 Bcl phosphorylation 57
2.8.3 CB_1 receptor expression 57
2.8.4 Cytochrome c expression 58
2.8.5 JNK phosphorylation 58
2.8.6 JNK1/2 expression 59
2.8.7 p53 expression 59
2.8.8 Phosphorylated p53 expression 60
2.8.9 Total JNK expression 60
2.8.10 Total actin expression 61
2.8.11 Densitometry 62
2.9 Immunocytochemistry 63
2.9.1 Anti-active caspase-3 immunocytochemistry 63
2.9.2 Poly(ADP-ribose) polymerase (PARP) immunocytochemistry 64
2.10 Fluorescence immunocytochemistry 64
2.10.1 Phospho-JNK fluorescence immunocytochemistry 64
2.10.2 Bax fluorescence immunocytochemistry 65
2.11 Evaluation of neuronal viability 66
2.11.1 Terminal deoxinucleotidyltransferase-mediated biotinylated

UTP nick end labeling (TUNEL) 66
2.11.2 DNA fragmentation using agarose gel electrophoresis 67
2.12 Measurement of caspase-3 activity using biochemical assay 68
2.13 Antisense treatments 69
2.13.1 Cellular antisense oligonucleotide uptake 69
2.13.2 JNK antisense oligonucleotides 69
2.14 Isolation of RNA 70
2.14.1 Precautions 70
2.14.2 RNA extraction from cultured cortical neurons 71
2.14.3 Analysis of isolated RNA by Gel Electrophoreis 71
2.14.4 DNAse 1 treatment of RNA 72
2.14.5 Quantitation of RNA 72
2.15 Reverse Transcription-Polymerase Chain Reaction (RT-PCR) 73
2.15.1 Reverse Transcription 73
2.15.2 Polymerase Chain Reaction 73
2.15.3 Densitometry 74
2.16 Statistical analysis 75

Chapter 3 THC induces apoptosis in cultured cortical neurons via the cytochrome *c*/caspase-3 cell death pathway

3.1 Introduction 76
3.2 Results 79
3.2.1 THC induces DNA fragmentation in cultured cortical neurons 79
3.2.2 THC induces DNA fragmentation in cultured cortical neurons in a dose-dependent manner 79
3.2.3 Effect of THC on ladder-patterned DNA fragmentation 81
3.2.4 THC-induced DNA fragmentation in cultured cortical neurons is mediated by the CB_1 receptor 81
3.2.5 THC-induced release of mitochondrial cytochrome *c* into the cytoplasm is AM 251-sensitive 82

3.2.6 THC increases caspase-3 activity in a time-dependent manner in cultured cortical neurons 83
3.2.7 THC stimulates an increase in caspase-3 activity in an AM 251-sensitive manner in cultured cortical neurons 84
3.2.9 THC increases PARP cleavage in cultured neurons 86
3.3 Discussion 87

Chapter 4 An investigation of the role of c-Jun N-terminal Kinase in THC-induced apoptosis of cultured cortical neurons

4.1 Introduction 94
4.2 Results 97
4.2.1 THC increases JNK phosphorylation in cultured cortical neurons 97
4.2.2 THC activates JNK1 and JNK2 isoforms at different time points 97
4.2.3 THC does not regulate JNK1 and JNK2 protein expression 99
4.2.4 JNK3 protein expression is moderate in cultured cortical neurons 99
4.2.5 Dose-dependency of THC-induced JNK1 and JNK2 activation 100
4.2.7 AM 251 pre-treatment prevents THC-induced JNK activation 101
4.2.9 PTX abrogates THC-induced JNK1/2 activation 102
4.2.11 Cellular antisense oligonucleotide uptake 103
4.2.12 Time course of JNK1/2 downregulation in JNK antisense oligonucleotide treated neurons 103
4.2.13 AS1 selectively downregulates JNK1 protein expression 105
4.2.14 AS2 selectively downregulates JNK2 protein expression 105
4.2.15 JNK antisense prevents THC-induced caspase-3 activation in cultured cortical neurons 106
4.2.16 JNK antisense prevents THC-induced DNA fragmentation in cortical cells 108

4.2.17 AS1 pre-treatment has no effect on THC-induced JNK2 activity 110
4.3 Discussion 111

Chapter 5 Determination of the involvement of p53 signalling in THC-induced apoptosis of cultured cortical neurons

5.1 Introduction 118
5.2 Results 121
5.2.1 THC induces an increase in p53 protein expression in cultured cortical neurons 121
5.2.2 Effect of THC on p53 mRNA expression 121
5.2.3 THC induces the phosphorylation of p53 at residue serine-15 in cultured cortical neurons 122
5.2.4 THC increases p53 protein expression in a dose-dependent manner 123
5.2.5 Dose-dependency of THC-induced p53 phosphorylation on serine-15 123
5.2.6 THC increases p53 protein expression via the CB_1 cannabinoid receptor 124
5.2.7 AM 251 pre-treatment prevents THC-induced phosphorylation of p53 on serine-15 124
5.2.8 THC increases cytosolic Bax protein expression in cultured neurons 125
5.2.9 THC increases Bax mRNA expression 125
5.2.10 THC-induced cytosolic Bax expression is dependent on the CB_1 receptor 127
5.2.11 THC has no effect on mitochondrial Bax expression 127
5.2.12 THC-induced Bax protein expression is p53-dependent 129
5.2.13 THC induces Bcl-2 phosphorylation in cultured cortical neurons 130
5.2.14 THC-induced phosphorylation of Bcl-2 is p53-dependent 131
5.2.15 THC-induces caspase-3 activation via p53 132

5.2.16 THC induction of DNA fragmentation is reliant on p53 133
5.3 Discussion 134

Chapter 6 A study of the effect of developmental influences on THC-induced apoptosis in cortical neuronal slices – An *ex vivo* study

6.1 Introduction 141
6.2 Results 140
6.2.1 The expression of CB_1 cannabinoid receptor in rat cortex is dependent on postnatal development 144
6.2.2 Effect of THC on ladder-patterned DNA fragmentation in cortical slices 145
6.2.3 Effect of THC on JNK1 expression in cortical slices obtained from neonatal rats 146
6.2.4 Dose-dependent analysis of the effects of THC on JNK1 expression in rat cortical slices obtained from adolescent rats 146
6.2.5 Effect of THC dose on JNK1 expression in rat cortical slices obtained from adult rats 147
6.2.6 THC induces JNK2 phosphorylation in cortical slices obtained from neonatal rats in a dose-dependent manner 148
6.2.7 THC increases JNK2 phosphorylation in cortical slices obtained from neonatal rats via CB_1 148
6.2.8 Effect of THC on JNK2 expression in cortical slices obtained from adolescent rats 149
6.2.9 Effect of THC on JNK2 in cortical slices obtained from adults 149
6.2.10 p53 protein expression is not modulated by THC in cortical brain slices obtained from neonatal, adolescent and adult animals 151
6.2.11 THC has no effect on phosphorylated $p53^{ser15}$ in cortical brain slices isolated from neonatal, adolescent and adult

rats 152
6.2.12 THC induces caspase-3 activation in cortical slices obtained from neonatal rats in a dose-dependent manner 153
6.2.13 THC increases caspase-3 activity in cortical slices obtained from neonatal rats via CB_1 153
6.2.14 Dose-dependent analysis of the effects of THC on caspase-3 activity in rat cortical slices obtained from adolescent animals 155
6.2.15 Dose-dependent effect of THC on caspase-3 activity in cortical slices obtained from adult rats 155
6.2.16 Effect of postnatal development on basal caspase-3 activity in rat cortical brain slices 156
6.3 Discussion 157

Chapter 7 The effect of postnatal development on THC-induced apoptosis in the rat cortex – An *in vivo* study

7.1 Introduction 165
7.2 Results 167
7.2.1 THC induces DNA fragmentation in the neonatal, but not the adult, cortex *in vivo* 167
7.2.2 Dose-dependency of THC-induced DNA fragmentation in the neonatal cortex *in vivo* 168
7.2.3 AM 251 prevents THC-induced DNA fragmentation in the neonatal cortex *in vivo* 168
7.2.4 THC induces DNA fragmentation in the neonatal, but not the adult, hippocampus *in vivo* 169
7.2.5 THC increases JNK phosphorylation in the neonatal cortex, but not the adult cortex, *in vivo* 170
7.2.6 Dose-dependency of THC-induced regulation of JNK phosphorylation in the neonatal and adult cortex *in vivo* 171
7.2.7 THC induces the differential regulation of JNK1 and

JNK2 isoforms in the neonatal cortex *in vivo* 172
7.2.8 THC does not regulate JNK1/JNK2 activity in the adult cortex *in vivo* 173
7.2.9 THC induces JNK activation in the neonatal cortex *in vivo* via the CB_1 cannabinoid receptor 174
7.2.10 THC induces JNK phosphorylation in the neonatal, but not the adult, hippocampus *in vivo* 174
7.2.11 THC increases caspase-3 activity in the neonatal cortex, but not the adult cortex, *in vivo* 176
7.2.13 Dose-dependency of THC-induced caspase-3 activation in the neonatal cortex *in vivo* 177
7.2.14 Effect of THC concentrations on caspase-3 activity in the adult cortex *in vivo* 178
7.2.15 THC induces caspase-3 activation in the neonatal cortex *in vivo* via the CB_1 cannabinoid receptor 179
7.2.16 THC increases caspase-3 activity in the neonatal, but not the adult, hippocampus *in vivo* 180
7.2.17 Effect of THC on Bax expression in the neonatal and adult cortex *in vivo* 181
7.2.18 Effect of THC on Bcl-2 phosphorylation in the neonatal and adult cortex *in vivo* 182
7.3 Discussion 183

Chapter 8 Final Discussion

8.1 General discussion 189
8.2 Future experiments 198

VIII Bibliography 200

IX Appendix I: Solutions 260

X **Appendix II: Suppliers** 268

XI **Publications** 271

II List of Figures

Figure 1.1 The structure of THC.

Figure 1.2 Distribution of cannabinoid CB_1 receptor in rat brain.

Figure 1.3 The Bcl-2 family members.

Figure 1.4 The activation of caspases.

Figure 1.5 The structure of PARP.

Figure 1.6 Structure of the MAPK signal transduction pathways.

Figure 1.7 p53 regulation of apoptosis.

Figure 1.8 Mechanism of antisense action.

Figure 2.1 Cultured cortical neuronal morphology.

Figure 2.2 Sample photo of total rat RNA.

Figure 3.1 THC induces DNA fragmentation in cultured cortical neurons.

Figure 3.2 Dose-dependency of THC-induced DNA fragmentation in cultured cortical neurons.

Figure 3.3 Assessment of DNA fragmentation in cell culture using DNA ladder technique.

Figure 3.4 AM 251 prevents THC-induced DNA fragmentation.

Figure 3.5 THC promotes translocation of cytochrome *c* from the mitochondria to the cytoplasm.

Figure 3.6 THC increases caspase-3 activity in a time-dependent manner in cultured cortical neurons.

Figure 3.7 THC increases caspase-3 via CB_1 in cultured cortical neurons.

Figure 3.8 THC increases caspase-3 activity in cortical neurons via the CB_1 cannabinoid receptor.

Figure 3.9 THC cleaves PARP following CB_1 receptor activation.

Figure 4.1 THC activates JNK in cultured cortical neurons.

Figure 4.2 Time course of THC-induced activation of JNK.

Figure 4.3 Effect of THC on JNK1/2 total protein expression.

Figure 4.4 Relative expression levels of the JNK isoforms in cultured cortical neurons.

Figure 4.5 THC induces JNK1 activation in a dose-dependent manner.

Figure 4.6 THC induces JNK1 activation in a dose-dependent manner.

Figure 4.7 THC-induced activation of JNK1 is mediated by the CB_1 cannabinoid receptor.
Figure 4.8 THC-induced activation of JNK1 is mediated by the CB_1 cannabinoid receptor.
Figure 4.9 THC-induced JNK1 activation is mediated by G-protein subtypes $G_{i/o}$.
Figure 4.10 THC induces JNK2 activation via G-protein subtypes $G_{i/o}$.
Figure 4.11 Antisense oligonucleotides are actively taken up by cortical neuronal cultures after 1hr of incubation.
Figure 4.12 Time course of JNK antisense mediated JNK depletion.
Figure 4.13 AS1 effectively reduce total JNK1 protein expression.
Figure 4.14 AS2 downregulates total JNK2 protein expression.
Figure 4.15 JNK1 and JNK2 are required for caspase-3 activity in THC-induced apoptosis.
Figure 4.16 JNK1 and JNK2 isoforms are required for THC-induced DNA fragmentation.
Figure 4.17 Activation of JNK1 is not upstream of THC-induced JNK2 activation.
Figure 5.1 Time course of THC-induced increase in p53 protein expression.
Figure 5.2 THC does not regulate transcription of p53 mRNA expression at 5 min.
Figure 5.3 Time course of THC-induced phosphorylation of p53 at serine-15.
Figure 5.4 THC increases p53 expression in a dose-dependent manner.
Figure 5.5 THC increases p53 phosphorylation on serine-15 in a dose-dependent manner.
Figure 5.6 THC increases p53 protein expression via the CB_1 receptor.
Figure 5.7 THC increases p53 phosphorylation on serine-15 via the CB_1 receptor.
Figure 5.8 THC increases cytosolic Bax protein expression at 60 and 120 min.
Figure 5.9 THC increases Bax mRNA expression.
Figure 5.10 THC increases cytosolic Bax protein expression via the CB_1 receptor.
Figure 5.11 Effect of THC on mitochondrial Bax protein expression.

Figure 5.12 THC increases Bax protein expression via p53.
Figure 5.13 Time course of THC-induced phosphorylation of Bcl-2.
Figure 5.14 Bcl-2 phosphorylation by THC is p53-dependent.
Figure 5.15 p53 is required for caspase-3 activity in THC-induced apoptosis.
Figure 5.16 p53 is required for THC-induced DNA fragmentation.
Figure 6.1 CB_1 cannabinoid receptor expression increases with postnatal development.
Figure 6.2 Assessment of DNA fragmentation using DNA ladder technique.
Figure 6.3 Effect of THC on phospho-JNK1 expression in brain slices obtained from the cortex of neonatal rats.
Figure 6.4 Effect of THC on phospho-JNK1 expression in brain slices obtained from the adolescent rat cortex.
Figure 6.5 Effect of THC on JNK1 expression in cortical brain slices from adult rats.
Figure 6.6 THC induces JNK2 activation in cortical slices obtained from neonatal rats in a dose-dependent manner.
Figure 6.7 THC induces JNK2 activation via CB_1 in neonatal cortical brain slices.
Figure 6.8 THC induces JNK2 activation in cortical slices obtained from adolescent rats at high THC concentrations.
Figure 6.9 JNK2 activity in cortical slices obtained from adult rats is regulated by THC in a dose-dependent manner.
Figure 6.10 THC has no effect on p53 in cortical brain slices obtained from neonatal, adolescent and adult rats.
Figure 6.11 Effect of THC on p53 phosphorylation in cortical brain slices isolated from neonatal, adolescent and adult rats.
Figure 6.12 THC increases caspase-3 activity in cortical brain slices obtained from neonatal animals in a dose-dependent manner.
Figure 6.13 THC increases caspase-3 activity in cortical brain slices obtained from neonatal rats via CB_1.
Figure 6.14 Dose-dependent analysis of the effect of THC on caspase-3 in cortical brain slices isolated from adolescent rats.
Figure 6.15 Dose-dependent analysis of the effect of THC on caspase-3 in cortical brain slices obtained from adult animals.

Figure 6.16 Basal caspase-3 activity is associated with postnatal development.
Figure 7.1 THC induces apoptosis in the neonatal cortex *in vivo*.
Figure 7.2 Dose-dependency of THC-induced apoptosis in the neonatal/adult cortex *in vivo*.
Figure 7.3 The *in vivo* apoptotic actions of THC in the neonatal cortex are CB_1 receptor-dependent.
Figure 7.4 THC induces DNA fragmentation in the neonatal hippocampus *in vivo*.
Figure 7.5 THC activates JNK in the neonatal cortex *in vivo*.
Figure 7.6 Effect of THC on JNK1/2 activity in neonatal cortex *in vivo*.
Figure 7.7 THC has no effect on JNK1/2 in adult cortex *in vivo*.
Figure 7.8 Dose-dependency of THC-induced JNK phosphorylation in the neonatal/adult cortex *in vivo*.
Figure 7.9 The proclivity of THC to regulate JNK activity in the neonatal cortex *in vivo* is CB_1 receptor-dependent.
Figure 7.10 THC activates JNK in the neonatal, but not adult, hippocampus *in vivo*.
Figure 7.11 Effect of THC on caspase-3 activity in neonatal and adult cortex.
Figure 7.12 THC activates caspase-3 in the neonatal cortex *in vivo*.
Figure 7.13 THC activates caspase-3 in the neonatal cortex *in vivo* in a dose-dependent manner.
Figure 7.14 A dose-response analysis of the effect of THC on caspase-3 activity in the adult cortex *in vivo*.
Figure 7.15 The *in vivo* apoptotic actions of THC in the neonatal cortex are CB_1 receptor-dependent.
Figure 7.16 Caspase-3 activity is regulated by THC in the neonatal, but not the adult, hippocampus *in vivo*.
Figure 7.17 Effect of THC on Bax expression in the neonatal and adult cortex *in vivo*.
Figure 7.18 Effect of THC on phospho-Bcl-2 expression in the neonatal and adult cortex *in vivo*.

Figure 8.1 Proposed model contributing to THC-induced neuronal apoptosis in cultured rat cortical neurons, cortical brain slices obtained from neonatal rats and the neonatal rat cortex *in vivo*.

III List of Tables

Table 2.1 Antibodies used for Western blotting.

Table 2.2 Primer pairs used for PCR.

IV Acknowledgements

I would first like to thank my supervisor Dr. Veronica Campbell. I still consider myself very lucky that you changed your mind that day and rustled up an undergraduate project for me. You have been very inspirational to work with in terms of your dedication, patience, knowledge and particularly your enthusiasm. Thank you for giving me the opportunity and I hope that your research continues to gain the international appraisal that it deserves.

There are many people whom I have worked with over the past three years that I wish to acknowledge, but I must first thank Dr. Barry Boland and Dr. Marie Fogarty, who both had a huge influence on my decision to pursue my Ph.D studies in Veronica's lab. Thank you both for all you taught me and making the VC lab such a good place to work. I must thank my present lab co-workers, Eric Farrell and Roisín McCormack. I am sad that I will not work with you more and wish you both success with your projects. I am also indebted to the students who have worked directly with me on my project, including Ingrid Redmond, Áine Murphy and Laura Kelly.

I would like to thank Prof. Marina Lynch for her personal inspiration and the use of her lab equipment. I wish also to thank all members of the MAL lab, both past and present, for making my time in the lab such an enjoyable one. They are Dr. Aileen Lynch, Dr. Francis Oliver Maher, Dr. Darren Martin, Dr. Yvonne Nolan, Dr. Rachel Nally, Aedín Minogue, Claire Barry, Michelle Moore, Michelle Walsh, Céire Costelloe, Rachael Clarke, Thady Kavanagh, Anto Lyons and Peter Lonergan. A special thanks to Aedín and Darren for their help with the *in vivo* work.

I would like to acknowledge Prof. Chris Bell for affording me the privilege of carrying out my research in the Physiology Department. Sincere thanks to Dr. Alan Tuffery for his support, particularly during my undergraduate years.

I would also like to thank other students in the Department (past and present) including Noreen Boyle, Amy Hennigan, Joan Sullivan, Laurence O'Dwyer, Jaime O'Dwyer and Mikel Egana, who all created a pleasant atmosphere in the Department. I also thank the technical staff including Kieran, Alice, Quentin, Dave, Ann, Aidan, Siobhán and Doreen for their kindness.

Special thanks to Leslie Penney for her suggestions and assistance with sectioning.

I wish to thank my parents, Elizabeth and Kieran, and my sister, Ciara, for being so patient and encouraging, particularly through difficult times at the beginning of my studies. Special thanks to my brother, Rob, who has had such a big influence on me over the last years. Finally, I dedicate this thesis to Jane to thank you for all your support, patience and belief. I am very grateful.

V Declaration

This thesis is submitted by the undersigned for the degree of Doctor in Philosophy at the University of Dublin, Trinity College and had not been submitted to any other university as an exercise for a degree. I declare that this thesis is entirely my own work and I give permission to the library to lend or copy this thesis upon request.

Eric Downer

VI Abstract

Δ^9-Tetrahydrocannabinol (THC), the principle psychoactive component of marijuana (*Cannabis sativa*), elicits diverse psychological effects in humans. THC exerts its central effects through the CB_1 cannabinoid receptor, a G-protein-coupled receptor distributed throughout the central nervous system. We report that THC induces DNA fragmentation in a dose- and time-dependent manner in cultured cortical neurons. THC-induced apoptosis was inhibited by the CB_1 receptor antagonist AM 251, suggesting that THC-induced neurotoxicity in cortical neurons is mediated by the central CB_1 cannabinoid receptor. THC promoted translocation of mitochondrial cytochrome *c* to the cytosol and increased the activity of caspase-3, in an AM 251-sensitive manner. Use of the CB_1 receptor inhibitor has also identified that cleavage of the DNA-repair enzyme poly(ADP-ribose) polymerase (PARP) as a downstream consequence of THC-induced CB_1 activation. Furthermore, THC induced the activation of the stress-activated protein kinase, c-Jun N-terminal kinase (JNK), via the CB_1 receptor and its associated G-protein, $G_{i/o}$. Treatment of cultured cortical neurons with THC resulted in the time-dependent activation of JNK1 and JNK2 isoforms that preceded neuronal cell death. Use of specific JNK1 and JNK2 antisense oligonucleotides has identified activation of caspase-3 and DNA fragmentation as a downstream consequence of JNK1 and JNK2 activation. Time course experiments also revealed that THC induces an early increase in the expression of the nuclear phospho-protein, p53. This increase was via the central CB_1 receptor and its associated G-protein and was dependent on THC-induced phosphorylation of p53 on residue serine-15. THC was also found to increase the cytosolic expression of the pro-apoptotic mitochondria-associated protein Bax, and induce the phosphorylation of its anti-apoptotic protein partner, Bcl-2, events presumably contributing to cytochrome *c* translocation and apoptosis. Treatment of cortical neurons with the p53 inhibitor, pifithrin-α, blocked the modulatory effects of THC on Bax and phospho-Bcl-2 protein expression, caspase-3 activity and DNA fragmentation, indicating that p53 neuronal signalling is pivotal in THC-induced neuronal apoptosis of cultured cortical cells.

The inter-relationship between neuronal maturity and THC apoptotic signal transduction was determined by examining the *ex vivo* effects of THC on the viability of cortical slices obtained from three rat age groups; neonatal (4-7-day old), adolescent (20-30-day old) and adult (3-4 month old) rats. For *ex vivo* experiments, cortical brain slices were incubated with THC (5nM-50μM) for a 2hr period. Interestingly, the expression of CB_1 receptor varied considerably in rat cortical slices depending on developmental age. THC produced a dose-dependent increase in JNK2 phosphorylation and caspase-3 activity via CB_1 in cortical slices obtained from neonatal, but not adolescent or adult animals, indicating that the proclivity of THC to regulate these apoptotic molecules in the rat cortex are dependent on postnatal development. THC had no effect on JNK1 and p53 phosphorylation in any rat age group at the time point tested.

The influence of postnatal development on the apoptotic actions of THC in the rat cortex was also determined in an *in vivo* system. For *in vivo* experiments, neonatal (4-7-day old) rat pups and adult (3-4-month old) rats received subcutaneous injections of THC (1, 10, 30mg/kg) for 3hr. The role of the CB_1 receptor in modulating the *in vivo* effects of THC was determined by administering intraperitoneal injections of AM 251 for 30 min prior to THC exposure. Following THC exposure, a dose-dependent increase in the level of DNA fragmentation, JNK2 and caspase-3 activity was observed in the neonatal, but not the adult, cortex. These effects were mediated by the CB_1 receptor. The apoptotic effects of THC on the neonatal cortex *in vivo* did not involve an increase in JNK1 activity or an alteration of the mitochondria-associated proteins, Bax and Bcl-2.

The experimental evidence presented in this study indicate that damaging effects of THC in neonatal cortical cells are operative in *in vitro*, *ex vivo* and *in vivo* systems. The data highlights signal transduction pathways that contribute directly to the neurotoxic effects of THC. Interestingly, the apoptotic actions of THC are influenced by postnatal development, with the damaging consequences of THC restricted to the neonatal brain. Overall, these finding suggest a cannabinoid-induced molecular mechanism culminating in the demise of neonatal cortical cells.

VII List of Abbreviations

Ab	antibody
AFC	Ac-DEVD-7-amino-4-trifluoromethylcoumarin
2-AG	2-arachidonyl-glycerol
AIF	apoptosis-inducing-factor
Anandamide	*N*-arachidonyl-ethanolamide
ANOVA	analysis of variance
APAF	apoptotic protease activating factor
APS	ammonium persulphate
ARA-C	cytosine-arabino-furanoside
AS	antisense oligonucleotides
AS1	JNK1 antisense oligonucleotides
AS2	JNK2 antisense oligonucleotides
ATF-2	activating transcription factor-2
Aβ	beta-amyloid
Bcl-2	B-cell leukaemia/lymphoma 2-like proteins
BH	Bcl-2 homology
Bp	base pairs
BSA	bovine serum albumin
Ca^{2+}	calcium ion
$CaCl_2$	calcium chloride
CAD	caspase-activated deoxyribonuclease
cAMP	cyclic AMP
CARD	caspase recruitment domain
CB	cannabinoid
cDNA	copy deoxyribonucleic acid
CHO	chinese hamster ovary
cm	centimetre
CNS	central nervous system
CO_2	carbon dioxide
DAB	diaminobenzidine
DEPC	diethylpyrocarbonate

DEVD	aspartic-glutamic-valine-aspartic residue
DFF	DNA fragmentation factor
DMSO	dimethyl sulphoxide
DNA	deoxyribonucleic acid
DNAse	deoxyribonucleic acid
dNTP	deoxynucleotidetriphosphate
DOTMA/DOPE	N-[1-(2,3-dioleoylooxy)propyl]-N,N,N-trimethylammonium/dioleotlphosphatidyletha nolamine
DTT	dithiothreitol
ECL	enhanced chemiluminescence
EDTA	ethylenediamine-tetraacetic acid
EF	executive function
EGTA	ethylene glycol bis (□-amionethyether) N,N 'tetraacetic acid
ERK	extracellular signal regulated kinase
EtBr	ethidium bromide
EtOH	ethanol
FADD	Fas-associated death domain
FITC	flourescein isothiocyanate
GCK	germinal center kinase
G-protein	GTP-binding protein
GTP	guanosine 5'-diphosphate
HEPE	N-[2-Hydroxyethyl]piperazine-N'-[2-ethane-sulfonic acid]
H_20_2	hydrogen peroxide
hr	hour
HRP	horseradish peroxidase
ICE	interleukin 1β-converting enzyme
IgG	immunoglobulin G
IL	interleukin
JIP	JNK-interacting protein
JNK	c-Jun N-Terminal kinase

K^+	potassium ion
KCl	potassium chloride
kDa	kilo Dalton
KH_2PO_4	potassium phosphate
µl	microlitre
LTP	long-term potentiation
µM	micromolar
µm	micrometer
mA	milliamp
MAPK	mitogen-activated protein kinase
MAPKK	MAPK kinase
MAPKKK	MAPK kinase kinase
Mg	milligram
$MgCl_2$	magnesium chloride
Mg_2SO_4	magnesium sulphate
min	minute
mm	millimetre
mM	millimolar
mRNA	messenger ribonucleic acid
Na^+	sodium ion
NaCl	sodium chloride
NAD	nicotinamide adenine dinucleotide
Na_2HPO_4	sodium phosphate (dibasic anhydrous)
NBM	neurobasal medium
NF-κB	nuclear factor-κB
NGF	nerve growth factor
$-NH_2$	amino terminal
nm	nanometre
p53AIP1	p53-regulated apoptosis-inducing protein 1
PAGE	polyacrylamide gel electrophoresis
PAK	p21-activated kinase
PAR	poly (ADP) ribose
PARP	poly(ADP) ribose polymerase

PBS	phosphate-buffered saline
PC12	phaeochromocytoma cell line
PCR	polymerase chain reaction
PKB	protein kinase B
PKC	protein kinase C
PLA_2	phospholipase A_2
PMSF	phenylmethylsulphonyl fluoride
PTP	permeability transition pore
PTX	pertussis toxin
RNA	ribonucleic acid
RNAse	ribonuclease
ROS	reactive oxygen species
RT	room temperature
SAPK	stress-activated protein kinase
SC	scrambled control oligonucleotides
SC1	JNK1 scrambled control oligonucleotides
SC2	JNK2 scrambled control oligonucleotides
SDS	sodium dodecyl sulphate
SDS-PAGE	SDS-polyacrylamide gel electrophoresis
SEM	standard error of the mean
TBE	tris borate edta
TBS	tris-buffered saline
TBS-T	TBS-Tween
TdT	terminal deoxynucleotidyl transferase
TE	Tris-EDTA
TEMED	N,N,N,-N-tetramethylenediamine
THC	Δ^9-Tetrahydrocannabinol
TNF-α	tumour necrosis factor α
Tris-HCl	Trizma-hydrochloride
TUNEL	TdT-mediated-UTP-end nick labelling
Tyr	tyrosine
U	unit
UV	ultraviolet

VEGF	vascular endothelial growth factor

Chapter 1

General Introduction

1.1 Marijuana

Marijuana, the common name for cannabis, is one of the oldest and most widely used of all psychoactive drugs in the world today with 4.2% of individuals over the age of 15 abusing marijuana (Gatley *et al.*, 1996; Huestis and Choo, 2002). It has a long history of consumption in human societies for both medicinal and recreational purposes (Mailleux and Vanderhaeghen, 1992; Grinspoon and Bakalar, 1995) and its prevalence of use continues to increase, particularly in young people (Ashton, 2001). The drug is derived from the Indian hemp plant, *Cannabis sativa*, which has been cultivated in China for its fibre for over 5000 years (Reisine and Brownstein, 1994). All parts of both the male and female plant contain psychoactive cannabinoids (Abood and Martin, 1992) with the highest concentrations found in the resinous exudate of the female flower head, with lower concentrations also found in the leaves, stem and roots (Ameri, 1999). The seed does not contain any cannabinoids (Iversen, 2000). The most potent preparations of marijuana (hashish) are made by scraping the resin from the flower heads (Iversen, 2000). Most commonly the plant is cut, dried and incorporated into cigarettes, allowing it be smoked, the preferred route of administration in Western countries (Katzung, 2001). The psychoactive compound in marijuana is soluble in fats and alcohol, which ensures that marijuana is also commonly taken orally in various foodstuffs and drinks (Iversen, 2000).

The behavioural and pharmacological effects of marijuana involve the central nervous system (CNS). Behavioural effects have been studied extensively in humans over the past 30 years, and although subjective effects of the drug vary from individual to individual depending on the dose of the drug, the environment in which the drug is taken, expectations of the subject and the route of administration, there are several identified behavioural effects that typically accompany marijuana use (Abood and Martin, 1992). The most pertinent feature is an initial period of euphoria that is frequently followed by a period of sedation (Azorlosa *et al.*, 1992; Abood and Martin, 1992). The subjective effect of marijuana use usually reaches a maximum level approximately 20 min after smoking and slowly declines to baseline over 3-4hr

(Chiang and Barnett, 1984). Marijuana has also been demonstrated to impair functioning in cognitive and performance tasks, including the impairment of short-term memory consolidation (Block and Ghoneim, 1993; Heyser *et al.*, 1993; Hampson and Deadwyler, 1999) and results in decrements in tasks such as reaction time, concept formation and motor coordination (Ashton, 2001). Indeed, studies have linked marijuana use with increased incidence of road traffic accidents (Buchan *et al.*, 1998). At high doses, acute panic reactions or mild paranoia have also been observed (Hollister, 1986). Marijuana is often co-abused with other drugs such as alcohol, and there is evidence that the impairment produced by alcohol is additive to that induced by marijuana (Lukas and Orozco, 2001). It has been suggested that some of the behavioural manifestations of marijuana are associated with an alteration in functional activity of the cortex (Matthew *et al.*, 1997). This is supported by evidence that abusers of marijuana display deficits in tasks dependent on the frontal cortex, particularly working memory (Jentsch *et al.*, 1998), suggesting that some dysfunction in frontal cortical functioning may contribute to the behavioural effects that are typically ascribed to marijuana usage.

In addition to the central actions of marijuana, cannabinoids exert a variety of biological effects outside the CNS. The most consistent cardiovascular effects of marijuana are tachycardia, hypotension and dilation of conjuctival blood vessels (Cavero *et al.*, 1974; Ashton, 2001). Furthermore, acute cardiovascular death in young adults has been reported following cannabis use (Bachs and Morland, 2001). Marijuana has no effect on respiratory rate but is associated with bronchitis and emphysema (Fligiel *et al.*, 1997; Roth *et al.*, 1998). There is also evidence that marijuana modulates immune functions, including the regulation of antibody production and lymphocyte proliferation (Nahas *et al.*, 1974; Klein *et al.*, 1998; Schwarz *et al.*, 1994) and is furthermore involved in the regulation of the reproductive system (Wenger *et al.*, 1999).

As with most drugs of abuse, tolerance has been reported to develop to many of the effects of marijuana in both animals and man, even with modest doses of marijuana (Pertwee, 1991). It is established that chronic marijuana use does not result in withdrawal (Abood and Martin, 1992). Although few reports have established experimental models for self-administration of cannabinoids,

an indicator of abuse potential, the occurrence of some form of psychological dependence or craving is thought to occur rather than physical dependence (Abood and Martin, 1992). Hence, there is evidence that many marijuana users are now seeking treatment for cannabis dependence (Ashton, 2001).

1.2 Δ^9-Tetrahydrocannabinol

The predominant active ingredient in preparations of marijuana is Δ^9-Tetrahydrocannabinol (THC), a compound now considered to be the major psychoactive component of marijuana (Gaoni and Mechoulam, 1964). THC is a highly lipophilic molecule, which allows it to permeate the plasma membrane and sequester in the lipid compartments of the body (Di Marzo *et al.*, 1998). Indeed, within seconds of inhaling marijuana smoke THC is present at its site of action in the brain (Agurell *et al.*, 1986). The hemp plant synthesizes over 400 bioactive chemical molecules, of which more than 60 are known as cannabinoids due to their structural similarity to THC (Abood and Martin, 1992). These include the extensively studied naturally occurring cannabinoids, cannabinol and canabidiol, whose discovery led to the production of cannabinoid derivatives including THC (Iversen, 2000). The content of THC varies considerably among plants, so that special genetic lines may produce as much as 4-6% THC content, while most marijuana plants have a THC content ranging from trace amounts to 2.7% (Katzung, 2001). Furthermore, hashish contains 4-10% THC (Samuelsson, 1999). Makriyannis and Rapaka (1990) have shown that the structure of THC includes several molecular fragments that contribute to its cannabimimetic activity (Figure 1.2). Loss of the phenolic hydroxyl on the A ring eliminates THC activity. However the side chain at the C-3 position is crucial for cannabimimetic activity. Lengthening of this side enhances cannabinoid affinity for its receptor (see section 1.3), and this has been shown to occur *in vivo* when THC is converted to 11-hydroxy-THC, the centrally active metabolite of THC (Abood and Martin, 1992). However, this compound is not nearly as abundant as THC, and the predominant activity of marijuana is derived from THC itself (Cone and Huestis, 1993).

Smoking marijuana results in the rapid appearance of THC in the plasma, appearing after the first marijuana puff and reaching a peak within 10 min (Huestis *et al.*, 1992). Interestingly, the physiological and behavioural effects of marijuana lag behind plasma THC levels, reaching a maximum at approximately 30 min (Chiang and Barnett, 1984). This may be due to evidence that the excretion of THC and its metabolites occurs over extended periods (Huestis and Cone, 1998). Indeed, the plasma half-life of THC has been determined to be as long as 4.1 days (Cone and Huestis, 1993) ensuring that traces of THC are evident in the brain several days after marijuana consumption.

The discovery of THC was followed by the production of synthetic analogues of THC such as CP-55, 940 (Devane *et al.*, 1988), HU-210 (Mechoulam *et al.*, 1988) and WIN 55212-2 (D'Ambra *et al.*, 1996). These products were developed as compounds possessing desirable medicinal properties. However, only one synthetic cannabinoid, nabilone, in addition to THC which is prescribed in capsules (Marinol), has been developed and approved as a medicine (Lemberger, 1999; Tramer *et al.*, 2001). Despite this, synthetic cannabinoids serve as invaluable research tools in the study of cannabinoid pharmacology.

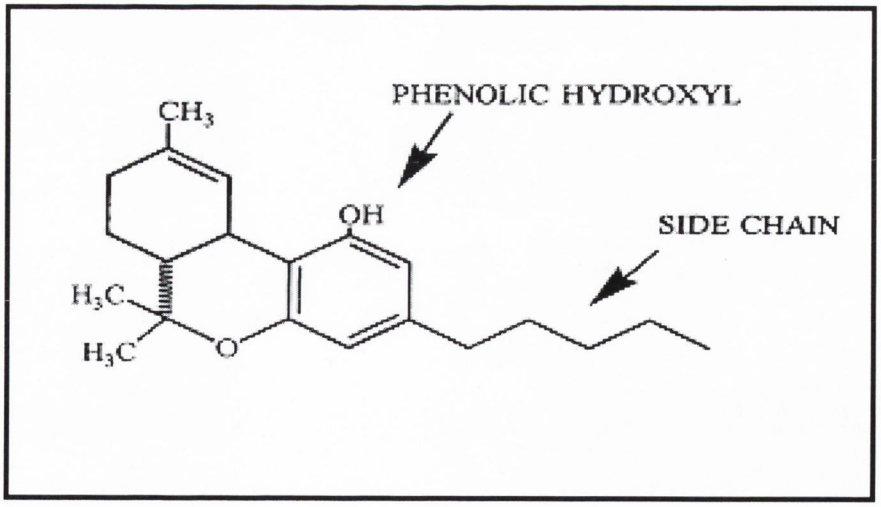

Figure 1.1: The structure of THC (Adapted from Iversen, 2000).

1.3 Cannabinoid receptor

Owing to the lipophilicity and cell membrane-perturbating actions of THC (Di Marzo *et al.*, 1998) it was considered that this compound acted non-specifically by dissolving into the lipid-rich plasma membranes of neurons and disrupting CNS functioning. Speculation about the cellular actions of THC was resolved when it was found that the addition of THC to neuroblastoma cells inhibited the activity of adenylate cyclase and decreased cellular levels of cyclic AMP (cAMP), therefore indicating that its actions were mediated by a member of the GTP-binding protein (G-protein) receptor family (Howlett and Fleming, 1984). Furthermore, sensitivity to pertussis toxin (PTX) provided evidence that THC acts through a $G_{i/o}$-protein-coupled cannabinoid receptor mechanism (Howlett *et al.*, 1986). Receptor-binding studies have also provided direct evidence that THC exerts most of its central and peripheral effects by binding to cannabinoid receptors (Devane *et al.*, 1988; Howlett, 1995). Cannabinoid receptors have an amino acid sequence consistent with the tertiary structure of G-protein-coupled receptors (Porter and Felder, 2001). The receptors consist of an extracellular N-terminal and intracellular C-terminal, with seven hydrophobic transmembrane-spanning domains that couple to the receptor G-protein (Reisine and Brownstein, 1994).

1.3.1 Cannabinoid receptor subtypes

To date, two different subtypes of cannabinoid receptor have been characterised and cloned from mammalian tissues: CB_1 (Matsuda *et al.*, 1990) and CB_2 (Munro *et al.*, 1993). A splice variant of the CB_1 receptor has also been isolated and designated as $CB_{1(b)}$ (Shire *et al.*, 1995). The first cannnabinoid receptor, CB_1, was reported by Matsuda and colleagues (1990) after the cloning and expression of a complementary DNA from a rat cDNA library that encoded the receptor. The second cannabinoid receptor subtype, CB_2, was derived three years later by Munro and co-workers (1993) from a human promyelocytic leukaemia cell HL60 cDNA library. Both subtypes have an amino acid sequence consistent with the tertiary structure typical of G-protein-coupled receptors (Porter and Felder, 2001). As with many G-protein coupled receptors,

the CB_1 receptor contains conserved cysteine residues in the third extracellular loop which stabiles the tertiary structure of the receptor (Matsuda, 1997). CB_1 also differs from most G-protein-coupled receptors in that it lacks highly conserved proline residues (Ameri, 1999). The CB_2 receptor exhibits 68% sequence homology with the CB_1 receptor within the transmembrane domain, and 44% homology throughout the entire receptor (Munro *et al.*, 1993). There are considerable differences in the size of both receptor subtypes. While the CB_1 receptor consists of 472 amino acids (53kDa) the CB_2 receptor consists of 360 amino acids (40kDa) due to the difference in the length of the extracellular domain (Matsuda, 1997). The CB_1 receptor sequence and pharmacology appear to be conserved across species, with the rat CB_1 receptor sharing 97.3% homology at the amino acid level and 93% identity at the nucleic acid level with the human CB_1 receptor (Gérard *et al.*, 1991). Furthermore, an amphibian cannabinoid receptor has been cloned recently, suggesting evolutionary conservation of the cannabinoid system (Soderstrom *et al.*, 2000). However, the CB_2 receptor subtype exhibits pharmacological differences between species (Griffin *et al.*, 2000). Pharmacological and physiological evidence suggests that there may be other cannabinoid receptor subtypes that have yet to be cloned and characterised. Indeed, Breivogel and co-workers (2001) have provided evidence for an additional cannabinoid receptor family in mouse brain. This is a G-protein-coupled receptor that is related to both CB_1 and CB_2 but is insensitive to plant-derived cannabinoids. However, the cloning and expression of the receptor gene has not been determined. In addition, endogenous cannabinoids have been demonstrated to act via vanilloid receptors (Maccarrone et al., 2000). Indeed, recent evidence suggests that vasoactive effects are exerted by endogenous (Pacher *et al.*, 2004; Ross, 2003; see Section 1.4) and synthetic (Baker and McDougall, 2004) cannabinoids by acting via vanilloid TRPV(1) receptors, highlighting TRPV(1) as a potential cannabinoid receptor.

Although the ligand binding selectivities of the CB_1 and CB_2 receptors are similar (Ameri, 1999), there is evidence that the enodogenous cannabinoid, anandamide (see Section 1.4), exhibits higher affinity for CB_1 than for CB_2 receptors (Showalter *et al.*, 1996). It is also accepted that, despite anandamide binding to both receptors, it has the characteristics of a partial cannabinoid

agonist (Hillard, 2000). In contrast, a second endogenous cannabinoid, 2-arachidonyl-glycerol (2-AG; see Section 1.4), binds with low affinity to CB_1 and CB_2, but exhibits full efficacy (Hillard, 2000; Sugiura *et al.*, 2000). Research on the cannabinoid receptors has also suggested that THC acts as a partial agonist at the CB_1 cannabinoid receptor (Devane *et al.*, 1988). There is also evidence that cannabinoid receptors downregulate after a chronic cannabinoid exposure (Oviedo *et al.*, 1993) which may underlie the development of tolerance after prolonged cannabinoid exposure (Rodriquez de Fonseca *et al.*, 1994).

1.3.2 Cannabinoid receptor distribution

The CB_1 cannabinoid receptor is one of the most abundantly expressed of neuronal receptors (Iversen, 2000) and exhibits the same general pattern of distribution in several mammalian species, including man (Herkenham *et al.*, 1991). CB_1 is distributed mainly in the CNS and is responsible for mediating the psychoactive effects of THC (Matsuda *et al.*, 1990). Areas such as the cortex (layers I and IV), hippocampus (CA pyramidal cell layers and dentate gyrus), basal ganglia (substantia nigra and globus pallidus) and cerebellum (molecular layer) represent regions of the brain in which high densities of the CB_1 receptor subtype have been identified (Tsou *et al.*, 1998; Mailleux and Vanderhaeghen, 1992; Figure 1.2). The high density in these regions demonstrates an involvement of cannabinoids in the impairment of cognition and memory. Within these brain regions immunohistochemical analysis has revealed that the CB_1 receptor appears to be expressed on cell bodies, dendrites and axons of neuronal cell fibres (Tsou *et al.*, 1998). Furthermore, CB_1 expression is sparse or absent in areas of the brain stem and hypothalamus (Ameri, 1999). Expression of the CB_1 cannabinoid receptor does not occur exclusively in the brain but also in several peripheral tissues, including lung (Rice *et al.*, 1997), testis (Gérard et al., 1991) and presynaptically on sympathetic nerve terminals (Ishac *et al.*, 1996).

In contrast, the expression of the CB_2 receptor is almost exclusively restricted to cells and organs of the immune system (Munro *et al.*, 1993) being primarily expressed in macrophages from the marginal zone of the spleen (Munro *et al.*, 1993). The CB_2 receptor is also highly expressed in the tonsils

and immune cells (Schatz *et al.*, 1997; Galiegue *et al.*, 1995). To date, no CB_2 receptor transcripts have been reported in brain tissue (Reggio, 1999).

There is growing evidence that cannabinoid receptor expression levels in the brain vary with developmental age (Fernández-Ruiz *et al.*, 2000; see section 1.6). Based on expression patterns in key brain regions it has been shown that the human CB_1 receptor expression is higher in the fetal and neonatal brain when compared with expression levels in the adult human brain (Glass *et al.*, 1997). Similarly, Berrendero and colleagues (1998) have observed that CB_1 receptor mRNA expression appear atypically distributed in the fetal rat brain as compared to the adult brain. This evidence suggests that the cannabinoid system may play a modulatory role in neurobiological processes, in particular neural development.

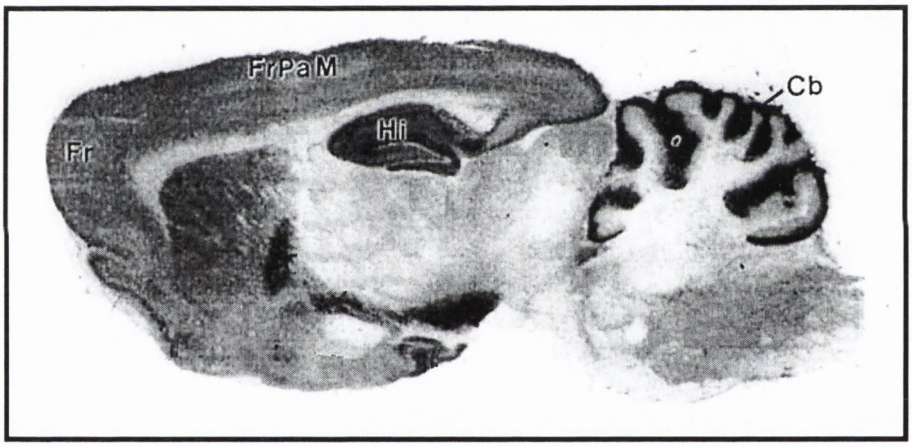

Figure 1.2: Distribution of cannabinoid CB_1 receptor in rat brain.
An autoradiograph of the binding of radioactively labelled CP-55, 940 to a brain section. Cb=cerebellum; Fr=frontal cortex; FrPaM=frontoparietal cortex; Hi=hippocampus (adapted from Herkenham *et al.*, 1991).

1.3.3 Cannabinoid receptor signal transduction

The CB_1 receptor has been shown to modulate a number of neuronal functions following activation, including ion channel activity (Caulfield and Brown, 1992; Turkanis *et al.*, 1991; Deadwyler *et al.*, 1993; Twitchell *et al.*, 1997) and neurotransmitter release (Jentsch *et al.*, 1998; Gessa *et al.*, 1998;

Shen *et al.*, 1996; Schlicker *et al.*, 1997). CB_1 receptor agonists inhibit voltage-gated calcium currents in neuroblastoma cells (Caulfield and Brown, 1992). Furthermore, CB_1 receptors inhibit N- and P/Q-type Ca^{2+} channels in cultured rat hippocampal neurons (Twitchell *et al.*, 1997). The effect of CB_1 cannabinoid receptors on calcium currents is slow in onset and recovery and is PTX-sensitive, implicating a role for G-protein subtypes G_i or G_o (Twitchell *et al.*, 1997). THC has also been shown to inhibit voltage-gated Na^+ channels in neuroblastoma cells (Turkanis *et al.*, 1991). Cannabinoid receptors are also involved in activating inwardly rectifying K^+ channels in murine tumour cells expressing CB_1 (Mackie *et al.*, 1995) and voltage-dependent K^+ A currents in hippocampal cells (Deadwyler *et al.*, 1993). Again, these actions are blocked by PTX. Ion channel modulation appears to be a feature associated with CB_1 and not CB_2 receptor subtypes (Felder *et al.*, 1995).

There is also evidence that neurotransmitter systems are modulated by cannabinoid receptors and this may account for some of the psychoactive effects of marijuana use. The CB_1 receptor has been shown to decrease acetylcholine in the rat cortex and hippocampus *in vivo* (Gessa *et al.*, 1998; Carta *et al.*, 1998; Nava *et al.*, 2001). THC has also been shown to reduce dopamine transmission in the rat frontal cortex *in vivo* (Jentsch *et al.*, 1998). However, there is also evidence that cannabinoid receptors stimulate dopamine release in the frontal cortex *in vivo* (Pistis *et al.*, 2001) and *in vitro* (French, 1997). Cannabinoids have also been shown to inhibit, via CB_1, noradrenaline release in slices from human and rat hippocampus (Schlicker *et al.*, 1997) and glutamatergic transmission in cultured rat hippocampal cells (Shen *et al.*, 1996) and cerebellar Purkinje cells (Levenes *et al.*, 1998). Since calcium channels are required to evoke neurotransmitter release in the CNS (Wheeler *et al.*, 1994), cannabinoids may inhibit neurotransmission by modulating the influx of Ca^{2+} into the nerve terminal.

The signalling pathways activated by cannabinoid receptors are continuing to be elucidated. The proclivity of cannabinoids to inhibit adenylate cyclase was first indentified by Howlett and Fleming (1984). Indeed, it was this finding that was the basis of the concept that the effects of cannabinoids are mediated by G-protein coupled membrane receptors. Cannabinoids have been shown to couple to the inhibition of adenylate cyclase in a neuroblastoma cell

line (Dill and Howlett, 1988) and in the rat cortex and hippocampus (Bidaut-Russell *et al.*, 1990). The inhibitory effects of cannabinoids on adenylate cyclase involve both CB_1 (Felder *et al.*, 1995) and CB_2 (Slipetz *et al.*, 1995) cannabinoid receptors. Recently the CB_1 has also been linked to the activation of the mitogen-activated protein kinase (MAPK) pathway, a signalling network involved in the mediation of cell differentiation and death (Mielke and Herdegen, 2000; see section 1.9). The CB_1 receptor has also been shown to activate extracellular signal-regulated kinase (ERK) in hippocampus *in vitro* and *in vivo* (Derkinderen *et al.*, 2003), in astrocytoma cells in culture (Galve-Roperh *et al.*, 2002), in Chinese hamster ovary (CHO) cells transfected with CB_1 (Bouaboula *et al.*, 1995b) and in MCF-7 cells (Melck *et al.*, 1999). In contrast, cannabinoids have been shown to mediate ERK inhibition in PC12 cells via CB_1 (Rueda *et al.*, 2002). CB_2 receptor inhibitors also prevent cannabinoid-induced ERK activation in CHO cells transfected with CB_2 (Bouaboula *et al.*, 1996). CB_1-dependent regulation of ERK has also been shown to modulate the Na^+/H^+ exchanger in CHO cells (Bouaboula *et al.*, 1999). Furthermore, it has been established that the CB_1 receptor couples to the stress related kinase, p38, in hippocampal slices (Derkinderen *et al.*, 2001) and in CHO cells transfected with CB_1 (Rueda *et al.*, 2000). Recent reports have also shown that CB_1 couples to the c-Jun N-terminal kinase (JNK; see section 1.9.1) pathway in CHO cells transfected with CB_1 (Rueda *et al.*, 2000). The CB_1 receptor also been shown to activate the protein kinase B (PKB) pathway in CHO cells (Gómez del Pulgar *et al.*, 2000b) and oligodendrocytes (Molina-Holgado *et al.*, 2002) and inhibit PKB expression in glioma cell cultures (Gómez del Pulgar *et al.*, 2002). Finally, the CB_1 receptor regulates sphingomyelin metabolising pathways in primary astrocytes (Sánchez *et al.*, 2001b).

It should be noted that cannabinoid receptor antagonist studies have revealed that there is a constant tonic level of signalling at both the CB_1 (Landsman *et al.*, 1997) and CB_2 (Portier *et al.*, 1999) cannabinoid receptors. This constitutive activity has important implications when analysing cannabinoid-induced cellular signalling networks.

1.4 Endogenous cannabinoids

The identification of specific membrane-bound cannabinoid receptors responsible for mediating the central and peripheral effects of THC and other cannabinoids raised the question about the existence of endogenous cannabinoid agonists to which the receptors must respond. To date, two major families of endogenous ligands of cannabinoid receptors have been isolated from the nervous and peripheral tissues, *N*-arachidonyl-ethanolamide (anandamide; Devane *et al.*, 1992) and 2-arachidonyl-glycerol (2-AG; Mechoulam *et al.*, 1995; Stella *et al.*, 1997; Sugiura *et al.*, 1996), although other endogenous cannabinoids such as adrenylethanolamide and meadethanolamide have also been identified (Hanus *et al.*, 1993; Priller *et al.*, 1995). Endogenous cannabinoids are unsaturated fatty acid derivatives of arachidonic acid that differ structurally from THC (Martin *et al.*, 2002). Anandamide and 2-AG are found in different regions of the brain including the cortex, hippocampus and cerebellum (Felder *et al.*, 1993), areas with a high density of cannabinoid receptors (Tsou *et al.*, 1998; Figure 1.2). Furthermore, 2-AG is present in brain in amounts 170 times greater than anandamide (Stella *et al.*, 1997). Endogenous cannabinoids are also found in peripheral tissues such as the spleen and heart (Di Marzo *et al.*, 1998) and their lipophilic nature and short half-life (Piomelli *et al.*, 2000) suggest that they act near their sight of synthesis. They are commonly synthesized following membrane depolarization and Ca^{2+} influx into the cell. A rise in intracellular Ca^{2+} activates an *N*-acyltransferase, promoting the transfer of arachidonate from arachidonyl phospholipids to phosphatidylethanolamine, which serves as a substrate for Ca^{2+}-activated phospholipase D, producing anandamide (Sugiura *et al.*, 1996). Endogenous cannabinoids undergo rapid degradation through neuronal re-uptake by a saturable transmembrane carrier and enzymatic degradation by an amidase and fatty-acid amidohydrolase (Deutsch and Chin, 1993; Di Marzo *et al.*, 1994; Di Marzo *et al.*, 1998; Beltramo *et al.*, 1997). Although endogenous cannabinoids bind to both the CB_1 and CB_2 receptor subtypes, their affinity for the CB_1 receptor is approximately four-fold greater than for CB_2 (Showalter *et al.*, 1996; Mechoulam *et al.*, 1995).

Although the physiological role of endogenous cannabinoids has not yet been completely clarified they do appear to mimic many of the effects of THC, including the inhibition of memory consolidation (Di Marzo *et al.*, 1998), induction of apoptosis (Schwarz *et al.*, 1994; Maccarrone *et al.*, 2000; Sarker *et al.*, 2003), neuroprotection (Panikashvili *et al.*, 2001; Nagayama *et al.*, 1999), inhibition of adenylate cyclase (Stella *et al.*, 1997), inhibition of neurotransmission (Piomelli, 2003: Wilson and Nicoll, 2001), inhibition of cancer cell growth (De Petrocellis *et al.*, 1998; Melck *et al.*, 1999; Melck *et al.*, 2000) and the regulation of the ERK (Galve-Roperh *et al.*, 2002; Derkinderen *et al.*, 2003; Kobayashi *et al.*, 2001; Melck *et al.*, 1999), JNK (Sarker *et al.*, 2003; Rueda *et al.*, 2000), p38 MAPK (Sarker *et al.*, 2003; Derkinderen *et al.*, 2001) and PKB (Gómez del Pulgar *et al.*, 2002) pathways. In addition to these functions of the endogenous system, endogenous cannabinoids appear to play a role in events related to neural development (Fernández-Ruiz *et al.*, 1999; see section 1.6). This is supported by evidence that the endogenous cannabinoids and receptors appear early during neuronal development (Berrendero *et al.*, 1998; Rodriguez de Fonseca *et al.*, 1993) and, similar to developmental expression patterns of the cannabinoid receptors, anandamide levels in the rat brain vary at different developmental stages (Fernández-Ruiz *et al.*, 2000). Furthermore, the cannabinoid receptor and endogenous cannabinoid system appear to be conserved across species, suggesting evolutionary conservation of the endogenous cannabinoid system (Soderstrom *et al.*, 2000; Gérard *et al.*, 1991).

1.5 Cannabinoids and cell viability

One of the most intriguing actions of cannabinoids is their ability to control cell survival. Long-term toxicology studies with THC or marijuana extracts have claimed that harmful toxic effects of cannabinoids do not exist (Braude, 1972; Scallet, 1991; Chan *et al.*, 1996). Particularly, Hollister (1986) found that marijuana does not cause structural damage to the brains of laboratory animals or long-term damage to the human brain. Similarly, Chan and colleagues (1996) have shown that rats and mice exposed to THC 5 days a week for 2 years show no evidence of significant alterations in the brain. Indeed, the bulk of evidence also suggests that cannabinoids are neuroprotectants (see section 1.5.3). Contrary to the prevalent opinion of an absence of harmful toxic effects of cannabinoids, numerous recent studies have characterised varying degrees of tissue and cellular injury following cannabinoid exposure (Guzmán *et al.*, 2002), indicating that detrimental effects of cannabinoids exist.

1.5.1 Neuronal toxicity/regression

Administration of cannabinoids causes alterations in cognitive processes, specifically an impairment in learning and memory. For example, THC reduces maze learning (Fehr *et al.*, 1976) and acquisition and retention in the radial arm maze in rats (Lichtman *et al.*, 1995). The memory effects of cannabinoids are thought to be due to an alteration in synaptic function in the hippocampus, a brain region containing a large number of cannabinoid receptors (Tsou *et al.*, 1998; Mailleux and Vanderhaeghen, 1992; Figure 1.2). Indeed, THC has been shown to depress Schaffer collateral long-term potentiation (LTP) in the rat hippocampus (Collins *et al.*, 1994). There is also evidence that the endogenous cannabinoid system regulates LTP via the phenomenon of depolarisation-induced suppression of inhibition (Wilson and Nicoll, 2001). Furthermore, cannabinoids regulate a number of neurotransmitter systems, inducing a variety of behavioural symptoms that can be ascribed to marijuana use (Jentsch *et al.*, 1998; Gessa *et al.*, 1998; Shen *et al.*, 1996; Schlicker *et al.*, 1997). However, since cell death in the CNS leads to significant

dysfunction (Raffay and Cohen, 1997), it is possible that the modulatory effects of marijuana on cognitive processes are attributable to cannabinoid-induced neurotoxicity.

Studies have persistently shown that chronic exposure to THC or marijuana extracts alters the structure of the rat hippocampus (Scallet, 1991). Scallet and colleagues (1987) have shown that adult rats dosed orally for 90 days with THC (20mg/kg/day) display morphological changes in the hippocampus indicative of neurotoxicity. Specifically, THC decreases the mean volume of neurons and the number of synapses per unit volume in the hippocampal CA3 region and these structural changes were present 7 months after treatment. Furthermore, Lawston and co-workers (2000) have shown that adult rats injected twice daily with the synthetic cannabinoid, WIN 55,212-2 (2mg/kg), for 21 days show dendritic degradation in CA1 of the hippocampus and retraction from the pyramidal cells. In addition, several recent studies have revealed that cannabinoids can induce neurotoxic effects in hippocampal neurons in a cultured cell system. Chan and colleagues (1998) have shown that THC (0.5-20μM) induces cell body shrinkage, nuclear condensation and DNA fragmentation, features associated with apoptosis (see Section 1.7), in cultured hippocampal neurons following a 15 min exposure. The apoptotic actions of THC on hippocampal cultures were reliant on CB_1-dependent generation of reactive oxygen species (ROS) via the activation of phospholipase A_2 (PLA_2; Chan *et al.*, 1998). Furthermore, THC, anandamide and the synthetic cannabinoid WIN 55,212-2, prevent the formation of new synapses in hippocampal cultures in a manner dependent on the CB_1 receptor (Kim and Thayer, 2001). This effect is also exerted by the synthetic cannabinoid, HU-210, following CB_1 activation in neuroblastoma cells *in vitro* (Zhou and Song, 2001). The morphoregulatory function of cannabinoids in the hippocampus may contribute to cannabinoid-induced memory deficits as changes in the strength of connections between neurons is thought to underlie memory formation (Bolshakov *et al.*, 1997).

Neonatal rats injected on the 2nd postnatal day with a pharmacologically relevant dose (1mg/kg) of anandamide show evidence of mitochondrial damage of the B-type neurons of the trigeminal ganglia and dorsal root ganglia (Szöke

et al., 2002). This effect is detected 1 week post-treatment and was progressive up to at least the 20th week (Szöke *et al.*, 2002). This finding is significant since mitochondrial function is commonly perturbed early during the apoptotic process (Zamzami *et al.*, 1996; see section 1.8.1).

Toxic effects of cannabinoids also exist in other transformed neural cells. Anandamide (0.25-1μM) has been shown to induce apoptotic body formation and DNA fragmentation in cultured neuroblastoma cells following a 24hr incubation (Maccarrone *et al.*, 2000). This neurotoxic effect is independent of CB_1 activation and involves an increase in intracellular calcium concentration, cytochrome *c* release from the mitochondria and caspase-3 activation (Maccarrone *et al.*, 2000). Anandamide (5μM; 1hr incubation) has also been shown to induce apoptosis in cultured PC12 cells via cytochrome *c* translocation and caspase-3 activation in a CB_1-independent manner (Sarker *et al.*, 2003). Anandamide (5μM) has recently been shown to inhibit neurogenesis, preventing cortical progenitor cell, neural stem cell and PC12 cell differentiation to the mature neuronal phenotype (Rueda *et al.*, 2002). In the same study by Rueda and colleagues (2002), methanandamide, an analogue of anandamide, inhibited adult rat neurogenesis in the subgranular zone of the dentate gyrus.

In addition to the proclivity of cannabinoids to regulate neuronal growth arrest and apoptosis, there is a large amount of experimental evidence suggesting that cannabinoids are involved in the regression of gliomas *in vitro* and *in vivo* (Velasco *et al.*, 2004; Guzmán, 2003). Sánchez and colleagues (1998) have shown that exposure to THC (1μM) for 5 days induces cell shrinkage and DNA fragmentation and in cultured C6.9 glioma (a subclone of rat glioma cells) cells in a CB_1-independent mechanism that is dependent on the rapid induction of sphingomyelin hydrolysis. In the same study, THC (1μM; 5 day incubation) induced apoptosis in neuroblastoma and astrocytoma cell lines. Similarly, Jacobsson and co-workers (2000) found that THC (1μM) and the naturally occurring cannabinoid, canabidiol, but not anandamide (6 day incubation), reduced C6 glioma cell viability. Galve-Roperh and colleagues (2000) have reported that intratumoural injection of THC (1mg/kg/day) for 7 days eradicated tumour growth in 3/15 animals. The anti-tumoural actions of THC involved the regression of glioma cell growth via CB_2 receptor-induced

ceramide production (Sánchez *et al.*, 2001a; Galve-Roperh *et al.*, 2000) and inhibiting vascular endothelial migration and survival by inhibiting the expression of the proangiogenic molecule, vascular endothelial growth factor (VEGF; Blázquez *et al.*, 2003; Blázquez *et al.*, 2004).

1.5.2 Non-neuronal cell toxicity/regression

Several studies have shown that cannabinoids have damaging effects on non-neuronal cells. THC (5μM) induces apoptosis in murine bone marrow-derived dendritic cells via the cytochrome *c*/caspase cell death pathway (Do *et al.*, 2004). Furthermore, THC (15-30μM) induces DNA fragmentation in cultured splenocytes (2hr incubation) and macrophages (4hr incubation) by downregulating Bcl-2 expression and enhancing the activity of the interleukin (IL)-1β converting enzyme, caspase-1 (Zhu *et al.*, 1998). This apoptotic effect is also exerted by anandamide on cultured T and B lymphocytes (Schwarz *et al.*, 1994). Non-psychotropic cannabinoids induce apoptosis in myeloid leukemia cell lines (24hr treatment) and human T lymphocytes (4hr incubation) in a manner that involves caspase-3 activation (Gallily *et al.*, 2003; Bidinger *et al.*, 2003). McKallip and colleagues (2002b) have shown that THC (10μM) induces apoptosis in cultured splenocytes (16hr) and thymocytes (24hr) in a CB_2-dependent manner involving caspases. In the same study, *in vivo* administration of 10mg/kg THC was shown to induce atrophy and apoptosis in the thymus and spleen as early as 6hr after treatment. It should also be considered that several reports have shown proliferative effects of cannabinoids at low concentrations, notably in human B-cells (Derocq *et al.*, 1995) and murine hematopoietic cell line (Valk *et al.*, 1997), indicating that cannabinoid dose may determine the neurotoxic/neuroprotective outcome.

The effect of cannabinoids on cancer cell growth has been extensively studied. In lung tumour cells, THC (60μg/ml) induces necrotic death at 24hr of treatment by decreasing ATP levels and disrupting mitochondrial function (Sarafian *et al.*, 2002). Similarly, exposure of lung tumour cells to THC (10μg/ml; 4-8hr incubation) can partially activate components of the apoptotic pathway involving caspase-3 (Sarafian *et al.*, 2001). Furthermore, THC at concentrations of 4μM induces apoptosis in lung cancer cells at 6hr (Hart *et al.*,

2004). THC induces proliferation in a gliomablastoma cell line at low concentrations (100mM; 18hr incubation) but induces apoptosis in a lung carcinoma cell line at higher concentrations (4-10μM; 6hr incubation) via ERK and PKB pathway regulation (Hart *et al.*, 2004). THC (5μM; 4hr incubation) has been shown to decrease the viability of murine tumour cells in culture and induce apoptosis in murine tumour cells *in vivo* (5mg/kg; 24hr treatment; McKallip *et al.*, 2002a). THC (1μM) also induces DNA fragmentation in human prostate cancer cells PC-3, after 2-3 days of treatment via a cannabinoid receptor-independent mechanism (Ruiz *et al.*, 1999). Similarly, endogenous cannabinoids suppress the proliferation of the prostate cancer cell line DU-145 by downregulating the levels of prolactin via CB_1 (Melck *et al.*, 2000). Anti-proliferative actions of endogenous cannabinoids are also exerted on human breast cancer cell proliferation (De Petrocellis *et al.*, 1998) by inhibition of nerve growth factor (NGF)- and prolactin-induced proliferation via suppression of Trk and prolactin receptors, respectively (Melck *et al.*, 2000). The effects of cannabinoids on human breast cancer cells are reliant on CB_1-induced inhibition of adenylate cyclase and activation of the ERK cascade (Melck *et al.*, 1999). Synthetic and non-psychoactive cannabinoids inhibit skin tumor growth *in vitro* and *in vivo* by attenuating epidermal growth factor receptor (EGFR) activity and preventing angiogenesis (Casanova *et al.*, 2003). Overall, these studies highlight the possible development of cannabinoids as novel anti-cancer drugs.

1.5.3 Neuroprotection

It should be considered that in contrast to the data supporting cannabinoid-induced neurodegeneration, the bulk of experimental evidence suggests that cannabinoids act as neuroprotectants in certain systems *in vitro* an *in vivo* (Guzmán *et al.*, 2002). The protective effects of cannabinoids have principally been determined in cultured neurons *in vitro*. However, it is not clear if this is a CB_1 receptor-dependent process. Endogenous cannabinoids protect cultured cortical neurons from hypoxia and glucose deprivation independent of CB_1 and CB_2 receptor activation (Sinor *et al.*, 2000; Nagayama *et al.*, 1999). In addition, THC and canabidiol decrease glutamate toxicity in rat cortical

neuronal cultures in a receptor-independent process that is not blocked by CB_1 receptor antagonists (Hampson *et al.*, 1998). The non-psychotropic cannabinoid, HU-211, also protects rat forebrain cultures (Nadler *et al.*, 1993) and cortical neuronal cultures (Eshhar *et al.*, 1993) from amino acid neurotoxicity. Similarly, Abood and co-workers (2001) have shown that THC protects mouse spinal neurons against kainite toxicity via activation of the CB_1 receptor. A similar neuroprotective effect has been observed using the synthetic cannabinoid CP-55, 940 (Hampson and Grimaldi, 2001). Likewise, synthetic cannabinoids have also been shown to protect cultured hippocampal neurons from glutamate-induced excitotoxicity by a mechanism involving CB_1 receptor activation (Shen and Thayer, 1998). Protective effects of CB_1 agonists were observed in a mouse hippocampal cell line and in primary cerebellar cell cultures (Marsicano *et al.*, 2002). Furthermore, synthetic cannabinoids also promote the survival of oligodendrocytes progenitors in culture via CB_1 and CB_2 receptors (Molina-Holgado *et al.*, 2002) and CB_1-dependent protective effects of THC and synthetic cannabinoids have been observed in primary astrocytes exposed to pro-apoptotic lipid ceramide (Gómez del Pulgar *et al.*, 2002). Finally, the non-psychoactive cannabinoid, cannabidiol, protects cultured rat PC12 cells from toxic beta-amyloid (Aβ)-induced toxicity (Iuvone *et al.*, 2004).

Neuroprotective effects of cannabinoids have also been found *in vivo*. Nagayama and co-workers (1999) have shown that WIN 55212-2 decreases hippocampal loss in adult rats following transient global cerebral ischemia via the CB_1 receptor. THC has also been shown to protect the neocortex and striatum, but not the hippocampus, from an ischemic insult in adult rats (Louw *et al.*, 2000). Furthermore, THC reduces neuronal injury via CB_1 in neonatal rats injected with ouabain (van der Stelt *et al.*, 2001). 2-AG has been shown to reduce brain odema, infarct volume and hippocampal damage via the CB_1 cannabinoid receptor in mice following closed head injury (Panikashvili *et al.*, 2001). Furthermore, WIN 55,212-2 has been shown to protect hippocampal astrocytes from the toxic effects of focal administration of ceramide (Gómez del Pulgar et al., 2002). It is also interesting to note that in infant rat models of *in vivo* neurodengeneration, anandamide precursors (Hansen *et al.*, 2001a) and anandamide concentrations and CB_1 receptor density are increased in the

cortex (Hansen *et al.*, 2001b), which may represent a putative neuroprotective response. The neuroprotective effects of cannabinoids may be exerted a variety of mechanisms, including the scavenging of ROS (Hampson *et al.*, 1998; Iuvone *et al.*, 2004; Marsicano *et al.*, 2002), inhibition of caspase-3 processing (Iuvone *et al.*, 2004) or by the closing of voltage sensitive calcium channels and the reduction of calcium influx into the cell (Shen and Thayer, 1996). These experimental findings suggest that cannabinoids may have potential therapeutic value in disorders resulting from cerebral ischemia, including stroke, and may slow the progression of neurodegenerative diseases.

Overall it appears that neurotoxic and neuroprotective effects of cannabinoids can be observed. These differences are likely to depend on a variety of influences, apparently including the nature of the toxic insult (cannabinoid concentration, duration of exposure), the origin of the cell type under study and the particular cannabinoid used.

1.6 Cannabinoids and development

As described in section 1.5, the influence of marijuana on neuronal cell viability is complex as both neurotoxic (Scallet, 1991; Lawston *et al.*, 2000; Kim and Thayer, 2001; Chan *et al.*, 1998) and neuroprotective (Sinor *et al.*, 2000; Nagayama *et al.*, 1999; Hampson *et al.*, 1998) properties have been determined. The effects of cannabinoids on neuronal viability are complicated further by data obtained from neuronal cultures *in vitro* and from *in vivo* experiments. Specifically, while the bulk of experimental evidence demonstrating a neurotoxic effect of cannabinoids has been obtained from cultured neurons prepared from neonatal animals (Chan *et al.*, 1998; Kim and Thayer, 2001), cannabinoids fail to induce damage related to necrosis or apoptosis in the brain of adult animals (Galve-Roperh *et al.*, 2000). Furthermore, there is no direct evidence that marijuana is toxic to the adult human brain (Chan *et al.*, 1998). These experimental data suggest that the proclivity of cannabinoids to regulate neuronal viability may be influenced by postnatal development. This evidence also supports the view that marijuana

use may underlie some of the CNS abnormalities that occur in infants exposed to marijuana *in utero* (Huestis and Choo, 2002), and may furthermore reflect a role for the endogenous cannabinoid system in CNS developmental processes (Fernández-Ruiz *et al.*, 1999).

Despite the fact that marijuana is the most widely used illicit drug by pregnant women (Huestis and Choo, 2002), there are few studies on the prevalence of *in utero* drug exposure. Marijuana smoking during pregnancy is associated with a reduction in head circumference (Fried *et al.*, 1999), lower birth weight (Abel, 1984) and fetal length (Day *et al.*, 1994). Newborns exposed prenatally to marijuana also have withdrawal (Hutchings, 1990), increased tremors (Fried, 1982), a high-pitched cry (Lester *et al.*, 1989) and reduced quiet sleep (Scher *et al.*, 1988). Furthermore, prenatal exposure of rodents to cannabinoids produces a large list of malformations including exencephaly, hydronephrosis, body edema, spina bifida and fused ribs (Abel, 1984). More recent studies have assessed the effects of perinatal marijuana exposure on cognitive and behavioural outcomes. It has been demonstrated that the consumption of cannabinoids by rodents during gestational and lactational periods produces marked effects on the development and differentiation of the CNS of its offspring (Dalterio, 1986; Fernández-Ruiz *et al.*, 1992; Fernández-Ruiz *et al.*, 1994; Fernández-Ruiz *et al.*, 1996). Cannabinoids can readily be transferred from the mother to the offspring through placental blood during gestation (Martin *et al.*, 1977) or through milk during lactation (Jakubovic *et al.*, 1973). In both cases, cannabinoids can reach the fetal and neonatal brain in substantial amounts due to the immaturity of the blood-brain barrier at these ages (Fernández-Ruiz *et al.*, 1992; Fernández-Ruiz *et al.*, 1994). Indeed, several studies have shown that prenatal and early postnatal exposure to THC or THC in combination with other cannabinoids produces long-term abnormalities in brain function (Dalterio, 1986; Fernández-Ruiz *et al.*, 1992; Nahas and Frick, 1986; Mokler *et al.*, 1986; Navarro *et al.*, 1995). In particular, cannabinoid-exposure during prenatal and early postnatal periods has been shown to alter the temporally-ordered sequence of events that occur during neurotransmitter development. A large list of studies have revealed modulatory effects of cannabinoids on the maturation of dopamine (Fernández-Ruiz *et al.*, 1992; Fernández-Ruiz *et al.*, 1994; Fernández-Ruiz *et al.*, 1996), serotonin

(Molina-Holgado *et al.*, 1996), and opioidergic neurons (Kumar *et al.*, 1990). These modifications during perinatal periods are followed by long-term effects on adult behaviour.

A study by Fried (1995) examined the association between human marijuana consumption during pregnancy and effects upon offspring (up to early school age) in the areas of cognitive development and behaviour. In this study, marijuana use was associated with increased tremors and startles in 7-, 9- and 30-day-old infants and poorer habituation to visual stimuli was observed in newborns less than a week of age. Interestingly, this study failed to find a relationship between prenatal marijuana exposure and cognitive deficits during early childhood, particularly between the ages of 1 and 3 years. Indeed, this finding is consistent with other studies (Tennes *et al.*, 1985; Astley and Little, 1990) and suggests that CNS abnormalities may be sub clinical in early childhood, surfacing at a later age and manifesting in cognitive and learning difficulties, a suggestion supported by other reports (Griffith *et al.*, 1994). Indeed, this initial, apparent absence of effect should not be considered as *in utero* exposure having transient effects for, as the children became older, a number of cognitive variables appeared to distinguish between marijuana and control children (Fried, 1995; Fried and Smith, 2001). At 4 years, tests of verbal ability and memory discriminated between the offspring of marijuana users and regular children and at 6-9 years visual perception and memory, language comprehension and sustained attention also discriminated between the two groups. Other studies have shown memory impairments in children at 2 years of age prenatally exposed to marijuana (Fried and Watkinson, 1990) and impairments in short-term memory, verbal and abstract reasoning in 3-year-old offspring of marijuana users (Griffith *et al.*, 1994). The areas of vulnerability affected by prenatal marijuana exposure appear to be involved in neurocognitive functioning, suggesting that exposure to marijuana *in utero* may impact, in a negative manner, on aspects of executive function (EF; Fried and Smith, 2001). Interestingly, EF is considered a marker of prefrontal cortical function (Lezak, 1995), a region of the CNS implicated in marijuana effects (Pope and Yurgelin-Todd, 1996). Indeed, the frontal lobes have a high CB_1 receptor density (Tsou *et al.*, 1998; Mailleux and Vanderhaeghen, 1992; Figure 1.2) and heavy abusers of marijuana display deficits in tasks dependent on

prefrontal lobe functioning, particularly short-term memory and attention (Pope and Yurgelin-Todd, 1996).

As mentioned in section 1.4, there is evidence that the system constituted by CB_1 receptors and the endogenous cannabinoids have a role in specific events of brain development (Fernández-Ruiz *et al.*, 1999; Ramos *et al.*, 2002). This is suggested by the ample evidence that the endogenous cannabinoids (Berrendero *et al.*, 1999) and the CB_1 receptor (Berrendero *et al.*, 1998; Rodriguez de Fonseca *et al.*, 1993; McLaughlin *et al.*, 1994; Belue *et al.*, 1995; Garcia-Gil *et al.*, 1999b) are expressed in the fetal and early postnatal brain. Furthermore, these elements are atypically located in the CNS during postnatal periods (Berrendero *et al.*, 1998; Romero *et al*, 1997; Fernández-Ruiz *et al.*, 2000) suggesting that this system plays a functional role in brain development. For example, functional CB_1 receptors have been located in fetal white matter areas (Berrendero *et al.*, 1998), areas that display low CB_1 receptor density in the adult brain (Berrendero *et al.*, 1998). Furthermore, CB_1 receptors have been associated with transverse or commissural fibre tracts, such as the corpus callosum, indicating that they are involved in axonal migration and synaptogenesis (Shivacher *et al.*, 1996). Similarly, anandamide and 2-AG are found in the fetal and early postnatal brain and the distribution of both cannabinoids varies during development (Berrendero *et al.*, 1999). Evidence from cultured neuronal and glial cells also support a role for the endogenous cannabinoid system in developmental processes, particularly the expression of growth-related genes (Bouaboula *et al.*, 1995a), energy metabolism (Gómez del Pulgar *et al.*, 2000), proliferative signal tranduction pathways (Galve-Roperh *et al.*, 2002; Derkinderen *et al.*, 2003) and apoptosis (Sarker *et al.*, 2003).

1.7 Apoptosis

Cells of multicellular organisms have the ability to activate an internal sequence of events of programmed cell death, known as apoptosis (Raffay and Cohen, 1997). The apoptosis theory, first proposed by Kerr and colleagues (1972), has challenged conceptual thinking in all aspects of cell biology. Apoptosis occurs in both vertebrates and invertebrates and is distinguished by unique morphological alterations such as blebbing of the plasma membrane, cell shrinkage without membrane rupture, chromatin condensation and migration to the nuclear membrane, packaging of cellular contents into membrane bound bodies for deletion, presentation of epitopes identifying the cell as a phagocytic target and specific DNA cleavage into oligonucleosomal fragments (Behl, 2000). Organelles within the shrunken apoptotic cytoplasm retain a normal appearance except for the dilation of the endoplasmic reticulum and swelling of the mitochondria (Zörnig *et al.*, 2001). Throughout the apoptotic process the plasma membrane does not rupture, allowing phagocytic deletion of the apoptotic cells by neighbourbouring cells without pro-inflammatory changes (Williams and Smith, 1993). Furthermore, apoptosis is an active process with organised and regulated biochemical events, including intracellular signal transduction, ordered enzyme cascades and gene transcription (Kerr and Harmon, 1991). Despite the diversity in signal transduction, all apoptotic pathways are believed to converge ultimately with the activation of caspases (Blatt and Glick, 2001; see section 1.8.3). Multiple inducers of apoptosis have been identified including ionising radiation, oxidative stress, sustained increases in $[Ca^{2+}]_i$, addition or withdrawal of steroid hormones, cytokines and chemotherapeutic drugs (Gerschenson and Rotello, 1992; Raff, 1998). During normal embryonic and adult development, cells that are unnecessary or deleterious undergo apoptosis (Raffay and Cohen, 1997). Indeed, in the nervous system approximately 50% of total neurons die by the apoptotic process during embryonic and fetal development of rats, mice and humans (Lo *et al.*, 1995).

Apoptosis is commonly identified using biochemical methods that detect key events in the apoptotic process (Blatt and Glick, 2001). Two methods, the

Terminal deoxinucleotidyltransferase-mediated biotinylated nick end labeling (TUNEL) and DNA laddering techniques can be used to assess the internucleosomal cleavage of DNA. The TUNEL system provides an accurate quantitative method of determining cell death in cultured cell populations by providing a colorimetric DAB based system to isolate cells containing fragmented DNA. In addition to this staining technique, fragmented DNA may be visualised on an agarose gel as distinct fragments of oligonucleosomal size (180-200bp lengths; Arends *et al.*, 1990). The DNA ladder formation results from the nucleolytic cuts in linker DNA between nucleosomes within chromatin (Arends *et al.*, 1990). The 180bp periodicity of the DNA fragments is a telltale sign of apoptosis.

Conversely, necrotic cell death is induced following high amplitude cellular injury resulting from blunt trauma, toxin exposure or loss of blood supply (Raffay and Cohen, 1997; Blatt and Glick, 2001). The necrotic cells undergo swelling, their chromatin takes on the appearance of a flocculant mass, and the cells rupture, resulting in failure of cellular homeostasis (Lee *et al.*, 1993; Blatt and Glick, 2001). The resulting leakage of the cellular contents results in a host inflammatory response (Raff, 1998; Raffay and Cohen, 1997). Apoptosis and necrosis also differ in that within hours after the administration of the death signal the plasma membrane in apoptosis remains intact (Cohen *et al.*, 1992). In contrast, in necrotic cells the membrane is damaged within minutes following the administration of the noxious agent.

It is worth noting that in complex cellular systems such as neuronal networks, it is unlikely that a simple linear cascade of events is sufficient to promote cell death (Nicotera *et al.*, 1999). It is more likely that individual intricately connected pathways self-amplify or delete each other to execute the apoptotic programme. Furthermore, although the vast majority of cell death literature suggests that all cases of cell death can be classified as either apoptosis or necrosis, aspects of both mechanisms can exist in a variety of cell death paradigms (Pieper *et al.*, 1999).

1.8 The apoptotic pathway

1.8.1 Cytochrome *c*

The electron transport protein, cytochrome *c*, resides in the space between the outer and inner membranes of mitochondria where it participates in electron transport (Reed, 1997). In addition to cytochrome *c*, the inter-membrane space contains several other pro-apoptotic proteins including apoptotic-inducing-factor (AIF), and in some cells, caspases 2, 3 and 9 have been detected (Blatt and Glick, 2001). It has been shown that a common event associated with apoptosis involves the translocation of cytochrome *c* from the mitochondria to the cytoplasm (Rosse *et al.*, 1998). Indeed, cytochrome *c* release from the mitochondria has been shown to accompany apoptosis in every circumstance and cell line where it has been studied (Reed, 1997). The mechanism for mitochondrial cytochrome *c* translocation continues to be debated, but at least two competing theories have been advanced. First, it has been hypothesized that the translocation of cytochrome *c* from the mitochondria into the cytoplasm results from the opening of a mitochondrial channel termed the permeability transition pore (PTP; Eskes *et al.*, 1998; Zamzami *et al.*, 1996). This channel consists primarily of the adenine nucleotide translocator (ANT) and the voltage-dependent anion channel (VDAC) located in the inner and outer mitochondrial membranes respectively (Zoratti and Szabo, 1995). Many data has reported that opening of the PTP results in mitochondrial inner membrane potential ($\Delta\psi m$) collapse, mitochondrial swelling, matrix Ca^{2+} release, ROS generation, rupture of the outer membrane and leakage of many mitochondrial proteins including cytochrome *c* (Susin *et al.*, 1996; Eskes *et al.*, 1998; Zamzami *et al.*, 1996). An alternative model predicts that cytochrome *c* translocation is regulated by a specific channel located in the outer mitochondrial membrane (Reed, 1997). Potential effectors in this system may be members of the Bcl family of mitochondria-associated proteins (see section 1.8.2), which have been shown to possess channel-forming properties (Schlesinger *et al.*, 1997). However, there is also evidence that the mitochondria-associated proteins can induce the opening (Marzo *et al.*, 1998; Shimizu *et al.*, 1999; Pastorino *et al.*, 1998) or closure (Kroemer *et al.*, 1997;

Shimizu *et al.*, 1999) of the PTP. Once released from mitochondria, cytochrome *c* complexes with a cytosolic factor designated as apoptotic protease activating factor-1 (APAF-1), a human homologue of the nematode *Caenorhabditis elegans* (*C. elegans*) cell death protein CED-4 (Zou *et al.*, 1997), and caspase-9 (APAF-3; Zörnig *et al.*, 2001; Porter, 1999). This complex is formed by an interaction between the caspase recruitment domain (CARD) domain of APAF-1 and the prodomain of caspase-9 (Zörnig *et al.*, 2001). In the presence of cytochrome *c* and either ATP or ADP (Li *et al.*, 1997), the caspase is autocatalytically activated and has the proclivity to activate a common protease cascade that terminates in cellular apoptosis (Slee *et al.*, 1999).

It should be noted that a direct mechanistic link between an apoptotic stimulus and caspase regulation also exists via the death receptor pathway. Death receptors are members of the nerve growth factor receptor family and include tumour necrosis factor receptor 1 (TNF-R1), Fas (CD95) and DR-3, -4 and –5 (Blatt and Glick, 2001; Zörnig *et al.*, 2001). Upon activation, the cytoplasmic death domain (DD) of these receptors recruit adaptor molecules which in turn recruit pro-caspases (Herr and Debatin, 2001; Blatt and Glick, 2001; Zörnig *et al.*, 2001), initiating the caspase-dependent apoptotic programme.

1.8.2 Bcl-2 protein family

The Bcl-2 family (B-cell leukaemia/lymphoma 2-like proteins) of mitochondria-associated proteins register diverse forms of intracellular damage and regulate cell death by controlling the integrity of the outer mitochondrial membrane (Korsmeyer, 1995). At least 15 Bcl-2 family members have been identified (Adams and Cory, 1998) and all members have conserved regions known as Bcl-2 homology (BH) domains, which allow interaction between family members (Oltvai *et al.*, 1993). The Bcl-2 family consist of two opposing groups that regulate apoptosis: pro-apoptotic members that induce cytochrome *c* release from mitochondria and anti-apoptotic members that counteract the pro-apoptotic members and prevent cytochrome *c* translocation from the mitochondria (Korsmeyer, 1999; Figure 1.3). Four conserved BH domains (BH1-4) are found in the anti-apoptotic members (Bcl-2, Bcl-x_L, Bcl-w, Mcl-1, A1/BFL-1, BOO/DIVA), while the pro-apoptotic members are split into two

groups, those that possess BH1, BH2 and BH3 regions (Bax, BAK, BOK/MTD, Bcl-x_S) and those that possess only the short BH3 domain (BID, Bad, BIK/NBK, BLK, Hrk, BIM/BOD; Nechushtan *et al.*, 1999; Figure 1.3). A striking characteristic of the Bcl-2 family members is their ability to form homo- and heterodimers through BH domain interaction (Oltvai *et al.*, 1993; Korsmeyer, 1995; Yin *et al.*, 1994). The BH1, BH2 and BH3 regions are in close proximity and form a hydrophobic pocket capable of binding a BH3 region of another family member (Figure 1.3B). The cell death/survival decision depends on the relative expression levels of the pro-apoptotic and anti-apoptotic members. Overexpression of the anti-apoptotic members has been shown to protect cells against apoptosis involving cytochrome *c* release from the mitochondria (Choi *et al.*, 2001; Murphy *et al*, 2000). Similarly, overexpression of the pro-apoptotic members culminates in the demise of the cell (Wolter *et al.*, 1997; Gross *et al.*, 1998). The structural similarity between Bcl-X_L and pore-forming domains of certain bacterial toxins (Muchmore *et al.*, 1996), in addition to the evidence that Bcl-x, Bcl-2 and Bax can form ion channels in synthetic lipid membranes (Antonsson *et al.*, 1997; Minn *et al.*, 1998; Schendel *et al.*, 1997) has strengthened the suggestion that mitochondria-associated proteins control cytochrome *c* release by forming specific channels in the outer mitochondrial membranes. Indeed, there is evidence that Bcl-2 can prevent channel formation by Bax *in vitro* (Antonsson *et al.*, 1997). However, it has also been suggested that pro-survival mitochondria-associated proteins may function downstream of cytochrome *c* release by directly inhibiting the activities of APAF-1 (Rosse *et al.*, 1998; Zou *et al.*, 1997).

Bax is a cytosolic protein that translocates to the mitochondria during apoptosis (Gross *et al.*, 1998; Wolter *et al.*, 1997). Various apoptotic stimuli induce the translocation of Bax to the mitochondrial membrane where it inserts as a homodimer (Gross *et al.*, 1998). It is unclear whether Bax homodimerization is a cause of its translocation or a consequence of its insertion, however dimerization is strongly associated with cell death (Gross *et al.*, 1998). There is also evidence that in its inactive state the C- and N-termini of Bax interact and that upon triggering of apoptosis there is a conformational change in Bax, exposing these two domains to enable Bax insertion into the mitochondria (Nechushtan *et al.*, 1999; Choi *et al.*, 2001; Gross *et al.*, 1998).

This conformation change possibly involves cleavage of Bax at its N-terminus by the cysteine protease, calpain (Choi *et al.*, 2001; Wood and Newcomb, 2000; Gao and Dou, 2000; Wood *et al.*, 1998). Furthermore, the BH3-domain-only proteins such as Bid have the proclivity to induce a structural changes in Bax to enhance its apoptotic actions (Desagher *et al.*, 1999). This conformational change is inhibited by Bcl-2 (Murphy *et al.*, 2000) and it precedes Bax translocation (Godlewski *et al.*, 2001; Nechushtan *et al.*, 1999). In contrast, Bcl-2 resides on the cytoplasmic surface of the mitochondrial outer membrane, endoplasmic reticulum and nuclear envelope (Adams and Cory, 1998). Bcl-2 prevents cytochome *c* release by blocking the redistribution of Bax to the mitochondria (Gross *et al.*, 1998) and preventing the conformational changes that manifest in its translocation (Murphy *et al.*, 2000; Choi *et al.*, 2001). However the pro-survival function of Bcl-2 is inhibited following phosphorylation of the Bcl-2 protein (Yamamoto *et al.*, 1999).

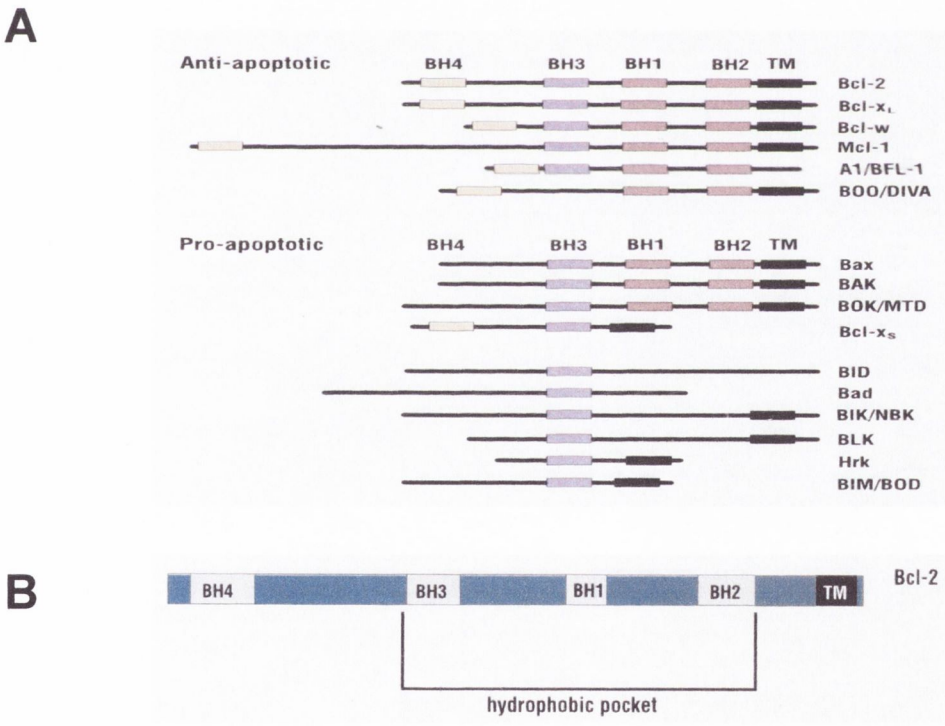

Figure 1.3: The Bcl-2 family members.

(A) The anti- and pro-apoptotic Bcl-2 proteins. TM is the membrane-anchoring region.

(B) Position of the Bcl-2 homology regions (BH1-4) in Bcl-2. The region forming the hydrophobic pocket is indicated (taken from Adams and Cory, 1998).

In addition to cytochrome *c*, several other proteins are released from mitochondria during apoptosis including apoptosis-inducing factor (AIF) and Smac/Diablo (Zörnig *et al.*, 2001). AIF redistributes from the mitochondria to the nucleus during apoptosis and induces some of the nuclear morphological changes associated with apoptosis in a caspase-independent manner (Zörnig *et al.*, 2001; Herr and Debatin, 2001). The Smac/Diablo molecule inactivates caspase inhibitors (IAPs) and thereby relieves inhibition of caspase activation by IAP inactivation (Zörnig *et al.*, 2001).

1.8.3 Caspase-3

Caspases are specialised cysteine proteases that are common effectors of apoptosis (Martin and Green, 1995). Caspases are extremely specific proteases, cleaving their substrates after aspartic acid residues (Janicke *et al.*, 1998). To date, at least 14 different caspases have been identified in mammalian tissues (Nicotera, 2000). These proteases, initially characerised from the interleukin 1β-converting enzyme (ICE/Caspase-1; Black *et al.*, 1989), are homologues to cell death proteases identified in the nematode, *C. elegans* (Yuan and Horvitz, 1990). The caspase family function as either effectors (caspases 2, 3, and 7) or initiators (caspases 6, 8, 9, and 10) of apoptosis (Blatt and Glick, 2001). Various apoptotic stimuli, such as ultraviolet light, oxidative stress and chemotherapeutic drugs, activate early phase initiator caspases which procedes to activate the executioner caspases (Hoffman, 1999).

Caspases are synthesized as a single polypeptide chain mainly in the cytoplasm that is cleaved at two aspartic acids into a large and small subunit (Raff, 1998; Figure 1.4). The N-terminal polypeptide known as the pro-domain is discarded and the large and small subunits dimerize to form the active enzyme (Figure 1.4). In the case of caspase-3 (CPP32/Yama/Apopain), the most widely studied executioner caspase, this involves the cleavage and processing of an inactive pro-enzyme (32kDa) in the cytoplasm to a 17kDa–12kDa heterodimer (Slee *et al.*, 1999). Caspase-3 activity is regulated by several mechanisms. Firstly, following death receptor activation, caspase-8 is modulated as a result of its interaction with Fas-associated death domain (FADD), which can then cleave pro-caspase-3 to its active form (Schmitz *et al.*,

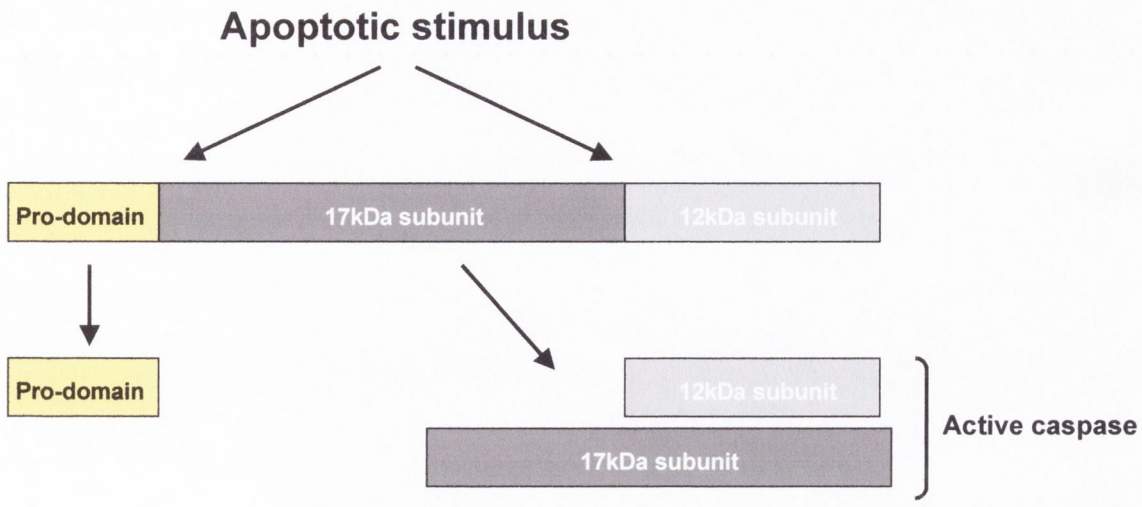

Figure 1.4: The activation of caspases.

The active form of a caspase consists of large and small chains released from a precursor by proteolysis (adapted from Raff, 1998).

2000). The accumulation of cytochrome *c* in the cytoplasm also plays a pivotal role in the activation of caspase-3 (Reed, 1997). The complexing of mitochondrially released cytochrome *c* and APAF-1 to caspase-9 leads to its dimerization and autolytic activation which in turn processes and activates the 32kDa pro-enzyme to its herterodimeric form (Wang, 2000). Finally, caspase-3 is activated by direct cleavage by the serine protease, granzyme B, or the lysosomal protease, cathepsin-L (Ishisaka *et al.*, 1999). Once activated, caspase-3 is capable of autocatalysis as well as cleaving and activating other members of the caspase family, resulting in rapid and irreversible apoptosis (Zou *et al.*, 1997; Slee *et al.*, 1999).

Caspases contribute to the drastic morphological changes associated with apoptosis by proteolysing and disabling a number of key substrates including structural, nuclear and signalling proteins (Blatt and Glick, 2001). Cytoskeletal proteins cleaved by caspases include actin and α-fodrin, which is responsible for many of the morphological changes that occur during apoptosis (Wang, 2000). Caspase-3 is also known to cleave the DNA repair-associated protein poly(ADP-ribose) polymerase (see section 1.8.4) and the cytosolic factor DNA fragmentation factor (DFF), producing sustained DNA fragmentation

(Lazebnik *et al.*, 1994; Kim *et al.*, 1999; Janicke *et al.*, 1998; Liu *et al.*, 1996). Furthermore, caspase-3 mediated cleavage of its endogenous inhibitor, ICAD, enables caspase-activated deoxyribonuclease (CAD) translocation to the nucleus and resultant DNA fragmentation (Enari *et al.*, 1998). Caspases also regulate other proteins including Protein Kinase C (PKC), PLA_2, mitogen-activated protein kinase kinase 1 (MEKK1) and the mitochondria-associated proteins Bcl-2 and Bax (Goping *et al.*, 1998; Shiah *et al.*, 2001; Wang, 2000). The consequences of these cleavage events are now emerging and suggest that they are for many of the phenotypic changes that occur during apoptosis.

1.8.4 Poly(ADP-ribose) polymerase

In addition to the morphological changes associated with caspase-3 activation and apoptosis, this protease is also responsible for DNA fragmentation, a hallmark of apoptosis (Liu *et al.*, 1996). An early target for caspase-3 is the DNA repair enzyme, poly(ADP-ribose) polymerase (PARP; Kaufmann *et al.*, 1993), whose structure is shown in Figure 1.5. Nuclear PARP is selectively activated by DNA strand breaks to participate in DNA repair (Pieper *et al.*, 1999). PARP is a 113kDa polypeptide that binds to both double- and single-stranded DNA strand breaks via its DNA binding domain consisting of two zinc-fingers located at the N-terminal of the protein (Menissier-de Murcia *et al.*, 1989). Upon binding, the catalytic domain located at the C-terminal generates long branched chains of poly (ADP-ribose) (PAR) from the PARP substrate nicotinamide adenine dinucleotide (NAD) and transfers them to various nuclear proteins, most notably onto the central automodification domain of PARP itself (Pieper *et al.*, 1999). Poly (ADP-ribosyl)ation of proteins generally leads to their inhibition (Lautier *et al.*, 1993). Hence, it is the auto-poly(ADP-ribosyl)ation of PARP that inactivates the enzyme, allowing its release from DNA and the binding and action of DNA repair enzymes (Alvarez-Gonzalez *et al.*, 1994).

Following a death stimulus the PARP polypeptide (113kDa) is cleaved by apoptotic proteases such as caspase-3 (Tewari *et al.*, 1995; Lazebnik *et al.*, 1994) to 89kDa and 24kDa PARP fragments that are considered to be apoptotic markers (Nicotera *et al.*, 1999; Kaufmann *et al.*, 1993). This apoptosis-associated cleavage of PARP removes the amino-terminal domain of

the protein to yield the 89kDa fragment that still retains basal catalytic activity but lacks the DNA binding domain (Nicholson *et al.*, 1995; Figure 1.5). Hence, apoptosis associated cleavage of PARP precludes the catalytic domain from being recruited to the sites of DNA damage, and hence disables PARP from coordinating subsequent DNA repair (Nicholson *et al.*, 1995). There is also evidence that the 24kDa cleavage product binds to fragmented DNA following an apoptotic insult, inhibiting DNA repair by physically blocking access of repair proteins to fragmented DNA (Pieper *et al.*, 1999). Although PARP is centrally involved in apoptosis, it also has a pivotal role in classical necrotic cell death (Pieper *et al.*, 1999). However the necrosis-associated PARP cleavage produces a major 50kDa fragment and minor 40kDa and 35kDa fragments (Shah *et al.*, 1996). It should also be considered that following extensive DNA damage as typically occurs in necrosis, the resultant increase in PARP activity rapidly depletes NAD stores, a key co-enzyme in energy metabolism (Sims *et al.*, 1983). The resultant decrease in ATP levels culminates in cell death (Sims *et al.*, 1983).

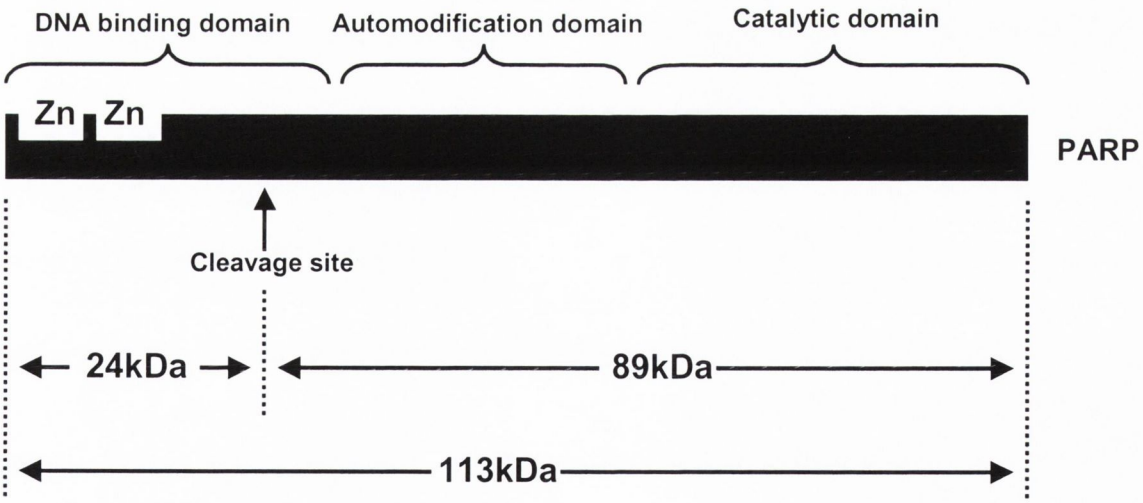

Figure 1.5: The structure of PARP.

Apoptosis-associated cleavage of PARP produces a 24kDa fragment containing the DNA binding domain and an 89kDa fragment that is the automodification and catalytic domains (adapted from Nicholson *et al.*, 1995).

1.9 Mitogen-activated protein kinases

Mitogen-activated protein kinases (MARKs) represent a group of enzymes that are activated by cytokines and environmental stresses (Ip and Davis, 1998). The function of these kinases is to convert extracellular stimuli to intracellular signals that, in turn, control the expression of genes that are essential for many cellular responses, including cell growth and death (Marshall, 1995). Signalling cascades involving MAPKs are found in all eukaryotic organisms (Derkinderen *et al.*, 1999) and have been conserved through evolution demonstrating their importance in intracellular signalling (Sugde and Clerk, 1997). These widely distributed kinases are activated by dual phosphorylation on threonine and tyrosine residues by upstream kinases (Derkinderen *et al.*, 1999). Information transfer by MAPK pathways is hierarchical, involving cascades of kinases (Figure 1.6). Typical MAPK cascades are composed of three enzymes, which are sequentially activated by phosphorylation; a MAPK kinase kinase (MAPKKK/MEKK); a MAPK kinase (MAPKK/MEK); and a MAPK (Carboni *et al.*, 1998; Figure 1.6). In mammalian cells, three main subfamilies of MAPK have been described to date; extracellular signal regulated kinases (ERKs), p38-MAPK and c-Jun-N-terminal kinase (JNK; Derkinderen *et al.*, 1999; see section 1.9.1) although the ERK5 MAPK is also recognised as a distinct subfamily (Buschbeck and Ullrich, 2005). They are distinguished by the nature of the amino acid residue located between the phosphorylated threonine/tyrosine residues in the catalytic core of the proteins (Whitmarsh and Davis, 1996). The ERK cascade is commonly activated in response to growth factors and is involved in cell growth and differentiation, whereas the p38-MAPKs and JNKs, termed stress kinases, typically mediate cellular responses to proinflammatory cytokines such as tumour necrosis factor α (TNF-α) and interleukin 1, and a variety of environmental stresses including heat shock, ultraviolet light and ischemia (Schaeffer and Weber, 1999). Although the kinase cascade leading to the activation of a specific MAPK is distinct, there is also the potential of cross-talk at each level of the signal-transduction coupling (Minden and Karin, 1997).

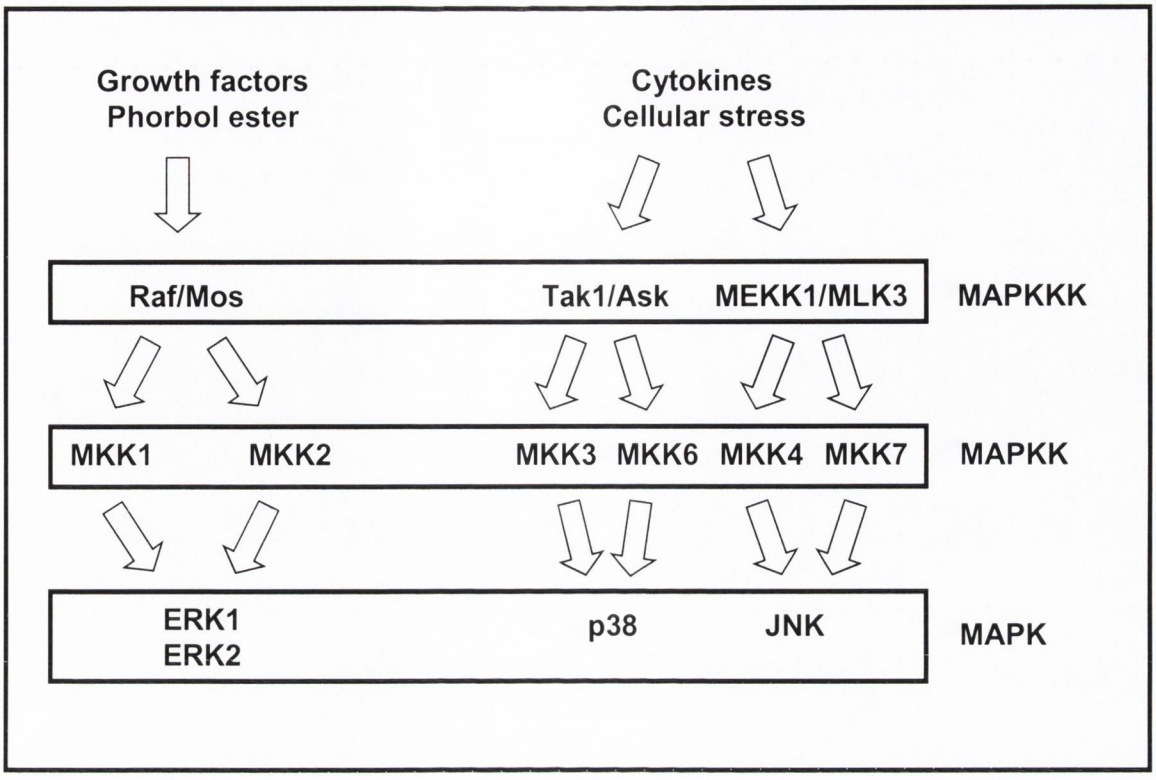

Figure 1.6: Structure of the MAPK signal transduction pathways (adapted from Ip and Davis, 1998; Xia *et al.*, 1995).

1.9.1 c-Jun N-terminal kinase

The c-Jun N-terminal kinases (JNKs) are classic stress-activated protein kinases (SAPKs). Although the precise physiological role of JNK remains to be elucidated, they constitute a family of kinases that act in the signal transduction coupling of cellular stress and apoptosis (Hochedlinger *et al.*, 2002), regeneration and repair (Mielke and Herdegen, 2000), differentiation (Kuan *et al.*, 1999) and physiological stimuli (Xu *et al.*, 1997). JNKs are activated by an array of stressful stimuli, including ionising radiation, heat and osmotic shock, inflammatory cytokines, deprivation of trophic factors and lipid messengers such as ceramide (Mielke and Herdegen, 2000). JNK is also activated in response to cell stress induced by certain DNA damaging agents (Deng *et al.*, 2001). The expression and activity of JNK in the nervous tissue under basal conditions strongly argues for a physiological role of JNKs in the nervous system (Mielke *et al.*, 1999). Activation of the JNK signalling pathway is mediated by dual phosphorylation on threonine/tyrosine residues in position 183 and 185 in JNK1/2 and positions 221 and 223 in JNK3, by two MAPKKs,

MKK4 and MKK7 (Ip and Davis, 1998; Figure 1.6). In addition, other protein kinases, such as p21-activated kinase (PAK) and germinal center kinase (GCK), and the cysteine protease, caspase-3 (Ozaki *et al.*, 1999), activate the JNK pathway via an unknown mechanism leading to confusion concerning the definition of the upstream elements of the JNK pathway. Once the JNK pathway is activated, the final cellular responses depends on a variety of influences, namely the cell type and the state of activation of other transduction pathways within the cell (Herdegen *et al.*, 1997).

JNKs are encoded by three different genes *jnk1*, *jnk2* and *jnk3* and the products of each gene reveal isoforms with approximate molecular weight of 46kDa (JNK1), 54kDa (JNK2) and 57kDa (JNK3), all of which are found in the mammalian brain (Gupta *et al.*, 1996). Furthermore, at least 10 JNK isoforms exist as a result of alternative splicing (Gupta *et al.*, 1996). The JNK genes, *jnk1* and *jnk2* are ubiquitously expressed, while *jnk3* is largely restricted to brain, heart and testis (Ip and Davis, 1998). In comparison with other tissues, the brain displays a higher baseline activation of JNK (Xu *et al.*, 1997). In the brain, JNK expression is in ontogenetic development regulated (Carboni *et al.*, 1998; Yang *et al.*, 1997). Carboni and colleagues (1998) have shown that JNK2 and JNK3 are the main isoforms expressed in the adult brain and that the expression patterns of these isoforms does not vary during development. In contrast, JNK1 displays high and diffuse expression in the newborn rat brain but its expression progressively declines during post-natal development to become restricted to the endopiriform nucleus and the medial habenula (Carboni *et al.*, 1998). The different distributions of JNK in the CNS suggests the existence of separate functions for the JNK isoforms. Indeed, this is supported by evidence that the JNK isoforms exhibit diverse selectivity for their substrates (Gupta *et al.*, 1996).

Despite uncertainty over the precise functions of JNK signalling, it is firmly established that JNK is required for apoptosis, particularly in neuronal tissue. This is supported by evidence that JNK is involved in the induction of apoptosis in rat PC12 cells (Xia *et al.*, 1995), that neurons are protected from apoptosis in JNK knockout animals (Yang *et al.*, 1997; Kuan *et al.*, 1999) and that JNK inhibitors prevent apoptosis (Dickens *et al.*, 1997). Despite these findings the mechanism by which JNK activation may trigger apoptosis is

largely unknown. It should also be noted that in contrast to the damaging effects of JNK on neuronal tissue, anti-apoptotic functions of JNK exist (Wisdom *et al.*, 1999). This may reflect the different properties of cells, the existence of separate functions of the JNK isoforms or may depend on the duration of JNK activation (Ip and Davis, 1998; Chen *et al.*, 1996). Therefore, JNKs may play a dual role (both positive or negative) in regulating apoptosis.

JNK proteins are anchored in the cytoplasm by JNK-interacting proteins (JIPs; Dickens *et al.*, 1997). These proteins act as a scaffold and following dissociation from the JIP anchor complex, JNK has the proclivity to translocate to the nucleus and associate with their substrates (Gupta *et al.*, 1995). JNKs have a number of nuclear substrates, and there is growing evidence that different JNK isoforms vary in there interaction with transcripition factors (Yin *et al.*, 1997). The nuclear substrates for JNK include c-jun (Herdegen *et al.*, 1997), activating transcripition factor-2 (ATF-2; Gupta *et al.*, 1995) and ELK-1 (Cavigelli *et al.*, 1995). Once phosphorylated within their activation domains, these transcription factors control the expression of genes that mediate the cellular response to stress. In addition to nuclear substrates, JNKs regulate the expression of a variety of cytoplasmic substrates including the tumour suppressor p53 (Buschmann *et al.*, 2001; Kobayashi and Tsukamoto, 2001; Potapova *et al.*, 2000; Metzler *et al.*, 2000; Wang and Friedman, 2000; see section 1.10), caspase-3 (Seimiya *et al.*, 1997; Bozyczko-Coyne *et al.*, 2001), the cytoskeletal proteins, tau (Reynolds et al., 1997) and neurofilament heavy chains (Giasson and Mushynski, 1997) and the mitochondria-associated proteins Bcl-X_L (Ito *et al.*, 2001), Bcl-2 (Park *et al.*, 1997; Kang *et al.*, 1998), Bax (Lei *et al.*, 2002) and BH3-only proteins (Harris and Johnson, 2001). Indeed JNK signalling can modulate p53 expression resulting in the suppression of Bcl-2 and enhancement of Bax induction, both critical events in the apoptotic cascade (Miyashita and Reed, 1995).

1.10 p53

The p53 tumour suppressor protein plays an important role in the regulation of stress-mediated G1 cell-cycle arrest to enable DNA repair, or if this is not possible, promoting cell deletion by apoptosis (Levine, 1997). The decision whether an individual cell undergoes p53-induced growth arrest or apoptosis depends on a variety of factors, including the cell type and the environment conditions (Zörnig *et al.*, 2001). The proclivity of p53 to induce growth arrest depends on its activity as a sequence-specific activator of $P21^{WAF1/CIP-1}$ protein, which inhibits cell proliferation by regulating cyclin-dependent kinases (Zörnig *et al.*, 2001). However, as most neurons are in a post-mitotic state (Miller *et al.*, 2000), the cell cycle regulatory function of p53 is absent in these cells. Hence, in post-mitotic neurons in which DNA fragmentation is occurring following a toxic insult, the regulation of p53 expression is associated with mechanisms underlying cellular apoptosis rather than recovery from the insult (Enokido *et al.*, 1996; Jordan *et al.*, 1997). Indeed, accumulating evidence now suggests that p53 is involved in neuronal apoptosis (Jordan *et al.*, 1997; Xiang *et al.*, 1996; Napieralski *et al.*, 1999; Aloyz *et al.*, 1998).

Although various stress stimuli such as cytotoxic drugs, metabolite deprivation and heat shock lead to p53 activation, the primary stimulus for inducing p53 activation are DNA single strand breaks (Blatt and Glick, 2001; Jayaraman and Prives, 1995). Although it is still largely unknown how p53 regulates apoptosis, it seems that transcription-dependent and -independent pathways are involved (Attardi *et al.*, 1996). The p53 substrates involved in regulating the cell cycle and apoptosis are shown in Figure 1.7. At the gene level, p53 has been shown to upregulate Bax transcription and repress Bcl-2 transcription, favouring mitochondrial-dependent apoptosis (Miyashita and Reed, 1995; Cregan *et al.*, 1999). Furthermore, p53 transcriptionally induces the TRAIL receptor DR5 and the Fas receptor (CD95), priming the cell for apoptosis (Kastan, 1997; Owen-Schaub *et al.*, 1995; Bennett *et al.*, 1998). p53 also targets other apoptotic genes including, *c-fos* (Elkeles *et al.*, 1999), *MCG10* (Zhu and Chen, 2000), and *p53AIP1* (p53-regulated apoptosis-inducing

protein 1; Oda *et al.*, 2000). ROS may also be produced by the p53-inducible gene, *PIG3*, resulting in apoptosis (Johnson *et al.*, 1997). Transcriptionally-independent mechanisms of p53-induced apoptotic death include increased surface expression of the CD95 death receptor (Bennet *et al.*, 1998) and direct signalling at the mitochondria (Marchenko *et al.*, 2000; Bonini *et al.*, 2004), promoting cytochrome *c* translocation and procaspase-3 activation.

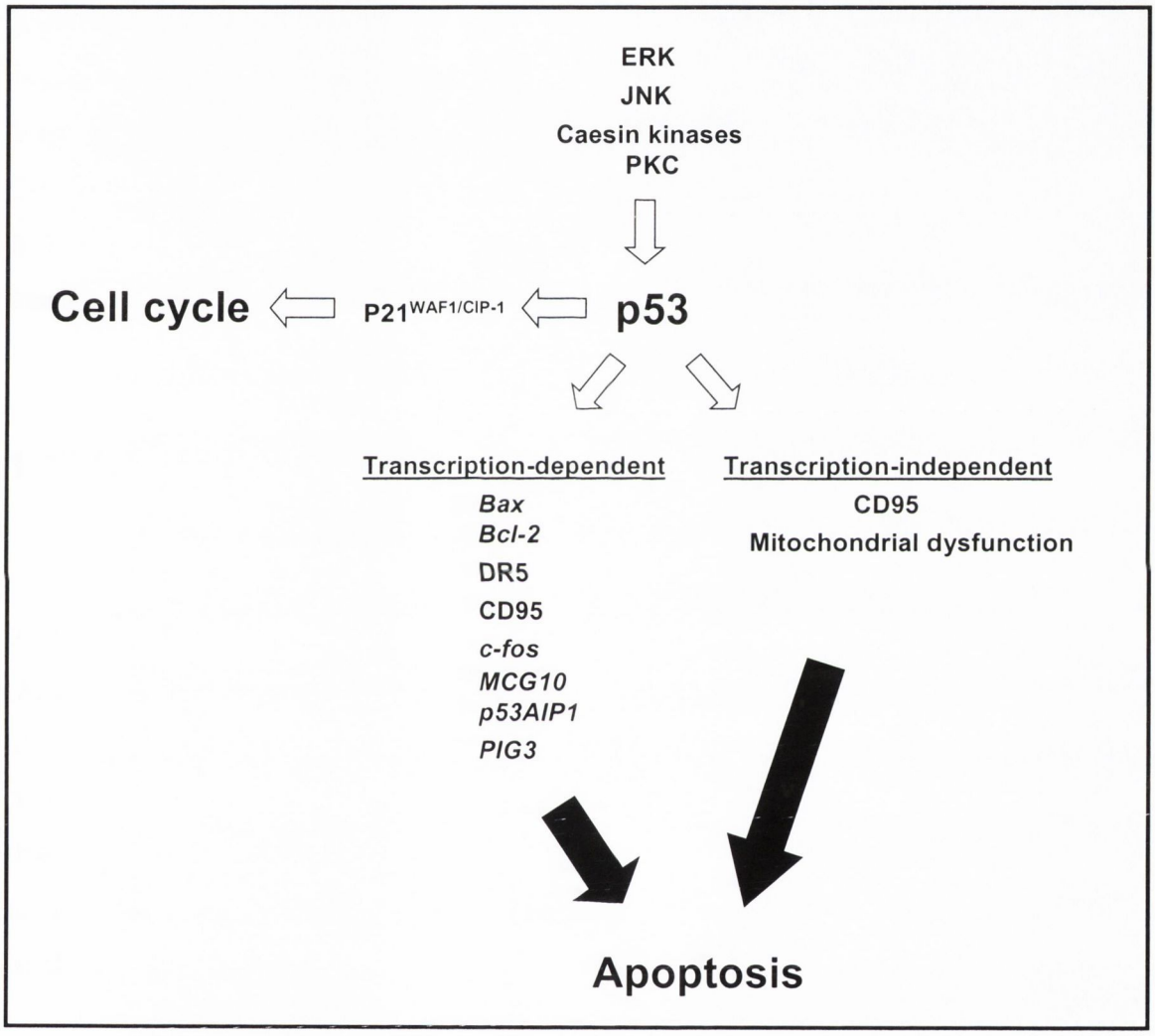

Figure 1.7: p53 regulation of apoptosis (adapted from Herr and Debatin, 2000).

Normal cellular p53 concentrations are low, due to its short half-life and metabolic instability when inactivated (Evan and Littlewood, 1997). It has been shown that phosphorylation plays an important role in regulating the biological

activities of p53 following DNA damage or cellular stress (Herr and Debatin, 2001). Although more than a dozen phosphorylation sites have been mapped on p53 depending on the phosphorylating kinase and the stress-inducing stimulus, the phosphorylation of p53 on residue serine-15 at the p53 N-terminus has been shown to be a critical signal required to regulate the p53 response to stress signals (Appella and Anderson, 2001). The phosphorylation state of p53 is controlled by a large number of proteins including JNK, ERKs, caesin kinases and PKC (Blatt and Glick, 2001). Stress-mediated phosphorylation of p53 at residue 15 disrupts its association with its negative regulator, the oncoprotein Mdm-2, preventing ubiquitin-mediated p53 degradation (Shieh *et al.*, 1997). Once phosphorylated the stability of the p53 protein is increased, allowing it to act as a transcripition factor to enhance and repress genes involved in the apoptotic process (Herr and Debatin, 2000).

1.11 Antisense technology

A useful approach toward evaluating the function of a particular protein is to prevent the expression of that protein by using antisense oligonucleotides (AS). It is a particularly useful technique for investigating a protein for which an inhibitor does not exist and also offers the potential to inhibit the expression of a particular isoform of the same protein family without affecting the expression of the related isoforms. Hence, in the absence of available inhibitors for the various isoforms of the stress kinase, JNK, AS targeted to the specific JNK1 and JNK2 isoforms were employed in this thesis.

Antisense technology employs the use of single stranded RNA or DNA sequences to alter the metabolism of specific mRNA, thereby modulating the transfer of information from gene to protein in a sequence-specific manner (Scanlon *et al.*, 1995; Cioffi and Monia, 1999). AS hybridise to the complementary mRNA of the gene of interest and provide a steric obstacle to the ribosome translating the protein of interest (Figure 1.8). As a result, the production of the protein is temporarily inhibited allowing the biological function of the protein to be approached by loss-of-function analysis. The biological

effect of the oligonucleotides can only be observed after enough pre-existing target protein has been degraded and also after the AS has inhibited the synthesis of enough target new protein. This varies depending on antisense uptake efficacy and target protein half-life. Furthermore, the degree of target protein downregulation by most AS ranges from 50-90%. However, pronounced biological effects can often be detected at inhibition rates of as little as 20%. In our experiments (Chapter 4), JNK1 and JNK2 protein expression was significantly reduced by 79% and 70% respectively, following AS exposure. Appropriate controls are an intricate part of antisense experiments and serve to eliminate substance-related side effects and the possibility that the effects of the AS are related to a non-sequence-specific mechanism. Commonly, scrambled control oligonucleotides (SC) are used, which are obtained by incorporating nonhybridizing base mismatches (typically one to six) into the oligonucleotide sequence. Hence, SC have no ability to hybidise to the target mRNA.

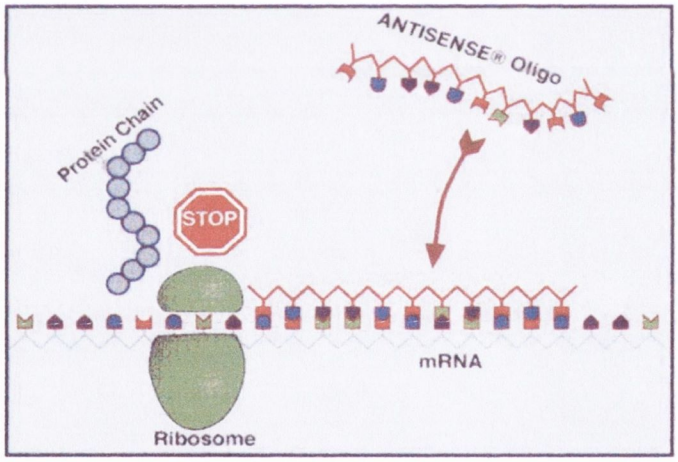

Figure 1.8: Mechanism of antisense action.
AS hybridise to the target complementary mRNA, preventing the translation of the target protein (taken from Biognostik antisense edition, 2001/2002).

In a cell culture system, AS are added directly into the culture medium and are taken up into the cells by fluid-phase endocytosis and also through a putative receptor protein, p80. Cellular uptake can be enhanced by

preincubating the oligonucleotides with a cationic lipid formulation such as lipofectin transfection reagent. The cationic charge masks the anion charge of the oligonucleotide backbone, allowing the lipid/oligonucleotide complex to pass the cell membrane efficiently. Once in the cell, the oligonucleotides are first entrapped in the endosomes and are steadily released into the cytosol where they bind to target mRNA sequences.

Natural oligonucleotides consist of phosphodiester links that are extremely sensitive to nucleases present intracellularly and hence are not very stable (Crooke, 1992). Chemical modifications have been introduced to AS to increase their half-life. Oligonucleotides commonly contain sulphur in place of an oxygen atom in the DNA backbone, producing phosphorothioated oligonucleotides that are resistant to exo- and endonucleases. In our experiments phosphorothioate oligodeooxynucleotides were used to deplete JNK1 and JNK2 isoforms in rat cortical neuronal cultures.

1.12 Objectives

The objectives of this study are to assess the effects of THC on the viability of rat primary cultured cortical neurons and determine the intracellular molecular mechanisms underlying THC-induced apoptosis in this cultured cell system. The influence of postnatal development (neuronal maturity) on regulating the apoptotic actions of THC will also be assessed in the rat cortex both *ex vivo* and *in vivo*.

- The effect of THC on cultured cortical neuronal viability will be determined by monitoring DNA fragmentation using the TUNEL and DNA laddering techniques. The impact of THC on classical apoptotic events including cytochrome *c* translocation, caspase-3 activation and PARP cleavage, will be addressed using western immunblotting, immunocytochemistry and biochemical assays.

- The effect of THC on the activation of the MAPK family member, JNK, will also be monitored in cultured cortical neurons by western immunoblotting and fluorescence microscopy using phospho-specific antibodies. Characterisation of the role of JNK1 and JNK2 isoforms in THC-induced neurotoxicity will be assessed using antisense technology. JNK1 and JNK2 antisense will be used to investigate the upstream roles of both JNK isoforms in the THC-induced activation of caspase-3 and subsequent DNA fragmentation.

- The proclivity of THC to impact on p53 signalling in cultured cortical cells will be determined using RT-PCR and western immunblotting. It will also be determined if regulatory effects of THC on the expression patterns of the mitochondria-associated proteins, Bax and Bcl-2, exist in cultured rat cortical neurons using western immunoblotting and RT-PCR. Downstream apoptotic consequences of p53 induction will be investigated using the synthetic p53 inhibitor, pifithrin-α. The role of p53 in THC-induced Bax and phosphorylated Bcl-2 expression, caspase-3

activation and DNA fragmentation will be assessed in cultured neurons exposed to pifithrin-α prior to THC exposure.

- In order to determine if the apoptotic actions of THC on the rat cortex are reliant on postnatal development, cortical brain slices obtained from neonatal (4-7-day old), adolescent (20-30-day old) and adult (3-4 month old) rats will be exposed to THC and the apoptotic consequences assessed. Targets for investigation include DNA fragmentation using agarose gel electrophoresis, JNK and p53 activation using western immunoblotting and caspase-3 activation using a biochemical assay.

- The *in vivo* effects of THC on two rat age groups (4-7-day old rat pups and 3-4 month old adult rats) will be ascertained to determine if the apoptotic actions of THC on the rat cortex are reliant on postnatal development. Following subcutaneous injections of THC it will be determined if apoptotic actions of THC exist *in vivo*, and if so, if this is influenced by development. Following treatment the level of DNA fragmentation, JNK and caspase-3 activation will be determined in cryostat sections prepared of the cortex using TUNEL and immunocytochemistry. JNK and caspase-3 activity will also be analysed using western immunoblotting and a biochemical assay, respectively. The *in vivo* effects of THC on the expression of Bax and Bcl-2 will also be ascertained using western immunoblotting.

Overall this study will isolate neuronal signal transduction pathways contributing to the apoptotic actions of THC in the rat cortex. It will also highlight the influence of neuronal development in determining the apoptotic consequences of THC exposure.

Chapter 2

Methods

2.1 Cell culture

2.1.1 Aseptic technique

The culturing of cells requires the use of sterile techniques to prevent both bacterial and fungal infection. An aseptic technique is required to maintain the sterility of any areas that the cultured cells are exposed to, including the internal areas of culture flasks, bottles, plastics and dissection instruments. The following aseptic technique procedures were adhered to for all cell culture procedures.

2.1.2 Sterilisation of glassware, plastics and dissection instruments

All glassware, pipette tips, dissection instruments, deionised H_2O and microfuge tubes (Sarstedt, Leicester, UK) were wrapped in aluminum foil, sealed with autoclave tape (Sigma-Aldrich, Dorset, UK) and autoclaved at 121°C for 30 min (Priorclave Ltd., Model #EH150, London, UK). To ensure sterility, all equipment used in the dissection procedure was oven baked at 200°C (Sanyo-Gallenkamp Hotbox Oven, Model #OHG050, Loughborough, UK) for 1 hr prior to use.

2.1.3 Sterility of work environment

All cell culture work was carried out in a laminar flow hood (Astec-Microflow laminar flow workstation, Florida, USA). In the laminar flow workstation air passes through HEPA (high efficiency particle air) filters at the top of the flowhood and flows downwards. The airflow creates a downward barrier in front of the open portion of the hood preventing the entry of external airborne contaminants into the laminar flow hood. Before using the laminar flow hood, the interior was sterilized by wiping down all accessible surfaces with 70% ethanol (EtOH), followed by a 15 min exposure to ultraviolet (UV) light. Disposable latex gloves (sprayed with 70% EtOH) were worn at all times when cell manipulations were being performed in the hood. Gloves were changed regularly to avoid contamination.

2.1.4 Reagents and medium formulation

Solutions such as phosphate buffered saline (PBS; 100mM NaCl, 80mM Na_2HPO_4, 20mM NaH_2PO_4, pH 7.4) were hand filtered into autoclaved glass bottles or sterile 15/50ml plastic tubes (BD Biosciences Pharmingen, San Diego, USA) using a 0.2μm cellulose acetate membrane syringe filter (Pall Corporation, Michigan, USA) attached to a 10ml sterile syringe (B.Braun Medical Ltd., Melsungen, Germany). Neurobasal medium (NBM; Invitrogen, Paisley, UK) supplemented with heat inactivated horse serum (10%), penicillin (100 U/ml), streptomycin (100 U/ml) and glutamax (2mM; Invitrogen, Paisley, UK) was filtered through a 0.2μm cellulose acetate membrane (Millipore Ireland B.V, Cork, Ireland) in a Millipore Sterifil unit (Sigma-Aldrich, St. Louis, USA.) connected to a vacuum pump. Care was taken to ensure that the side and tip of a pipette did not contact anything except the sterile interiors of the sterile containers that were in use. Pipettes were placed on sterile racks (Bell-Art Products, New Jersey, USA) between use and were regularly wiped down with 70% EtOH.

2.1.5 Disposal

All used plastic ware was discarded in autoclavable plastic bags (Bibby Sterilin Ltd., Staffordshire, UK) and autoclaved.

2.2 Primary culture of cortical neurons

The culturing of primary cortical neurons is an *in vitro* technique involving dissection of the brain, removal of the cortex and dissociation of the cortical tissue to obtain a population of neurons. Primary neuronal cell cultures are superior to cell line models as they represent non-transformed unaltered phenotypes.

2.2.1 Preparation of sterile coverslips

To ensure sterility 13mm diameter glass coverslips (Chance Propper, West Midlands, UK) were soaked in 70% EtOH for 24hr followed by an overnight exposure to UV light in the laminar flow hood. Sterile coverslips were then coated with poly-L-lysine (60μg/ml in sterile H_20) in a final volume of 25ml for 1hr at 37°C to provide a suitable surface to which dissociated neurons would adhere. Coated coverslips were then air-dried in the laminar flow workstation, placed in sterile 24-well plates (Greiner Bio One Gmbh, Kremsmuenster, Austria) and stored at 4°C until required for use (maximum 2 week storage).

2.2.2 Animals

Postnatal 1-day old Wistar rats were born at the BioResources Unit (Trinity College, Dublin 2, Ireland). Animals were maintained under a 12hr light/dark cycle at an ambient temperature of 22-23°C. On the day of birth, animals were removed from the litter cage and placed in a ventilated box containing suitable cotton wool bedding. The animals were then taken to the Physiology Department and kept in the cell culture room until dissection.

2.2.3 Dissection

Primary cortical neurons were established from postnatal 1-day old Wistar rats. Dissection of one rat brain yielded a preparation of 2 individual 24-well plates. Working in a laminar flow hood, rats were decapitated using a large sterile scissors and the skull exposed by cutting the skin in a straight line from the neck to the top of the head with a smaller sterile scissors. To remove the skull the small

sterile scissors was used, cutting around the skull on each side of the head, ensuring that the inside point of the scissors remained against the inside of the skull at all times. A sterile forceps was used to lift back the skull and expose the brain. The cerebral cortices were removed with the forceps and placed in a sterile petri dish (Greiner Bio One Gmbh, Kremsmuenster, Austria) containing sterile PBS. Any meninges were carefully removed using a fine forceps and cortices were chopped into 3-4mm pieces with a sterile disposable scalpel (Schwann-Mann, Sheffield, UK).

2.2.4 Dissociation procedure

Cortical tissue was incubated in 5ml of sterile PBS containing trypsin (0.3% w/v, Sigma-Aldrich, Dorset, UK) for 25 min at 37°C. Trypsin digestion of connective tissue was followed by trituration (x5) of the dissociated neurons in sterile PBS containing soyabean trypsin inhibitor (0.1% w/v, Sigma-Aldrich, Dorset, UK), DNAse (0.2mg/ml; Sigma-Aldrich, Dorset, UK) and $MgSO_4$ (0.1M; Sigma-Aldrich, Dorset, UK). The cell suspension was then gently filtered through a sterile 40µm nylon mesh filter (Becton Dickinson Labware Europe, France) to remove tissue clumps and centrifuged (Sigma-Aldrich, Model #2K15C, St. Louis, USA) at 2, 000 x *g* for 3 min at 20°C. The pellet was resuspended in neurobasal medium (NBM; Invitrogen, Paisley, UK) supplemented with 10% heat inactivated horse serum (Invitrogen, Paisley, UK), penicillin (100 U/ml; Invitrogen, Paisley, UK), streptomycin (100 U/ml; Invitrogen, Paisley, UK), glutamax (2mM; Invitrogen, Paisley, UK) and B27 (1:50 dilution; Invitrogen, Paisley, UK). B27 was added to the NBM due to its neuroprotective antioxidant properties.

2.2.5 Plating of resuspended neurons

Resuspended neurons in NBM were placed on the centre of each coverslip at a density of 0.25 x 10^6 cells and allowed to adhere to the glass coverslip for 2-3hr in a humidified incubator containing 5% CO_2: 95% air at 37°C (Model # 394-048, Jencons Scientific Ltd., Bedfordshire, UK) prior to each well being flooded with 300µl of supplemented pre-warmed NBM. Cells were incubated for 3 days *in*

vitro. Media was then replaced with supplemented NBM containing 5ng/ml cytosine-arabino-furanoside (ARA-C; Sigma-Aldrich, Dorset, UK) to prevent proliferation of non-neuronal cells and maintain the purity of the cortical neuronal culture. This ensured that microglia and astrocyte contamination was less than 5% in culture preparations. Media containing ARA-C was removed after 24hr and replaced with supplemented NBM (200µl/well). Cells were grown in culture for up to 7 days prior to treatments and culture media was replaced every 3 days depending on treatment conditions. Cultured neurons were monitored daily by light microscopy (Nikon Labophot, Nikon Instech Co., Ltd, Kanagawa, Japan) to ensure that the cells appeared healthy and to ensure that fungal or bacterial infection was not occurring. A sample photo of cultured cortical neurons at 4 days *in vitro* is shown in Figure 2.1.

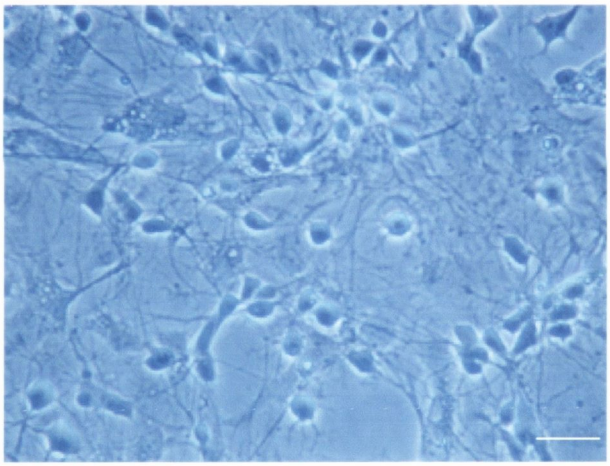

Figure 2.1: Cultured cortical neuronal morphology.

At day 4 *in vitro* there is a dense population of neurons, displaying oval cell bodies and an extensive neurite network representative of mature neurons. Scale bar is 50µm.

2.3 Cell treatments

2.3.1 THC

THC was obtained from Sigma-Aldrich Company Ltd. (Dorset, UK). The drug was initially dissolved in methanol and stored at –20°C as an 80mM stock solution. For culture use, the stock drug was diluted to final concentrations (0.5nM-50μM) in pre-warmed supplemented NBM and 0.007% methanol (v/v) was used as vehicle control.

2.3.2 CB_1 cannabinoid receptor inhibitor

The selective CB_1 receptor antagonist ^{123}I-labeled *N*-piperidin-1-yl)-5-(4-idophenyl)-1-(2,4 dichlorophenyl)-4-methyl-I *H*-pyrazole-3-carboxamide (AM 251; Gatley *et al.*, 1996) (Tocris Cookson Ltd., Bristol, UK) was stored as a 10mM stock solution in dimethylsulfoxide (DMSO; Sigma-Aldrich, Dorset, UK) and diluted to a final concentration of 10μM in warm culture media for addition to cultures; 0.1% DMSO (v/v) used as a vehicle control for AM 251. Neurons were pre-incubated with AM 251 for 30 min before treating with THC. AM 251 is a structural analogue of SR 141716A, a compound considered to be the prototypical CB_1 anatagonist (Rinaldi-Carmona *et al.*, 1994). It is a selective, high affinity inhibitor exhibiting slightly better affinity for the CB_1 receptor than SR 141716A and is approximately two-fold more selective for CB_1 than SR 141716A. Furthermore, AM 251 is 306-fold selective for CB_1 over CB_2 (Lan *et al.*, 1999).

2.3.3 p53 inhibitor

The p53 inhibitor pifithrin-α (Calbiochem International, Darmstadt, Germany) was made up as a stock solution of 1mM in DMSO and was used at a final concentration of 100nM. Cells were exposed to the p53 inhibitor for 60 min prior to THC treatment. This inhibitor is a cell permeable highly lipophilic molecule that efficiently inhibits p53-dependent transactivation of p53-responsive genes and reversibly blocks p53-mediated apoptosis (Culmsee *et al.*, 2001).

2.3.4 Pertussis toxin

Pertussis toxin (PTX; Sigma-Aldrich, Dorset, UK) was reconstituted in PBS and neurons were incubated with 200ng/ml PTX for 24hr prior to THC treatment. PTX is a G-protein inhibitor, blocking the dissociation of the α and β/γ subunits of G_i/G_o-proteins (Kaslow *et al.*, 1987).

2.3.5 Etoposide

Etoposide (Sigma-Aldrich, Dorset, UK) was made up as a stock solution of 1mM in sterile H_2O. It was diluted to a final concentration of 10μM in NBM for addition to cell cultures. Etoposide is a DNA damaging agent that has neurotoxic effects (Nakajima *et al.*, 1994). The target for etoposide is DNA topoisomerase II, an enzyme involved in DNA replication, recombination and chromosome segregation (Jiang, 2005). Cells were exposed to etoposide for 24hr to induce apoptosis.

2.4 *Ex vivo* studies

2.4.1 Animals

Neonatal (4-7-day old), adolescent (20-30-day old) and adult (3-4 month old) male Wistar rats were supplied by the Bio Resources Unit, Trinity College, Dublin. All rats were maintained under a 12hr light-dark cycle in the Bio Resources Unit and food (normal laboratory chow, unless otherwise stated) and water was available *ad libitum*. Ambient temperature was controlled between 22 and 23°C.

2.4.2 Cortical slice preparation

Rats were killed by decapitation and the right cortex removed and dissected on ice. Freshly dissected cortex from neonatal (4-7-day old), adolescent (20-30-day old) and adult (3-4 month old) Wistar rats was sliced bidirectionally to a thickness of 350μm using a McIlwain tissue chopper (Mickle Laboratory Engineering Co., Surrey, UK) and placed in microfuge tubes containing 1ml ice-

cold sterile HEPES-buffered saline (145mM NaCl, 5mM KCl, 1mM $MgCl_2$, 2mM $CaCl_2$, 1mM Mg_2SO_4, 1mM KH_2PO_4, 10mM glucose, 30mM HEPES, pH 7.4). Slices were vortexed and allowed to settle. Excess solution was removed and replaced with 0.5ml pre-warmed sterile drug solution under sterile conditions.

2.4.3 Drug treatment of cortical slices

For *ex vivo* use, THC was diluted to concentrations of (5nM-50μM) in sterile pre-warmed HEPES-buffered saline and 0.007% methanol (v/v) was used as vehicle control. Slices were incubated with THC for 2hr with agitation in a humidified incubator containing 5% CO_2: 95% air at 37°C (Model # 394-048, Jencons Scientific Ltd., Bedfordshire, UK). Cortical slices were pre-incubated with AM 251 (10μM; diluted in sterile pre-warmed HEPES-buffered saline) for 30 min before treating with THC.

2.5 *In vivo* studies

2.5.1 Animals

All animals used were male Wistar rats supplied by the Bio Resources Unit, Trinity College, Dublin. Two rat age groups were used, 4-7-day old rat pups (8-13g) and 3-4 month old adult rats (180-300g). Animals were maintained under conditions outlined in section 2.4.1. All animal experimentation was performed under a licence granted by the Minister for Health and Children (Ireland) under the Cruelty to Animals Act, 1876 and the European Community Directive, 86/609/EC.

2.5.2 THC administration

In all experiments rats were anaesthetised by intraperitoneal (ip) injection of urethane (1.5g/kg, 33% w/v; Sigma-Aldrich, Dorset, UK). The absence of a pedal reflex was used to confirm deep anaesthesia and if needed a further top-up dose was administered (to a maximum of 2.5g/kg). While away from the litter the ambient temperature maintained at approximately 33°C using a heated blanket

and lamp. The THC group received subcutaneous injections (5μl/g body weight) of 1mg/kg, 10mg/kg or 30mg/kg THC in vehicle and the control group received injections of vehicle alone (5% absolute alcohol, 5% Cremophor EL and 90% sterile saline; Sigma-Aldrich, Dorset, UK). Rats were killed 3hr post-treatment by decapitation.

2.5.3 AM 251 administration

In some experiments, 4-7-day old rat pups (8-13g) received intraperitoneal injections (5μl/g body weight) of the CB_1 receptor antagonist AM 251 (10mg/kg) in vehicle (5% absolute alcohol, 5% Cremophor EL and 90% sterile saline) 30 min before THC injection (10mg/kg; 3hr treatment). The control CB_1 receptor inhibitor group received an ip injection (5μl/g body weight) of AM 251 (10mg/kg) in vehicle alone for 3hr.

2.5.4 Dissection

Rats were killed by decapitation and the right cortex removed and dissected on ice. The left half of the brain was dissected on ice, the cerebellum discarded and the brain frozen. This procedure took approximately 2 min.

2.5.5 Preparation of slices for freezing

Freshly dissected cortex was sliced bidirectionally to a thickness of 350μm using a McIlwain tissue chopper (Mickle Laboratory Engineering Co., Surrey, UK) and placed in microfuge tubes containing 1ml Krebs solution (composition in mM: NaCl 136, KCl 2.54, KH_2PO_4 1.18, $MgSO_4$ 1.18, $NaHCO_3$ 16, glucose 10, pH 7.4) with added $CaCl_2$ (2mM final concentration). Slices were allowed to settle and were rinsed once more with Krebs solution containing $CaCl_2$. The slices were rinsed a further two times with Krebs solution containing 2mM $CaCl_2$ and 10% DMSO (v/v) and stored at -80°C until required for later analyses.

2.5.6 Preparation of cryostat sections

For cryostat sectioning the dissected half brain was covered in OCT compound (R.A. Lamb Ltd, Sussex, UK), quickly frozen in liquid nitrogen onto cork discs for sectioning and stored at -80°C. Glass slides (76x26mm) were coated with subbing solution (0.5% gelatine (w/v), 0.05% chrome alum (w/v) in deionised H_20; BDH, Dorset, UK) for 10 sec at 60°C and allowed to dry overnight at RT. This provided a suitable surface to which sections could adhere. On the day of the experiment the half brain was equilibrated to -20°C for 20-30 min. Saggital sections (10μm) were cut, stained with methylene green for 2 min and viewed by light microscopy (Nikon Labophot, Nikon Instech Co., Ltd, Kanagawa, Japan) for detection of the hippocampus. For each animal, 21 sections (10μm) were cut onto 7 subbed slides (3 sections/slide), allowed to dry (10 min) and stored at -20°C until required.

2.6 Protein quantification using the Bradford assay

Protein concentration in cultured cell samples and in cortical slices was assessed according to Bradford (1976). Standards were prepared from stock solution of 1000μg/ml bovine serum albumin (BSA; Sigma-Aldrich, Dorset, UK). This was diluted in dH_2O to prepare a range of standards (including a blank of dH_2O) from 1000μg/ml to 3.125μg/ml. Samples (10μl) and standards (10μl) were added to a 96-well plate (Sarstedt, Wexford, Ireland) in duplicate and Bio-Rad dye reagent concentrate (1:5 dilution in dH_2O, 200μl; Bio-Rad, Hertfordshire, UK) was added to both and absorbance was assessed at 600nm using a 96-well plate reader (EIA Multiwell reader, Sigma-Aldrich, Dorset, UK). The concentration of protein in samples was calculated from the regression line plotted (Instat 2.03) from the absorbance of the BSA standards.

2.7 Sodium Dodecyl Sulphate-Polyacrylamide Gel Electrophoresis (SDS-PAGE)

2.7.1 Preparation of cell culture protein

(i) Preparation of total protein

To analyse total expression of protein neuronal cell cultures were washed in Tris Buffered Saline (TBS; 20mM Tris-HCl; 150mM NaCl; pH 7.6) before harvesting by scraping coverslips in lysis buffer (80µl/well; 25mM HEPES, 5mM $MgCl_2$, 5mM dithiothreitol, 5mM EDTA, 2mM PMSF, 10µg/ml leupeptin, 10µg/ml pepstatin, 10µg/ml aprotinin, pH 7.4) on ice using the rubber end of a 1ml syringe piston (B.Braun Medical Ltd., Melsungen, Germany). Lysates were homogenised (x10 strokes) in lysis buffer on ice using a 1ml glass homogeniser (Jencons, Bedfordshire, UK). Samples were then centrifuged (13, 000 x *g* for 15 min at 4°C) and the supernatant collected as the whole cell protein.

(ii) Preparation of cytosolic and mitochondrial fraction

To obtain cytosolic and mitochondrial protein fractions cells were washed in TBS before 100µl of permeabilisation buffer (250mM sucrose, 70mM KCL, 137mM NaCl, 4.5mM Na_2HPO_4, 1.4mM kH_2P0_4, 0.1mM PMSF, 10µg/ml leupeptin, 2µg/ml aprotinin, 200µg/ml digitonin; pH 7.4) was added to each well and left on ice for 5 min. The permeabilisation buffer was then removed and collected as the cytosolic fraction. Mitochondrial buffer (100µl; 50mM Tris Base, 150mM NaCl, 2mM EGTA, 0.2% Triton-X-100, 0.3% Igepal p-40 (v/v), 0.1mM PMSF, 10µg/ml leupeptin, 2µg/ml aprotinin; pH 7.2) was then added to each well before harvesting the mitochondrial protein by scraping coverslips using the rubber end of a 1ml syringe piston (B.Braun Medical Ltd., Melsungen, Germany). Cells were centrifuged (15, 000 x *g* for 20 min at 4°C) and the supernatant containing the mitochondrial fraction was collected.

2.7.2 Preparation of cortical slice protein

Cortical slices were thawed rapidly, washed 3 times in Krebs solution (composition in mM: NaCl 136, KCl 2.54, KH_2PO_4 1.18, $MgSO_4$ 1.18, $NaHCO_3$ 16, glucose 10) containing 2mM $CaCl_2$ and homogenised (x30 strokes) in lysis buffer (500µl; 20mM HEPES, 10mM KCl, 1.5mM $MgCl_2$, 1mM EGTA, 1mM EDTA, 1mM DTT, 0.1mM PMSF; 2µg/ml leupeptin; 2µg/ml aprotinin; 200mM sucrose; pH 7.4) using a 1ml glass homogeniser (Jencons, Bedfordshire, UK).

Total expression of protein (section 2.7.1 (i)) was assessed in all cases unless otherwise stated. All samples were prepared for SDS-polyacrylamide gel electrophoresis. Protein concentration was assessed (see section 2.6) and samples equalised with lysis buffer. An equal volume of sodium dodecyl sulphate (SDS) sample buffer (150mM Tris-HCl pH 7.4, 10% glycerol (v/v), 10% SDS (w/v), 5% β-mercaptoethanol (v/v), 0.05% Bromophenol Blue (w/v)) to sample was added to a microfuge tube and samples boiled for 5 min. In the case of CB_1 receptor expression analysis, samples were not treated with drug and were homogenised on ice in 400µl sterile ice-cold HEPES-buffered saline following dissection. These samples were equalised in HEPES-buffered saline and suspended in sample buffer. All samples were stored at -20°C until required.

2.7.3 Preparation of polyacrylamide gels

Polyacrylamide separating gels (1mm thick) with a monomer concentration of either 10% or 12% overlaid with 4% stacking gel were cast by setting them between two 10cm wide glass plates (Sigma-Aldrich, Dorset, UK), which were mounted on an electrophoresis unit (Sigma Techware, Dorset, UK) using spring clamps. The upper and lower reservoirs of the unit were flooded with electrode running buffer (25mM Tris-base, 200mM glycine, 0.1% SDS (w/v)). Samples (10µl) were loaded into the wells and proteins were separated by the application of a 32mA current to the gel apparatus. Pre-stained molecular standards (5µl; Sigma-Aldrich, Dorset, UK and Santa Cruz Biotechnology Inc, Santa Cruz, CA, USA) were used to confirm the molecular weight of protein bands. The migration

of the bromophenol blue was monitored and the current switched off when the dye reached the bottom of the gel (20-30 min).

2.7.4 Semi-dry electrophoretic blotting of proteins

The gel was removed from the apparatus and placed on top of a sheet of nitrocellulose blotting paper (0.45μm pore size; Sigma-Aldrich, Dorset, UK), which had been cut to the approximate size of the gel and soaked in ice-cold transfer buffer (25mM Tris-base pH 8.3, 192mM glycine, 20% methanol (v/v), 0.05% SDS (w/v)). A sandwich was made by placing one piece of filter paper (Standard Grade No. 3, Whatman, Kent, UK) on top of the gel and one piece beneath the nitrocellulose paper. This sandwich was soaked in transfer buffer and placed on the platinum-coated titanium electrode (anode) of a semi-dry blotter (Sigma-Aldrich, Dorset, UK). The lid of the blotter (stainless steel cathode) was moistened with transfer buffer, placed on top of the sandwich and sealed. The uncovered portion of the cathode was shielded with a mylar cut-out (Sigma-Aldrich, Dorset, UK), ensuring that all applied current passed through the sandwich. A constant current of 225mA was applied for 90 min.

2.8 Western immunoblotting

The nitrocellulose blotting paper was blocked for non-specific binding and probed with an antibody raised against the appropriate protein. This was washed off with TBS containing 0.05% Tween (TBS-T, v/v) and incubated with a secondary antibody that was horseradish peroxidase (HRP)-conjugated. A chemiluminescent detection chemical (SuperSignal Ultra; Pierce, Leiden, Netherlands) or Enhanced Cheminluminescence (ECL) detection reagent (Amersham, Buckinghamshire, UK) was added and the blotting paper exposed to 5 x 7 inch photographic film (Hyperfilm, Amersham, Buckinghamshire, United Kingdom) and developed using a Fuji X-ray film processor (Model # RGII, FUJJIFILM Medical Systems, Stamford, USA).

2.8.1 Bax expression

Bax expression was assessed in cytosolic and mitochondrial fractions. Non-specific binding was blocked by incubating the nitrocellulose in TBS containing 2% BSA (w/v) overnight at 4°C. The membrane was washed for 10 min 2 times in TBS-T. The primary antibody used was a rabbit polyclonal Bax antibody (DAKO Corporation, Carpinteria, CA, USA) that recognizes amino acids 43-61 of human Bax (1:200 dilution in TBS-T containing 0.1% BSA; w/v). This was incubated for 2hr at RT and then washed for 20 min 3 times in TBS-T. The secondary antibody (anti-rabbit IgG-HRP, 1:2000 dilution in TBS-T containing 0.1% BSA (w/v); Sigma, Dorset, UK) was incubated for 90 min at RT and washed for 10 min 12 times in TBS-T. Supersignal (Pierce, Leiden, Netherlands) was added to membranes, incubated for 3 min and the membranes exposed to photographic film for 5 sec in the dark prior to being developed.

2.8.2 Bcl phosphorylation

Bcl-2 phosphorylation was assessed by incubating the nitrocellulose in TBS containing 2% BSA (w/v) overnight at 4°C and then washing for 10 min 2 times in TBS-T. The primary antibody used was a rabbit polyclonal anti-phospho-Bcl-2 antibody (Oncogene, Boston, MA, USA) that recognises a peptide corresponding to amino acids 81-94 of human *bcl-2* (1:250 dilution in TBS-T containing 0.1% BSA; w/v). This was incubated for 2hr at RT and then washed for 20 min 3 times in TBS-T. The secondary antibody (goat anti-rabbit IgG-HRP, 1:1000 dilution in TBS-T containing 0.1% BSA (w/v); Santa Cruz Biotechnology Inc, Santa Cruz, CA, USA) was incubated for 1hr at RT and washed for 10 min 12 times in TBS-T. Supersignal (Pierce, Leiden, Netherlands) was added to membranes, incubated for 3 min and the membranes exposed to photographic film for 2 sec in the dark prior to being developed.

2.8.3 CB_1 receptor expression

In the case of CB_1 receptor expression, non-specific binding was blocked by incubating the nitrocellulose in TBS containing 2% BSA (w/v) overnight at 4°C

and then washing for 10 min 2 times in TBS-T. The primary antibody used was a goat polyclonal CB_1 receptor antibody (Santa Cruz Biotechnology Inc, Santa Cruz, CA, USA) raised against a peptide mapping the amino terminus of CB_1 of human origin (1:400 dilution in TBS-T containing 0.1% BSA; w/v). This was incubated for 2hr at RT and then washed for 20 min 3 times in TBS-T. The secondary antibody (anti-goat IgG-HRP, 1:1500 dilution in TBS-T containing 0.1% BSA (w/v); Santa Cruz Biotechnology Inc, Santa Cruz, CA, USA) was incubated for 1hr at RT and washed for 10 min 12 times in TBS-T. Supersignal (Pierce, Leiden, Netherlands) was added to membranes, incubated for 3 min and the membranes exposed to photographic film for 2 sec in the dark prior to being developed.

2.8.4 Cytochrome *c* expression

Cytochrome *c* expression was assessed by incubating the nitrocellulose in PBS containing 10% Marvel (w/v) for 2hr at RT with gentle shaking. The membrane was washed for 10 min 2 times in PBS containing 0.05% Tween (PBS-T; v/v). The primary antibody used was a rabbit polyclonal cytochrome *c* antibody (Santa Cruz Biotechnology Inc, Santa Cruz, CA, USA) raised against recombinant protein corresponding to amino acids 1-104 representing full length cytochrome *c* of horse origin (1:250 dilution in PBS-T containing 2% Marvel; w/v). This was incubated overnight at 4°C and then washed for 20 min 3 times in PBS-T. The secondary antibody (goat anti-rabbit IgG-HRP, 1:1000 dilution in PBS-T containing 2% Marvel (w/v); Sigma, Dorset, UK) was incubated for 1hr at RT and washed for 10 min 12 times in PBS-T. ECL detection reagent (Amersham, Buckinghamshire, UK) was added to membranes, incubated for 5 min and the membranes exposed to photographic film for 20 min at 4°C in the dark before being developed.

2.8.5 JNK phosphorylation

In the case of phosphorylation JNK expression, non-specific binding was blocked by incubating the nitrocellulose in TBS containing 2% BSA (w/v) overnight at 4°C and then washing for 10 min 2 times in TBS-T. The primary antibody for phosphorylated JNK used was a mouse polyclonal anti-phospho-specific JNK

antibody (Santa Cruz Biotechnology Inc, Santa Cruz, CA, USA) that recognises JNK1 and JNK2 isoforms of human origin phosphorylated on Thr-183 and Tyr-185 (1:200 dilution in TBS-T containing 0.1% BSA; w/v). This was incubated for 2hr at RT and then washed for 20 min 3 times in TBS-T. The secondary antibody (goat anti-mouse IgG-HRP, 1:400 dilution in TBS-T containing 0.1% BSA (w/v); Sigma-Aldrich, Dorset, UK) was incubated for 90 min at RT and washed for 10 min 12 times in TBS-T. Supersignal (Pierce, Leiden, Netherlands) was added to membranes, incubated for 3 min and the membranes exposed to photographic film for 1 sec in the dark prior to being developed.

2.8.6 JNK1/2 expression

To assess JNK1 and JNK2 expression, non-specific binding was blocked by incubating the nitrocellulose in TBS containing 2% BSA (w/v) overnight at 4°C. The membrane was washed for 10 min 2 times in TBS-T. The primary antibodies used were a mouse monoclonal JNK1 antibody (Santa Cruz Biotechnology Inc, Santa Cruz, CA, USA) that recognises the epitope corresponding to amino acids 1-384 representing full length JNK1 (1:200 dilution in TBS-T containing 0.1% BSA; w/v), and a mouse monoclonal JNK2 antibody (Santa Cruz Biotechnology Inc, Santa Cruz, CA, USA) that recognizes the epitope corresponding to amino acids 1-424 representing full length JNK2 (1:200 dilution in TBS-T containing 0.1% BSA; w/v) of human origin. This was incubated for 2hr at RT and then washed for 20 min 3 times in TBS-T. The secondary antibody (goat anti-mouse IgG-HRP, 1:400 dilution in TBS-T containing 0.1% BSA (w/v); Sigma-Aldrich, Dorset, UK) was incubated for 1hr at RT and washed for 10 min 12 times in TBS-T. Supersignal (Pierce, Leiden, Netherlands) was added to membranes, incubated for 3 min and the membranes exposed to photographic film for 2 sec in the dark prior to being developed.

2.8.7 p53 expression

To assess p53 expression, non-specific binding was blocked by incubating the nitrocellulose in TBS containing 2% BSA (w/v) overnight at 4°C. The

membrane was washed for 10 min 2 times in TBS-T. The primary antibody used was a goat polyclonal antibody raised against the epitope mapping the carboxy terminus of p53 of human origin (1:500 dilution in TBS-T containing 0.1% BSA (w/v); Santa Cruz Biotechnology Inc, Santa Cruz, CA, USA). This was incubated for 2hr at RT and then washed for 20 min 3 times in TBS-T. The secondary antibody (donkey anti-goat IgG-HRP, 1:1800 dilution in TBS-T containing 0.1% BSA (w/v); Santa Cruz Biotechnology Inc, Santa Cruz, CA, USA) was incubated for 1hr at RT and washed for 10 min 12 times in TBS-T. Supersignal (Pierce, Leiden, Netherlands) was added to membranes, incubated for 3 min and the membranes exposed to photographic film for 1 sec in the dark prior to being developed.

2.8.8 Phosphorylated p53 expression

In the case of phosphorylated p53 (serine (ser) 15) expression, non-specific binding was blocked by incubating the nitrocellulose in TBS containing 2% BSA (w/v) overnight at 4°C. The membrane was washed for 10 min 2 times in TBS-T. The primary antibody used was a rabbit monoclonal antibody that detects endogenous levels of p53 only when phosphorylated at residue serine-15 (1:400 dilution in TBS-T containing 0.1% BSA (w/v); Cell Signalling Technologies, Massachusetts, USA). This was incubated for 2hr at RT and then washed for 20 min 3 times in TBS-T. The secondary antibody (goat anti-rabbit IgG-HRP, 1:1000 dilution in TBS-T containing 0.1% BSA (w/v); Sigma-Aldrich, Dorset, UK) was incubated for 1hr at RT and washed for 10 min 12 times in TBS-T. Supersignal (Pierce, Leiden, Netherlands) was added to membranes, incubated for 3 min and the membranes exposed to photographic film for 3 sec in the dark prior to being developed.

2.8.9 Total JNK expression

Following Western immunoblotting for JNK phosphorylation, blots were stripped with an antibody stripping solution (1:10 dilution in deionised H_20; Reblot Plus Strong antibody stripping solution; Chemicon, California, USA) and reprobed

for total JNK expression in order to confirm equal loading of protein. As before, non-specific binding was blocked by incubating the nitocellulose membrane in TBS containing 2% BSA (w/v) for 2 hours at RT. The primary antibody used was a rabbit JNK polyclonal antibody recognising JNK1, JNK2 and JNK3 (1:1000 dilution in TBS-T containing 0.2% BSA (w/v); Santa Cruz, California, USA). Membranes were incubated overnight at 4°C in the presence of the antibody and washed for 15 min 3 times in TBS-T. The secondary antibody (1:1000 dilution; goat anti-rabbit IgG-HRP in TBS-T containing 0.2% BSA (w/v); Amersham, Buckinghamshire, UK) was added and membranes were incubated for 1hr at RT. Membranes were washed for 15 min 5 times in TBS-T. Supersignal (Pierce, Leiden, Netherlands) was added to membranes, incubated for 3 min and the membranes exposed to photographic film for 3 sec in the dark prior to being developed.

2.8.10 Total actin expression

Following Western immunoblotting for Bax, CB_1, p53, phosphorylated p53 and Bcl-2, blots were stripped with an antibody stripping solution as before (see Section 2.8.9) and reprobed for analysis of total actin expression to confirm equal loading of protein. As before, non-specific binding was blocked by incubating the nitrocellulose membrane overnight at 4°C in TBS containing 2% BSA (w/v). The membrane was washed for 15 min 4 times in TBS-T. The primary antibody used was a mouse monoclonal actin antibody corresponding to amino acid sequence mapping at the carboxy terminus of actin of human origin (1:200 dilution in TBS containing 0.1% BSA (w/v); Santa Cruz, California, USA). Membranes were incubated for 2hr at RT in the presence of the antibody and washed for 15 min 4 times in TBS-T. The secondary antibody (1:400 dilution; goat anti-mouse IgG HRP in TBS-T containing 0.1% BSA (w/v); Sigma-Aldrich, Dorset, UK) was added and incubation proceeded for 1hr at RT. Membranes were washed for 15 min 4 times in TBS-T. SuperSignal (Pierce, Leiden, Netherlands) was added for 5 min and membranes were exposed to photographic film for 1 sec in the dark after which time the film was developed.

Protein Target	Antibody Source	2° Antibody	Antibody Dilution % BSA in TBS-T	Protein Band Size
Phosphorylated JNK1/2	Mouse	Goat anti-mouse IgG	1° 1/200 0.1% BSA 2° 1/400 0.1% BSA	JNK1 46 kDa JNK2 54 kDa
JNK1	Mouse	Goat anti-mouse IgG	1° 1/200 0.1% BSA 2° 1/400 0.1% BSA	46 kDa
JNK2	Mouse	Goat anti-mouse IgG	1° 1/200 0.1% BSA 2° 1/400 0.1% BSA	54 kDa
Total JNK	Rabbit	Goat anti-rabbit IgG	1° 1/1000 0.2% BSA 2° 1/1000 0.2% BSA	JNK1 46 kDa JNK2 54 kDa
p53	Goat	Donkey anti-goat IgG	1° 1/500 0.1% BSA 2° 1/1800 0.1% BSA	53 kDa
$p53^{ser15}$ phosphorylation	Rabbit	Goat anti-rabbit IgG	1° 1/400 0.1% BSA 2° 1/1000 0.1% BSA	53 kDa
Bax	Rabbit	Goat anti-rabbit IgG	1° 1/200 0.1% BSA 2° 1/2000 0.1% BSA	21 kDa
Cytochrome *c* *	Rabbit	Goat anti-rabbit IgG	1° 1/250 2% Marvel 2° 1/1000 2% Marvel	11.4 kDa
Actin	Mouse	Goat anti-mouse IgG	1° 1/200 0.1% BSA 2° 1/400 0.1% BSA	46 kDa
CB_1	Goat	Donkey anti-goat IgG	1° 1/400 0.1% BSA 2° 1/1500 0.1% BSA	53 kDa
Phosphorylated Bcl-2	Rabbit	Goat anti-rabbit IgG	1° 1/250 0.1% BSA 2° 1/1000 0.1% BSA	24-26 kDa

Table 2.1 Antibodies used for Western blotting. * Antibody dilution in PBS-T

2.8.11 Densitometry

In all cases quantification of protein bands exposed onto photographic film was achieved by densitometric analysis using ZERO-Dscan Image Analysis system (Scanalytics, Fairfax, USA). Values are expressed as arbitrary units. In some cases where actin/expression loading controls were not equal, expression of the target protein was normalised to total actin/expression in the same sample.

2.9 Immunocytochemistry

2.9.1 Anti-active caspase-3 immunocytochemistry

Treated cell cultures and cryostat sections were washed in TBS and fixed with 4% paraformaldehyde (Sigma-Aldrich, Dorset, UK) in TBS (w/v) for 30 min at RT. Fixed cells were permeabilised by incubating in 0.2% Triton X-100 (v/v; Sigma-Aldrich, Dorset, UK). Cells were washed 3 times in TBS and endogenous peroxidases blocked with 0.03% (v/v) hydrogen peroxide (Sigma-Aldrich, Dorset, UK). Cells were again washed with TBS and non-specific staining blocked with blocking buffer (5% goat serum in TBS containing 0.1% Triton X-100; v/v) for 2hr at RT. Cells were then incubated overnight at 4°C with a goat polyclonal anti-active caspase-3 antibody (Promega Corporation, Madison, WI, USA) purified from rabbit serum, diluted 1:200 in blocking buffer. This antibody recognizes the p17 cleaved active form of the protease. The cells were then washed in TBS and incubated with biotinylated anti-goat IgG (diluted 1:50 in blocking buffer; Biosource International Inc, California, USA) for 1hr at RT. Cells were incubated with streptavidin conjugated to HRP (Amersham, UK), diluted 1:50 in TBS, for 40 min at RT. Cells were washed in TBS before detection using the peroxidase substrate H_2O_2 and the stable chromogen diaminobenzidine (DAB, Dako Corporation, Carpinteria, USA) solution (1ml; 958µl DAB, 40µl of saturated Nikel Aluminum Sulphate ($(NH)_4SO_4NiSO_4.6H_2O$) and 2µl of H_2O_2, Sigma-Aldrich, Dorset, UK). Incubation proceeded until cells had taken on a stained appearance (approximately 10 min). Cells were counterstained with Eosin, washed in deionised H_2O, dehydrated through graded alcohols and mounted on slides with DPX mounting medium (a mixture of distyrene (a polystyrene), tricresyl phosphate (plasticiser) and xylene with a refractive index of 1.5; BDH Laboratory Supplies, Dorset, UK). Cells were then viewed under light microscopy (Nikon Labophot, Nikon Instech Co., Ltd, Kanagawa, Japan) at x100 magnification where the caspase-3-positive cells stained dark purple. Cells displaying active caspase-3 immunoreactivity were counted and expressed as a percentage of the total number cells examined (250-350 cells/coverslip).

2.9.2 Poly(ADP-ribose) polymerase (PARP) immunocytochemistry

Cultures treated with THC±AM 251 were fixed in 4% paraformaldehyde (w/v) for 30 min at RT and permeabilised with 0.2% Triton X-100 (v/v) and Proteinase K (0.2%; w/v). Endogenous peroxidases were blocked with 0.03% hydrogen peroxide (v/v) and cells washed repeatedly in TBS. Cultures were then blocked with 5% BSA in TBS (w/v) for 30 min at RT and incubated with an anti-cleavage site specific PARP polyclonal antibody purified from goat serum (1:50 dilution in blocking buffer, 1hr incubation; Biosource International Inc, California, USA) which recognises the cleaved 85kDa PARP fragment. The cells were washed in TBS and immunoreactivity was detected by incubating the cells with biotinylated anti-goat IgG secondary antibody (1:50 dilution in blocking buffer, 1hr; Biosource International Inc, California, USA) and streptavidin conjugated to HRP (1:50 dilution in TBS, 40 min incubation at RT; Amersham, Buckinghamshire, UK). Immunoreactive cells were visualised after incubation using the DAB solution (1ml; 958µl DAB, 40µl of saturated Nikel Aluminum Sulphate ($(NH)_4SO_4NiSO_4.6H_2O$) and 2µl of H_2O_2, Sigma-Aldrich, Dorset, UK) for 10 min, washed several times in dH_2O and mounted onto microscope slides with DPX medium (BDH Laboratory Supplies, Dorset, UK). Cells were then viewed under light microscopy at x100 magnification (Nikon Labophot, Nikon Instech Co., Ltd, Kanagawa, Japan), where cleaved PARP immunoreactive cells stained dark purple. Cells with cleaved PARP were counted and expressed as a percentage of the total number of cells examined (250-350 cells/coverslip).

2.10 Fluorescence immunocytochemistry

2.10.1 Phospho-JNK fluorescence immunocytochemistry

Treated cell cultures or cryostat sections of brain were fixed with 4% paraformaldehyde in TBS (w/v) for 30 min at RT. Fixed cells were permeabilised by incubating in 0.2% Triton X-100 (v/v) and Proteinase K (0.2%; w/v). Cells were washed in TBS and non-reactive sites blocked with blocking buffer (5% goat

serum in TBS; v/v) for 2hr at RT. To determine the intracellular distribution of active-JNK (phosphorylated JNK), cells were incubated overnight at 4°C with a mouse polyclonal anti-phospho-specific JNK antibody (Santa Cruz Biotechnology Inc, Santa Cruz, CA, USA) that recognizes JNK1 and JNK2 isoforms phosphorylated on Thr-183 and Tyr-185 (1:500 dilution in TBS containing 2.5% goat serum; v/v). The cells were then washed in TBS and incubated in the dark with goat anti-mouse IgG conjugated to flourescein isothiocyanate (FITC) (diluted 1:100 in 2.5% goat serum in TBS (v/v); Sigma-Aldrich, Dorset, UK) for 1hr at 37°C. Cells were washed several times in dH_2O before mounting on microscope slides using a mounting medium for fluorescence (Vector Laboratories Inc., California, USA). The perimeter of each coverslip/slide was then sealed using nail varnish. Care was taken to minimise exposure of cells to light in order to prevent the fluorescent tag from bleaching. Mounted coverslips/cryostats were viewed under x40 magnification by fluorescence microscopy (Leitz Orthoplan Microscope, Leica Microsystems AG, Wetzlar, Germany) using Improvision software (Improvision, Coventry, UK). Cells were observed under excitation, 490 nm; emission, 520 nm for FITC labelled antibodies.

2.10.2 Bax fluorescence immunocytochemistry

Treated cultures were fixed with 4% paraformaldehyde in TBS (w/v) for 30 min at RT. Fixed cells were permeabilised by incubating in 0.2% Triton X-100 (v/v). Cells were washed in TBS and non-reactive sites blocked with blocking buffer (5% goat serum in TBS; v/v) for 2hr at RT. Cells were incubated overnight with a monoclonal primary antibody raised against amino acids 1-171 of Bax of mouse origin (1:50 dilution in TBS containing 10% blocking buffer (v/v); Santa Cruz Biotechnology Inc, Santa Cruz, CA, USA). The cells were then washed in TBS and incubated in the dark with biotinylated horse anti-mouse IgG (1:50 in 10% blocking buffer (v/v); Vector Laboratories Inc., CA, USA) for 1hr at RT. Coverslips were then washed with TBS and incubated with extra-avidin-conjugated FITC (diluted 1:50 in 2.5% goat serum in TBS (v/v); Sigma-Aldrich, Dorset, UK) for 40 min at RT. Coverslips were washed several times in dH_2O to

remove unbound FITC before mounting on microscope slides using a mounting medium for fluorescence (Vector Laboratories Inc., California, USA). The perimeter of each coverslip was then sealed using nail varnish. Care was taken to minimise exposure of cells to light in order to prevent the fluorescent tag from bleaching. Mounted coverslips were viewed under x40 magnification by fluorescence microscopy (Leitz Orthoplan Microscope, Leica Microsystems AG, Wetzlar, Germany) using Improvision software (Improvision, Coventry, UK). Cells were observed under excitation, 490 nm; emission, 520 nm for FITC labelled antibodies.

2.11 Evaluation of neuronal viability

2.11.1 Terminal deoxinucleotidyltransferase-mediated biotinylated UTP nick end labeling (TUNEL)

Apoptotic cell death was determined in cell cultures and cryostat brain sections by monitoring DNA fragmentation using TUNEL staining according to manufacturers instructions (DeadEnd Colorimetric Apoptosis Detection System; Promega Corporation, Madison, WI, USA). Following treatment cells were washed in TBS and fixed with paraformaldehyde (4%; w/v) for 30 min at RT. Cells were permeabilised with Triton-X100 (0.2%; v/v) and Proteinase K (0.2%; w/v). Cells were then refixed in 4% paraformaldehyde (w/v) for 10 min and incubated in equilibration buffer (200mM potassium cacodylate (pH 6.6 at 25°C), 25mM Tris-HCl (pH 6.6 at 25°C), 0.2mM DTT, 0.25mg/ml BSA, 2.5mM cobalt chloride) for 10 min. A Reaction buffer (100µl; 1µl biotinylated nucleotide mix (25µM biotinylated nucleotide mix, 10mM Tris-HCl, pH7.6, 1mM EDTA), 1µl Terminal deoxynucleotidyl Transferase (TdT) enzyme and 98µl equilibration buffer, Promega Corporation, Madison, USA) was applied for 60 min at 37°C to incorporate biotinylated nucleotide at the 3′-OH DNA ends of fragmented DNA. Endogenous peroxidases were blocked using 0.3% H_2O_2 (v/v) and HRP-labelled

streptavidin was bound to the biotinylated nucleotides (1:100 dilution in TBS for 1hr at RT). Apoptotic cells (TUNEL positive) were detected using the DAB (DAKO Corporation, Carpinteria, CA, USA) solution (1ml; 958μl DAB, 40μl of saturated Nikel Aluminum Sulphate ($(NH)_4SO_4NiSO_4.6H_2O$) and 2μl of H_2O_2, Sigma-Aldrich, Dorset, UK). This solution stains the apoptotic nuclei of TUNEL positive cells dark brown after approximately 10 min. The cells were washed in dH_2O and dehydrated through graded alcohols. After mounting coverslips/cryostats on slides with DPX mounting medium (BDH Laboratory Supplies, Dorset, UK) the neurons were viewed under light microscopy (Nikon Labophot, Nikon Instech Co., Ltd, Kanagawa, Japan) at x100 magnification. Cells displaying apoptotic nuclei were counted and expressed as a percentage of the total number of cells examined (400-500 cells/coverslip).

2.11.2 DNA fragmentation using agarose gel electrophoresis

Following treatment, cortical slices and cortical cell cultures were lysed. To determine if DNA fragmentation was occurring, slices were centrifuged in lysis buffer (500μl; 10mM Tris-HCl, 5mM EDTA, 100mM NaCl, 0.5% SDS, pH 8) at 200 x *g* for 10 min at 4°C. Lysis buffer was removed and replaced with ice-cold sterile PBS (1ml) and centrifuged at 200 x *g* for 10 min at 4°C. PBS was removed and the pellet homogenised (x10 strokes) on ice in lysis buffer (500μl) containing Proteinase K (100μg/ml) using a 1ml glass homogeniser (Jencons, Bedfordshire, UK). Samples were left overnight at 50°C. Following treatment, cultured cells were washed in ice-cold PBS before harvesting on ice by scraping coverslips in lysis buffer (75μl/well). Samples were centrifuged at 1, 500 x *g* for 8 min at 4°C and the pellet homogenised in lysis buffer (500μl) containing Proteinase K (100μg/ml) using a 1ml glass homogeniser (Jencons, Bedfordshire, UK) and left overnight at 50°C. The fragmented DNA was extracted using phenol and chloroform (Sigma-Aldrich, Dorset, UK), and centrifuged at 13, 000 x *g* for 5 min at 4°C. The aqueous phase was transferred into a new microfuge tube, and incubated with isopropanol and NaCl (500mM) overnight at -20°C to precipitate DNA. After centrifugation at 14, 000 x *g* for 30 min at 4°C, the supernatant was removed, the DNA pellet was

washed with 70% EtOH (Sigma-Aldrich, Dorset, UK) and centrifuged at 15, 000 x *g* for 20 min at 4°C. The supernatant was removed and the pellet allowed to air dry for 30 min. The DNA pellet was dissolved in 25μl Tris-EDTA (TE) buffer (10mM Tris-HCl, pH 8.0, and 5mM EDTA) containing Ribonuclease A (50μg/ml; Sigma-Aldrich, Dorset, UK) at 37°C for 1hr. Equal volumes of DNA samples (20μl) were prepared for electrophoresis on a 1.5% (w/v) agarose gel by mixing with 6x gel loading buffer (4μl; 60% glycerol (v/v), 0.4% bromophenol blue (w/v)). The gel was prepared by boiling the appropriate quantity of agarose (Promega Corporation, Madison, USA) in 100ml of 1x tris borate EDTA (TBE) buffer (0.08M Tris Base; 0.04M boric acid; 1mM EDTA; pH 8). Ethidium Bromide (EtBr; Sigma-Aldrich, Dorset, UK) was added to give a final concentration of 0.5μg/ml and the gel cast into the horizontal gel system and allowed to set. Samples were heated to 65°C for 10 min, loaded (10μl) into the wells and the gel electrophoresed at 70V for 2hr. Migration of the bromophenol blue was monitored and the voltage was switched off when the blue dye band reached the bottom of the gel. The DNA was visualized under UV light and photographed using a UV transluminator (Chromato-vue, model TL-33, UVP INC, California, USA). The lengths of the DNA fragments were compared to a 100bp DNA ladder (Promega Corporation, Madison, WI, USA).

2.12 Measurement of caspase-3 activity using biochemical assay

Cleavage of the fluorogenic caspase-3 substrate (Ac-DEVD-7-amino-4-trifluoromethylcoumarin peptide (AFC); Alexis Corporation, Nottingham, UK) to its fluorescent product was used as a measure of caspase-3 activity. Following treatment cell cultures/cortical slices were homogenised in lysis buffer (25mM HEPES, 5mM $MgCl_2$, 5mM dithiothreitol, 5mM EDTA, 2mM PMSF, 10μg/ml leupeptin, 10μg/ml pepstatin, 10μg/ml aprotinin, pH 7.4) on ice. Samples (50μl) were incubated with the DEVD peptide (10μM; 4μl) or incubation buffer (50μl;

50mM HEPES, 10mM dithiothreitol, 20% glycerol (v/v), pH 7.4) for 1hr at 37°C and the fluorescence assessed (excitation, 400nm; emission, 505nm) using a Fluoroscan Ascent FL platereader (MSC Medical Supply Co. Ltd, UK).

2.13 Antisense treatments

2.13.1 Cellular antisense oligonucleotide uptake

To monitor the uptake pattern of antisense oligonucleotides (AS), cell cultures were maintained in supplemented media in the presence of FITC-labelled control oligonucleotides (2μM; Biognostik, Gottingen, Germany) for several different timepoints ranging from 1-24hr. Coverslips were washed several times in dH_2O to remove unbound FITC before mounting on microscope slides using a mounting medium for fluorescence (Vector Laboratories Inc., California, USA). The perimeter of each coverslip was then sealed using nail varnish and care was taken to minimise exposure of cells to light in order to prevent the fluorescent tag from bleaching. Mounted coverslips were viewed under x40 magnification by fluorescence microscopy (Leitz Orthoplan Microscope, Leica Microsystems AG, Wetzlar, Germany) using Improvision software (Improvision, Coventry, UK). Cells were observed under excitation, 490 nm; emission, 520 nm for FITC labelled antibodies.

2.13.2 JNK antisense oligonucleotides

To evoke a transient downregulation in expression of JNK1 or JNK2 an antisense approach was used. JNK AS and scrambled control (SC) phosphorothioated oligonucleotides were synthesized by Biognostik (Gottingen, Germany). These oligonucleotides contain sulphur in the internucleotide phosphate linkages of the DNA backbone, which increases resistance to exo and endonucleases present in serum and intracellularly respectively. The sequences used were according to previously published work (Hreniuk *et al.*, 2001) and are complementary to the mRNA encoding rat JNK1 and JNK2 protein: JNK1

antisense (AS1), 5′-CTCATGATGGCAAGCAATTA-3′; JNK1 scrambled control (SC1), 5′-ACTACTACACTAGACTAC-3′; JNK2 antisense (AS2), 5′-GCTCAGTGGACATGGATGAG-3′ and JNK2 scrambled control (SC2), 5′-GGACTACTACACTAGACTAC-3′. Antisense oligonucleotides were made up as a 100μM stock solution in a provided antisense dilution buffer (Biognostik, Gottingen, Germany). Neurons were maintained in supplemented media in the presence of the oligonucleotides for 48hr prior to treatment with THC. N-[1-(2,3-dioleoylooxy)propyl]-N,N,N-trimethylammonium / dioleotlphosphatidylethanolamine (DOTMA/DOPE 5μg/ml; Life Technologies, Paisley, UK) was incorporated into serum-free media for the first 4hr of oligonucleotide treatment to ensure sufficient oligonucleotide uptake. Downregulation of JNK1 and JNK2 protein expression was achieved by using AS1 and AS2 at a final concentration of 2μM.

2.14 Isolation of RNA

2.14.1 Precautions

For RNA analysis certain precautions were taken since ubiquitous RNAse enzymes easily degrade RNA. RNase enzymes are resistant to autoclaving but can be inactivated by diethylpyrocarbonate (DEPC; 0.1% (v/v) Sigma-Aldrich, Dorset, UK). Hence, all solutions used for RNA work were treated with DEPC. Solutions containing amines, such as Tris, cannot be DEPC-treated directly as DEPC is inactivated by such chemicals. These solutions were prepared in DEPC-treated water. Gloves and disposable sterile plastics were used at all times and any glassware used was baked overnight at 200°C. Following the extraction procedure, manipulations with RNA were carried out quickly on ice to prevent degradation of RNA by endogenous RNAses.

2.14.2 RNA extraction from cultured cortical neurons

Total RNA was isolated from cultured cortical cells using TRI reagent (Sigma-Aldrich, Dorset, UK). This is a modified version of the single step method of acid guanidine thiocyanate-phenol-chloroform extraction (Chomczynski and Sacchi, 1987). Cultured neurons were rinsed with DEPC-treated PBS and lysed directly in 24-well culture plates by adding 50μl reagent/well and scraping coverslips using the rubber end of a 1ml syringe piston (B.Braun Medical Ltd., Melsungen, Germany). Cells were incubated for 5 min at RT to permit the complete dissociation of nucleoprotein complexes. Phase separation was achieved by adding 0.2ml of chloroform reagent (Sigma-Aldrich, Dorset, UK) per 1ml of TRI reagent. Samples were mixed by inversion and incubated at RT for 2-15 minutes. The resulting mixture was centrifuged at 12, 000 x *g* for 15 min. Following centrifugation the mixture separates into a lower red, phenol-chloroform phase, an interphase, and a colour-less upper aqueous phase. RNA remains exclusively in the upper phase while DNA and proteins partition to the interphase and lower organic phase. The aqueous phase was transferred to a fresh microfuge tube. RNA was precipitated by adding 0.5ml of isopropanol (Sigma-Aldrich, Dorset, UK) per 1ml of reagent used. Samples were incubated at RT for 10 min then centrifuged at 12, 000 x *g* for 20 min. RNA pellets were then washed once with 75% EtOH (Sigma-Aldrich, Dorset, UK), allowed to air dry for 30 min and dissolved in sterile DEPC treated water. RNA samples were stored at -80°C until required for use.

2.14.3 Analysis of isolated RNA by Gel Electrophoresis

To check that isolated RNA was intact, samples were run on a 1% (w/v) agarose gel. The gel was prepared by boiling the appropriate quantity of agarose (Promega Corporation, Madison, USA) in 100ml of 1x tris borate EDTA (TBE) buffer (0.08M Tris; 0.04M boric acid; 1mM EDTA; pH 8.3). EtBr (Sigma-Aldrich, Dorset, UK) was added to give a final concentration of 0.5μg/ml and the gel cast into the horizontal gel system and allowed to set. RNA samples (1.5μl) were prepared for electrophoresis by mixing with H_2O (3.5μl) and of 6x gel loading

buffer (1μl; 60% glycerol (v/v), 0.4% bromophenol blue (w/v)). Samples (6μl) were loaded into the wells and RNA was separated by application of a 90V voltage to the gel apparatus. Migration of the bromophenol blue was monitored and the voltage was switched off when the blue dye band reached the bottom of the gel. The gel was visualized under UV light and photographed using a UV transluminator (Chromato-vue, model TL-33, UVP INC, California, USA).

2.14.4 DNAse 1 treatment of RNA

Contaminating DNA was removed from RNA preparations using Deoxyribonuclease 1 (DNAse 1; Invitrogen, Paisley, UK). DNAse 1 digests single and double-stranded DNA to oligonucleotides. RNA sample (1.5μg) was incubated for 15 min at RT with DNAse 1 (1.5μl; 1U/ml) and 10x DNAse 1 (1μl) reaction buffer. EDTA (1μl; 25mM) solution was added to the reaction mixture in order to inactivate the DNAse and the tube contents incubated at 65°C for 10 min.

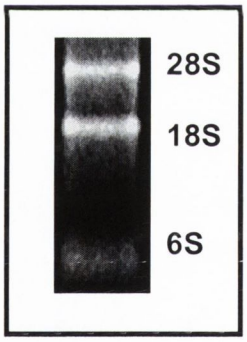

Figure 2.2: Sample photo of total rat RNA.
An intact preparation of total RNA exhibits distinct ribosomal RNA bands of 28S, 18S and 6S.

2.14.5 Quantitation of RNA

The quantity of RNA was determined spectrophotometrically by measuring the RNA at a wavelength of 260nm. An absorbance value of 1 at this wavelength corresponds to 40μg/ml of RNA.

2.15 Reverse Transcription-Polymerase Chain Reaction (RT-PCR)

Reverse-transcription polymerase chain reaction (RT-PCR) is a powerful technique that allows analysis of small quantities of specific messenger ribonucleic acid (mRNA). Total RNA is converted to complementary DNA (cDNA) using a reverse transcriptase enzyme. Specific cDNA's are then amplified by PCR using appropriate primer sequences. This PCR is semi-quantitative as a constitutively expressed gene (housekeeping gene), β-actin, is amplified in parallel with each PCR reaction. This acts as an internal control and by calculating ratios of the target gene to β-actin, relative amounts of the target gene can be determined.

2.15.1 Reverse Transcription

First strand cDNA synthesis of the mRNA was carried out using Superscript II RNASE H- Reverse-Transcriptase enzyme (Invitrogen, Paisley, UK). Sample RNA (1μg) was mixed with oligo dT Primer (1μl; Invitrogen, Paisley, UK) and dNTP mix (1μl; containing 10mM each of dATP, dTTP, dCTP and dGTP; Promega Corporation, Madison, USA). This mixture was incubated at 65°C for 5 min (to uncoil the RNA) then moved to ice. To this reaction mixture, 5x reaction buffer (4μl), 0.1M dithiothreitol (2μl) and Ribonuclease (RNAse) Inhibitor (1μl; Promega Corporation, Madison, USA) were added and the reaction was preheated to 42°C for 2 min before adding Superscript Reverse-Transcription enzyme (1μl; 200 units). The reaction was incubated at 42°C for 50 min for cDNA synthesis and then at 75°C for 10 min to inactivate the reverse transcriptase.

2.15.2 Polymerase Chain Reaction

A mastermix PCR reaction (final volume 25μl) was made up containing 2.5μl of 10x reaction buffer, 2.5-3μl (2.5-3mM) magnesium chloride ($MgCl_2$), 1μl dNTP mix (Promega Corporation, Madison, USA), 1μl of each of the upstream and downstream primers (40 pmoles; MWG Biotech, Ebersberg, Germany), 12.5-13μl

sterile H_2O and 0.5μl (5 units) Taq polymerase enzyme (Promega Corporation, Madison, USA). 2.5μl of sample cDNA was added to this mastermix. The reaction contents were then overlaid with mineral oil (Sigma-Aldrich, Dorset, UK; to prevent evaporation of the reaction contents) and placed in the thermocycler (Biometra GmbH, Gottingen, Germany). The PCR was run with an initial denaturing step of 95°C followed by 25-35 cycles consisting of a denaturing step of 95°C for 1 min, an annealing step of 50-55°C (see table 2.1 for optimal annealing temperature) for 1 min and an extension step of 72°C for 1 min 30 seconds. A final extension step of 72°C for 10 min was carried out to ensure complete extension of the PCR products. The PCR products (5μl) were loaded into the wells and separated on a 1.5% (w/v) agarose gel containing Etbr (0.5μg/ml) and visualized under UV light using a UV transilluminator (Chromato-vue, model TL-33, UVP INC, California, USA). In all cases a DNA 100bp ladder (Promega Corporation, Madison, WI, USA) was also loaded to determine the size of DNA bands.

2.15.3 Densitometry

In all cases quantification of PCR bands was achieved by densitometric analysis using the Zero-Dscan Image Analysis System (Scanalytics Inc., Fairfax, USA). Values are expressed as arbitrary units.

Target Gene	Primer Sequence	Annealing Temperature (°C)	Fragment Size (Base-Pairs)
p53	Fw: 5′ GGCCATCTACAAGAAGTCAC 3′ Rv: 5′ CCAGAAGATTCCCACTGGAG 3′	53	317bp
β-actin*	Fw: 5′ GAAATCGTGCGTGACATTAAAGAGAAGCT 3′ Rv: 5′ TCAGGAGGAGCAATGATCTTGA 3′	52	360bp
Bax**	Fw: 5′ GCAGAGAGGATGGCTGGGGAGA 3′ Rv: 5′ TCCAGACAAGCAGCCGCTCACG 3′	52	352bp

Table 2.2 Primer pairs used for PCR.

* Primers from Nakajima-Iijima *et al.*, 1985

** Primers from Ray *et al.*, 2000

2.16 Statistical analysis

Data are expressed as means ± standard error of the means (SEM) of the number of experiments indicated in every case. Statistical analysis was performed by use of a Student's *t* test or one-way analysis of variance (ANOVA). When the statistical test indicated significance (i.e. where $p<0.05$), *post hoc* student Neumann-Keuls test analysis was used to determine which conditions were significantly different from each other. All statistical analysis was carried out using Instat 2.03 software.

Chapter 3

THC induces apoptosis in cultured cortical neurons via the cytochrome c/caspase-3 cell death pathway

3.1 Introduction

The use of marijuana by humans can induce behavioural deficits characterised by cognitive and memory impairments (Block and Ghoeim, 1993). In particular, heavy abusers of marijuana display deficits on tasks dependent on cortical cognitive functions, particularly working memory (Jentsch *et al.*, 1998). Despite these findings, the precise molecular mechanisms for these affects have not been fully elucidated. It is accepted that in contrast to many other cell types, neurons possess a very limited capacity for self-renewal and repair (Raffay and Cohen, 1997). Consequently, cell death in the nervous system can result in neuronal dysfunction or very significantly reduced functional reserves. Hence, the possibility that the proclivity of THC to induce the degeneration of cultured cortical neurons contributing to some of the behavioural deficits accompanying marijuana use is a pertinent issue.

The effects of THC and other cannabinoids on the brain are exerted through the central CB_1 cannabinoid receptor, a receptor distributed mainly in the CNS and displaying an intense pattern of expression in the rat cortex, particularly in frontal regions where the CB_1 receptor subtype is found in cortical axons, cell bodies and dendrites (Tsou *et al.*, 1998). The CB_1 receptor is responsible for mediating the central effects of THC. Indeed CB_1 is more responsive to psychoactive cannabinoids than to non-psychoactive cannabinoids (Matsuda *et al.*, 1990) and is localised in brain regions most likely involved in the psychoactive effects of THC (Twitchell *et al.*, 1997).

Apoptosis is distinguished by specific DNA cleavage into oligonucleosomal fragments, features atypical of the processes associated with necrotic cell death (Lee *et al.*, 1993). Furthermore, apoptosis is an active process with organised and regulated biochemical events (Raffay and Cohen, 1997). Recently cannabinoids have been shown to control the cell survival/death decision (Guzmán *et al.*, 2002). Indeed, there has been growing evidence suggesting a role for THC in the regulation of neuronal viability. Indeed, THC promotes degeneration of cultured hippocampal neurons (Chan *et al.*, 1998), hippocampal neurons *in vivo* (Scallet *et al.*, 1987), cultured C6 glioma cells (Sánchez *et al.*, 1998; Jacobsson *et al.*, 2000), glioma cell growth

in vivo (Galve-Roperh *et al.*, 2000) and immune cells *in vitro* (Zhu *et al.*, 1998) and *in vivo* (McKallip *et al.*, 2002b). Some of the proposed intracellular mechanisms accounting for the apoptotic effects of THC in these systems have included the generation of free radicals by cyclooxygenase, sustained ceramide accumulation and caspase-1 activation. Furthermore, there is evidence that endogenous cannabinoid anandamide induces apoptosis in cultured neuroblastomas (Maccarrone *et al.*, 2000), PC12 cells (Sarker *et al.*, 2003) and lymphocytes (Schwarz *et al.*, 1994) and causes damage to neurons in neonatal rats *in vivo* (Szöke *et al.*, 2002).

Apoptotic events are typically accompanied by the activation of caspase-3, an extensively studied cysteine protease that has been shown to be of importance in the induction of apoptosis (Janicke *et al.*, 1998). Caspase-3 is normally held in check as a 32kDa inactive precursor in the cytosolic fraction of mammalian cells (Nicholson *et al.*, 1995), requiring aspartate motif cleavage for activation, producing a 17kDa and a 12kDa active heterodimer when the cell is signalled to die (Janicke *et al.*, 1998). Once activated, caspase-3 is capable of autocatalysis as well as cleaving and activating other members of the caspase family (Zou *et al.*, 1997). The consequences of these cleavage events are now emerging and suggest that they are responsible for many of the phenotypic changes that occur during neuronal apoptosis.

Under normal physiological conditions, the electron transport protein cytochrome *c* is located between the inner and outer mitochondrial membranes where it participates in the production of ATP (Reed, 1997). A common event in the regulation of the caspase-3 cascade involves the translocation of mitochondrial cytochrome *c* across the outer mitochondrial membrane into the cytosol (Rosse *et al.*, 1998). Once released from mitochondria, cytochrome *c* complexes with a cytosolic factor, APAF-1, inducing conformational changes that in turn trigger the activation of caspase-3 and the resultant apoptotic cascade (Zou *et al.*, 1997).

The DNA repair enzyme PARP is selectively activated by DNA strand breaks to participate in DNA repair (Pieper *et al.*, 1999). PARP is proteolytically cleaved by caspase-3 at the onset of apoptosis (Kaufmann *et al.*, 1993). This apoptosis-associated cleavage of PARP removes the amino-terminal domain of the protein to yield an 89kDa fragment that still retains basal catalytic activity

but lacks the DNA binding domain (Nicholson *et al.*, 1995). Hence a consequence of PARP inactivation would be sustained DNA strand breakage.

The aim of this chapter was to assess the effect of THC on the viability of cultured cortical neurons and to characterise the signal transduction pathways that underlie THC-induced neurotoxicity in this cultured cell system. Given that the CB_1 cannabinoid receptor has been shown to be responsible for mediating the central effects of THC, the role of this receptor in THC-induced cell death in primary cultures of cortical neurons was assessed using a selective CB_1 receptor antagonist, AM 251. The ability of THC, acting through the CB_1 receptor, to impact on the cytochrome *c*/caspase-3 system was evaluated. Furthermore, the contribution of PARP cleavage, presumably as a downstream consequence of caspase-3 activation, to this apoptotic pathway was also assessed.

3.2 Results

3.2.1 THC induces DNA fragmentation in cultured cortical neurons

To determine whether THC is neurotoxic to neurons we assessed its ability to induce DNA fragmentation in cultured rat cortical neurons. DNA cleavage into oligonucleosomal fragments is a distinguishing feature of apoptosis (Lee *et al.*, 1993) that can readily be detected using the colorimetric TUNEL system. Neurons were exposed to THC (5μM) for various time points ranging from 5-360 min, cells were fixed and analysed for levels of DNA fragmentation using TUNEL (Figure 3.1). In untreated neurons, 9.2 ± 2.1% (mean ± SEM) of cells displayed fragmented DNA in the nucleus (TUNEL positive) and this was unaffected by THC exposure for 5 min (9.2 ± 3.1%) and 15 min (15.6 ± 1.5%). However, this was significantly increased to 33.2 ± 5.2% ($p<0.05$, ANOVA, n=5 observations), 34.4 ± 8.6% ($p<0.05$, ANOVA, n=5), 57.0 ± 4.8% ($p<0.01$, ANOVA, n=5), 63.3 ± 2.7% ($p<0.01$, ANOVA, n=5) and 67.3 ± 5.3% ($p<0.01$, ANOVA, n=5) in neurons treated with THC for 30, 60, 120, 180 and 360 min respectively. This finding demonstrates that THC induces apoptosis in cultured cortical neurons in a time-dependent manner. Sample TUNEL images displaying the apoptotic effect of THC on cultured cortical neurons at 120 min is shown in Figure 3.1B.

3.2.2 THC induces DNA fragmentation in cultured cortical neurons in a dose-dependent manner

To determine the dose-dependency of THC-induced DNA fragmentation, cultured cortical cells were exposed to THC at a range of concentrations (0.01-10μM) for 2hr, a time point at which a maximal level of DNA fragmentation was observed (Figure 3.1). Figure 3.2 demonstrates that in untreated neurons, 20.2 ± 2.4% (mean ± SEM) of cells were TUNEL positive. The percentage of cells staining TUNEL positive was unaffected by THC exposure at 0.01μM (19.5 ± 4.1%) for 2hr. However, treatment of cells with THC at concentrations of 0.1μM, 1μM, 5μM and 10μM for 2hr significantly increased the percentage of apoptotic cells to 28.7 ± 2.8% ($p<0.05$, ANOVA, n=5 observations), 35.4 ± 4.8% ($p<0.05$, ANOVA, n=5), 49.5 ± 1.9% ($p<0.01$,

ANOVA, n=5) and 55.8 ± 8.0% ($p<0.01$, ANOVA, n=5), respectively. This indicates that THC doses as low as 0.1μM are neurotoxic to cultured neurons.

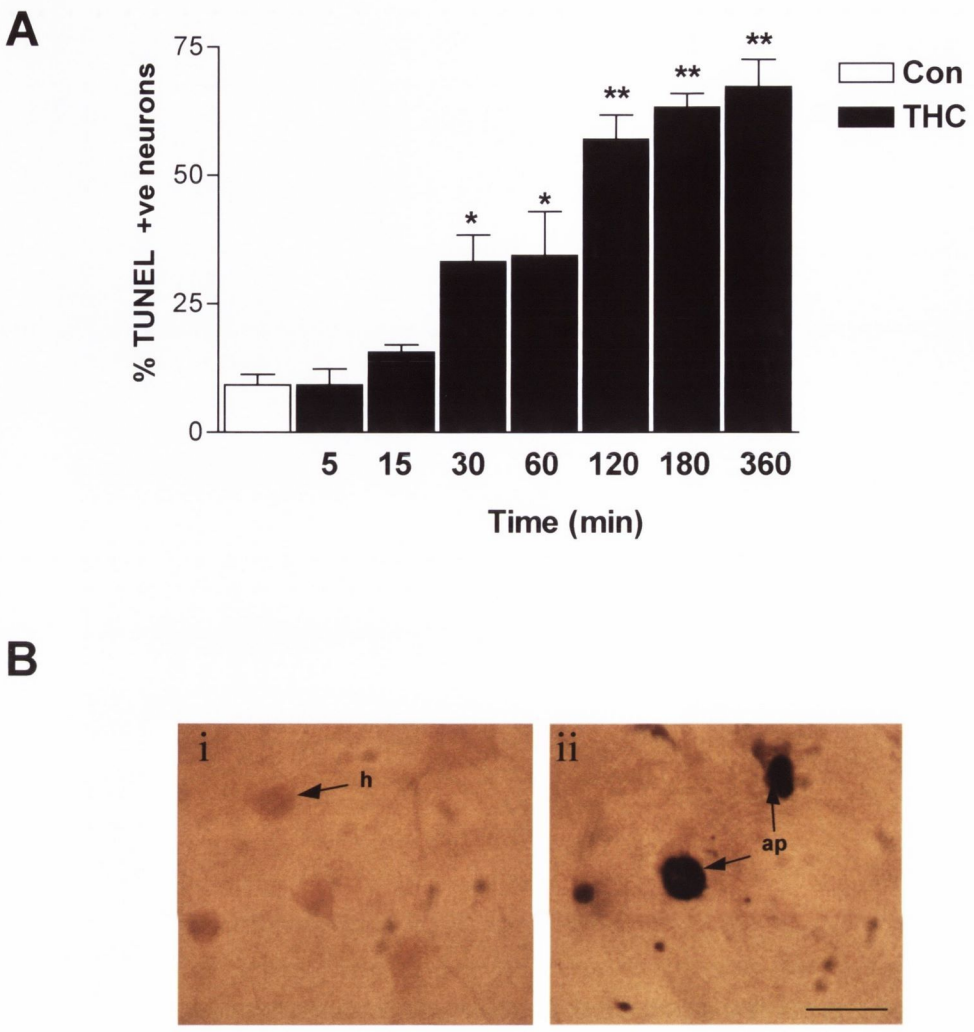

Figure 3.1: THC induces DNA fragmentation in cultured cortical neurons

A: Primary cortical neurons were treated with THC (5μM) for 5-360 min. A significant increase in DNA fragmentation (% TUNEL +ve neurons) was found following treatment with THC for 30, 60, 120, 180 and 360 min. Results are expressed as mean ± SEM for 5 independent observations, **p<0.01, *p<0.05.
B: Light microscopic images of TUNEL staining of (i) vehicle-treated and (ii) neurons treated with THC for 120 min. Arrows indicate representative examples of healthy (h) and apoptotic (ap) neurons. Scale bar is 20μm.

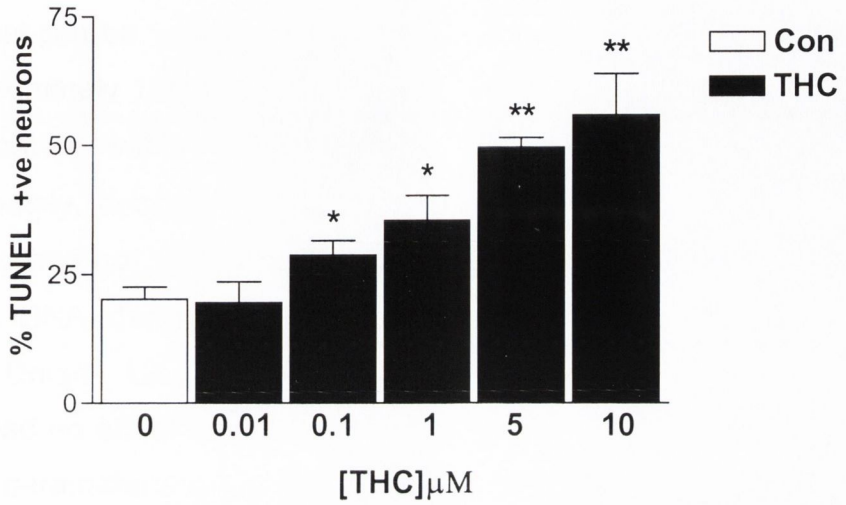

Figure 3.2: Dose-dependency of THC-induced DNA fragmentation in cultured cortical neurons

Primary cortical neurons were treated with THC (0.1-10μM) for 120 min, cells were fixed and analysed for DNA fragmentation using TUNEL. A significant increase in DNA fragmentation (% TUNEL +ve neurons) was found following treatment with THC at concentrations of 0.1μM, 1μM, 5μM and 10μM. Results are expressed as mean ± SEM for 5 observations, **p<0.01, *p<0.05.

3.2.3 Effect of THC on ladder-patterned DNA fragmentation

The role of THC in neuronal cell death was also assessed by agarose gel electrophoresis in cortical cell cultures (Figure 3.3). The formation of distinct DNA fragments of oligonucleosomal size (180-200bp lengths) is a biochemical hallmark of apoptosis (Arends *et al.*, 1990; Spooren and Hengerer, 2000) that can be visualised on a gel as a distinct ladder of bands at multiples of approximately 180 base pairs. DNA fragmentation was assessed in cultured cells treated with THC (5μM) for various time points (30-300 min). Unfortunately, despite the successful extraction of DNA from cultures, DNA laddering was not visualised in cortical cultures treated with THC. It is notable that the DNA damaging agent, etoposide (10μM, 24hr treatment; Sigma-Aldrich, Dorset, UK), despite its known neurotoxic effects (Nakajima *et al.*, 1994), had no effect on DNA fragmentation in cell cultures. This indicates that various parameters within the protocol remain to be optimised. A sample agarose gel demonstrating DNA laddering attempts is shown in Figure 3.3.

3.2.4 THC-induced DNA fragmentation in cultured cortical neurons is mediated by the CB_1 receptor

Due to the lipophilic nature of THC (Di Marzo *et al.*, 1998), some of its effects may be attributable to interactions with membrane lipids rather than as a result of receptor activation. However, treatment of cortical neurons with AM 251 (10μM), a selective high affinity CB_1 receptor antagonist, prevented the THC-induced DNA fragmentation (Figure 3.4) as indicated by the TUNEL method. In cortical neurons treated with THC (5μM) for 2hr the percentage of apoptotic cells was significantly increased from 22.1 ± 1.5% (mean ± SEM) to 49.1 ± 0.8% ($p<0.001$, ANOVA, n=5 observations). While treatment of cells with AM 251 alone had no effect on neuronal viability (22.1 ± 1.5% neurons with fragmented DNA), it prevented the THC-induced increase in DNA fragmentation (25.8 ± 0.7% TUNEL positive neurons). This indicates that in cultured cortical neurons the apoptotic effects of THC are mediated by the CB_1 receptor. Representative images of neurons stained for DNA fragmentation using the TUNEL technique are shown in Figure 3.4B.

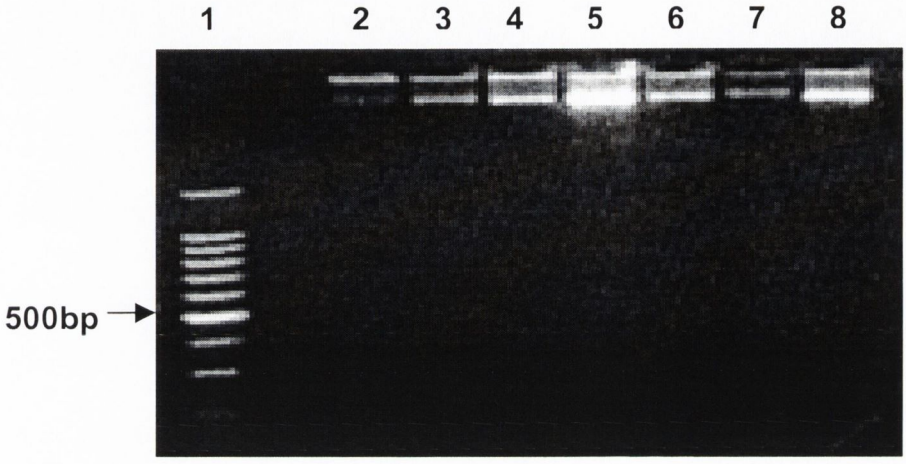

Figure 3.3: Assessment of DNA fragmentation in cell culture using DNA ladder technique

Cultured cortical neurons were treated with THC (5μM) for various times. After incubation, DNA was extracted and elctrophoresed in agarose/EtBr gels. Lane 1, DNA ladder; Lane 2, etoposide (10μM; 24hr treatment); Lane 3, untreated neurons; Lane 4, THC (30 min treatment); Lane 5, THC (1hr treatment); Lane 6, THC (2hr treatment); Lane 7, THC (3hr treatment); Lane 8, THC (5hr treatment). The DNA ladder (lane 1) consists of 11 double stranded DNA fragments with sizes of 100-1500bp. The 500bp fragment is present at triple the intensity of other DNA fragments, serving as a reference indicator. Data represent one of three experiments with similar results.

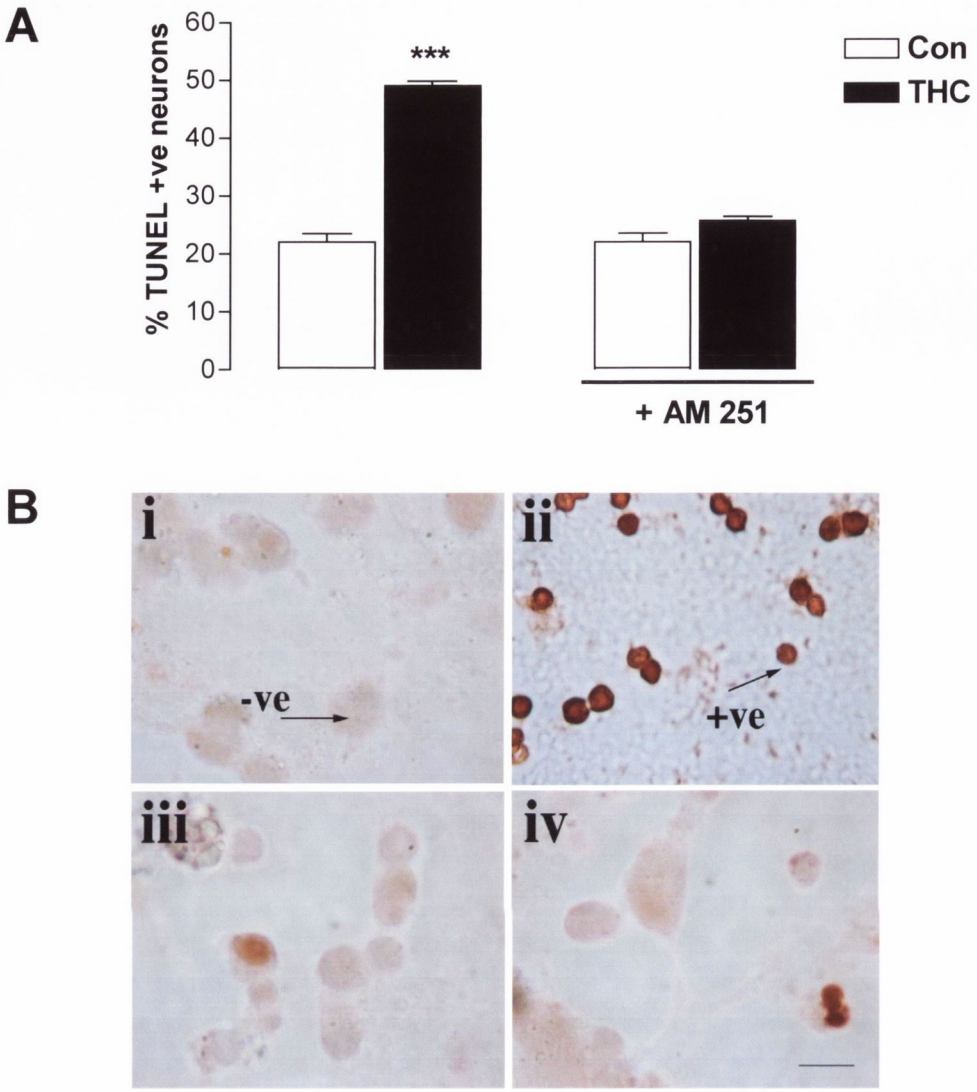

Figure 3.4: AM 251 prevents THC-induced DNA fragmentation

A: Cultured cortical neurons were treated with THC (5μM) in the presence or absence of the CB_1 receptor antagonist AM 251 (10μM) for 2hr. Cell viability was assessed by the TUNEL assay. Neurons were pre-incubated with AM 251 (10μM) for 30 min before treating with THC (5μM). THC significantly increased DNA fragmentation and this was prevented by AM 251. Results are expressed as mean ± SEM for 5 observations, ***$p<0.001$.

B: Light microscopic images of TUNEL staining of (i) vehicle-treated neurons, (ii) THC-treated neurons, (iii) AM 251-treated cultures and (iv) cultures treated with THC in the presence of AM 251. Arrows indicate TUNEL-negative (-ve) and TUNEL-positive (+ve) cells. Scale bar is 25μm.

3.2.5 THC-induced release of mitochondrial cytochrome *c* into the cytoplasm is AM 251-sensitive

A key event in the apoptotic cascade involves the translocation of mitochondrial cytochrome *c* into the cytoplasm (Rosse *et al.*, 1998). Cytochrome *c* release from the mitochondria is a known mechanism of caspase-3 activation (Zou *et al.*, 1997). The ability of THC (5μM) to promote the translocation of mitochondrial cytochrome *c* into the cytoplasm was assessed by western immunoblot on cytosolic samples using an anti-cytochrome *c* antibody in conjunction with densitometric analysis (Figure 3.5). In vehicle-treated cells the mean band width was 2220.9 ± 206.4 arbitrary units (mean ± SEM) and this was significantly increased by treating cortical neuronal cultures with THC to 2867.6 ± 228.2 ($p<0.05$, ANOVA, n=9 observations) for 2hr. Exposure to AM 251 (10μM) had no effect on mean cytochrome *c* expression (2128.5 ± 179.8) and prevented the THC-induced increase in cytochrome *c* (2140.9 ± 182.4). These data indicate that treatment of cortical neurons with THC for 2hr promotes the translocation of cytochrome *c* into the cytoplasm from the mitochondria. Furthermore, this event was blocked by AM 251, implicating the involvement of the CB_1 receptor in the THC-induced release of cytochrome *c*. A sample immunoblot demonstrating the effect of THC on cytochrome *c* release is shown in Figure 3.5B.

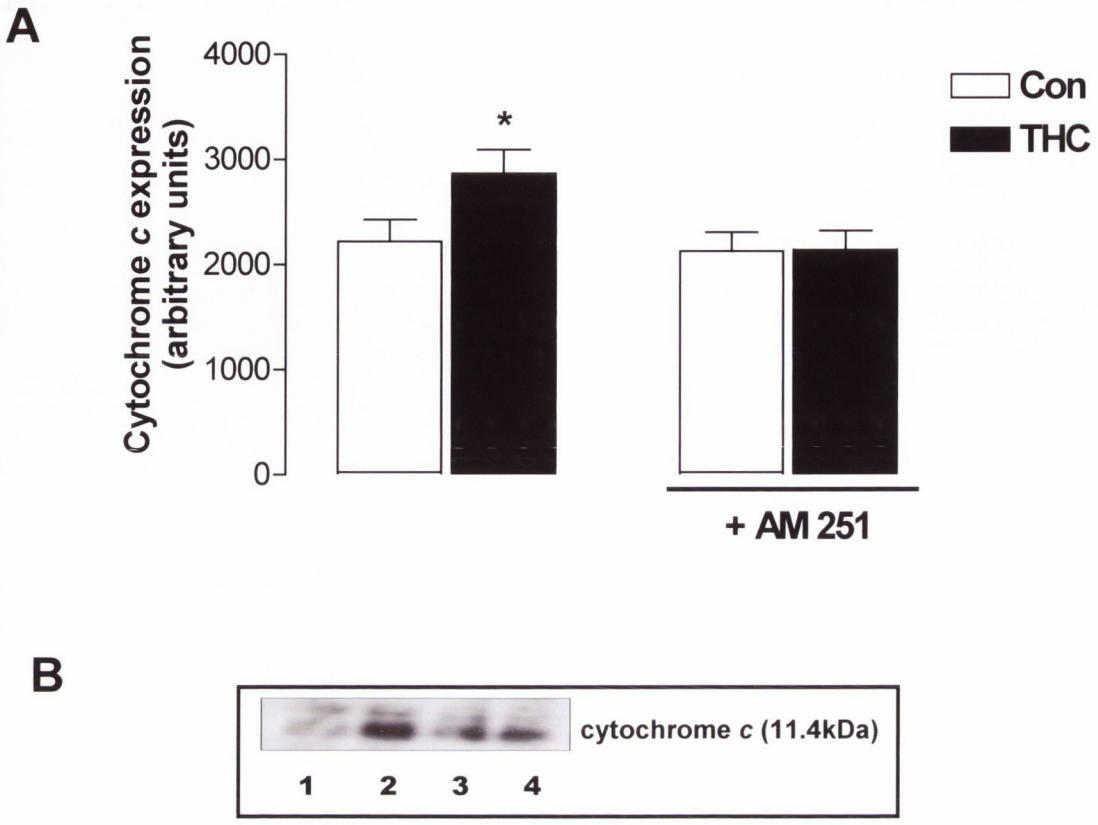

Figure 3.5: THC promotes translocation of cytochrome *c* from the mitochondria to the cytoplasm

A: Cultured cortical neurons were incubated with THC (5μM) ± AM 251 (10μM) for 2hr, cell protein was harvested in lysis buffer and analysed for cytochrome *c* expression using western immunoblotting. THC significantly increased cytochrome *c* expression in the cytoplasm. Although AM 251-treatment had no effect on cytosolic cytochrome *c* expression, it inhibited the THC-induced increase in cytosolic expression of cytochrome *c*. Results are expressed as mean ± SEM for 9 independent observations, *$p<0.05$.

B: A sample western immunoblot demonstrating the increase in cytosolic cytochrome *c* expression in THC-treated cortical neurons (lane 2) at 2hr compared to control cells (lane 1). While AM 251 had no effect on cytosolic cytochrome *c* expression (lane 3) it abolished the ability of THC (5μM) to evoke an increase in cytosolic expression of cytochrome *c* (lane 4).

3.2.6 THC increases caspase-3 activity in a time-dependent manner in cultured cortical neurons

Apoptotic cell death is typically accompanied by the activation of the cysteine protease caspase-3 (Janicke *et al.*, 1998). The ability of THC (5μM) to impact on caspase-3 activation was assessed by monitoring the cleavage of the fluorogenic caspase-3 peptide DEVD to its fluorescent product following THC exposure (Figure 3.6). Since activation of caspase-3 is likely to precede apoptosis the time course of THC-induced activation of caspase-3 was examined by incubating neurons with THC for a range of time points (5-120 min). Caspase-3 activity was 0.09 ± 0.03 pmoles AFC produced/mg protein/min (mean ± SEM) in untreated cells and this was not significantly affected by exposure to THC for 5 min (0.15 ± 0.06 pmoles AFC produced/mg protein/min) or 15 min (0.19 ± 0.05 pmoles AFC produced/mg protein/min). However, exposure of neurons to THC for 30 min significantly increased caspase-3 activity to 0.23 ± 0.06 pmoles AFC produced/mg protein/min ($p<0.05$, ANOVA, n=5 observations) and a 120 min exposure to THC significantly increased caspase-3 activity to 0.25 ± 0.04 pmoles AFC produced/mg protein/min ($p<0.05$, ANOVA, n=5). Hence, THC-induced activation of caspase-3 occurs prior to the morphological features of apoptosis and reaches a maximal level at 2hr of THC exposure.

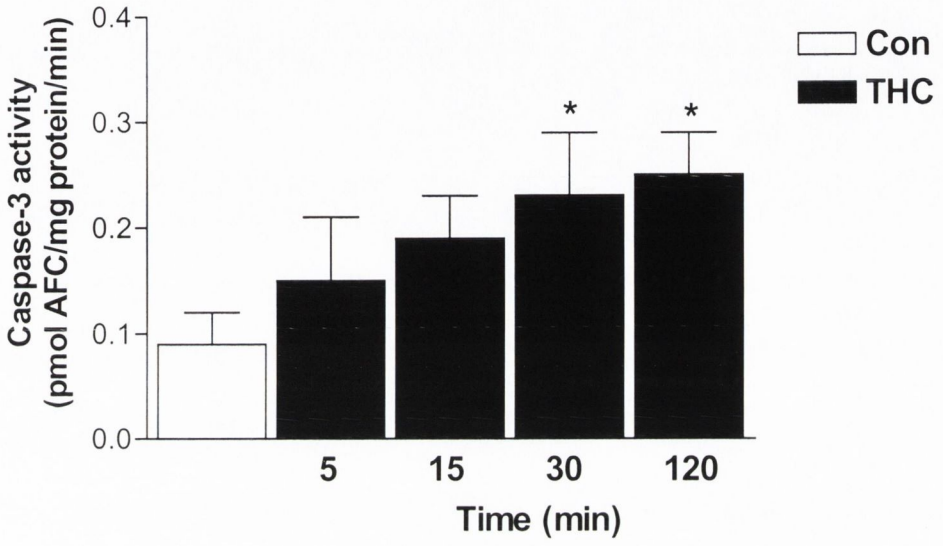

Figure 3.6: THC increases caspase-3 activity in a time-dependent manner in cultured cortical neurons

Cultured cortical neurons were treated with THC (5μM; 2-120 min) and caspase-3 activity as assessed by the cleavage of the fluorogenic DEVD substrate. Treatment of neurons with THC for 30 min and 120 min significantly increased caspase-3 activity compared to vehicle-treated cells. Exposure to THC for shorter time periods did not significantly affect caspase-3 activity. Results are expressed as the mean ± SEM for 5 observations, *$p<0.05$.

3.2.7 THC stimulates an increase in caspase-3 activity in an AM 251-sensitive manner in cultured cortical neurons

Since the apoptotic effects of THC involve the CB_1 cannabinoid receptor (Figure 3.4) the involvement of this receptor in THC-induced caspase-3 activation was determined. The ability of THC (5μM) to impact on caspase-3 activation via CB_1 was assessed by monitoring the cleavage of the fluorogenic caspase-3 peptide DEVD to its fluorescent product (Figure 3.7) and by determining the level of active caspase-3 immunoreactivity in neurons using an anti-active caspase-3 antibody (Figure 3.8). Treatment of neurons with THC for 2hr, a time point at which a maximal increase in caspase-3 activity was observed, significantly increased caspase-3 activity as reported in Figure 3.7. Caspase-3 activity was 21.1 ± 2.2 pmoles AFC produced/mg protein/min (mean ± SEM) in vehicle-treated cells and this was significantly increased to 47.1 ± 5.9 pmoles AFC produced/mg protein/min in cells treated with THC for 2hr ($p<0.05$, ANOVA, n=4 observations). To test the specificity of the central CB_1 cannabinoid receptor involvement in THC-induced caspase-3 activation, cell cultures were pre-treated with AM 251 (10μM) prior to THC exposure and caspase-3 activity assessed. In the presence of AM 251, THC failed to increase caspase-3 activity (15.7 ± 4.8 pmoles AFC produced/mg protein/min). Furthermore, neurons treated with AM 251 alone showed a level of caspase-3 activity comparable to that measured in control cells (15.9 ± 7.7 pmoles AFC produced/mg protein/min).

The pivotal role of caspase-3 in THC signal transduction was also assessed by immunocytochemistry in fixed cell cultures (Figure 3.8). Exposure of cultured cortical neurons to THC (5μM) for 2hr produced a significant increase in the percentage of cells displaying active caspase-3 immunoreactivity as determined using an anti-active caspase-3 antibody. In cells treated with vehicle alone, 11.3 ± 2.2% (mean ± SEM) of cells showed evidence of active caspase-3 immunoreactivity. Addition of THC to cortical neurons for 2hr produced a significant increase in the percentage of neurons stained positive for the active form of caspase-3 (34.6 ± 3.9%, $p<0.01$, ANOVA, n=7 observations). Although exposure of neurons to the CB_1 receptor antagonist AM 251 (10μM) alone had no effect on the percentage of cells

displaying active caspase-3 immunoreactivity (14.5 ± 2.7%), it prevented the THC-induced increase in caspase-3 activity (14.9 ± 2.8%). Representative images of neurons treated with THC in the absence or presence of AM 251 and stained for caspase-3 activity using an anti-active caspase-3 antibody are shown in Figure 3.8B.

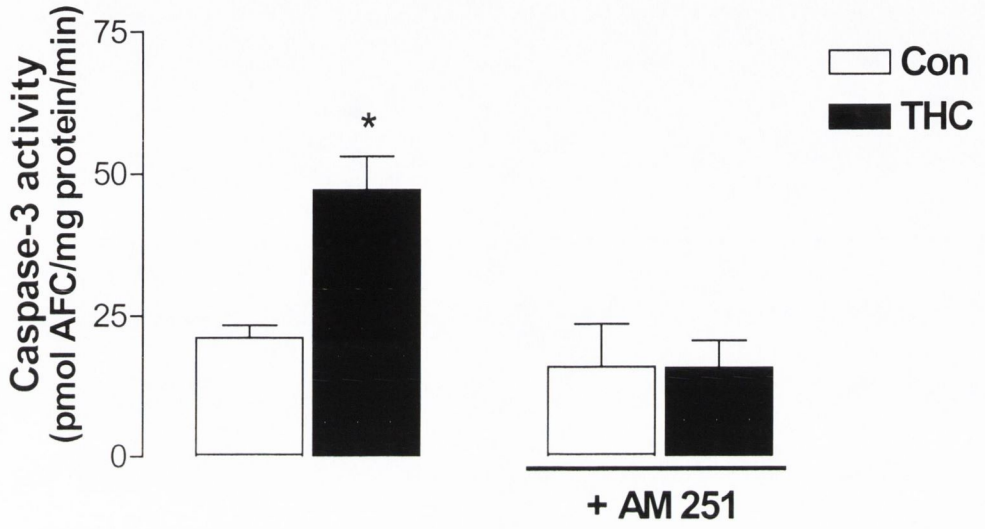

Figure 3.7: THC increases caspase-3 via CB_1 in cultured cortical neurons

Treatment of primary cortical neurons with THC (5μM) for 2hr significantly increased caspase-3 activity as assessed by the cleavage of the fluorogenic DEVD substrate. The stimulatory effect of THC on caspase-3 activity was prevented by AM 251 (10μM), indicating the involvement of the CB_1 cannabinoid receptor. Exposure of cells to the CB_1 inhibitor alone had no effect on caspase-3 activity. Results are expressed as the mean ± SEM for 4 observations, *$p<0.05$.

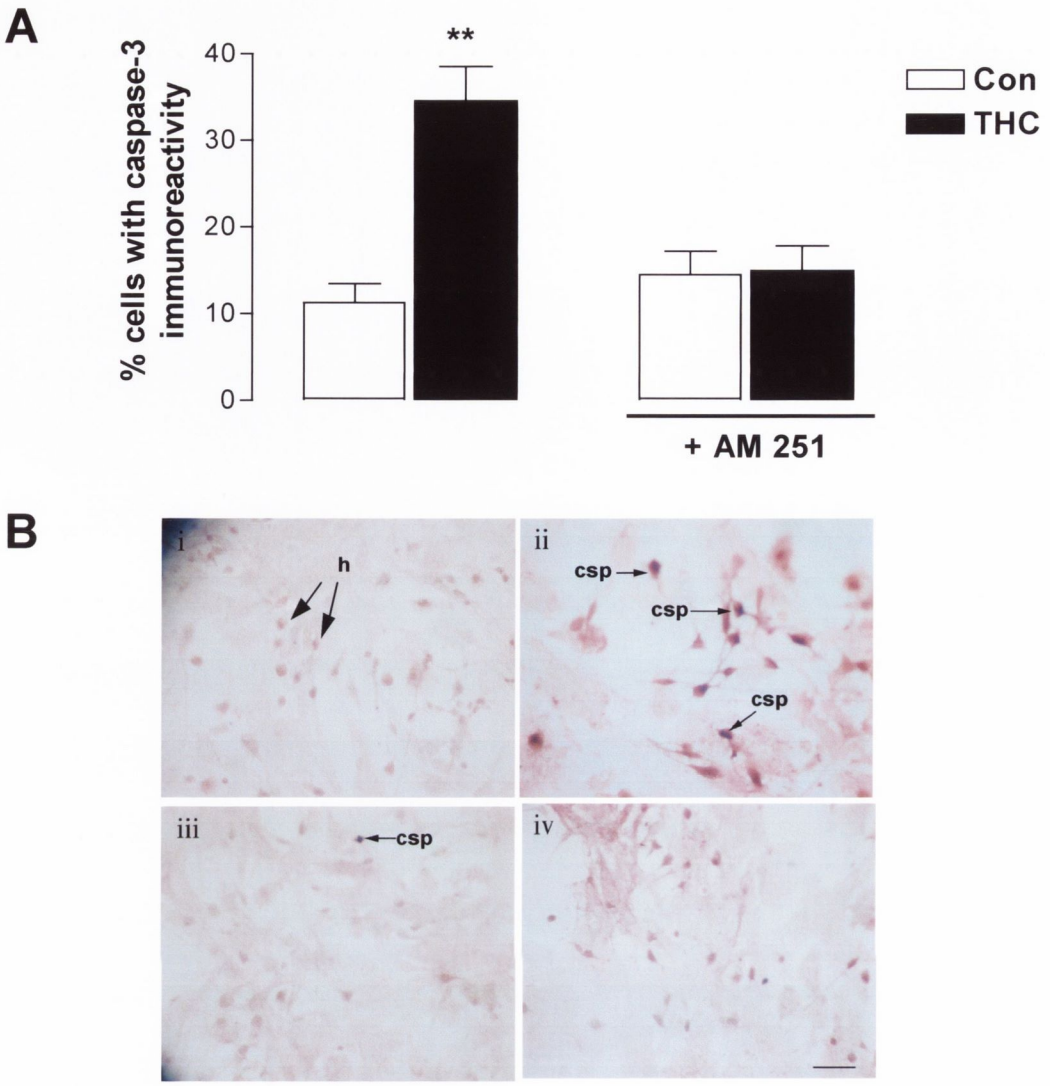

Figure 3.8: THC increases caspase-3 activity in cortical neurons via the CB_1 cannabinoid receptor

A: Assessment of active caspase-3 immunoreactivity was made after treatment of neurons with THC (5μM) alone, THC (5μM) with the CB_1 antagonist AM 251 (10μM) or with AM 251 (10μM) alone for 2hr. THC significantly increased the percentage of neurons displaying active caspase-3 immunoreactivity. AM 251 abolished the THC-induced increase in active caspase-3 immunoreactivity. Results are expressed as mean ± SEM for 7 observations, **$p<0.01$.

B: Sample photos of (i) vehicle-treated cells, (ii) THC-treated cells, (iii) AM 251-treated cultures and (iv) cultures treated with THC in the presence of AM 251, which were stained using an anti-active caspase-3 antibody. Arrows indicate healthy (h) and caspase-3 immunoreactive (csp) neurons. Scale bar is 50μm.

3.2.9 THC increases PARP cleavage in cultured neurons

PARP cleavage is considered a biochemical marker of apoptosis and occupies a central position in the apoptotic pathway (Kaufmann *et al.*, 1993). The ability of THC (5μM) to cleave the PARP polypeptide (113kDa) to an 89kDa fragment was assessed by immunocytochemistry using a cleavage site-specific PARP antibody (Figure 3.9). Addition of THC to cortical cultures for 2hr produced a significant increase in the percentage of cells displaying immunoreactivity for the cleaved form of PARP from 8.5 ± 0.5% (mean ± SEM) to 40.1 ± 3.9% ($p<0.01$, ANOVA, n=5 observations). AM 251 (10μM) had no effect on basal levels of cleaved PARP immunoreactivity (8.3 ± 0.8%) in neurons but it prevented the stimulatory effect of THC on PARP cleavage (8.1 ± 0.9% of cells displayed cleaved-PARP immunoreactivity following THC treatment in the presence of AM 251 for 2hr). This indicates that the transduction pathway contributing to THC-induced apoptosis of cultured cortical neurons involves the cleavage of the PARP enzyme. Representative examples of healthy neurons and neurons displaying immunoreactivity for cleaved PARP following THC exposure are shown in Figure 3.9B.

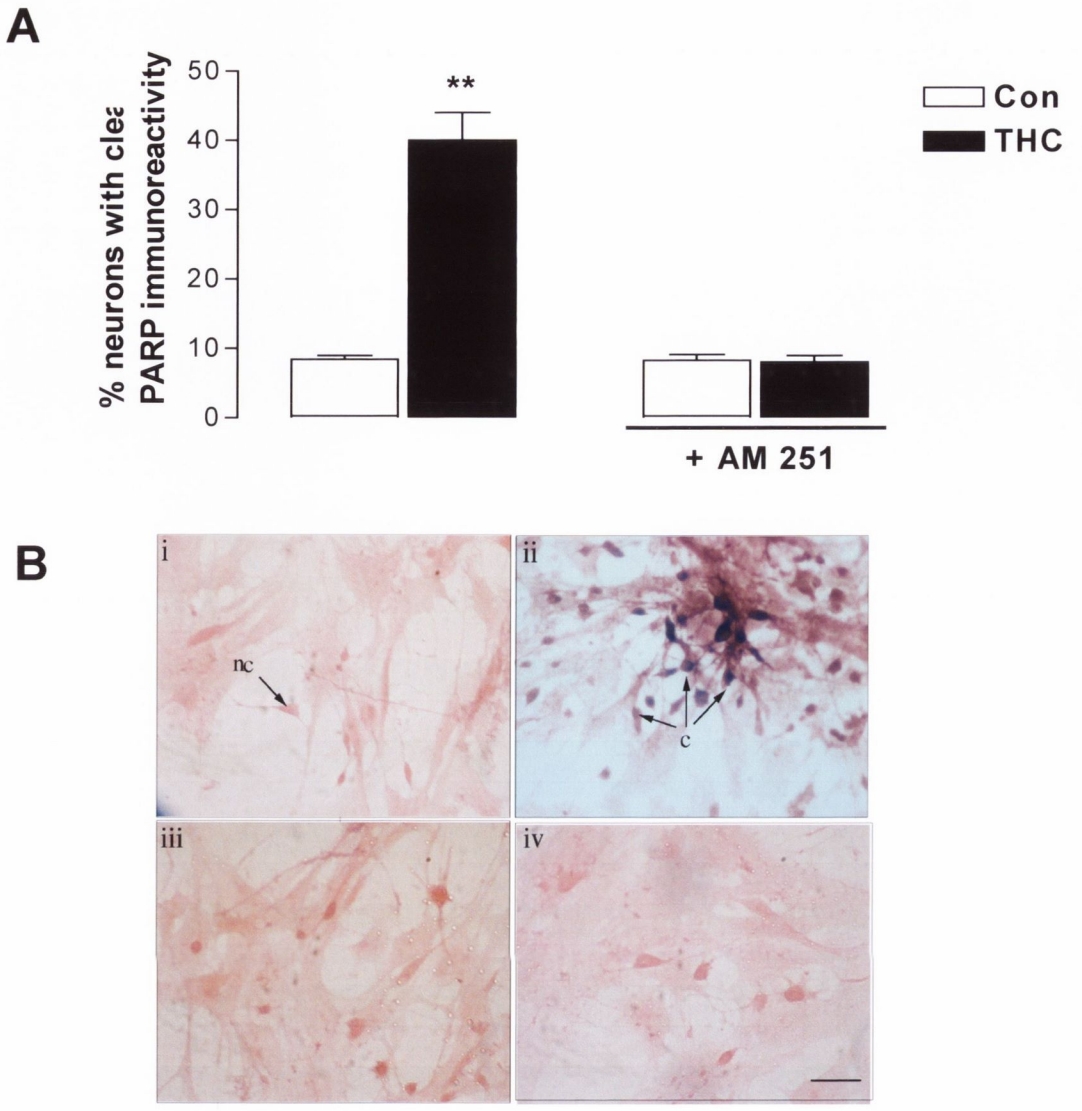

Figure 3.9: THC cleaves PARP following CB_1 receptor activation

A: Cultured cortical neurons were treated with THC (5μM) in the presence or absence of AM 251 (10μM) for 2hr. The level of cleaved PARP immunoreactivity was determined by immunocytochemistry. THC significantly increased the percentage of neurons expressing the cleaved form (89kDa) of PARP. Treatment with AM 251 prevented this increase. Results are expressed as mean ± SEM for 5 observations, **$p<0.01$.

B: Immunocytochemistry using the cleavage site-specific anti-PARP antibody in (i) control, (ii) THC-treated, (iii) AM 251-treated and (iv) THC + AM 251-treated cultures. Arrows indicate healthy non-cleaved (nc) PARP neurons and neurons displaying immunoreactivity for cleaved (c) PARP. Scale bar is 25μm.

3.3 Discussion

The aim of this study was to examine the effects of THC on neuronal viability and to characterise the intracellular mechanisms that underlie THC-induced neurotoxicity in cultured cortical neurons. THC neurotoxicity *in vitro* was examined using cultured cortical neurons to identify signal transduction pathways contributing to toxicity. THC induced DNA fragmentation in the nucleus of cultured neurons, reflecting an apoptotic response profile to THC. The ability of THC to induce DNA fragmentation was blocked by AM 251, indicating that THC neurotoxicity is mediated through the central CB_1 cannabinoid receptors in cortical neurons. THC was found to induce cleavage of the DNA-repair enzyme PARP in an AM 251-dependent manner. Furthermore, THC significantly increased cytochrome *c* release from the mitochondria into the cytoplasm and produced an increase in the activity of the cell death protease, caspase-3. Again, the proclivity of THC to impact on the cytochrome *c*/caspase-3 system was abated by AM 251. Data herein suggest that the CB_1 cannabinoid receptor is coupled to effectors involved in the regulation of cytochrome *c* release and caspase-3 activation, and hence may be pertinent in mediating the neurotoxic properties of THC.

Apoptosis, or programmed cell death, is a normal physiological process in which a cell actively participates in its own destruction without triggering an inflammatory response (Kerr *et al.*, 1972). This process is characterised by distinct morphological and biochemical changes to the cell, including the internucleosomal cleavage of DNA (Behl, 2000). The ability of THC to induce DNA fragmentation was assessed by two techniques, TUNEL staining and by assessing DNA laddering using agarose gel electrophoresis. The TUNEL system provides an accurate quantitative method of determining cell death in cultured cell populations. In addition to providing a colorimetric DAB based system to isolate cells containing fragmented DNA, the occurrence of apoptosis can be observed morphologically (membrane blebbing, cell shrinkage). In addition to this staining technique, fragmented DNA may be visualised on an agarose gel as distinct fragments of oligonucleosomal size (180-200bp lengths; Arends *et al.*, 1990). The DNA ladder formation results

from the nucleolytic cuts in linker DNA between nucleosomes within chromatin (Arends *et al.*, 1990). The 180bp periodicity of the DNA fragments is a tell-tale sign of apoptosis. As the source of DNA for DNA laddering using agarose gel electrophoresis may be cellular or from tissues, this technique was used to analyse apoptosis in cultured cells exposed to THC. Unfortunately, DNA laddering was not observed in THC-treated cell cultures. Furthermore, the assessment of apoptosis using DNA laddering did not reveal evidence of DNA fragmentation in etoposide-treated cell cultures, which suggests that the technique remains to be optimised as etoposide has been shown consistently to in induce neuronal apoptosis (Nakajima *et al.*, 1994). It should be noted that in systems in which apoptosis is occurring asynchronously, genomic DNA ladders may not be visible or may appear as a smear pattern which may account for this effect. Furthermore, the ability to visualise a DNA ladder is dependent on the amount and quality of fragmented DNA. This can partly be controlled by preventing DNA degradation, which can occur in thawed tissue or during the extraction process due to shearing. It is also possible that the DNA failed to move out of the well following loading, which may be prevented by ensuring that DNA is sufficiently cleaned with phenol/chloroform.

At a cellular level THC has been shown to modulate a number of neuronal functions, including ion channel activity (Turkanis *et al.*, 1991; Mackie *et al.*, 1995; Twitchell *et al.*, 1997; Caulfield and Brown, 1992; Deadwyer *et al.*, 1993) and neurotransmitter release (Jentsch *et al.*, 1998; Gessa *et al.*, 1998; Shen *et al.*, 1996; Schlicker *et al.*, 1997), and there is increasing evidence suggesting a role for THC in the regulation of neuronal viability. Indeed, there has been growing evidence for a role of cannabinoids in controlling the cell survival/death decision. The finding that THC promotes degeneration of cultured cortical neurons is consistent with the effects of THC on cultured hippocampal neurons (Chan *et al.*, 1998), hippocampal neurons *in vivo* (Scallet *et al.*, 1987), cultured C6 glioma cells (Sánchez *et al.*, 1998; Jacobsson *et al.*, 2000), glioma cell growth *in vivo* (Galve-Roperh *et al.*, 2000) and immune cells *in vitro* (Zhu *et al.*, 1998) and *in vivo* (McKallip *et al.*, 2002b). Some of the proposed intracellular mechanisms accounting for the apoptotic effects of THC in these systems have included the generation of free radicals by cyclooxygenase, sustained ceramide accumulation and caspase-1 activation.

Furthermore, there is evidence that endogenous cannabinoid anandamide induces apoptosis in cultured neuroblastomas (Maccarrone *et al.*, 2000), PC12 cells (Sarker *et al.*, 2000) and lymphocytes (Schwarz *et al.*, 1994) and causes damage to neonatal neurons *in vivo* (Szöke *et al.*, 2002).

Cannabinoid-induced psychoactive effects are rapid, typically reaching a maximum 20-30 min after the marijuana cigarette has been finished and declining to baseline over 3-4hr (Chiang and Barnett, 1984). Data presented in this chapter suggests that the duration of cannabinoid exposure determines if neurotoxic consequences exist. Indeed, a 30 min exposure to THC was required to induce a significant increase in caspase-3 activity and DNA fragmentation and a maximal level of apoptosis was observed at 2-3hr post THC treatment. The time course of THC-induced cortical cell death was similar to that found in hippocampal cultures. Indeed, Chan and colleagues (1998) have found that a 15 min THC exposure is neurotoxic to hippocampal cultures. Furthermore, THC-induces apoptosis in cultured splenocytes and macrophages (Zhu *et al.*, 1998) and murine bone marrow-derived dendritic cells (Do *et al.*, 2004) after 2hr. However these findings contrast with the apoptotic actions of THC in glioma C6.9 cell, in which apoptotic features are observed after a 3-5 day THC exposure (Sánchez *et al.*, 1998; Rueda *et al.*, 2000). Our findings suggest that cortical cells are particularly susceptible to THC-induced apoptosis, undergoing degeneration within the first hour of cannabinoid exposure, which may contribute to the drug-induced behavioural deficits.

The results presented in this study demonstrate that THC neurotoxicity in cultured cortical neurons is blocked by AM 251, a potent and selective CB_1 receptor antagonist (Lan *et al.*, 1999), indicating that THC neurotoxicity is dependent on CB_1 receptor activation in cortical neurons. However, the precise role of the cannabinoid receptors in regulating neuronal viability is poorly understood. The finding that neuronal cell death involving THC is a direct consequence of CB_1 receptor activation has previously been implicated in cultured hippocampal neurons by Chan and colleagues (1998). The implications of this finding are significant considering that the central CB_1 cannabinoid receptor is localised in brain regions whose functionality is associated with the pharmacological action of cannabinoids (Twitchell *et al.*,

1997). Specifically, areas such as the cerebral cortex (layers I and VI) and the hippocampus (CA3 field of Ammons horn and the molecular layer of the dentate gyrus), brain regions associated with memory and cognition, represent regions of the CNS in which the CB_1 receptor is densely located (Mailleux and Vanderhaeghen, 1992). Hence, the possibility that the CB_1-mediated neurotoxicity, identified in this study, may contribute to the compromised neuronal function associated with marijuana use is a relevant issue.

There is also evidence that THC and other cannabinoids act as a neuroprotectants in certain systems. Cannabinoid receptor agonists are neuroprotective in excitotoxic cell death *in vivo* (van der Stelt *et al.*, 2001; Panikashvili *et al.*, 2001) and *in vitro* (Abood *et al.*, 2001; Shen & Thayer, 1998), which is dependent on CB_1 receptor activation. Furthermore, THC and nonpsychotropic cannabinoids decrease glutamate toxicity in rat cortical neuronal cultures in a receptor-independent process that is not blocked by CB_1 receptor antagonists (Hampson *et al.*, 1998). Furthermore, synthetic cannabinoids protect cultured cortical neurons from *in vitro* hypoxia and glucose deprivation in a CB_1-independent manner (Nagayama *et al.*, 1999). Hence, the precise role of the cannabinoid receptors in regulating these neuroprotective effects is poorly understood, with CB_1-dependent and independent effects being observed. Overall it appears that neurotoxic and neuroprotective effects of cannabinoids can be observed, and these differences are likely to depend on a variety of influences, including the nature of the toxic insult, the cell type under study and the particular cannabinoid used.

Mitochondrial function is commonly perturbed early during the apoptotic process (Zamzami *et al.*, 1996) and there is evidence that cannabinoids induce mitochondrial damage in neurons (Szöke *et al.*, 2002), liver cells (Mahoney and Harris, 1974), dendritic cells (Do *et al.*, 2004), and lung tumour cells (Sarafian *et al.*, 2002). Furthermore, it has also been shown that THC is an effective inhibitor of NADH-oxidase activity in the rat brain (Bartova and Birmingham, 1976), indicating that THC may have an apoptotic effect by interrupting electron-chain transport, thus preventing oxidative phosphorylation. Following exposure of cells to stimuli that trigger apoptosis the electron transport protein cytochrome *c* is rapidly released from the mitochondria into the cytoplasm

(Rosse *et al.*, 1998). The finding that THC caused the release of cytochrome *c* from the mitochondria supports a role for this protein in THC toxicity. Indeed, the apoptotic actions of anandamide on neuroblastoma and lymphoma cells involves cytochrome *c* release from the mitochondria (Maccarrone *et al.*, 2000). Furthermore, THC induction of dendritic cell apoptosis involves a collapse of the mitochondrial membrane potential and cytochrome *c* release (Do *et al.*, 2004). The ability of THC to impact on this component of the cell death pathway was blocked by AM 251, suggesting that the neurotoxic effects of THC are mediated by the coupling of CB_1 to the translocation of cytochrome *c* from the mitochondria. Once in the cytoplasm, cytochrome *c* binds to the WD repeats of the cytosolic factor APAF-1 (Zou *et al.*, 1997; Reed, 1997) a human homologue of the nematode *C. elegans* cell death protein CED-4 (Zou *et al.*, 1997). This induces a conformational change that allows APAF-1 to recruit and complex with caspase-9 through the interaction of CARD domains (Reed, 1997). The clustering of caspase-9 with APAF-1 stimulates the processing of inactive caspase-9 to its active form, which presumably triggers a cascade of caspase activation involving caspase-3 (Slee *et al.*, 1999).

Caspases act as molecular instigators of apoptosis (Zou *et al.*, 1997; Janicke *et al.*, 1998; Rosse *et al.*, 1998). Caspase-3 is the most intensively studied apoptotic caspase. The enzyme exists as a proenzyme (32kDa) in most cells, including neurons, and is processed and activated by caspase-9 to the herterodimeric form (17kDa and 12kDa) during apoptosis (Slee *et al.*, 1999). The accumulation of cytochrome *c* in the cytoplasm plays a pivotal role in the activation of caspase-3 (Reed, 1997). In this study THC was found to activate caspase-3 in cultured cortical neurons, presumably as a downstream consequence of the THC-induced liberation of cytochrome *c* from the mitochondria into the cytoplasm. This is consistent with the apoptotic effects of cannabinoids on splenocytes and thymocytes (Mckallip *et al.*, 2002b), neuroblastoma and lymphoma cells (Maccarrone *et al.*, 2000), myeloblastic leukemia cells (Gallily *et al.*, 2003), bone-marrow-derived dendritic cells (Do *et al.*, 2004) and PC-12 cells (Sarker *et al.*, 2000), which involves caspases. THC-induced caspase-3 activation was blocked by AM 251, suggesting that the neurotoxic effects of THC are mediated by coupling of the CB_1 receptor to cytochrome *c* release and caspase-3 activation. There is also evidence that the

toxic effects of THC in immune cells involves caspase-1 (Zhu *et al.*, 1998), the interleukin (IL)-1β converting enzyme. Despite the apoptotic actions of caspase-1 in neurons (Vereker *et al.*, 2000), THC-does not regulate caspase-1 in cultured cortical neurons (Campbell, 2001).

In vitro, caspase-3 is known to cleave a number of structural proteins, as well as RNA splicing and DNA repair-associated proteins (Janicke *et al.*, 1998; Liu *et al.*, 1996). The consequences of these cleavage events are now emerging and suggest that they are responsible for many of the phenotypic changes that occur during neuronal apoptosis. The DNA repair enzyme PARP is proteolytically cleaved by caspase-3 at the onset of apoptosis (Kaufmann *et al.*, 1993). Nuclear PARP is selectively activated by DNA strand breaks to participate in DNA repair (Pieper *et al.*, 1999). THC was found to degrade the 113kDa PARP protein to a distinct 89kDa fragment, a recognised marker of apoptosis. This finding is consistent with the apoptotic effects of anandamide on PC12 cells which involves PARP cleavage (Do *et al.*, 2004). The apoptosis-associated cleavage of PARP removes the amino-terminal domain of the protein to yield the 89kDa fragment that still retains basal catalytic activity but lacks the DNA binding domain (Nicholson *et al.*, 1995). Hence a consequence of PARP inactivation would be sustained DNA strand breakage and this is consistent with the data obtained in this study where increased occurrence of the cleaved 89kDa PARP fragment and DNA fragmentation was detected in cells exposed to THC.

The exact nature of the link between the CB_1 receptor and cytochrome *c* release was not addressed in this study. However, previous studies have demonstrated that the toxic effects of THC involve a PTX sensitive G-protein (Campbell, 2001). Furthermore, PTX partially inhibits THC-induced apoptosis in dendritic cells (Do *et al.*, 2004). These findings are consistent with the evidence that links the CB_1 receptor to activation of G-protein subtypes $G_{i/o}$ (Howlett, 1995). To date, the role of G-proteins in neuronal cell death has not been completely clarified since PTX-sensitive G-proteins have been found to exert both pro-apoptotic (Farkas *et al.*, 1998) and anti-apoptotic effects (Jakob and Krieglstein, 1997). However the data presented by our laboratory

demonstrate that the coupling of the CB_1 receptor, presumably to PTX-sensitive G-proteins, as facilitators of apoptosis.

In summary, treatment of cultured cortical neurons with THC induces cell death via the CB_1 cannabinoid receptor. Data from this study show that the apoptotic pathway triggered by THC in cultured cortical neurons involves cytochrome *c* translocation from the mitochondria, caspase-3 activation and PARP cleavage. The dose of THC used in the present study is consistent with the human plasma concentrations of THC (low μM; Chiang and Barnett, 1984; Giroud *et al.*, 2001). Indeed, Azorlosa and colleagues (1992) have found THC concentrations of 1μM in the human plasma during recreational use. Therefore, it may be possible to reach THC levels of as high as 15-20μM in the brain as THC can be concentrated 15- to 20-fold in some tissues (Johansson *et al.*, 1989). Considering that THC is a highly lipophilic molecule and will readily cross the blood-brain barrier, this study suggests that some of the impairments in cortical function associated with marijuana use may be attributable to the activation cytochrome *c*/caspase-3 cell death pathway in cortical neurons. Furthermore, although the precise physiological role of endogenous cannabinoids is not known, our findings suggest that the proclivity of THC to induce apoptosis in neonatal cortical neurons may reflect the role of endogenous cannabinoids in CNS development.

Chapter 4

An investigation of the role of c-Jun N-terminal Kinase in THC-induced apoptosis of cultured cortical neurons

4.1 Introduction

It has been established that cannabinoids exert most of their effects in the central and peripheral nervous system through the CB_1 and CB_2 cannabinoid receptors, which are coupled to heterotrimeric $G_{i/o}$-proteins (Matsuda *et al.*, 1990; Munro *et al.*, 1993). The cellular mechanisms through which cannabinoids exert their effects are continuing to be identified and include several signal transduction pathways. Cannabinoid receptors have been shown to couple to the protein kinase B/Akt (PKB) pathway (Gómez del Pulgar *et al.*, 2000b), the extracellular signal-regulated kinase (ERK) pathway (Bouaboula *et al.*, 1995b; Bouaboula *et al.*, 1996; Derkinderen *et al.*, 1999; Derkinderen *et al.*, 2003), the p38 mitogen-activated protein kinase (MAPK) pathway (Derkinderen *et al.*, 2001) and the c-Jun N-terminal kinase (JNK) pathway (Rueda *et al.*, 2000). Due to cannabinoid receptor coupling to mitogen- and stress-activated kinase transduction systems, it is accepted that cannabinoids are involved in regulating cell fate in certain cells by modulating these pathways. While there is growing evidence that the JNK pathway is central to cell death in the nervous system (Mielke and Herdegen, 2000), the precise role of JNK in cannabinoid signalling is unclear. Although THC increases JNK phosphorylation in Chinese hamster ovary (CHO) cells transfected with CB_1 receptor cDNA, cultured astrocytes and glioma cells (Rueda *et al.*, 2000), the role of JNK in cannabinoid signal transduction in cortical neurons remains to be established. Furthermore, the contribution of JNK signalling to CB_1 receptor-dependent induction of cortical neuronal apoptosis was investigated.

The widely distributed JNKs belong to the family of MARKs along with ERK1/2, p38 and ERK5, and represent a group of enzymes that are activated by cytokines and environmental stresses (Ip and Davis, 1998; Buschbeck and Ullrich, 2005). The MAPK cascades function to convert extracellular stimuli to intracellular signals that are vital for many cellular responses, including cell growth and death (Marshall, 1995). Activation of JNK signalling is mediated by dual phosphorylation on threonine/tyrosine residues by upstream kinases as part of the cellular response to stress (Derkinderen *et al.*, 1999). Once

activated, the final cellular response varies with cell type and the state of activation of other transduction pathways within the cell (Herdegen et al., 1997). JNKs are encoded by three different genes, *jnk1*, *jnk2* and *jnk3*, and the products of each gene reveal isoforms with approximate molecular weight of 46kDa (JNK1), 54kDa (JNK2) and 57kDa (JNK3), all of which are found in the mammalian brain (Gupta *et al.*, 1996). Although it is recognised that the JNK3 isoform is distributed throughout the rat cerebral cortex (Carboni *et al.*, 1998), JNK3 protein expression was moderate in our cell culture model. Hence, the relative contribution of the JNK1 and JNK2 isoforms to the apoptotic process was investigated.

JNK has the proclivity to phosphorylate a variety of nuclear and cytoplasmic substrates, some of which are vital for the apoptotic actions of JNK. It is established that JNK phosphorylates the transcriptional activation domains of transcription factors (Ip and Davis, 1998). JNK also phosphorylates a number of cytoplamic substrates. JNK regulates the stablility and transcriptional activities of the cell cycle regulatory protein p53 via phosphorylation (Buschmann *et al.*, 2001). It has also been reported that JNK promotes cell death by promoting cytochrome *c* release from the mitochondria (Tournier *et al.*, 2000). In the nervous system the pro-apoptotic mitochondria-associated protein Bax acts downstream of JNK in regulating the translocation of mitochondrial cytochrome *c* into the cytosol (Kang *et al.*, 1998), and there is evidence to support an interaction between JNK and Bax in the cell death cascade (Lei *et al.*, 2002). JNK can also regulate the expression of the anti-apoptotic mitochondria-associated protein Bcl-2, inhibiting its pro-survival function possibly via phosphorylation (Park *et al.*, 1997; Kang *et al.*, 1998), and regulate caspase activity (Seimiya *et al.*, 1997).

The experiments in this chapter were therefore undertaken to examine the nature of the link between the CB_1 receptor, activation of JNK and downstream apoptotic consequences in cultured cortical neurons. In addition to determining the time- and dose-dependency of THC-induced JNK activation, the involvement of the CB_1 cannabinoid receptor and its associated G-protein in the THC-dependent regulation of JNK signalling was investigated in cultured cortical neurons. Downstream apoptotic consequences of JNK activation included the activation of caspase-3 and the induction of DNA fragmentation,

presumably as a consequence of JNK-induced regulation of cytochrome *c* translocation. Since commercially available JNK inhibitors prevent activity of the JNK1, JNK2 and JNK3 isoforms, it is impossible to determine the contribution of each isoform to the JNK mediated effects when using these inhibitors. Hence, to elucidate the respective roles of JNK1 and JNK2 in THC-induced apoptosis, antisense technology was employed to temporarily downregulate JNK1 and JNK2 expression. This technique employs the use of specific phosphorothioated oligonucleotides designed to bind specifically to a complementary sequence of mRNA on the target gene, causing a conformational obstacle for protein translation. As a result, the production of the specific protein is temporarily inhibited without affecting the expression of other genes. Treatment of neurons with specific antisense oligonucleotides that target rat JNK1 or JNK2 mRNA allowed the investigation of the upstream roles of both JNK isoforms in the THC-induced activation of caspase-3 and subsequent DNA fragmentation.

4.2 Results

4.2.1 THC increases JNK phosphorylation in cultured cortical neurons

Cultured cortical neurons were exposed to THC (5μM) for 5 min and 120 min and JNK activity (phosphorylation) assessed by fluorescence immunocytochemistry (Figure 4.1). Phospho-JNK immunofluorescence was detected using an anti-phospho-specific JNK antibody, which recognises JNK1 and JNK2 isoforms phosphorylated on residues Thr-183 and Tyr-185, in addition to a FITC-conjugated secondary antibody. Cells were viewed by fluorescent microscopy at an excitation wavelength of 490nm. In vehicle-treated neurons, phospho-JNK immunoreactivity was detectable at (i) 5 min and (iii) 120 min, indicating a tonic level of JNK activation in cell cultures. However, in cultures treated with THC for (ii) 5 min and (iv) 120 min a higher intensity of phospho-JNK immunoreactivity was observed within the cytosol and nucleus of cultured neurons.

4.2.2 THC activates JNK1 and JNK2 isoforms at different time points

To delineate the time course of THC-induced JNK phosphorylation and to furthermore characterise the role of the JNK isoforms in THC-induced neuronal signalling, cultured cortical neurons were exposed to THC (5μM) for various time points (5-120 min). Expression levels of the phosphorylated (active) form of JNK1 and JNK2 were measured by western immunoblot using a polyclonal anti-phospho-specific JNK antibody, and band widths were quantified using densitometry (Figure 4.2). Interestingly, there was a differential activation of both JNK1 and JNK2 isoforms depending on the duration of treatment with THC. First, for the JNK1 time course (Figure 4.2A), in untreated neurons the mean band width was 7.3 ± 0.8 (arbitrary units; mean ± SEM) and this was significantly increased to 13.4 ± 1.6 ($p<0.001$, ANOVA; n=7 observations) following treatment with THC for 5 min. However, no change in JNK1 activity was observed at subsequent time points of 30 min (8.5 ± 0.7) and 60 min (7.0 ± 0.6), and JNK1 was in fact significantly reduced to (4.2 ± 0.4) following treatment with THC for 2hr ($p<0.05$, ANOVA, n=7).

In contrast, the mean band width of phosphorylated JNK2 expression in untreated cortical neuronal cultures was 21.4 ± 3.9 (Figure 4.2B) and this was significantly increased to 38.8 ± 6.3 when neurons were cultured in media containing THC for 120 min ($p<0.01$, ANOVA; $n=7$). At earlier time points of 5 min (20.1 ± 2.9), 30 min (16.2 ± 3.0) and 60 min (17.7 ± 3.9), treatment with THC had no effect on JNK2 activity. This result indicates that the proclivity of THC to regulate JNK1/2 isoforms follows a distinct temporal pattern. A sample immunoblot demonstrating the activation of JNK1 and JNK2 after 5 min and 120 min of THC treatment respectively, is shown in Figure 4.2C.

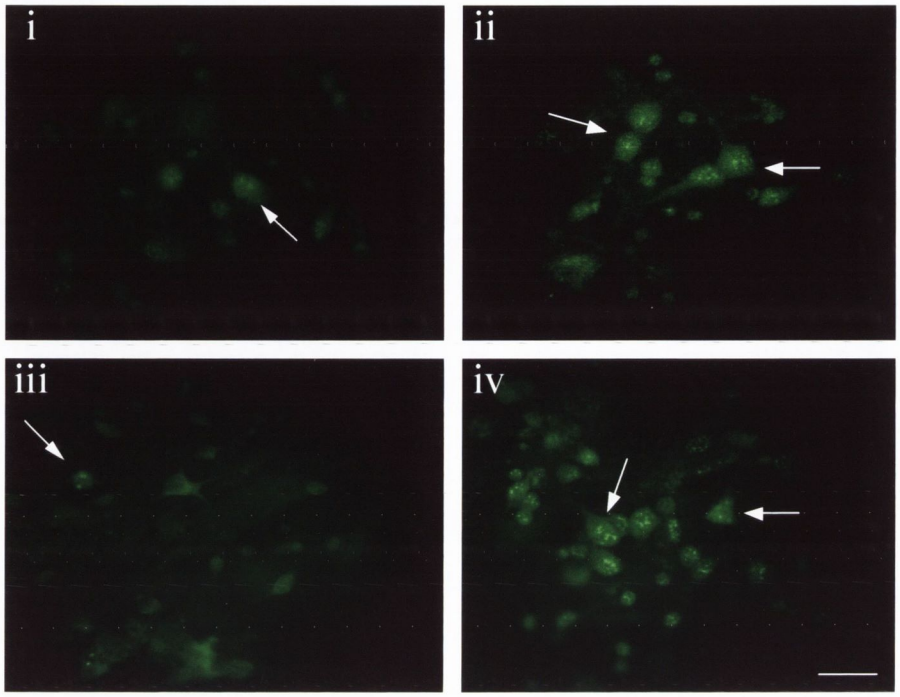

Figure 4.1: THC activates JNK in cultured cortical neurons

Cortical cultures were exposed to THC (5μM) for 5 min and 2hr, cells were fixed and the expression of the phosphorylated form of JNK assessed by immunofluorescence. In control neurons (i, iii), phospho-JNK immunoreactivity is apparent in neuronal subpopulations. Neurons exposed to THC for (ii) 5 min and (iv) 120 min display intense phospho-JNK immunostaining in the nucleus and in discrete areas of the cytoplasm. Arrows indicate neurons displaying phospho-JNK immunoreactivity. Scale bar is 25μm.

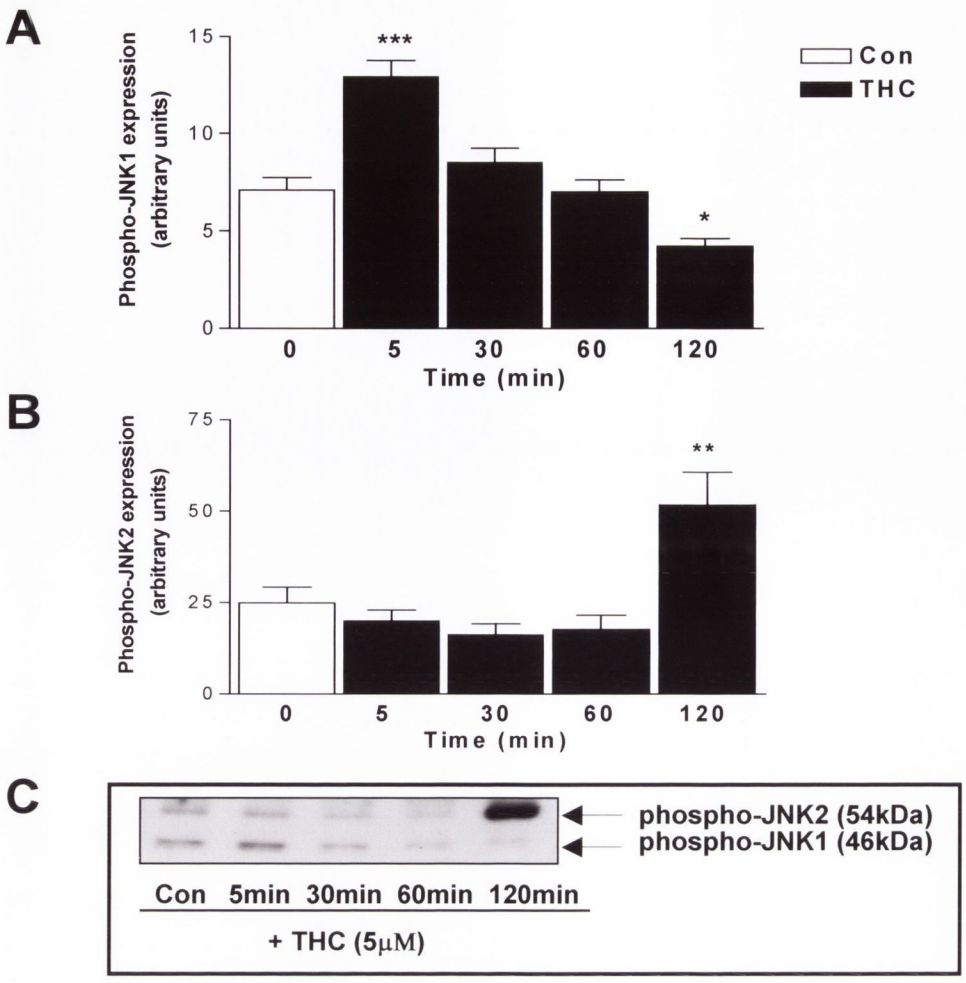

Figure 4.2: Time course of THC-induced activation of JNK

Cultured cortical neurons were exposed to THC (5μM) for 5-120 min, cells were harvested and fractions analysed for the expression levels of the phosphorylated active forms of JNK1 and JNK2 using western immunoblot.

A: A significant increase in JNK1 activity was found following treatment with THC for 5 min. Treatment with THC for 120 min significantly decreased JNK1 activity. Results are expressed as mean ± SEM for 7 observations, ***$p<0.001$, *$p<0.05$.

B: JNK2 activity was significantly increased when neurons were treated with THC for 120 min. Results are mean ± SEM for 7 observations, **$p<0.01$.

C: A sample western immunoblot demonstrating the increase in JNK1 activity at 5 min of THC treatment (lane 2) and the corresponding increase in JNK2 activity following treatment with THC for 2hr (lane 5). Lane 1 represents untreated neurons, neurons treated with THC for 30 min (lane 3) and neurons treated with THC for 60 min (lane 4).

4.2.3 THC does not regulate JNK1 and JNK2 protein expression

To ensure that the increase in expression of phosphorylated JNK1 at 5 min and phosphorylated JNK2 at 120 min (Figure 4.2) is not attributable to a THC-induced increase in total JNK protein expression JNK phosphorylation blots were stripped and reprobed for total JNK expression using a JNK polyclonal antibody that recognises total JNK1 and JNK2 protein expression (Figure 4.3). In control cells, JNK1 total expression at 5 min was 46.5 ± 1.2 arbitrary units (mean ± SEM) and exposure of neurons to THC (5μM) for 5 min had no effect on total JNK1 expression (46.9 ± 2.7; Figure 4.3A). In untreated neurons at 120 min, total JNK2 expression was 56.3 ± 7.3, and this was unaffected when neurons were cultured in media containing THC for 120 min (56.3 ± 9.1; Figure 4.3B). Sample immunoblots demonstrating that total JNK1 and JNK2 protein expression was unaffected by THC are shown as insets in Figure 4.3A, B.

4.2.4 JNK3 protein expression is moderate in cultured cortical neurons

JNKs are encoded by three different genes, *jnk1*, *jnk2* and *jnk3* all of which are found in the mammalian brain (Gupta *et al.*, 1996). To dertermine the tonic expression levels of JNK1, JNK2 and JNK3 isoforms in cortical cells, untreated cultured cortical neurons were analysed for the expression levels of total JNK protein by western immunoblotting using a JNK polyclonal antibody that recognises total JNK1, JNK2 and JNK3 protein expression (Figure 4.4). Although it is recognised that the JNK3 isoform is distributed throughout the rat cerebral cortex (Carboni *et al.*, 1998), JNK3 protein expression was moderate in cultured cortical neurons and could not be analysed densitometrically.

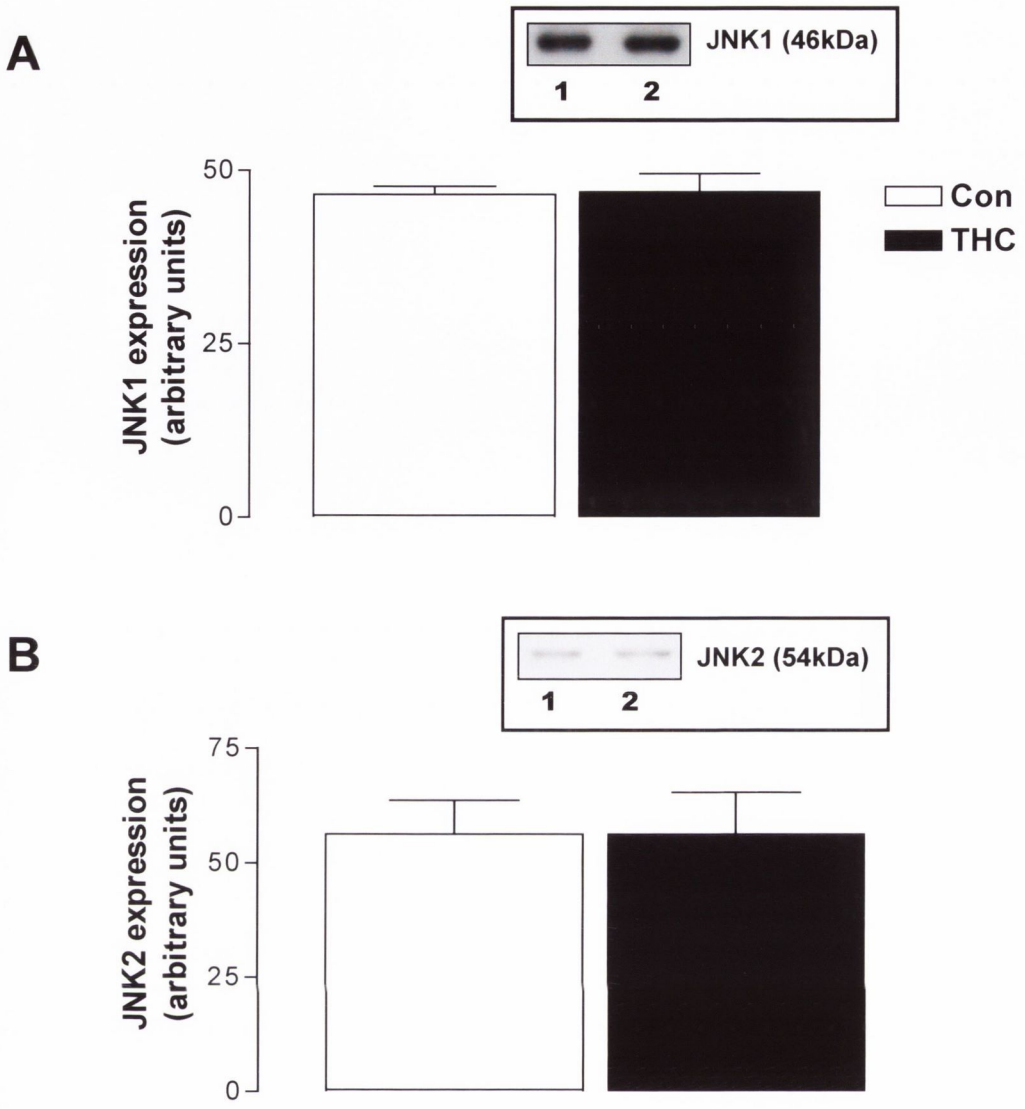

Figure 4.3 Effect of THC on JNK1/2 total protein expression

JNK phosphorylation blots were stripped and reprobed for total JNK expression using a JNK antibody that recognises total JNK1 and JNK2 protein expression.

A: THC had no effect on JNK1 protein expression at 5 min. Results are mean ± SEM for 6 observations. Inset: Sample western immunoblot showing that THC treatment (5 min) had no effect on JNK1 expression (lane 2) as compared to vehicle-treated neurons (lane 1).

B: Incubation of cells with THC for 2hr did not effect JNK2 protein expression. Results are mean ± SEM for 6 observations. Inset: A sample western immunoblot demonstrating total JNK2 expression in vehicle-treated neurons (lane 1) and neurons treated with THC (5μM) for 2hr (lane 2).

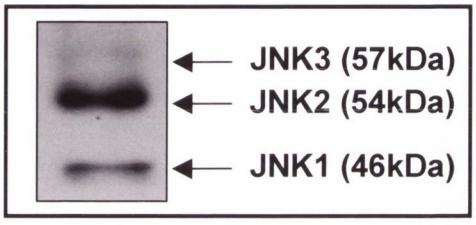

Figure 4.4 Relative expression levels of the JNK isoforms in cultured cortical neurons

Untreated cortical neurons were harvested and analysed for JNK1, JNK2 and JNK3 expression by western immunoblotting. JNK3 expression was moderate compared to JNK1 and JNK2 protein expression.

4.2.5 Dose-dependency of THC-induced JNK1 and JNK2 activation

Since it has previously been demonstrated in our lab that 5μM is the concentration of THC required to induce maximal neuronal degeneration (Campbell, 2001), a dose-response analysis of THC-induced JNK1 (Figure 4.5) and JNK2 (Figure 4.6) activation was performed to determine the concentration of THC required to evoke maximal activation of the JNK isoforms at each of their respective time points of activation.

Figure 4.5 demonstrates that in cell cultures treated with vehicle for 5 min phosphorylated JNK1 expression was 51.6 ± 1.3 arbitrary units (mean ± SEM). Treatment of neurons with 5nM THC (63.2 ± 4.5) or 0.5μM THC (69.5 ± 6.2) for 5 min had little effect on JNK1 activity. However, JNK1 activity was significantly increased to 72.7 ± 6.9 when neurons were treated with 5μM THC for 5 min ($p<0.05$, ANOVA, n=9 observations), the time point at which maximal JNK1 activity was observed. This indicates that the regulatory effect of THC on JNK1 activity is dose-dependent. A sample western immunoblot demonstrating the dose-dependency of THC-induced phosphorylation of JNK1 is shown in Figure 4.5B.

Figure 4.6 demonstrates that phosphorylated JNK2 expression was 28.9 ± 2.2 in control cells and was not significantly affected by treating cells for 120 min with THC at 5nM (33.7 ± 2.5) or 0.5μM (36.4 ± 2.9). However, exposure of neurons to THC at a concentration of 5μM significantly increased phosphorylated JNK2 expression to 40.1 ± 4.2 ($p<0.05$, ANOVA, n=9 observations) and a 50μM THC dose significantly increased phosphorylated JNK2 expression to 42.8 ± 4.1 ($p<0.05$, ANOVA, n=3), indicating that THC increases JNK2 activity at 120 min in a dose-dependent manner. A sample western immunoblot demonstrating the dose-dependency of THC-induced actiavtion JNK2 at 120 min is shown in Figure 4.6B.

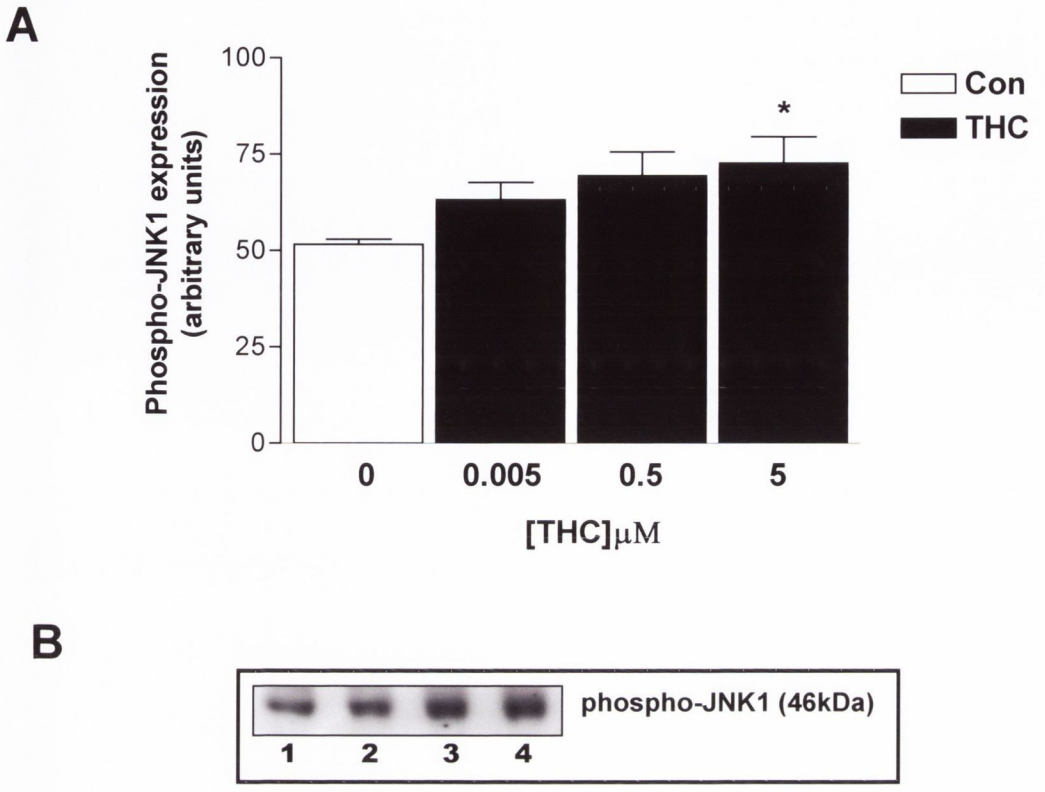

Figure 4.5: THC induces JNK1 activation in a dose-dependent manner

Cultured cortical neurons were treated with increasing concentrations of THC for 5 min. Following treatment cells were harvested and the analysed for the expression levels of the phosphorylated active form of JNK1 using western immunoblotting.

A: A significant increase in JNK1 activity was found following treatment with THC at a concentration of 5μM. Exposure to THC at 5nM and 0.5μM had no effect on JNK1 activity. Results are expressed as mean ± SEM for 9 observations, *$p<0.05$.

B: A sample western immunoblot showing that a 5 min treatment with 5μM THC significantly increased JNK1 activity (lane 4) as compared to vehicle-treated neurons (lane 1). Exposure of cells to 5nM (lane 2) and 0.5μM (lane 3) THC for 5 min had little effect on JNK1 activity.

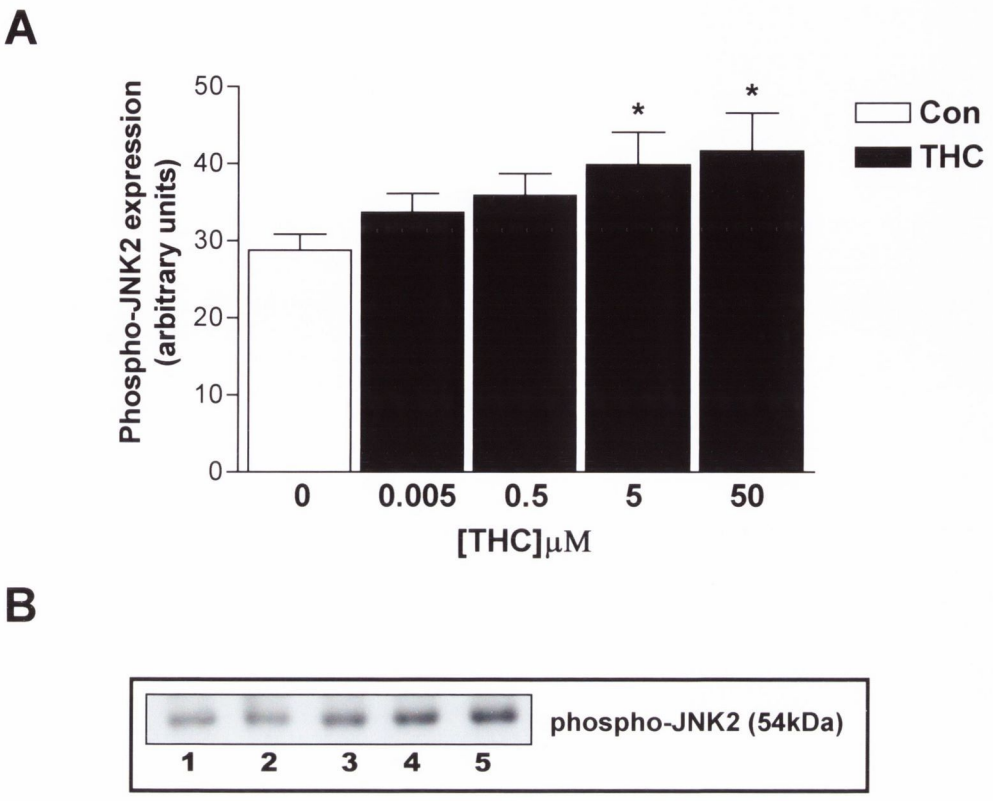

Figure 4.6: THC induces JNK2 activation in a dose-dependent manner

Cultured cortical neurons were treated with THC (5nM-50μM) for 120 min. Following treatment cells were harvested and the analysed for the expression levels of the phosphorylated active form of JNK2 using western immunoblotting.

A: A significant increase in JNK2 activity at 120 min was found following treatment with THC at concentrations of 5μM and 50μM. Exposure to THC at 5nM and 0.5μM had no effect on JNK2 activity. Results are expressed as mean ± SEM for 9 observations, *$p<0.05$.

B: A sample immunoblot showing JNK2 activity in neurons treated with THC for 120 min at concentrations of 5nM (lane 2), 0.5μM (lane 3), 5μM (lane 4), and 50μM (lane 5). Lane 1 is JNK2 activity in neurons treated with methanol vehicle for 120 min.

4.2.7 AM 251 pre-treatment prevents THC-induced JNK activation

To determine whether THC-induced JNK activation was reliant on signalling through the CB_1 cannabinoid receptor, cultured cortical neurons were pre-treated with the selective CB_1 receptor antagonist AM 251 (10μM) for 30 min prior to THC (5μM) exposure. Since THC (5μM) was found to activate JNK1 at 5 min and JNK2 at 120 min (Figure 4.2), the effect of AM 251 (10μM) on JNK activation at these time points was evaluated.

Figure 4.7 shows that in neurons treated with methanol vehicle for 5 min the phosphorylated JNK1 expression was 44.9 ± 4.9 arbitrary units (mean ± SEM) and this was significantly increased following THC treatment (5 min) to 58.7 ± 3.6 ($p<0.05$, ANOVA, n=6 observations). While pre-treatment with AM 251 alone had no effect on phosphorylated JNK1 expression (37.4 ± 3.4), it prevented the THC-induced increase in JNK1 activity (38.1 ± 5.9). This result provides evidence of a role for the CB_1 cannabinoid receptor in the THC-induced activation of JNK1. A sample immunoblot demonstrating the activation of JNK1 following THC treatment for 5 min, and the abolition of this effect in AM 251-treated cells is shown in Figure 7.7B.

Figure 4.8 demonstrates that phosphorylated JNK2 expression in vehicle-treated control neurons was significantly increased from 12.8 ± 0.5 to 15.7 ± 0.3 following treatment with THC (5μM) for 120 min ($p<0.01$, ANOVA, n=6 observations). Exposure to AM 251 (10μM) alone had no effect on phosphorylated JNK2 expression (11.6 ± 1.8) and it prevented the THC-induced increase in phosphorylated JNK2 expression (12.6 ± 0.5), indicating that THC-induces JNK2 activation via CB_1. A sample immunoblot demonstrating the CB_1-dependent activation of JNK2 following THC treatment is shown in Figure 4.8B.

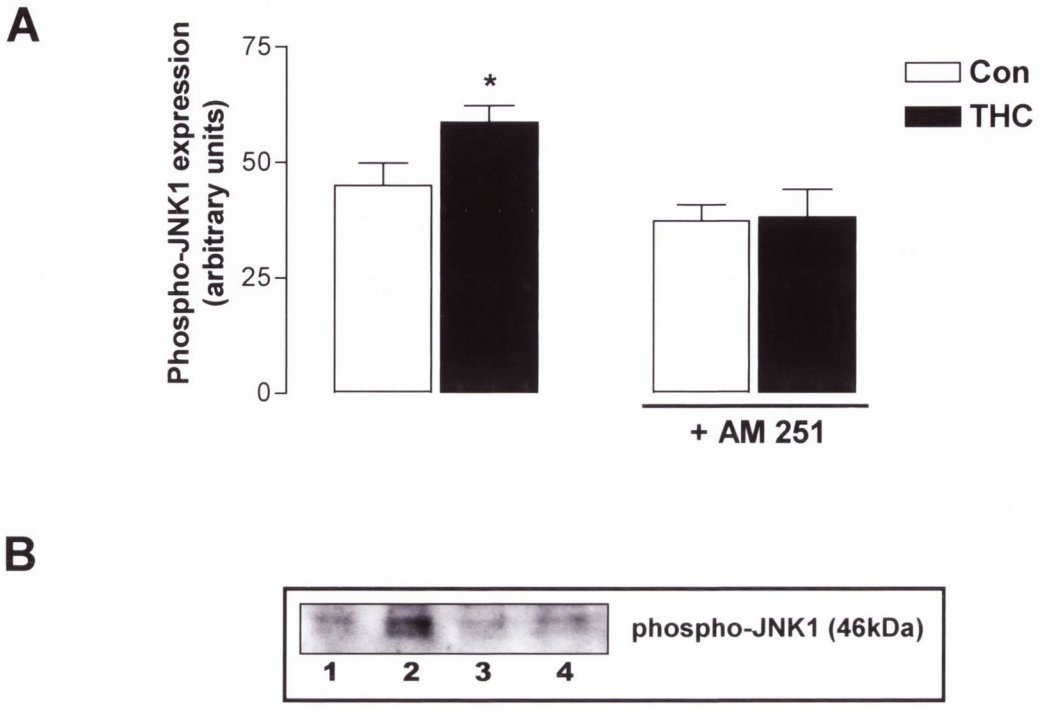

Figure 4.7: THC-induced activation of JNK1 is mediated by the CB_1 cannabinoid receptor

Cultured cortical neurons were pre-incubated with the CB_1 receptor antagonist AM 251 (10μM) for 30 min prior to THC (5μM) treatment for 5 min. Following treatment cell protein was harvested and analysed for the expression levels of phosphorylated JNK1 using western immunoblot.

A: Pre-incubation of cortical neurons with AM 251 abolished the THC-induced increase in JNK1 activity observed at 5 min. Results are expressed as mean ± SEM for 6 observations, *$p<0.05$.

B: A sample western immunoblot demonstrating the increase in JNK1 activity after 5 min of THC treatment in lane 2 compared to JNK1 activity in control neurons (lane 1). While AM 251 had no effect on JNK1 activity (lane 3), it abolished the ability of THC to induce JNK1 activation (lane 4).

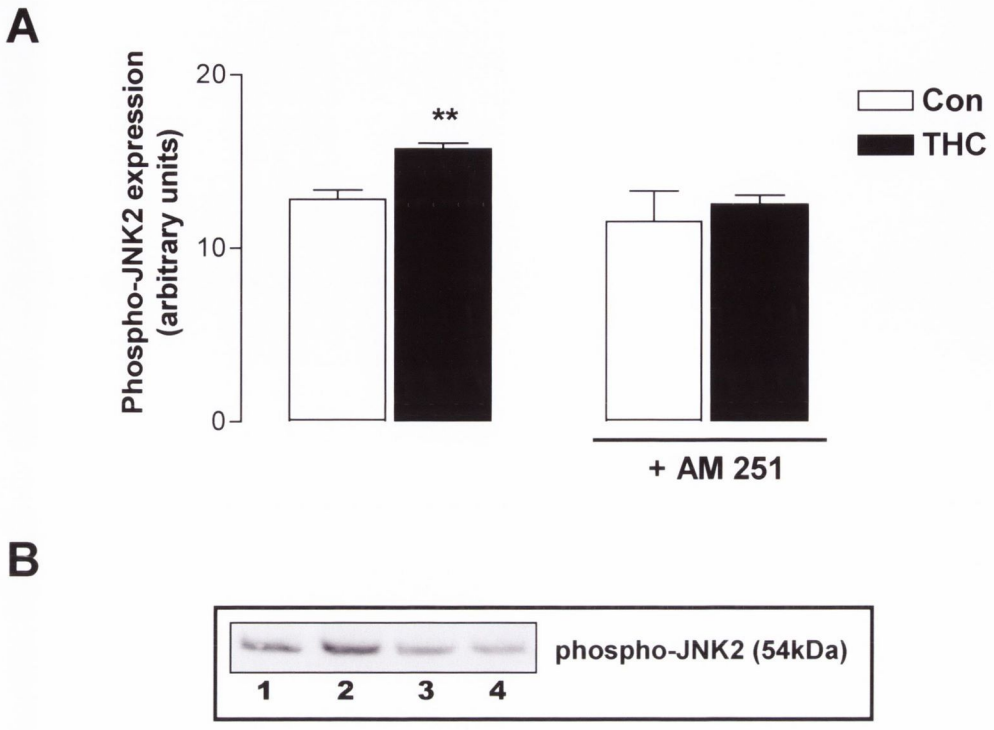

Figure 4.8: THC-induced activation of JNK2 is mediated by the CB_1 cannabinoid receptor

Cultured cortical neurons were pre-incubated with the CB_1 receptor antagonist AM 251 (10μM) for 30 min prior to THC (5μM) treatment for 120 min. Cell protein was harvested and analysed for the expression levels of phosphorylated JNK2 using western immunoblot.

A: Pre-incubation with AM 251 prevented the THC-induced activation of JNK2 at 120 min of treatment. Results are expressed as mean ± SEM for 6 observations, **$p<0.01$.

B: A sample western immunoblot showing that THC treatment for 120 min significantly increases JNK2 activity (lane 2) as compared to vehicle-treated neurons (lane 1). The stimulatory effect of THC on JNK2 activity was prevented by AM 251 (lane 4). Exposure of cells to the CB_1 inhibitor alone had no effect on JNK2 activity (lane 3).

4.2.9 PTX abrogates THC-induced JNK1/2 activation

The central CB_1 cannabinoid receptor is coupled to $G_{i/o}$-proteins (Howlett, 1995). The involvement of G-protein subtypes $G_{i/o}$ in coupling the CB_1 receptor to JNK activation in cultured cortical neurons was assessed using PTX (200ng/ml). As shown in Figure 4.9, PTX pre-treatment prior to THC (5μM) exposure for 5 min (31.9 ± 5.6 arbitrary units; mean ± SEM) prevented THC-induced JNK1 activation at 5 min (55.9 ± 4.7; $p<0.05$, ANOVA, n=5 observations). Incubation of neurons with methanol vehicle for 5 min (41.4 ± 2.7) or PTX alone for 24hr (35.1 ± 3.7) had no effect on JNK1 activity. A sample immunoblot demonstrating the activation of JNK1 following THC treatment, and the abolition of this effect in PTX-treated cells is shown in Figure 4.9B.

Similarly, Figure 4.10 demonstrates that phospho-JNK2 expression was significantly increased from 13.9 ± 0.5 to 22.3 ± 2.8 arbitrary units (mean ± SEM) following treatment with THC (5μM) for 120 min ($p<0.05$, ANOVA, n=5 observatiosn). Treatment with PTX alone had no effect on phosphorylated JNK2 expression (16.1 ± 1.9) but prevented the THC-induced increase in JNK2 activity at 120 min (14.7 ± 2.1). A sample immunoblot demonstrating the G-protein-dependent activation of JNK2 following THC treatment is shown in Figure 4.10B. These data suggest that the coupling of the CB_1 receptor to G-protein subtypes $G_{i/o}$ facilitates THC-induced JNK1 and JNK2 activation.

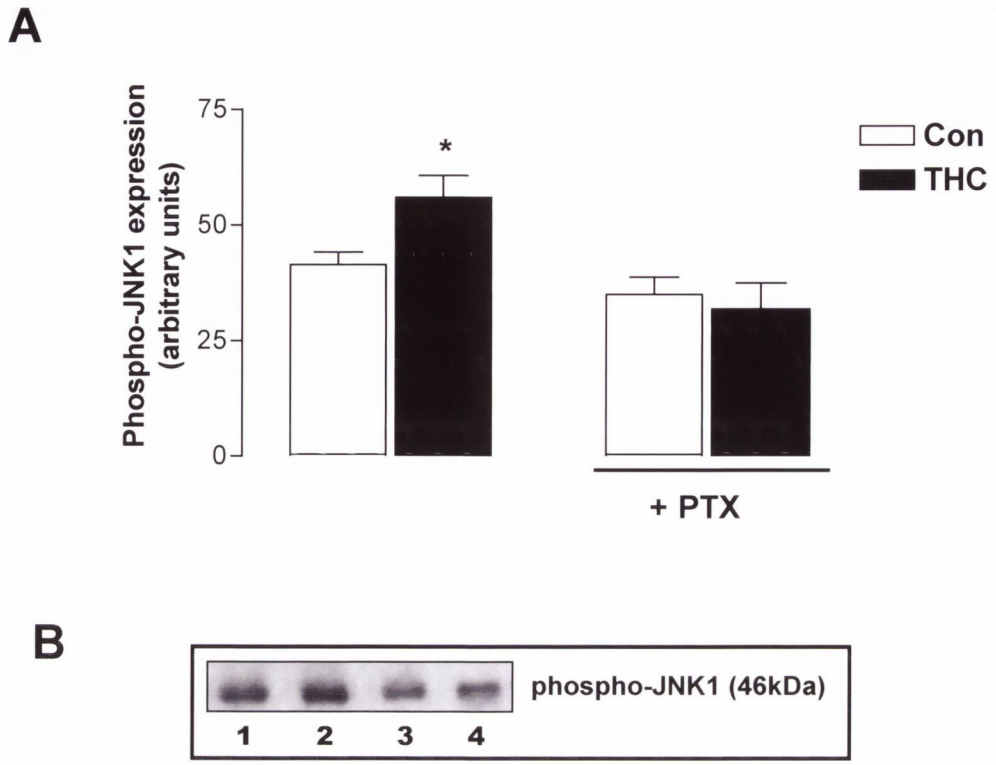

Figure 4.9: THC-induced JNK1 activation is mediated by G-protein subtypes $G_{i/o}$

Cultured cortical neurons were pre-treated with PTX (200ng/ml; 24hr) prior to THC (5μM) incubation for 5 min. Following treatment cell protein was harvested and analysed for the expression levels of phosphorylated JNK1 using western immunoblot.

A: THC significantly increased phospho-JNK1 expression and this was prevented by pre-treatment with PTX. Results are expressed as mean ± SEM for 5 observations, *$p<0.05$.

B: A sample western immunoblot demonstrating the increase in JNK1 activity (5 min) following THC exposure in lane 2 compared to JNK1 activity in control neurons (lane 1). While PTX had no effect on JNK1 activity (lane 3), it abolished the ability of THC to induce JNK1 activation (lane 4).

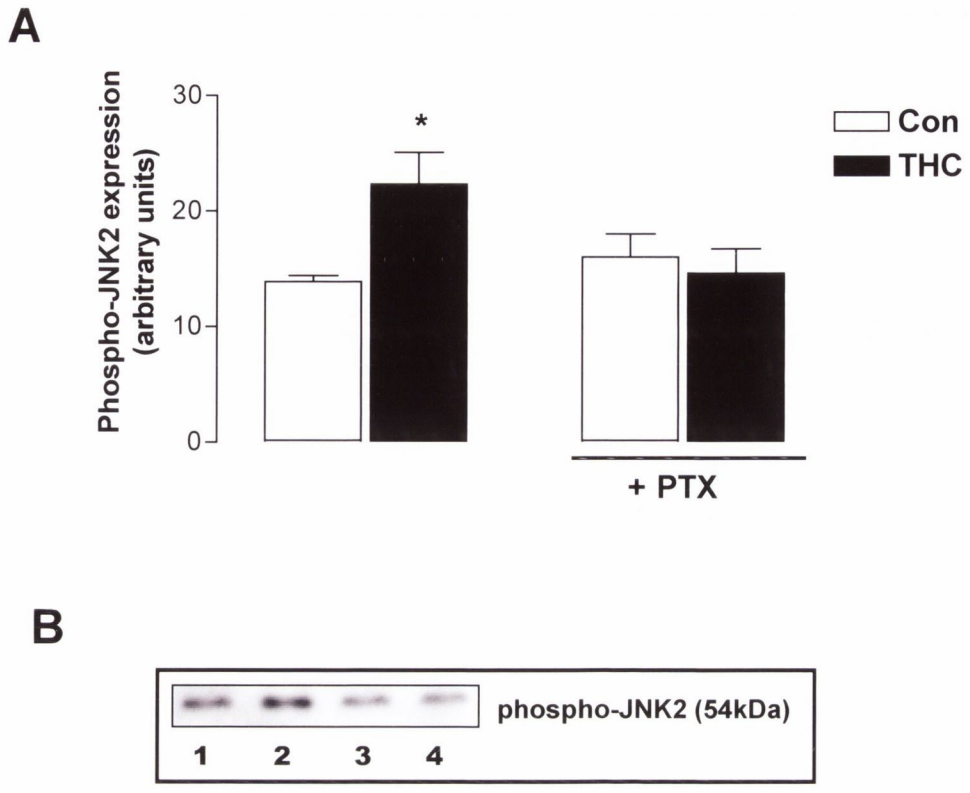

Figure 4.10: THC induces JNK2 activation via G-protein subtypes $G_{i/o}$

Cultured cortical neurons were pre-treated with PTX (200ng/ml; 24hr) prior to THC (5μM) incubation for 120 min. Cell protein was harvested and analysed for the expression levels of phosphorylated JNK2 using western immunoblot.

A: THC significantly increased phospho-JNK2 expression and this was prevented by pre-treatment with PTX. Results are expressed as mean ± SEM for 5 observations, *$p<0.05$.

B: Sample immunoblot demonstrating the increase in JNK2 activity (2hr) in lane 2 following THC exposure compared to vehicle-treated control neurons (lane 1). PTX abrogated the ability of THC to induce JNK2 activation (lane 4). PTX-treatment alone had no effect on JNK2 activity (lane 3).

4.2.11 Cellular antisense oligonucleotide uptake

Since commercially available JNK inhibitors such as CEP-1347 (Cephalon, USA), D-JNKI1 and SP600125 (Alexis Biochemicals, UK) prevent activity of the JNK1, JNK2 and JNK3 isoforms, it is impossible to determine the contribution of each isoform to the JNK mediated effects when using these inhibitors. Hence, to elucidate the respective roles of JNK1 and JNK2 in THC-induced apoptosis, antisense technology was employed to temporarily downregulate JNK1 and JNK2 expression. Specific phosphorothioated oligonucleotides, designed to evoke a transient downregulation in protein expression of JNK1 and JNK2 isoforms were incorporated into the culture medium. To monitor the uptake pattern of antisense oligonucleotides, neurons were incubated with FITC-labelled control oligonucleotides (2μM) for several different time points ranging from 1-24hr. It was found that a 1hr treatment was sufficient to ensure sufficient oligonucleotide uptake (Figure 4.11). Immunofluorescence was detected throughout the neuronal cell cultures, indicating oligonucleotide partitioning into cytoplasmic and nuclear compartments. Within these subcellular zones oligonucleotides have the proclivity to bind specifically to the complementary sequence of mRNA on the target gene, causing a conformational obstacle for protein translation. Since control oligonucleotide uptake was observed at 1hr, it was accepted that cortical neuronal treatment with JNK1/2 antisense oligonucleotides ensured adequate uptake of antisense.

4.2.12 Time course of JNK1/2 downregulation in JNK antisense oligonucleotide treated neurons

To determine to optimal time point required to selectively reduce JNK1 and JNK2 protein expression, neuronal cell cultures were exposed to 2μM of either JNK1 antisense oligonucleotides (AS1) or JNK2 antisense oligonucleotides (AS2) for various time points ranging from 1-72hr and JNK protein expression assessed by western immunoblotting using antibodies specific for total JNK1/2 protein expression. Upon treatment with AS1 (Figure 4.12A) and AS2 (Figure 4.12B) for at least 48hr, cellular levels of JNK1 and JNK2 protein were markedly reduced when compared to neurons treated with

JNK1 scrambled control oligonucleotides (SC1; Figure 4.12A) and JNK2 scrambled control oligonucleotides (SC2; Figure 4.12B), respectively. No observable downregulation in JNK1/2 protein expression was observed at the earlier time points of 1hr, 6hr, 12hr and 24hr indicating that a 48hr treatment with antisense was required to ensure sufficient downregulation of the JNK1 and JNK2 proteins.

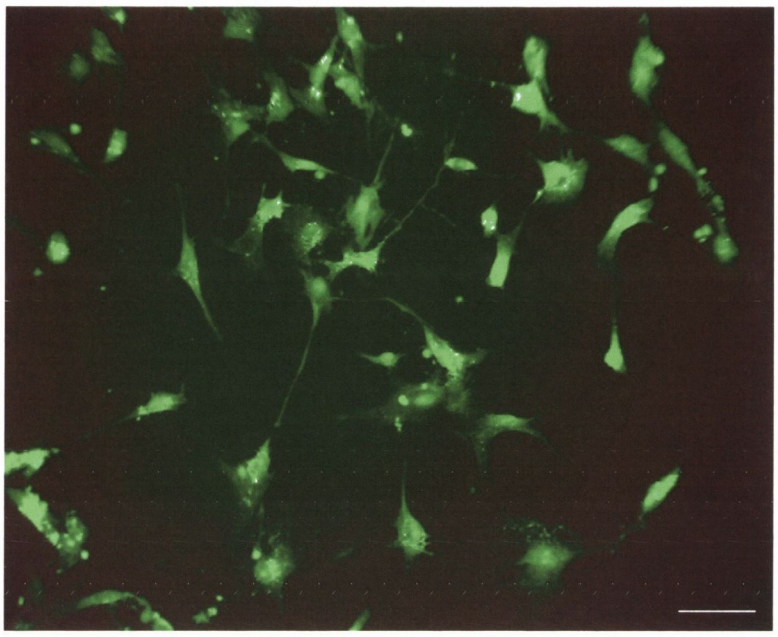

Figure 4.11: Antisense oligonucleotides are actively taken up by cortical neuronal cultures after 1hr of incubation

Cortical neuronal cultures were incubated with FITC-labelled control oligonucleotides (2μM) for 1-24hr. Efficient oligonucleotide uptake was observed at all time points using fluorescent immunocytochemistry. Scale bar is 25μm.

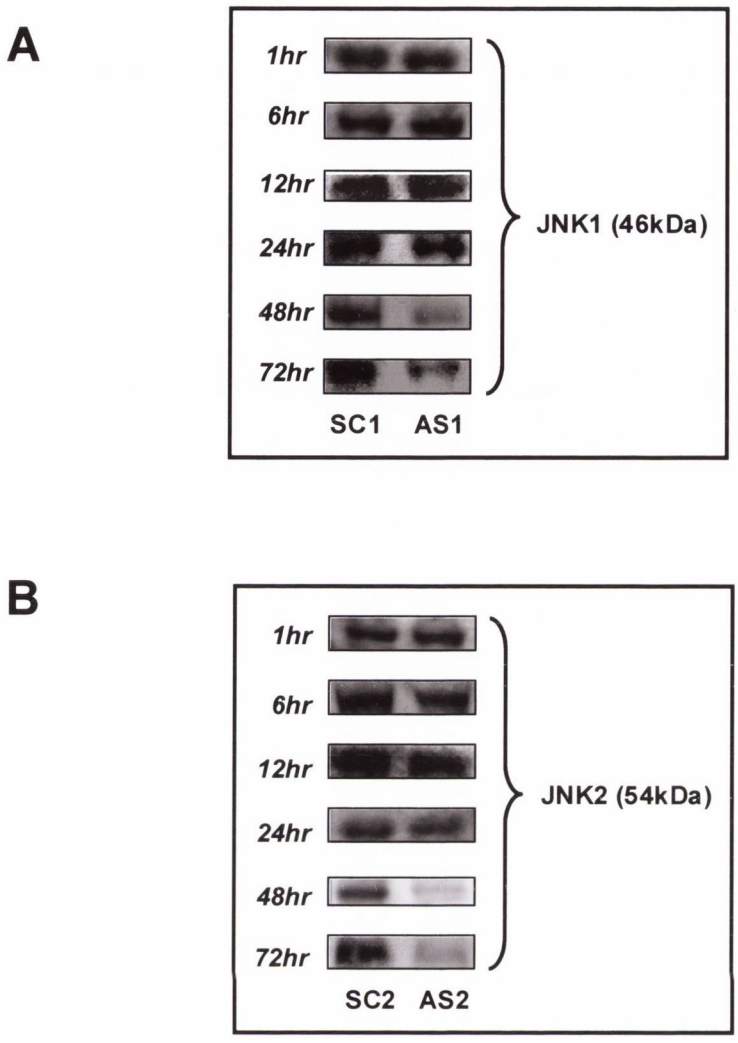

Figure 4.12: Time course of JNK antisense mediated JNK depletion

Cultured cortical neurons were exposed to AS1 or AS2 for various time points ranging from 1-72hr and JNK protein expression assessed by western immunoblotting. Expression of JNK1 and JNK2 was effectively downregulated following incubation with the relevant antisense sequence for 48hr.

A: Sample western immunoblots demonstrating JNK1 protein expression in SC1- and AS1-treated neurons at 1hr, 6hr, 12hr, 24hr, 48hr and 72hr.

B: Sample immunoblots demonstrating JNK2 protein expression in SC2-treated neurons and neurons treated with AS2 for various time points (1-72hr).

4.2.13 AS1 selectively downregulates JNK1 protein expression

The extent of JNK1 protein depletion was assessed in neuronal cell cultures exposed to 2μM of AS1 and SC1 for 48hr (Figure 4.13). JNK1 protein expression was determined by western immunoblot using a JNK1 monoclonal antibody in conjunction with densitometric analysis. Upon treatment with AS1, cellular levels of JNK1 protein were markedly reduced. In cells treated with SC1 for 48hr, JNK1 expression was 19.2 ± 2.9 arbitrary units (mean ± SEM) and this was significantly decreased by 79% to 3.9 ± 1.5 when AS1 was incorporated into the media for 48hr ($p<0.05$, Student's *t* test, n=4 observations). JNK1 protein expression in untreated neuronal cells (17.5 ± 0.3) was comparable to SC1-treated cells. The antisense-mediated depletion of JNK1 was specific since AS2 (19.1 ± 0.3) had no effect on JNK1 protein expression. A sample immunoblot demonstrating the antisense-mediated downregulation of JNK1 protein expression at 48hr is shown Figure 4.13B.

4.2.14 AS2 selectively downregulates JNK2 protein expression

The extent of JNK2 protein depletion was assessed by western immunoblot using a JNK2 monoclonal antibody following exposure to 2μM of AS2 and SC2 for 48hr (Figure 4.14). AS2 significantly decreased JNK2 protein expression by 70% to 11.7 ± 3.7 arbitrary units (mean ± SEM) when compared to the cells treated with SC2 for 48hr (34.1 ± 4.1, Student's *t* test, n=4 observations). JNK2 protein expression in untreated neuronal cells (30.7 ± 0.9) was comparable to SC2-treated cells. Furthermore, the antisense-mediated depletion of JNK2 was specific since AS1 (27.5 ± 3.7) had no effect on JNK1 protein expression. A sample immunoblot demonstrating the antisense-mediated downregulation of JNK2 protein expression at 48hr is shown Figure 4.14B.

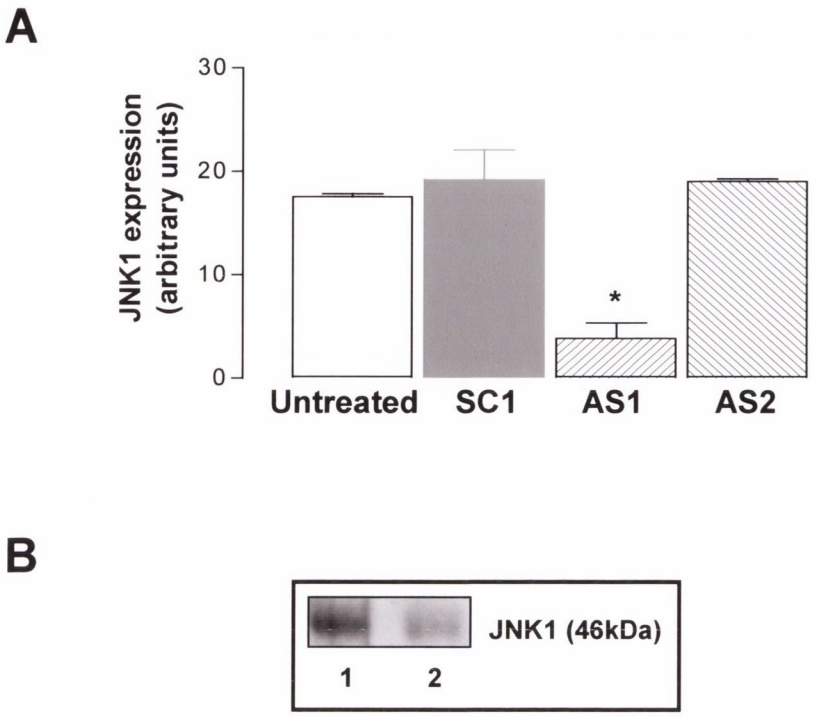

Figure 4.13: AS1 effectively reduce total JNK1 protein expression

Neurons were incubated with JNK1 antisense oligonucleotides (AS1; 2μM) or JNK1 scrambled control oligonucleotides (SC1; 2μM) for 48hr. Cells were harvested in lysis buffer and the total expression of JNK1 protein was examined by western blot analysis.

A: Treatment with AS1 for 48hr significantly decreased JNK1 protein expression in comparison to untreated cells and cells treated with SC1 for the same time course. AS2 treatment for 48hr had no effect on JNK1 protein expression. Results are expressed as mean ± SEM for 4 experiments, *$p<0.05$.

B: A sample immunoblot demonstrating that AS1 treatment for 48hr (lane 2) significantly reduces JNK1 protein expression as compared to SC1-treated neurons (lane 1).

A

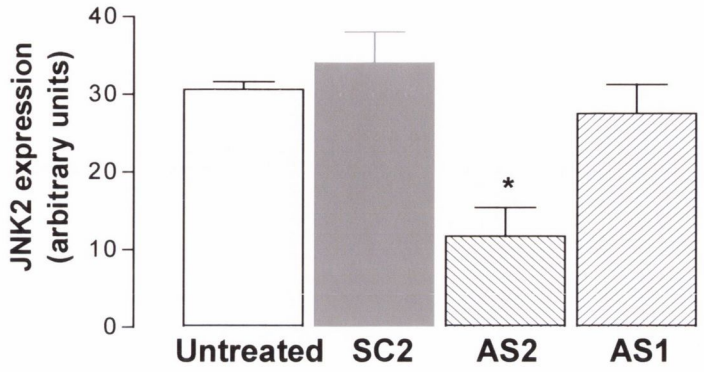

B

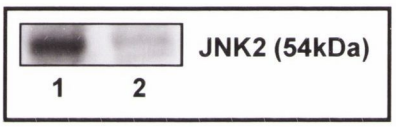

Figure 4.14: AS2 downregulates total JNK2 protein expression

Neuronal cells were incubated with JNK2 antisense oligonucleotides (AS2; 2μM) or JNK2 scrambled control oligonucleotides (SC2; 2μM) for 48hr. Cells were harvested in lysis buffer and the total expression JNK2 protein was determined by western blot analysis.

A: AS2 treatment for 48hr significantly reduced JNK2 expression. AS1 had no effect on JNK2 protein expression. Results are expressed as mean ± SEM for 4 experiments, *$p<0.05$.

B: A sample immunoblot demonstrating the significant reduction in JNK2 protein expression in AS2-treated neurons (lane 2) as compared to SC2-treated cells (lane 1).

4.2.15 JNK antisense prevents THC-induced caspase-3 activation in cultured cortical neurons

Apoptotic cell death is typically accompanied by the activation of the cysteine protease caspase-3 (Janicke *et al.*, 1998) and there is evidence that JNK regulates caspases (Seimiya *et al.*, 1997). Caspase-3 is cleaved and activated in cultured cortical neurons following treatment with THC (5μM) for 2hr (Chapter 3). Since caspase-3 is known to have a pivotal role in the cell death pathway triggered by THC within the cortex (Chapter 3; Campbell, 2001), it was determined whether JNK1 or JNK2 are involved upstream of caspase-3 activation using the JNK antisense approach. Following downregulation of each of the JNK isoforms, the role of JNK1 and JNK2 in THC-induced caspase-3 activation was assessed by monitoring the cleavage of the fluorescently labelled caspase-3 substrate, DEVD, to its fluorescent product (Figure 4.15).

The data presented in Figure 4.15A indicate that treatment with THC (5μM) for 2hr significantly increased caspase-3 activity from 22.5 ± 1.7 pmol AFC produced/mg protein/min (mean ± SEM) in vehicle-treated neurons to 50.7 ± 6.9 pmol AFC produced/mg protein/min ($p<0.05$, ANOVA; n=7 observations). In cells treated with SC1 alone for 48hr, caspase-3 activity was comparable to control values (25.1 ± 5.8 pmol AFC produced/mg protein/min). In neurons pre-incubated with SC1 for 48hr prior to THC treatment for 2hr, THC-induced caspase-3 activation was retained (55.1 ± 11.2 pmol AFC produced/mg protein/min, $p<0.05$, ANOVA; n=7). However, pre-treatment with AS1 for 48hr prior to THC treatment prevented the THC-induced increase in caspase-3 enzyme activity (31.8 ± 6.5 pmol AFC produced/mg protein/min). This result demonstrates that JNK1 is pertinent in THC-induced activation of caspase-3 in cultured cortical neurons.

Figure 4.15B demonstrates that a 2hr exposure of cortical neurons to THC (5μM) significantly increased basal caspase-3 activity from 22.1 ± 1.5 pmol AFC produced/mg protein/min (mean ± SEM) to 63.1 ± 11.1 pmol AFC produced/mg protein/min ($p<0.05$, ANOVA, n=8 observations). Neurons incubated with SC2 for 48hr showed a level of caspase-3 activity similar to that measured in vehicle-treated neurons (32.7 ± 8.7 pmol AFC produced/mg

protein/min). Pre-treatment with AS2 for 48hr prior to THC treatment prevented the THC-induced increase in caspase-3 activity (26.1 ± 5.2 pmol AFC produced/mg protein/min). Furthermore, exposure to SC2 for 48hr prior to THC treatment failed to prevent the THC-induced increase in caspase-3 activity (58.3 ± 5.9 pmol AFC produced/mg protein/min; $p<0.05$ ANOVA, n=8). This finding demonstrates a role for JNK2 in the THC-induced activation of caspase-3.

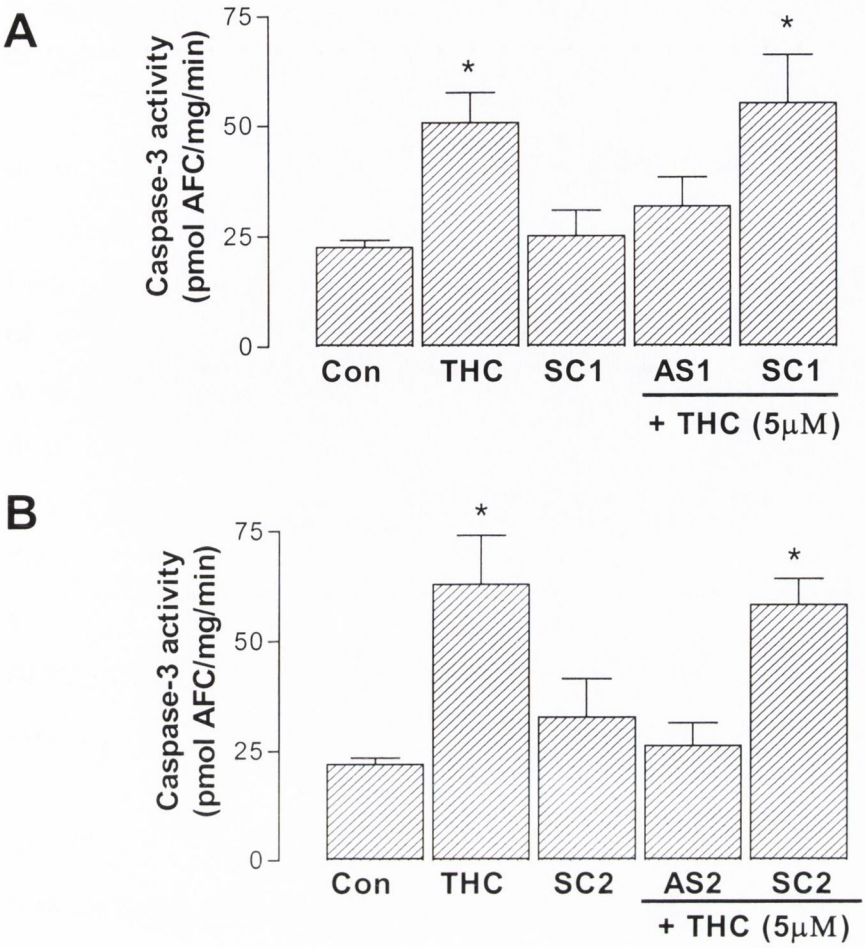

Figure 4.15: JNK1 and JNK2 are required for caspase-3 activity in THC-induced apoptosis

Neuronal cells were incubated with 2μM AS1/2 or SC1/2 for 48hr. Antisense oligonucleotides were then removed and cells incubated with THC (5μM) for 2hr. Following treatment cells were harvested in lysis buffer and caspase-3 activity assessed by monitoring the cleavage of the fluorogenic DEVD peptide.

A: Treatment of cortical neurons with THC for 2hr significantly increased caspase-3 activity. The stimulatory effect of THC on caspase-3 activity was prevented by pre-treatment with AS1 for 48hr prior to THC treatment. In SC1-treated cells, THC also evoked an increase in caspase-3 activity. Results are expressed as mean ± SEM for 7 observations, *$p<0.05$.

B: Pre-treatment of cells with AS2 for 48hr prior to THC treatment abolished the stimulatory effect of THC on caspase-3 activity. Results are expressed as mean ± SEM for 8 observations, *$p<0.05$.

4.2.16 JNK antisense prevents THC-induced DNA fragmentation in cortical cells

Apoptosis is distinguished by specific DNA cleavage into oligonucleosomal fragments (Lee *et al.*, 1993). THC causes a maximal increase in DNA fragmentation in cultured cortical neurons 2-3hr post-treatment (Chapter 3), therefore this time point was used to determine the roles of JNK1 and JNK2 in THC-induced DNA fragmentation. The TUNEL technique was used to assess the levels of DNA fragmentation in cultured cortical neurons following antisense-mediated depletion of JNK1 and JNK2 (Figure 4.15). In vehicle-treated control cells, 19.1 ± 2.0% (mean ± SEM) of cells displayed fragmented DNA (TUNEL positive) and this was significantly increased to 50.0 ± 5.9% in cells treated with THC (5μM) for 3hr ($p<0.001$, ANOVA, n=5 observations). Antisense-mediated depletion of either JNK1 or JNK2 prevented the THC-induced increase in DNA fragmentation.

Exposure of cells to AS1 (2μM) for 48hr prior to THC (5μM) treatment prevented the THC-induced increase in TUNEL staining (26.2 ± 6.6% TUNEL positive cells). In contrast, in cells pre-treated with SC1 (2μM) the THC-induced increase in DNA fragmentation was retained (46.4 ± 5.6% TUNEL positive cells, $p<0.001$, ANOVA, n=5 observations). Treatment with SC1 (2μM) alone for 48hr had no effect on the level of DNA fragmentation (23.0 ± 1.9% TUNEL positive cells).

In neurons pre-treated with AS2 (2μM) for 48hr before THC (5μM) exposure for 3hr, 19.8 ± 2.7% (mean ± SEM) of cells were TUNEL positive. In contrast, neurons pre-incubated with SC2 (2μM) for 48hr prior to treatment with THC showed a significant increase in DNA fragmentation (56.3 ± 3.4% TUNEL positive cells, $p<0.001$, ANOVA, n=5 observations). Again, treatment with SC2 (2μM) alone for 48hr had no effect on the level of DNA fragmentation (26.8 ± 2.6% TUNEL positive cells). Representative images of neurons stained for DNA fragmentation using the TUNEL technique are shown in Figure 4.15B, C.

These results demonstrate that depletion of either JNK1 or JNK2 prevents the THC-induced DNA fragmentation. This data is consistent with caspase-3 activity data and suggests that both JNK1 and JNK2 are intricately

involved in regulating the THC-induced activation of caspase-3 and resultant DNA fragmentation in the cannabinoid-induced apoptotic pathway.

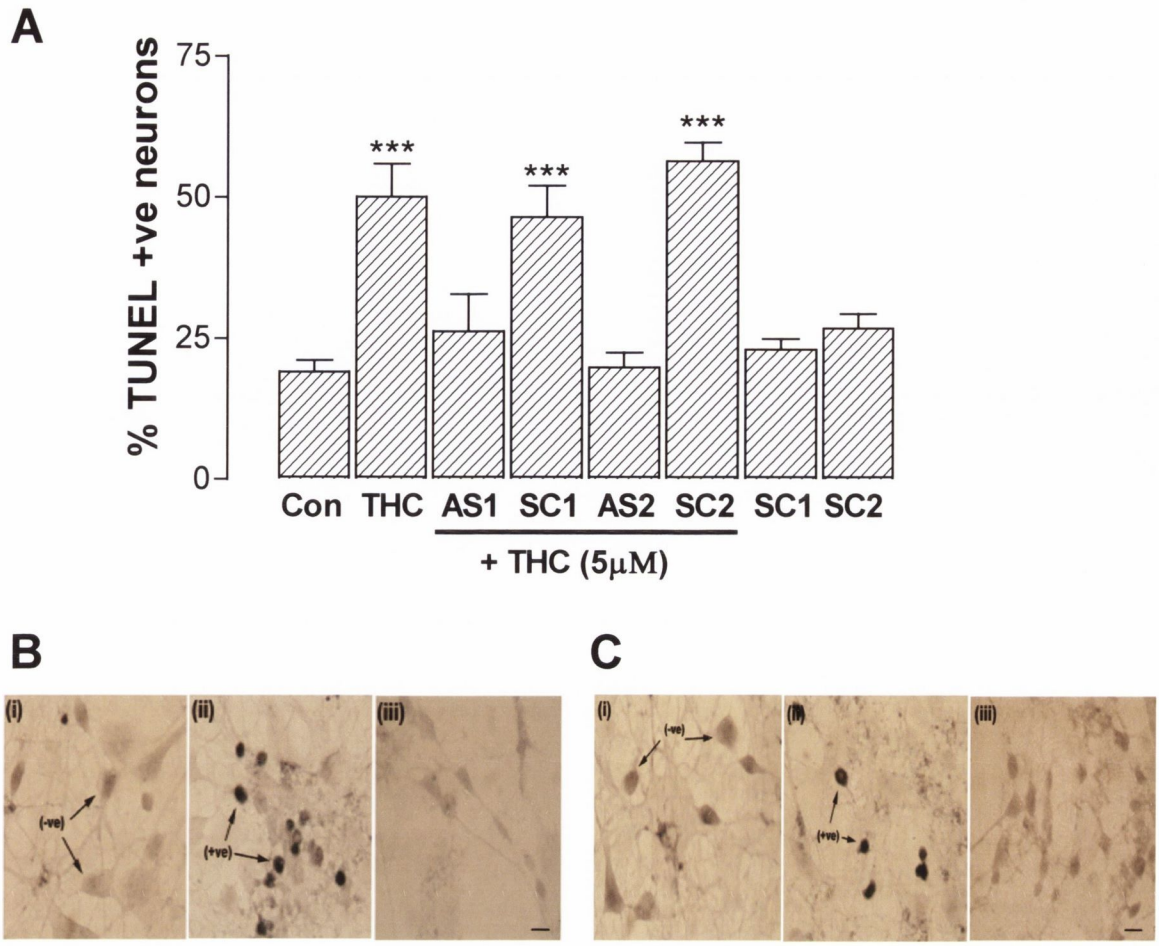

Figure 4.16: JNK1 and JNK2 isoforms are required for THC-induced DNA fragmentation

A: Exposure of neurons to THC (5μM) for 3hr significantly increased the percentage of TUNEL-positive neurons displaying fragmented DNA in the nucleus, relative to the control. Treatment with AS1 and AS2 for 48hr prior to THC treatment prevented the THC-induced increase in the level of DNA fragmentation. Results are expressed as mean ± SEM for 5 observations, ***$p<0.001$. Neurons treated with SC1 and SC2 for 48hr failed to prevent the THC-induced increase in the percentage of TUNEL-positive neurons. Exposure to SC1/2 alone was not neurotoxic.

B: Representative images of (i) control, (ii) THC-treated and (iii) THC/AS1-treated cortical neurons following TUNEL staining. Arrows indicate TUNEL-negative (-ve) and TUNEL-positive (+ve) cells. Scale bar is 25μm.

C: Representative images of TUNEL staining of (i) vehicle-treated, (ii) THC-treated and (iii) THC/AS2-treated cortical neurons. Scale bar is 25μm.

4.2.17 AS1 pre-treatment has no effect on THC-induced JNK2 activity

Since THC was found to increase JNK1 activity (at 5 min) prior to JNK2 activity (at 120 min), the use of antisense technology was employed to analyse whether JNK1 was involved upstream in the regulation of JNK2 activity (Figure 4.16). Neurons were treated with AS1 (2μM) for 48hr to downregulate JNK1 protein expression prior to exposure to THC (5μM) for 2hr. Treatment of cells with THC for 2hr significantly increased JNK2 phosphorylation to 31.1 ± 2.9 arbitrary units (mean ± SEM) compared to vehicle-treated neurons (21.9 ± 2.4; $p<0.05$, ANOVA, n=4 observations). Pre-treatment with AS1 failed to prevent the THC-induced significant increase in JNK2 activity (32.5 ± 1.9; $p<0.05$, ANOVA, n=4). Neurons treated with AS1 alone for 48hr showed a level of JNK2 activity comparable to that found in methanol vehicle-treated control neurons (23.9 ± 2.3). This data suggests that JNK1 does not occupy an upstream role in the regulation of JNK2 activity in the THC-induced apoptotic pathway. A sample western immunoblot demonstrating the activation of JNK2 following THC treatment, and the failure of AS1 to abolish this increase is shown in Figure 4.16B.

A

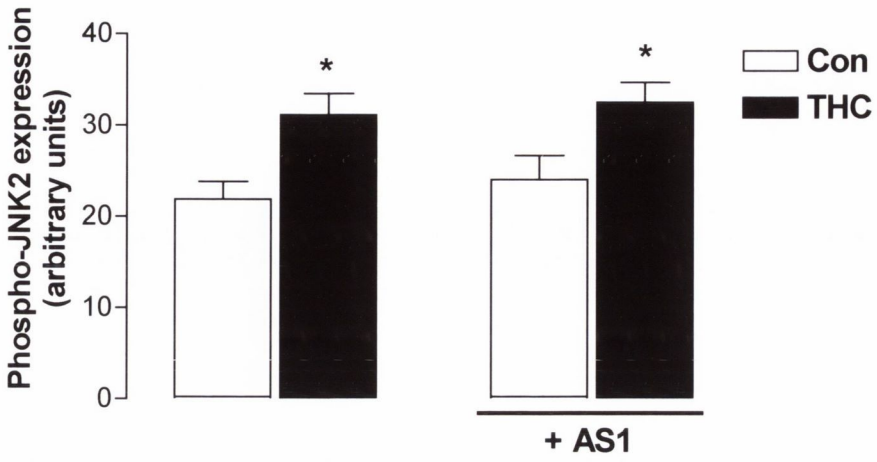

B

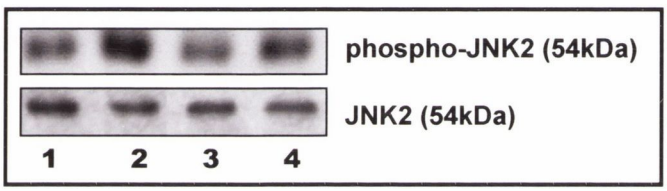

Figure 4.17: Activation of JNK1 is not upstream of THC-induced JNK2 activation

Neurons were pre-incubated with AS1 (2μM) for 48hr, treated with THC (5μM) for 2hr and analysed for phosphorylated JNK2 expression using western immunoblotting.

A: Exposure to AS1 failed to prevent the THC-induced increase in JNK2 activity observed at 2hr. Results are expressed as mean ± SEM for 4 observations, *$p<0.05$.

B: A sample western immunoblot showing that THC treatment for 2hr increases JNK2 activity (lane 2) as compared to vehicle-treated neurons (lane 1). The stimulatory effect of THC on JNK2 activity was not prevented by AS1 pre-treatment (lane 4). Exposure of cells to AS1 alone had no effect on JNK2 activity (lane 3). Also present is a sample immunoblot showing JNK2 total protein expression to confirm that changes in JNK2 activity are not due to changes in JNK2 protein expression.

4.3 Discussion

The aim of this study was to examine the ability of the central CB_1 cannabinoid receptor to couple to the JNK signalling pathway, and to assess the role of JNK in THC-induced neurotoxicity in cultured cortical neurons. THC was found to induce the activation of JNK1 and JNK2 at 5 min and 120 min respectively in a dose-dependent manner. The ability of THC to induce activation of both JNK isoforms was blocked by AM 251 and PTX, implicating the involvement of CB_1 cannabinoid receptors and G-protein subtypes, $G_{i/o}$, in this pathway. An antisense approach was used to delineate the contribution of JNK1 and JNK2 in THC-induced cell death. Treatment of cortical neurons with specific antisense oligonucleotides targeted to rat JNK1 or JNK2 mRNA effectively reduced the protein expression of the respective JNK isoform. Antisense oligonucleotide-mediated reduction of JNK1 and JNK2 protein expression prevented THC-induced caspase-3 activation and downstream DNA fragmentation. Data herein suggest that the CB_1 cannabinoid receptor is coupled to JNK in cortical neurons, and that both JNK1 and JNK2 are involved in the regulation of downstream effectors that are pertinent in the THC-induced apoptotic pathway.

In this study, the time course of THC-induced activation of JNK1 and JNK2 in cultured cortical neurons was assessed. It was found that THC increases JNK1 and JNK2 activity after 5 min and 120 min of treatment, respectively, using fluorescence microscopy and western immunoblotting. Half-maximal stimulation of JNK1 occurred at a lower dose of THC than JNK2, indicating that THC-induced JNK2 activation was more reluctant than JNK1 activation in our cell culture model. The punctate pattern of phospho-JNK immunostaining detected in the cytoplasm of cell cultures following exposure to THC may reflect an association of JNK with the mitochondria or cytoplasmic substrates such as p53, Bax and Bcl-2 (Buschmann *et al.*, 2001; Park *et al.*, 1997; Kang *et al.*, 1998). It has been established that JNK activation may occur early (Xia *et al.*, 1995) or late (Virdiee *et al.*, 1997) in apoptosis, and the finding that THC activates JNK1 and JNK2 within dissimilar timeframes suggests that the JNK isoforms may mediate different signals in cultured cortical neurons. A

potential function of JNK may be to initiate programmed cell death (Johnson *et al.*, 1996), and the data demonstrating the early activation of JNK1 (within 5 min), may reflect a role for JNK1 in regulating downstream apoptotic effectors. Furthermore, the finding that THC activates JNK2 at 120 min of treatment is consistent with the time point at which maximal neuronal cell death has been previously shown in cultured cortical neurons (Chapter 3). It is therefore possible that JNK2 activation may have occurred in response to DNA fragmentation, which is consistent with other studies (Ghahremani *et al.*, 2002). In addition, considering that JNK activity may be regulated by caspase-3 (Ozaki *et al.*, 1999; Hatai *et al.*, 2000) and we have previously shown that caspase-3 is activated as early as 30 min after exposure to THC in cortical neurons (Chapter 3), it is possible that JNK2 activity is modulated by caspase-3 in this system. In refute of this hypothesis, antisense-mediated downregulation of JNK2 reduced the THC-induced increase in caspase-3 activation and DNA fragmentation, suggesting that the late activation of JNK2 still plays a key role in the apoptotic cascade. It is of note that although JNK2 activity was increased at 120 min, a concomitant decline in JNK1 activity was observed at this time point. This suggests a functional interaction between JNK1 and JNK2 isoforms and this is supported by evidence that JNK2 negatively regulates JNK1 phosphorylation (Hochedlinger *et al.*, 2002). However, the finding that antisense-induced depletion of JNK1 failed to prevent the THC-induced increase in JNK2 activity, suggests that JNK1 does not occupy an upstream role in regulating JNK2 activity.

Although three JNK isoforms exists, encoded by three different genes *jnk1*, *jnk2* and *jnk3* (Gupta *et al.*, 1996), the detailed distribution of these isoforms, particularly during development, is largely unknown. However, it has been determined that the *jnk1* and *jnk2* genes are ubiquitously expressed, while the *jnk3* gene is selectively expressed in brain (Martin *et al.*, 1996). There is also evidence that the JNK3 isoform is involved in apoptotic signalling in the brain (Yang *et al.*, 1997). Unfortunately, JNK3 protein expression was virtually undetectable in our cell culture model, hence the relative contribution of the JNK1 and JNK2 isoforms to the apoptotic process was investigated. Carboni and colleagues (1998) have reported that JNK3 expression can vary in the cortex depending on developmental age, particularly during the early stages of

postnatal development which may account for the low levels of JNK3 expression found in cultured cortical neurons obtained from 1-day old rat pups.

The involvement of JNK cascades in the regulation of cell proliferation via G-proteins has been demonstrated (Coso *et al.*, 1996). Our previous studies have demonstrated that the toxic effects of THC involve a PTX sensitive G-protein (Campbell, 2001). This is consistent with evidence that links the central CB_1 receptor to activation of G-protein subtypes $G_{i/o}$ (Howlett, 1995). To date the role of G-proteins in neuronal cell death has not been completely clarified since PTX-sensitive G-proteins have been found to exert both pro-apoptotic (Farkas *et al.*, 1998) and anti-apoptotic (Jakob & Krieglstein, 1997) effects. However, data presented here demonstrate that coupling of the CB_1 receptor to PTX-sensitive G-proteins facilitates JNK activation in cortical cells.

JNK has the proclivity to regulate the expression of a number of cytoplasmic substrates, including the mitochondria-associated proteins Bax and Bcl-2 (Park *et al.*, 1997; Kang *et al.*, 1998; Lei *et al.*, 2002), and it has been shown that these proteins can act downstream of JNK in regulating the translocation of mitochondrial cytochrome *c* into the cytosol (Kang *et al.*, 1998). Once in the cytosol, cytochrome *c* complexes with a cytosolic factor designated as APAF-1, which in turn triggers the activation of the cysteine protease caspase-3, which contributes to the drastic morphological changes associated with apoptosis by disabling a number of key substrates (Zou *et al.*, 1997). We have previously shown that caspase-3 is central to the apoptotic cascade triggered by THC in cortical neurons (Chapter 3). Use of JNK pathway inhibitors has been demonstrated to inhibit caspase-3 activation in neuronal populations (Bozyczko-Coyne *et al.*, 2001) indicating that JNK can directly regulate caspase-3 activity. However, since commercially available JNK inhibitors such as CEP-1347 (Cephalon, USA), D-JNKI1 and SP600125 (Alexis Biochemicals, UK) prevent activity of the JNK1, JNK2 and JNK3 isoforms, it is impossible to determine the contribution of each isoform to the JNK mediated effects when using these inhibitors. Hence, to elucidate the respective roles of JNK1 and JNK2 in THC-induced caspase-3 activation, antisense technology was employed to temporarily downregulate JNK1 and JNK2 expression. This technique employs the use of specific phosphorothioated oligonucleotides

designed to bind specifically to a complementary sequence of mRNA on the target gene, causing a conformational obstacle for protein translation. As a result, the production of the target protein is temporarily inhibited without affecting the expression of other genes. The antisense oligonucleotides used in our experiments contain sulphur in the internucleotide phosphate linkages of the DNA backbone, making the antisense resistant to breakdown and increasing the half-life to greater than 48hr compared to 5 min in unmodified oligonucleotides. Antisense oligonucleotides are actively taken up by most eukaryotic cells by endocytosis and a putative receptor protein. In our experiments, cellular uptake of antisense was enhanced by pre-treating neurons with DOTMA/DOPE lipofectin reagent, a cationic lipid formulation that enables the efficient passage of antisense into the cell. Antisense uptake into cortical neurons was confirmed using FITC-labelled olignucleotides in conjunction with fluorescence microscopy. Although the antisense procedure can be technically difficult, we were successful in optimising conditions and were able to induce a selective antisense-mediated depletion of JNK1 and JNK2 in our cultured cell system, and hence to characterise the role of the respective JNK isoforms in the cannabinoid-induced cell death pathway. In neurons treated with JNK1 and JNK2 antisense oligonucleotides for 48hr, JNK1 and JNK2 protein expression was significantly reduced by 79% and 70%, respectively. Depletion of JNK1 and JNK2 prevented the THC-induced activation of caspase-3, indicating that both JNK1 and JNK2 isoforms are upstream of caspase-3 in the THC-induced apoptotic cascade.

Data presented in Chapter 3 showed that THC promotes degeneration of cultured cortical neurons in a time-dependent manner, with a maximal effect occurring 2-3hr post-treatment. The evidence presented here and by others (Rueda *et al.*, 2000; Sarker *et al.*, 2003), supports an early interaction between cannabinoids and JNK, indicating that JNK activation is an upstream event in the degenerative pathway. The finding that the downregulation of JNK1 and JNK2 using antisense technology effectively blocked THC-induced activation of caspase-3 and downstream DNA fragmentation indicates that both JNK1 and JNK2 are intricately involved in the transduction of THC-induced apoptotic signals. It is of particular note that depletion of either JNK1 or JNK2 isoforms completely abrogated the THC-induced caspase-3 activation and DNA

fragmentation. One would expect that since THC has the proclivity to couple to both JNK1 and JNK2, depletion of one isoform may result in THC-coupling to the remaining isoform to evoke caspase-3 activation and resultant DNA fragmentation. This clearly was not the case and our results may reflect an interaction between JNK1 and JNK2 with respect to the regulation of upstream effectors involved in caspase-3 activation. Indeed, a requirement for both JNK1 and JNK2 has been implicated in the phosphorylation of the p53 tumour suppressor protein (Buschmann *et al.*, 2001), a potential upstream event in the regulation of caspase-3 activity. Furthermore, it has been shown that inhibition of the active forms of both JNK1 and JNK2 prevents cytochrome *c* release from the mitochondria and activation of enzymes upstream of caspase-3 (Bozyczko-Coyne *et al.*, 2001). This study provides evidence of a requirement for both JNK1 and JNK2 in the THC-induced activation of caspase-3 and DNA fragmentation, and may reflect co-operativity between JNK1 and JNK2 in relation to these aspects of the cell death cascade.

To date, little is known about the role of JNK in THC signalling. Rueda and colleagues (2000) have found that JNK1/2 are activated within 5 min of THC treatment and that sustained JNK activation over 3 days of THC insult is required to induce cell death in glioma C6.9 cells, suggesting that the duration of JNK induction may be the determining factor in the cell death decision. This is supported by evidence that the duration of JNK activation determines its apoptotic characteristics (Chen *et al.*, 1996). Furthermore, these differences may reflect differential cellular responses of neuronal populations to THC, with cortical neurons being susceptible to early insult of cannabinoid exposure due to the differential activation of the JNK1/2 signalling cascades. We are aware that in the same study of Rueda and colleagues (2000) and in other studies (Sánchez *et al.*, 1998a), rat cortical primary neurons were not susceptible to a 3-5-day exposure to THC, which may reflect the lower dose of THC used in these studies. It has also been recently found that the endogenous cannabinoid, anandamide, induces apoptosis in PC12 cells, and this is accompanied by the early (within 30 min) activation of the JNK pathway and downstream cytochrome *c* translocation and caspase-3 activation (Sarker *et al.*, 2003). A very recent study by Do and co-workers (2004) has shown that THC induces apoptosis 2-3hr after exposure in dendritic cells independently of

JNK activation. However, the authors failed to examine levels of phosphorylated JNK expression at the 5 min and 2hr time points, the times at which JNK1 and JNK2 are induced in cultured cortical cells, respectively. Furthermore, THC does not affect JNK activity in hippocampal slices prepared from the adult rat brain (Derkinderen *et al.*, 2001). Thus, the effects of cannabinoids may be dependent on neuronal maturity with neonatal cultures being susceptible to JNK activation following cannabinoid challenge.

In addition to JNK, cannabinoids have been shown to regulate the other MAPK family members, p38 and ERK. Similar to JNK, the p38 MAPK family mediate cellular responses to stress, regulating cell responses to inflammatory and osmotic stress (Herlarr and Brown, 1999). In contrast, the ERK family members are involved in regulating cell growth and differentiation in response to growth factors and other intracellular messengers (Derkinderen *et al.*, 1999). However, there is also data showing that ERK mediates growth arrest and apoptosis in many cells (Grewal *et al.*, 1999). THC activates p38 MAPK in hippocampal slices (Derkinderen *et al.*, 2001) and in CHO cells transfected with CB_1 receptor cDNA (Rueda *et al.*, 2000). Furthermore, endogenous cannabinoids regulate p38 in hippocampal slices (Derkinderen *et al.*, 2001) and in PC12 cells (Sarker *et al.*, 2003). THC has also been shown to activate ERK in hippocampal slices (Derkinderen *et al.*, 2003) and in CHO cells transfected with CB_1 receptor cDNA (Bouaboula *et al.*, 1995). Endogenous cannabinoids have also been shown to regulate ERK phosphorylation, particularly in hippocampal slices (Derkinderen *et al.*, 2003), HL-60 cells (Kobayashi *et al.*, 2001a), MCF-7 cells (Melck et al., 1999) and in a human teratocarcinoma cell line (Milton, 2002). Overall, these findings show that MAPK signalling has a pertinent role in cannabinoid-induced cellular responses.

In summary, the results from this study demonstrate that treatment of cortical cultures with THC activates the JNK1 and JNK2 pathways via the CB_1 cannabinoid receptor and its associated G-protein. There was a distinct temporal pattern of JNK1 and JNK2 phosphorylation. An antisense approach revealed that both JNK1 and JNK2 are required for the activation of caspase-3 and DNA fragmentation in cultured cortical neurons. Overall, these findings demonstrate that THC activates JNK in neonatal cortical cells and that JNK

signalling is directly involved in regulating the apoptotic effects of THC in cultured cortical neurons.

Chapter 5

Determination of the involvement of p53 signalling in THC-induced apoptosis of cultured cortical neurons

5.1 Introduction

p53 is a nuclear phospho-protein that acts as a tumour suppressor providing a protective effect against tumour growth (Zörnig *et al.*, 2001). The p53 tumour suppressor gene is functionally inactivated in some 70% of human tumours (Evan *et al.*, 1995). Although various stress stimuli such as cytotoxic drugs, metabolite deprivation, physiological damage and heat shock lead to p53 activation, the primary stimulus for inducing p53 activation is DNA damage (Blatt and Glick, 2001). Depending on the stimulus and state of activation of the cell, the p53 protein plays an important role in the regulation of stress-mediated G1 cell cycle arrest after DNA damage to enable DNA repair, or to apoptosis (Levine, 1997). However, as most neurons are in a post-mitotic state (Miller *et al.*, 2000), the cell cycle regulatory function of p53 in neurons is absent. Hence, in post-mitotic neurons in which DNA fragmentation is occurring following a toxic insult, the regulation of p53 expression is associated with mechanisms underlying cellular apoptosis rather than recovery from the insult (Enokido *et al.*, 1996; Jordan *et al.*, 1997). Indeed, accumulating evidence now suggests that p53 is involved in neuronal apoptosis. For example, p53 induces apoptosis in post-mitotic hippocampal (Jordan *et al.*, 1997) and cortical neurons (Xiang *et al.*, 1996) and expression of the p53 protein is increased in neuronal tissue following experimental traumatic brain injury (Napieralski *et al.*, 1999). To date there is no evidence that cannabinoids regulate p53 expression. However, there is evidence that cannabinoids induce the regression of malignant gliomas *in vivo* (Sánchez *et al.*, 2001; Galve-Roperh *et al.*, 2000), one of the most malignant forms of cancer. These findings indicate that p53 signalling may be involved in canabinoid-induced effects in the brain.

Normal cellular p53 concentrations are low due to its short half-life and metabolic instability when inactivated (Evan and Littlewood, 1998). Although it is still largely unknown how p53 regulates growth arrest and apoptosis, it has been shown that phosphorylation plays an important role in regulating the biological activities of p53 (Herr and Debatin, 2001). The phosphorylation state of p53 is controlled by a large number of proteins including JNK, ERKs, casein kinases and PKC (Blatt and Glick, 2001). Although more than a dozen

phosphorylation sites have been mapped on p53 depending on the phosphorylating kinase and the stress-inducing stimulus, the phosphorylation of p53 on residue serine-15 at the p53 N terminus has been shown to be a critical signal required to regulate the p53 response to stress signals (Appella and Anderson, 2001). Stress-mediated phosphorylation of p53 at residue 15 disrupts its association with its negative regulator Mdm-2, preventing ubiquitin-mediated degradation of p53 (Shieh *et al.*, 1997). Once phosphorylated the stability of the p53 protein is increased, allowing it to act as a transcripition factor to enhance and repress genes involved in the apoptotic process. Indeed phosphorylation of p53 on serine-15 has been shown to occur following DNA damage (Siliciano *et al.*, 1997) and this is also associated with an increase in p53 transcriptional activities (Dumaz and Meek, 1999). This includes an up-regulation of the pro-apoptotic Bcl-2 family member, Bax, and repression of the anti-apoptotic Bcl-2 gene, both events favouring apoptosis in a mitochondrial-dependent manner (Miyashita and Reed, 1995). The Bax gene promoter region contains p53-binding sites (Mihara *et al.*, 2003) and it is generally assumed that Bax is involved in p53-induced cell death (Aloyz *et al.*, 1998; Culmsee *et al.*, 2002). Bax is an integral membrane protein bound to organelles or a soluble protein found in the cytoplasm (Wolter *et al.*, 1997). Following cell damage, Bax can translocate to the mitochondrial membrane (Wolter *et al.*, 1997) and regulate cytochrome *c* translocation to the cytosol (Kim *et al.*, 2001). In contrast to Bax, Bcl-2 is an anti-apoptotic mitochondria-associated protein that prevents Bax-induced cytochrome *c* translocation and resultant cell death by inhibiting Bax redistribution from the cytoplasm to the mitochondria (Murphy *et al.*, 2000). Interestingly, the pro-survival function of Bcl-2 can be switched off following phosphorylation of the Bcl-2 protein (Yamamoto *et al.*, 1999) and there is evidence that JNK (Yamamoto *et al.*, 1999) and p53 (Pucci *et al.*, 1999) have the proclivity to induce Bcl-2 phosphorylation. Despite the evidence that THC regulates Bcl-2 expression in splenocytes (Zhu *et al.*, 1998) there is no evidence to date to suggest that the mitochondria-associated proteins are involved in THC-induced apoptosis in neuronal tissue.

The experimental work in this chapter was therefore undertaken to determine if THC impacts on p53 signalling in cultured cortical neurons and to determine the contribution of p53 to THC-induced apoptosis. In addition to

determining the time-and dose-dependency of THC-induced regulation of p53 expression, the involvement of the CB_1 cannabinoid receptor in the THC-dependent regulation of p53 signalling was investigated. The contribution of Bax and Bcl-2, the pro- and anti-apoptotic substrates for JNK and p53 (Yamamoto *et al.*, 1999; Culmsee *et al.*, 2002; Miyashita and Reed, 1995), to this CB_1-sensitive transduction pathway was also examined. Downstream apoptotic consequences of p53 induction were investigated using the synthetic p53 inhibitor, pifithrin-α. This inhibitor acts by inhibiting p53 DNA binding activity thereby preventing the transcription of p53-responsive genes. The role of p53 in THC-induced Bax and phosphorylated Bcl-2 expression, caspase-3 activation and DNA fragmentation was assessed in neurons exposed to pifithrin-α prior to THC exposure.

5.2 Results

5.2.1 THC induces an increase in p53 protein expression in cultured cortical neurons

To determine if THC regulates the tumour suppressor protein, p53, cultured cortical neurons were exposed to THC (5μM) for various time points (5-180 min). Expression levels of total cellular p53 protein was measured by western immunoblot using a polyclonal antibody raised against the epitope mapping the carboxy terminus of p53, and band widths were quantified using densitometry (Figure 5.1A). Following THC exposure for 5 min, p53 expression was significantly increased from 82.1 ± 2.5 arbitrary units (mean ± SEM) in untreated cortical neurons to 102.8 ± 6.6 ($p<0.05$, ANOVA; n=5 observations). However, no change in total p53 expression was observed at 30 min (72.3 ± 8.5), 60 min (73.6 ± 4.6), 120 min (68.7 ± 12.3) and 180 min (65.1 ± 7.2). This indicates that THC induces an early increase in p53 protein expression. A sample immunoblot demonstrating the transient increase in p53 protein expression following THC exposure is shown in Figure 5.1B.

5.2.2 Effect of THC on p53 mRNA expression

To determine if the THC-induced increase in p53 protein expression at 5 min (Figure 5.1) was transcription-dependent, cultured cortical neurons were incubated with THC (5μM) for 5 min and levels of p53 mRNA expression assessed by PCR using gene-specific primers for p53 and β-actin (Figure 5.2). In methanol vehicle-treated cells, p53 mRNA expression was 13.2 ± 1.8 arbitrary units (mean ± SEM; n=4 experiments) and exposure to THC for 5 min had no effect on p53 mRNA expression (14.9 ± 1.9). In all experiments, p53 mRNA expression was normalised to the mRNA expression of the housekeeping gene, β-actin. This indicates that the THC-induced increase in p53 protein expression (Figure 5.1) is not dependent on increased transcription of the p53 gene. A sample agarose gel demonstrating that p53 mRNA expression was unaffected by THC exposure is shown in Figure 5.2B.

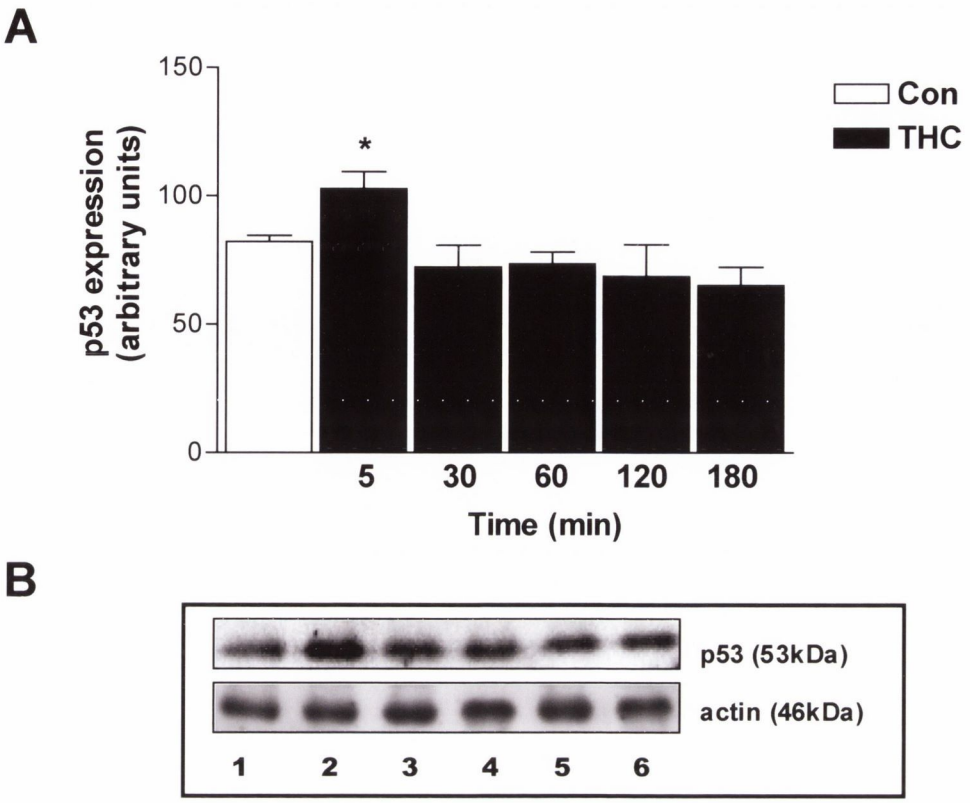

Figure 5.1: Time course of THC-induced increase in p53 protein expression

Cultured cortical neurons were treated with THC (5μM) for 5-180 min, cell protein was harvested and analysed for the expression levels of p53 using western immunoblot.

A: A significant increase in p53 expression was found following treatment with THC for 5 min. Exposure to THC for subsequent time points (30-180 min) had no effect on p53 expression. Results are expressed as mean ± SEM for 5 observations, *$p<0.05$.

B: A sample western immunoblot demonstrating the increase in p53 protein expression at 5 min of THC treatment (lane 2). Lane 1 represents untreated neurons, neurons treated with THC for 30 min (lane 3), 60 min (lane 4), 120 min (lane 5) and 180 min (lane 6). Actin immunoblot confirms equal protein loading.

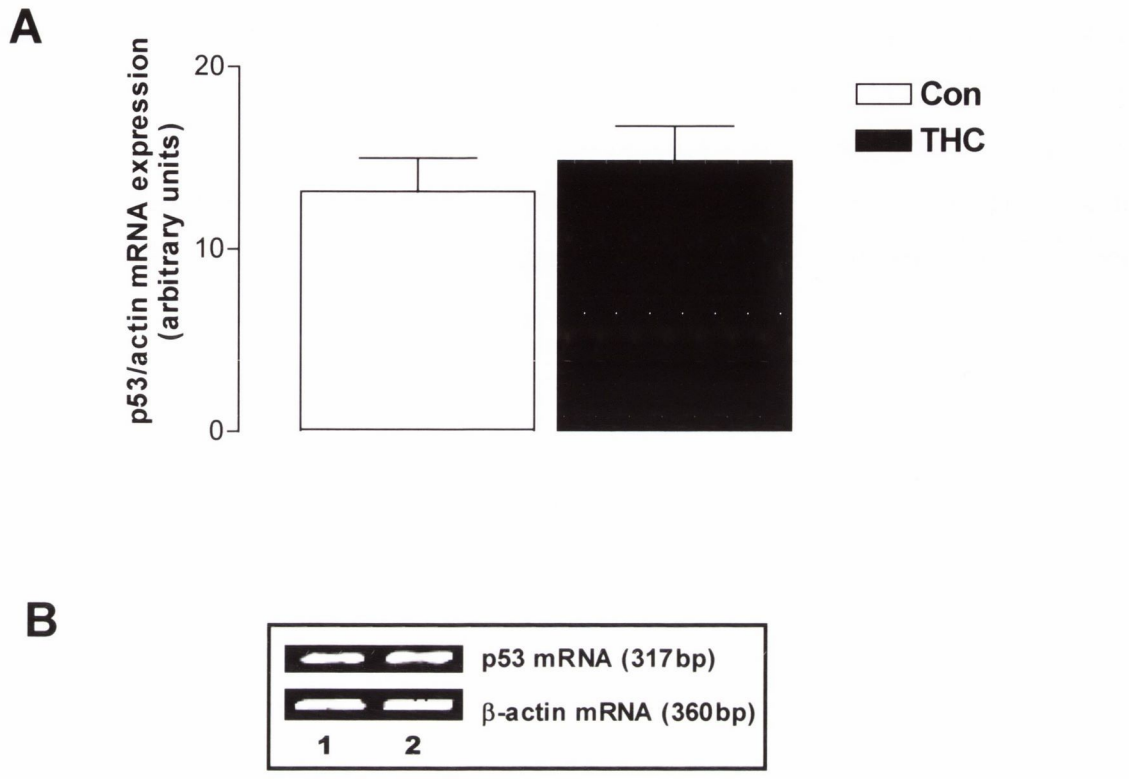

Figure 5.2: THC does not regulate transcription of p53 mRNA expression at 5 min

Cultured cortical neurons were treated with vehicle or THC (5μM) for 5 min and expression of p53 mRNA assessed using RT-PCR.

A: Exposure to THC for 5 min had no effect on p53 mRNA expression. Results are expressed as mean ± SEM for 4 observations.

B: Sample agarose gels demonstrating expression levels of p53 and β-actin mRNA at 5 min in control neurons (lane 1) and THC-treated cells (lane 2).

5.2.3 THC induces the phosphorylation of p53 at residue serine-15 in cultured cortical neurons

Since THC-induced increased p53 protein expression at 5 min was a transcription-independent event, it was determined if a post-translation modification in p53 accounted for the effects of THC on p53 protein expression. It has been shown that phosphorylation plays an important role in regulating the biological activities of p53 (Herr and Debatin, 2001). Once phosphorylated the stability of the p53 protein is increased allowing it to act as a transcripition factor to enhance and repress genes involved in the apoptotic process (Miyashita and Reed, 1995). Phosphorylation of p53 at residue serine-15, a key site for p53 stabilisation (Appella and Anderson, 2001) was assessed following treatment with THC (5μM) for 5 min using an antibody that detects endogenous levels of p53 only when phosphorylated at residue serine-15 (Figure 5.3). Following THC treatment for 5 min, phospho-p53^{ser15} expression was significantly increased from 25.6 ± 1.6 arbitrary units (mean ± SEM) in untreated cortical neurons to 35.9 ± 1.8 ($p<0.05$, ANOVA; n=5 observations). Phospho-p53^{ser15} expression was not changed in neurons exposed to THC for 30 min (23.1 ± 3.1), 60 min (26.6 ± 1.4), 120 min (23.1 ± 2.0) and 180 min (24.3 ± 3.5). This finding suggests that THC increases p53 protein expression at 5 min by stabilising the p53 protein via phosphorylation at residue serine-15. A sample immunoblot demonstrating the increase in phospho-p53^{ser15} expression following THC exposure for 5 min is shown in Figure 5.3B.

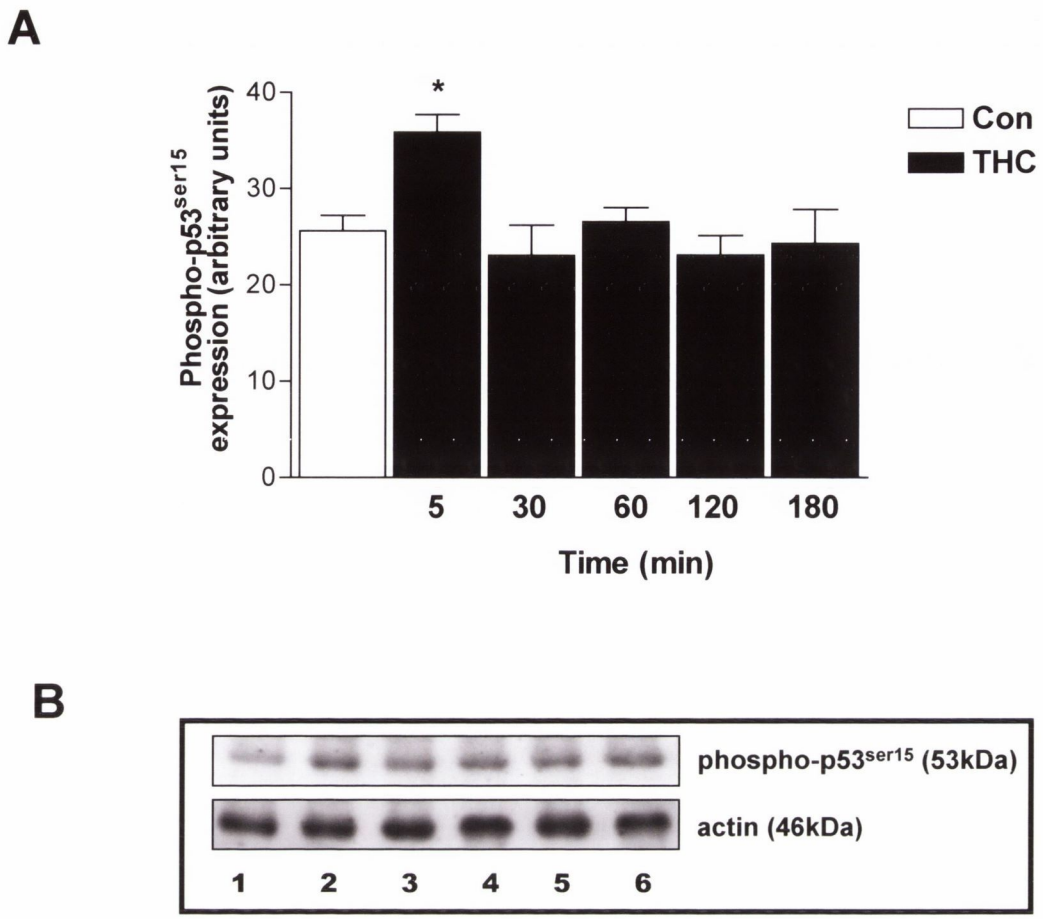

Figure 5.3: Time course of THC-induced phosphorylation of p53 at serine-15

Cultured cortical neurons were treated with THC (5μM) for 5-180 min, cell protein was harvested and analysed for the expression levels of p53 phosphorylated on serine-15 using western immunoblotting.

A: THC significantly increased phospho-p53^{ser15} expression at 5 min but not at subsequent time points (30-180 min). Results are expressed as mean ± SEM for 5 observations, *$p<0.05$.

B: A sample western immunoblot demonstrating the increase in phospho-p53^{ser15} expression at 5 min of THC treatment (lane 2) compared to untreated neurons (lane 1), neurons treated with THC for 30 min (lane 3), 60 min (lane 4), 120 min (lane 5) and 180 min (lane 6). Actin expression was monitored to ensure equal protein loading.

5.2.4 THC increases p53 protein expression in a dose-dependent manner

A dose-response analysis of the effects of THC on p53 protein expression at 5 min was performed to determine the concentration of THC required to evoke a significant increase in expression of the p53 protein (Figure 5.4). Neuronal cell cultures treated with vehicle for 5 min showed a level of p53 expression (10.3 ± 0.4 arbitrary units; mean ± SEM) comparable to that found in cells treated with 0.5μM THC (11.6 ± 1.1) for 5 min. However, p53 protein expression was significantly increased to 15.3 ± 1.9 when neurons were treated with 5μM THC for 5 min ($p<0.05$, ANOVA, n=5 observations). Similarly, a 50μM THC dose (15.3 ± 1.3) significantly increased p53 protein expression at 5 min ($p<0.05$, ANOVA, n=5). This finding indicates that the effect of THC on p53 regulation is reliant on THC concentration. A sample western immunoblot demonstrating the dose-dependency of the THC-induced increase in p53 protein expression is shown in Figure 5.4B.

5.2.5 Dose-dependency of THC-induced p53 phosphorylation on serine-15

Figure 5.5 demonstrates that phospho-p53^{ser15} expression was 29.5 ± 2.3 arbitrary units (mean ± SEM) in neurons treated with methanol vehicle for 5 min and was not significantly affected by treating neurons for 5 min with THC at a concentration of 0.5μM (31.9 ± 2.9). However, exposure of neurons to THC at a concentration of 5μM for 5 min significantly increased phospho-p53^{ser15} expression to 42.9 ± 4.4 ($p<0.05$, ANOVA, n=5 observations) and a 50μM THC dose significantly increased phospho-p53^{ser15} expression to 49.1 ± 7.0 ($p<0.05$, ANOVA, n=5). A sample western immunoblot demonstrating the dose-dependency of the THC-induced increase in phosphorylation of p53 on serine-15 is shown in Figure 5.5B.

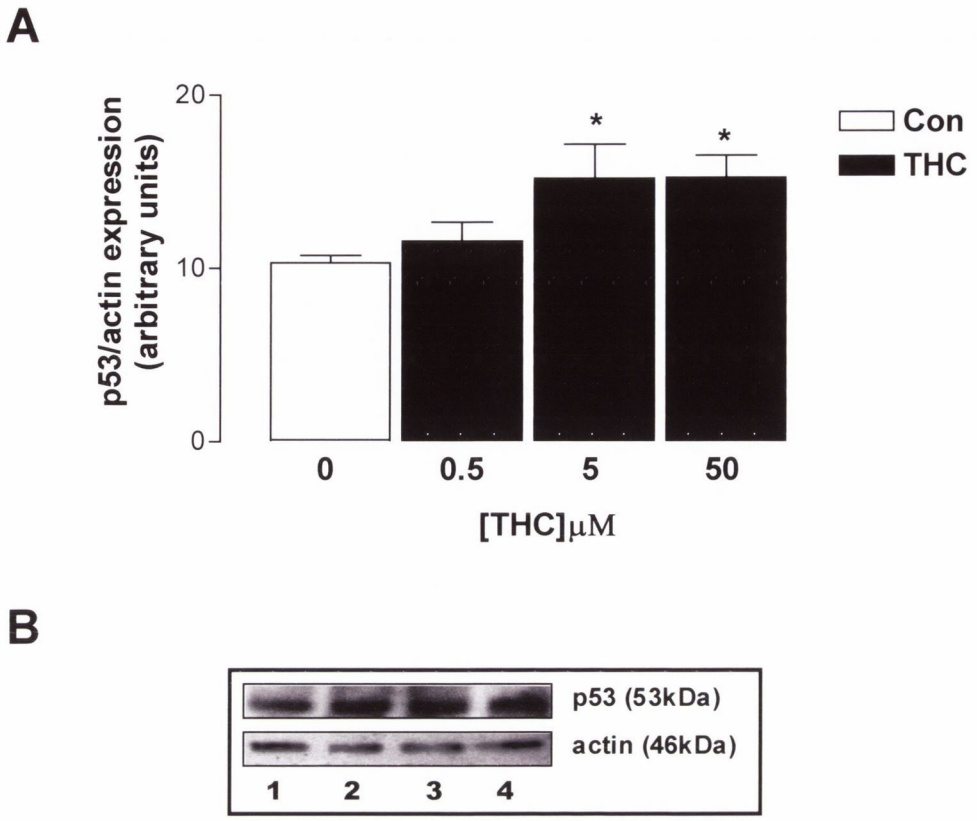

Figure 5.4: THC increases p53 expression in a dose-dependent manner

Cultured cortical neurons were treated with increasing concentrations of THC for 5 min. Following treatment cell protein was harvested and analysed for the expression levels of p53 protein using western immunoblot.

A: A significant increase in p53 protein expression was found following treatment with THC at concentrations of 5μM and 50μM. Exposure to THC at a concentration of 0.5μM had little effect on the expression levels of p53 protein. Results are expressed as mean ± SEM for 5 observations, *$p<0.05$.

B: A sample western immunoblot demonstrating that a 5 min treatment with THC at doses of 5μM (lane 3) and 50μM (lane 4) significantly increased p53 expression as compared to vehicle-treated neurons (lane 1). Exposure of cells to 0.5μM THC (lane 2) for 5 min had little effect on p53 expression. Actin expression confirms that changes in p53 protein expression are not due unequal protein loading.

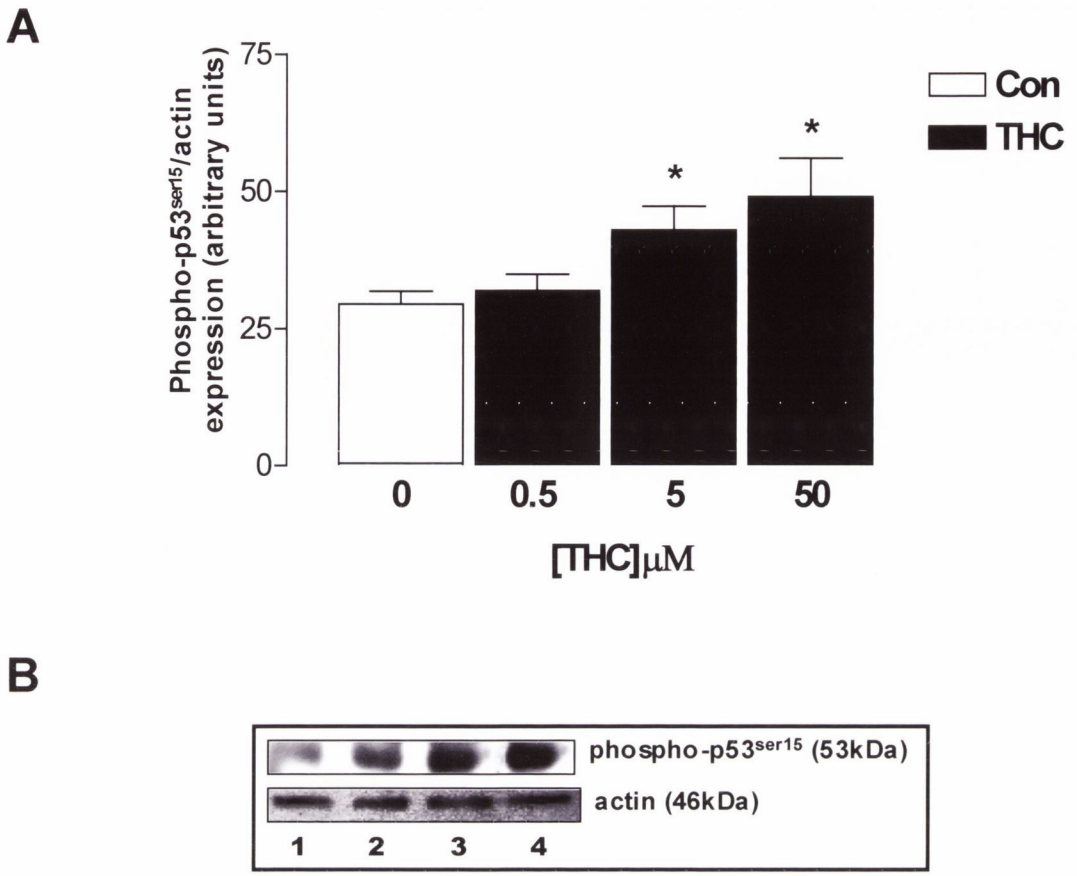

Figure 5.5: THC increases p53 phosphorylation on serine-15 in a dose-dependent manner

Cultured cortical neurons were treated with increasing concentrations of THC for 5 min. Following treatment cell protein was harvested and analysed for the expression levels of phospho-p53^{ser15} expression using western immunoblot.

A: THC significantly increased phospho-p53^{ser15} expression at 5 min at concentrations of 5μM and 50μM. Results are expressed as mean ± SEM for 5 observations, *$p<0.05$.

B: A sample western immunoblot showing that a 5 min treatment with 5μM THC (lane 3) and 50μM THC (lane 4) significantly increased phospho-p53^{ser15} expression as compared to vehicle-treated neurons (lane 1) and neurons exposed to 0.5μM THC (lane 2) for 5 min. Also present is a sample immunoblot showing actin expression for each treatment group.

5.2.6 THC increases p53 protein expression via the CB_1 cannabinoid receptor

To assess the role of the CB_1 receptor in coupling THC to p53 signalling, cultured cortical neurons were pre-treated with the selective CB_1 receptor antagonist AM 251 (10μM) for 30 min prior to THC (5μM) exposure for 5 min. AM 251 prevented the THC-induced increase in p53 protein expression at 5 min (Figure 5.6). In cortical neurons treated with methanol vehicle for 5 min p53 expression expression was 12.7 ± 11.3 arbitrary units (mean ± SEM) and this was significantly increased following THC treatment (5 min) to 19.0 ± 2.1 ($p<0.05$, ANOVA, n=4 observations). While pre-treatment with AM 251 alone had no effect on the level of p53 protein expression (10.2 ± 2.3), it prevented the THC-induced increase in p53 expression (13.3 ± 1.4) indicating that the modulation of p53 by THC is CB_1 receptor-dependent. A sample western immunoblot demonstrating the CB_1 receptor-dependent increase in p53 protein expression following THC treatment is shown in Figure 5.6B.

5.2.7 AM 251 pre-treatment prevents THC-induced phosphorylation of p53 on serine-15

To determine whether THC-induced p53 phosphorylation on serine-15 was reliant on signalling through the CB_1 cannabinoid receptor, cultured cortical neurons were again pre-treated with the selective CB_1 receptor antagonist AM 251 (10μM) prior to THC exposure (5μM) for 5 min (Figure 5.7). Phospho-$p53^{ser15}$ expression in vehicle-treated control neurons was significantly increased from 46.2 ± 2.0 to 59.4 ± 5.1 arbitrary units (mean ± SEM) following treatment with THC (5μM) for 5 min ($p<0.05$, ANOVA, n=6 observations). Exposure to AM 251 alone had no effect on phospho-$p53^{ser15}$ expression (40.2 ± 3.2) and it prevented the THC-induced increase in phospho-$p53^{ser15}$ expression (35.9 ± 7.4). This result indicates that the phosphorylation of p53 by THC is dependent on CB_1 receptor activation. A sample western immunoblot demonstrating the CB_1 receptor-dependent increase in phospho-$p53^{ser15}$ expression following THC treatment is shown in Figure 5.7B.

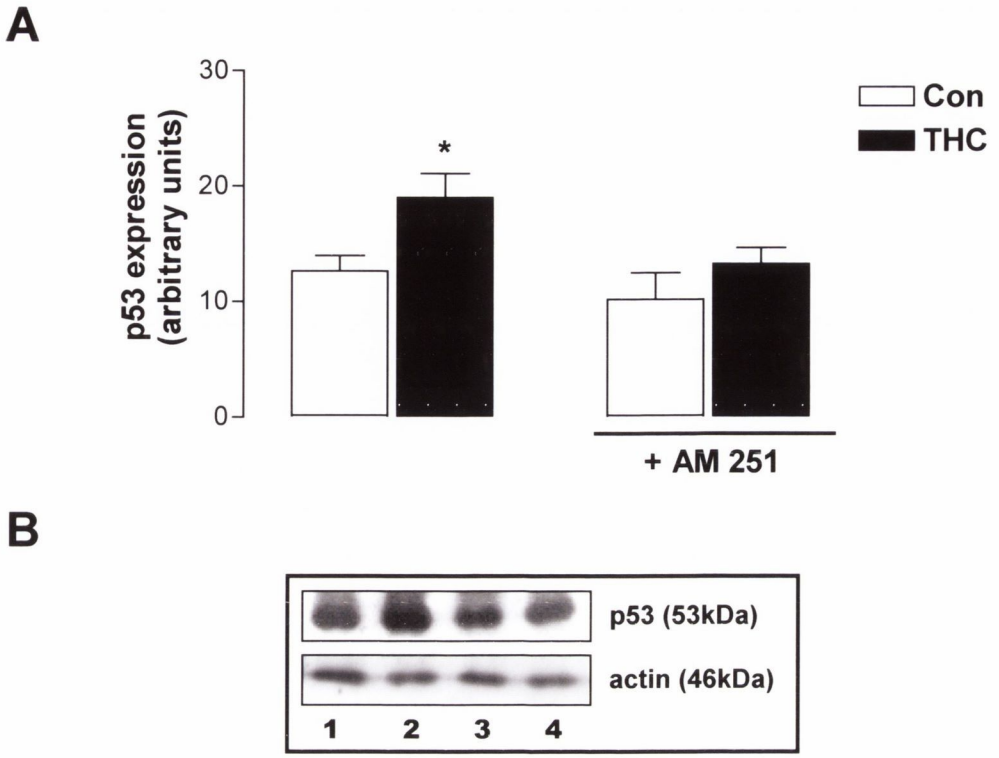

Figure 5.6: THC increases p53 protein expression via the CB_1 receptor

Cultured cortical neurons were pre-incubated with the CB_1 receptor antagonist AM 251 (10μM) for 30 min prior to THC (5μM) treatment for 5 min. Following treatment cell protein was harvested and analysed for the expression levels of p53 protein using western immunoblot.

A: Pre-incubation of cortical neurons with AM 251 prior to THC exposure abolished the THC-induced increase in p53 expression observed at 5 min. Results are expressed as mean ± SEM for 4 observations, *$p<0.05$.

B: A sample western immunoblot demonstrating the increase in p53 protein expression after 5 min of THC treatment in lane 2 compared to p53 expression in control neurons (lane 1). While AM 251 had no effect on p53 protein expression (lane 3), it abolished the ability of THC to increase p53 expression (lane 4). Also present is a sample immunoblot showing actin loading controls.

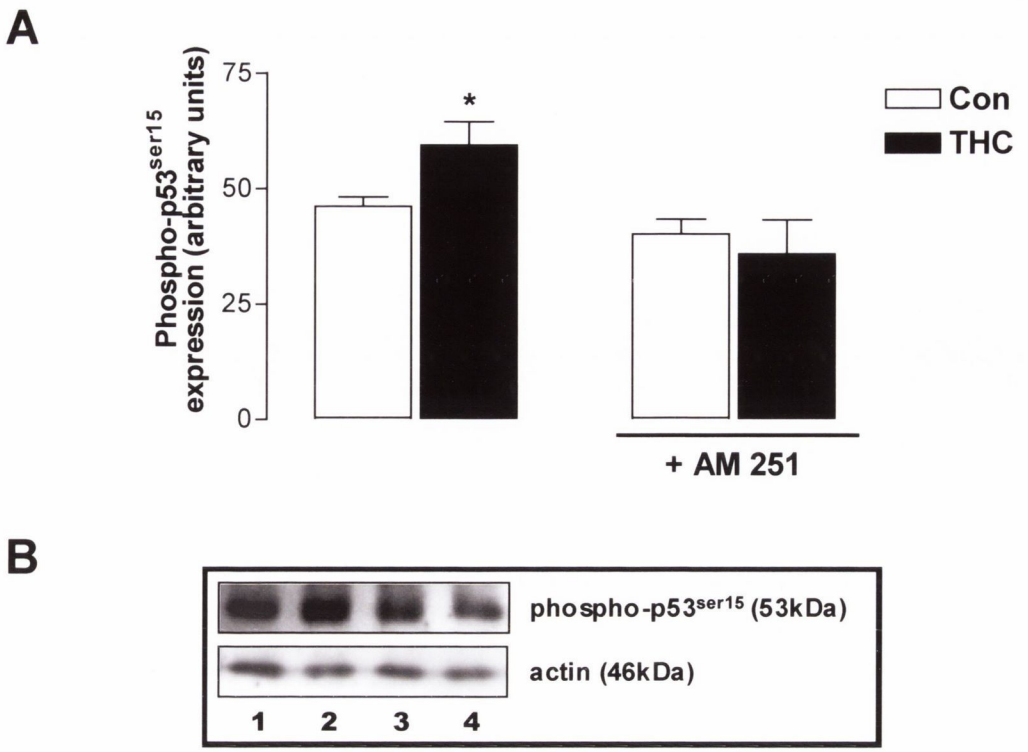

Figure 5.7: THC increases p53 phosphorylation on serine-15 via the CB_1 receptor

Cultured cortical neurons were pre-incubated with the CB_1 receptor antagonist AM 251 (10μM) for 30 min prior to THC (5μM) treatment for 5 min. Neuronal protein was harvested and analysed for phospho-p53^{ser15} expression using western immunoblot.

A: Pre-incubation of cortical neurons with AM 251 prior to THC exposure abolished the THC-induced increase in phospho-p53^{ser15} expression observed at 5 min. Results are expressed as mean ± SEM for 6 observations, *$p<0.05$.

B: Sample western immunoblots demonstrating phospho-p53^{ser15} and actin expression. THC increased phospho-p53^{ser15} expression after 5 min of THC treatment in lane 2 compared to phospho-p53^{ser15} expression in control neurons (lane 1). AM 251 abolished the ability of THC to increase phospho-p53^{ser15} (lane 4). Furthermore, AM 251 alone had no effect on phospho-p53^{ser15} expression (lane 3).

5.2.8 THC increases cytosolic Bax protein expression in cultured neurons

Although the mechanism of p53-mediated apoptosis is poorly understood there is evidence that p53 induces apoptosis by altering the expression of the Bcl family of mitochondria-associated proteins (Marchenko *et al.*, 2000). Furthermore, p53 has been shown to up-regulate the transcription of the pro-apoptotic protein, Bax (Miyashita and Reed, 1995). In this study, expression levels of cytosolic Bax were measured by western immunoblot using an antibody that recognises amino acids 43-61 of Bax in cell cultures treated with THC (5μM) for 60 min and 120 min (Figure 5.8). THC significantly increased cytosolic Bax expression from 11.0 ± 1.2 arbitrary units (mean ± SEM) in vehicle-treated control neurons to 16.7 ± 2.1 following 60 min of THC exposure ($p<0.05$, Student's *t*-test, n=5 experiments). Furthermore, THC treatment for 120 min significantly increased cytosolic Bax expression from 9.3 ± 2.0 to 19.0 ± 2.2 ($p<0.01$, Student's *t*-test, n=5). This demonstrates that the pro-apoptotic mitochondria-associated protein, Bax, is involved in THC neuronal signalling. Figure 5.8B shows sample western immunoblots demonstrating THC-induction of cytosolic Bax protein expression at 60 and 120 min of THC exposure.

5.2.9 THC increases Bax mRNA expression

To determine if the increase in cytosolic Bax protein expression (Figure 5.8) was a consequence of THC-induced regulation of transcription of the bax gene, Bax mRNA expression was assessed by RT-PCR following THC (5μM) treatment for 60 min using gene-specific primers for Bax and β-actin (Figure 5.9). Bax mRNA expression was assessed at 60 min of THC exposure as this was a time point at which THC significantly increased Bax protein expression (Figure 5.8). In vehicle-treated control neurons at 60 min, Bax mRNA expression was 8.5 ± 0.3 arbitrary units (mean ± SEM). Incubation of cortical cells with THC for 60 min significantly increased Bax mRNA expression to 10.8 ± 0.9 ($p<0.05$, Student's *t*-test, n=5 experiments). This indicates that THC regulates Bax expression in neurons at a transcriptional level, increasing the transcription of the *bax* gene, which accounts for the corresponding increase in cytosolic Bax protein expression at 60 min of THC exposure. Bax mRNA

expression was normalised to the mRNA expression of the housekeeping gene, β-actin. A sample agarose gel demonstrating the modulatory effect of THC on Bax mRNA expression is shown in Figure 5.9B.

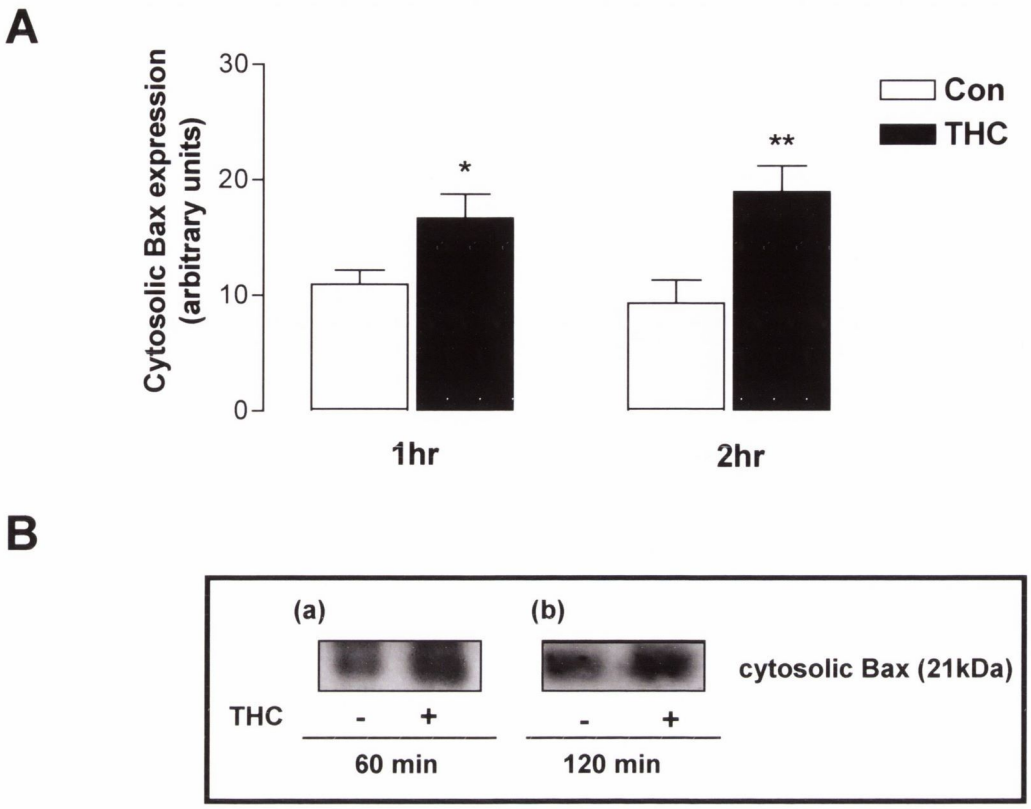

Figure 5.8: THC increases cytosolic Bax protein expression at 60 and 120 min

Cultured cortical neurons were exposed to THC (5μM) or vehicle for 60 min or 120min. Following treatment cytosolic proteins were assessed for the expression of Bax protein by western immunoblotting.

A: THC exposure for 60 and 120 min significantly increased cytosolic Bax protein expression. Results are expressed as mean ± SEM for 5 observations, *$p<0.05$, **$p<0.01$.

B: Sample immunoblots demonstrating cytosolic Bax protein expression. Neurons were treated with THC for 60 min (panel a) and 120 min (panel b).

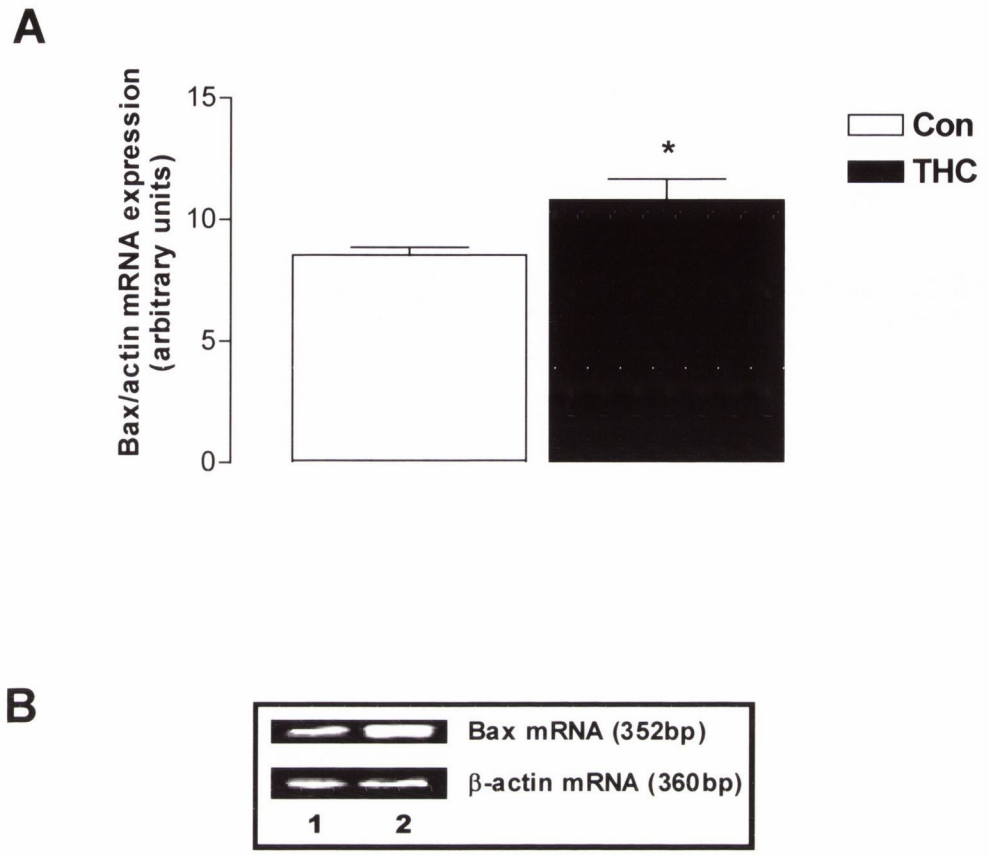

Figure 5.9: THC increases Bax mRNA expression

Cultured cortical neurons were treated with vehicle or THC (5μM) for 60 min and expression of Bax mRNA assessed using RT-PCR.

A: Exposure to THC for 60 min significantly increased Bax mRNA expression. Results are expressed as mean ± SEM for 5 observations, *$p<0.05$.

B: Agarose gels showing Bax and β-actin mRNA expression levels at 60 min in control neurons (lane 1) and THC-treated cells (lane 2).

5.2.10 THC-induced cytosolic Bax expression is dependent on the CB_1 receptor

In this experiment, expression levels of cytosolic Bax were measured following pre-treatment with the selective CB_1 receptor antagonist AM 251 (10μM) for 30 min and exposure to THC (5μM) for 2hr. Figure 5.10 demonstrates that in control cells cytosolic Bax protein expression was 23.8 ± 4.9 arbitrary units (mean ± SEM) and this was significantly increased following THC treatment for 120 min to 50.2 ± 6.4 ($p<0.01$, ANOVA, n=5 observations). AM 251 alone had no effect on cytosolic Bax expression (15.4 ± 4.9), however it prevented the THC-induced increase in cytosolic Bax expression (22.7 ± 6.0). This indicates that THC induces an increase in cytosolic Bax protein expression by activating the CB_1 receptor. A sample western immunoblot demonstrating the CB_1-dependent increase in THC-induced Bax protein expression is shown in Figure 5.10B.

5.2.11 THC has no effect on mitochondrial Bax expression

There is evidence that following a death signal, a dramatic change occurs in the intracellular localisation of Bax, specifically, Bax moves from the cytosol to the mitochondrial membrane (Wolter *et al.*, 1997; Gross *et al.*, 1998). Once at the mitochondria, there is evidence that Bax inserts in the mitochondrial membrane and orchestrates a programme of mitochondrial dysfunction that results in apoptosis (Gross *et al.*, 1998). In this study, expression levels of mitochondrial Bax protein were measured by western immunoblot using an antibody that recognises amino acids 43-61 of Bax in cell cultures treated with THC (5μM) for 120 min (Figure 5.11). Neurons were also pre-treated with AM 251 (10μM) prior to THC exposure to determine if the effect of THC on mitochondrial Bax expression was CB_1 cannabinoid receptor mediated. In methanol vehicle-treated cells, mitochondrial Bax protein expression was 24.2 ± 0.3 arbitrary units (mean ± SEM; n=5 experiments) and exposure to THC for 120 min had no effect on Bax protein expression at the mitochondria (19.7 ± 4.6). Neurons treated with AM 251 alone (21.0 ± 0.8) and THC in the presence of AM 251 (20.6 ± 3.3) for 120 min displayed a level of mitochondrial Bax protein expression comparable to the control cells. This

demonstrates that THC does not induce Bax translocation to the mitochondria in cortical neurons and that the effect of THC on Bax expression is restricted to the cytoplasm. Figure 5.11B shows a sample immunoblot demonstrating the effects of THC on mitochondrial Bax protein expression at 120 min.

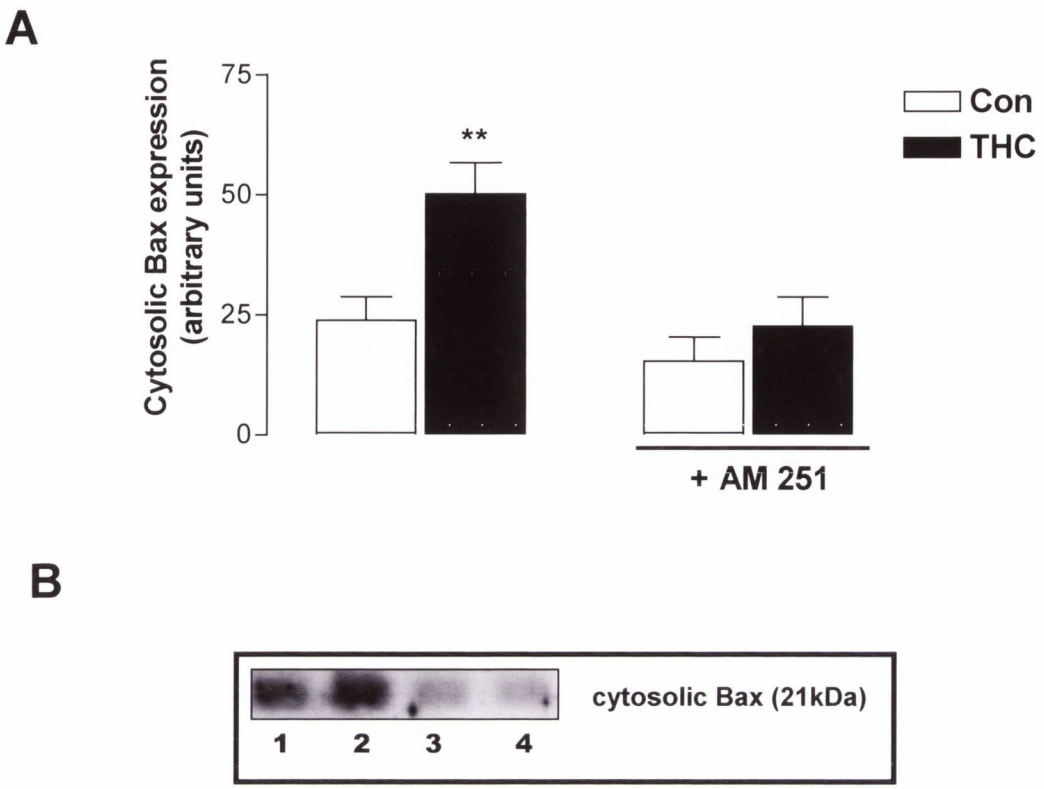

Figure 5.10: THC increases cytosolic Bax protein expression via the CB_1 receptor

Neurons were pre-incubated with AM 251 (10μM) for 30 min, treated with THC (5μM) for 120 min and analysed for the expression levels of cytosolic Bax protein using western immunoblotting.

A: Exposure to AM 251 abolished the THC-induced increase in Bax expression. Results are expressed as mean ± SEM for 5 observations, **$p<0.01$.

B: A sample western immunoblot showing that THC treatment for 120 min increases cytosolic Bax protein expression (lane 2) as compared to vehicle-treated neurons (lane 1). The stimulatory effect of THC on Bax expression was prevented by AM 251 (lane 4). Exposure of cells to AM 251 alone had no effect on Bax expression (lane 3).

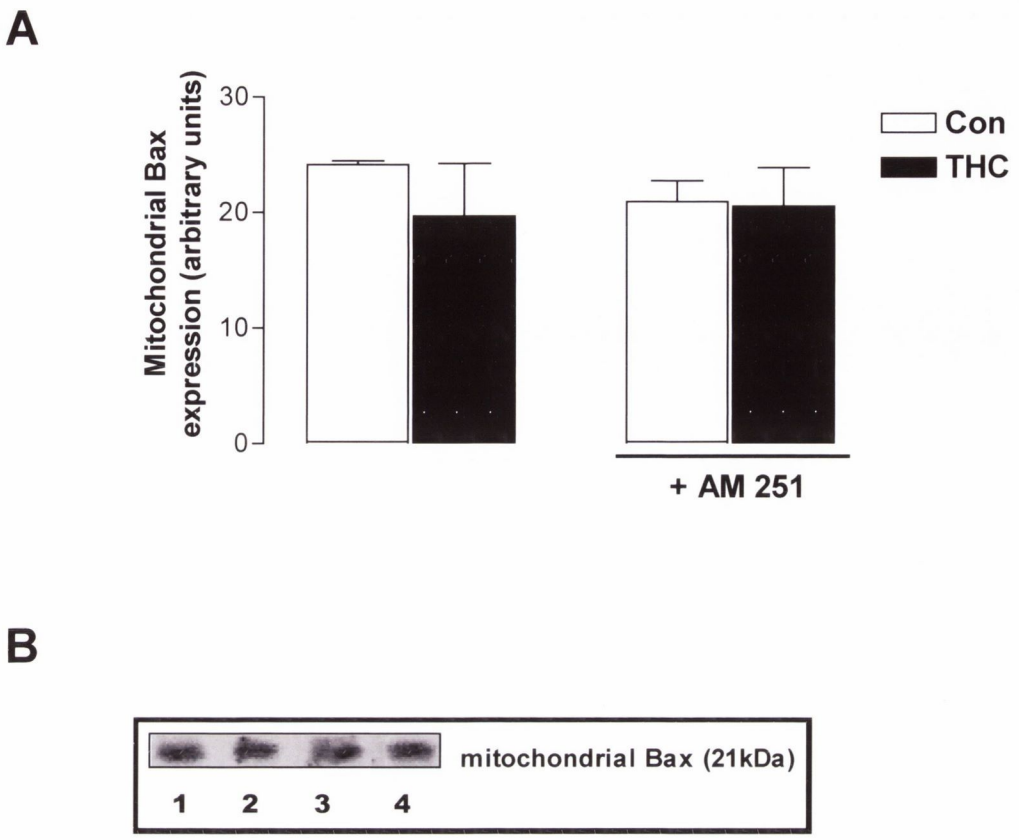

Figure 5.11: Effect of THC on mitochondrial Bax protein expression

Cortical neurons were pre-treated with AM 251 (10μM) for 30 min, exposed to THC (5μM) for 120 min and analysed for the expression levels of mitochondrial Bax protein by western immunoblotting.

A: THC had no effect on mitochondrial Bax protein expression at 120 min. Results are expressed as mean ± SEM for 5 observations.

B: A sample western immunoblot showing equal expression levels of mitochondrial Bax protein in vehicle-treated neurons (lane 1), THC-treated (lane 2), AM 251-treated (lane 3) and AM 251+THC-treated (lane 4) cortical neurons.

5.2.12 THC-induced Bax protein expression is p53-dependent

To determine if p53 is involved in THC-induced apoptosis by regulating the expression of the pro-apoptotic protein, Bax, cultured neurons were treated with the p53 inhibitor, pifithrin-α (100nM) prior to THC (5μM) exposure for 120 min, a time point at which THC-induces an increase in Bax protein expression (Figure 5.8). Expression levels of Bax protein were then measured by western immunoblot (Figure 5.12A) and by determining the level of Bax expression using Bax fluorescence immunocytochemistry in stained cells (Figure 5.12C). Figure 5.12A shows that Bax expression in vehicle-treated control neurons was significantly increased from 1.2 ± 0.1 to 1.4 ± 0.1 arbitrary units (mean ± SEM) following treatment with THC for 120 min ($p<0.05$, ANOVA, n=5 observations). Exposure to pifithrin-α alone had no effect on Bax expression (1.1 ± 0.1) and it prevented the THC-induced increase in Bax expression (1.0 ± 0.1). A sample western immunoblot illustrating the p53-dependent increase in Bax protein expression following THC treatment is shown in Figure 5.12B.

The role of p53 in THC-mediated regulation of Bax expression was also assessed by fluorescence immunocytochemistry in fixed cell cultures (Figure 5.12C). Bax immunofluorescence was detected using a monoclonal primary antibody raised against amino acids 1-171 of Bax, a secondary antibody and extra-avidin-conjugated FITC. Cells were viewed by fluorescent microscopy at an excitation wavelength of 490nm. In vehicle-treated neurons, Bax immunoreactivity was detectable (Figure 5.12C(i)), indicating a tonic level of Bax expression in cell cultures. However, in cultures treated with THC for 120 min (Figure 5.12C (ii)) a higher intensity of Bax immunoreactivity was observed throughout the neurons. Bax expression in neurons treated with pifithrin-α alone (Figure 5.12C (iii)) and THC in the presence of pifithrin-α (Figure 5.12C (iv)) display a level of Bax expression comparable to vehicle-treated neurons. These findings indicate that the THC-induced increase in Bax protein expression at 120 min is dependent on p53 signalling.

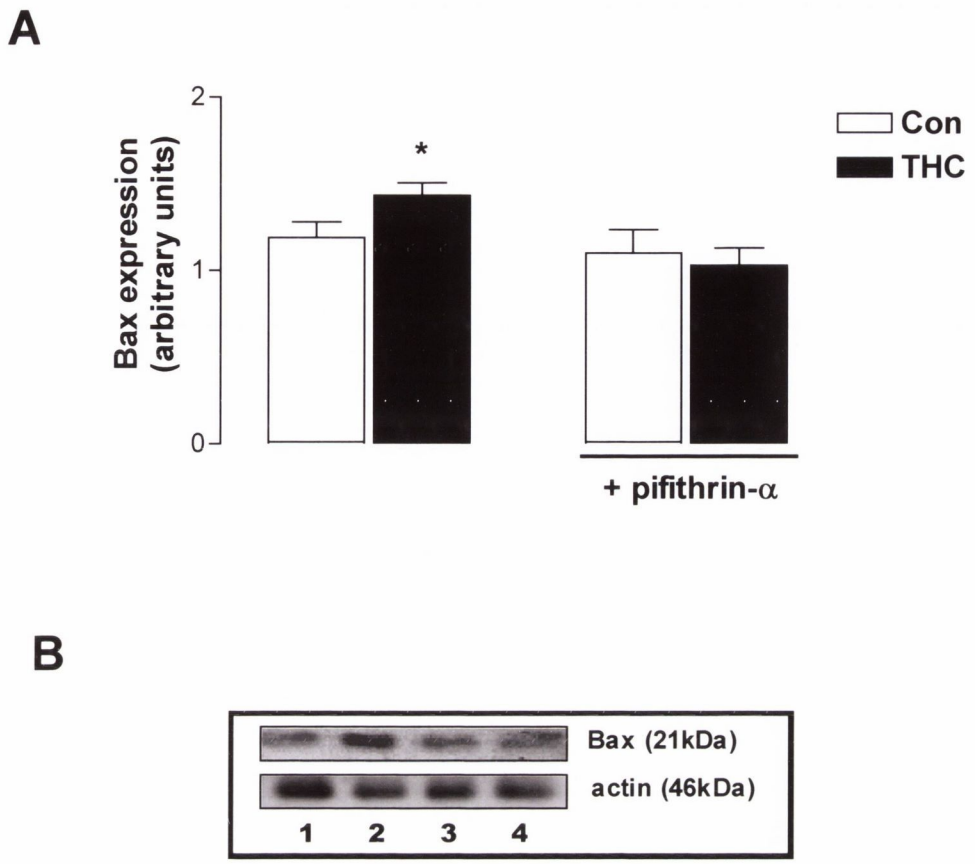

Figure 5.12: THC increases Bax protein expression via p53

Cultured cortical neurons were pre-incubated with the p53 inhibitor pifithrin-α (100nM) for 60 min prior to THC (5μM) treatment for 120 min. Following treatment cell protein was harvested and analysed for the expression levels of Bax protein using western immunoblot.

A: Pre-incubation of cortical neurons with pifithrin-α prior to THC exposure abolished the THC-induced increase in Bax expression observed at 120 min. Results are expressed as mean ± SEM for 5 observations, *$p<0.05$.

B: A sample western immunoblot demonstrating the increase in Bax protein expression after 120 min of THC exposure (lane 2) compared to Bax expression in control neurons (lane 1). While pifithrin-α had no effect on Bax protein expression (lane 3), it abolished the ability of THC to increase Bax expression (lane 4). Also present is a sample immunoblot showing actin loading controls.

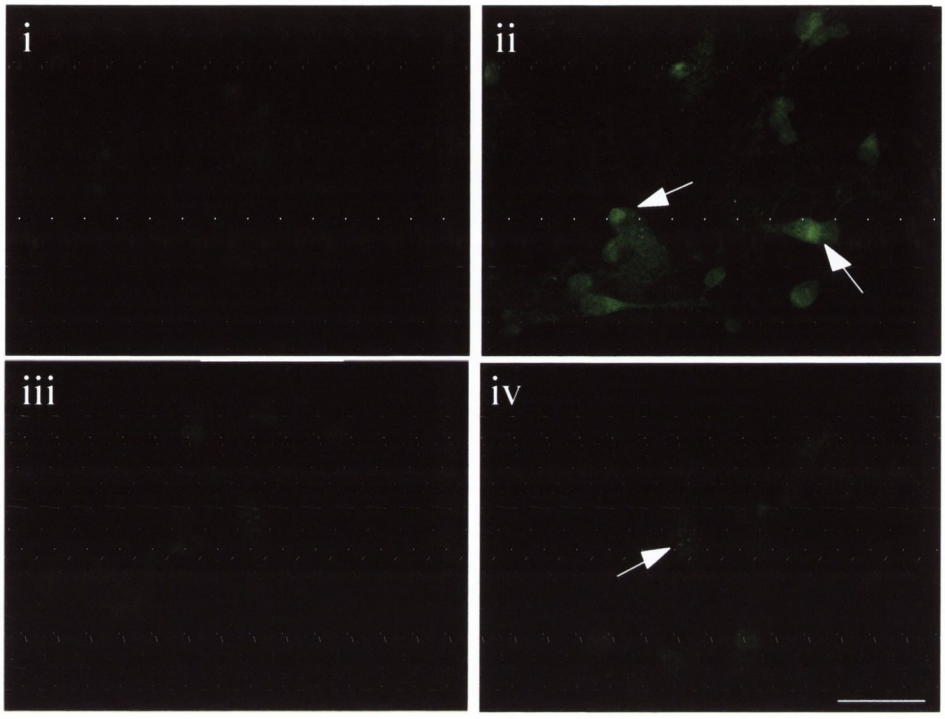

C: Cortical cultures were pre-incubated with pifithrin-α (100nM) for 60 min prior to THC (5μM) treatment for 120 min. Cells were fixed and the expression of the Bax assessed by immunofluorescence. In (i) control neurons, Bax immunoreactivity is apparent in neuronal subpopulations. Neurons exposed to (ii) THC for 120 min display intense Bax immunostaining. Bax expression in (iii) pifithrin-α-treated cells and (iv) pifithrin-α+THC-treated neurons is moderate. Arrows indicate neurons displaying Bax immunoreactivity. Scale bar is 50μm.

5.2.13 THC induces Bcl-2 phosphorylation in cultured cortical neurons

In addition to the evidence suggesting that p53 induces apoptosis by up-regulating the transcription of the pro-apoptotic protein, Bax (Miyashita and Reed, 1995), there is evidence linking p53 and JNK kinases to neuronal apoptosis by altering the expression of other members of the Bcl family of mitochondria-associated proteins (Pucci *et al.*, 1999; Mielke and Herdegen, 2000). In contrast to Bax, the anti-apoptotic protein, Bcl-2, represses cell death (Korsmeyer, 1999). However, p53 and JNK kinases can antagonise the function of Bcl-2 by phosphorylation, inhibiting its pro-survival function (Pucci *et al.*, 1999; Yamamoto *et al.*, 1999). To determine whether THC induces the phosphorylation of Bcl-2, cultured cortical neurons were exposed to THC (5μM) for various time points (5-120 min). Expression levels of the phosphorylated form of Bcl-2 were measured by western immunoblot using an anti-phospho-Bcl-2 antibody, and band widths were quantified using densitometry (Figure 5.13). No change in Bcl-2 phosphorylation was observed at 5 min (78.9 ± 13.1 arbitrary units; mean ± SEM), 30 min (74.8 ± 11.7) and 60 min (105.0 ± 14.4) when compared to untreated cortical cells (74.1 ± 3.6). However, following THC exposure for 120 min, Bcl-2 phosphorylation was significantly increased to 170.0 ± 23.3 ($p<0.05$, ANOVA; n=6 observations). This indicates that THC possibly inhibits the pro-survival function of Bcl-2 via phosphorylation. A sample immunoblot demonstrating the increase in phospho-Bcl-2 expression following THC exposure for 120 min is shown in Figure 5.13B.

A

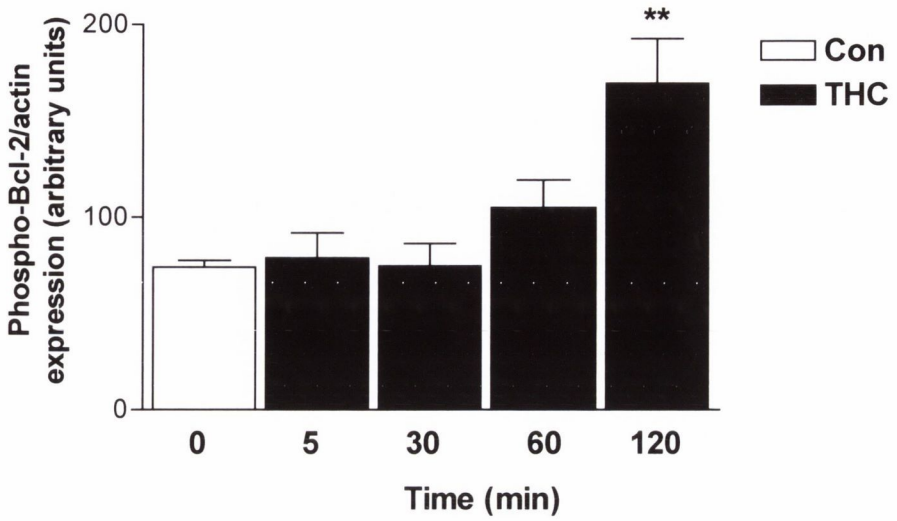

B

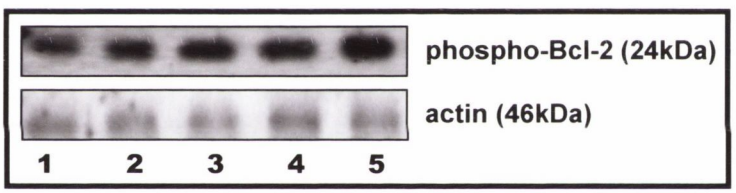

Figure 5.13: Time course of THC-induced phosphorylation of Bcl-2

Cultured cortical neurons were treated with THC (5μM) for 5-120 min, cell protein was harvested and analysed for the expression levels of phosphorylated Bcl-2 protein using western immunoblot.

A: THC significantly increased phospho-Bcl-2 expression at 120 min but not at earlier time points (5-60 min). Results are expressed as mean ± SEM for 6 observations, **$p<0.01$.

B: A sample western immunoblot demonstrating the increase in phospho-Bcl-2 expression at 120 min of THC treatment (lane 5) compared to untreated neurons (lane 1), neurons treated with THC for 5 min (lane 2), 30 min (lane 3) and 60 min (lane 4). Actin expression was monitored to ensure equal protein loading.

5.2.14 THC-induced phosphorylation of Bcl-2 is p53-dependent

Phosphorylation of the anti-apoptotic protein, Bcl-2, inhibits its pro-survival function (Yamamoto *et al.*, 1999). It is the decreasing ratio of active Bcl-2 to Bax at the mitochondrial membrane that determines cytochrome *c* translocation to the cytosol and the advancement of the cell death cascade (Korsmeyer *et al.*, 1995). Hence, to determine if p53 is involved in regulating the expression of the phosphorylated form of the Bcl-2 protein, cultured cortical neurons were treated with pifithrin-α (100nM) prior to THC (5μM) exposure for 120 min (Figure 5.14). In cortical neurons treated with methanol vehicle for 120 min, phosphorylated Bcl-2 protein expression was 1.1 $\pm$ 0.1 (arbitrary units; mean $\pm$ SEM) and this was significantly increased following THC treatment (120 min) to 1.5 $\pm$ 0.1 ($p<0.05$, ANOVA, n=6 observations). While pre-treatment with pifithrin-α alone had no effect on the level of phosphorylated Bcl-2 protein expression (0.9 $\pm$ 0.1), it prevented the THC-induced increase in p53 expression (1.2 $\pm$ 0.1), indicating that the modulation of Bcl-2 phosphorylation by THC is p53-dependent. A sample immunoblot showing the p53-dependent increase in phosphorylated Bcl-2 protein expression following THC exposure is shown in Figure 5.14B.

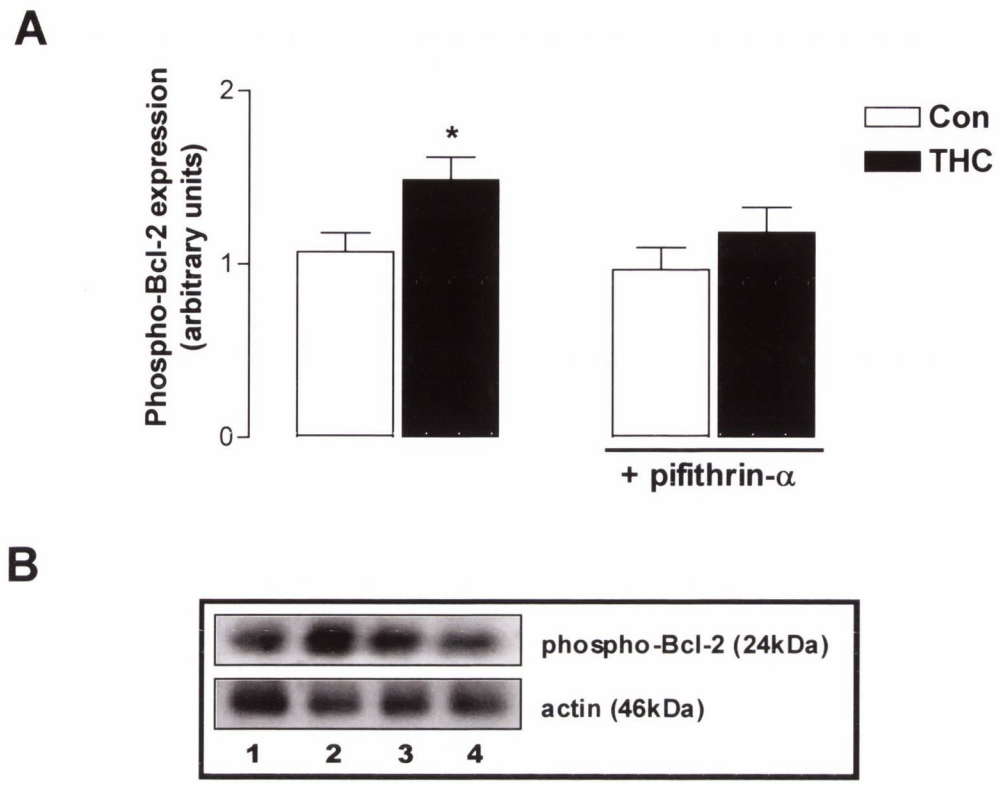

Figure 5.14: Bcl-2 phosphorylation by THC is p53-dependent

Cortical neurons were pre-treated with pifithrin-α (100nM) for 60 min prior to THC (5μM; 120 min) treatment. Cell protein was harvested and analysed for the expression levels of the phosphorylaed form of Bcl-2 protein using western immunoblotting.

A: Pifithrin-α prevented THC-induced phosphorylation of Bcl-2 at 120 min. Results are expressed as mean ± SEM for 6 observations, *$p<0.05$.

B: A sample western immunoblot demonstrating phosphorylated Bcl-2 protein expression at 120 min in control neurons (lane 1), THC-treated neurons (lane 2), pifithrin-α-treated cells (lane 3) and cells treated with pifithrin-α prior to THC exposure. Actin immunoblots display equal protein loading of samples.

5.2.15 THC-induces caspase-3 activation via p53

Since caspase-3 has a central role in the cell death pathway triggered by THC in the rat cortex (Chapter 3, 4), it was determined if p53 signalling was involved in regulating caspase-3 activity. Following the inhibition of p53 by exposing cultured cortical neurons to pifithrin-α, caspase-3 activity was assessed following THC exposure by monitoring the cleavage of the fluorescently labelled caspase-3 substrate, DEVD, to its fluorescent product (Figure 5.15). Neurons were pre-treated with pifithrin-α (100nM) for 60 min prior to THC (5μM; 120 min) treatment. In control conditions, caspase-3 activity was 5.5 $\pm$ 0.9 nmol AFC produced/mg protein/min (mean $\pm$ SEM) and this was significantly increased to 9.4 $\pm$ 1.2 nmol AFC produced/mg protein/min when neurons were incubated with THC for 120 min ($p<0.05$, ANOVA, n=6 observations). Caspase-3 activity in neurons treated with pifithrin-α alone (4.5 $\pm$ 0.9 nmol AFC produced/mg protein/min) for 120 min was comparable to control levels of caspase-3 activity. The THC-induced increase in caspase-3 activity was reduced to 5.0 $\pm$ 1.2 nmol AFC produced/mg protein/min in neurons treated with pifithrin-α+THC, indicating that the THC-induced activation of caspase-3 is p53-dependent.

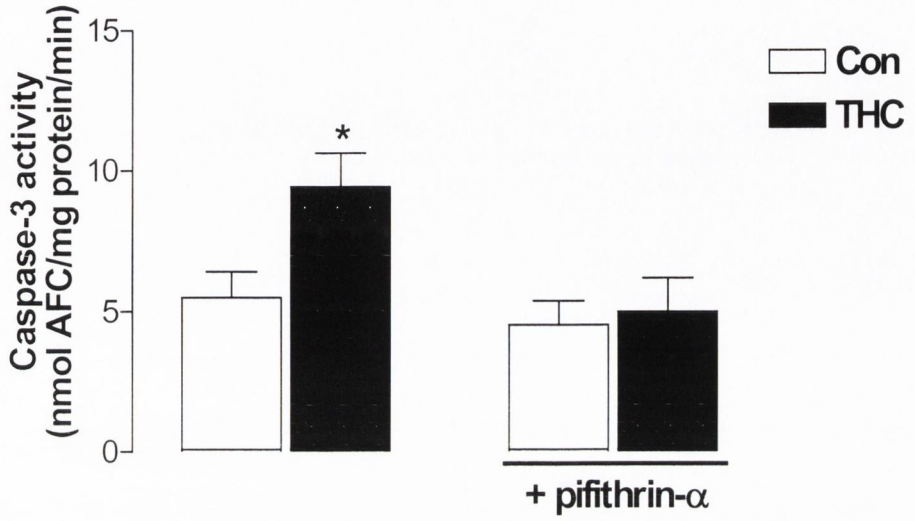

Figure 5.15: p53 is required for caspase-3 activity in THC-induced apoptosis

Treatment of primary cortical neurons with THC (5μM; 120 min) significantly increased caspase-3 activity as assessed by the cleavage of the fluorogenic DEVD substrate. The stimulatory effect of THC on caspase-3 activity was prevented by pifithrin-α (100nM). Exposure of cells to pifithrin-α had no effect on caspase-3 activity. Results are expressed as the mean ± SEM for 4 observations, *$p<0.05$.

5.2.16 THC induction of DNA fragmentation is reliant on p53

THC causes a maximal increase in DNA fragmentation 2-3hr post-treatment (Chapter 3), therefore this time point was used to determine if p53 was involved directly in mediating THC-induced DNA fragmentation. Following p53 inhibition by exposing cultured cortical neurons to pifithrin-α (100nM), the TUNEL technique was used to assess the levels of THC-induced DNA fragmentation at 120 min (Figure 5.16). In vehicle-treated control cells, 16.9 $\pm$ 2.7% (mean $\pm$ SEM) of cells displayed fragmented DNA in the nucleus (TUNEL positive). This was significantly increased to 41.3 $\pm$ 3.4% in cells treated with THC for 120 min ($p<0.001$, ANOVA, n=4 observations). While treatment of cells with pifithrin-α alone for 120 min had no effect on neuronal viability (22.6 $\pm$ 2.3% neurons with fragmented DNA), it prevented the THC-induced increase in DNA fragmentation (23.8 $\pm$ 4.1% TUNEL positive neurons). This finding suggests that p53 is directly involved in THC-induced DNA fragmentation. Representative TUNEL images of neurons are shown in Figure 5.16B.

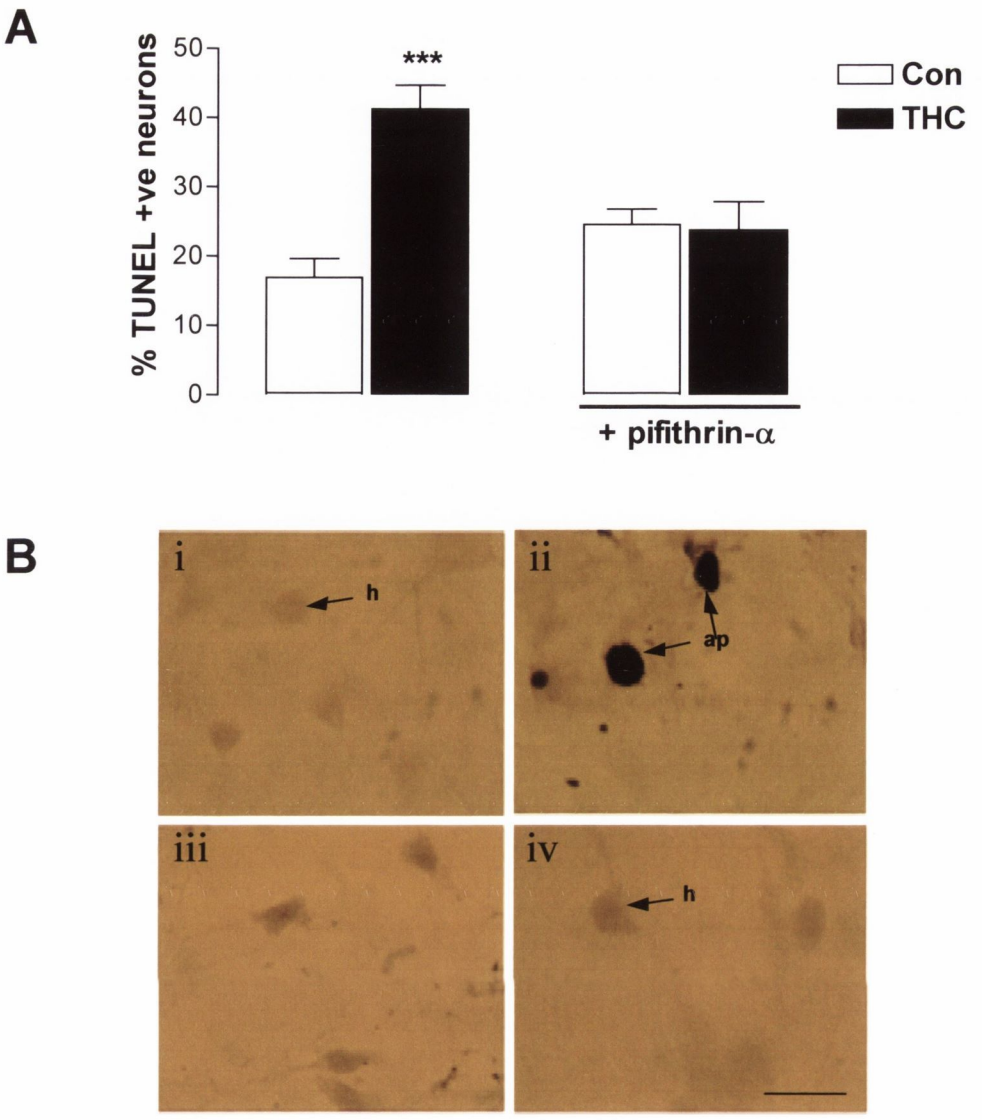

Figure 5.16: p53 is required for THC-induced DNA fragmentation

Cultured cortical neurons were treated with THC (5μM; 120 min) in the presence or absence of pifithrin-α (100nM). Cell viability was assessed using the TUNEL technique.

A: THC significantly increased DNA fragmentation and this was prevented by pifithrin-α pre-incubation. Results are expressed as mean ± SEM for 4 observations, ***p<0.001.

B: Images of TUNEL staining of (i) vehicle-treated neurons, (ii) THC-treated neurons, (iii) pifithrin-α-treated cultures and (iv) cultures treated with THC in the presence of pifithrin-α. Arrows indicate representative examples of healthy (h) and apoptotic (ap) neurons. Scale bar is 25μm.

5.3 Discussion

The experimental work in this chapter examined the ability of THC to couple to the nuclear phospho-protein p53, and to determine if p53 signalling contributes to the apoptotic actions of THC in cultured cortical neurons. Time course experiments revealed that THC induces an early increase in p53 protein expression at 5 min. This increase was via the central CB_1 cannabinoid receptor and was dose-dependent. Furthermore, the proclivity of THC to regulate p53 protein expression was not dependent on increased transcription of *p53* as THC had no effect on p53 mRNA expression as determined by RT-RCR. THC increased phosphorylation of p53 on residue serine-15 at 5 min, stabilising the p53 protein and possibly accounting for the increase in p53 protein expression at the same time point. Again the ability of THC to induce the phosphorylation of p53 on serine-15 was blocked by AM 251 implicating the involvement of CB_1 cannabinoid receptors in this pathway. THC was also found to increase the cytosolic expression of the pro-apoptotic mitochondria-associated protein Bax, and induce the phosphorylation of its anti-apoptotic protein partner Bcl-2, an event presumably contributing to cytochrome *c* translocation and apoptosis. THC-induced regulation of Bax protein was dependent on increased transcription of *bax* by THC and was also reliant on CB_1 receptor activation. The p53 inhibitor, pifithrin-α, was used to determine the role of p53 in regulating downstream effectors in THC-induced cell death. Treatment of cortical neurons with pifithrin-α blocked the effects of THC on Bax and phospho-Bcl-2 protein indicating that the mitochondria-associated proteins are regulated by p53 in THC-induced neuronal signalling. Use of pifithrin-α also revealed that p53 contributes directly to the THC regulation of apoptosis as the p53 inhibitor prevented THC-induced caspase-3 activation and downstream DNA fragmentation. Overall, this study indicates that THC regulates p53 signal transduction in cultured cortical cells and that this pathway contributes directly to the apoptotic effects of THC.

A recent report by Do and colleagues (2004) demonstrated that the p53 gene is upregulated in dendritic cells following THC exposure for 45 min. As far as we are aware this is the first report that THC or other cannabinoids regulate

the expression of the p53 tumour suppressor. Data presented herein demonstrate that THC induces an increase in p53 expression and phosphorylation on serine-15 at 5 min post THC-treatment. The increase in expression and phosphorylation of p53 protein were dependent on THC signalling through the CB_1 cannabinoid receptor. THC had no effect on p53 mRNA expression, indicating that THC increases p53 expression in a transcription-independent manner. The level of p53 is kept low in normal healthy cells due its short half-life, but increases in response to cellular stress (Levine, 1997; Miller *et al.*, 2000). There is evidence that p53 becomes phosphorylated on residue serine-15 following cellular stress, disrupting the association of p53 with its negative regulator, Mdm-2, which in turn prevents the degradation of the p53 protein (Shieh *et al.*, 1997). Hence, the finding that THC rapidly phosphorylates p53 on serine-15 provides a mechanism for the THC-mediated increase in p53 protein expression.

Data from the previous chapter indicated that THC regulates the JNK family of MAPKs. Several mechanisms for p53 stabilisation have been suggested including ERK, casein kinases and JNK (Blatt and Glick, 2001). THC induces the differential activation of JNK1 and JNK2 at 5 min and 2hr of THC treatment in cultured cortical cells, respectively (Chapter 4). Since we have demonstrated the early activation of JNK1 and p53 after 5 min of THC treatment, it is possible that JNK1 regulates p53 expression in this cultured cell system. This is supported by evidence that JNK1, but not JNK2, induces phosphorylation of p53 on serine-15 following exposure of cultured cortical neurons to the toxic Aβ peptide (Fogarty *et al.*, 2003). There is also evidence in non-neuronal cells that JNK1 has the ability to regulate p53 phosphorylation (Wang and Friedman, 2000). Hu and colleagues (1997) have also found that JNK2 and JNK3 isoforms can act as p53 N-terminal kinases in response to cellular stress. However, since we have found that JNK2 is activated at the later time point of 2hr following THC exposure (Chapter 4), it is unlikely that JNK2 is pertinent in the THC-mediated activation of p53. Furthermore, although several papers indicate that JNK functions upstream of p53, Inamaura and colleagues (2001) have found that p53 can recognise DNA damage prior to stimulating the JNK pathway, with phosphorylated JNK then up-regulating

the expression of p53. Overall, these findings indicate that the interplay between the JNK and p53 pathways vary with the stress stimulus and the state of activation of the signal transduction pathways within the cell.

The mechanism of p53-induced apoptosis has been extensively studied and involves the activation of the mitochondrial/caspase pathway (Marchenko *et al.*, 2000; Bonini *et al.*, 2004), regulation of the Fas receptor (Bennett *et al.*, 1998) and the transcription of genes involved in regulating the redox state of the cell (Polyak et al., 1997). A growing and diverse list of genes are involved in the apoptotic actions of p53, including the *bax* gene (Miyashita and Reed, 1997; Cregan *et al.*, 1999). Bax is involved in apoptotic cascades utilising the mitochondria-dependent pathway (Reed, 1997). The mitochondria undergo critical changes during the cell death process, including inner mitochondrial transmembrane potential ($\Delta\Psi_m$) collapse, interruption of electron-chain transport and prevention of oxidative phosphorylation, free radical production, permeability transition pore opening and outer mitochondrial membrane rupture (Reed, 1997). A consequence of these events is the translocation of cytochrome *c* from the mitochondrial intermembrane space into the cytoplasm, the site of cytochrome c-induced caspase-3 activation via APAF-1 (Slee *et al.*, 1999). Bax is a pro-apoptotic mitochondria-associated by virtue of its ability to promote cytochrome *c* release from the mitochondria. The Bax protein has homology with its anti-apoptotic protein partner Bcl-2 in conserved regions known as Bcl-2 homology (BH) domains, which allow interaction between both family members (Oltvai *et al.*, 1993). A striking characteristic of the Bcl-2 family members is their ability to form homo- and heterodimers through BH domain interaction (Oltvai *et al.*, 1993; Korsmeyer, 1995). This ensures that the cell death/survival decision depends on the relative expression levels of the pro-apoptotic and anti-apoptotic members. Overexpression of the anti-apoptotic members has been shown to protect cells against apoptosis involving cytochrome *c* release from the mitochondria (Choi *et al.*, 2001; Murphy *et al*, 2000). Similarly, overexpression of the pro-apoptotic members culminates in the demise of the cell (Wolter *et al.*, 1997; Gross *et al.*, 1998).

Bax normally resides in the cytoplasm and translocates to the mitochondria during apoptosis (Gross *et al.*, 1998). In its inactive state there is

evidence suggesting that the C- and N-termini interact and that upon triggering of apoptosis there is a conformational change in Bax, exposing these two domains to enable Bax insertion into the mitochondria (Nechushtan *et al.*, 1999; Choi *et al.*, 2001; Gross *et al.*, 1998). Indeed, there is evidence that Bax can form channels in artificial membranes (Schlesinger *et al.*, 1997). In this context, it is possible that Bax may form channels in the mitochondrial membrane, allowing the release of cytochrome *c*. To determine if THC promotes Bax translocation from the cytosol to the mitochondria, expression of Bax protein was assessed in cytosolic and mitochondrial fractions from cortical neurons exposed to THC by western immunoblot. THC was found to increase cytosolic Bax expression, ensuring that Bax homodimers predominate in cortical cells exposed to THC and contributing to the apoptotic actions of THC. The increase in Bax expression was due to a transcriptional event since THC directly up-regulated expression of the bax gene as assessed by RT-PCR. Furthermore, THC-induced Bax expression was dependent on p53 induction as pre-treatment of neurons with the p53 inhibitor pifithrin-α, abolished the stimulatory effect of THC on Bax induction. It is interesting to note that despite the modulatory effect of THC on cytosolic Bax expression, THC had no effect on mitochondrial Bax expression. This suggests that THC may evoke Bax translocation to other intracellular organelles and this is supported by evidence that Bax translocates to the endoplasmic reticulum (Zong *et al.*, 2003) and nucleus (Salah-Eldin *et al.*, 2003) during apoptosis. Furthermore, Choi and colleagues (2001) have shown that the apoptotic actions of Bax involve a conformational change via cleavage at the Bax N-terminal. Interestingly, this cleavage event occurred only in mitochondrial fractions, suggesting that the failure of THC to induce Bax expression in cortical neuronal mitochondrial fractions may be due to the inability of the Bax antibody used in our study to recognise the cleaved form of Bax located in the mitochondrial fractions of cortical neurons.

In support of the evidence presented herein suggesting that p53 induces apoptosis by up-regulating the transcription of Bax, Do and co-workers (2004) have recently shown that THC induces an upregulation of the p53 and Bax genes in bone marrow-derived dendritic cells. However, the authors fail to

identify if these events contribute directly to the apoptotic actions of THC in dendritic cells (Do *et al.*, 2004). There is also evidence that p53 can regulate the expression of the anti-apoptotic protein, Bcl-2, a members of the Bcl family of mitochondria-associated proteins (Mielke and Herdegen, 2000). In contrast to Bax, Bcl-2 represses cell death (Korsmeyer, 1999) by preventing cytochrome *c* translocation from the mitochondria (Shimizu *et al.*, 1999) and there is evidence that Bcl-2 is involved in cannabinoid-induced cell death in immune cells (Zhu *et al.*, 1998) and PC12 cells (Sarker *et al.*, 2003). Bcl-2 prevents cytochome *c* release by blocking the redistribution of Bax to the mitochondria (Gross *et al.*, 1998) and the conformational changes that manifest in its translocation (Murphy *et al.*, 2000; Choi *et al.*, 2001). However, the pro-survival function of Bcl-2 is inhibited following phosphorylation of the Bcl-2 protein (Yamamoto *et al.*, 1999) and there is evidence that Bcl-2 phosphorylation can be regulated by p53 (Pucci *et al.*, 1999). Evidence presented here demonstrate that THC induces the phosphorylation of Bcl-2 protein within the same timeframe of Bax induction, and this phosphorylation event was dependent on p53 as the p53 inhibitor, pifithrin-α, prevented THC-induced Bcl-2 phosphorylation.

In addition to the proposed regulatory effects of p53 on Bax and phospho-Bcl-2 induction, Marchenko and colleagues (2000) have shown that p53 can target directly to the mitochondria to induce apoptosis. The accumulation of p53 at the mitochondria is rapid, occurring 1hr after p53 induction and precedes changes in the mitochondrial membrane potential and the release of mitochondrial cytochrome *c* and caspase-3 activation, and is blocked by overexpressing Bcl-2 protein. Hence, p53 can contribute to apoptosis by direct signalling at the mitochondria in addition to modulating the expression pattern of the mitochondria-associated proteins.

The apoptotic events that are evoked by THC in cortical neurons include the release of mitochondrial cytochrome *c* into the cytosol following CB_1 receptor activation (Chapter 3), and our finding that THC induces Bax and phopho-Bcl-2 expression via p53 induction is a likely mechanism for this event. Once in the cytosol, cytochrome *c* complexes with the cytosolic factor, APAF-1, which in turn triggers the activation of the cysteine protease caspase-3, which

contributes to the drastic morphological changes associated with apoptosis by disabling a number of key substrates (Zou *et al.*, 1997). We have previously shown that caspase-3 is central to the apoptotic cascade triggered by THC in cortical neurons (Campbell, 2001; Chapter 3) and caspase-3 induction is dependent on JNK1 and JNK2 signalling (Chapter 4). In Chapter 4 it was found that the downregulation of JNK1 and JNK2 using antisense technology effectively blocked THC-induced activation of caspase-3 and downstream DNA fragmentation, indicating that both JNK1 and JNK2 are intricately involved in the transduction of THC-induced apoptotic signals. It was of particular note that depletion of either JNK1 or JNK2 isoforms completely abrogated the THC-induced caspase-3 activation and DNA fragmentation, which may reflect an interaction between JNK1 and JNK2 with respect to the regulation of upstream effectors involved in caspase-3 activation. Indeed, a requirement for both JNK1 and JNK2 has been implicated in the phosphorylation of p53 (Buschmann *et al.*, 2001), and p53 has been shown to contribute directly to caspase-3 activity (Cregan *et al.*, 1999) and DNA fragmentation (Chi *et al.*, 2004). The involvement of p53 in the regulation of JNK-induced caspase-3 activation and DNA fragmentation following THC exposure is supported by the finding that pifithrin-α prevents THC-induced caspase-3 activation and the fragmentation of DNA.

Despite the relative absence of evidence that cannabinoids regulate p53 expression, it has been shown that cannabinoids induce the regression of malignant gliomas *in vivo* (Sánchez *et al.*, 2001a; Galve-Roperh *et al.*, 2000). Indeed, Galve-Roperh and colleagues (2000) have shown that rats bearing tumours survive significantly longer when treated with THC for 1 week when compared to untreated healthy rats, and furthermore, THC-induced the complete regression of tumour growth in approximately 30% of the THC-treated animals. The molecular mechanisms accounting for glioma regression in these systems involved an increase in the pro-apoptotic lipid ceramide and ERK activation (Galve-Roperh *et al.*, 2000). Data reported in this chapter suggest that the proclivity of THC to up-regulate the expression of the tumour suppressor p53 may contribute to the anti-tumoural actions of cannabinoids in the brain.

In summary, the results from this study demonstrate that treatment of cortical cultures with THC induces a transcription-independent increase in p53 expression. This increase was dependent on CB_1 cannabinoid receptor activation and was possibly reliant on THC-induced phosphorylation of p53 on residue serine-15. THC-induces an increase in cytosolic Bax expression via CB_1 by increasing the expression of the bax gene. Furthermore, THC-induces the phosphorylation of Bcl-2, blocking its anti-apoptotic function. Application of pifithrin-α, an inhibitor of p53, attenuated the THC-induced increase in Bax and phosphorylated Bcl-2 expression, caspase-3 activation and DNA fragmentation. These results demonstrate that THC regulates p53 in cultured cortical cells and that p53 is involved in regulating the neurotoxic actions of THC.

Chapter 6

A study of the effect of developmental influences on THC-induced apoptosis in cortical neuronal slices – An ex vivo study

6.1 Introduction

The influence of cannabinoids on neuronal viability remains a complex issue since neurotoxic (Chan *et al.*, 1998; Kim and Thayer, 2001; Sarker *et al.*, 2003) and neuroprotective properties have been determined in cultured neurons *in vitro* (Nadler *et al.*, 1993; Eshhar *et al.*, 1993; Nagayama *et al.*, 1999; Iuvone *et al.*, 2003). Indeed, data from the previous chapters have shown that THC has deleterious effects on cultured cortical neurons. The influence of THC on neuronal survival is further compounded by differential results obtained from *in vitro* and *in vivo* experiments. Hence, while several studies have demonstrated a neurotoxic effect of THC in cultured neurons (which are prepared from embryonic or neonatal rodent brain), there is no direct evidence suggesting that cannabinoids are neurotoxic to the mature adult CNS (Scallet, 1991; Hollister, 1986; Galve-Roperh *et al.*, 2000). Furthermore, in human adults that abuse marijuana, neurodegenerative changes have not been found (Hollister, 1986). In contrast, numerous reports have identified neuroprotective effects of cannabinoids *in vivo* (Nagayama *et al.*, 1999; Louw *et al.*, 2000). Hence, the influence of neurodevelopment on the ability of THC to induce the activation of intracellular events that underlie the apoptotic effects of THC was investigated. This study was undertaken in an *ex vivo* system, analysing apoptotic consequences of THC exposure in freshly dissected cortex from neonatal (4-7-day old), adolescent (20-30-day old) and adult (3-4 month old) rats. Cortical brain slices were exposed to THC for 2hr, the time point at which THC induces a maximal level of DNA fragmentation in cultured cortical neurons (Chapter 3).

The central CB_1 cannabinoid receptor is one of the most abundantly expressed of neuronal receptors (Iversen, 2000) and is localised in brain regions most likely involved in the psychoactive effects of THC, including the cortex (Tsou *et al.*, 1998; Mailleux and Vanderhaeghen, 1992; Twitchell *et al.*, 1997). Furthermore, the apoptotic actions of THC on cultured cortical neurons are reliant on the activation of this receptor (Chapter 3, 4, 5). Interestingly, there is increasing evidence that the CB_1 receptor is expressed in the fetal and early postnatal brain (Berrendero *et al.*, 1998; Rodriguez de Fonseca *et al.*,

1993; McLaughlin *et al.*, 1994; Belue *et al.*, 1995; Garcia-Gil *et al.*, 1999) but its expression pattern varies during development (Fernández-Ruiz *et al.*, 2000; Glass *et al.*, 1997; Berrendero *et al.*, 1998). Although this may have important implications in terms of a modulatory role of the cannabinoid system in neurobiological processes, in particular neural development, overstimulation of cannabinoid receptors at critical stages of development may have damaging consequences on nervous system functioning. Indeed, several studies have shown that prenatal and early postnatal exposure to THC, or THC in combination with other cannabinoids, produces long-term abnormalities in brain function (Dalterio, 1986; Fernández-Ruiz *et al.*, 1992; Nahas and Frick, 1986; Mokler *et al.*, 1986; Navarro *et al.*, 1995).

The apoptotic actions of THC on cultured cortical neurons obtained from neonatal rat pups involve the activation of the stress kinase, JNK (Chapter 4). It was found that THC increases the activity of JNK isoforms, JNK1 and JNK2, in cortical cells after 5 min and 120 min of treatment, respectively (Chapter 4). The nuclear phospho-protein p53 is a target for JNK regulation (Blatt and Glick, 2001) and experimental evidence presented in Chapter 5 demonstrates that THC enhances the stability of the p53 protein via phosphorylation of p53 on residue serine-15. Both of these molecules have the proclivity to regulate the expression of a number of cytoplasmic substrates, including the mitochondria-associated proteins Bax and Bcl-2 (Park *et al.*, 1997; Kang *et al.*, 1998; Lei *et al.*, 2002) which can regulate the translocation of mitochondrial cytochrome *c* into the cytosol (Kang *et al.*, 1998), a central apoptotic event (Reed, 1997; Rosse *et al.*, 1998). Once released from mitochondria, cytochrome *c* complexes with a cytosolic factor, APAF-1, inducing conformational changes that in turn trigger the activation of the cell death protease, caspase-3, and the resultant apoptotic cascade (Zou *et al.*, 1997). Experimental work presented in previous chapters has identified Bax and Bcl-2 (Chapter 5), cytochrome *c* (Chapter 3), and caspase-3 (Chapter 3, 4, 5) as targets for regulation by THC in cultured cortical neurons. THC-induced regulation of these apoptotic events were mediated by CB_1 cannabinoid receptors and contributed directly to the apoptotic actions of THC on cultured cortical neurons

The experiments in this *ex vivo* study were aimed at providing further insight into the signalling events that couple to the CB_1 receptor in the rat

cortex. Particular focus was on the contribution of developmental influences (maturity of neurons) to influencing the apoptotic actions of THC in cortical neurons. The contribution of the CB_1 receptor and its differential expression in relation to postnatal development and THC-induced neurotoxicity was assessed in cortical brain slices obtained from neonatal, adolescent and adult rats. The ability of THC, acting through the CB_1 receptor, to impact on the phosphorylated forms of JNK1, JNK2 and p53 were assessed. Furthermore, the proclivity of THC to regulate caspase-3 activity and DNA fragmentation in each rat age group was also determined. In all cases, dose-response studies were performed to determine the efficiency of CB_1 coupling to its associated signalling molecules during neuronal development.

6.2 Results

6.2.1 The expression of CB_1 cannabinoid receptor in rat cortex is dependent on postnatal development

There is evidence to support that the expression of the central cannabinoid CB_1 receptor changes in the CNS at different stages of development (Berrendero *et al.*, 1998). To assess the expression pattern of the CB_1 receptor during brain development, cortical brain slices obtained from neonatal (4-7-day old), adolescent (20-30-day old) and adult (3-4 month old) rats were homogenised in sterile HEPES-buffered saline following dissection and the expression of the CB_1 receptor determined by western immunoblotting using a polyclonal CB_1 receptor antibody raised against a peptide mapping the amino terminus of CB_1, in conjunction with densitometry (Figure 6.1). CB_1 cannabinoid receptor expression was 33.2 ± 3.3 arbitrary units (mean ± SEM) in cortical slices obtained from neonatal rats. Expression of the CB_1 receptor was significantly increased to 70.8 ± 9.7 in cortical brain slices obtained from adolescent rats ($p<0.01$, ANOVA; n=6 observations). Similarly, CB_1 receptor expression was significantly higher in adult cortical tissue (61.4 ± 7.0) compared to neonatal samples ($p<0.05$, ANOVA; n=6). This finding suggests that the expression pattern of the CB_1 receptor in the rat cortex varies at different stages of development and may influence the actions of cannabinoids on the brain. A sample immunoblot demonstrating the increase in CB_1 cannainoid receptor expression in the rat cortex with postnatal development is shown in Figure 6.1B.

A

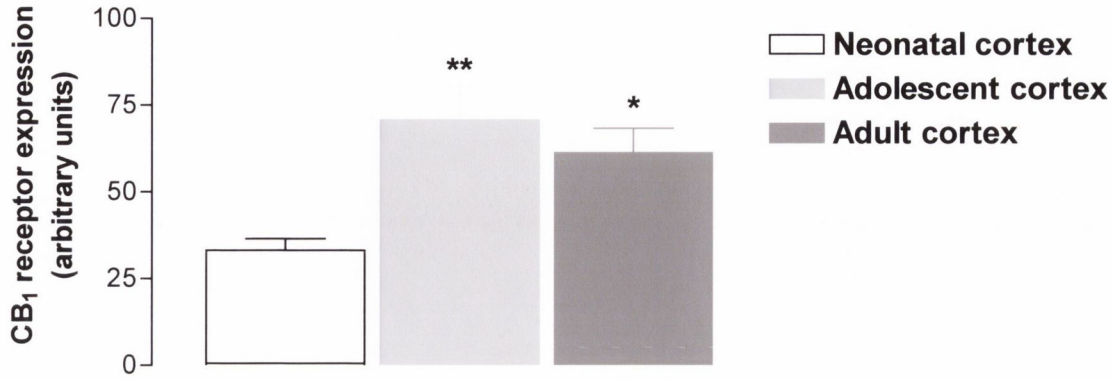

B

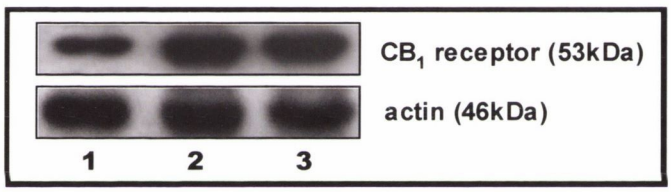

Figure 6.1: CB_1 cannabinoid receptor expression increases with postnatal development

Cortical brain slices obtained from neonatal (4-7-day old), adolescent (20-30-day old) and adult (3-4 month old) rats were homogenised in HEPES-buffered saline and the expression of the CB_1 receptor determined by western immunoblotting.

A: A significant increase in CB_1 receptor expression was found in cortical slices obtained from adolescent and adult rats compared to neonatal slices. Results are expressed as mean ± SEM for 6 observations, **$p<0.01$, *$p<0.05$.

B: A sample western immunoblot demonstrating CB_1 receptor expression in cortical brain slices obatained from neonatal (lane 1), adolescent (lane 2) and adult (lane 3). Actin immunoblots confirm equal protein loading.

6.2.2 Effect of THC on ladder-patterned DNA fragmentation in cortical slices

The role of postnatal development on THC-induced neuronal cell death was assessed by agarose gel electrophoresis in cortical slices (Figure 6.2). The formation of distinct DNA fragments of oligonucleosomal size (180-200bp lengths) is a biochemical hallmark of apoptosis (Arends *et al.*, 1990; Spooren and Hengerer, 2000) that can be visualised on a gel as a distinct ladder of bands at multiples of approximately 180 base pairs. DNA laddering was determined in cortical slices obtained from neonatal (4-7-day old), adolescent (20-30-day old) and adult (3-4 month old) Wistar rats treated with THC (5μM) in the absence/presence of AM 251 (10μM) for 2hr in sterile HEPES-buffered saline. Cortical slices were treated with 0.007% methanol (v/v) for 2hr as vehicle control. DNA laddering was not visualised in either slices treated with THC. However, It is notable that the DNA damaging agent, etoposide (10μM, 24hr treatment; Sigma-Aldrich, Dorset, UK), despite its neurotoxic effects (Nakajima *et al.*, 1994), had no effect on DNA fragmentation in cell cultures (Chapter 3). This indicates that various parameters within the protocol remain to be optimised. A sample agarose gel demonstrating DNA laddering attempts is shown in Figure 6.2.

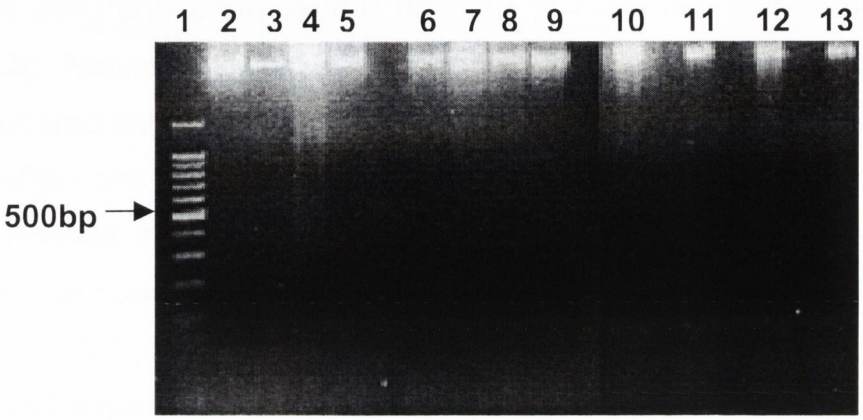

Figure 6.2: Assessment of DNA fragmentation using DNA ladder technique

Cortical slices isolated from neonatal (4-7-day old), adolescent (20-30-day old) and adult (3-4 month old) rats were treated with THC (5μM) in the absence/presence of AM 251 (10μM) for 2hr and DNA expression assessed. Lane 1, DNA ladder. Neonatal cortical tissue: Lane 2, methanol vehicle control (0.007%; v/v); Lane 3, THC; Lane 4, AM 251; Lane 5, THC+AM 251. Adolescent cortical tissue: Lane 6, methanol control (0.007%; v/v); Lane 7, THC; Lane 8, AM 251; Lane 9, THC+AM 251. Adult cortical tissue: Lane 10, methanol control (0.007%; v/v); Lane 11, THC; Lane 12, AM 251; Lane 13, THC+AM 251. Data represent one of three experiments with similar results.

6.2.3 Effect of THC on JNK1 expression in cortical slices obtained from neonatal rats

In previous chapters it has been shown that the effects of THC on apoptotic molecules in cultured cortical neurons are dose-dependent. Hence, a dose-response analysis of the effects of THC on phospho-JNK1 expression was performed to determine if the dose of THC influences its regulatory effects on JNK1 phosphorylation in neonatal (4-7-day old) cortical brain slices (Figure 6.3). Neonatal slices were exposed to THC (5nM-5μM) in sterile HEPES-buffered saline for 2hr. Following treatment, slices were homogenised in lysis buffer and phosphorylated/non-phosphorylated JNK1 protein expression assessed by western immunoblot. Figure 6.3 demonstrates that exposure to THC at concentrations of 5nM (2.4 ± 0.1 arbitrary units; mean ± SEM), 0.5μM (2.4 ± 0.2), 5μM (2.3 ± 0.3), and 50μM (2.3 ± 0.2) showed a level of phospho-JNK1 expression comparable to phosphorylated JNK1 expression in vehicle-treated slices (2.7 ± 0.2) obtained from neonatal rats. This suggests that various concentrations of THC have no effect on phospho-JNK1 expression in the neonatal cortex.

6.2.4 Dose-dependent analysis of the effects of THC on JNK1 expression in rat cortical slices obtained from adolescent rats

A dose-response analysis of the effects of THC on phospho-JNK1 expression in cortical slices obtained from adolescent (20-30-day old) rats was performed to determine if the dose of THC influences JNK1 phosphorylation in the adolescent cortex (Figure 6.4). Cortical slices obtained from young rats were exposed to increasing concentrations of THC for 2hr. Phosphorylated JNK1 expression in vehicle-treated slices was (1.2 ± 0.1 arbitrary units; mean ± SEM). Exposure of cortical slices obtained from adolescent rats to THC at concentrations of 5nM (1.5 ± 0.1), 0.5μM (1.3 ± 0.2), 5μM (1.2 ± 0.1), and 50μM (1.2 ± 0.1) did not affect the expression pattern of the phosphorylated active JNK1 isoform.

6.2.5 Effect of THC dose on JNK1 expression in rat cortical slices obtained from adult rats

A dose-response analysis of the effects of THC on the level of JNK1 phosphorylation in adult (3-4 month old) cortical slices was performed to determine if the concentration of THC influences JNK1 phosphorylation in the mature cortex (Figure 6.5). Cortical slices obtained from adult rats were exposed to concentrations of THC ranging from 5nM-50μM for 2hr. Phospho-JNK1 expression in slices exposed to methanol vehicle for 2hr was 1.2 ± 0.1 arbitrary units (mean ± SEM). Treatment with 5nM THC (1.1 ± 0.1), 0.5μM THC (1.1 ± 0.1), 5μM THC (1.2 ± 0.1) and 50μM THC (1.3 ± 0.2) did not affect the expression of the phosphorylated form of the JNK1 isoform, indicating that JNK1 activity is not modulated by THC in mature cortical brain slices.

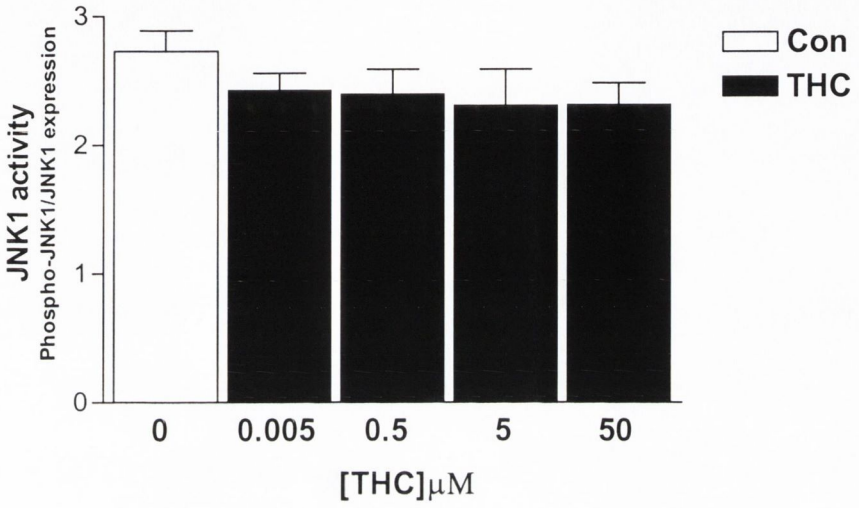

Figure 6.3: Effect of THC on phospho-JNK1 expression in brain slices obtained from the cortex of neonatal rats

Neonatal (4-7-day old) brain slices were treated with increasing concentrations of THC (5nM-50μM) for 2hr. Following treatment cell protein was harvested and analysed for the expression levels of the active (phosphorylated) and inactive (non-phosphorylated) forms of JNK1 protein using western immunoblotting. THC had no effect on phospho-JNK1 expression at concentrations of 5nM, 0.5μM, 5μM and 50μM at 2hr. Results are expressed as mean ± SEM for 6 observations.

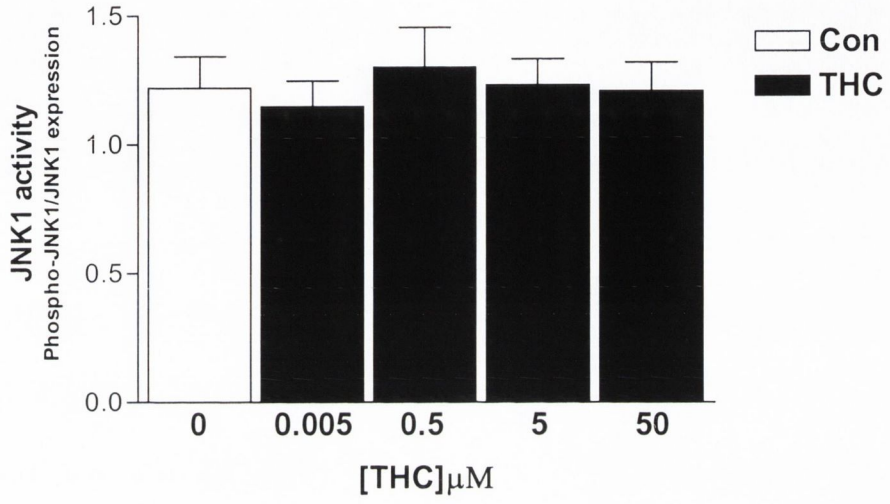

Figure 6.4: Effect of THC on phospho-JNK1 expression in brain slices obtained from the adolescent rat cortex

Cortical brain slices from obtained from adolescent (20-30-day old) rats were treated for 2hr with concentrations of THC ranging from 5nM-50μM. Following treatment cell protein was harvested and analysed for the expression levels of the active and inactive forms of JNK1 protein using western immunoblotting. THC had no effect on phospho-JNK1 expression at concentrations of 5nM, 0.5μM, 5μM and 50μM when compared to vehicle-treated slices. Results are expressed as mean ± SEM for 6 observations.

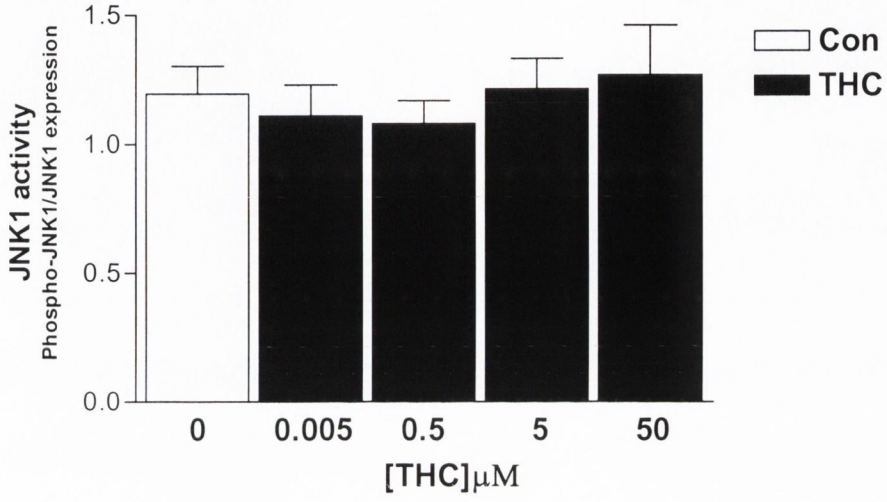

Figure 6.5: Effect of THC on JNK1 expression in cortical brain slices from adult rats

Cortical brain slices from adult (3-4 month old) rats were treated for 2hr with concentrations of THC ranging from 5nM-50μM and the expression levels of the phosphorylated and non-phosphorylated form of JNK1 protein determined by western immunoblotting. Incubation of slices with THC at concentrations of 5nM, 0.5μM, 5μM and 50μM had no effect on phospho-JNK1 expression when compared to vehicle-treated slices at 2hr. Results are expressed as mean ± SEM for 4 experiments.

6.2.6 THC induces JNK2 phosphorylation in cortical slices obtained from neonatal rats in a dose-dependent manner

THC induction of apoptosis of neonatal cultured cortical neurons involves the activation of the JNK2 isoform (Chapter 4). To determine if THC induces JNK2 activation in neonatal cortical tissue, cortical slices obtained from neonatal (4-7-day old) rats were incubated with THC in sterile HEPES-buffered saline for 2hr. Following treatment, slices were homogenised in lysis buffer and phosphorylated/non-phosphorylated JNK2 protein expression assessed by western immunoblot Since we have previously shown that 5μM is the concentration of THC required to induce maximal JNK2 activation in cultured cells (Chapter 4), a dose-response analysis of THC-induced JNK2 activation was performed to determine the concentration of THC required to evoke maximal activation of the JNK2 isoform. Figure 6.6 shows that in neonatal slices exposed to vehicle for 2hr phosphorylated JNK2 expression was 2.0 ± 0.1 arbitrary units (mean ± SEM). Slices exposed to THC at concentrations of 5nM (1.9 ± 0.2) or 0.5μM (1.9 ± 0.2) for 2hr displayed a level of JNK2 activity comparable to control values. However, JNK2 activity was significantly increased to 2.6 ± 0.2 when cortical slices obtained from neonatal rats were treated with 5μM THC for 2hr ($p<0.05$, ANOVA, n=5 observations). A 50μM THC dose further increased JNK2 activity to the significant value of 2.8 ± 0.4 ($p<0.05$, ANOVA, n=5). This result demonstrates that THC modulates JNK2 activity in cortical slices obtained from neonatal rats in a dose-dependent manner, with a minimal concentration of 5μM THC required to induce JNK2 activation.

6.2.7 THC increases JNK2 phosphorylation in cortical slices obtained from neonatal rats via CB_1

To determine if THC induces JNK2 activation in neonatal cortical tissue following CB_1 receptor activation, cortical slices obtained from neonatal (4-7-day old) rats were pre-incubated with AM 251 (10μM; diluted in sterile pre-warmed HEPES-buffered saline) for 30 min before treating with THC (5μM) for 2hr. In cortical slices obtained from neonatal rats treated with methanol vehicle for 2hr phosphorylated JNK2 expression was 91.0 ± 0.5 arbitrary units (mean ±

SEM) and this was significantly increased following THC treatment for 2hr to 124.3 ± 11.4 ($p<0.05$, ANOVA, n=5 observations; Figure 6.7). While pre-treatment with AM 251 alone had no effect on phosphorylated JNK2 expression (82.6 ± 11.7), it prevented the THC-induced increase in JNK2 activity (73.7 ± 14.7). This result demonstrates the involvement of the CB_1 receptor in mediating JNK2 activity in neonatal cortical brain slices.

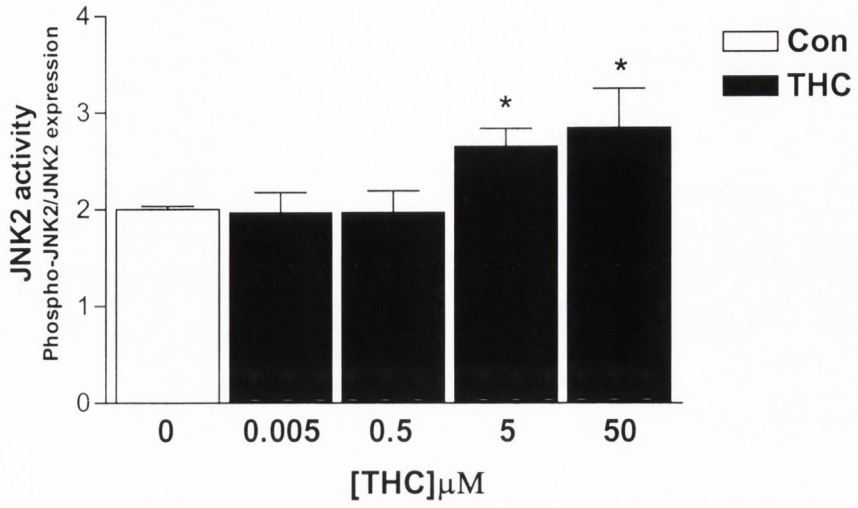

Figure 6.6: THC induces JNK2 activation in cortical slices obtained from neonatal rats in a dose-dependent manner

Cortical neuronal slices obtained from neonatal (4-7-day old) rat pups were treated with increasing concentrations of THC (5nM-50μM) for 2hr. Following treatment cell protein was harvested and the analysed for the expression levels of the phosphorylated active form and non-phosphorylated inactive form of JNK2 using western immunoblotting. A significant increase in JNK2 activity was found following treatment with THC at concentrations of 5μM and 50μM. Exposure of slices to 5nM and 0.5μM THC had no effect on JNK2 activity. Results are expressed as mean ± SEM for 5 observations, *$p<0.05$.

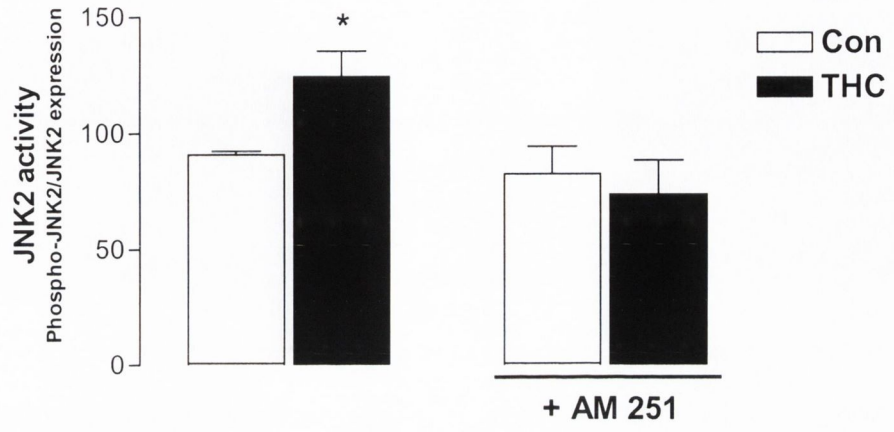

Figure 6.7: THC induces JNK2 activation via CB_1 in neonatal cortical brain slices

Cortical slices obtained from neonatal (4-7-day old) rats were pre-incubated with AM 251 (10μM) for 30 min prior to THC (5μM) treatment for 2hr. Protein was harvested and analysed for the expression levels of the phosphorylated and non-phosphorylated form of JNK2 using western immunoblot. Pre-incubation of cortical neurons with AM 251 abolished the THC-induced increase in JNK2 activity observed at 2hr. Results are expressed as mean ± SEM for 5 observations, *$p<0.05$.

6.2.8 Effect of THC on JNK2 expression in cortical slices obtained from adolescent animals

To determine if the regulatory effects of THC on phospho-JNK2 are dependent on neuronal maturity, cortical slices obtained from adolescent (20-30-day old) rats were exposed to a range of THC concentrations (5nM-50μM) for 2hr (Figure 6.8). Interestingly, exposure of cortical slices obtained from adolescent rats to THC at a concentration of 50μM significantly increased JNK2 phosphorylation to 3.3 ± 0.5 arbitrary units (mean ± SEM) from 1.4 ± 0.2 in vehicle-treated control slices ($p<0.01$, ANOVA, n=6 observations). Exposure of cortical slices to THC at concentrations of 5nM (1.8 ± 0.3), 0.5μM (1.8 ± 0.2) and 5μM (1.9 ± 0.3) did not affect the level of JNK2 phosphorylation in rat cortical slices obtained from adolescent rats. This finding suggests that THC has the proclivity to regulate JNK2 in the adolescent rat cortex, but that this effect requires high concentrations of THC.

6.2.9 Effect of THC on JNK2 in cortical slices obtained from adults

A dose-dependent study was used to determine if THC regulates JNK2 activity in cortical slices obtained from adult rats in a dose-dependent manner. Cortical slices obtained from adult (3-4 month old) rats were exposed to THC (5nM-50μM) for 2hr and JNK2 phosphorylation determined (Figure 6.9). JNK2 expression in adult slices exposed to vehicle for 2hr was 1.2 ± 0.1 arbitrary units (mean ± SEM). Slices exposed to THC at doses of 5nM (1.2 ± 0.3), 0.5μM (1.2 ± 0.1) and 5μM (1.4 ± 0.2) for 2hr displayed a level of JNK2 activity comparable to control values. However, JNK2 activity in cortical slices obtained from adult rats was significantly increased to 2.2 ± 0.3 when slices were treated with 50μM THC for 2hr ($p<0.05$, ANOVA, n=5 observations). This finding suggests that high concentrations of THC induce JNK2 activation in the adult rat cortex.

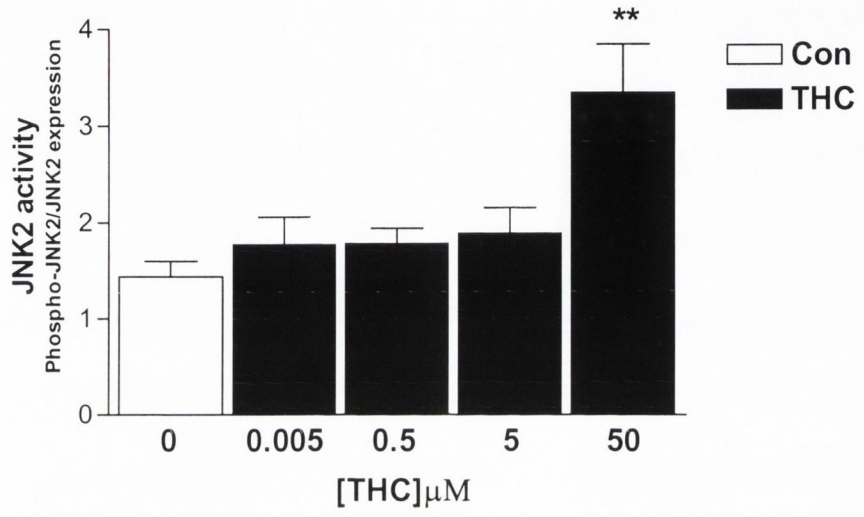

Figure 6.8: THC induces JNK2 activation in cortical slices obtained from adolescent rats at high THC concentrations

Cortical neuronal slices obtained from adolescent (20-30-day old) rats were treated with THC (5nM-5μM) for 2hr, cell protein was harvested and the analysed for the expression levels of the phosphorylated/non-phosphorylated form of JNK2 using western immunoblotting. A significant increase in JNK2 activity was found following treatment with THC at a concentration of 50μM. Exposure of slices to 5nM, 0.5μM and 5μM THC had no effect on JNK2 activity. Results are expressed as mean ± SEM for 6 observations, **p<0.01.

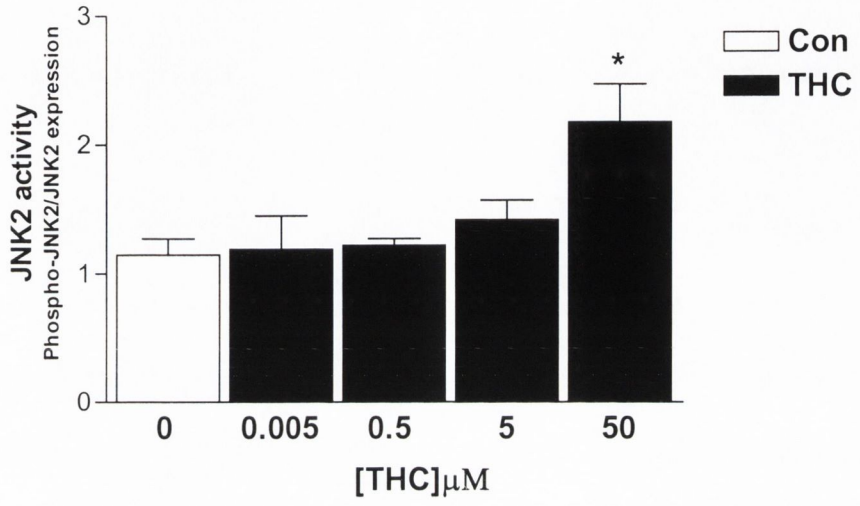

Figure 6.9: JNK2 activity in cortical slices obtained from adult rats is regulated by THC in a dose-dependent manner

Rat cortical neuronal slices obtained from adult (3-4 month old) animals were treated with THC (5nM-5μM) for 2hr, cell protein was harvested and the analysed for the expression levels of JNK2 using western immunoblotting. A 50μM THC dose significantly increased JNK2 activity. Exposure to 5nM, 0.5μM and 5μM THC had no effect on JNK2 activity. Results are expressed as mean ± SEM for 5 observations, *$p<0.05$.

6.2.10 p53 protein expression is not modulated by THC in cortical brain slices obtained from neonatal, adolescent and adult animals

In chapter 5 it was shown that THC regulates the expression and phosphorylation of the tumour suppressor protein, p53, in cultured cortical neurons prepared from neonatal rat pups. To determine if THC modulates p53 expression in the rat cortex *ex vivo*, cortical brain slices obtained from neonatal (4-7-day old), adolescent (20-30-day old), and adult (3-4 month old) rats were exposed to THC (5μM) in sterile HEPES-buffered saline for 2hr. Cortical slices were also incubated with 0.007% methanol (v/v) for 2hr as vehicle control. Following treatment, slices were homogenised in lysis buffer and total p53 protein expression assessed by western immunoblot using an antibody that recognises the non-phosphorylated form of p53.

Figure 6.10A demonstrates that exposure to THC (22.5 ± 1.2 arbitrary units, mean ± SEM) for 2hr had no effect on p53 protein expression in cortical slices obtained from neonatal rats when compared to slices exposed to methanol vehicle control (24.2 ± 1.0) for 2hr. Figure 6.10B demonstrates that THC exposure for 2hr increases p53 protein expression in cortical brain slices obtained from adolescent rats, but not significantly so. Thus, p53 expression was 26.9 ± 1.6 arbitrary units (mean ± SEM) in control and 35.7 ± 4.8 in THC-treated slices (p=0.176, student's *t* test; n=4 observations). Again, Figure 6.10C demonstrates that treatment of slices obtained from adult rat cortex with THC (22.0 ± 1.2 arbitrary units, mean ± SEM) for 2hr had no effect on p53 protein expression when compared to the levels of p53 expression observed in vehicle controls (23.4 ± 1.6) for 2hr. These results suggest that a 2hr exposure to THC does not affect total p53 protein expression in the neonatal, adolescent and adult cortex.

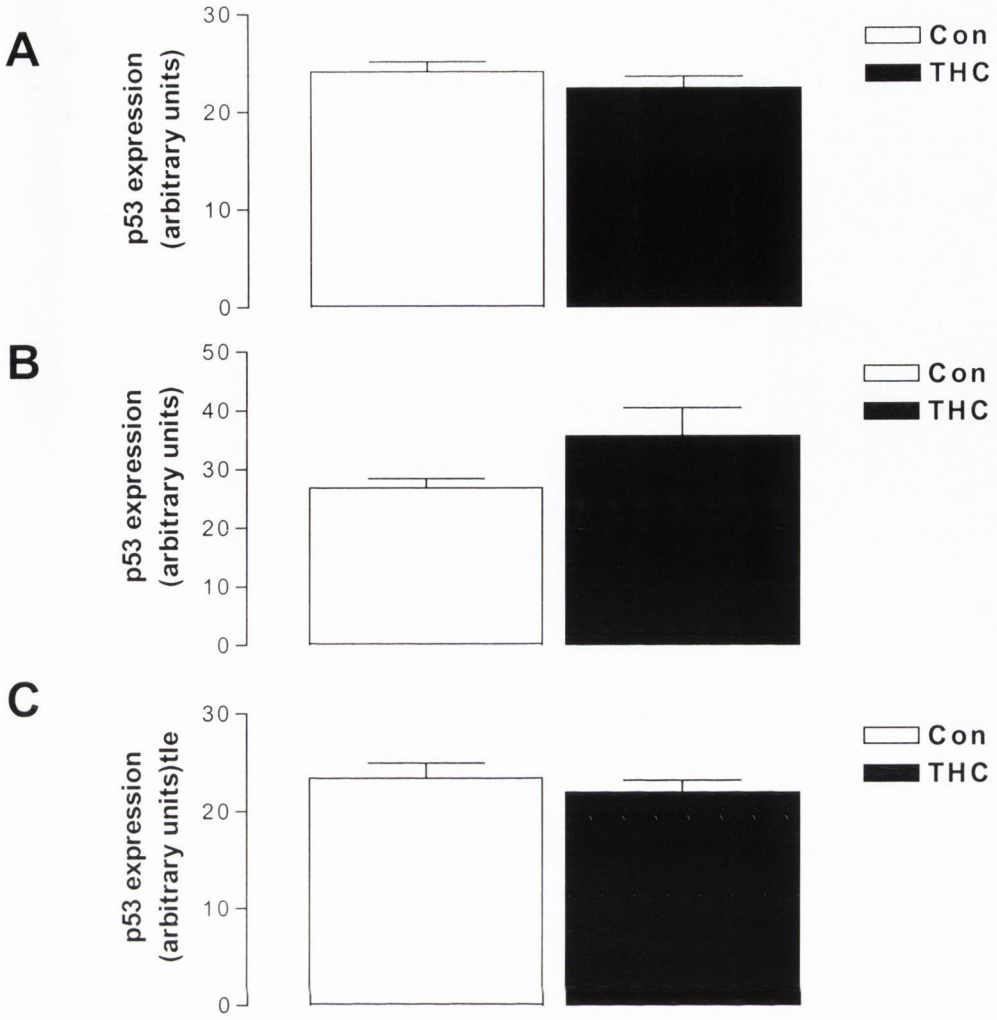

Figure 6.10: THC has no effect on p53 in cortical brain slices obtained from neonatal, adolescent and adult rats

Cortical slices from neonatal (4-7-day old), adolescent (20-30-day old) and adult (3-4 month old) rats were treated with THC (5μM) treatment for 2hr. Following treatment cell protein was harvested and analysed for the expression levels of p53 protein using western immunoblot.

A: THC had no effect on total p53 expression in neonatal cortical slices. Results are expressed as mean ± SEM for 6 observations.

B: THC increased p53 protein expression, but not significantly so, in adolescent cortical slices. Results are expressed as mean ± SEM for 4 observations, p=0.176.

C: THC had no effect on total p53 protein expression in adult cortical slices. Results are expressed as mean ± SEM for 6 observations.

6.2.11 THC has no effect on phosphorylated $p53^{ser15}$ in cortical brain slices isolated from neonatal, adolescent and adult rats

To determine if THC modulates phosphorylated $p53^{ser15}$ expression in the rat cortex *ex vivo*, cortical brain slices obtained from neonatal (4-7-day old), adolescent (20-30-day old), and adult (3-4 month old) rats were exposed to THC (5μM) in sterile HEPES-buffered saline for 2hr. Cortical slices were also incubated with 0.007% methanol (v/v) for 2hr as vehicle control. Following treatment, slices were homogenised in lysis buffer and phosphorylated p53 protein expression assessed by western immunoblot using an antibody that recognises p53 when phosphorylated on serine-15.

Figure 6.11A demonstrates that exposure of cortical slices obtained from neonatal rats to THC for 2hr does not modulate phospho-$p53^{ser15}$ expression. Phosphorylated $p53^{ser15}$ expression in control slices treated with methanol vehicle for 2hr was 47.5 ± 5.6 arbitrary units (mean ± SEM) and this was unaffected by THC treatment 42.5 ± 3.0 for 2hr. Data in Figure 6.11B demonstrates that THC exposure for 2hr does not modulate phospho-$p53^{ser15}$ expression in cortical slices obtained from adolescent rats. Phosphorylated $p53^{ser15}$ expression in control slices exposed to methanol vehicle for 2hr was 31.2 ± 3.4 arbitrary units (mean ± SEM). Exposure of immature slices to THC (33.4 ± 3.8) for 2hr displayed a level of phospho-$p53^{ser15}$ expression comparable to basal controls. Similarly, Figure 6.11C demonstrates that exposure of mature cortical slices obtained from adult rats to THC for 2hr had no effect on phospho-$p53^{ser15}$ expression. Control phosphorylated p53 expression was 22.1 ± 2.0 arbitrary units (mean ± SEM) in mature slices obtained from adult rats treated with methanol vehicle for 2hr and this was unaffected by THC treatment (21.7 ± 1.9) for 2hr. These results suggest that a 2hr exposure to THC does not affect phospho-$p53^{ser15}$ expression in the neonatal, adolescent or adult rat cortex.

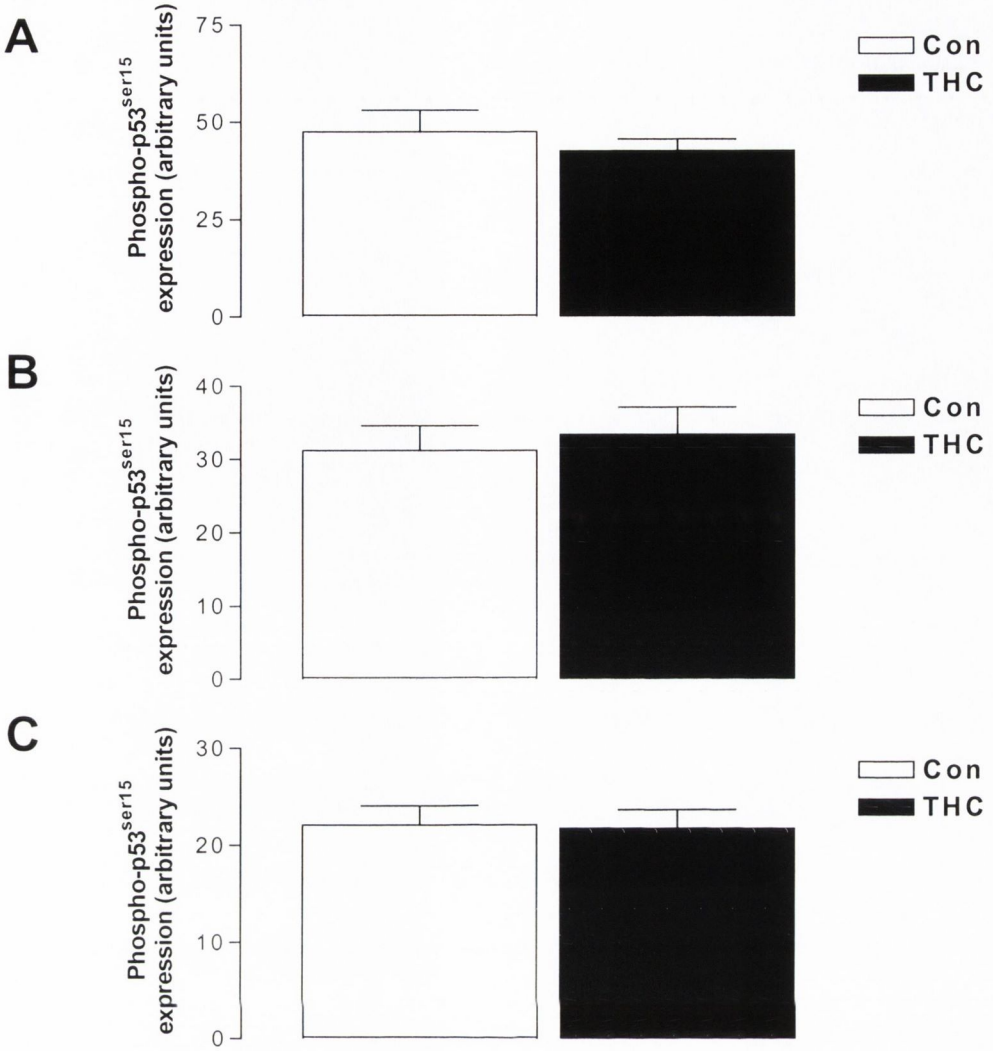

Figure 6.11: Effect of THC on p53 phosphorylation in cortical brain slices isolated from neonatal, adolescent and adult rats

Cortical slices from neonatal (4-7-day old), adolescent (20-30-day old), and adult (3-4 month old) rats were treated with THC (5μM) treatment for 2hr. Following treatment cell protein was harvested and analysed for the expression levels of phospho-p53^{ser15} using western immunoblot.

A: THC exposure for 2hr had no effect on phospho-p53^{ser15} in neonatal cortical slices. Results are expressed as mean ± SEM for 6 observations.

B: Phospho-p53^{ser15} expression was not affected by THC treatment of adolescent slices. Results are expressed as mean ± SEM for 4 observations.

C: THC had no effect on phospho-p53^{ser15} expression in adult slices. Results are expressed as mean ± SEM for 5 observations.

6.2.12 THC induces caspase-3 activation in cortical slices obtained from neonatal rats in a dose-dependent manner

The apoptotic protease caspase-3 is cleaved and activated in neonatal cultured cortical neurons following treatment with THC (5μM) for 2hr (Chapter 3). THC-induced caspase-3 activity in cultured cells is regulated by JNK1/2 (Chapter 4) and p53 (Chapter 5). Since we have previously shown that caspase-3 activity in neuronal cultures requires THC at a dose of 5μM (Chapter 3, 4, 5), a dose-response analysis of THC-induced caspase-3 activation was performed to determine the concentration of THC required to evoke maximal activation of the protease in cortical slices obtained from neonatal rats. Cortical slices obtained from neonatal (4-7-day old) rats were incubated with THC (5nM-5μM) in sterile HEPES-buffered saline for 2hr. Following treatment, slices were homogenised in lysis buffer and caspase-3 activity determined by monitoring the cleavage of the fluorescently labelled caspase-3 substrate, DEVD, to its fluorescent product.

Figure 6.12 shows that in slices obtained from neonatal rats exposed to vehicle for 2hr caspase-3 activity was 277.9 ± 99.1 pmol AFC produced/mg protein/min (mean ± SEM). Neonatal slices exposed to THC at concentrations of 5nM (575.6 ± 189.0 pmol AFC produced/mg protein/min) or 0.5μM (978.0 ± 166.0 pmol AFC produced/mg protein/min) for 2hr had no significant effect on the level of caspase-3 activity. However, caspase-3 activity was significantly increased to 1417.0 ± 161.1 pmol AFC produced/mg protein/min when cortical slices obtained from neonatal rats were treated with 5μM THC for 2hr ($p<0.05$, ANOVA, n=5 observations). A 50μM THC dose further increased caspase-3 activity to the significant value of 1756.0 ± 490.7 pmol AFC produced/mg protein/min in slices obtained from neonatal rats ($p<0.01$, ANOVA, n=5). This result demonstrates that THC modulates caspase-3 activity in neonatal cortical slices in a dose-dependent manner.

6.2.13 THC increases caspase-3 activity in cortical slices obtained from neonatal rats via CB_1

Involvement of the CB_1 receptor in THC-induced caspase-3 activation in neonatal cortical brain slices was monitored by pre-incubated cortical slices

with AM 251 (10μM; diluted in HEPES-buffered saline) for 30 min before treating with THC (5μM). Treatment with THC for 2hr significantly increased caspase-3 activity from 4.2 ± 1.8 pmol AFC produced/mg protein/min (mean ± SEM) in vehicle-treated neonatal slices to 43.1 ± 14.1 pmol AFC produced/mg protein/min ($p<0.01$, ANOVA, n=6 observations; Figure 6.13). Cortical slices obtained from neonatal rats treated with AM 251 alone for 2hr displayed a level of caspase-3 activity comparable to control values (4.1 ± 1.8 pmol AFC produced/mg protein/min). Furthermore, pre-treatment with AM 251 prior to THC exposure (4.7 ± 1.2 pmol AFC produced/mg protein/min) prevented the THC-induced increase in caspase-3 activity observed at 2hr, indicating that it was CB_1 receptor mediated. This result provides evidence that, in addition to increasing caspase-3 activity following CB_1 receptor activation in neonatal cultured cortical neurons, THC has the proclivity to activate caspase-3 via CB_1 in neonatal cortical brain slices.

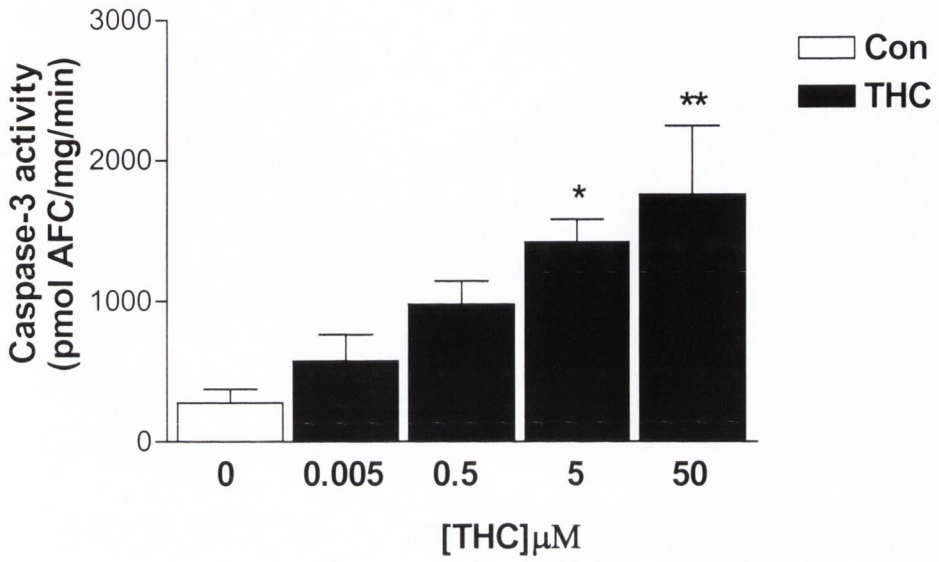

Figure 6.12: THC increases caspase-3 activity in cortical brain slices obtained from neonatal animals in a dose-dependent manner

Cortical neuronal slices obtained from neonatal (4-7-day old) rat pups were treated with increasing concentrations of THC (5nM-50μM) for 2hr, slices were lysed and caspase-3 activity was assessed by the cleavage of the fluorogenic DEVD substrate. A significant increase in caspase-3 activity was found following treatment with THC at concentrations of 5μM and 50μM. Results are expressed as mean ± SEM for 5 observations, **p<0.01, *p<0.05.

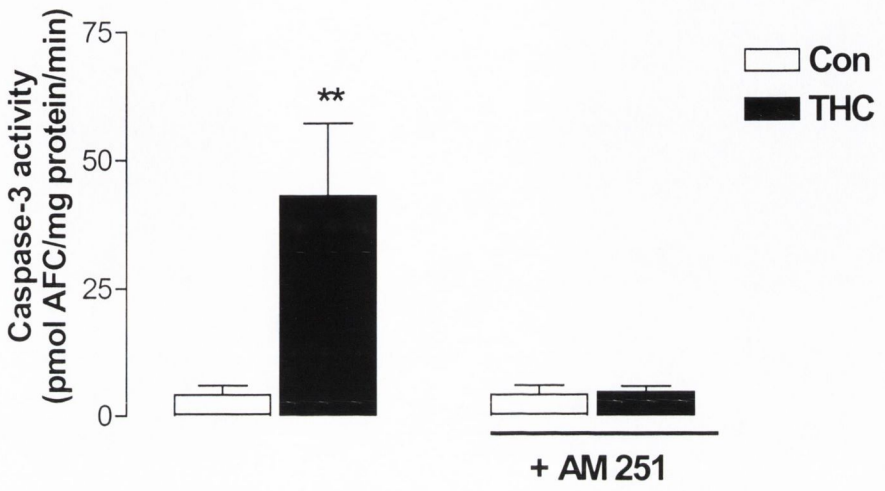

Figure 6.13: THC increases caspase-3 activity in cortical brain slices obtained from neonatal rats via CB_1

Treatment of cortical brain slices obtained from neonatal (4-7-day old) rats with THC (5μM) for 2hr significantly increased caspase-3 activity as assessed by the cleavage of the fluorogenic DEVD substrate. The stimulatory effect of THC on caspase-3 activity was prevented by AM 251 (10μM), indicating the involvement of the CB_1 cannabinoid receptor. Exposure of slices to the CB_1 inhibitor alone had no effect on caspase-3 activity. Results are expressed as the mean ± SEM for 6 observations, **$p<0.01$.

6.2.14 Dose-dependent analysis of the effects of THC on caspase-3 activity in rat cortical slices obtained from adolescent animals

To determine if the stimulatory effects of THC on caspase-3 activity are dependent on neuronal maturity, a dose-response analysis of the effects of THC on caspase-3 in cortical slices obtained from adolescent (20-30-day old) rats was performed to determine if the concentration of THC influences the state of activation of the caspase-3 enzyme in adolescent cortex (Figure 6.14). Cortical slices obtained from adolescent rats were exposed to increasing concentrations of THC for 2hr and caspase-3 activity assessed. Caspase-3 activity in vehicle-treated slices was 409.7 ± 48.7 pmol AFC produced/mg protein/min (mean ± SEM). Exposure of cortical slices obtained from adolescent rats to THC at concentrations of 5nM (388.9 ± 60.2 pmol AFC produced/mg protein/min), 0.5μM (433.0 ± 142.8 pmol AFC produced/mg protein/min), 5μM (406.1 ± 67.4 pmol AFC produced/mg protein/min), and 50μM (396.0 ± 92.1 pmol AFC produced/mg protein/min) did not affect caspase-3 activity, confirming that the proclivity of THC to induce caspase-3 activation depends on neuronal maturity, with the adolescent cortex being insensitive to cannabinoid exposure.

6.2.15 Dose-dependent effect of THC on caspase-3 activity in cortical slices obtained from adult rats

A dose-dependent analysis was used to determine if THC regulates caspase-3 activity in the adult cortex *ex vivo*. Cortical slices obtained from adult (3-4 month old) rats were exposed to THC (5nM-50μM) for 2hr and caspase-3 activity determined (Figure 6.15). Caspase-3 activity in adult slices exposed to methanol vehicle for 2hr was 311.2 ± 49.9 pmol AFC produced/mg protein/min (mean ± SEM). THC incubation for 2hr at doses of 5nM (307.5 ± 43.2 pmol AFC produced/mg protein/min), 0.5μM (304.4 ± 57.5 pmol AFC produced/mg protein/min), 5μM (293.2 ± 55.2 pmol AFC produced/mg protein/min) and 50μM (282.2 ± 37.7 pmol AFC produced/mg protein/min) had no effect on caspase-3 activation. This finding suggests that mature cortical slices obtained from adult rats are resistant to THC-induced caspase-3 activation.

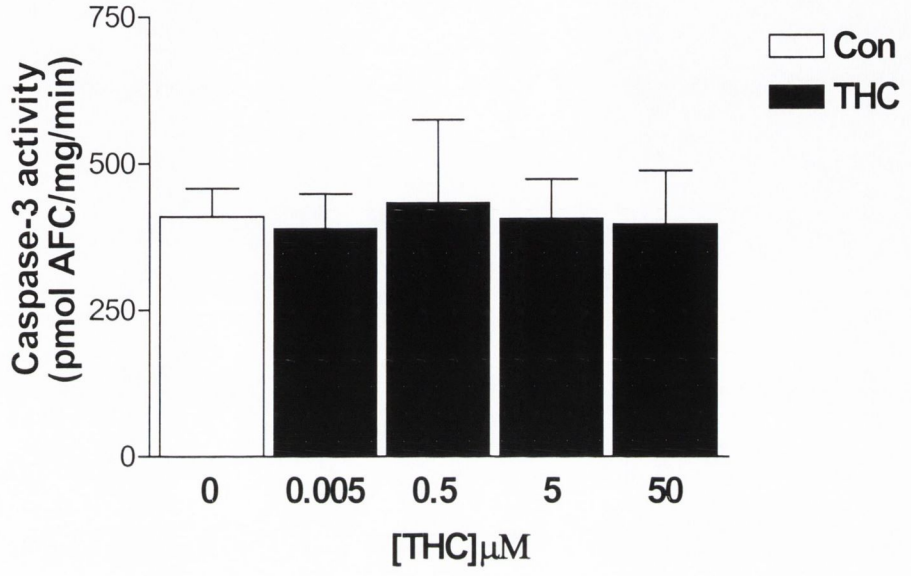

Figure 6.14: Dose-dependent analysis of the effect of THC on caspase-3 in cortical brain slices isolated from adolescent rats

Cortical neuronal slices obtained from adolescent (20-30-day old) rats were treated with increasing concentrations of THC (5nM-50μM) for 2hr, lysed and caspase-3 activity assessed. The doses of THC examined exerted no effect on caspase-3 activity. Results are expressed as mean ± SEM for 5 observations.

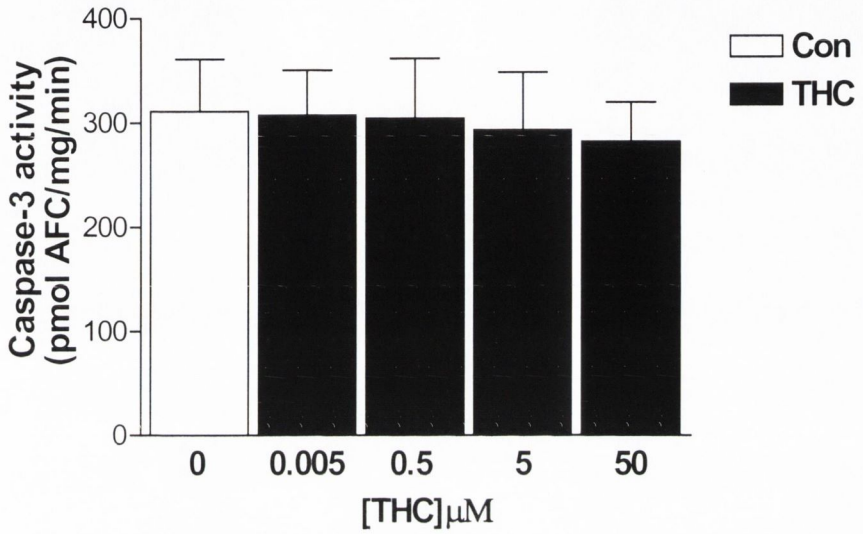

Figure 6.15: Dose-dependent analysis of the effect of THC on caspase-3 in cortical brain slices obtained from adult animals

Cortical neuronal slices obtained from adult (3-4 month old) rats were treated with increasing concentrations of THC (5nM-50μM) for 2hr, lysed and caspase-3 activity assessed. THC had no effect on caspase-3 activity at all the doses tested. Results are expressed as mean ± SEM for 4 observations.

6.2.16 Effect of postnatal development on basal caspase-3 activity in rat cortical brain slices

During embryonic and fetal development of rats, approximately 20-80% of neurons in a developing population die by the apoptotic process (Oppenheim *et al.*, 1991). Apoptosis is commonly associated with an increase in the activity of the caspase-3 enzyme (Janicke *et al.*, 1998). To determine if mean basal caspase-3 activity varies with postnatal development, cortical neuronal slices isolated from healthy neonatal (4-7-day old), adolescent (20-30-day old) and adult (3-4 month old) rats were homogenised in lysis buffer and caspase-3 activity determined by monitoring the cleavage of the fluorescently labelled caspase-3 substrate, DEVD, to its fluorescent product (Figure 6.16). In cortical slices obtained from neonatal rat pups, mean basal caspase-3 activity was 2.9 ± 0.1 pmol AFC produced/mg protein/min (mean ± SEM). There was a significant reduction in basal caspase-3 activity in cortical tissue isolated from adolescent rats (0.9 ± 0.2 pmol AFC produced/mg protein/min; $p<0.01$, ANOVA, n=4 observations) and adult rats (0.4 ± 0.1 pmol AFC produced/mg protein/min; $p<0.001$, ANOVA, n=6 observations). This finding provides evidence that the tonic level of caspase-3 activity and apoptosis is higher in neonatal rats than in adolescent and adult rats due to cortical neuronal development in the neonate.

Figure 6.16: Basal caspase-3 activity is associated with postnatal development

Cortical brain slices obtained from neonatal (4-7-day old), adolescent (20-30-day old) and adult (3-4 month old) rats were homogenised in lysis buffer and caspase-3 activity determined by monitoring the cleavage of the fluorescent caspase-3 substrate, DEVD, to its fluorescent product. A significant decrease in caspase-3 activity was found cortical slices isolated from adolescent and adult animals as compared to basal levels in cortical slices from neonatal rats. Results are expressed as mean ± SEM for 4-6 observations, ***$p<0.001$, **$p<0.01$.

6.3 Discussion

The aim of this study was to examine the *ex vivo* effects of THC on the viability of cortical slices obtained from three rat age groups; neonatal (4-7-day old), adolescent (20-30-day old) and adult (3-4 month old) rats. These age groups were selected following an examination of the studies by Fernández-Ruiz and colleagues, which have comprehensively determined the effects of perinatal cannabinoid exposure on the neonatal, immature and mature adult nervous system (Fernández-Ruiz *et al.*, 1992; Fernández-Ruiz *et al.*, 1994; Fernández-Ruiz *et al.*, 1996; Fernández-Ruiz *et al.*, 1999; Fernández-Ruiz *et al.*, 2000; Garcia-Gil *et al.*, 1999a; Garcia-Gil *et al.*, 1998). The inter-relationship between neuronal maturity and THC apoptotic signal transduction was determined. In all experiments, cortical brain slices were incubated with THC (5nM-50μM) for a 2hr period, a time point at which THC actively regulates the apoptotic machinery in cultured cortical neurons (Chapter 3, 4, 5). At this time point THC induced a dose-dependent increase in the activity of the JNK2, but not the JNK1, isoform in cortical slices obtained from neonatal rats. Furthermore, a regulatory effect of THC on JNK2 activity was determined in cortical slices obtained from adolescent and adult rats, but only at the highest concentrations tested. The ability of THC to induce activation of JNK2 in the neonate was blocked by AM 251, implicating the involvement of CB_1 cannabinoid receptors. THC (2hr incubation) had no effect on the expression levels of p53 phosphorylated on serine-15 in cortical slices obtained from the three rat age groups. However, THC significantly increased caspase-3 activity via CB_1 in cortical slices obtained from neonatal, but not adolescent or adult animals. The proclivity of THC to induce caspase-3 activation in the neonatal cortex was dose-dependent. Interestingly, the expression of CB_1 receptor varied considerably in rat cortical slices depending on developmental age, which may have important implications for cannabinoid-induced effects during postnatal development. Overall, this study indicates that the proclivity of THC to regulate apoptotic molecules in the rat cortex are dependent on postnatal development.

Apoptotic and anti-proliferative actions of cannabinoids on cultured neurons (Chan *et al.*, 1998; Kim and Thayer, 2001; Sarker *et al.*, 2003) and glioma cells (Sánchez *et al.*, 1998) are well characterised. *In vivo* studies examining the neurotoxic properties of cannabinoids in the adult brain have concluded that cannabinoids can induce morphological changes in brain structures that are indicative of toxicity (Scallet *et al.*, 1987; Lawston *et al.*, 2000). However, these studies have failed to identify apoptotic markers in the brain of cannabinoid-treated adult animals. Indeed, Galve-Roperh and colleagues (2000) have shown an absence of apoptosis using the TUNEL technique in the subventricular zone of the adult rat brain exposed to THC for 7 days. Furthermore, Hollister (1986) found that marijuana does not cause structural damage to the brains of laboratory animals or long-term damage to the human brain. These studies are consistent with our findings in cortical slices obtained from adolescent and adult rats exposed to THC *ex vivo*. Specifically, data presented in this chapter has shown that THC has no effect on key components of the THC-induced apoptotic pathway, including JNK and caspase-3, in cortical slices obtained from adolescent and adult rats.

Exposure of neonatal rats to THC can alter behaviour (Meyer and Kunkle, 1999). Although there is indirect evidence that the neonatal brain is susceptible to THC-induced apoptosis from *in vitro* studies (Chan *et al.*, 1998), our findings demonstrate that cortical slices obtained from neonatal rats are susceptible to THC-induced JNK2 and caspase-3 activation. This suggests that the neonatal brain may be more vulnerable to the neurodegenerative effects of THC and is consistent with the findings of Do and colleagues (2004). In this study, mature dendritic cells were more resistant to the apoptotic actions of THC than immature cells (Do *et al.*, 2004). It is noteworthy that, in the present study, the highest concentrations THC tested induced an increase in JNK2 activity in cortical slices obtained from the adolescent and adult animals, which may indicate a non-apoptotic function of JNK2 in the mature cortex following cannabinoid exposure. This does not eliminate the possibility that apoptotic effects of cannabinoids exist in the mature cortex following exposure to THC at high doses. However, the 50μM dose of THC is not reflective of human plasma concentratrions following recreational marijuana use (Azorlosa *et al.*, 1992).

The ability of THC to induce DNA fragmentation was determined by assessing DNA laddering using agarose gel electrophoresis. Unfortunately, DNA laddering was not observed in any treatment groups, but as discussed in Chapter 3, this technique remains to be optimised in the laboratory. However, the modulatory effects of THC on JNK2 and caspase-3 activity is evidence that the neonatal brain is sensitive to cannabinoid-induced cell death. The stimulatory effects of THC on JNK2 and caspase-3 activity in cortical slices obtained from neonatal animals were CB_1- and dose-dependent. This finding is supported by the recent study by McKallip and co-workers (2002). In this study it was shown that neonatal rats injected on the 2^{nd} postnatal day with a pharmacologically relevant dose (1mg/kg) of anandamide show evidence of mitochondrial damage of the B-type neurons of the trigeminal ganglia and dorsal root ganglia (Szöke *et al.*, 2002). This effect is detected 1 week post-treatment and was progressive up to at least the 20^{th} week (Szöke *et al.*, 2002). This finding is significant since mitochondrial function is commonly perturbed early during the apoptotic process (Zamzami *et al.*, 1996). Indeed, the apoptotic events responsible for THC-induced apoptosis of cultured cortical neurons involve an alteration in the expression of the mitochondria-associated proteins (Chapter 5) and the increased translocation of mitochondrial cytochrome *c* (Chapter 3). It is also interesting to note that, despite the stimulatory effects of THC on JNK2 activity in neonatal cortical slices, THC had no effect on JNK1 phosphorylation in the neonatal rat age group. This may be due to a differential time frame of JNK1 and JNK2 activation following THC treatment. Indeed, in Chapter 4 data was presented demonstrating THC-induced activation of JNK1 at 5 min and JNK2 at 2hr in cultured cortical neurons, which may account for the effects of THC on JNK2 activity at 2hr in neonatal cortical brain slices. Similarly, time course experiments have revealed that the apoptotic actions of THC in cultured cortical neurons involve an early transient increase in the phosphorylation of p53 on residue serine-15 at 5 min, stabilising the p53 protein and accounting for the increase in p53 protein expression at the same time point (Chapter 5). In the present study, THC exposure for 2hr had no effect on normal p53, or phospho-$p53^{ser15}$, protein expression, mirroring the effects of THC on p53 in cultured cortical neurons at

2hr and suggesting an alternative time course of p53 induction in the rat cortex *ex vivo*.

It is worth noting that in the brain, JNK expression varies during development (Carboni *et al.*, 1998; Yang *et al.*, 1997). Carboni and colleagues (1998) have shown that JNK2 and JNK3 are the main isoforms expressed in the adult brain and that the expression patterns of these isoforms does not vary during development. In contrast, JNK1 displays high and diffuse expression in the newborn rat brain but its expression progressively declines during post-natal development to become restricted to the endopiriform nucleus and the medial habenula (Carboni *et al.*, 1998). Despite the high expression patterns of JNK1 in the neonatal rat brain, this isoform does not appear to be involved in THC-induced apoptotic signalling in the neonatal cortex at the 2hr time point.

THC was found to activate caspase-3, an executioner protease in the apoptotic pathway (Martin and Green, 1995), in cortical tissue isolated from neonatal, but not adolescent or adult rats. This again suggests that the neonatal brain may be more vulnerable to the neurodegenerative effects of THC as the proclivity of THC to activate caspase-3 was eliminated as postnatal development progressed. The ability of THC to induce the activation of caspase-3 in neonatal cortical tissue was blocked by AM 251, implicating the involvement of CB_1 cannabinoid receptors. Again, this finding and timeframe of activation is concurrent with the apoptotic actions of THC on cultured cortical neurons prepared from neonatal rats (Chapter 3, 4, 5). Experimental evidence in Chapter 4 revealed that the transduction pathway contributing to THC-induced apoptosis of cultured neurons involves JNK isoforms acting upstream in the regulating the activity of caspase-3, a finding supported by other studies (Bozyczko-Coyne *et al.*, 2001). Hence, a reasonable model predicts that, in the neonatal cortex *ex vivo*, THC couples to the CB_1 cannabinoid receptor to induce JNK2 phosphorylation and subsequent caspase-3 activation, resulting in the demise of the cortical cells. In addition, considering that JNK activity may be regulated by caspase-3 (Ozaki *et al.*, 1999; Hatai *et al.*, 2000) and we have previously shown that caspase-3 is activated as early as 30 min after exposure to THC in cortical neurons (Chapter 3), it is possible that JNK2 activity is modulated by caspase-3 in this *ex vivo* system.

In contrast to our evidence that the neonatal cortex is sensitive to the damaging effects of THC exposure, a recent report has shown that THC is neuroprotective in an *in vivo* model of excitotoxicity (van der Stelt *et al.*, 2001). In this study, THC reduced neuronal injury elicited by the inhibition of the Na^+/K^+-ATPase in 7- to 8-day-old neonatal rats. This effect was CB_1 receptor-dependent and occurred following a 30 min exposure to THC prior to toxin injection. It is also interesting to note that in infant rat models of *in vivo* neurodengeneration, anandamide precursors (Hansen *et al.*, 2001a) and anandamide concentrations and CB_1 receptor density are increased in the cortex (Hansen *et al.*, 2001b), which may represent a putative neuroprotective response. These studies, in conjunction with the experimental data presented in this chapter, indicate the complex regulatory effects of cannabinoids on neuronal viability, with neurotoxic and neuroprotective effects of cannabinoids being observed.

A recent study by Schneider and Koch (2003) has shown that the pubertal period in rats (postnatal day 40-65) is a vulnerable period for the effects of cannabinoids. Indeed, chronic peripubertal treatment with the synthetic cannabinoids led to long-lasting deficits in sensorimotor gating and object recognition memory in adult animals. This finding is consistent with behavioural studies in humans subjects which have shown attentional deficits in adults following marijuana abuse in early-onset users (before age 16; Ehrenreich *et al.*, 1999). Furthermore, chronic exposure of immature rats to THC has been shown to produce residual effects on different behaviours (Stiglick and Kalant, 1985). It is suggested that these disturbances are due to a persistent imbalance in various neurotransmitter systems induced by cannabinoid exposure during pubertal development (Schneider and Koch, 2003). Overall these results suggest that immature nervous system may be susceptible to the physiological effects of cannabinoid administration. Despite these findings, data presented in this chapter indicate that the adolescent rat cortex is insensitive to THC-induced activation of apoptotic signalling molecules. This does not eliminate the possibility that chronic THC treatments or cannabinoid exposure *in vivo* may influence neuronal viability in the adolescent cortex.

The data presented in this and previous chapters (Chapter 3, 4, 5) indicate that the apoptotic pathway triggered by THC in rat cortical neurons is reliant on THC coupling to the central CB_1 cannabinoid receptor. Indeed, western immunoblot analysis in this chapter has shown the presence of CB_1 receptors in cortical slices obtained from neonatal rat pups, which is consistent with the published distribution patterns of this receptor in the brain (Tsou *et al.*, 1998; Mailleux and Vanderhaeghen, 1992). However, there is growing evidence that cannabinoid receptor expression levels in the brain vary with developmental age (Fernández-Ruiz *et al.*, 2000). Indeed, the results presented here demonstrate that the level of CB_1 receptor expression increases with postnatal development. This is consistent with the findings of Rodriguez de Fonseca and co-workers (1993), which demonstrate a progressive increase in cannabinoid receptor expression in rats from postnatal day 10 to maximum values between postnatal day 30 in the forebrain and postnatal day 40 in the striatum. Cannabinoid receptor expression was shown to decrease after postnatal day 40 to reach the adult values at postnatal day 70 (Rodriguez de Fonseca *et al.*, 1993). However, these findings differ from other studies that have shown that the density of the receptor is markedly higher in the developing brain. For example, based on expression patterns in key brain regions it has been shown that the human CB_1 receptor expression is higher in the fetal and neonatal brain when compared with expression levels in the adult human brain (Glass *et al.*, 1997). Similarly, functional CB_1 receptors have been located in fetal white matter areas (Berrendero *et al.*, 1998), areas that display low CB_1 receptor density in the adult brain (Berrendero *et al.*, 1998). The transient nature of this phenomenon has been interpreted as related to the possible involvement of the cannabinoid system in developmental events, such as cell proliferation and migration, axonal elongation and synaptogenesis (Fernández-Ruiz *et al.*, 1999). The role of the endogenous cannabinoid system in brain development is also supported by evidence of the progressive increase in anandamide levels in the cerebrum, cerebellum and hippocampus during development (Koga *et al.*, 1997). It is reasonable to hypothesize that overstimulation of cannabinoid receptors at critical stages of development in the neonatal cortex may have damaging consequences on nervous system functioning. Indeed, several studies have shown that prenatal and early

postnatal exposure to THC or THC in combination with other cannabinoids produces long-term abnormalities in brain function (Dalterio, 1986; Fernández-Ruiz *et al.*, 1992; Nahas and Frick, 1986; Mokler *et al.*, 1986; Navarro *et al.*, 1995).

Several studies have shown that prenatal and early postnatal exposure to THC or THC in combination with other cannabinoids produces long-term abnormalities in brain function (Dalterio, 1986; Fernández-Ruiz *et al.*, 1992; Nahas and Frick, 1986; Mokler *et al.*, 1986; Navarro et al., 1995). Indeed, Mirmiran and Swaab (1987) have suggested that the last week of prenatal and the first three weeks of postnatal life in the rat is a period of increased vulnerability to drug actions. Indeed, data presented herein has shown that cortical slices prepared from 4-7-day old rats are sensitive to cannabinoid-induced apoptosis. Cannabinoids can readily be transferred from the mother to the offspring through placental blood during gestation (Martin *et al.*, 1977) or through milk during lactation (Jakubovic *et al.*, 1973). In both cases, cannabinoids can reach the fetal and neonatal brain in substantial amounts due to the immaturity of the blood-brain barrier at these ages (Fernández-Ruiz *et al.*, 1992; Fernández-Ruiz *et al.*, 1994). Cannabinoid-exposure during prenatal and early postnatal periods has been shown to alter the temporally-ordered sequence of events that occur during neurotransmitter development (Fernández-Ruiz *et al.*, 2000). Furthermore, cannabinoid exposure during perinatal periods affects the maturation of dopaminergic systems at immature rat ages (postnatal days 15-40; Rodriguez de Fonseca *et al.*, 1991). A large list of studies have revealed modulatory effects of cannabinoids on the maturation of dopamine, (Fernández-Ruiz *et al.*, 1992; Fernández-Ruiz *et al.*, 1994; Fernández-Ruiz *et al.*, 1996), serotonin (Molina-Holgado *et al.*, 1996), and opioidergic neurons (Kumar *et al.*, 1990). These modifications during perinatal periods are followed by long-term effects on adult behaviour.

Overall, the findings from this preliminary *ex vivo* study of the influence of neuronal development on THC-induced apoptosis indicate that the neonatal cortex may be more susceptible to the neurodegenerative actions of THC. This is indicated by the proclivity of THC to modulate key apoptotic transduction molecules in cortical tissue isolated from neonatal, but not the adolescent or adult, animals. Specifically, THC-induced an increase in JNK2 phosphorylation

and caspase-3 activity in cortical slices obtained from neonatal rat pups, central molecules in transduciing apoptotic signals in the neonatal cortex *in vitro*. In summary, these findings indicate an inter-relationship between neuronal maturity and the impact of THC on neural fate.

Chapter 7

The effect of postnatal development on THC-induced apoptosis in the rat cortex – An in vivo study

note that the regulatory effects of THC on apoptotic signal transduction in cortical slices obtained from neonatal animals was absent in the adolescent and adult cortex (Chapter 6). This finding suggests that the immature cortex may be more vulnerable to the effects of THC on apoptotic parameters. The present study expanded this investigation to an *in vivo* system. Specifically, neonatal and adult animals received subcutaneous injections of THC for 3hr, a time point at which THC induces a significant level of apoptosis in cultured cortical neurons (Chapter 3). Rats were then sacrificed and the ability of THC, acting through the CB_1 receptor, to impact on the active forms of JNK1/JNK2 and caspase-3 were determined. Furthermore DNA fragmentation was determined using the TUNEL technique in cryostat sections prepared of the rat cortex. Finally, the contribution of the mitochondria-associated proteins, Bax and Bcl-2, to the *in vivo* effects of THC were assessed.

7.2 Results

7.2.1 THC induces DNA fragmentation in the neonatal, but not the adult, cortex *in vivo*

Since we have shown that THC induces DNA fragmentation in cultured cortical neurons (Chapter 3) and that the proclivity of THC to induce the activation of apoptotic molecules in cortical slices is dependent upon postnatal development (Chapter 6), the ability of THC to induce DNA fragmentation in the rat cortex *in vivo* was assessed. Neonatal (4-7-day old) rat pups and adult (3-4 month old) rats received subcutaneous injections of 10mg/kg THC in vehicle (5% absolute alcohol, 5% Cremophor EL and 90% sterile saline) for 3hr. A control group received injections of vehicle alone for 3hr. Following treatment, cryostat sections were prepared and the level of DNA fragmentation determined using the TUNEL technique (Figure 7.1). Neonatal rats treated with THC for 3hr showed a higher level of DNA fragmentation than neonatal rats exposed to vehicle alone (n=4 observations; Figure 7.1A). Interestingly, there was no difference in the occurrence of DNA fragmentation in THC-treated adult rats and vehicle-treated adult rats (Figure 7.1B). This suggests that the apoptotic actions of THC in the cortex are prevalent *in vivo* and that the proclivity of THC to induce apoptosis is dependent on neuronal maturity, with the neonatal cortex being susceptible to the damaging effects of THC. Representative images of cryostat sections of the cortex stained for DNA fragmentation using the TUNEL technique are shown in Figure 7.1.

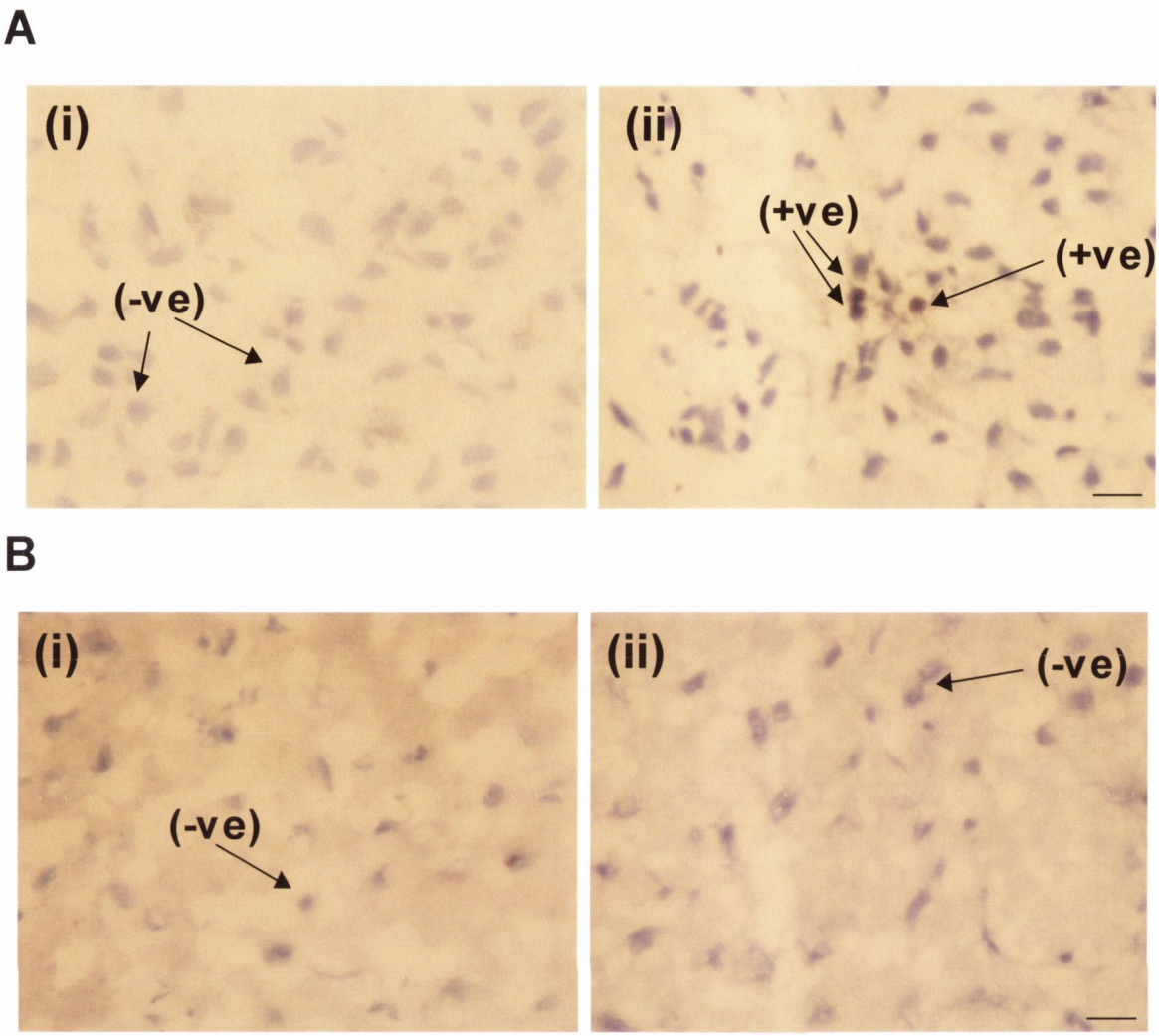

Figure 7.1: THC induces apoptosis in the neonatal cortex *in vivo*

Neonatal (4-7-day old) and adult (3-4 month old) rats received subcutaneous injections of 10mg/kg THC in vehicle or vehicle alone for 3hr and cryostat sections prepared. The level of DNA fragmentation was determined in the cortex using the TUNEL technique.

A: Exposure of neonatal animals to (ii) THC for 3hr increased the number of TUNEL-positive neurons displaying fragmented DNA in the nucleus relative to the (i) control. Arrows indicate TUNEL-negative (-ve) and TUNEL-positive (+ve) cells. Scale bar is 25μm.

B: Representative images of TUNEL staining of cryostat sections obtained from (i) vehicle-treated adult rats and (ii) THC-treated adult rats. THC had no effect on the level of DNA fragmentation in the adult cortex. Scale bar is 25μm.

7.2.2 Dose-dependency of THC-induced DNA fragmentation in the neonatal cortex *in vivo*

Since THC (10mg/kg) was shown to induce DNA fragmentation in the neonatal cortex but not the adult cortex (Figure 7.1) the dose-dependency of this effect was assessed to determine if higher THC concentrations are required to induce apoptosis in the adult cortex *in vivo*. Neonatal (4-7-day old) rat pups and adult (3-4 month old) rats received subcutaneous injections of 1, 10 and 30mg/kg THC in vehicle (5% absolute alcohol, 5% Cremophor EL and 90% sterile saline) or vehicle alone for 3hr, cryostat sections were prepared and DNA fragmentation assessed using TUNEL staining (Figure 7.2). Neonatal rats treated with THC at concentrations of 10mg/kg and 30mg/kg showed a higher level of DNA fragmentation than rats exposed to 1mg/kg THC and vehicle alone (n=4 observations; Figure 7.2A), although there was evidence of apoptosis in rats exposed to 1mg/kg THC (n=4). Treatment of adult rats with 1mg/kg THC, 10mg/kg THC and 30mg/kg THC had no effect on the level of DNA fragmentation in the cortex when compared to sections taken from the cortex of vehicle-treated adult animals (Figure 7.2B). This result suggests that the apoptotic actions of THC in the neonatal cortex *in vivo* are dose-dependent. Representative TUNEL images of cryostat sections of the neonatal and adult cortex are shown in Figure 7.2.

7.2.3 AM 251 prevents THC-induced DNA fragmentation in the neonatal cortex *in vivo*

The apoptotic effects of THC on cultured cortical neurons (Chapter 3) and cortical slices obtained from neonates exposed to THC (Chapter 6) are dependent on the activation of the CB_1 cannabinoid receptor. To determine if the *in vivo* apoptotic effects of THC in the neonatal cortex are dependent on THC coupling to CB_1, neonatal (4-7-day old) rats received intraperitoneal injections of the CB_1 antagonist AM 251 (10mg/kg) in vehicle (5% absolute alcohol, 5% Cremophor EL and 90% sterile saline) for 30 min prior to THC (10mg/kg; 3hr) treatment (Figure 7.3). The control CB_1 receptor inhibitor group received an intraperitoneal injection of AM 251 (10mg/kg) alone for 3hr. In cryostat sections taken from neonatal animals treated with THC for 3hr the level of DNA fragmentation was high compared to sections from vehicle-

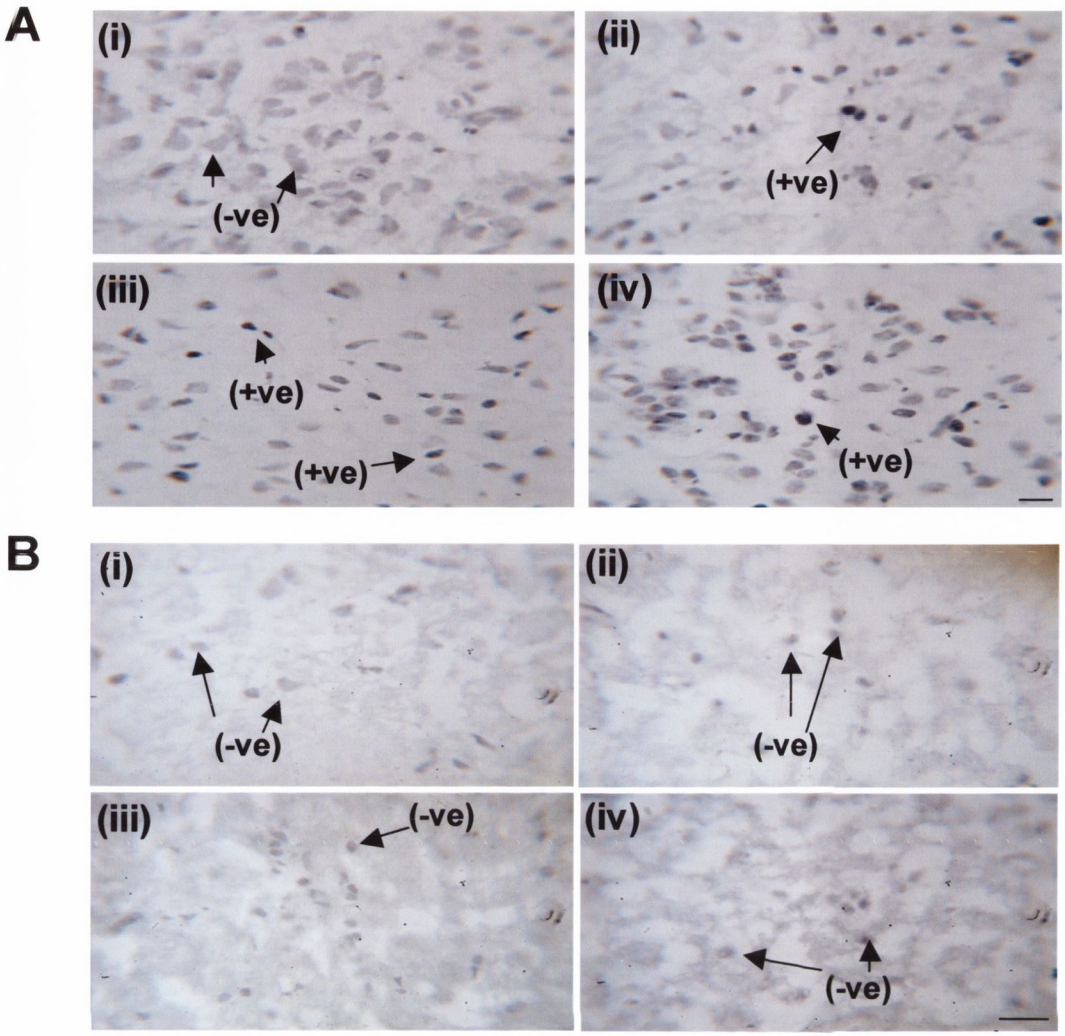

Figure 7.2: Dose-dependency of THC-induced apoptosis in the neonatal/adult cortex *in vivo*

Neonatal (4-7-day old) and adult (3-4 month old) rats received subcutaneous injections of THC (1, 10, 30mg/kg) for 3hr and the level of DNA fragmentation was assessed in cryostat sections using the TUNEL technique.

A: Exposure of neonatal rats to (ii) 1mg/kg, (iii) 10mg/kg and (iv) 30mg/kg THC for 3hr increased the number of TUNEL-positive neurons in the cortex displaying fragmented DNA in the nucleus relative to the (i) control. Arrows indicate TUNEL-negative (-ve) and TUNEL-positive (+ve) cells. Scale bar is 25μm.

B: Adult crytostat sections taken from animals treated with (ii) 1mg/kg, (iii) 10mg/kg and (iv) 30mg/kg THC had no effect on the level of DNA fragmentation in the cortex when compared to sections taken from (i) control adult animals. Scale bar is 25μm.

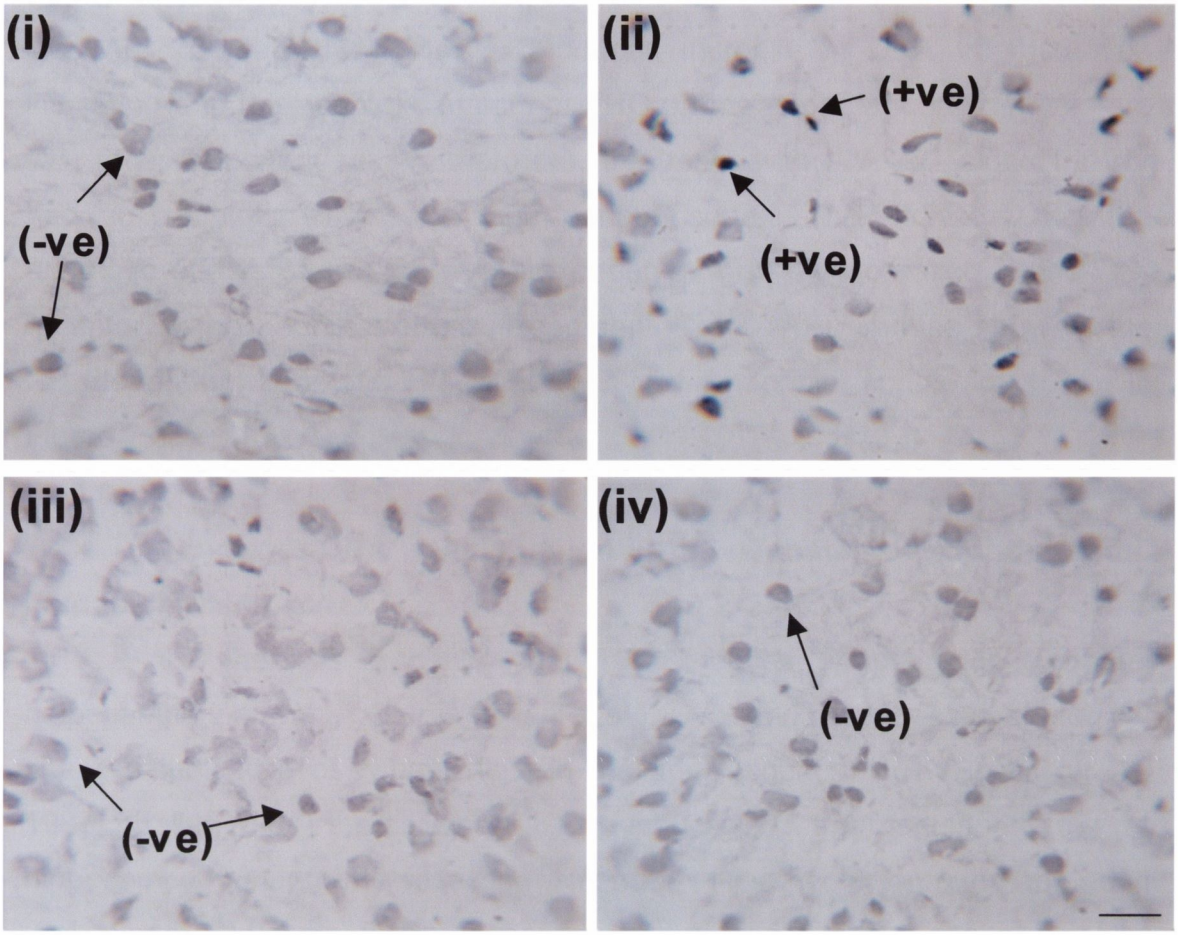

Figure 7.3: The *in vivo* apoptotic actions of THC in the neonatal cortex are CB_1 receptor-dependent

Neonatal (4-7-day old) rats received intraperitoneal injections of the CB_1 antagonist AM 251 (10mg/kg) for 30 min prior to THC (10mg/kg; 3hr) treatment. Control groups received subcutaneous injections of vehicle or AM 251 (10mg/kg) alone for 3hr. The level of DNA fragmentation in the cortex was assessed in cryostat sections using the TUNEL technique. Representative images of TUNEL staining of cryostat sections from (i) vehicle-treated neonatal rats, (ii) THC-treated neonatal rats, (iii) AM 251-treated neonates and (iv) THC+AM 251-treated neonatal rats show that THC increases the level of DNA fragmentation in a CB_1-dependent manner. Arrows indicate TUNEL-negative (-ve) and TUNEL-positive (+ve) cells. Scale bar is 25μm.

treated animals (n=4 observations), as was shown in Figure 7.1. Pre-treatment with AM 251 prevented the THC-induced increase in DNA fragmentation indicating that the apoptotic effects of THC on the neonatal cortex *in vivo* are CB_1 receptor-dependent. Furthermore, treatment with AM 251 alone for 3hr had no apoptotic effects on the neonatal cortex. This indicates that the apoptotic effects of THC *in vivo* are dependent on the activation of the CB_1 receptor in the neonatal cortex. Representative TUNEL images showing the CB_1-dependent apoptotic effects of THC in the neonatal cortex are shown in Figure 7.3.

7.2.4 THC induces DNA fragmentation in the neonatal, but not the adult, hippocampus *in vivo*

Since there is evidence that THC induces apoptosis in neonatal hippocampal neuronal cultures (Chan *et al.*, 1998) and produces morphological changes indicative of neurotoxicity in the adult hippocampus (Scallet *et al.*, 1987; Scallet, 1991) the ability of THC to induce DNA fragmentation in the rat hippocampus *in vivo* was assessed. Neonatal (4-7-day old) rat pups and adult (3-4 month old) rats were assessed to determine if the age of the rat determined if neurotoxic effects of THC exist in the hippocampus. Animals received subcutaneous injections of 10mg/kg THC in vehicle (5% absolute alcohol, 5% Cremophor EL and 90% sterile saline) for 3hr. A control group received injections of vehicle alone for 3hr. Following treatment, cryostat sections were prepared and the level of DNA fragmentation in the hippocampus determined using the TUNEL technique (Figure 7.4). Neonatal rats treated with vehicle for 3hr showed little evidence of apoptosis in the hippocampus. However THC-treated neonatal rats showed a high level of DNA fragmentation in the hippocampus (n=4 observations; Figure 7.4A). Interestingly, THC had no effect on the number of hippocampal neurons displaying fragmented DNA in sections prepared from adult rats (Figure 7.4B). This suggests that THC induces apoptosis in the neonatal, but not the adult, hippocampus *in vivo*. Representative images of hippocampal cryostat sections stained for DNA fragmentation using the TUNEL technique are shown in Figure 7.4.

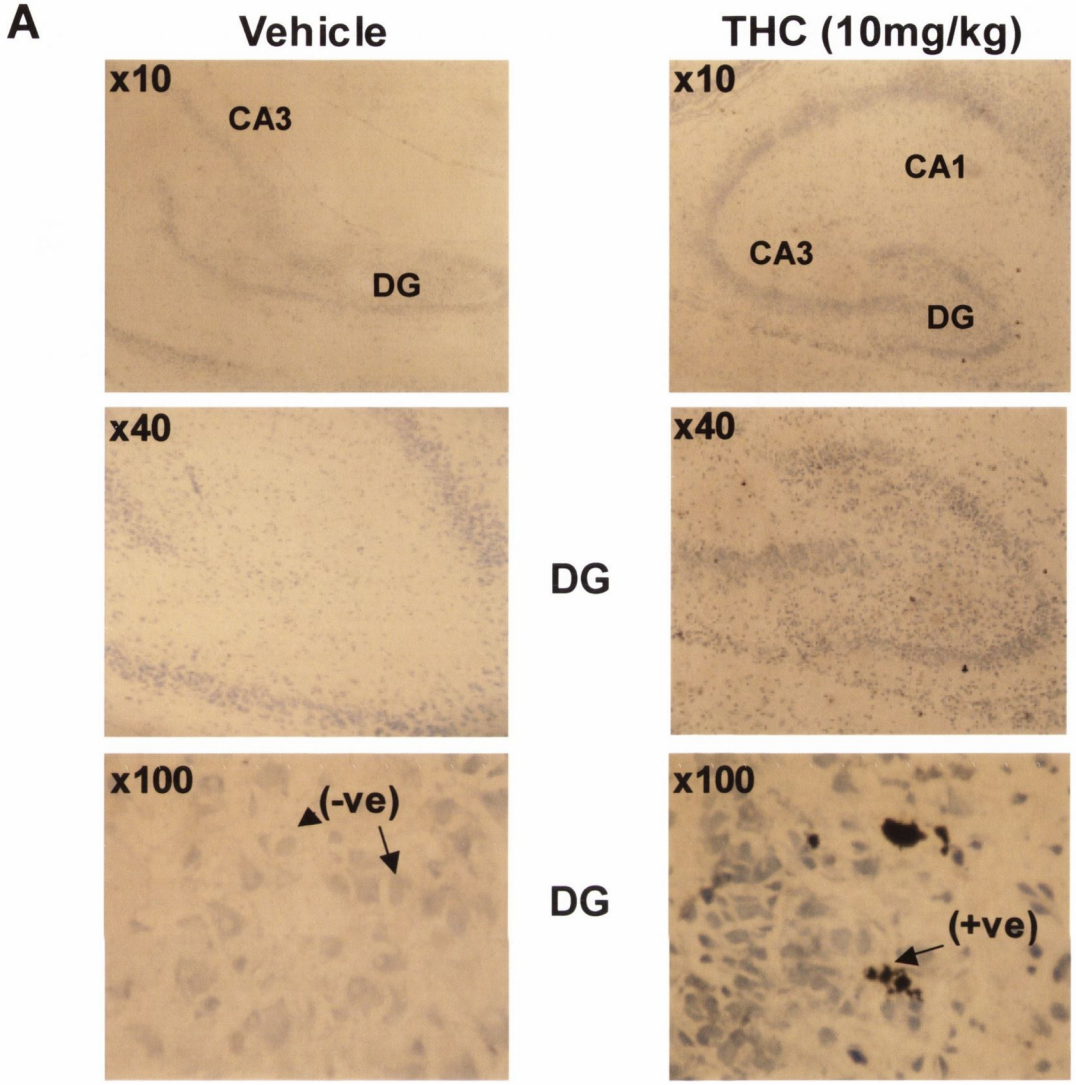

Figure 7.4: THC induces DNA fragmentation in the neonatal hippocampus *in vivo*

Neonatal (4-7-day old) and adult (3-4 month old) rats received subcutaneous injections of 10mg/kg THC in vehicle or vehicle alone for 3hr and cryostat sections prepared. The level of DNA fragmentation was determined in the dentate gyrus (DG) of the hippocampus using the TUNEL technique.

A: Exposure of neonatal rats to THC induced DNA fragmentation in the hippocampus. The lefthand panels are representative images showing TUNEL staining of the hippocampus from vehicle-treated neonates and the righthand panel are representative images from THC-treated animals. Arrows indicate TUNEL-negative (-ve) and TUNEL-positive (+ve) cells.

B

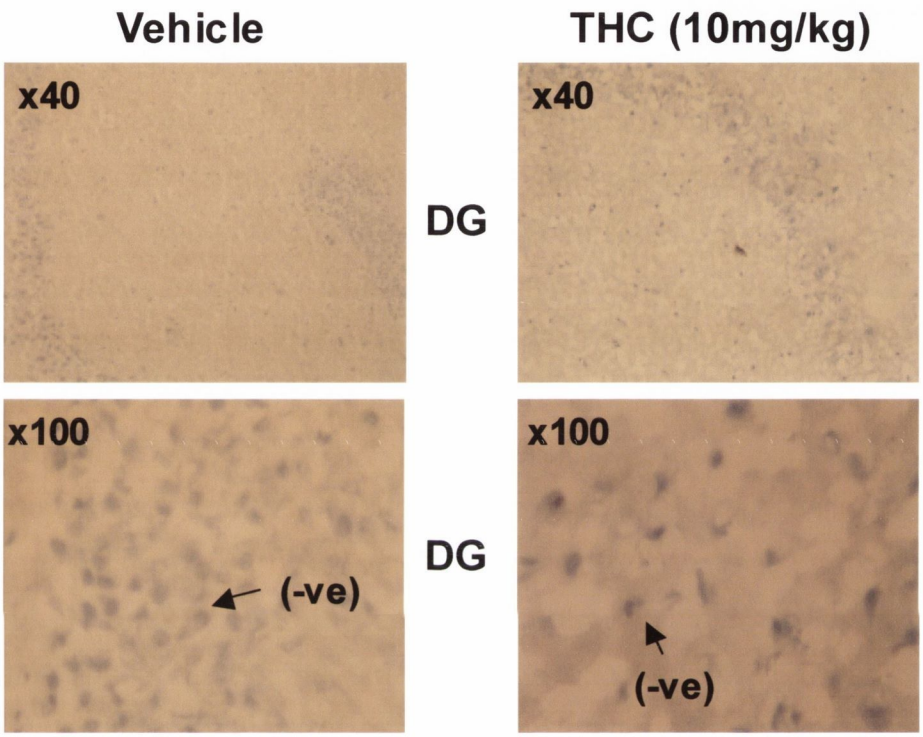

B: Representative images of TUNEL staining of the dentate gyrus (DG) of the hippocampus from vehicle-treated (lefthand panel) and THC-treated (righthand panel) adult rats. THC had no effect on the level of DNA fragmentation in the adult hippocampus. Arrows indicate TUNEL-negative (-ve) and TUNEL-positive (+ve) cells.

7.2.5 THC increases JNK phosphorylation in the neonatal cortex, but not the adult cortex, *in vivo*

The apoptotic effects of THC in cultured cortical neurons involve the activation of the MAPK family member, JNK (Chapter 4). To determine if THC regulates JNK activity (phosphorylation) in an *in vivo* system, neonatal (4-7-day old) rat pups and adult (3-4 month old) rats received subcutaneous injections of THC (10mg/kg; 3hr) in vehicle (5% absolute alcohol, 5% Cremophor EL and 90% sterile saline). A control group received injections of vehicle alone for 3hr. Following treatment, cryostat sections were prepared and JNK phosphorylation assessed in the cortex by fluorescence immunocytochemistry (Figure 7.5). Phospho-JNK immunofluorescence was detected using an anti-phospho-specific JNK antibody which recognises JNK1 and JNK2 isoforms phosphorylated on residues Thr-183 and Tyr-185, in addition to a FITC-conjugated secondary antibody. Cells were viewed by fluorescence microscopy at an excitation wavelength of 490nm. In vehicle-treated animals, phospho-JNK immunoreactivity was detectable in the cortex of cryostat sections taken from neonatal (Figure 7.5A(i)) and adult (Figure 7.5B(i)) animals, indicating a tonic level of JNK activation in the cortex of control animals. However, in cryostat sections obtained from neonatal animals exposed to THC for 3hr (Figure 7.5A(ii)) a higher intensity of phospho-JNK immunoreactivity was observed in the cortical neurons. In contrast, sections from adult animals treated with THC for 3hr (Figure 7.5B(ii)) displayed a level of phospho-JNK immunofluoresence in the cortex comparable to control adult animals. This indicates that THC regulates JNK signalling in the neonatal cortex *in vivo*.

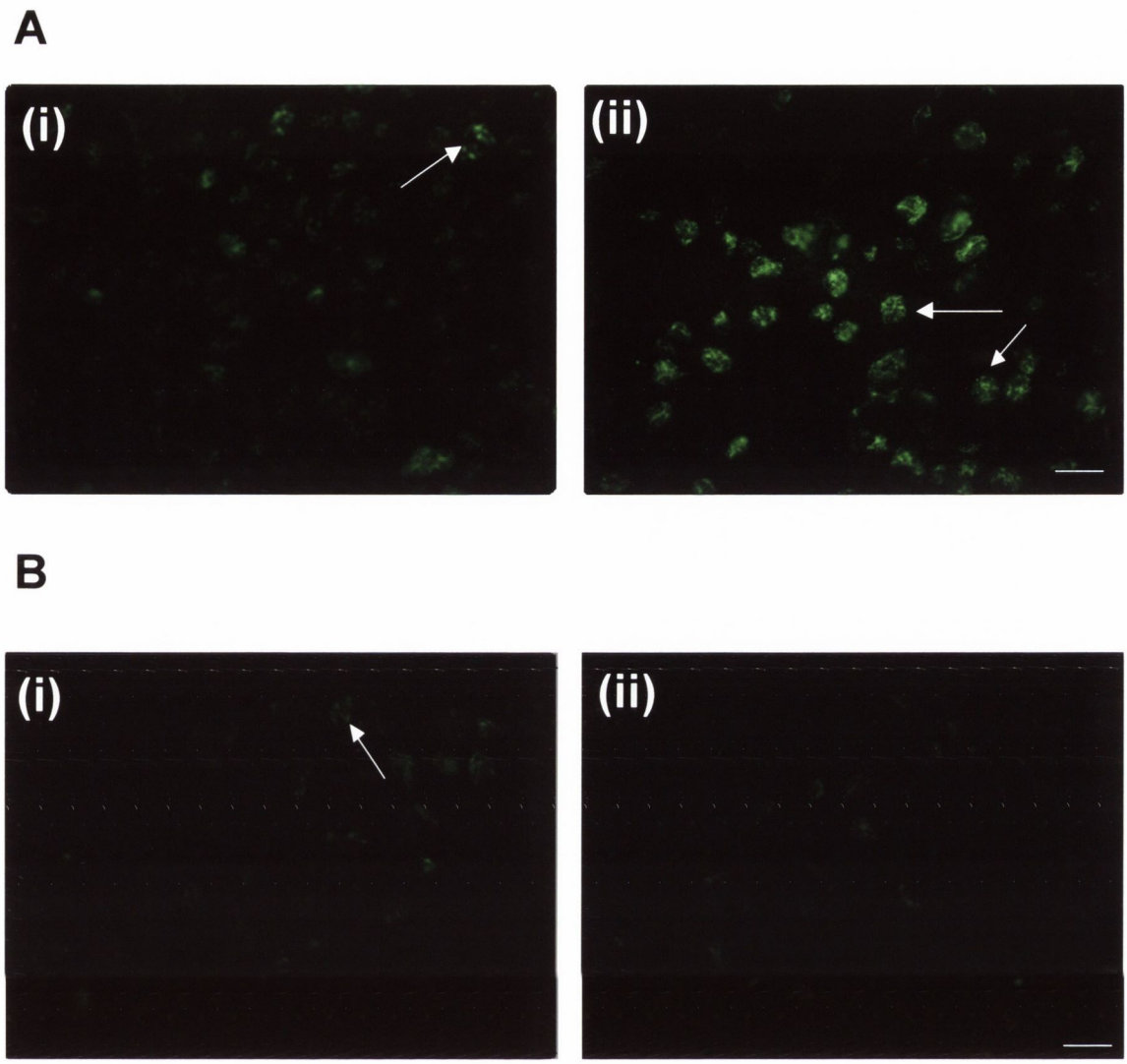

Figure 7.5: THC activates JNK in the neonatal cortex *in vivo*

Neonatal (4-7-day old) and adult (3-4 month old) rats received subcutaneous injections of THC (10mg/kg; 3hr) in vehicle or vehicle alone for 3hr and cryostat sections prepared. The expression of the phosphorylated form of JNK was assessed by immunofluorescence.

A: Neonatal cryostat sections. In sections from (i) control animals, phospho-JNK immunoreactivity is apparent in neuronal subpopulations. Sections from (ii) THC-treated animals display intense phospho-JNK immunostaining. Arrows indicate neurons displaying phospho-JNK immunoreactivity. Scale bar is 25μm.

B: Adult cryostat sections. Phospho-JNK immunostaining is low in sections from (i) vehicle-treated and (ii) THC-treated animals. Scale bar is 25μm.

7.2.6 Dose-dependency of THC-induced regulation of JNK phosphorylation in the neonatal and adult cortex *in vivo*

Since THC (10mg/kg) was shown to increase JNK phosphorylation in the neonatal cortex but not the adult cortex (Figure 7.5) the dose-dependency of this effect was assessed. Neonatal (4-7-day old) rat pups and adult (3-4 month old) rats received subcutaneous injections of THC (1, 10 and 30mg/kg) in vehicle (5% absolute alcohol, 5% Cremophor EL and 90% sterile saline) or vehicle alone for 3hr and cryostat sections were prepared. JNK phosphorylation was assessed in the cortex by fluorescence immunocytochemistry (Figure 7.6). Figure 7.6A demonstrates that phospho-JNK immunoreactivity was increased in the cortex of cryostat sections taken from neonatal rats treated with THC at concentrations of (ii) 1mg/kg, (iii) 10mg/kg and (iv) 30mg/kg THC for 3hr when compared to (i) vehicle-treated animals (n=4 observations). Cryostat sections prepared from adult rats treated with vehicle alone (Figure 7.6B(i)) for 3hr showed a level of phospho-JNK immunostaining, indicating a tonic level of JNK activation in the cortex of control animals. Furthermore, Figure 7.6B demonstrates that exposure of adult animals to THC at concentrations of (ii) 1mg/kg, (iii) 10mg/kg and (iv) 30mg/kg had no effect on the level of phospho-JNK immunostaining. This indicates that JNK signalling is regulated by THC in the neonatal cortex *in vivo* in a dose-dependent manner. Representative fluorescent images of cryostat sections stained for phospho-JNK are shown in Figure 7.6.

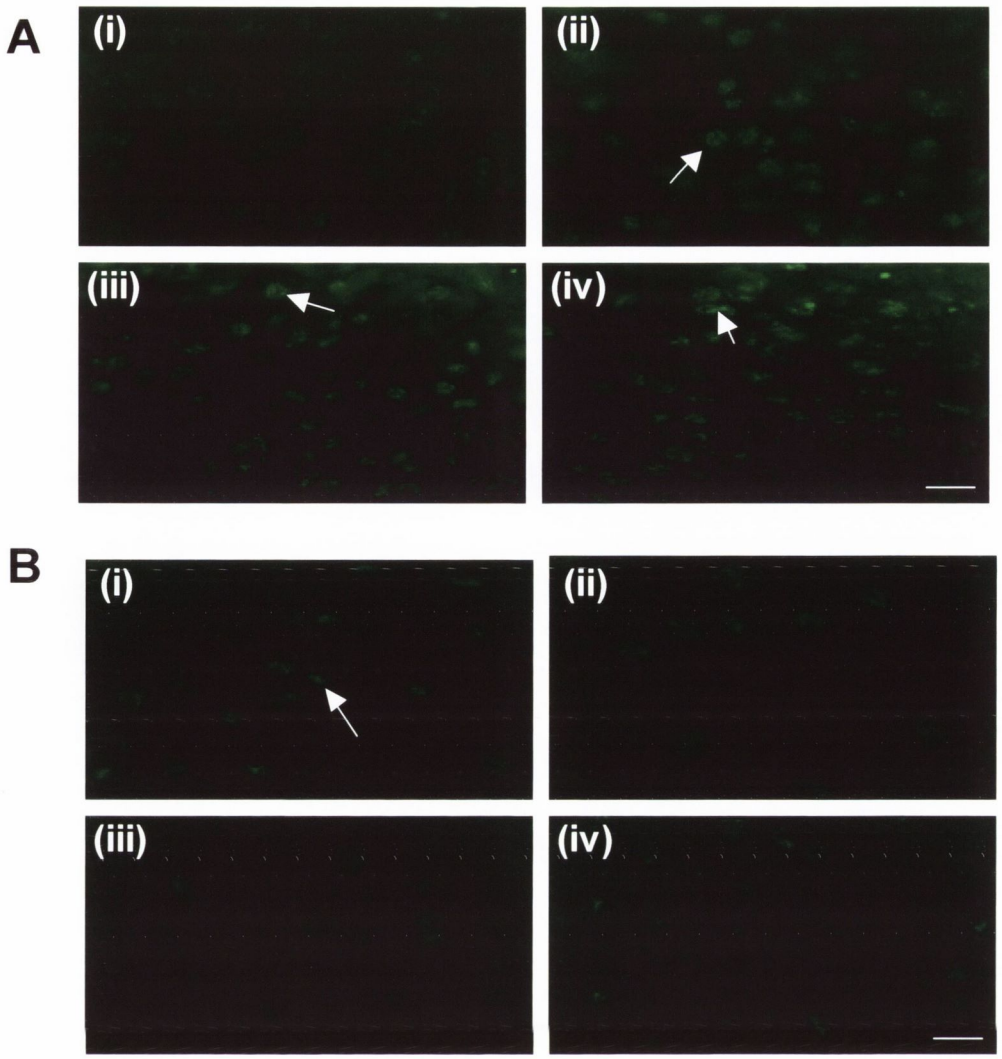

Figure 7.6: Dose-dependency of THC-induced JNK phosphorylation in the neonatal/adult cortex *in vivo*

Neonatal (4-7-day old) and adult (3-4 month old) rats received subcutaneous injections of THC (1, 10, 30mg/kg) for 3hr and the expression of the phosphorylated form of JNK was assessed by immunofluorescence.

A: Neonatal cryostat sections. Exposure to (ii) 1mg/kg THC, (iii) 10mg/kg THC and (iv) 30mg/kg THC for 3hr increased the number of phospho-JNK immunoreactive neurons in the neonatal cortex. Treatment with (i) vehicle for 3hr had little effect on JNK. Arrows indicate phospho-JNK immunoreactive cells. Scale bar is 25μm.

B: Adult cryostat sections taken from animals treated with (ii) 1mg/kg, (iii) 10mg/kg and (iv) 30mg/kg. THC had no effect on phospho-JNK in the cortex when compared to sections taken from (i) control animals. Scale bar is 25μm.

7.2.7 THC induces the differential regulation of JNK1 and JNK2 isoforms in the neonatal cortex *in vivo*

In chapter 4 it was found that THC regulates the expression levels of the phosphorylated form of JNK1 and JNK2 in a time-dependent manner in cultured neurons. Furthermore, it was shown that the differential activation of JNK1 (at 5 min) and JNK2 (at 2hr) contributed directly to the apoptotic actions of THC in cultured cortical cells. To determine if THC differentially induces the phosphorylation of the JNK1 and JNK2 isoforms *in vivo*, neonatal (4-7-day old) rats received subcutaneous injections of 10mg/kg THC in vehicle (5% absolute alcohol, 5% Cremophor EL and 90% sterile saline) for 3hr. A control group received injections of vehicle alone for 3hr. Following treatment, freshly dissected cortex was sliced and homogenised in lysis buffer. Expression levels of the phosphorylated (active) form of JNK1 and JNK2 were measured by western immunoblot using a polyclonal anti-phospho-specific JNK antibody, and band widths were quantified using densitometry (Figure 7.7). Figure 7.7A demonstrates that in the neonatal cortex from vehicle-treated animals phospho-JNK1 expression was 75.0 ± 3.6 arbitrary units (mean ± SEM) and that phospho-JNK1 expression was comparable in THC-treated animals (83.8 ± 4.5) at 3hr. In contrast, phospho-JNK2 expression was increased from 136.1 ± 2.0 in vehicle-treated neonates to 172.5 ± 5.0 following THC treatment for 3hr ($p<0.01$, Student's *t* test, n=6 observations; Figure 7.7B). This indicates that, in accordance with the effect of THC on JNK regulation in cultured cortical cells and cortical slices, THC-induces JNK2 activation in the neonatal cortex at 3hr *in vivo*. Sample western immunoblots demonstrating the effect of THC on neonatal JNK1 and JNK2 activity are shown as insets in Figure 7.7A, B.

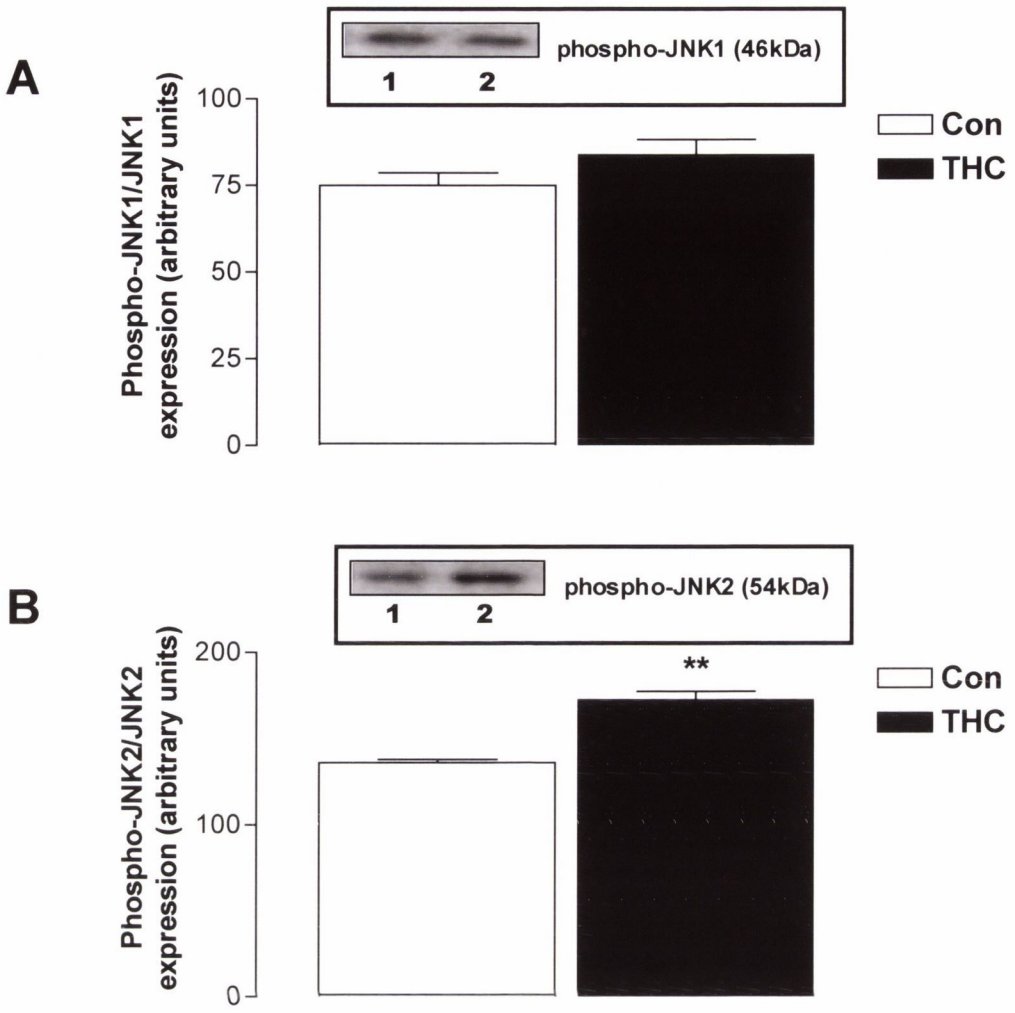

Figure 7.7: Effect of THC on JNK1/2 activity in neonatal cortex *in vivo*

Neonatal (4-7-day old) rats received injections of THC (10mg/kg; 3hr) in vehicle or vehicle alone for 3hr. Following treatment cortical slices were prepared, lysed and analysed for the expression levels of the phosphorylated active forms of JNK1 and JNK2 using western immunoblot.

A: THC has no effect on phospho-JNK1 expression in the neonatal cortex. Results are expressed as mean ± SEM for 9 observations. Inset: Sample western immunoblot demonstrating JNK1 activity in vehicle-treated (lane 1) and THC-treated (lane 2) neonatal animals.

B: THC significantly increases JNK2 activity in the neonatal cortex. Results are expressed as mean ± SEM for 6 observations, **$p<0.01$. Inset: Sample immunoblot demonstrating the increase in JNK2 activity in THC-treated (lane 2) neonatal animals compared to vehicle-treated (lane 1) rats.

7.2.8 THC does not regulate JNK1/JNK2 activity in the adult cortex *in vivo*

To determine if THC induces the phosphorylation of the JNK1 and JNK2 isoforms in the adult cortex *in vivo*, adult (3-4 month old) rats received subcutaneous injections of 10mg/kg THC in vehicle (5% absolute alcohol, 5% Cremophor EL and 90% sterile saline) for 3hr and a control group received injections of vehicle alone for 3hr. Following treatment, the cortex was homogenised in lysis buffer and expression of phosphorylated JNK1 and JNK2 were measured by western immunoblot using a polyclonal anti-phospho-specific JNK antibody, and band widths were quantified using densitometry (Figure 7.8). Figure 7.8A demonstrates that phospho-JNK1 expression in the cortex from vehicle-treated adult rats was 109.4 ± 4.4 arbitrary units (mean ± SEM) and this was unaffected by exposure of adult rats to THC (110.8 ± 11.1). Unlike the neonatal cortex, the adult cortex was insensitive to THC-induced JNK2 activation (Figure 7.8B). JNK2 activity in the cortex of vehicle-treated adult rats was 200.8 ± 4.4 and THC treatment for 3hr did not affect JNK2 phosphorylation (211.6 ± 14.3; Figure 7.8B). This indicates that at the 3hr time point, JNK activity is not sensitive to cannabinoid exposure in the adult cortex. Sample western immunoblots demonstrating the effect of THC on JNK1 and JNK2 activity in the adult cortex are shown as insets in Figure 7.8A, B.

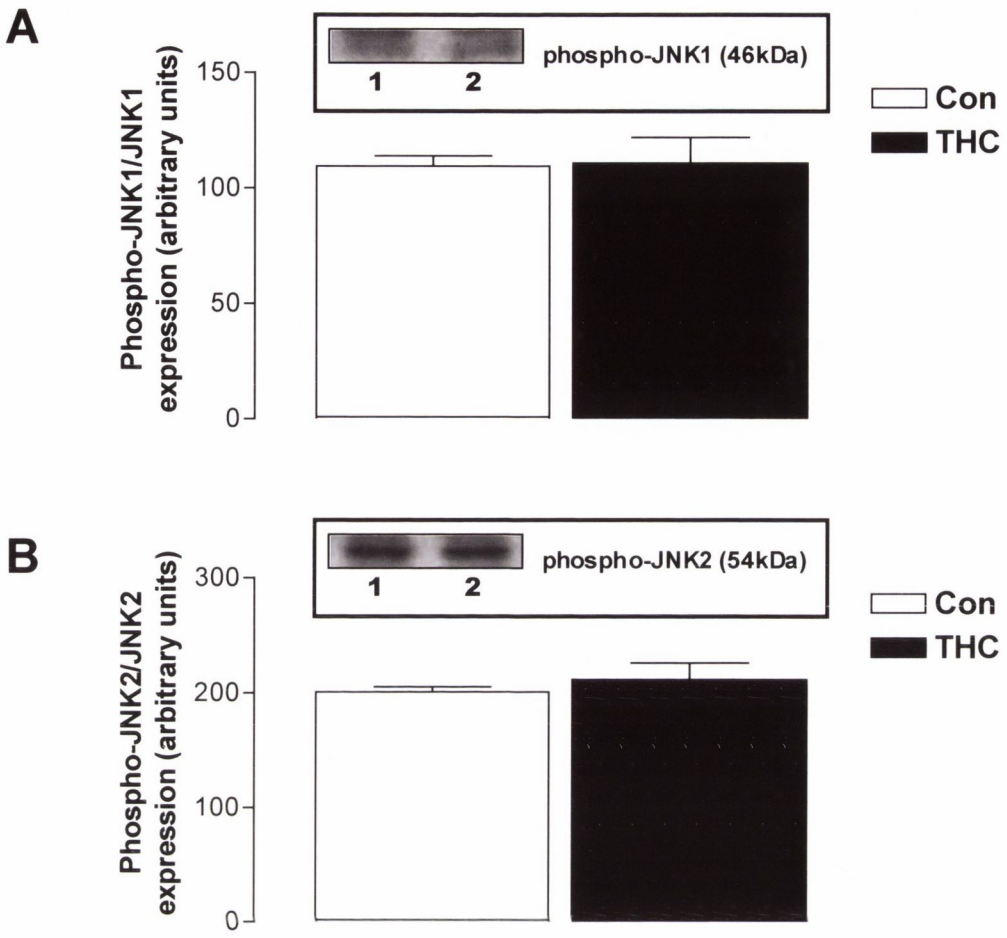

Figure 7.8: THC has no effect on JNK1/2 in adult cortex *in vivo*

Adult (3-4 month old) rats received injections of THC (10mg/kg; 3hr) in vehicle or vehicle alone for 3hr. Cortical slices were lysed and analysed for the active forms of JNK1 and JNK2 using western immunoblotting.

A: THC has no effect on JNK1 activity in the adult cortex. Results are expressed as mean ± SEM for 9 observations. Inset: Sample western immunoblot demonstrating JNK1 activity in vehicle-treated (lane 1) and THC-treated (lane 2) adult animals at 3hr.

B: THC has no effect on JNK2 phosphorylation in the adult cortex. Results are expressed as mean ± SEM for 9 observations. Inset: Sample western immunoblot demonstrating JNK2 activity in vehicle-treated (lane 1) and THC-treated (lane 2) adult animals at 3hr.

7.2.9 THC induces JNK activation in the neonatal cortex *in vivo* via the CB_1 cannabinoid receptor

THC-induced JNK activation in neonatal cortical cultures requires the activation of CB_1 (Chapter 4). To determine if the proclivity of THC to activate JNK in the neonatal cortex *in vivo* involves the CB_1 cannabinoid receptor, neonatal (4-7-day old) rats received intraperitoneal injections of the CB_1 antagonist AM 251 (10mg/kg) in vehicle (5% absolute alcohol, 5% Cremophor EL and 90% sterile saline) for 30 min prior to THC (10mg/kg) treatment for 3hr (Figure 7.9). As found in Figure 7.5, THC exposure for 3hr increased the level of active JNK immunofluoresence in cryostat sections taken from neonatal animals when compared to sections from vehicle-treated animals (n=4 observations). Pre-treatment with AM 251 prevented the THC-induced increase in the degree of phospho-JNK immunostaining. AM 251 alone had no effect on JNK activity. This indicates that THC regulates JNK activity in the neonatal cortex *in vivo* via the CB_1 cannabinoid receptor. Examples of phospho-JNK immunostaining in neonatal cryostat section are shown in Figure 7.9.

7.2.10 THC induces JNK phosphorylation in the neonatal, but not the adult, hippocampus *in vivo*

Despite the regulatory effects on THC on ERK (Derkinderen *et al.*, 2003) and p38 MAPK (Derkinderen *et al.*, 2001) in hippocampus, THC fails to activate JNK in hippocampal slices (Derkinderen *et al.*, 2001). To determine if THC regulates JNK in the hippocampus, neonatal (4-7-day old) and adult (3-4 month old) rats received subcutaneous injections of 10mg/kg THC in vehicle (5% absolute alcohol, 5% Cremophor EL and 90% sterile saline) for 3hr, cryostat sections were prepared and the level of phospho-JNK immunostaining in the dentate gyrus determined by fluorescence microscopy (Figure 7.10). Figure 7.10A demonstrates that neonatal rats treated with THC for 3hr showed a high level of active JNK immunofluoresence in the hippocampus when compared to vehicle-treated neonatal rats (n=4 observations). Interestingly, the adult hippocampus showed no sign of JNK activation in THC-treated animals (Figure 7.10B). This suggests that the neonatal, but not the adult, hippocampus is susceptible to THC-induced JNK activation. Representative fluorescent

images of hippocampal cryostat sections from neonatal and adult rats are shown in Figure 7.10.

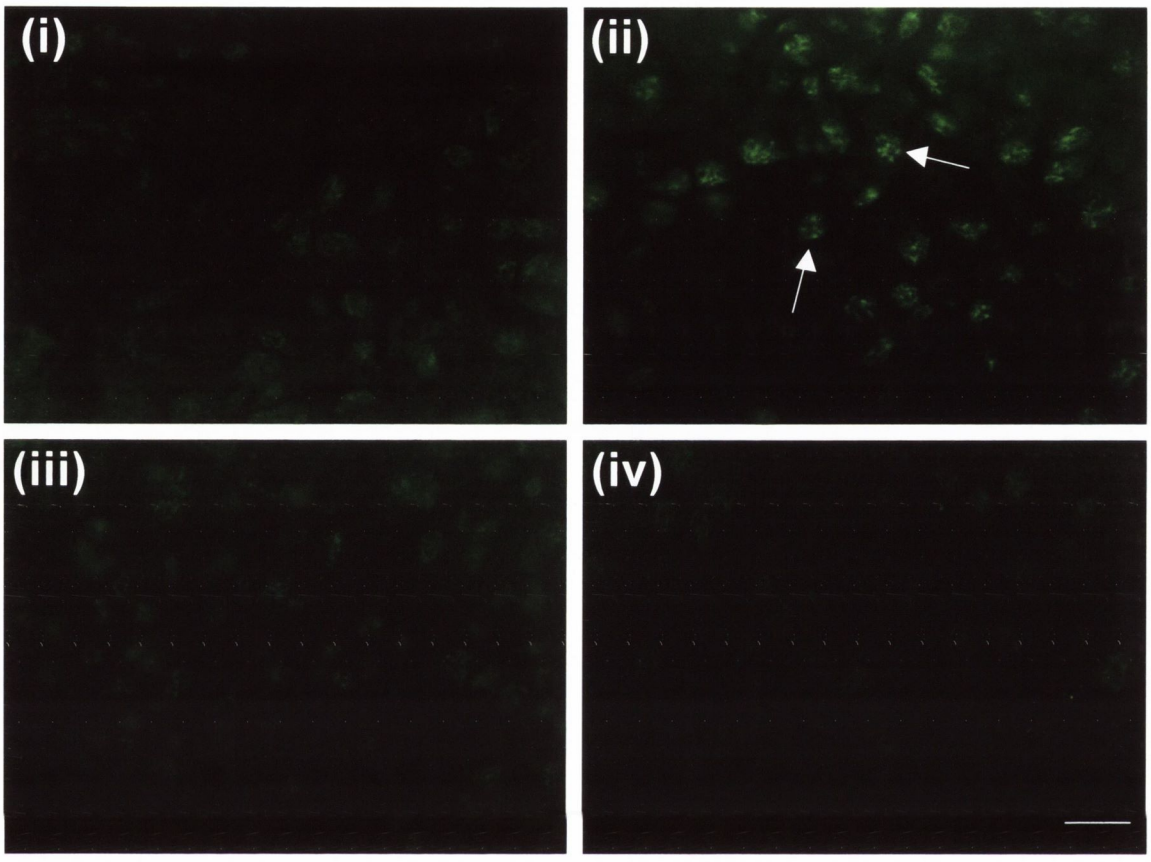

Figure 7.9: The proclivity of THC to regulate JNK activity in the neonatal cortex *in vivo* is CB_1 receptor-dependent

Neonatal (4-7-day old) rats received intraperitoneal injections of AM 251 (10mg/kg) for 30 min prior to THC (10mg/kg; 3hr) treatment. JNK activity in the cortex was assessed in cryostat sections using fluorescence microscopy. Fluorescent images of cryostat sections displaying a low level of JNK activity in (i) vehicle-treated neonatal rat sections when compared to (ii) THC-treated neonatal rats which show an increase in phospho-JNK immunostaining. (iii) AM 251-treated and (iv) THC+AM 251-treated neonatal rats show a level of JNK staining comparable to vehicle-treated neonatal rats. Arrows indicate phospho-JNK immunoreactive cells. Scale bar is 25μm.

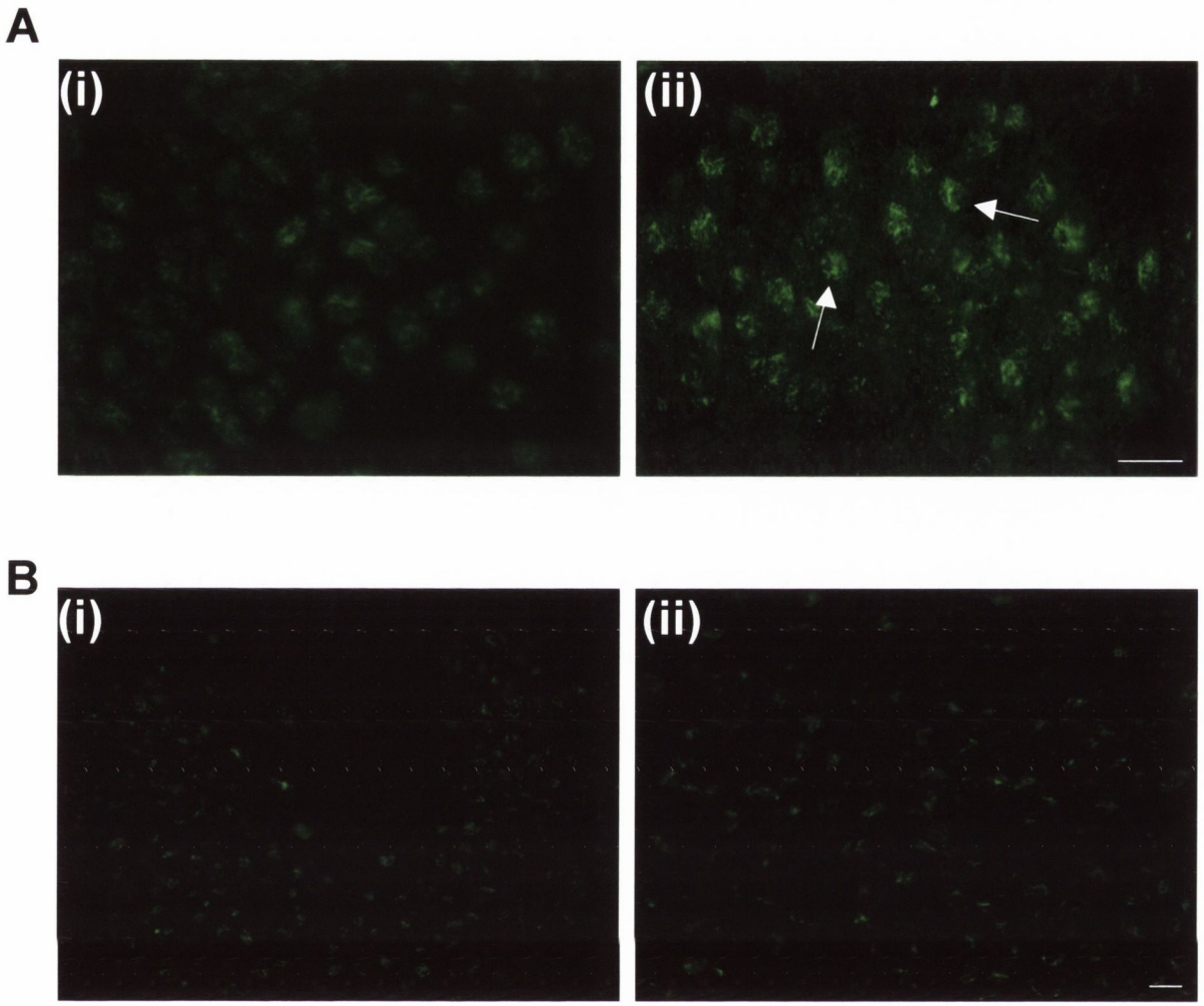

Figure 7.10: THC activates JNK in the neonatal, but not adult, hippocampus *in vivo*

Neonatal (4-7-day old) and adult (3-4 month old) rats received subcutaneous injections of 10mg/kg THC in vehicle or vehicle alone for 3hr and cryostat sections prepared. The expression of the phosphorylated form of JNK was assessed in the dentate gyrus by immunofluorescence.

A: Representative images displaying cryostat sections from (i) vehicle-treated and (ii) THC-treated neonatal rats. Exposure of neonatal rats to THC induced JNK phosphorylation in the hippocampus. Arrows indicate phospho-JNK immunoreactive cells. Scale bar is 25μm.

B: Representative images of adult cryostat sections of hippocampus from (i) vehicle-treated and (ii) THC-treated adult rats. THC had no effect on the level of JNK activity in the adult hippocampus. Scale bar is 25μm.

7.2.11 THC increases caspase-3 activity in the neonatal cortex, but not the adult cortex, *in vivo*

Caspase-3 is central to the cell death pathway triggered by THC in cultured neurons (Chapter 3, 4) and cortical slices *ex vivo* (Chapter 6). To determine if THC regulates caspase-3 *in vivo* and to furthermore assess the contribution of postnatal development to THC-induced caspase-3 activation, neonatal (4-7-day old) and adult (3-4 month old) rats received subcutaneous injections of THC (10mg/kg; 3hr) in vehicle (5% absolute alcohol, 5% Cremophor EL and 90% sterile saline) or vehicle alone for 3hr. Following treatment, cortical slices were prepared, homogenised in lysis buffer and caspase-3 activity determined by monitoring the cleavage of the fluorescently labelled caspase-3 substrate, DEVD, to its fluorescent product (Figure 7.11). Caspase-3 activity was also determined in cryostat sections prepared following treatment and assessed for the level of active caspase-3 immunoreactivity using an anti-active caspase-3 antibody (Figure 7.12).

Figure 7.11A demonstrates that in vehicle-treated neonatal rats caspase-3 activity was 396.6 ± 55.4 pmoles AFC produced/mg protein/min (mean ± SEM) and this was significantly increased to 818.8 ± 94.9 pmoles AFC produced/mg protein/min in neonatal rats exposed to THC for 3hr ($p<0.01$, Student's *t* test, n=9 observations). In contrast, in the adult cortex of THC-treated animals (65.1 ± 7.8 pmoles AFC produced/mg protein/min), caspase-3 activity was similar to control animal values (67.9 ± 12.8 pmoles AFC produced/mg protein/min; Figure 7.11B).

This result was confirmed by immunocytochemical analysis of cryostat sections from vehicle/THC-treated neonatal (Figure 7.12A) and adult (Figure 7.12B) animals. In vehicle-treated neonatal animals (Figure 7.12A(i)) caspase-3 immunoreactivity was not detectable. However exposure of neonates to THC for 3hr increased the number of caspase-3 immunoreactive cells in the cortex (Figure 7.12A(ii); n=4 observations). Figure 7.12B demonstrates that in adult animals (ii) THC treatment did not affect caspase-3 immunoreactivity when compared to (i) vehicle-treated control adults. These findings indicate that THC induces caspase-3 activation in the cortex *in vivo* and that this increase is dependent on postnatal development.

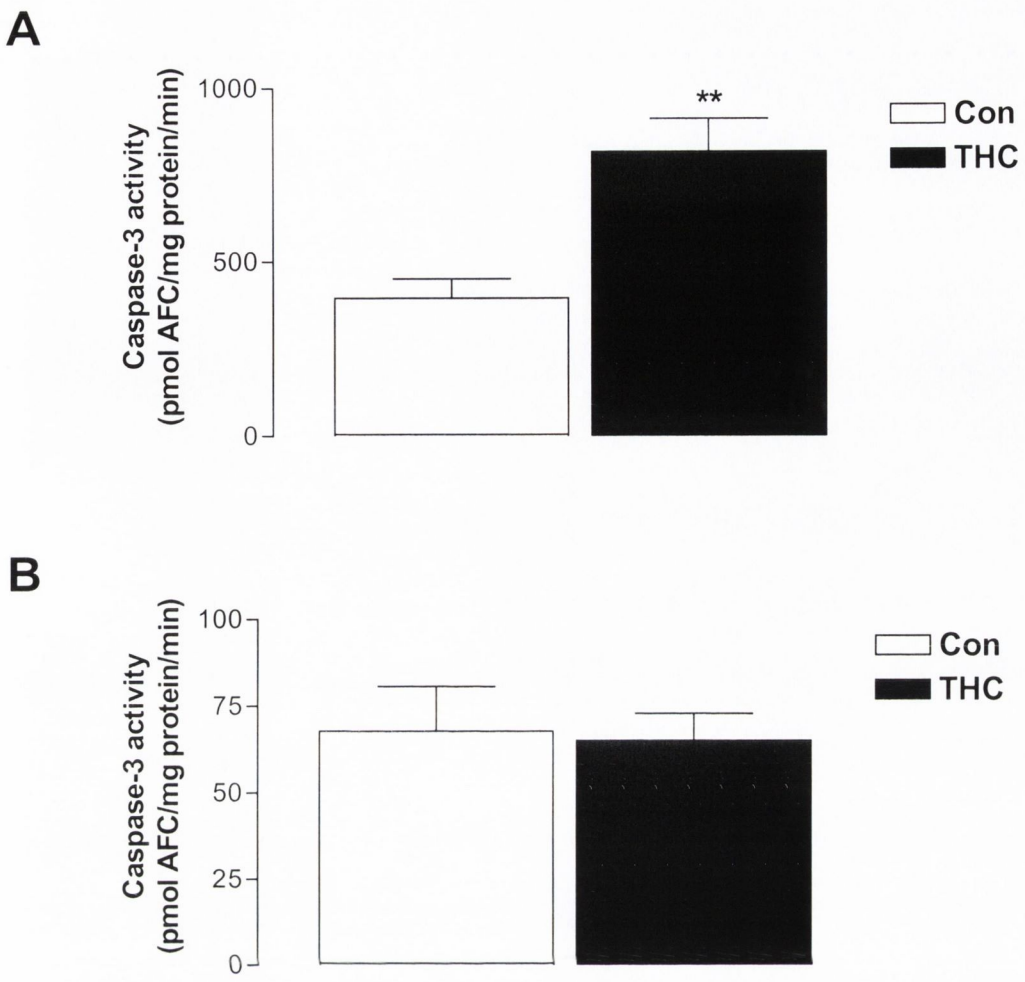

Figure 7.11: Effect of THC on caspase-3 activity in neonatal and adult cortex

Neonatal (4-7-day old) and adult (3-4 month old) rats received subcutaneous injections of 10mg/kg THC in vehicle or vehicle alone for 3hr. Cortical slices were prepared, homogenised in lysis buffer and analysed for caspase-3 activity by monitoring the cleavage of the fluorogenic DEVD substrate.

A: Treatment of neonatal rats with THC significantly increased caspase-3 activity. Results are expressed as the mean ± SEM for 9 observations, **$p<0.01$.

B: THC had no effect on caspase-3 activity in adult rats. Results are expressed as the mean ± SEM for 9 observations.

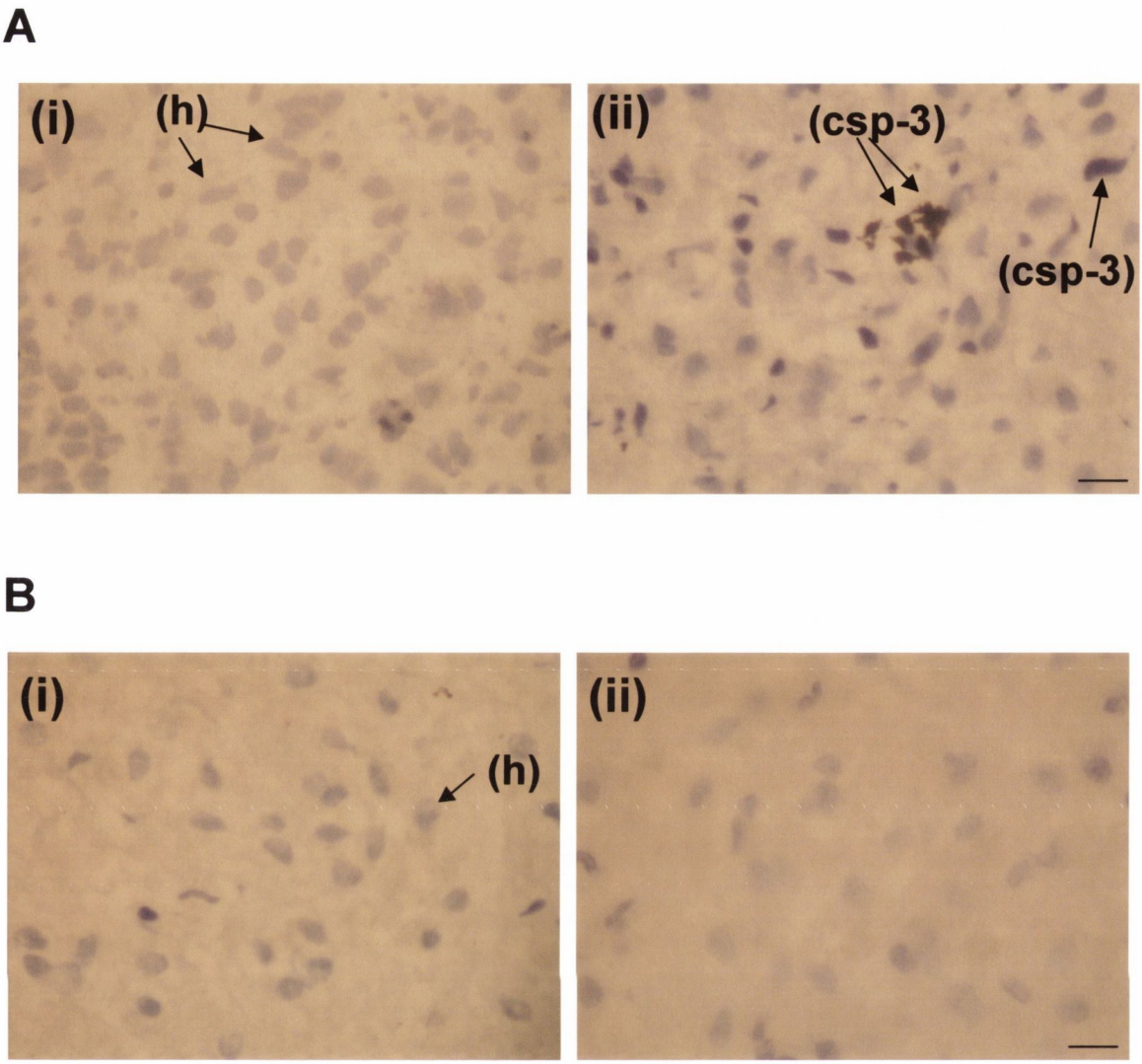

Figure 7.12: THC activates caspase-3 in the neonatal cortex *in vivo*

Neonatal (4-7-day old) and adult (3-4 month old) rats received subcutaneous injections of THC (10mg/kg; 3hr) in vehicle or vehicle alone for 3hr and cryostat sections were prepared. The expression of the active form of JNK in the cortex was assessed by immunocytochemistry using an anti-active caspase-3 antibody.

A: Neonatal cryostat sections. Caspase-3 activity in sections from (i) vehicle-treated animals is low. Capase-3 immunoreactivity is apparent in the cortex of sections from (ii) THC-treated animals. Arrows indicate examples of healthy (h) and caspase-3 immunoreactive (csp) neurons. Scale bar is 20μm.

B: Adult cryostat sections. Caspase-3 immunoreactivity is low in sections from (i) vehicle-treated and (ii) THC-treated adult animals. Scale bar is 20μm.

7.2.13 Dose-dependency of THC-induced caspase-3 activation in the neonatal cortex *in vivo*

Since there is evidence that THC induces caspase-3 activation in the neonatal cortex *in vivo* (Figure 7.11), the dose-dependency of this effect was determined. Neonatal (4-7-day old) rat pups received subcutaneous injections of THC (1, 10 and 30mg/kg) in vehicle (5% absolute alcohol, 5% Cremophor EL and 90% sterile saline) or vehicle alone for 3hr. Following treatment, caspase-3 activity was assessed in cortical slices by monitoring the cleavage of the fluorescently labelled caspase-3 substrate, DEVD, to its fluorescent product (Figure 7.13A). Caspase-3 activity was also determined in cryostat sections prepared following treatment and assessed for the level of active caspase-3 using immunocytochemistry (Figure 7.13B).

Figure 7.13A demonstrates that caspase-3 activity was 6.7 ± 0.9 nmoles AFC produced/mg protein/min (mean ± SEM) in vehicle-treated neonatal rats and this was increased to 9.3 ± 0.9 nmoles AFC produced/mg protein/min in neonatal rats exposed to THC (1mg/kg) for 3hr, but not significantly so ($p=0.09$, n=7 observations). However, treatment of neonatal animals with THC at concentrations of 10mg/kg and 30mg/kg significantly increased caspase-3 activity to 10.5 ± 1.2 nmoles AFC produced/mg protein/min ($p<0.05$, ANOVA, n=7) and 12.4 ± 1.0 nmoles AFC produced/mg protein/min ($p<0.01$, ANOVA, n=7), respectively.

Similarly, immunocytochemical analysis of cryostat sections from neonatal animals exposed to vehicle alone for 3hr or THC at concentrations of 1, 10 and 30mg/kg for 3hr revealed that the effects of THC on caspase-3 activity in the neonatal rat *in vivo* are dose-dependent (Figure 7.13B). In vehicle-treated (Figure 7.13B(i)) neonatal animals caspase-3 immunoreactivity was low. However exposure of neonates to THC at concentrations of 1mg/kg (Figure 7.13B(ii) n=4), 10mg/kg (Figure 7.13B(iii); n=4) and 30mg/kg (Figure 7.13B(iv); n=4) for 3hr increased the number of caspase-3 immunoreactive cells in the neonatal cortex. These findings indicate that the THC induced activation of caspase-3 in the neonatal cortex *in vivo* is dose-dependent.

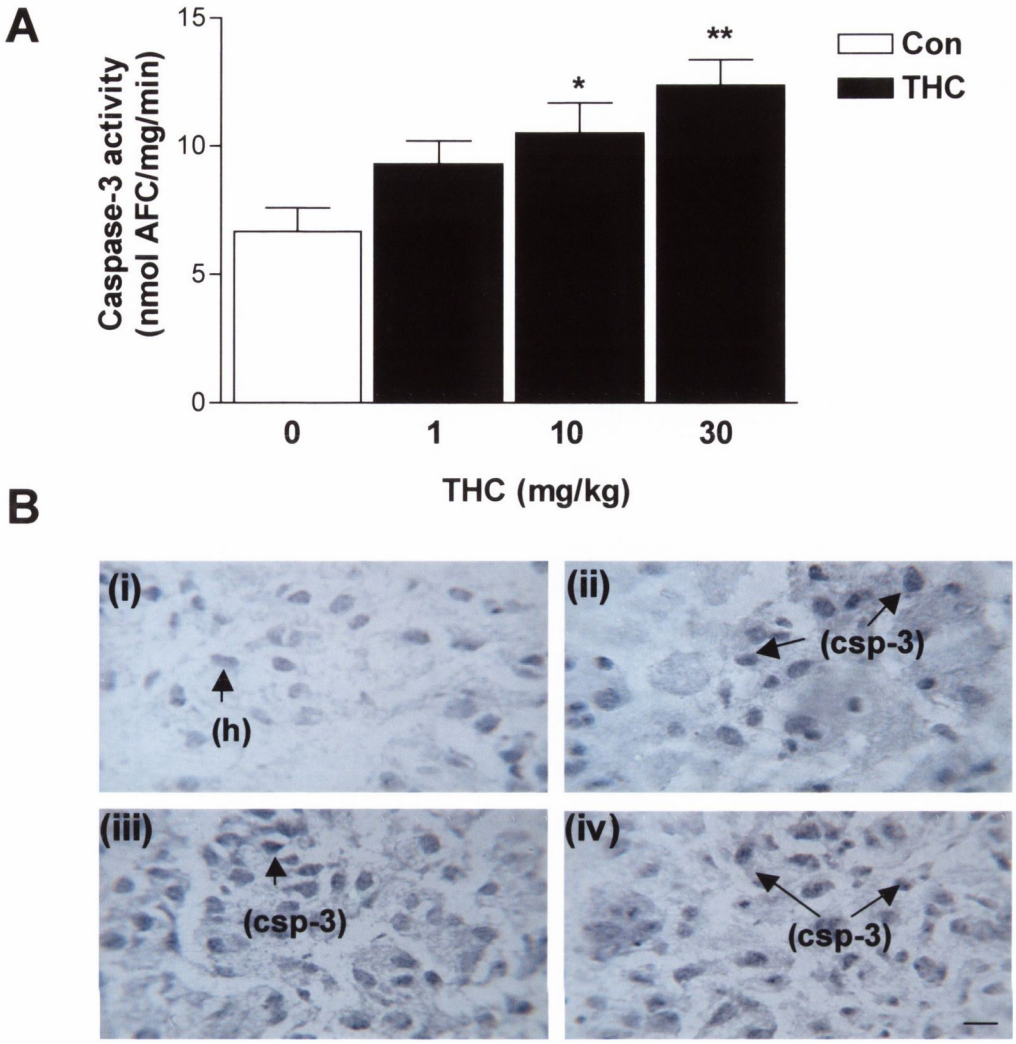

Figure 7.13: THC activates caspase-3 in the neonatal cortex *in vivo* in a dose-dependent manner

Neonatal (4-7-day old) rats received subcutaneous injections of THC (1, 10, 30mg/kg; 3hr) in vehicle or vehicle alone for 3hr and the level of caspase-3 activity assessed.

A: Caspase-3 assay. Treatment of rats with THC at concentrations of 10mg/kg and 30mg/kg significantly increased the cleavage of the fluorescent caspase-3 substrate. Results are expressed as the mean ± SEM for 7 observations, **$p<0.01$, *$p<0.05$.

B: Caspase-3 immunocytochemistry. Caspase-3 activity in cryostat sections from (i) vehicle-treated animals is low. Caspase-3 immunoreactivity is apparent in the cortex of animals treated with THC at concentrations of (ii) 1mg/kg THC, (iii) 10mg/kg THC and (iv) 30mg/kg THC. Arrows indicate examples of healthy (h) and caspase-3 immunoreactive (csp) neurons. Scale bar is 20μm.

7.2.14 Effect of THC concentrations on caspase-3 activity in the adult cortex *in vivo*

The adult cortex is not susceptible to THC-induced caspase-3 activation at a concentration of 10mg/kg (Figure 7.11). The dose-dependency of this effect was assessed to determine if higher THC concentrations induce caspase-3 activation in the adult cortex. Adult (3-4 month old) rats received subcutaneous injections of THC (1, 10 and 30mg/kg) in vehicle (5% absolute alcohol, 5% Cremophor EL and 90% sterile saline) or vehicle alone for 3hr and caspase-3 activity was assessed in cortical slices by the caspase-3 fluorogenic assay (Figure 7.14A). Caspase-3 activity was also determined in cryostat sections using caspase-3 immunocytochemistry (Figure 7.14B).

Figure 7.14A demonstrates that the activity of the caspase-3 enzyme in control adult rats was 1.9 ± 0.3 nmoles AFC produced/mg protein/min (mean ± SEM). Caspase-3 activity was unaffected by THC exposure at 1mg/kg (2.2 ± 0.1 nmoles AFC produced/mg protein/min), 10mg/kg (1.9 ± 0.3 nmoles AFC produced/mg protein/min) and 30mg/kg (2.0 ± 0.2 nmoles AFC produced/mg protein/min) for 3hr.

Similarly, Figure 7.14B shows that immunocytochemical analysis of cryostat sections from adult animals exposed to THC at concentrations of (ii) 1, (iii) 10 and (iv) 30mg/kg for 3hr had no effect on the level of caspase-3 activity in the cortex when compared to (i) vehicle-treated animals. These results suggest the adult rat cortex is not susceptible to THC-induced caspase-3 activation.

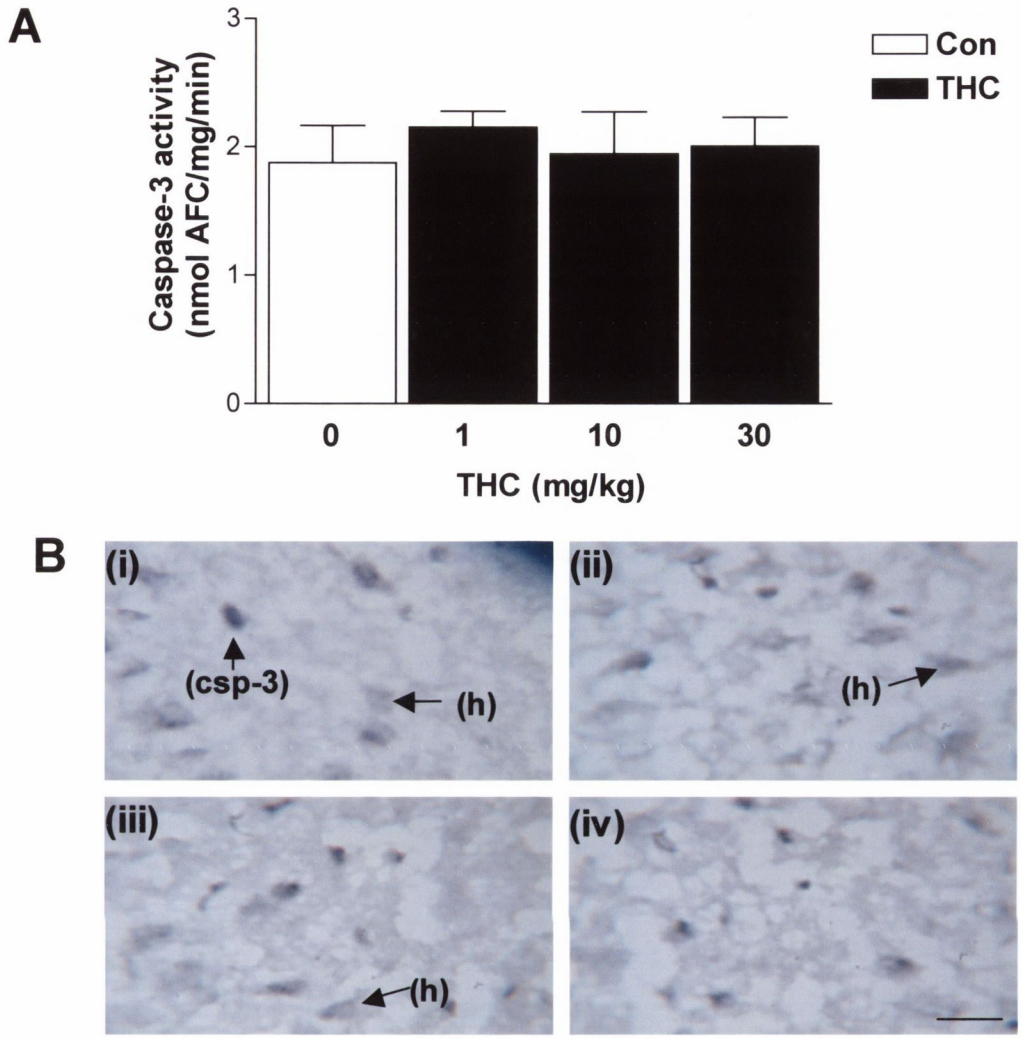

Figure 7.14: A dose-response analysis of the effect of THC on caspase-3 activity in the adult cortex *in vivo*

Adult (3-4 month old) rats received subcutaneous injections of THC (1, 10, 30mg/kg; 3hr) in vehicle and the level of caspase-3 activity assessed.

A: Caspase-3 assay. Treatment of rats with THC at concentrations of 1, 10 and 30mg/kg had no effect on the cleavage of the fluorescent caspase-3 substrate. Results are expressed as the mean ± SEM for 7 observations.

B: Caspase-3 immunocytochemistry. Caspase-3 immunoreactivity in adult cryostat sections from (i) vehicle-treated animals and adult animals treated with THC at concentrations of (ii) 1mg/kg (iii) 10mg/kg and (iv) 30mg/kg. THC had no effect on caspase-3 activity in the cortex at the concentrations tested. Arrows indicate examples of healthy (h) and caspase-3 immunoreactive (csp) neurons. Scale bar is 25μm.

7.2.15 THC induces caspase-3 activation in the neonatal cortex *in vivo* via the CB_1 cannabinoid receptor

THC-induced caspase-3 activation in neonatal cortical cultures (Chapter 3) and neonatal cortical slices (Chapter 6) requires the activation of the central CB_1 cannabinoid receptor. To determine if the CB_1 receptor is involved in the stimulatory effects of THC on caspase-3 *in vivo*, neonatal (4-7-day old) rats received intraperitoneal injections of the CB_1 antagonist AM 251 (10mg/kg) in vehicle (5% absolute alcohol, 5% Cremophor EL and 90% sterile saline) for 30 min prior to THC (10mg/kg) treatment for 3hr (Figure 7.15). Caspase-3 activity was assessed in cortical slices by the caspase-3 fluorogenic assay (Figure 7.15A) and also determined in cryostat sections using caspase-3 immunocytochemistry (Figure 7.15B).

Figure 7.15A demonstrates that exposure of neonatal rats in THC for 3hr increased caspase-3 activity from 6.7 ± 0.9 nmoles AFC produced/mg protein/min (mean ± SEM) in vehicle-treated animals to 10.5 ± 1.2 nmoles AFC produced/mg protein/min ($p<0.05$, ANOVA, n=7 observations). This increase in caspase-3 activity was CB_1 mediated as rats exposed to AM 251 in the presence of THC (6.6 ± 0.9 nmoles AFC produced/mg protein/min) displayed a level of caspase-3 activity in the cortex comparable to basal levels. Similarly, AM 251-treated (5.9 ± 0.5 nmoles AFC produced/mg protein/min) neonatal rats showed no change in caspase-3 activity in the cortex.

The role of the CB_1 receptor in THC-induced caspase-3 activation in the neonatal cortex was also assessed by immunocytochemistry using the anti-active caspase-3 antibody (Figure 7.15B). THC exposure for 3hr increased the level of active caspase-3 immunoreactive neurons in cryostat sections taken from neonatal animals when compared to sections from vehicle-treated animals (n=4 observations). Pre-treatment with AM 251 prevented the THC-induced increase in active caspase-3 staining. AM 251 alone had no effect on caspase-3 activity. This indicates that THC regulates caspase-3 activity in the neonatal cortex *in vivo* via the CB_1 cannabinoid receptor. Light microscopic images of the cortex in neonatal cryostat sections stained for active caspase-3 are shown in Figure 7.15B.

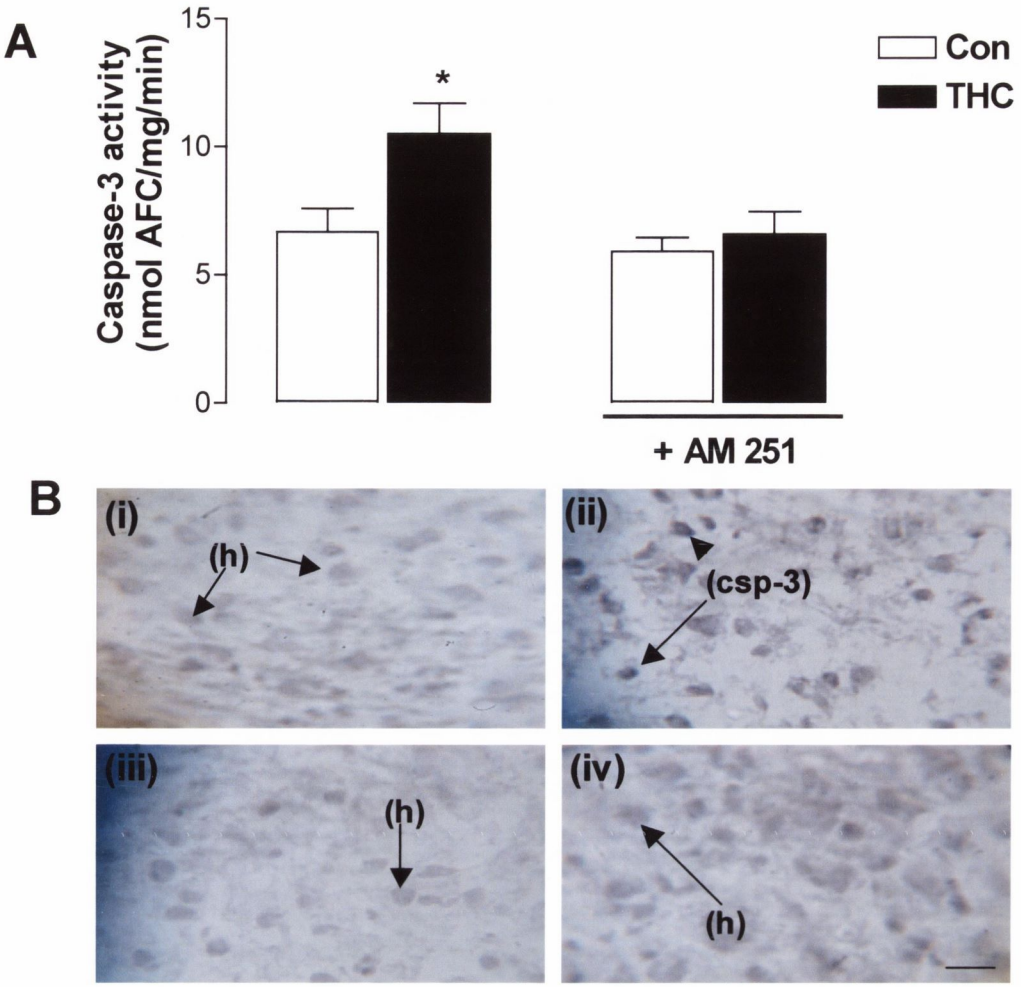

Figure 7.15: The *in vivo* apoptotic actions of THC in the neonatal cortex are CB_1 receptor-dependent

Neonatal (4-7-day old) rats received intraperitoneal injections of AM 251 (10mg/kg) for 30 min prior to THC (10mg/kg; 3hr) treatment. The level of caspase-3 activity was determined in the cortex using the caspase-3 biochemical assay and immunocytochemistry.

A: Caspase-3 assay. Treatment of rats with THC increased caspase-3 activity as determined by the cleavage of the fluorescent caspase-3 substrate. This was abrogated by AM 251. Results are expressed as the mean ± SEM for 7 observations, *$p<0.05$.

B: Caspase-3 immunocytochemical analysis. Caspase-3 immunoreactivity in cryostat sections from (i) vehicle-treated rats, (ii) THC-treated rats, (iii) AM 251-treated neonates and (iv) THC+AM 251-treated rats show that THC increases caspase-3 activity in a CB_1-dependent manner. Arrows indicate examples of healthy (h) and caspase-3 immunoreactive (csp) neurons. Scale bar is 25μm.

7.2.16 THC increases caspase-3 activity in the neonatal, but not the adult, hippocampus *in vivo*

To date there is no evidence that THC regulates caspase-3 activity in the hippocampus. Hence, the ability of THC to induce caspase-3 activation in the rat hippocampus *in vivo* was assessed. Furthermore, the contribution of postnatal influences to the THC-induced effects was determined. Neonatal (4-7-day old) rat pups and adult (3-4 month old) rats received subcutaneous injections of 10mg/kg THC in vehicle (5% absolute alcohol, 5% Cremophor EL and 90% sterile saline) for 3hr. A control group received injections of vehicle alone for 3hr. Following treatment, cryostat sections were prepared and the level of caspase-3 activity in the dentate gyrus determined using immunocytochemistry (Figure 7.16). THC-treated neonatal rats showed a higher level of caspase-3 immunoreactivity in the hippocampus at 3hr compared to vehicle-treated neonates (n=4 observations; Figure 7.16A). In contrast, THC had no effect on the level of caspase-3 immunoreactive neurons in the hippocampus of adult rats (Figure 7.16B). This suggests that the neonatal hippocampus is susceptible to THC-induced caspase-3 activation *in vivo*. Images of hippocampal cryostat sections stained for caspase-3 immunoreactivity are shown in Figure 7.16.

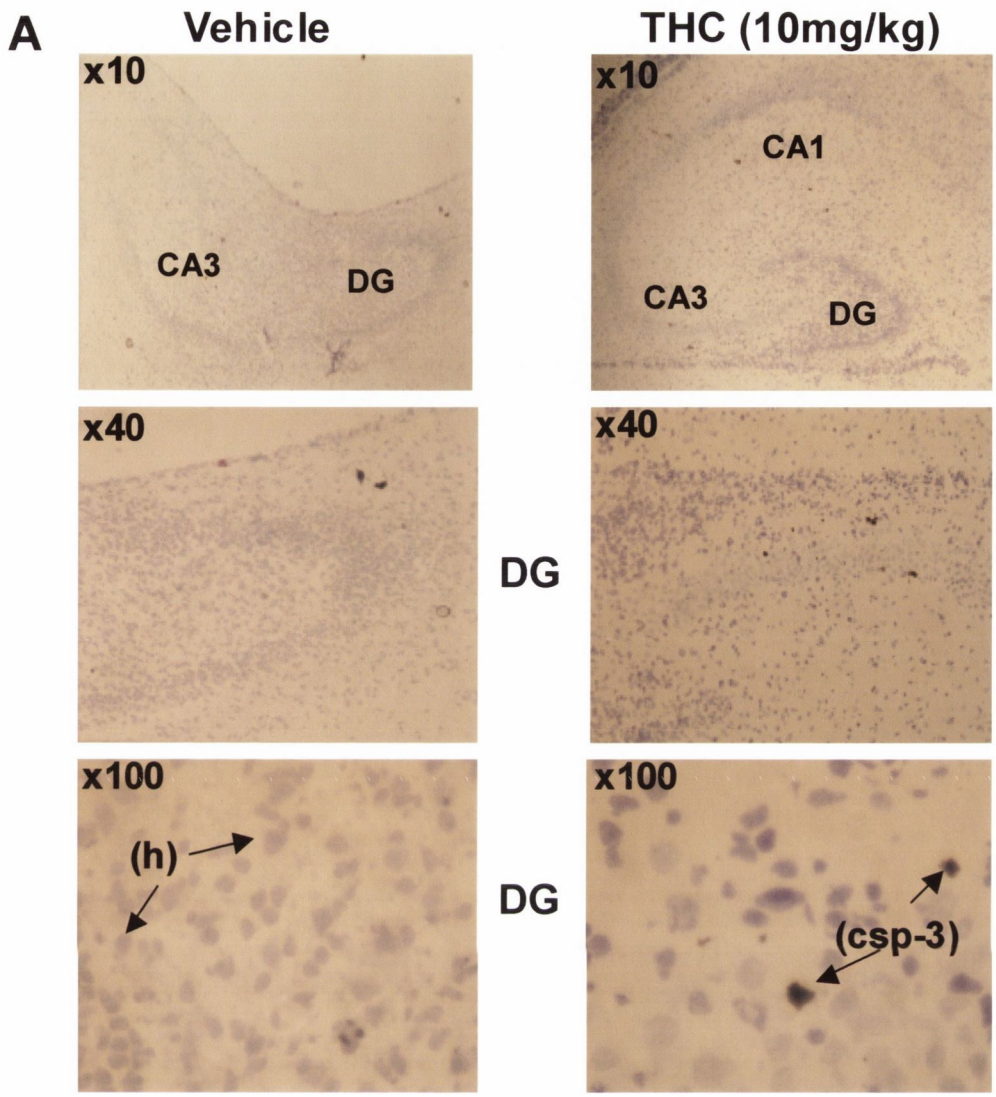

Figure 7.16: Caspase-3 activity is regulated by THC in the neonatal, but not the adult, hippocampus *in vivo*

Neonatal (4-7-day old) and adult (3-4 month old) rats received subcutaneous injections of 10mg/kg THC in vehicle or vehicle alone for 3hr and cryostat sections prepared. The level of caspase-3 immunoreactivity was determined in the dentate gyrus (DG) of the hippocampus by immunocytochemical analysis.

A: Exposure of neonatal rats to THC induced caspase-3 activation in the hippocampus as determined by immunocytochemistry. The lefthand panels are representative images showing caspase-3 immunostaining of the hippocampus from vehicle-treated neonates and the righthand panel are representative images from THC-treated animals. Arrows indicate examples of healthy (h) and caspase-3 immunoreactive (csp) neurons.

B

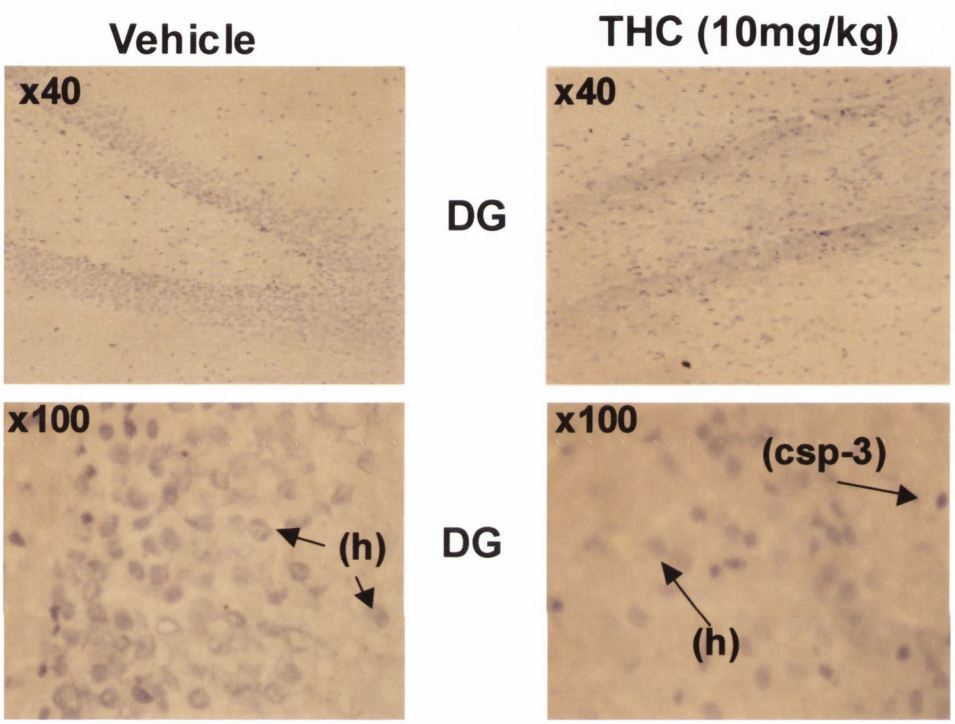

B: Representative images of caspase-3 immunostaining of the dentate gyrus (DG) of the hippocampus from vehicle-treated (lefthand panel) and THC-treated (righthand panel) adult rats. THC had no effect on caspase-3 activity in the adult hippocampus. Arrows indicate examples of healthy (h) and caspase-3 immunoreactive (csp) neurons.

7.2.17 Effect of THC on Bax expression in the neonatal and adult cortex *in vivo*

THC-induced apoptosis of cultured cortical neurons involves an increase in the expression of the pro-apoptotic mitochondria-associated protein Bax (Chapter 5; Miyashita and Reed, 1995). To determine if THC regulates Bax expression in the neonatal and adult cortex *in vivo*, neonatal (4-7-day old) and adult (3-4 month old) rats received subcutaneous injections of 10mg/kg THC in vehicle (5% absolute alcohol, 5% Cremophor EL and 90% sterile saline) for 3hr and a control group received injections of vehicle alone for 3hr. Following treatment, the cortex was dissected and homogenised in lysis buffer and expression of Bax determined by western immunoblot using an antibody that recognises amino acids 43-61 of Bax. Band widths were then quantified using densitometry (Figure 7.17). Figure 7.17A demonstrates that Bax expression in the cortex of vehicle-treated neonatal rats was 10.3 ± 0.4 arbitrary units (mean ± SEM) and this was unaffected by exposure of neonatal rats to THC (10.4 ± 1.1) for 3hr. Unlike the neonatal cortex, there was a trend towards an increase in Bax expression in the adult cortex, but not significantly so (Figure 7.17B). Bax expression in the cortex of vehicle-treated adult rats was 8.6 ± 0.9 and THC treatment for 3hr did not significantly affect Bax expression (11.0 ± 0.7; p=0.06). This indicates that at the 3hr time point, Bax expression is sensitive to cannabinoid exposure in the adult, but not the neonatal, cortex *in vivo*. Sample western immunoblots demonstrating the effect of THC on Bax expression in the neonatal and adult cortex *in vivo* are shown as insets in Figure 7.17A, B.

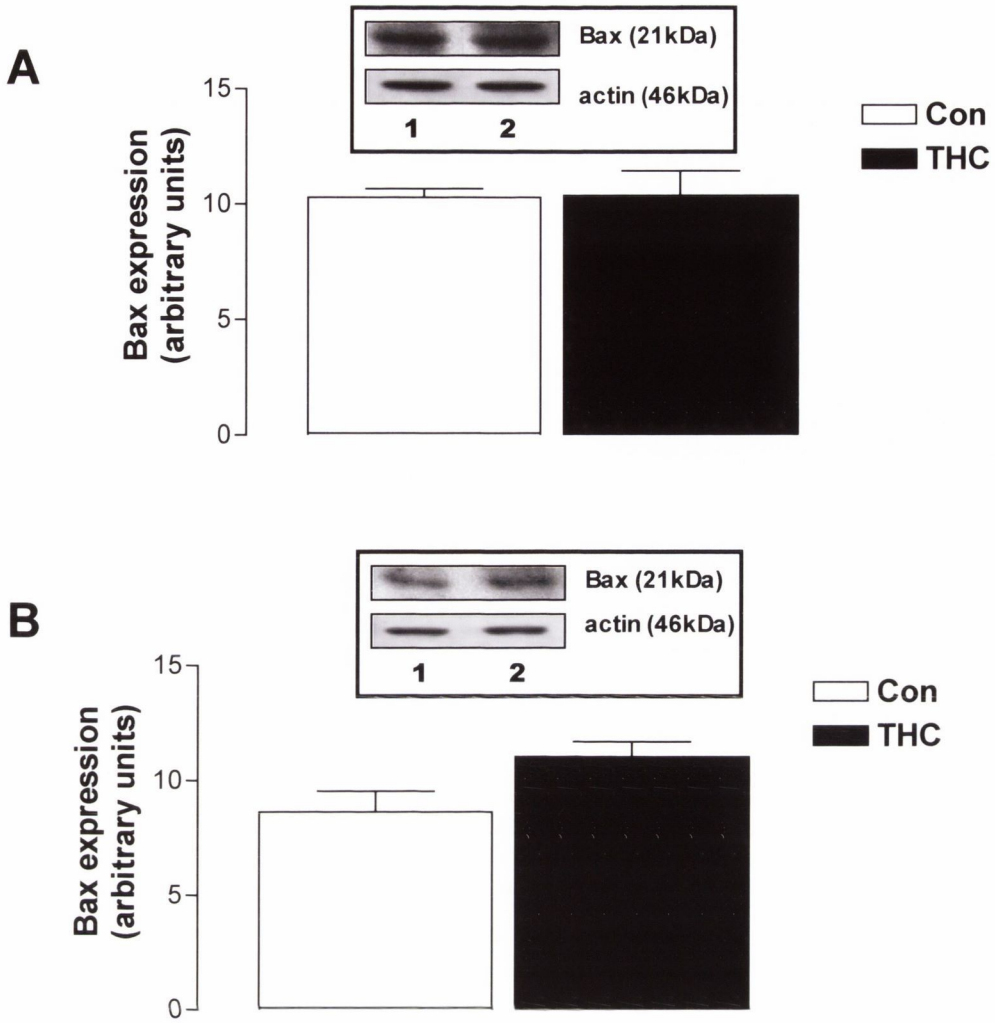

Figure 7.17: Effect of THC on Bax expression in the neonatal and adult cortex *in vivo*

Neonatal (4-7-day old) and adult (3-4 month old) rats received injections of THC (10mg/kg; 3hr) in vehicle or vehicle alone for 3hr. Following treatment cortical slices were prepared, lysed and assessed for the expression of Bax protein by western immunoblotting.

A: THC does not induce Bax expression in the neonatal cortex. Results are expressed as mean ± SEM for 8 observations. Inset: Sample western immunoblot demonstrating Bax expression in vehicle-treated (lane 1) and THC-treated (lane 2) neonatal animals.

B: THC increases Bax expression in the adult cortex, but not significantly. Results are expressed as mean ± SEM for 7 observations, p=0.06. Inset: Sample immunoblot demonstrating the increase in Bax expression in THC-treated (lane 2) adult animals compared to vehicle-treated (lane 1) adult rats.

7.2.18 Effect of THC on Bcl-2 phosphorylation in the neonatal and adult cortex *in vivo*

Data from Chapter 5 revealed that THC induces the phosphorylation of the anti-apoptotic mitochondria-associated protein Bcl-2 in cultured cortical neurons, inhibiting its pro-survival function (Yamamoto *et al.*, 1999). To determine if the proclivity of THC to phosphorylate Bcl-2 exists *in vivo*, neonatal (4-7-day old) and adult (3-4 month old) rats received subcutaneous injections of 10mg/kg THC in vehicle (5% absolute alcohol, 5% Cremophor EL and 90% sterile saline) or vehicle alone for 3hr. Following treatment, the cortex was dissected and homogenised in lysis buffer. The expression levels of the phosphorylated form of Bcl-2 were measured by western immunoblot using an anti-phospho-Bcl-2 antibody, and band widths were quantified using densitometry (Figure 7.18). No change in Bcl-2 phosphorylation was observed in the neonatal cortex exposed to THC for 3hr (12.6 ± 1.3 arbitrary units; mean ± SEM) when compared to the level of phospho-Bcl-2 expression in the cortex of vehicle-treated neonatal rats (12.0 ± 0.8; Figure 7.18A). In contrast, following exposure of adult rats to THC for 3hr, Bcl-2 phosphorylation was significantly increased from 10.4 ± 0.5 to 13.5 ± 1.2 ($p<0.05$, Student's *t* test; n=9 observations; Figure 7.18B). This indicates that the Bcl-2 protein is sensitive to cannabinoid-induced phosphorylation in the adult, but not the neonatal, cortex *in vivo*. Sample immunoblots demonstrating the effect of THC on phospho-Bcl-2 expression in the neonatal and adult cortex *in vivo* are shown as insets in Figure 7.18A, B.

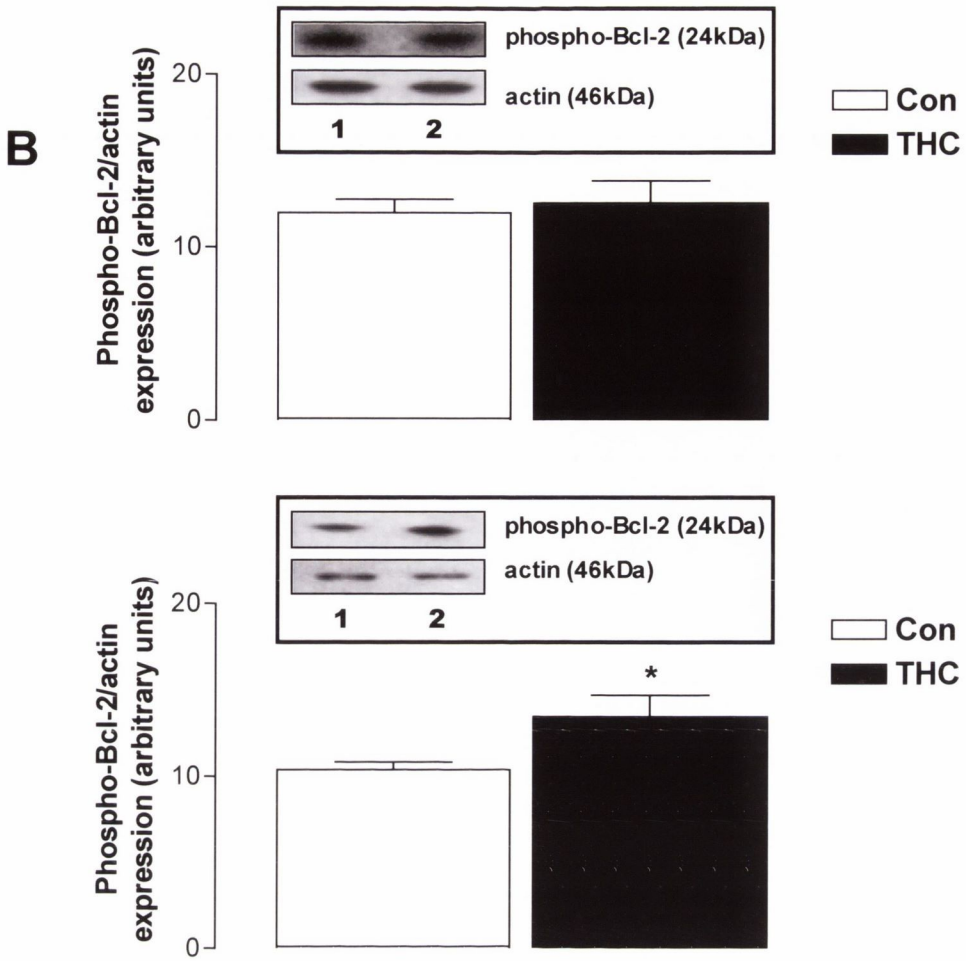

Figure 7.18: Effect of THC on phospho-Bcl-2 expression in the neonatal and adult cortex *in vivo*

Neonatal (4-7-day old) and adult (3-4 month old) rats received injections of THC (10mg/kg; 3hr) in vehicle or vehicle alone for 3hr. Following treatment cortical slices were prepared, lysed and assessed for the expression of the phosphorylated Bcl-2 protein by western immunoblotting.

A: THC has no effect on phospho-Bcl-2 expression in the neonatal cortex. Results are expressed as mean ± SEM for 8 observations. Inset: Sample western immunoblot demonstrating phospho-Bcl-2 expression in vehicle-treated (lane 1) and THC-treated (lane 2) neonatal animals.

B: THC significantly increases Bcl-2 phosphorylation in the adult cortex. Results are expressed as mean ± SEM for 9 observations, *$p<0.05$. Inset: Sample immunoblot demonstrating the increase in phospho-Bcl-2 expression in THC-treated (lane 2) adult animals compared to vehicle-treated (lane 1) adult rats.

7.3 Discussion

This study was aimed at determining if the development of the rat cortex influenced the ability of THC to activate components of the apoptotic cascade in the cortex *in vivo*. For all *in vivo* experiments, neonatal (4-7-day old) rat pups and adult (3-4-month old) rats received subcutaneous injections of THC (1, 10, 30mg/kg) for 3hr, a time point that THC induces apoptosis in cultured cortical cells (Chapter 3). The role of the CB_1 receptor in modulating the *in vivo* effects of THC was determined by administering intraperitoneal injections of AM 251 for 30 min prior to THC exposure. Following cannabinoid exposure for 3hr, a dose-dependent increase in the level of DNA fragmentation, JNK2 and caspase-3 activity was observed in the neonatal cortex. These effects were abrogated in neonatal animals pretreated with the CB_1 antagonist, AM 251, prior to THC exposure. The stimulatory effects of THC on this apoptotic pathway were also observed in the neonatal rat hippocampus. Interestingly, THC had no effect on the level of DNA fragmentation or the expression pattern of the apoptotic signalling molecules in the adult rat cortex or hippocampus *in vivo*. Furthermore, the apoptotic effects of THC on the neonatal cortex *in vivo* did not involve an alteration of the mitochondria-associated proteins, contradicting the role of these proteins in THC-induced apoptosis *in vitro*. Overall, results presented in this chapter indicate that the apoptotic effects of THC observed in neonatal cortical cultures are operative in the neonatal rat cortex *in vivo*, and that THC apoptotic signalling may be differentially regulated during neuronal development.

There is evidence to suggest that the doses of THC used in this study are behaviourally and pharmacologically active (Meyer and Kunkle, 1999; Mokler et al., 1987; Sim *et al.*, 1996; Jentsch *et al.*, 1998) and are comparable to concentrations of THC used in our *in vitro* experiments. Indeed, Chan and colleagues (1996) have shown that rats injected with 50mg/kg body weight of THC have a serum concentration of 10μM THC. The subcutaneous administration of THC was chosen as this route of administration has been successfully employed in other studies using neonatal rat pups (Meyer and Kunkle, 1999). Indeed, this route of administration best mimics marijuana

smoking (John A. Rosecrans, personal communication). The CB_1 receptor antagonist, AM 251, was used *in vivo* as it readily crosses the blood brain barrier (Samuel J. Gatley, personal communication). AM 251 was delivered intraperitoneally, the common route for cannabinoid receptor antagonists (van der Stelt *et al.*, 2001; Rueda *et al.*, 2002; Lichtman and Martin, 1997; Carta *et al.*, 1998; Nava *et al.*, 2001; Valijent *et al.*, 2001; Derkinderen *et al.*, 2003; Gessa *et al.*, 1998) and all *in vivo* treatment regimens had no effect on animal mortality.

The absence of neurotoxic changes in the adult hippocampus and cortex *in vivo* are supported by the findings of Chan and colleagues (1996). In this study no significant alterations were observed in the brains of mature animals dosed orally with high concentrations of THC (50-250mg/kg/day) for 2 years. In contrast, Scallet and colleagues (1987) have shown that chronic exposure to THC (20mg/kg/day) for 90 days affected the anatomical integrity of the hippocampus, decreasing the mean volume of neurons and the number of synapses per unit volume in the hippocampal CA3 region. Similarly, Lawston and co-workers (2000) have shown that adult rats injected twice daily with the synthetic cannabinoid, WIN 55,212-2, for 21 days show dendritic degradation in CA1 of the hippocampus and retraction from the pyramidal cells. The authors conclude that these structural changes may be indicative of cannabinoid-induced neurotoxicity and may underlie the learning and memory changes associated with marijuana use. A recent study by Rueda and colleagues (2002) has also shown that the anandamide analogue, methanandamide, reduces neuronal development in the subcellular zone of the dentate gyrus in adult rats, indicating that the endogenous system may modulate neurogenesis *in vivo*. The authors conclude that the cannabinoid-induced inhibition of neurogenesis may explain the cannabinoid disruption of cognitive processes. Furthermore, THC at concentration of 10mg/kg has been shown to induce apoptosis in extra neural organs *in vivo*, including the spleen and thymus (6-24hr incubations; McKallip *et al.*, 2002b; Do *et al.*, 2004). Despite these findings, data presented in this chapter indicate that THC is not toxic to the adult cortex or hippocampus *in vivo* at the 3hr time point. This may be due to the short-term duration of cannabinoid exposure in this study, with a chronic THC-exposure, as would occur in habitual marijuana users, required to

produce neurotoxicity in the adult brain. It must be noted however, that Galve-Roperh and colleagues (2000) have shown that a 7-day exposure to THC (1mg/kg) or WIN 55,212-2 does not induce any substantial apoptotic effect in the brain of adult rats *in vivo*. Overall, the effects of cannabinoids on neuronal viability in the adult brain *in vivo* are inconclusive. Differences in cannabinoid dose, route of administration and particularly the duration of exposure may account for the contrasting views.

The effects of THC on neuronal viability in the neonatal brain *in vivo* are unknown. Although it is established that cannabinoids possess neurotoxic properties in cultured cortical neurons obtained from neonatal animals (Chan *et al.*, 1998; Kim and Thayer, 2001; Chapter 3) there is no direct evidence that cannabinoids are toxic to the neonatal brain *in vivo*. Data herein show that a 3hr exposure to THC induces the morphological (DNA fragmentation, cell body shrinkage) and biochemical (JNK phosphorylation, caspase-3 activation) changes indicative of neurotoxicity in the neonatal cortex and hippocampus. It is surprising to note that THC exposure for 3hr, a time point at which THC induces apoptosis in cultured cortical neurons (Chapter 3), is neurotoxic *in vivo*, indicating that the consequences of cannabinoid exposure in the neonatal brain are severe, with cannabinoids possessing extensive apoptotic effects after short-term exposure at these early postnatal ages. Our findings in the neonatal brain are supported by a recent study by Szöke and colleagues (2002). In this study it was shown that exposure of newborn rats to anandamide induces mitochondrial damage in B-type neurons of trigeminal and dorsal root ganglia but not in interneurons of the dentate gyrus or Ammon's horn. This may reflect a neurotoxic response of the neonatal brain to cannabinoid exposure, as mitochondrial function is commonly perturbed during apoptosis (Reed, 1997).

The neurotoxicity of THC in the neonatal cortex *in vivo* was absent in neonatal animals pretreated with AM 251 prior to THC exposure, indicating that the *in vivo* apoptotic actions of THC require CB_1 cannabinoid receptors. Western blot analysis in the previous chapter verified the presence of CB_1 cannabinoid receptors in the neonatal rat cortex. Furthermore, radioligand binding studies have demonstrated that cannabinoid receptors are expressed in the cortex and hippocampus at postnatal day 5 (Romero *et al.*, 1997;

Fernández-Ruiz *et al.*, 2000). Thus, these data support CB_1 receptor-mediated apoptosis in the neonatal cortex.

In contrast to the data supporting cannabinoid-induced neurotoxicity in the neonatal brain *in vivo*, cannabinoids also act as neuroprotectants in the neonatal brain *in vivo*. For example, THC reduces neuronal injury via CB_1 in neonatal rats injected with ouabain (van der Stelt *et al.*, 2001). It is also interesting to note that in infant rat models of *in vivo* neurodengeneration, anandamide precursors (Hansen *et al.*, 2001a), anandamide concentrations and CB_1 receptor density (Hansen *et al.*, 2001b) are increased in the cortex, which may represent a putative neuroprotective response. It appears that, in support of the effects of THC on the viability of cultured neurons, neurotoxic and neuroprotective effects of cannabinoids are found *in vivo*, which may be determined by the nature of the toxic insult.

Experimental evidence in this chapter reveals that the transduction pathway contributing to THC-induced apoptosis in the neonatal cortex *in vivo* mirror the apoptotic consequences of THC exposure *in vitro* (Chapter 3, 4). Hence, a reasonable model predicts that, in the neonatal cortex *in vivo*, THC couples to the CB_1 cannabinoid receptor to induce JNK2 phosphorylation and subsequent caspase-3 activation at the 3hr time point, resulting in the fragmentation of the nuclear DNA and the demise of the cortical neurons. However, the apoptotic effects of THC in cortical neurons *in vitro* also involve the modulation of the mitochondria-associated proteins (Chapter 5). Specifically, THC induces an increase in Bax expression and Bcl-2 phosphorylation, both central apoptotic events (Yamamoto *et al.*, 1999; Gross *et al.*, 1998). However, the regulatory effect of THC on Bax/phospho-Bcl2 expression was absent in the neonatal cortex *in vivo*, suggesting that these molecules are not involved in THC-induced neurotoxicity *in vivo*. This may also reflect the dependency of the duration of cannabinoid exposure on regulating apoptotic signalling, which may vary between *in vitro* and *in vivo* systems. Interestingly, THC-induced regulation of the mitochondria-associated proteins was observed in the adult cortex *in vivo*, which may reflect a non-apoptotic role for these proteins in cannabinoid-induced effects on the adult CNS.

Perinatal exposure to drugs including marijuana (Fried and Watkinson, 1990), ethanol (Streissguth, 1983), nicotine (Peters and Tang, 1982),

methadone (Huthchings and Fitter, 1986), barbiturates (Swaab and Mirmiran, 1984), cocaine (Spear *et al.*, 1989) and diazepam (Gruen *et al.*, 1990) produces behavioural abnormalities in offspring. Indeed, direct administration of THC to neonatal animals produces pronounced behavioural changes (Meyer and Kunkle, 1999). The negative effects of THC on the neonatal brain presented in this chapter may have important implications in relation to known damaging effects of perinatal marijuana exposure on infants. Indeed, numerous reports by Fernández-Ruiz and co-workers have shown a number of effects of maternal THC or marijuana administration on dopaminergic functioning of the offspring (Fernández-Ruiz *et al.*, 1992; Fernández-Ruiz *et al.*, 1994; Fernández-Ruiz *et al.*, 1996). Cannabinoids readily disperse throughout the fetal brain due to the immaturity of the blood-brain barrier immature ages (Fernández-Ruiz *et al.*, 1994). Furthermore, THC metabolism is slower in the fetus (Nahas and Frick, 1986)) ensuring that the cannabinoid-induced effects are prolonged. Hence, cannabinoid-induced modifications during perinatal periods are likely to produce long-term effects on adult behaviour. Indeed, other studies have shown cognitive deficits such as memory impairments and attentional deficits in children perinatally exposed to marijuana (Fried and Watkinson, 1990; Griffith *et al.*, 1994; Fried, 1995; Fried and Smith, 2001). Hence, the finding that THC induces apoptosis in the neonatal cortex may contribute to the cognitive and behavioural deficits associated with perinatal marijuana exposure.

The endogenous cannabinoid system is considered to function in the regulation of brain development (Fernández-Ruiz *et al.*, 1999; Ramos *et al.*, 2002). This is suggested by the evidence that the endogenous cannabinoids (Berrendero *et al.*, 1999) and the CB_1 receptor (Berrendero *et al.*, 1998; Rodriguez de Fonseca *et al.*, 1993; McLaughlin *et al.*, 1994; Belue *et al.*, 1995; Garcia-Gil *et al.*, 1999b) are expressed in the fetal and early postnatal brain. Hence, it is reasonable to suggest that the damaging effects of THC in the neonatal brain, as revealed in this study, may interfere with normal endogenous cannabinoid signalling events, particularly during critical periods of pre- or early postnatal development. These effects may underlie some of CNS abnormalities found in offspring perinatally exposed to marijuana (Fried, 1995; Fried and Smith, 2001).

This chapter demonstrates that neurotoxic properties of THC exist in the neonatal rat cortex *in vivo*. These apoptotic actions mirror those which are found in the neonatal cortex *in vitro* and *ex vivo*. Specifically, THC induces DNA fragmentation, JNK phosphorylation and caspase-3 activation in the neonatal cortex following *in vivo* exposure to THC. Interestingly, the apoptotic actions of THC *in vivo* are absent in the adult rat cortex, indicating that the proclivity of THC to act as an apoptotic molecule in cortical cells depends on the maturity of the neurons. These findings, in addition to identifying an apoptotic transduction pathway induced by THC that is operative in an *in vivo* system, highlights the potential teratological effects of marijuana on the infant brain following cannabinoid exposure *in utero*. The findings presented herein may also reflect a role of the endogenous cannabinoid system in anti-proliferative events related to neuronal development.

Chapter 8

Final Discussion

8.1 General discussion

THC, the predominant psychoactive ingredient in preparations of marijuana, exerts a broad spectrum of effects on the CNS as well as on peripheral sites (Porter and Felder, 2001). It is widely accepted that most of these effects are exerted by the binding of cannabinoid constituents, including THC and endogenous cannabinoids, to specific G-protein-coupled cannabinoid receptors (Di Marzo *et al.*, 1998). Although the hemp plant synthesizes over 400 bioactive chemical molecules, of which more than 60 are known as cannabinoids due to their structural similarity to THC (Abood and Martin, 1992), it is impossible to evaluate the pharmacological and toxicological consequences of human and animal exposure to hundreds of compounds simultaneously. Hence, the scientific community has focused its attention on THC, which is considered an acceptable approach to evaluating the biochemical and molecular mechanisms that underlie cannabinoid actions.

Recently there has been growing interest in the role of cannabinoids in the control of the cell survival/death decision, particularly in neurons. Here we report that THC is neurotoxic in rat cortical cultures, cortical brain slices obtained from neonatal rats, and in the neonatal rat cortex *in vivo*. In all experiments this toxicity depended on the CB_1 receptor-dependent activation of the caspase-3 cell death pathway. The first part of the study identified some of the molecular targets for modulation by THC in cultured cortical neurons, with particular emphasis on the signalling molecules involved in regulating the caspase-3 cell death pathway. Targets for investigation included the apoptotic signalling molecules, p53 and JNK, and their substrates including, Bax, Bcl-2, cytochrome *c*, and caspase-3. Apoptotic markers assessed included PARP cleavage and DNA fragmentation. Having identified some of the molecular targets for modulation by THC in cultured cortical neurons, the next aspect of the study was concerned with determining if these events were operative in the rat brain *in vivo* and if so, were they influenced by the maturity if the CNS. This was first approached by an *ex vivo* study, designed to examine the effect of THC on the viability of cortical slices prepared from neonatal, adolescent and adult animals. Interesting, data from this study strongly suggested that the

apoptotic events triggered by THC in cultured cells *in vitro* were operative in neonatal cortical brain slices exposed to THC. Specifically, THC induced the activation of JNK2 and caspase-3 in cortical brain slices obtained from neonatal rats, key apoptotic events observed *in vitro*. Surprising, these apoptotic events were restricted to the neonatal cortical brain slices, with cortical slices obtained from adolescent and adult rats showing resistance to the apoptotic actions of THC. These findings were confirmed following administration of THC to neonatal and adult rats *in vivo*. Immunocytochemical and biochemical analysis of the cortex from these animals produced convincing evidence that THC increases the level of JNK phosphorylation, caspase-3 activity and DNA fragmentation in the neonatal, but not the adult cortex. Overall, the data presented in this study demonstrate that apoptotic actions of THC exist in the rat cortex and that there is an inter-relationship between neuronal maturity and THC apoptotic signal transduction.

Debate continues over the effects of cannabinoids on cell viability. The bulk of the experimental evidence indicates that cannabinoids may protect neurons from toxic insults both *in vitro* (Sinor *et al.*, 2000; Nagayama *et al.*, 1999; Hampson *et al.*, 1998; Nadler *et al.*, 1993; Marsicano *et al.*, 2002; Eshhar *et al.*, 1993; Abood *et al.*, 2001; Hampson and Grimaldi, 2001; Shen and Thayer, 1998; Milton, 2002; Iuvone *et al.*, 2004) and *in vivo* (van der Stelt *et al.*, 2001; Panikashvili *et al.*, 2000; Hansen *et al.*, 2001a). Furthermore, evidence that cannabinoids are neurotoxic is limited to isolated studies in primary neurons (Chan *et al.*, 1998) and transformed neural cells (Maccarrone *et al.*, 2000; Sarker *et al.*, 2003; Sánchez *et al.*, 1998; Jacobsson *et al.*, 2000). Although chronic exposure studies have revealed that THC produces morphological changes in the brain (Scallet, 1991, Scallet *et al.*, 1987) there is no direct evidence that neurotoxic effects of cannabinoids exist *in vivo*. Overall, the role of cannabinoids in controlling neuronal cell fate is a complex issue that is influenced by the nature of the toxic insult (dose, duration of exposure, route of administration), the cell type and the particular cannabinoid used.

Data presented in this study show that THC is neurotoxic to cultured cortical neurons. THC neurotoxicity *in vitro* was examined using cultured cortical neurons to identify signal transduction pathways contributing to toxicity. THC induced DNA fragmentation in the nucleus of cultured neurons, reflecting

an apoptotic response profile to THC. Apoptotic effects of THC were observed following exposure to THC for short time periods (30 min) and at submicromolar concentrations (0.1μM; Chapter 3). This is interesting considering that smoking marijuana results in the rapid appearance of THC in the plasma, appearing after the first marijuana puff and reaching a peak within 10 min (Huestis *et al.*, 1992). The dose of THC used in cultured neurons is also consistent with the human plasma concentrations of THC (low μM; Chiang and Barnett, 1984; Giroud *et al.*, 2001). Indeed, Azorlosa and colleagues (1992) have found THC concentrations of 1μM in the human plasma during recreational use, a concentration that produces apoptosis in 35% of cultured cells following a 2hr THC exposure (Chapter 3). Furthermore, THC may be concentrated in some tissues suggesting that cannabinoid concentrations may be higher in the brain after recreational use than the concentrations examined herein (Johansson *et al.*, 1989). It is also noteworthy that the potency (THC content) of marijuana has increased over the last number of years (Iversen, 2000), which may influence the apoptotic effects of THC.

The direct effect of THC on the activity of the most widely studied cell death protease, caspase-3 (Zou *et al.*, 1997; Janicke *et al.*, 1998; Rosse *et al.*, 1998), was observed throughout the study in cortical cells in culture, neonatal cortical brain slices and in the neonatal cortex *in vivo*. Indeed, a 30 min exposure to THC was sufficient to induce a significant increase in caspase-3 activity *in vitro*, the time point at which a significant increase in DNA fragmentation was also observed *in vitro* (Chapter 3). The regulatory effects of THC on this protease are consistent with the apoptotic effects of cannabinoids on splenocytes and thymocytes (Mckallip *et al.*, 2002b), neuroblastoma and lymphoma cells (Maccarrone *et al.*, 2000), myeloblastic leukemia cells (Gallily *et al.*, 2003), bone-marrow-derived dendritic cells (Do *et al.*, 2004) and PC-12 cells (Sarker *et al.*, 2000), in which the cannabinoid-induced apoptotic response profile involves caspases. The accumulation of cytochrome *c* in the cytoplasm plays a pivotal role in the activation of caspase-3 (Reed, 1997), and cytochrome *c* translocation is associated with cannabinoid-induced apoptosis in neuroblastoma (Maccarrone *et al.*, 2000) and dendritic (Do *et al.*, 2004) cells. Although not shown directly, we hypothesize that cytochrome *c* release

from the mitochondria is involved in the regulation of caspase-3 activity in cultured cortical cells, cortical brain slices obtained from neonatal rats and the neonatal rat cortex *in vivo*.

The results presented in this study provide strong evidence that the apoptotic actions of THC in cortical neurons involved an increase in the activity of the stress related kinase, JNK. It is of particular note that the time frame of JNK activation in cortical neurons varied considerably between different JNK isoforms. Indeed, maximal activation of JNK1 and JNK2 occurred after 5 min and 2hr of THC exposure, respectively, in cortical cultures (Chapter 4). Similarly JNK2, but not JNK1, activation was observed in the neonatal cortex *ex vivo* at 2hr post-THC treatment (Chapter 6) and in the neonatal cortex *in vivo* at the 3hr time point (Chapter 7). This suggests that functional diversity exists between the JNK isoforms in the neonatal rat cortex. However, despite the differential time course of JNK activation, both JNK1 and JNK2 appeared to directly contribute to THC-induced apoptosis in cultured cortical cells (Chapter 4). The regulatory effects of cannabinoids on JNK are supported by the findings of Rueda and colleagues (2000). In this study THC, synthetic cannabinoids and endogenous cannabinoids induced JNK1 and JNK2 phosphorylation in CHO cells stably transfected with CB_1 receptor cDNA following a 5 min incubation with the various cannabinoids. Furthermore, a 10 min exposure to THC induced JNK activation in neural cells endogenously expressing the CB_1 receptor (Rueda *et al.*, 2000). Interestingly, in the same study, a 3-day exposure to THC was associated with JNK activation and a significant decrease in cell viability in glioma C6.9 cells. It has also been recently found that the endogenous cannabinoid, anandamide, induces the early (within 30 min) activation of JNK in PC12 cells, and this contributes to apoptosis in these cells (Sarker *et al.*, 2003). It is also noteworthy that THC did not affect JNK phosphorylation in cortical slices obtained from adolescent and adult rats (Chapter 6) or in the adult cortex *in vivo* (Chapter 7). This finding concurs with the effects of cannabinoids on JNK1 and JNK2 phosphorylation in adult rat hippocampal slices (Derkinderen *et al.*, 2001). Overall, these findings suggest that JNK is involved in cannabinoid-induced neurotoxicity and suggest that the duration of JNK induction, in addition to the maturity of the neuronal

tissue, may be the determining factors in JNK transduction of cannabinoid-induced apoptotic signals.

Analysis of the nuclear phospho-protein, p53, revealed that p53 signalling contributes to the apoptotic actions of THC in cultured cortical neurons. THC was shown to stabilise the p53 protein in a transcription-independent manner via phosphorylation on residue serine-15 following a 5 min THC exposure (Chapter 5). THC had no effect on p53 induction in the neonatal cortex *ex vivo* (Chapter 6) and *in vivo* (Chapter 7) which may reflect the transient nature of cannabinoid-induced p53 expression. Despite the short-term nature of THC-induced p53 induction, p53 contributed directly to THC-induced apoptosis in cultured cells by influencing the expression of the mitochondria-associated proteins, caspase-3 activity and DNA fragmentation (Chapter 5). We also hypothesize that p53 is involved upstream in the regulation of THC-induced neurotoxicity in neonatal cortical brain slices and the neonatal cortex *in vivo*. Several mechanisms for p53 stabilisation have been suggested including JNK (Blatt and Glick, 2001), and since we have demonstrated the early activation of JNK1 and p53 after 5 min of THC treatment, it is possible that JNK1 regulates p53 expression in cortical cells following cannabinoid-exposure. Indeed, previous studies from our laboratory have identified p53 as a downstream target for JNK1 (Fogarty *et al.*, 2003). As far as we are aware, evidence that cannabinoids regulate p53 has previously only been reported by Do and colleagues (2004) who have demonstrated that the p53 gene is upregulated in dendritic cells following THC exposure for 45 min. Despite this evidence, the authors fail to identify if the modulatory effects of THC on p53 transcription contributes to THC-induced apoptosis of dendritic cells.

The mechanism of p53-induced apoptosis has been extensively studied and involves the activation of the mitochondrial/caspase pathway (Marchenko *et al.*, 2000; Bonini *et al.*, 2004). Analysis of the effects of THC on pro-apoptotic Bcl-2 family member, Bax, indicated that THC increases Bax transcription and protein expression in cultured cortical neurons (Chapter 5). Application of the p53 inhibitor, pifithrin-α, revealed that the THC-mediated increase in Bax protein expression was mediated by p53 signalling, placing Bax downstream of

p53, and possibly JNK1, in the THC-induced apoptotic cascade. THC was also shown to inhibit the pro-survival function of Bcl-2 via phosphorylation of the Bcl-2 protein. There is evidence that Bcl-2 phosphorylation can be regulated by p53 (Pucci *et al.*, 1999) and evidence presented in Chapter 5 demonstrated that THC induces the phosphorylation of Bcl-2 protein within the same timeframe of Bax induction This phosphorylation event was dependent on p53 as the p53 inhibitor, pifithrin-α, prevented THC-induced phosphorylation of Bcl-2. Again, there is limited evidence that cannabinoids regulate the mitochondria-associated proteins. Do and co-workers (2004) have recently shown that THC induces an upregulation of the Bax gene in bone marrow-derived dendritic cells. There is also evidence that THC inhibits Bcl-2 transcription in splenocytes (Zhu *et al.*, 1998a) and Bcl-inhibits anandamide-induced apoptosis of PC12 cells (Sarker *et al.*, 2003). Hence, cannabinoids have the proclivity to regulate the expression of mitochondria-associated proteins and regulate cell survival by altering the expression patterns of Bax and Bcl-2. It is recognised that THC had no effect on Bax and phospho-Bcl-2 expression in the neonatal cortex *in vivo* suggesting that the *in vitro* role of these proteins in cannabinoid-induced apoptosis may be absent *in vivo*.

The emerging cascade from the results in this study is of a THC-induced apoptotic pathway that is operative in neonatal cortical cultures, cortical slices obtained from neonatal animals and the neonatal cortex *in vivo* (proposed schematic in Figure 8.1). Cultured cortical neurons are susceptible to THC-induced apoptosis following exposure for 30 min and a maximal level of cell death is observed 2-3hr post-treatment. In cultured cells, THC induces the early phosphorylation of JNK1 and p53, which contribute to downstream apoptotic events including the induction Bax expression and Bcl-2 phosphorylation. These events presumably culminate in cytochrome *c* translocation and subsequent caspase-3 activation. JNK antisense oligonucleotides and the p53 inhibitor, pifithrin-α, have identified THC-induced p53, JNK1 and JNK2 phosphorylation as key events in the regulation of caspase-3 in this *in vitro* system. Caspase-3 results in cultured cortical cellular demise, possibly by inducing the cleavage of the PARP enzyme. The molecular events triggered by THC *in vitro* were reliant on CB_1 receptor

activation. Although the apoptotic events triggered by THC in the neonatal cortex in *ex vivo* and *in vivo* systems have not been characterised in as much detail in this study, there is strong evidence that CB_1-dependent JNK2 and caspase-3 activation, both pivotal events in THC-induced neurotoxicity *in vitro*, are central to the apoptotic actions of THC in the neonatal cortex *ex vivo* and *in vivo*.

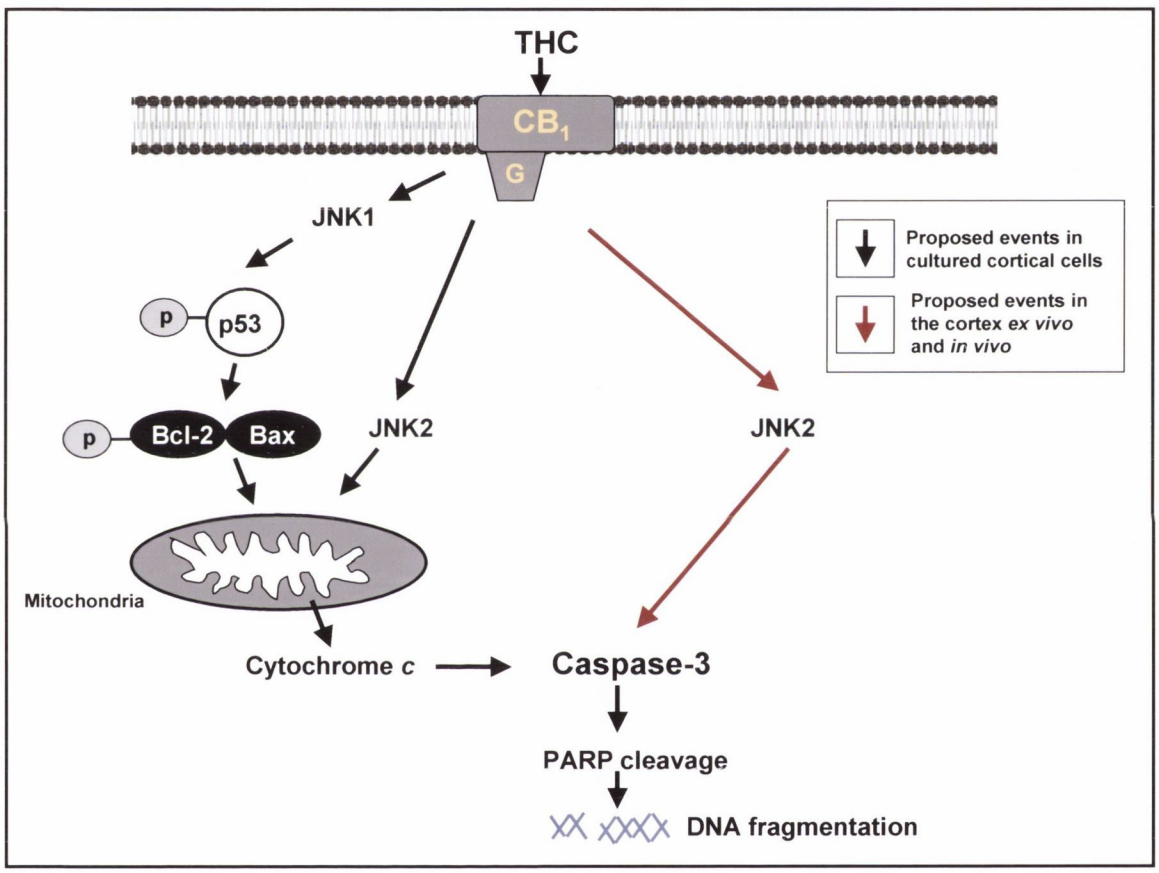

Figure 8.1: Proposed model contributing to THC-induced neuronal apoptosis in cultured rat cortical neurons, cortical brain slices obtained from neonatal rats and the neonatal rat cortex *in vivo*.

The findings in this study may have several important implications in cannabinoid research. Firstly, there is evidence to suggest that the doses of THC used in this study are behaviourally and pharmacologically active (Meyer and Kunkle, 1999; Mokler *et al.*, 1987; Sim *et al.*, 1996; Jentsch *et al.*, 1998)

and are comparable to concentrations of THC associated with recreational marijuana use (Nahas *et al.*, 1977; Chan *et al.*, 1996; Azorlosa *et al.*, 1992). Hence, it is reasonable to suggest that the cannabinoid-induced neurotoxicity identified in this study may contribute to the detrimental effects of marijuana on cognitive processes associated with cortical function. Indeed, it may be a combination of cannabinoid-induced alteration in a number of neurotransmitter systems (Jentsch *et al.*, 1998; Gessa *et al.*, 1998; Shen *et al.*, 1996; Schlicker *et al.*, 1997) and cannabinoid-induced neurotoxicity that induces the behavioural symptoms that can be ascribed to marijuana use. It is particularly noteworthy that the damaging effects of THC identified in this study are operative only in the neonatal cortex. This suggests that *in utero* exposure to marijuana may have marked effects on the development and differentiation of the CNS in the fetus. Hence, data presented in the present study may underlie the cognitive deficits, such as memory impairments and attentional deficits (Fried and Watkinson, 1990; Griffith *et al.*, 1994; Fried, 1995; Fried and Smith, 2001), that are found in children perinatally exposed to marijuana. Secondly, the apoptotic transduction pathway identified in this study may reflect a signalling pathway that is regulated by the endogenous cannabinoid system. Although the precise physiological role of the endogenous system is unknown, there is evidence that the endogenous cannabinoid system is involved in neural developmental events (Fernández-Ruiz *et al.*, 1999). Hence it is again reasonable to suggest that overstimulation of cannabinoid receptors at critical stages of development may have damaging consequences on nervous system functioning. Finally, cannabinoids have been shown to have therapeutic potential, particularly in the management of malignant gliomas (Velasco *et al.*, 2004; Blázquez *et al.*, 2004; Blázquez *et al.*, 2003; Galve-Roperh *et al.*, 2000) and the findings in the present study suggest a molecular mechanism that may be involved in the anti-tumoural actions of cannainoids.

In conclusion, this study suggests a molecular mechanism contributing to the neurotoxic effects of marijuana exposure. It is important to note that in complex cellular systems such as neuronal networks, it is unlikely that a simple linear cascade of events is sufficient to promote cell death. Hence, it is more likely that several transduction pathways self-amplify or delete each other to execute the apoptotic programme triggered by THC. Identification of the CB_1-

dependent transduction pathways is fundamental to understanding the effects of marijuana on neuronal function and provides further insight into the role of the endogenous cannabinoid system in neurobiological processes.

8.2 Future experiments

Although this study determined transduction pathways that are operative *in vitro* and *in vivo*, several important questions remain to be answered. Several mechanisms for p53 stabilisation have been suggested including JNK (Blatt and Glick, 2001). Considering that JNK1 and p53 are regulated by THC at the same time point in cultured neurons, it would be interesting to determine if JNK1 regulates p53 phosphorylation status in THC-induced apoptosis. Indeed, previous studies from our laboratory have demonstrated that JNK1 contributes directly to the stabilisation of p53 via phosphorylation on residue serine-15 (Fogarty *et al.*, 2003), strengthening the possibility of this proposal. It has also been demonstrated in our laboratory that during neuronal apoptosis, p53 accumulates at the lysosomal membrane (Fogarty and Campbell, manuscript in preparation). Indeed, p53 has been shown to have a role in destabilising the lysosomal membrane (Yuan *et al.*, 2002), resulting in the release of cathepsin proteases which have previously been demonstrated to result in cellular demise (Ditaranto-Desimone *et al.*, 2003; Turk *et al.*, 2000). Hence, it is reasonable to suspect that THC-induced neuronal apoptosis involves the p53 induced destabilisation of the lysosomal membrane and induction of apoptosis following the release of apoptotic cathepsin proteases.

Although it was determined that cytochrome *c* translocation occurred in cultured cortical cells, the mechanism for this event was not determined. Using the p53 inhibitor, pifithrin-α, and JNK antisense oligonucleotides, the role of p53 and JNK1/2, respectively, in cytochrome *c* translocation could be determined.

In this study, cannabinoid-induced apoptosis was investigated using the psychoactive cannabinoid, THC. However, several recent studies have shown that endogenous cannabinoids are neurotoxic molecules (Kim and Thayer, 2001; Sarker *et al.*, 2003; Maccarrone *et al.*, 2000), which may reflect an anti-proliferative function of the endogenous cannabinoid system in the CNS. Hence, the proclivity of endogenous to regulate the viability of cortical neurons, possibly via the pathway identified in the present study, warrants investigation.

Several aspects of the *ex vivo* and *in vivo* studies performed in the present investigation warrant further study. Firstly, time course experiments identifying the *in vivo* apoptotic actions of THC are essential. These studies will provide insight into the temporal sequence of apoptotic events activated by THC *in vivo*. Hence, such a study may clarify a role for signalling molecules such as p53, Bax, Bcl-2 and cytochrome *c* in the *in vivo* apoptotic actions of THC. It is also essential to determine the *in vivo* effects of THC on an adolescent rat age group. Furthermore, a chronic long-term THC exposure study would provide data reflective of habitual recreational use in human societies. Finally, given that the apoptotic actions of THC *in vivo* vary with postnatal development, it would be interesting to determine if apoptotic actions of THC exist in the cortex of offspring perinatally exposed to THC.

VIII Bibliography

Abel, E.L. (1984) Effects of delta 9-THC on pregnancy and offspring in rats. *Neurobehavioural Toxicology and Teratology*, **6(1)**, 29-32.

Abood, M.E. and Martin, B.R. (1992) Neurobiology of marijuana abuse. *Trends in Pharmacological Science,* **13**, 201-206.

Abood, M.E., Rizvi, G., Sallapudi, N. and McAllister, S. (2001) Activation of the CB_1 cannabinoid receptor protects cultured mouse spinal neurons against excitotoxicity. *Neuroscience Letters,* **309**, 197-201.

Adams, J. M. and Cory, S. (1998) The Bcl-2 protein family: Arbiters of cell survival. *Science,* **281**, 1322-1326.

Agurell, S., Halldin, M., Lindgren, J-.E., Ohlsson, A., Widman, M., Gillepie, H. and Hollister, L. (1986) Pharmacokinetics and metabolism of Δ^1-tetrahydrocannabinol and other cannabinoids with emphasis on man. *Pharmacology Review*, **38**, 21-38.

Aloyz, R.S., Bamji, S.X., Pozniak, C.D., Toma, J.G., Atwal, J., Kaplan, D.R. and Miller, F.D. (1998) P53 is essential for developmental neuron death as regulated by the TrkA and p75 neurotrophin receptors. *The Journal of Cell Biology*, **143(6)**, 1691-1703.

Alvarez-Gonzalez, R., Pacheco-Rodriguez, G. and Mendoza-Alvarez, H. (1994) Enzymology of ADP-ribose polymer synthesis. *Molecular and Cellular Biochemistry,* **138**, 33-37.

Ameri, A. (1999) The effects of cannabinoids on the brain. *Progress in Neurobiology*. **58**, 315-348.

Antonsson, B., Conti, F., Ciavatta, A., Montessuit, S., Lewis, S., Martinou, I., Bernasconi, L., Bernaird, A., Mermod, J-.J., Mazzei, G., Maundrell, K., Gambale, F., Sadoul, R. and Martinou, J-.C. (1997) Inhibition of Bax channel-forming activity by Bcl-2. *Science*, **277**, 370-372.

Appella, E. and Anderson, C. W. (2001) Post-translational modifications and activation of p53 by genotoxic stresses. *European Journal of Biochemistry,* **268**, 2764-2772.

Arends, M.J., Morris, R.G. and Wyllie, A.H. (1990) Apoptosis: the role of the endonuclease. *American Journal of Pathology*, **136**, 593-608.

Ashton, H.C. (2001) Pharmacology and effects of cannabis: a brief review. *British Journal of Psychiatry*, **178**, 181-186.

Astley, S. and Little, R. (1990) Maternal marijuana use during lactation and infant development at one year. *Neurotoxicology and Teratology*, **12**, 161-168.

Attardi, L. D., Lowe, S. W., Brugarolas, J. and Jacks, T. (1996) Transcriptional activation by p53, but not induction of the p21 gene, is essential for oncogene-mediated apoptosis. *European Molecular Biology Organization Journal,* **15**, 3693-3701.

Azorlosa, J.L., Heishman, S.J., Stitzer, M.L. and Mahaffey, J.M. (1992) Marijuana smoking: Effect of varying Δ^9-Tetrahydrocannabinol content and number of puffs. *The Journal of Pharmacology and Experimental Therapeutics*, **261(1)**, 114-122.

Bachs, L. and Morland, H. (2001) Acute cardiovascular fatalities following cannabis use. *Forensic Science International*, **124**, 200-203.

Baeuerie, B.A. and Baltimore, D. (1996) NF-κB: Ten years after. *Cell*, **87**, 13-20.

Baker, C.L. and McDougall, J.J. (2004) The cannabinomimetic arachidonyl-2-chloroethylamide (ACEA) acts on capsaicin-sensitive TRPV1 receptors but not cannabinoid receptors in rat joints. *British Journal of Pharmacology*, **142(8)**, 1361-1367.

Bartova, A. and Birmingham, M.K. (1976) Effect of Δ^9-Tetrahydrocannabinol on mitochondrial NADH-oxidase activity. *The Journal of Biological Chemistry*, **251(16)**, 5002-5006.

Behl, C. (2000) Apoptosis and Alzheimer's disease. *Journal of Neural Transmission,* **107**, 1325-1344.

Beltramo, M., Stella, N., Calignano, A., Lin, S.Y., Makriyannis, A. and Piomelli, D. (1997) Functional role of high-affinity anadamide transport, as revealed by selective inhibition. *Science*, **277**, 1094-1097.

Belue, R.C., Howlett, A.C., Westlake, T.M. and Hutchings, D.E. (1995) The ontogeny of cannabinoid receptors in the brain of postnatal and aging rats. *Neurotoxicology and Teratology*, **17(1)**, 25-30.

Bennet, M., Macdonald, K., Chan, S. W., Luzio, J. P., Simari, P. and Weissberg, P. (1998) Cell surface trafficking of Fas: a rapid mechanism of p53-mediated apoptosis. *Science,* **282**, 290-293.

Berdyshev, E.V., Boichot, E., Germain, N., Allain, N., Anger, J-.P. and Lagente, V. (1997) Influence of fatty acid ethanolamides and Δ^9-tetrahydrocannabinol on cytokine and arachidonate release by mononuclear cells. *European Journal of Pharmacology*, **330**, 231-240.

Berrendero, F., Garcia, L., Hernandez, M.L., Romero, J., Cebeira, M., de Miguel, R., Ramos, J.A. and Fernández-Ruiz, J.J. (1998) Localization of mRNA expression and activation of signal transduction mechanisms for cannabinoid receptor in rat brain during fetal development. *Development,* **125(6)**, 3179-3188.

Berrendero, F., Sepe, N., Ramos, J.A., Di Marzo, V. and Fernández-Ruiz, J.J. (1999) Analysis of cannabinoid receptor binding and mRNA expression and endogenous cannabinoid contents in the developing rat brain during late gestation and early postnatal period. *Synapse*, **33(3)**, 181-191.

Bidaut-Russell, M., Devane, W.A. and Howlett, A.C. (1990) Cannabinoid receptors and modulation of cyclic AMP accumulation in the rat brain. *Journal of Neurochemistry*, **55**, 21-26.

Bidinger, B., Torres, R., Rosseti, R.G., Brown, L., Beltre, R., Burstein, S., Lian, J.B., Stein, G.S. and Zurier, R.B. (2003) Ajulemic acid, a nonpsychoactive cannabinoid acid, induces apoptosis in human T lymphocytes. *Clinical Immunology*, **108**, 95-102.

Black, R.A., Kronheim, S.R., Merriam, J.E., March, C.J. and Hopp, T.P. (1989) A pre-aspartate-specific protease from human leukocytes that cleaves pro-interleukin-1 beta. *The Journal of Biological Chemistry*, **264**, 5323-5326.

Blatt, N. B. and Glick, G. D. (2001) Signaling pathways and effector mechanisms pre-programmed cell death. *Bioorganic and Medicinal Chemistry,* **9,** 1371-1384.

Blázquez, C., Casanova, M.L., Planas, A., Gómez Del Pulgar, T., Villanueva, C., Fernández-Acenero, M.J., Aragonés, J., Huffman, J.W., Jorcano, J.L. and Guzmán, M. (2003) Inhibition of tumor angiogenesis by cannabinoids. *FASEB Journal*, **15**, 274-2747.

Blázquez, C., González-Feria, L., Ávarez, L., Haro, A., Casanova, M.L. and Guzmán, M. (2004) Cannabinoids inhibit the vascular endothelial growth factor pathway in gliomas. *Cancer Research*, **64**, 5617-562

Block, R.I. and Ghoneim, M.M. (1993) Effects of chronic marijuana use on human cognition. *Psychopharmacology,* **110**, 219-228.

Bolshakov, V.Y., Golan, H., Kandel, E.R. and Siegelbaum, S.A. (1997) Recruitment of new sites of synaptic transmission during the cAMP-dependent late phase of LTP at CA3-CA1 synapses in the hippocampus. *Neuron*, **19**, 635-651.

Bonini, P., Cicconi, S., Cardinale, A., Vitale, C., Serafino, A.L., Ciotti, M.T. and Marlier, L.N. (2004) Oxidative stress induces p53-mediated apoptosis in glia: p53 transcription-independent way to die. *Journal of Neuroscience Research*, **75(1)**, 83-95.

Bouaboula, M., C., Bourrie, B., Rinaldi-Carmona, M., Shire, D., Le Fur, G. and Casellas, P. (1995a) Stimulation of cannabinoid receptor CB1 induces krox-24 expression in human astrocytoma clls. *The Journal of Biological Chemistry*, **270**, 13973-13980.

Bouaboula, M., Poinot-Chazel, C., Bourrie, B., Canat, X., Calandra, B., Rinaldi-Carmona, M., Le Fur, G. and Casellas, P. (1995b) Activation of mitogen-activated protein kinases by stimulation of the central cannabinoid receptor CB_1. *Biochemical Journal,* **312**, 637-641.

Bouaboula, M., Poinot-Chazel, C., Marchand, J., Canat, X., Bourrie, B., Rinaldi-Carmona, M., Calandra, B., Le Fur, G. and Casellas, P. (1996) Signaling pathway associated with stimulation of CB_2 peripheral cannabinoid receptor: Involvement of both mitogen-activated protein kinase and induction of Krox-24 expression. *European Journal of Biochemistry,* **237**, 704-711.

Bouaboula, M., Bianchini, F.R., Mckenzie, J., Pouyssegur, P. and Casellas, P. (1999) Cannabinoid receptor CB_1 activates the Na^+/H^+ exchanger NHE-1 isoform via G_i-mediated mitogen activated protein kinase signaling transduction patways. *FEBS Letters,* **449**, 61-65.

Bozyczko-Coyne, D., O'Kane, T. M., Wu, Z. L., Dobrzanski, P., Murthy, S., Vaught, J. L. and Scott, R. W. (2001) CEP-1347/KT-7515, an inhibitor of SAPK/JNK pathway activation, promotes survival and blocks multiple events. *Journal of Neurochemistry,* **77**, 849-863.

Bradford, M. (1976) A Rapid and Sensitive Method for the quantification of Microgram Quantities of Protein Utilizing the Principle pf Protein-Dye Binding. *Analytical Biochemistry,* **72,** 248-254.

Braude, M.C. (1972) Toxicology of cannabis. In: Cannabis and its Derivatives. Oxford University Press, pp. 89-99.

Breivogel, C.S., Griffin, G., Di Marzo, V. and Martin, B.R. (2001) Evidence for a new G protein-coupled cannabinoid revceptor in mouse brain. *Molecular Pharmacology*, **60**, 155-163.

Bryant, J.A., Hughes, S.G. and Garland, J.M. (2000) Regulation of cell cycle arrest and cell death-alternative responses to DNA damage. In: Programmed Cell Death in Animals and Plants. BIOS Scientific Publishers Ltd.

Buchan, B.J., Walsh, J.M. and Leaverton, P.E. (1998) Evaluation of the accuracy of on-site multi-analyte drug testing devices in the determination of the prevalence of illicit drugs in drivers. *Journal of Forensic Science*, **43**, 395-399.

Buschbeck, M. and Ullrich, A. (2005) The unique C-terminal of the mitogen-activated protein kinase ERK5 regulates its activation and nuclear shuttling. *The Journal of Biological Chemistry*, **280(4)**, 2659-2667.

Buschmann, T., Potapova, O., Bar-Shira, A., Ivanov, V., N. , Fuchs, S. Y., Henderson, S., Fried, V. A., Minamoto, T., Alarcon-Vargas, D., Pincus, M. R., Gaarde, W. A., Holbrook, N. J., Shiloh, Y. and Ronai, Z. (2001) Jun NH2-terminal kinase phosphorylation of p53 on Thr-81 is important for p53 stabilization and transcriptional activities in response to stress. *Molecular and Cellular Biology,* **21**, 2743-2754.

Campbell, V.A. (2001) Tetrahydrocannabinol-induced apoptosis in cultured cortical neurones is associated with cytochrome *c* release and caspase-3 activation. *Neuropharmacology,* **40**, 702-709.

Carboni, L., Carletti, R., Tacconi, S., Corrado, C. and Ferraguti, F. (1998) Differential expression of SAPK isoforms in the rat brain. An in situ hybridisation study in the adult rat brain and during post-natal development. *Molecular Brain Research,* **60**, 57-68.

Carta, G., Nava, F. and Gessa, G.L. (1998) Inhibition of hippocampal acetylcholine release after acute and repeated Δ^9-tetrahydrocannabinol in rats. *Brain Research*, **809**, 1-4.

Casanova, M.L., Blázquez, C., Martínez-Palacio, J., Villanueva, C., Fernández-Acenero, M.J. Huffman, J.W., Jorcano, J.L. and Guzmán, M. (2003) Inhibition of skin tumor and angiogenesis in vivo by activation of cannabinoid receptors. *The Journal of Clinical Investigation*, **111(1)**, 43-50.

Caulfield, M.P. and Brown, D.A. (1992) Cannabinoid receptor agonists inhibit Ca current in NG108-15 neuroblastoma cells via a pertussis toxin-sensitive mechanism. *British Journal of Pharmacology*, **106**, 231-232.

Cavero, I., Lokhandwala, M.F., Buckley, J.P. and Jandhyala, B.S. (1974) The effect of (-)-Δ^9-trans-Tetrahydrocannabinol on myocardial contractility and venous return in anesthetized dogs. *European Journal of Pharmacology*, **29**, 74-82.

Cavigelli, M., Dolfi, F., Claret, F.X. and Karin, M. (1995) Induction of c-fos expression through JNK-mediated TCF/Elk-1 phosphorylation. *EMBO Journal,* **14**, 5957-5964.

Chan, G.C., Hinds, T.R., Impey, S. and Storm, D.R. (1998) Hippocampal neurotoxicity of Δ^9-Tetrahydrocannabinol. *Journal of Neuroscience,* **18(14)**, 5322-5332.

Chan, P.C., Sills, R.C., Braun, A.G., Haseman, J.K. and Bucher, J.R. (1996) Toxicity and carcinogenicity of delta-9-tetrahydrocannabinol in Fischer rats and B6C3F1 mice. *Fundamental Applied Toxicology*, **30**, 109-117.

Chen, Y. R., Meyer, C. F. and Tan, T. H. (1996) Persistent activation of c-Jun N-terminal kinase 1 (JNK1) in gamma radiation-induced apoptosis. *The Journal of Biological Chemistry,* **271**, 631-634.

Chi, T.Y., Chen, G.G. and Lai, P.B. (2004) Eicosapentaenoic acid induces Fas-mediated apoptosis through a p53-dependent pathway in hepatoma cells. *Cancer Journal*, **10(3)**, 190-200.

Chiang, C.W. and Barnett, G. (1984) Marijuana effect and delta-9-tetrahydrocannabinol plasma level. *Clinical Pharmacology and Therapeutics,* **36(2)**, 234-238.

Choi, W-.S., Lee, E-.H., Chung, C-.W., Jung, Y-.K., Jin, B.K., Kim, S.U., Oh, T.H., Saido, T.C., and Oh, Y.J. (2001) Cleavage of Bax is mediated by caspase-dependent or -independent calpain activation in dopaminergic neuronal cells: protective role of Bcl-2. *Journal of Neurochemistry,* **77**, 1531-1541.

Chomczynski. P. and Sacchi, N. (1987) Single-step method of RNA isolation by acid guanidinium thiocyanate-phenol-chloroform extraction. *Analytical Biochemistry,* **162**, 156-159.

Cioffi, C.L. and Monia, B.P. (1999) Evaluation of biological role of c-jun N-terminal kinase using an antisense approach. *Methods in Enzymology*, **314**, 363-378.

Cohen, J.J., Duke, R.C., Fadok, V.A. and Sellins, K.S. (1992) Apoptosis and programmed cell death in immunity. *Annual Review of Immunology*, **10**, 267-293.

Collins, D.R., Pertwee, R.G. and Davies, S.N. (1994) The action of synthetic cannabinoids on the induction of long-term potentiation in the rat hippocampal slice. *European Journal of Pharmacology*, **259**, R7-R8.

Cone, E.J. and Huestis, M.A. (1993) Relating blood concentrations of Tetrahydrocannabinol and metabolites to pharmacologic effects and time of marijuana usage. *Therapeutic Drug Monitoring*, **15**, 527-532.

Coso, O.A., Teramoto, H., Simonds, W.F. and Gutkind, J.S. (1996) Signaling from G protein-coupled receptors to c-Jun kinase involves $\beta\gamma$ subunits of heterotrimeric G proteins acting on a Ras and Rac1-dependent pathway. *The Journal of Biological Chemistry,* **271(8)**, 3963-3966.

Cregan, S.P., MacLaurin, J.G., Craig, C.G., Robertson, G.S., Nicholson, D.W., Park, D.S. and Slack, R.S. (1999) Bax-dependent caspase-3 activation is a key determinant in p53-induced apoptosis in neurons. *Journal of Neuroscience*, **19(18)**, 7860-7869.

Crooke, S. T. (1992) Therapeutic applications of oligonucleotides. *Annual Review of Pharmacology and Toxicology,* **32**, 329-376.

Culmsee, C., Zhu, X., Yu, Q. S., Chan, S. L., Camandola, S., Guo, Z., Greig, N. H. and Mattson, M. (2001) A synthetic inhibitor of p53 protects neurons against death induced by ischemic and excitotoxic insults, and amyloid beta-peptide. *Journal of Neurochemistry,* **77**, 220-228.

Daaka, Y., Zhu, W., Friedman, H. and Klein, T.W. (1997) Induction of Interleukin-2 receptor α gene by Δ^9-tetrahydrocannabinol is mediated by nuclear factor κB and CB_1 cannabinoid receptor. *DNA Cell Biology*, **16**, 301-309.

Dalterio, S.L. (1986) Cannabinoid exposure: effects on development. *Neurobehavioural Toxicology and Teratology*, **8**, 345-352.

D'Ambra, M. (1996) Restoration of the normal coagulation process: advances in therapies to antagonize heparin. *Journal of Cardiovascular Pharmacology*, **1**, S58-63.

Day, N., Richardson, G., Goldschmidt, L., Robles, N., Taylor, P., Stoffer, D., Cornelius, M. and Geva, D. (1994) The effect of prenatal marijuana exposure on the cognitive development of offspring at age three. *Neurotoxicology and Teratology*, **16**, 169-175.

De Petrocellis, L., Melck, D., Palmiso, A., Bisogno, T., Laezza, C., Bifulco, M. and Di Marzo, V. (1998) The endogenous cannabinoid anandamide inhibits human breast cancer proliferation. *Proceedings of the National Academy of Science USA*, **95**, 8375-8380.

Deadwyler, S.A., Hampson, R.E., Bennet, B.A., Edwards, D.A., Mu, J., Pacheco, M.A., Ward, S.J. and Childers, S.R. (1993) Cannabinoids modulate potassium current in cultured hippocampal neurons. *Receptor Channels*, **1**, 121-134.

Deng, X., Xiao, L., Lang, W., Gao, F., Ruvolo, P. and May, W.S. (2001) Novel role for JNK as a stress-activated Bcl2 kinase. *The Journal of Biological Chemistry*, **276(26)**, 23681-23688.

Derkinderen, P., Enslen, H. and Girault, J.-A. (1999) The ERK/MAP-kinases cascade in the nervous system. *Neuroreport,* **10**, R24-R34.

Derkinderen, P., Ledent, C., Parmentier, M. and Girault, J.-A. (2001) Cannabinoids activate p38 mitogen-activated protein kinases through CB_1 receptors in hippocampus. *Journal of Neurochemistry,* **77**, 957-960.

Derkinderen, P., Valjent, E., Toutant, M., Corvol, J.-C., Enslen, H., Ledent, C., Trzaskos, J., Caboche, J. and Girault, J.-A. (2003) Regulation of Extracellular Signal-Regulated Kinase by cannabinoids in hippocampus. *Journal of Neuroscience,* **23(6)**, 2371-2382.

Derocq, J.M., Segui, M., Marchand, J., Le Fur, G. and Casellas, P. (1995) Cannabinoids enhance human B-cell growth at low nanomolar concentrations. *FEBS Letters*, **369**, 177-182.

Desagher, S., Osen-Sand, A., Nichols, A., Eskes, R., Montessuit, S., Lauper, S., Maundrell, K., Antonsson, B. and Martinou, J-.C. (1999) Bid-induced conformational change in Bax is responsible for mitochondrial cytochrome *c* release during apoptosis. *The Journal of Cell Biology*, **144(5)**, 891-901.

Deutsch, D.G. and Chin, S.A. (1993) Enzymatic synthesis and degradation of anandamide, a cannabinoid receptor agonist. *Biochemical Pharmacology*, **46(5)**, 791-796.

Devane, W.A., Dysarz, A., Johnson, M.R., Melvin, L.S. and Howlett, A. (1988) Determination and chacterisation of a cannabinoid receptor in rat brain. *Molecular Pharmacology*, **34**, 605-613.

Devane, W.A., Hanus, L., Breuer, A., Pertwee, R.G., Stevenson, L.A., Griff, C., Gibson, D., Mandelbaum, A., Etinger, A. and Mechoulam, R. (1992) Isolation and structure of a brain constituent that binds to the cannabinoid receptor. *Science,* **258**, 1946-1949.

Di Marzo, V., Fontana, A., Cadas, H., Schinell, S., Clmlno, G., Schwartz, J. and Plomell, D. (1994) Formaton and inactivation of endogenous cannabinoid anandamide in central neurones. *Nature,* **372**, 686-691.

Di Marzo, V., Melck, D., Bisogno, T. and De Petrocellis, L. (1998) Endocannabinoids: endogenous cannabinoid receptor ligands with neuromodulatory action. *Trends in Neuroscience,* **21(12)**, 521-528.

Dickens, M., Rogers, J. S., Cavanagh, J., Raitano, A., Xia, Z., Halpern, J. R., Greenberg, M. E., Sawyers, C. L. and Davis, R. J. (1997) A cytoplasmic inhibitor of the JNK signal transduction pathway. *Science,* **277**, 693-696.

Dill, J.A. and Howlett, A.C. (1988) Regulation of adenylate cyclase by chronic exposure to cannabimimetic drugs. *Journal of Pharmacology and Experimental Therapeutics,* **244(3)**, 1157-1163.

Ditaranto-Desimone, K., Saito, M., Tekirian, T. L., Saito, M., Berg, M., Dubowchik, G. M., Soreghan, B., Thomas, S., Marks, N. and Yang, A. J. (2003) Neuronal endosomal/lysosomal membrane destabilization activates caspases and induces abnormal accumulation of the lipid secondary messenger ceramide. *Brain Research Bulletin,* **59**, 523-531.

Do, Y., McKallip, R.J., Nagarkatti, M. and Nagarkatti, P.S. (2004) Activation through cannabinoid receptors 1 and 2 on dendritic cells triggers NF-κB-dependent apoptosis: Novel role for endogenous and exogenous cannabinoids in immunoregulation. *The Journal of Immunology*, **173(4)**, 2373-2382.

Dumaz, N. and Meek, D.W. (1999) Serine 15 phosphorylation stimulates p53 transactivation but does not directly influence intreaction with HDM2. *European Molecular Biology Organization Journal,* **14**, 7002-7010.

Ehrenreich, H., Rinn, T., Kunter, H.J., Moeller, M.R., Poser, W. and Schilling, L. (1999) Specific attentional dysfunction in adults following early start of cannabis use. *Psychopharmacology*, **142**, 295-301.

Elkeles, A., Juven-Gershon, T., Israeli, D., Wilder, S., Zalcenstein, A. and Oren, M. (1999) The c-fos proto-oncogene is a target for transactivation by the p53 tumor suppressor. *Molecular Cell Biology*, **19(4)**, 2594-2600.

Enari, M., Sakahira, H., Yokoyama, H., Okawa, K., Iwamatsu, A. and Nagata, S. (1998) A caspase-activated DNase that degrades DNA during apoptosis, and its inhibitor ICAD. *Nature*, **391**, 43-50.

Enokido, Y., Araki, T., Tanaka, K., Aizawa, S. and Hatanaka, H. (1996) Involvement of p53 in DNA strand break-induced apoptosis in postmitotic CNS neurons. *European Journal of Neuroscience,* **8**, 1812-1821.

Erlandsson, N., Baumann, B., Rossler, O.G., Kaufmann, K., Giehl, K.M., Wirth, T. and Thiel, G. (2002) Lack of correlation between NF-κB activation and induction of programmed cell death in PC12 pheochromocytoma cells treated with 6-hydroxydopamine or the cannabinoid receptor 1-agonist CP55,940. *Behavioural Pharmacology*, **64**, 487-495.

Eshhar, N., Streim, S. and Biegon, A. (1993) HU-211, a non-psychotropic cannabinoid, rescues cortrical neurones from excitatory amino acid toxicity in culture. *NeuroReport*, **5**, 237-240.

Eskes, R., Antonsson, B., Osen-Sand, A., Montessuit, S., Richter, C., Sadoul, R., Mazzei, G., Nichols, A. and Martinou, J. (1998) Bax-induced cytochrome *c* release from mitochondria is dependent on the permeability transition pore but highly dependent on mg^{2+} ions. *The Journal of Cell Biology,* **143(1)**, 217-224.

Evan, G.E., Brown, L., Whyte, M. and Harrington, E. (1995) Apoptosis and the cell cycle. *Current Opinion in Cell Biology*, **7**, 825-834.

Evan, G. and Littlewood, T. (1998) A matter of life and cell death. *Science,* **281**, 1317-1322.

Facchinetti, F., del Giudice, E., Furegato, S., Passarotto, M. and Leon, A. (2003) Cannabinoids ablate release of TNF-α in rat microglial cells stimulated with lypopolysaccharide. *Glia*, **41**, 161-168.

Farkas, I., Baranyi, L., Takahashi, M., Fukuda, A., Liposits, Zs., Yamamoto, T. and Okada, H. (1998) A neuronal C5a receptor and an associated apoptotic signal transduction pathway. *Journal of Physiology,* **507(3)**, 679-687.

Fehr, K.A., Kalant, H. and LeBlanc, A.E. (1976) Residual learning deficit after heavy exposure to cannabis or alcohol in rats. *Science*, **192**, 1249-1251.

Felder, C.C., Briley, E.M., Axelrod, J., Simpson, J.T., Mackie, K. and Devane, W.A. (1993) Anandamide, an endogenous cannabimimetic eicosanoid, binds to the cloned human cannabinoid receptor and stimulates receptor-mediated signal transduction. *Proceedings of the National Academy of Science USA*, **90**, 7656-7660.

Felder, C.C., Joyce, K.E., Briley, E.M., Mansouri, J., Mackie, K., Blonde, O., Lai, Y., Ma, A.L., and Mitchell, R.L. (1995) Comparison of the pharmacology and signal transduction of the human cannabinoid CB1 and CB2 receptors. *Molecular Pharmacology,* **48**, 443-450.

Fernández-Ruiz, J.J., Rodriguez de Fonseca, F., Navarro, M. and Ramos, J.A. (1992) Maternal cannabinoid exposure and brain development: changes in the ontogeny of dopaminergic neurons. In: Marihuana/Cannabinoids: Neurobiology and neurophysiology. CRC Press, pp. 119-164.

Fernández-Ruiz, J.J., Bonnin, A., Cebeira, M. and Ramos, J.A. (1994) Ontogenic and adult changes in the activity of the hypothalamic and extrahypothalamic dopaminergic neurons after perinatal cannabinoid exposure. In: Strategies for studying brain disorders. Farrand Press, pp. 357-390.

Fernández-Ruiz, J.J., Romero, J., Garcia-Gil, L., Garcia-Palomero, E. and Ramos, J.A. (1996) Dopaminergic neurons as neurochemical substrates of neurobehavioural effects of marihuana: developmental and adult studies. In: Dopamine Disease States. CYM Press, pp. 359-387.

Fernández-Ruiz, J.J., Berrendero, F., Hernandez, M.L., Romero, J. and Ramos, J.A. (1999) Role of endocannabinoids in brain development. *Life Sciences,* **65(6-7)**, 725-736.

Fernández-Ruiz, J., Berrendero, F., Hernandez, M.L. and Ramos, J.A. (2000) The endogenous cannabinoid system and brain development. *Trends in Neuroscience,* **23**, 14-20.

Fligiel, S.E.G., Roth, M.D., Kleerup, E.C., Barsky, S.H., Simmons, M.S. and Tashkin, D.P. (1997) Tracheobronchial histopathology in habitual smokers of cocaine, marijuana, and/or tobacco. *Chest*, **112**, 319-326.

Fogarty, M.P., Downer, E.J. and Campbell, V. (2003) A role for c-Jun N-terminal kinase 1 (JNK1), but not JNK2, in the β-amyloid-mediated stabilization of protein p53 and induction of the apoptotic cascade in cultured cortical neurons. *Biochemical Journal*, **371**, 789-798.

French, E.D. (1997) Δ^9-Tetrahydrocannabinol excites rat VTA dopamine neurons through activation of cannabinoid CB1 but not opioid receptors. *Neuroscience Letters*, **226**, 159-162.

Fried, P.A. (1982) Marihuana use by pregnant women and effects on offspring: an update. *Neurobehavioural Toxicology and Teratology*, **4**, 451-454.

Fried, P.A. and Watkinson, B. (1990) 36- and 48-month neurobehavioural follow-up of children prenatally exposed to marijuana, cigarettes and alcohol. *Journal of Developmental Behaviour and Pediatrics*, **11**, 49-58.

Fried, P.A. (1995) The ottawa prenatal prospective study (OPPS): methodological issues and findings - Its easy to throw the baby out with the bath water. *Life Sciences,* **56(24-27)**, 2159-2168.

Fried, P.A., Watkinson, R. and Gray, R. (1999) Growth from birth to early adolescence in offspring prenatally exposed to cigarettes and marijuana. *Neurotoxicology Teratology*, **21(5)**, 513-525.

Fried, P.A. and Smith, A.M. (2001) A literature review of the consequences of prenatal marihuana exposure. An emerging theme of a deficiency in aspects of executive function. *Neurotoxicology and Teratology*, **23**, 1-11.

Galiegue, S., Mary, S., Marchand, D., Dussossoy, D., Carriere, D., Carayon, P., Bouaboula, M., Shire, D., Le Fur, G. and Casellas, P. (1995) Expression of central and peripheral cannabinoid receptors in human immune tissues and leukocyte subpopulations. *European Journal of Biochemistry*, **232**, 54-61.

Gallily, R., Breuer, A. and Mechoulam, R. (2000) 2-arachidonylglycerol, an endogenous cannabinoid, inhibits tumour necrosis factor-alpha production in murine macrophages, and in mice. *European Journal of Pharmacology*, **406**, R5-R7.

Gallily, R., Even-Chena, T., Katzavian, G., Lehmann, D., Dagan, A. and Mechoulam, R. (2003) Gamma-irradiation enhances apoptosis induced by cannabidiol, a non-psychotropic cannabinoid, in cultured HL-60 myeloblastic leukemia cells. *Leukemia Lymphoma*, **44(10)**, 1767-1773.

Galve-Roperh, I., Sánchez, C., Luisa Cortes, M., Gómez del Pulgar, T., Izquierdo, M. and Guzmán, M. (2000) Anti-tumoral action of cannabinoids: Involvement of sustained ceramide accumulation and extracellular signal-regulated kinase activation. *Nature Medicine,* **6(3)**, 313-319.

Galve-Roperh, I., Rueda, D., Gómez del Pulgar, T., Velasco, G. and Guzmán, M. (2002) Mechanism of extracellular signal-regulated kinase activation by the CB_1 cannabinoid receptor. *Molecular Pharmacology,* **62**, 1385-1392.

Gao, G. and Dou, Q. P. (2000) N-terminal cleavage of bax by calpain generates a potent proapoptotic 18-kDa fragment that promotes bcl-2-independent cytochrome C release and apoptotic cell death. *Journal of Cellular Biochemistry,* **80**, 53-72.

Gaoni, Y. and Mechoulam, R. (1964) Isolation, structure, and partial synthesis of an active constituent of hashish. *Journal of the American Chemical Society,* **86**, 1646-1647.

Garcia-Gil, L., Ramos, J.A., Rubino, T., Parolaro, D. and Fernández-Ruiz, J.J. (1998) Perinatal Δ^9-Tetrahydrocannabinol exposure did not alter dopamine transporter and tyrosine hydroxylase mRNA levels in midbrain dopaminergic neurons of adult male and female rats. *Neurotoxicology and Teratology*, **20(5)**, 549-553.

Garcia-Gil, L., de Miguel, R., Romero, J., Perez, A., Ramos, J.A. and Fernández-Ruiz, J.J. (1999a) Perinatal Δ^9-Tetrahydrocannabinol exposure augmented the magnitude of motor inhibition caused by $GABA_B$, but not $GABA_A$, receptor agonists in adult rats. *Neurotoxicology and Teratology*, **21(3)**, 277-283.

Garcia-Gil, L., Romero, J., Ramos, J.A. and Fernández-Ruiz, J.J. (1999b) Cannabinoid receptor binding and levels in several brain regions of adult male and female rats perinatally exposed to delta-9-tetrahydrocannabinol. *Drug and Alcohol Dependency*, **55(1-2)**, 127-136.

Gatley, S.J., Gifford, A.N., Volkow, N.D., Lan, R. and Makriyannis, A. (1996) ^{123}I-labeled AM251: a radioiodinated ligand which binds *in vivo* to mouse brain cannabinoid CB_1 receptors. *European Journal of Pharmacology,* **307**, 331-338.

Gérard, C.M., Mollereau, C., Vassart, G. and Parmentier, M. (1991) Molecular cloning of a human cannabinoid receptor which is also expressed in testis. *Biochemical Journal,* **279**, 129-134.

Gerschenson, L.E. and Rotello, R.J. (1992) Apoptosis: A different type of cell death. *FASEB*, **6**, 2450-2455.

Gessa, G.L., Casu, M.A., Carta, G. and Mascia M.S. (1998) Cannabinoids decrease acetylcholine release in the medial-prefrontal cortex and hippocampus, reversal by SR 141716A. *European. Journal of Pharmacology,* **355**, 119-124.

Ghahremani, M.H., Keramaris, E., Shree, T., Xia, Z., Davis, R.J., Flavell, R., Slack, R.S. and Park, D.S. (2002) Interaction of the c-Jun/JNK pathway and cyclin-dependent kinase in death of embryonic cortical neurones evoked by DNA damage. *Journal of Biological Chemistry,* **277(38)**, 35586-35596.

Giasson, B.I. and Mushynski, W.E. (1997) Study of proline-directed protein kinases involved in phosphoryaltion of the heavy neurofilament subunit. *Journal of Neuroscience*, **17**, 9466-9472.

Giroud, C., Menetrey, A., Augsburger, M., Buclin, T., Sanchez-Mazas, P. and Mangin, P. (2001) Δ^9-THC, 11-OH-Δ^9-THC and Δ^9-THCCOOH plasma or serum to whole blood concentration distribution ratios in blood samples taken from living and dead people. *Forensic Science International*, **123**, 159-164.

Glass, M., Dragunow, M. and Faull, R.L. (1997) Cannabinoid receptors in the human brain: a detailed anatomical and quantitative autoradiographic study in the fetal, neonatal and adult human brain. *Neuroscience,* **77**, 299-318.

Godlewski, M.M., Motyl, M.A., Gajkowska, B., Wareski, P., Koronkiewicz, M. and Motyl, T. (2001) Subcellular redistribution of BAX during apoptosis induced by anticancer drugs. *Anticancer Drugs*, **12(7)**, 607-617.

Gómez del Pulgar, T., de Ceballos, M.L., Guzmán, M. and Velasco, G. (2000a) Cannabinoids protect astrocytes from ceramide-induced apoptosis through the phosphatidylinositol 3-kinase/Protein Kinse B pathway. *The Journal of Biological Chemistry*, **277(39)**, 36527-36533.

Gómez del Pulgar, T., Velasco, G. and Guzmán, M. (2000b) The CB_1 cannabinoid receptor is coupled to the activation of protein kinase B/Akt. *Biochemical Journal,* **347**, 369-373.

Gómez del Pulgar, T., Velasco, G., Sánchez, C., Haro, A. and Guzmán, M. (2002) *De novo*-synthesized ceramide is involved in cannabinoid-induced apoptosis. *Biochemical Journal,* **363**, 183-186.

Goping, I.S., Gross, A., Lavoie, J.N., Nguyen, M., Jemmerson, R., Roth, K., Korsmeyer, S.J. and Shore, G. (1998) Regulated targeting of BAX to mitochondria. *The Journal of Cell Biology*, **143(1)**, 207-215.

Grewal, S.S., York, R.D. and Stork, P.J.S. (1999) Extracellular-signal-regulated kinase signalling in neurons. *Current Opinions in Neurobiology*, **9**, 544-553.

Griffin, G., Tao, Q. and Abood, M.E. (2000) Cloning and pharmacological characterization of the rat CB(2) receptor. *Journal of Pharmacology and Experimental Therapeutics,* **292**, 886-894.

Griffith, D.R., Azuma, S.D. and Chasnoff, I.J. (1994) Three-year outcome of children exposed prenatally to drugs. *Journal of the American Academy of Child Adolescents Psychiatry*, **33**, 20-27.

Grinspoon, L. and Bakalar, J.B. (1995) Marihuana as Medicine: A Plea for Reconsideration. *Journal of the American Medical Association,* **273(23)**, 1875-1876.

Gross, A., Jockel, J., Wei, M.C. and Korsmeyer, S.J. (1998) Enforced dimerization of BAX results in its translocation, mitochondrial dysfunction and apoptosis. *European Molecular Biology Organization Journal,* **17(14)**, 3878-3885.

Gruen, R.J., Deutch, A.Y. and Roth, R.H. (1990) Perinatal diazepam exposure: alterations in exploratory behavior and mesolimbic dopamine turnover. *Pharmacology Biochemistry and Behaviour*, **36**, 169-175.

Gupta, S., Campbell, D., Derijard, B. and Davis, R. (1995) Transcription factor ATF2 regulation by the JNK signal transduction pathway. *Science,* **267**, 389-393.

Gupta, S., Barrett, T., Whitmarsh, A. J., Cavanagh, J., Sluss, H. K., Derijard, B. and Davis, R. J. (1996) Selective interaction of JNK protein kinase isoforms and transcription factors. *European Molecular Biology Organization Journal,* **15**, 2760-2770.

Guzmán, M., Sánchez, C. and Galve-Roperh, I. (2002) Cannabinoids and cell fate. *Pharmacology and Therapeutics*, **95**, 175-184.

Guzmán, M. (2003) Cannabinoids: potential anticancer agents. *Nat Rev Cancer*, **3(10)**, 745-755.

Hampson, A.J., Grimaldi, M., Axelrod, J. and Wink, D. (1998) Cannabidiol and (-)Δ^9-tetrahydrocannabinol are neuroprotective antioxidants. *Proceedings of the National Academy of Science USA*, **95**, 8268-8273.

Hampson, A.J. and Grimaldi, M. (2001) Cannabinoid receptor activation and elevated cyclic AMP reduce glutamate neurotoxicity. *Europoean Journal of Neuroscience*, **13**, 1529-1536.

Hampson, R.E. and Deadwyler, S.A. (1999) Cannabinoids, hippocampal function and memory. *Life Sciences*, **65(6/7)**, 715-723.

Hansen, H.H., Ikonomidou, C., Bittigau, P., Hansen, S.H. and Hansen, H.S. (2001a) Accumulation of the anandamide precursor and other *N*-acylethanolamine phospholipids in infant rat models of *in vivo* necrotic and apoptotic neuronal death. *Journal of Neurochemistry*, **76**, 39-46.

Hansen, H.H., Schmid, P.C., Bittigau, P., Lastres-Becker, I., Berrendero, F., Manzanares, J., Ikonomidou, C., Scmid, H.H.O., Fernandez-Ruiz, J.J. and Hansen, H.S. (2001b) Anandamide, but not 2-arachidonoylglycerol, accumulates during *in vivo* neurodegeneration. *Journal of Neurochemistry*, **78**, 1415-1427.

Hanus, L., Gopher, A., Almog, S. and Mechoulam, R. (1993) Two new unsaturated fatty acid ethanolamides in bain that bind to the cannabinoid receptor. *Journal of Medicinal Chemistry*, **36**, 3032-3034.

Harris, C.A. and Johnson, E.M. (2001) BH3-only Bcl-2 family members are coordinately regulated by the JNK pathway and require Bax to induce apoptosis in neurons. *The Journal of Biological Chemistry*, **276(41)**, 37754-37760.

Hart, S., Fischer, O.M. and Ullrich, A. (2004) Cannabinoids induce cancer cell proliferation via tumor necrosis factor α-converting enzyme (TACE.ADAM17)-mediated transactivation of epidermal growth factor receptor. *Cancer Research*, **64**, 1943-1950.

Hatai, T., Matsuzawai, A., Inoshita, S., Mochhida, Y., Kuroda, T., Sakamaki, K., Kuida, K., Yonehara, S., Ichijo, H. and Takeda, K. (2000) Execution of Apoptosis Signal-regulating Kinase 1 (ASK1)-induced apoptosis by mitochondria-dependent caspase activation. *The Journal of Biological Chemistry,* **275(34)**, 26576-26581.

Herdegen, T., Skene, P. and Bähr, M. (1997) The c-Jun transcription factor-bipotential mediator of neuronal cell death, survival and regeneration. *Trends in Neuroscience,* **20**, 227-231.

Herkenham, M., Lynn, A.B., Johnson, M.R., Melvin, L.S., de Costa, B.R. and Rice, K.C. (1991) Characterization and localization of cannabinoid receptors in rat brain: A quantitative in vitro autoradiographic study. *Journal of Neuroscience*, **11**, 563-583.

Herlarr, E. and Brown, Z. (1999) p38 MAPK signaling cascades in inflammatory disease. *Molecular Medicine Today*, **5**, 439-447.

Herr, I. and Debatin, K. M. (2001) Cellular stress response and apoptosis in cancer therapy. *Blood,* **98**, 2603-2614.

Herring, A.C. and Kaminski, N.E. (1999) Cannabinoid-mediated inhibition of nuclear factor-κB, cAMP response element-binding protein, and interleukin-2 secretion by activated thymocytes. *Journal of Pharmacology and Experimental Therapeutics*, **291**, 1156-1163.

Heyser, C.J., Hampson, R.E. and Deadwyler, S.A. (1993) Effects of Delta-9-Tetrahydrocannabinol on delayed match to sample performance in rats: alterations in short-term memory associated with changes in task specific firing of hippocampal cells. *The Journal of Pharmacology and Experimental Therapeutics*, **264(1)**, 294-306.

Hillard, C.J. (2000) Biochemistry and pharmacology of the endocannabinoids arachidonylethanolamide and 2-arachidonylglycerol. *Prostaglandins Other Lipid Mediators*, **61(1-2)**, 3-18.

Hochedlinger, K., Wagner, E. F. and Sabapathy, K. (2002) Differential effects of JNK1 and JNK2 on signal specific induction of apoptosis. *Oncogene,* **21**, 2441-2445.

Hoffman, K. (1999) The modular nature of apoptotic signaling proteins. *Cellular and Molecular Life Sciences*, **55**, 1113-1128.

Hollister, L.E. (1986) Health aspects of cannabis. *Pharmacology Review*, **38**, 1-20.

Howlett, A.C. and Fleming, R.M. (1984) Cannabinoid inhibition of adenylate cyclase. Pharmacology of the response in neuroblastoma cell membranes. *Molecular Pharmacology*, **29**, 532-538.

Howlett, A., Qualy, J. and Khachatrain, L. (1986) Involvement of G_i in the inhibition of adenylate cyclase by cannabinoid drugs. *Molecular Pharmacology,* **29**, 307-313.

Howlett, A.C. (1995) Pharmacology of cannabinoid receptors. *Annual Review of Pharmacological Toxicology,* **35**, 607-634.

Hreniuk, D., Garay, M., Gaarde, W., Monia, B., McKay, R. and Cioffi, C. L. (2001) Inhibition of c-Jun N-terminal kinase 1, but not c-Jun N-terminal kinase 2, suppresses apoptosis induced by ischemia/reoxygenation in rat cardiac myocytes. *Molecular Pharmacology,* **59**, 867-874.

Hu, M.C., Qui, W.R. and Wang, Y.P. (1997) JNK1, JNK2 and JNK3 are p53 N-terminal serine 34 kinases. *Oncogene*, **15**, 2277-2287.

Huestis, M.A., Sampson, A.H., Holicky, B.J., Henningfield, J.E. and Cone, E.J. (1992) Characterization of the absorption phase of marijuana smoking. *Clinical Pharmacology and Therapeutics*, **52(1)**, 31-41.

Huestis, M.A. and Cone, R.E. (1998) Urinary excretion half-life of 11-Nor-9-carboxy-Δ9-tetrahydrocannabinol in humans. *Therapeutic Drug Monitoring*, **20**, 570-576.

Huestis, M.A. and Choo, R.E. (2002) Drug abuse's smallest victims: in utero drug exposure. *Forensic Science International*, **128**, 20-30.

Hutchings, D.E. and Fitter, W.P. (1986) Neurobehavioural effects in human ad animal offspring following prenatal exposure to methadone. In: Handbook of Behavioural Teratology. Plenum Press, pp. 141.

Hutchings, D.E. (1990) Issues of risk assessment: lessons from the use and abuse of drugs during pregnancy. *Neurotoxicology Teratology*, **12(3)**, 183-189.

Inamaura, N., Enokido, Y. and Hatanaka, H. (2001) Involvement of c-jun N-terminal kinase and caspase-3-like protease in DNA damage-induced, p53-mediated apoptosis of cultured mouse cerebellar granule neurons. *Brain Research*, **904**, 270-278.

Ip, Y.T. and Davis, R.J. (1998) Signal transduction by the c-Jun N-terminal kinase (JNK) - from inflammation to development. *Current Opinion in Cellular Biology,* **10**, 205-219.

Ishac, E.J., Jiang, L., Lake, K.D., Varga, K., Abood, M.E. and Kunos, G. (1996) Inhibition of exocitotic noradrenaline release by presynaptic cannabinoid CB1 receptors on peripheral sympathetic nerves. *British Journal of Pharmacology*, **118**, 2023-2028.

Ishisaka, R., Utsumi, T., Kanno, T., Arita, K., Katunuma, N., Akiyama, J. and Utsumi, K. (1999) Participation of a cathepsin L-type protease in the activation of caspase-3. *Cell Structure and Function,* **24**, 465-470.

Ito, Y., Mishra, N. C., Yoshida, K., Kharbanda, S., Saxena, S. and D., K. (2001) Mitochondrial targeting of JNK/SAPK in the phorbol ester response of myeloid leukemia cells. *Cell Death and Differentiation,* **8**, 794-800.

Iuvone, T., Esposito, G., Esposito, R., Santamaria, R., Di Rosa, M. and Izzo, A.A. (2004) Neuroprotective effect of cannabidiol, a non-psychoactive component from *Cannabis sativa*, on β-amyloid-induced toxicity in PC12 cells. *Journal of Neurochemistry*, **89**, 134-141.

Iversen, L.L. (2000) Consumption of cannabis preparations for their psychoactive effects. In: The science of marijuana. Oxford University Press, pp. 14-17.

Jacobsson, S.O.P., Rongard, E., Stridh, M., Tiger, G. and Fowler, C.J. (2000) Serum-dependent effects of tamoxifen and cannabinoids upon C6 glioma cell viability. *Biochemical Pharmacology*, **69**, 1807-1813.

Jakob, R. and Kreiglsten, J. (1997) Influence of flupirtine on a G-protein coupled inwardly rectifying potassium current in hippocampal neurones. *British Journal of Pharmacology,* **122(7)**, 1333-1338.

Jakubovic, A., Hattori, T. and McGeer, P.L. (1973) Radioactivity in suckled rats after giving ^{14}C-tetrahydrocannabinol to the mother. *European Journal of Pharmacology*, **22**, 221-223.

Janicke, R.U., Sprengart, M.L., Wati, M.R. and Porter, A.G. (1998) Caspase-3 is required for DNA fragmentation and morphological changes associated with apoptosis. *The Journal of Biological Chemistry,* **273(16)**, 9357-9360.

Jayaraman, J.L. and Prives, C. (1995) Activation of p53 sequence-specific DNA binding by short single strands of DNA requires the p53 C-terminus. *Cell*, **81**, 1021-1029.

Jentsch, J.D., Verrico, C.D., Le, D. and Roth, R.H. (1998) Repeated exposure to Δ^9-Tetrahydrocannabinol reduces prefrontal cortical dopamine metabolism in the rat. *Neuroscience Letters,* **246**, 169-172.

Jiang, X. (2005) Random mutagenesis of B'A' core domain of yeast DNA topoisomerase II and large-scale screens of mutants resistant to the anticancer drug etoposide. *Biochemical and Biophysical Research Communications*, **327**, 597-603.

Johansson, E., Noren, K., Sjovall, J. and Halldin, M.M. (1989) Determination of delta-1-tetrahydrocannabinol in human fat biopsies from marihuana users by gas chromatography-mass spectrometry. *Biomedical Chromatography*, **3**, 35-38.

Johnson, N.L., Gardner, A.M., Diener, K.M., Lange-Carter, C.A., Gleavy, J., Jarpe, M.B., Minden, A., Karin, M., Zon, L.I. and Johnson, G.L. (1996) Signal transduction pathways regulated by mitogen-activated/extracellular response kinase kinase kinase induce cell death. *The Journal of Biological Chemistry,* **271(6)**, 3229-3237.

Johnson, T. M., Yu, Z. X., Ferrans, V. J., Lownstein, R. A. and Finkel, T. (1997) Reaction oxgen species are downstream mediators of p53-dependent apoptosis. *Proceedings of the National Acadamey of Sciences USA,* **93**, 11848-11852.

Jordan, J., Galindo, M. F., Prehn, J. H., Weichselbaum, R. R., Beckett, M., Ghadge, G. D., Roos, R. P., Leiden, J. M. and Miller, R. J. (1997) p53 expression induces apoptosis in hippocampal pyramidal neuron cultures. *Journal of Neuroscience,* **17**, 1397-1405.

Kang, C.-D., Jang, J.-H., Kim, K.-W., Lee, H.-J., Jeong, C.-S., Kim, C.-M., Kim, S.-H. and Chung, B.-S. (1998) Activation of c-Jun N-terminal kinase/stress-activated protein kinase and the decreased ratio of Bcl-2 to Bax are associated with the auto-oxidized dopamine-induced apoptosis in PC12 cells. *Neuroscience Letters,* **256**, 37-40.

Karpinich, N. O., Tafani, M., Rothman, R. J., Russo, M. A. and Farber, J. L. (2002) The course of etoposide-induced apoptosis from damage to DNA and p53 activation to mitochondrial release of cytochrome *c*. *The Journal of Biological Chemistry,* **277,** 16547-16552.

Kaslow, H.R., Lim, L.K., Moss, J. and Lesikar, D.D. (1987) Structure-activity analysis of the activation of pertussis toxin. *Biochemistry*, **26(1)**, 123-127.

Kassiotis, G., Bauer, J., Akassoglou, K., Lassmann, H., Kollias, G. and Probert, L. (1999) A tumour necrosis factor-induced model of human primary demyelinating diseases develops in immunodeficient mice. *European Journal of Immunology*, **29**, 912-917.

Kastan, M. (1997) On the TRAIL from p53 to apoptosis? *Nature Genetics*, **17(2)**,130-131.

Katzung, B.G. (2001) Marijuana. In: Basic and clinical pharmacology. Lange Medical Books/McGraw-Hill Medical Publishing Division, pp. 542-544.

Kaufmann, S.R., Desnoyers, S., Ottaviano, Y., Davidson, N.E. and Poirier, G.G. (1993) Specific proteolytic cleavage of poly(ADP-ribose) polymerase: An early marker of chemotherapy-induced apoptosis. *Cancer Research,* **53**, 3976-3985.

Kerr, J., Wyllie, A. H. and Currie, A. R. (1972) Apoptosis: a basic biological phenomenon with wide-ranging implications in tissue kinetics. *British Journal of Cancer,* **26**, 239-257.

Kerr, J.F.R. and Harmon, B.V. (1991) Definition and incidence of apoptosis: An historical perspective. In: Apoptosis: the molecular basis of cell death. Cold Spring Harbour Laboratory Press, pp. 5-29.

Kim, D. and Thayer, S.A. (2001) Cannabinoids inhibit the formation of new synapses between hippocampal neurons in culture. *The Journal of Neuroscience*, **21**, 1-5.

Kim, H.J., Mun, J.Y., Chun, Y.J., Choi, K.H. and Kim, M.Y. (2001) Bax-dependent apoptosis induced by ceramide in HL-60 cells. *FEBS Letters*, **505**, 264-268.

Kim, J-.E., Oh, J.H., Choi, W-.S., Chang, I.I., Sohn, S., Krajewski, S., Reed, J.C., O'Malley, K.L. and Oh, Y.J. (1999) Sequential cleavage of ploy(ADP-ribose)polymerase and appearance of a small Bax-immunoreactive protein are blocked by Bcl-X_L and caspase inhibitors during staurosporine-induced dopaminergic neuronal apoptosis. *Journal of Neurochemistry*, **72(6)**, 2456-2463.

Klein, T.W., Friedman, H. and Specter, S. (1998) Marijuana, immunity and infection. *Journal of Immunology*, **83**, 102-115.

Kobayashi, Y., Arai, S., Waku, K. and Sugiura, T. (2001) Activation of 2-Arachidonylglycerol, and endogenous cannabinoid receptor ligand, of p42/44 mitogen-activated protein kinase in HL-60 cells. *Journal of Biochemistry* **129**, 665-669.

Kobayashi, K and Tsukamoto, I. (2001) Prolonged Jun N-terminal kinase (JNK) activation and the upregulation of p53 and $p21^{WAF1/CIP1}$ preceded apoptosis in hepatocytes after partial hepatectomy and cisplatin. *Biochimic et Biophysica Acta*, **1537**, 79-88.

Koga, D., Santa, T., Fukushima, T., Homma, H. and Imai, K. (1997) Liquid chromatographic-atmospheric pressure chemical ionization mass spectrometric determination of anandamide and its analogs in rat brain and peripheral tissues. *Journal of Chromatographic and Biomedical Science Applications*, **690**, 7-13.

Korsmeyer, S. J. (1995) Regulators of cell death. *Trends in Genetics,* **11**, 101-105.

Korsmeyer, S. (1999) BCL-2 gene family and the regulation of programmed cell death. *Journal of Cancer Research,* **59**, 1693-1700.

Kroemer, G., Zamzami, N. and Susin, S. (1997) Mitochondrial conrol of apoptosis. *Immunology Today,* **18**, 44-51.

Kuan, C. Y., Yang, D. D., Samanta Roy, D. R., Davis, R. J., Rakic, P. and Flavell, R. A. (1999) The Jnk1 and Jnk2 protein kinases are required for regional specific apoptosis during early brain development. *Neuron,* **22**, 667-676.

Kumar, A.M., Haney, M., Becker, T., Thompson, M.L., Kream, R.M. and Miczek, K. (1990) Effect of early exposure on Δ^9-tetrahydrocannabinol on the levels of opioid peptides, gonadotropin-releasing hormone and substance P in the adult male rat brain. *Brain Research*, **525**, 78-83.

Lan, R., Liu, Q., Fan, P. (1999) Structure-activity relationships of pyrazole derivatives as cannabinoid receptor antagonists. *Journal of Medicinal Chemistry*, **42**, 769-776.

Landsman, R.S., Burkey, T.H., Consroe, P., Roeske, W.R. and Yamamura, H.I. (1997) SR141716A is an inverse agonist at the human cannabinoid CB1 receptor. *European Journal of Pharmacology*, **334**, R1-R2.

Lautier, D., Lagueux, J., Thibodeau, J., Menard, L. and Poirier, G.G. (1993) Molecular and biochemical features of poly (ADP-ribose) metabolism. *Molecular Cell Biochemistry*, **122**, 171-193.

Lawston, J., Borella, A., Robinson, J.K. and Whitaker-Azmitia, P.M. (2000) Changes in hippocampal morphology following chronic treatment with the synthetic cannabinoid WIN 55,212-2. *Brain Research*, **877**, 407-410.

Lazebnik, Y.A., Kaufmann, S.H., Desnoyers, S., Poirier, G.G. and Earnshaw, W.C. (1994) Cleavage of poly(AP-ribose) polymerase by a proteinase wih properties of ICE. *Nature*, **371**, 346-347.

Lee, S., Christakos, S. and Small, M.B. (1993) Apoptosis and signal transduction: clues to a molecular mechanism. *Current Opinion in Cell Biology,* **5**, 286-291.

Lei, K., Nimual, A., Zong, W.X., Kennedy, N.J., Flavell, R.A., Thompson, C.B., Bar-Sagi, D. and Davis, R.J. (2002) The Bax subfamily of Bcl2-related proteins is essential for apoptotic signal transduction by c-Jun NH(2)-terminal kinase. *Molecular Cell Biology,* **22(13)**, 4929-4942.

Lemberger, L. (1999) Nabilone: a synthetic cannabinoid of medicinal value. In: Marihuana and Medicine. Totowa: Humana Press, pp. 561-566.

Lester, B. and Dreher, M. (1989) Effects of marijuana use during pregnancy on newborn cry. *Child Development*, **60**, 765-771.

Levenes, C., Daniel, H., Soubrie, P. and Crepel, F. (1998) Cannabinoids decrease excitatory synaptic transmission and impair long-term depression in rat cerebellar Purkinje cells. *Journal of Physiology*, **510**, 867-879.

Levine, A. (1997) p53 the cellular gatekeeper for growth and division. *Cell,* **88,** 323-331.

Lezak, M.D. (1995) Neuropsychological assessment. Oxford University Press, pp, 650-685.

Li, P., Nijhawan, D., Budihardjo, I., Srinivasula, S. M., Ahmad, M., Alnemri, E. S. and Wang, X. (1997) Cytochrome c and dATP-dependent formation of Apaf-1/caspase-9 complex initiates an apoptotic protease cascade. *Cell,* **91**, 479-489.

Lichtman, A.H., Dimen, K.R. and Martin, B.R. (1995) Systemic or intrahippocampal cannabinoid administration impairs spatial memory in rats. *Psychopharmacology*, **119**, 282-290.

Lichtman, A.H. and Martin, B.R. (1997) The selective cannabinoid antagonist SR141716A blocks cannabinoid-induced antinociception in rats. *Pharmacology Biochemistry and Behaviour*, **57(1/2)**, 7-12.

Liu, X., Kim, C.N., Yang, J., Jemmerson, R. and Wang, X. (1996) Induction of apoptotic program in cell-free extracts: requirement of dATP and cytochrome *c*. *Cell,* **86**, 147-157.

Lo, A.C., Houenou, L.J. and Oppenheim, R.W. (1995) Apoptosis in the nervous system: morphological features, methods, pathology, and prevention. *Histological Cytology*, **58(2)**, 139-149.

Louw, D.F., Yang, F.W. and Sutherland, G.R. (2000) The effect of δ–9-tetrahydrocannabinol on forebrain ischemia in rat. *Brain Research*, **857**, 183-187.

Lukas, S.E. and Orozco, S. (2001) Ethanol increases plasma delta(9)-tetrahydrocannabinol (THC) levels and subjective effects after marihuana smoking in human volunteers. *Drug Alcohol Dependency*, **64(2)**, 143-149.

Maccarrone, M., Lorenzon, T., Bari, M., Melino, G. and Finazzi-Agro, A. (2000) Anandamide induces apoptosis in human cells via vanilloid receptors. *The Jounal of Bilogical Chemistry*, **275**, 31938-31945.

Mackie, K., Lai, Y., Westenbroek, R. and Mitchell, R. (1995) Cannabinoids activate an inwardly rectifying potassium conductance and inhibit Q-type currents in AtT20 cells transfected with rat brain cannabinoid receptor. *Journal of Neuroscience,* **15(10)**, 6552-6561.

Mailleux, P. and Vanderhaeghen, J.-J. (1992) Distribution of neuronal cannabinoid receptor in the adult rat brain: a comparative receptor binding radioautography and *in situ* hybridization histochemistry. *Neuroscience,* **48(3)**, 655-668.

Makriyannis, A. and Rapaka, R. (1990) The molecular basis of cannabinoid activity. *Life Sciences,* **47**, 2173-2184.

Marchenko, N., Zaika, A. and Moll, U. M. (2000) Death signal-induced localization of p53 protein to mitochondria. A potential role in apoptotic signaling. *The Journal of Biological Chemistry,* **275**, 16202-16212.

Marshall, C. J. (1995) Specificity of receptor tyrosine kinase signaling: transient versus sustained extracellular signal-regulated kinase activation. *Cell,* **80**, 179-185.

Marsicano, G., Moosmann, B., Hermann, H., Lutz, B. and Behl, C. (2002) Neuroprotective properties of cannabinoids against oxidative stress: role of the cannabinoid receptor CB1. *Journal of Neurochemistry*, **80**, 448-456.

Martin, B.R., Dewey, W.L., Harris, L.S. and Beckner, J.S. (1977) ^{3}H-delta-9-tetrahydrocannabinol distribution in pregnant dogs and their fetuses. *Research Communications of Chemical Pathology and Pharmacology*, **17**, 457-470.

Martin, B.R., Jefferson, R.G., Winckler, R., Wiley, J.L., Thomas, B.F., Crocker, P.J., Williams, W. and Razdan, R.K. (2002) Assessment of the structural commonality between tetrahydrocannabinol and anandamide. *European Journal of Pharmacology*, **435**, 35-42.

Martin, J.H., Mohit, A.A. and Miller, C.A. (1996) Developmental expression in the mouse nervous system of the p493^{F12} SAP kinase. *Molecular Brain Research*, **35**, 47-57.

Martin, S.J. and Green, D.R. (1995) Protease activation during apoptosis: Death by a thousand cuts? *Cell*, **82**, 349-352.

Marzo, I., Brenner, C., Zamzami, N., Susin, S.A., Beutner, G., Brdiczka, D., Remy, R., Xie, Z.-H., Reed, J.C. and Kroemer, G. (1998) The permeability transition pore complex: a target for apoptosis regulation by casases and Bcl-2-related proteins. *Journal of Experimental Medicine*, **187**, 1261-1271.

Matsuda, L.A., Loiait, S.J., Brownstein, M.J., Young, A.C. and Bonner, T.I. (1990) Structure of a cannabinoid receptor and functional expression of the cloned cDNA. *Nature,* **346**, 561-564.

Matsuda, L.A. (1997) Molecular aspects of cannabinoid receptors. *Critical Review of Neurobiology*, **11**, 143-166.

Matthew, R.J., Wilson, W.H., Coleman, R.E., Turkington, T.G. and DeGrado, T.R. (1997) Marijuana intoxication and brain activation in marijuana smokers. *Life Sciences,* **60(23)**, 2075-2089.

McKallip, R.J., Lombard, C., Fisher, M., Martin, B.R., Ryu, S., Grant, S., Nagarkatti, P.S. and Nagarkatti, M. (2002a) Targeting CB2 cannabinoid receptors as a novel therapy to treat malignant lymphatic disease. *Blood*, **100(2)**, 627-634.

McKallip, R.J., Lombard, C., Martin, B.R., Nagarkatti, M. and Nagarkatti, P.S. (2002b) Δ^9-Tetrahydrocannabinol-induced apoptosis in the thymus and spleen as a mechanism of immunosuppression *in vitro* and *in vivo*. *The Journal of Pharmacology and Experimental Therapeutics*, **302**, 451-465.

McLaughlin, C.R., Martin, B.R., Compton, D.R. and Abood, M.E. (1994) Cannabinoid receptors in developing rats: detection of mRNA and receptor binding. *Drug and Alcohol Dependency*, **36(1)**, 27-31.

Mechoulam, R., Feigenbaum. J.J., Lander, N., Segal, M., Jarbe, T.U., Hiltunen, A.J. and Consroe, P. (1988) Enantiomeric cannabinoids: stereospecificity of psychotropic activity. *Experientia*, **44(9)**, 762-764.

Mechoulam, R., Ben-Shabat, S., Hanus, L., Ligumsky, M., Kaminski, N.E., Schatz, A.R., Gopher, A., Almog, S., Martin, B.R., Compton, D.R., Pertwee, R.F., Griffin, G., Bayewitch, M., Barg, J. and Vogel, Z. (1995) Identification of an endogenous 2-monoglyceride, present in canine gut, that binds to cannabinoid receptors. *Biochemical Pharmacology*, **50**, 83-90.

Melck, D., Rueda, D., Galve-Roperh, I., De Petrocellis, L., Guzmán, M. and Di Marzo, V. (1999) Involvement of the cAMP/protein kinase A pathway and of mitogen-activated protein kinase in the anti-proliferative effects of anandamide in human breast cancer cells. *FEBS Letters*, **463**, 235-240.

Melck, D., De Petrocellis, L., Orlando, P., Bisogno, T., Laezza, C., Bifulco, M. and Di Marzo, V. (2000) Suppression of nerve growth factor Trk receptors and prolactin receptors by endocannabinoids leads to inhibition of human breast and prostate cancer proliferation. *Endocrinology*, **141**, 118-126.

Menissier-de Murcia, J., Molinete, M., Gradwohl, G., Simonin, F. and de Murcia, G. (1989) Zinc-binding domain of poly(ADP-ribose)polymerase participates in the recognition of single strand breaks of DNA. *Journal of Molecular Biology*, **210**, 229-233.

Metzler, B., Hu, Y., Dietrich, H. and Xu, Q. (2000) Increased expression and activation of stress-activated protein kinases/c-Jun NH_2-Terminal protein kinases in atherosclerotic lesions coincide with p53. *American Journal of Pathology*, **156(6)**, 1875-1886.

Meyer, J.S. and Kunkle, R. (1999) Behavioural responses to a D_1 dopamine agonist in weanling rats treated neonatally with cocaine and Δ^9-tetrahydrocannabinol. *Neurotoxicology and Teratology*, **21(4)**, 375-380.

Mielke, K., Brecht, S., Dorst, A. and Herdegen, T. (1999) Activation of JNK and p38 stress kinases, c-Jun phosphorylation and c-Jun/AP-1 DNA binding activity following kainic acid induced seizures. *Neuroscience*, **91**, 471-483.

Mielke, K. and Herdegen, T. (2000) JNK and p38 stress kinases-degenerative effectors of signal-transduction-cascades in the nervous system. *Progress in Neurobiology,* **61**, 45-60.

Mihara, M., Erster, S., Zaika, A., Petrenko, O., Chittenden, T., Pancoska, P. and Moll, U. M. (2003) p53 has a direct apoptogenic role at the mitochondria. *Molecular Cell,* **11**, 577-590.

Miller, F. D., Pozniak, C. D. and Walsh, G. S. (2000) Neuronal life and death: an essential role for the p53 family. *Cell Death Differentiation,* **7**, 880-888.

Milton, N.G. (2002) Anandamide and noladin ether prevent neurotoxicity of the human amyloid-beta peptide. *Neuroscience Letters*, **332(2)**, 127-130.

Minden, A. and Karin, M. (1997) Regulation and function of the JNK subgroup of MAP kinases. *Biochemica et Biophysica Acta,* **1333**, 85-104.

Minn, A.J., Velez, P., Schendel, S.L., Liang, H., Muchmore, S.W., Fesik, S.W., Fill, M. and Thompson, C.B. (1997) Bcl-X_L forms an ion channel in synthetic lipid membranes. *Nature*, **385**, 353-357.

Mirmiran, M. and Swaab, D.F. (1987) Influence of drugs on brain neurotransmitter and behavioural states during development. *Developmental Pharmacology and Therapeutics*, **10**, 377-384.

Miyashita, T. and Reed, J.C. (1995) Tumour suppressor p53 is a direct transcriptional activator of the human Bax gene. *Cell,* **80**, 293-299.

Mokler, D.J., Robinson, S.E., Johnson, J.H., Hong, J.S. and Rosecrans, J.A. (1986) Effects of postweaning administration of delta-9-tetrahydrocannabinol (THC) on adult behavioural and neuroendocrine function in Sprague-Dawley and Fischer-344 rats. *Neurobehavioural Toxicology and Teratology*, **8(4)**, 407-413.

Mokler, D.J., Robinson, S.E., Johnson, J.H., Hong, J.S. and Rosecrans, J.A. (1986) Neonatal administration of Delta-9-Tetrahydrocannabinol (THC) alters the neurochemical response to stress in the adult Fischer-344 rat. *Neurotoxicology and Teratology*, **9**, 321-327.

Molina-Holgado, F., Amaro, A., Gonzalez, M.I., Alvarez, F.J. and Leret, M.L. (1996) Effect of maternal Δ^9-tetrahydrocannabinol on developing serotonergic system. *European Journal of Pharmacology*, **316**, 39-42.

Molina-Holgado, E., Vela, J.M., Arevalo-Martin, A., Almazan, G., Molina-Holgado, F., Borrell, J. and Guaza, C. (2002) Cannabinoids promote oligodendrocyte progenitor survival: involvement of cannabinoid receptors and phosphatidylinositol-3 kinase/Akt signalling. *The Jounal of Neuroscience*, **22(22)**, 9742-9753.

Muchmore, S.W., Sattler, M., Liang, H., Meadows, R.P., Harlan, J.E., Yoon, H.S., Nettsheim, D., Chang, B.S. and Thompson, S.-L. (1996) X-ray and NMR structure of human Bcl-X_L, an inhibitor of programmed cell death. *Nature*, **381**, 335-341.

Munro, S., Thomas, K.L. and Abu-Shaar, M. (1993) Molecular characterization of a peripheral receptor for cannabinoids. *Nature,* **365**, 61-65.

Murphy, K.M., Streips, U.N., and Lock, R.B. (2000) Bcl-2 inhibits a Fas-induced conformational change in the Bax N-terminus and Bax mitochondrial translocation. *The Journal of Biological Chemistry,* **275(23)**, 17225-17228.

Nadler, V., Mechoulam, R. and Sokolovsky, M. (1993) The non-psychotropic cannabinoid (+)-3S,4S)-7-hydroxy-Δ^6-tetrahydrocannabinol 1,1-dimethylheptyl (HU-211) attenuates *N*-methyl-D-aspartate receptor-mediated neurotoxicity in primary cultures of rat forebrain. *Neuroscience Letters*, **162**, 43-45.

Nagayama, T., Sinor, A.D., Simon, R.P., Chen, J., Graham, S.H., Jin, K. and Greenberg, D.A. (1999) Cannabinoids and neuroprotection in global and focal cerebral ishcemia and in neuronal cultures. *The Journal of Neuroscience,* **19(8)**, 2987-2995.

Nahas, G., Suciv-Foca, G., Armand, J-.P. and Morishima, A. (1974) Inhibition of cellular mediated immunity in marihuana smokers. *Science*, **183**, 419-420.

Nahas, G.G., Morishima, A. and Desoize, B. (1977) Effects of cannabinoids on macromolecular synthesis and replication of cultured lymphocytes. *Federation Proceedings*, **36**, 1748-1752.

Nahas, G.G. and Frick, H.C. (1986) Developmental effects of cannabis. *Neurotoxicology*, **7**, 381-396.

Nakajima-Iijima S, Hamada H, Reddy P, Kakunaga T. (1985) Molecular structure of the human cytoplasmic beta-actin gene: interspecies homology of sequences in the introns. *Proceedings of the National Academy of Sciences USA,* **82,** 6133-7.

Nakajima, M., Kashiwagi, K., Ohta, J., Furukawa, S., Hayashi, K., Kawashima, T. and Hayashi, Y. (1994) Etoposide induces programmed death in neurons cultured from the fetal rat central nervous system. *Brain Research*, **641(2)**, 350-352.

Napieralski, J. A., Raghupathi, R. and McIntosh, T. K. (1999) The tumor-suppressor gene, p53, is induced in injured brain regions following experimental traumatic brain injury. *Brain Research Molecular Brain Research,* **71**, 78-86.

Nava, F. Carta, G., Colombo, G. and Gessa, G.L. (2001) Effects of chronic Δ^9-tetrahydrocannabinol treatment on hippocampal extracellular acetylcholine concentration and alternation performance in the T-maze. *Neuropharmacology*, **41**, 392-399.

Navarro, M., Rubio, P. and de Fonseca, F.R. (1995) Behavioural consequences of maternal exposure to natural cannabinoids in rats. *Psychopharmacology*, **122(1)**, 1-14.

Nechushtan, A., Smith, C.L., Hsu, Y-.T. and Youle, R.J. (1999) Conformation of the Bax C-terminus regulates subcellular location and cell death. *EMBO Journal,* **18(9)**, 2330-2341.

Nicholson, D.W., Ali, A., Thornberry, N.A., Vaillancourt, J.P., Ding, C.K., Gallant, M., Gareau, Y., Griffin, P.R., Labelle, M., Lazebnik, Y.A., Munday, N.A., Raju, S.M., Smulson, M.E., Yamin, T., Yu, V.L. and Miller, D.K. (1995) Identification and inhibition of the ICE/CED-3 protease necessary for mammalian apoptosis. *Nature,* **376**, 37-43.

Nicotera, P., Leist, M. and Manzo, L. (1999) Neuronal cell death: a demise with different shapes. *Trends in Pharmacological Science,* **20**, 46-51.

Nicotera, P. (2000) Caspase requirement for neuronal apoptosis and neurodegeneration. *International Union of Biochemistry and Molecular Biology Life*, **49**, 421-425.

Oda, K., Arakawa, H., Tanaka, T., Matsuda, K., Tanikawa, C., Mori, T., Nishimori, H., Tamai, K., Tokino, T., Nakamura, Y. and Taya Y. (2000) p53AIP1, a potential mediator of p53-dependent apoptosis, and its regulation by Ser-46-phosphorylated p53. *Cell*, **102(6)**, 849-862.

Oltvai, Z.N., Milliman, C.L. and Korsmeyer, S.J. (1993) Bcl-2 heterodimerizes *in vivo* with a conserved homolog, Bax, that accelerates cell death. *Cell,* **74**, 609-619.

Oppenheim, R.W. (1991) Cell death during development of the nervous system. *Annual Review of Neuroscience*, **14**, 453-501.

Oviedo, A., Glowa, J. and Herkenham, M. (1993) Chonic cannabinoid administration alters cannabinoid receptor binding in rat brain: A quantitative autoradiographic study. *Brain Research*, **616**, 293-302.

Owen-Schaub, L.B., Zhang, W., Cusack, J.C., Angelo, L.S., Santee, S.M., Fujiwara, T., Roth, J.A., Deisseroth, A.B., Zhang, W.W. and Kruzel, E. (1995) Wild-type human p53 and a temperature-sensitive mutant induce Fas/APO-1 expression. *Molecular Cell Biology*, **15(6)**, 3032-3040.

Ozaki, I., Tani, E., Ikemoto, H., Kitagawa, H. and Fujikawa, H. (1999) Activation of stress-activated protein kinase/c-Jun NH_2–terminal kinase and p38 kinase in calphostin c-induced apoptosis requires caspase-3-like proteases but is dispensable for cell death. *The Journal of Biological Chemistry,* **274(9)**, 5310-5317.

Pacher, P., Batkai, S. and Kunos, G. (2004) Haemodynamic profile and responsiveness to anandamide of TRPV1 receptor knock-out mice. *Journal of Physiology*, **558(2)**, 67-657.

Panikashvili, D., Simeonidou, C., Ben-Shabat, S., Hanus, L., Breuer, A., Mechoulam, R. and Shohami, E. (2001) An endogenous cannabinoid (2-AG) is neuroprotective after brain injury. *Nature,* **413**, 527-531.

Park, J., Kim, I. O. Y., Lee, K., Han, P. L. and Choi, E. J. (1997) Activation of c-Jun N-terminal kinase antagonizes an anti-apoptotic action of Bcl-2. *The Journal of Biological Chemistry,* **272**, 16725-16728.

Pastorino, J.G., Chen, S.T., Tafani, M., Snyder, J.W. and Farber, J.L. (1998) The overexpression of Bax produces cell death upon induction of the mitochondrial permeability transition pore. *The Journal of Biological Chemistry*, **273(13)**, 7770-7775.

Pertwee, R.G. (1991) Tolerance to and dependence on psychotropic cannabinoids. In: The Biological Basis of Drug Tolerance. London Academic Press Ltd., pp. 231-265.

Pertwee, R.G., Joe-Adigwe, G. and Hawksworth, G.M. (1996) Further evidence for the presence of cannabinoid CB1 receptors in mouse vas deferens. *European Journal of Pharmacology,* **296**, 169-172.

Peters, D.A.V. and Tang, S. (1982) Sex-dependent biological changes following prenatal nicotine exposure in the rat. *Pharmacology Biochemistry and Behaviour*, **17**, 1077-1082.

Pieper, A.A., Verma, A., Zhang, J. and Snyder, S.H. (1999) Poly (ADP-ribose) polymerase, nitric oxide and cell death. *Trends in Pharmacological Science,* **20**, 171-181.

Piomelli, D., Giuffrida, A., Calignano, A. and de Fonseca, R. (2000) The endocannabinoid system as a target for therapeutic drugs. *Trends in Pharmacological Science*, **21**, 218-224.

Piomelli, D. (2003) The molecular logic of endocannabinoid signalling. *Nature Review of Neuroscience*, **4**, 873-878.

Pistis, M., Porcu, G., Melis, M., Diana, M. and Gessa, G.L. (2001) Effects of cannabinoids on prefrontal neuronal responses to ventral tegmental area stimulation. *European Journal of Neuroscience*, **14**, 96-102.

Polyak, K., Xia, Y., Zweler, J.L., Kinzler, K.W. and Vogelstein, B. (1997) A model for p53-induced apoptosis. *Nature*, **389**, 300-305.

Pope, H.G. and Yurgelin-Todd, D. (1996) The residual cognitive effects of heavy marijuana use in college students. *Journal of the American Medical Association*, **275**, 521-527.

Porter, A.C. and Felder, C.C. (2001) The endocannabinoid nervous system: unique opportunities for therapeutic intervention. *Pharmacology and Therapeutics,* **90**, 45-60.

Porter, A.G. (1999) Protein translocation in apotosis. *Trends in Cell Biology*, **9**, 394-401.

Portier, M., Rinaldi-Carmona, M., Pecceu, F., Combes, T., Poinot-Chazel, C., Calandra, B., Barth, F., le Fur, G. and Casellas, P. (1999) SR 144528, an antagonist for the peripheral cannabinoid receptor that behaves as an inverse agonist. *Journal of Pharmacology and Experimental Therapeutics*, **288**, 582-589.

Potapova, O., Gorospe, M., Dougherty, R.H., Dean, N.M., Gaarde, W.A. and Holbrook, N.J. (2000) Inhibition of c-Jun N-terminal kinase 2 expression suppresses growth and induces apoptosis of human tumour cells in a p53-dependent manner. *Molecular and Cellular Biology*, **20(5)**, 1713-1722.

Priller, J., Briley, E.M., Mansouri, J., Devane, W.A., Mackie, K. and Felder, C.C. (1995) Mead ethanolamide, a novel eicosanoid, is an agonist for the central (CB1) and peripheral (CB2) cannabinoid receptors. *Molecular Pharmacology*, **48**, 288-292.

Pucci, B., Bellincampi, L., Tafani, M., Masciullo, V., Melino, G. and Giordano, A. (1999) Paclitaxel induces apoptosis in Saos-2 cells with CD95L upregulation and Bcl-2 phosphorylation. *Experimental Cell Research*, **252(1)**, 134-143.

Puffenbarger, R.A., Boothe, A.C. and Cabral, G.A. (2000) Cannabinoids inhibit LPS-inducible cytokine mRNA expression in rat microglial cells. *Glia*, **29**, 58-69.

Raff, M. (1998) Cell suicide for beginners. *Nature,* **396**, 119-122.

Raffay, M. and Cohen, G.M. (1997) Apoptosis and necrosis in toxicology: A continuum or distinct modes of cell death? *Pharmacology and Therapeutics,* **75(3)**, 153-177.

Ramos, J.A., De Miguel, R., Cebeira, M., Hernandez, M. and Fernández-Ruiz, J.J. (2002) Exposure to cannabinoids in the development of endogenous cannabinoid system. *Neurotoxicology Research*, **4(4)**, 363-372.

Ray, S. K., Fidan, M., Nowak, M. W., Wilfor, G. G., Hogan, E. L. and Banik, N. L. (2000) Oxidative stress and Ca2+ influx upregulate calpain and induce apoptosis in PC12 cells. *Brain Research,* **852**, 326-334.

Reed, J. C. (1997) Cytochrome c: can't live with it--can't live without it. *Cell,* **91**, 559-562.

Reggio, P.H. (1999) Ligand-ligand and ligand-receptor approaches to modeling the cannabinoid CB_1 and CB_2 receptors: achievements and challenges. *Current Medicinal Chemistry,* **6(8)**, 665-683.

Reisine, T. and Brownstein, M.J. (1994) Opioid and cannabinoid receptors. *Current Biology,* **4**, 406-412.

Reynolds, C.H., Utton, M.A., Gibb, G.M., Yates, A. and Anderton, B.H. (1997) Stress-activated protein kinase/c-jun [it]N[rm]-terminal kinase phosphorylates tau protein. *Journal of Neurochemistry*, **68**, 1736-1744.

Rice, W., Shannon, J.M., Burton, F. and Fiedeldey, D. (1997) Expression of a brain-type cannabinoid receptor (CB1) in alveolar Type II cells in the lung: regulation by hydrocortisone. *European Journal of Pharmacology,* **327**, 227-232.

Rinaldi-Carmona, M., Barth, F., Heaulme, M., Shire, D., Calandra, B., Congy, C., Martinez, S., Maruani, J., Neliat, G., Caput, D., Ferrara, P., Soubrie, P., Breliere, J.C. and Lefur, G. (1994) SR 141716A, a potent and selective antagonist of the brain cannabinoid receptor. *FEBS Letters*, **350**, 240-244.

Rodriguez de Fonseca, F., Cebeira, M., Fernández-Ruiz, J.J., Navarro, M. and Ramos, J.A. (1991) Effects of pre- and perinatal exposure to hashish extracts on the ontogeny of brain dopaminergic neurons. *Neuroscience*, **43**, 713-723.

Rodriguez de Fonseca, F., Ramos, J.A., Bonnin, A. and Fernández-Ruiz, J.J. (1993) Presence of cannabinoid binding sites in the brain from early postnatal ages. *Neuroreport*, **4**, 135-138.

Rodriguez de Fonseca, F., Gorriti, M.A., Fernández-Ruiz, J.J., Palomo, T. and Ramos, J.A. (1994) Down-regulation of rat brain cannabinoid receptor binding sites after chronic Δ^9-tetrahydrocannabinol. *Pharmacology Biochemistry and Behaviour*, **47**, 33-40.

Romero, J., Garcia-Palomero, E., Berrendero, F., Garcia-Gil, L., Hernandez, M.L., Ramos, J.A. and Fernández-Ruiz, J.J. (1997) Atypical location of cannabinoid receptors in white matter areas during rat brain development. *Synapse*, **26(3)**, 317-323.

Ross, R.A. (2003) Anandamide and vanilloid TRPV1 receptors. *British Journal of Pharmacology*, **140(5)**, 790-801.

Rosse, T., Olivier, R., Monney, L., Rager, M., Conus, S., Fellay, I., Jansen, B. and Borner, C. (1998) Bcl-2 prolongs cell survival after Bax-induced release of cytochrome c. *Nature,* **391**, 441-442.

Roth, M.D., Arora, A., Barsky, S.H., Kleerup, E.C., Simmons, M., Tashlin, D.P. (1998) Airway inflammation in young marijuana and tobacco smokers. *American Journal of Respiratory Critical Care Medicine*, **157**, 928-937.

Rueda, D., Galve-Roperh, I., Haro, A. and Guzmán, M. (2000) The CB_1 cannabinoid receptor is coupled to the activation of c-Jun N-Terminal kinase. *Molecular Pharmacology,* **58(4)**, 814-820.

Rueda, D., Navarro, B., Martinez-Serrano, A., Guzmán, M. and Galve-Roperh, I., (2002) The endocannabinoid anandamide inhibits neuronal progenitor cell differentiation through attenuation of the Rap1/B-Raf/ERK pathway. *The Journal of Biological Chemistry,* **277(48)**, 46645-46650.

Ruiz, L., Miguel, A. and Diaz-Laviada, I. (1999) Δ^9-Tetrahydrocannabinol induces apoptosis in human prostate PC-3 cells via a receptor-independent mechanism. *FEBS Letters*, **458**, 400-404.

Salah-Eldin, A.E., Inoue, S., Tsukamoto, S., Aoi, H. and Tsuda, M. (2003) An association of Bcl-2 phosphorylation and Bax localization with their functions after hyperthermia and paclitaxel treatment. *International Journal of Cancer*, **103(1)**, 53-60.

Samuelsson, G. (1999) Drugs of Natural Origin. Swedish Pharmaceutical Press.

Sánchez, C., Galve-Roperh, I., Canova, C., Brachet, P. and Guzmán, M. (1998) Δ^9-Tetrahydrocannabinol induces apoptosis in C6 glioma cells. *FEBS Letters,* **436**, 6-10.

Sánchez, C., de Ceballos, M., Gómez del Pulgar, T., Rueda, D., Corbacho, C., Velasco, G., Galve-Roperh, I., Huffman, J., Ramón y Cajal, S. and Guzmán, M. (2001a) Inhibition of glioma growth *in vivo* by selective activation of the CB_2 cannabinoid receptor. *Cancer Research*, **61**, 5784-5789.

Sánchez, C., Rueda, D., Segui, B., Galve-Roperh, I., Levade, T. and Guzmán, M. (2001b) The CB(1) cannabinoid receptor of astrocytes is coupled to sphingomyelin hydrolysis through the adaptor protein fan. *Molecular Pharmacology*, **59(5)**, 955-959.

Sarafian, T.A., Tashkin, D.A. and Roth, M.D. (2001) Marijuana smoke and Δ^9-Tetrahydrocannabinol promote necrotic cell death but inhibit fas-mediated apoptosis. *Toxicology and Applied Pharmacology*, **174**, 264-272.

Sarafian, T.A., Kouyoumjian, S., Tashkin, D.A. and Roth, M.D. (2002) Synergistic cytotoxicity of Δ^9-tetrahydrocannabinol and butylated hydroxyanisole. *Toxicology Letters*, **133**, 171-179.

Sarker, K.P., Biswas, K.K., Yamakuchi, M., Lee, K.-Y., Hahiguchi, T., Krach, M., Kitajima, I. & Maruyama, I. (2003) ASK1-p38 MAPK/JNK signaling cascade mediates anandamide-induced PC12 cell death. *Journal of Neurochemistry,* **85**, 50-61.

Scallet, A.C., Uemura, E., Andrews, A., Ali, S.F., McMillan, D.E., Paule, M.G., Brown, R.M. and Slikker Jr, W. (1987) Morphometric studies of the rat hippocampus following chronic delta-9-tetrahydrocannabinol (THC). *Brain Research,* **436**, 193-198.

Scallet, A.C. (1991) Neurotoxicology of cannabis and THC: a review of chronic exposure studies in animals. *Pharmacology Biochemistry Behaviour*, **40(3)**, 671-676.

Scanlon, K. J., Ohta, Y., Ishida, H., Kijima, H., Ohkawa, T., Kaminski, A., Tsai, J., Horng, G. and Kashani-Sabet, M. (1995) Oligonucleotide-mediated modulation of mammalian gene expression. *Federation of American Societies for Experimental Biology Journal,* **9**, 1288-1296.

Schaeffer, H. J. and Weber, M. J. (1999) Mitogen-activated protein kinases: specific messages from ubiquitous messengers. *Molecular and Cellular Biology,* **19**, 2435-2444.

Schatz, A.R., Lee, M., Condie, R.B., Pualaski, J.T. and Kaminski, N.E. (1997) Cannabinoid receptors CB1 and CB2: a characterization of expression and adenylate cyclase modulation within the immune system. *Toxicology Applied Pharmacology*, **142**, 278-287.

Schendel, S.L., Xie, Z., Montal, M.O., Matsuyama, S., Montal, M. and Reed, J.C. (1997) Channel formation by antiapoptotic protein Bcl-2. *Proceedings of the National Academy of Science USA*, **94**, 5113-5118.

Scher, MS., Richardson, G.A., Coble, P.A., Day, N.L. and Stoffer, D.S. (1988) The effects of prenatal alcohol and marijuana exposure: disturbances in neonatal sleep cycling and arousal. *Pediatric Research*, **24**, 101-105.

Schlesinger, P.H., Gross, A., Yin, X-.M., Yamamoto, K., Saito, M., Waksman, G. and Korsmeyer, S.J. (1997) Comparison of the ion channel characteristics of proapoptotic BAX and antiapoptotic BCL-2. *Proceedings of the National Academy of Sciences USA,* **94**, 11357-11362.

Schlicker, E., Timm, J., Zentner, J. and Gothert, M. (1997) Cannabinoid CB_1 receptor-mediated inhibition of noradrenaline release in the human and guiea-pig hippocampus. *Naunyn-Schmiedebergs Arch Pharmacologie*, **356**, 583-589.

Schmitz, I., Kirchhoff, S. and Krammer, P. H. (2000) Regulation of death receptor-mediated apoptosis pathways. *International Journal of Biochemistry and Cell Biology,* **32**, 1123-1136.

Schneider, M. and Koch, M. (2003) Chronic pubertal, but not adult chronic cannabinoid treatment impairs sensorimotor gating, recognition memory, and performance in a progressive ratio task in adult rats. *Neuropsychopharmacology*, **28**, 1760-1769.

Schwarz, H., Blanco, F.J. and Lotz, M. (1994) Anandamide, an endogenous cannabinoid receptor agonist inhibits lymphocyte proliferation and induces apoptosis. *Journal of Neuroimmunology*, **55**, 107-115.

Seimiya, H., Mashima, T., Toho, M. and Tsuruo, T. (1997) c-Jun NH_2-terminal kinase-mediated activation of interleukin-1β converting enzyme/CED-3-like protease during anticancer drug-induced apoptosis. *The Journal of Biological Chemistry*, **272(7)**, 4631-4636.

Shah, G.M., Shah, R.G. and Poirier, G.G. (1996) Different cleavage pattern for poly(ADP-ribose) polymerase during necrosis and apoptosis in HL-60 cells. *Biochemical and Biophysical Research Commuications*, **229**, 838-844.

Shen, M., Piser, T.M., Seybold, V.S. and Thayer, S.A. (1996) Cannabinoid receptor agonists inhibit glutamatergic synaptic transmission in rat hippocampal cultures. *Journal of Neuroscience,* **16(14)**, 4322-4334.

Shen, M. and Thayer, S.A. (1998) Cannabinoid receptor agonists protect cultured mouse hippocampal neurons from excitotoxicity. *The American Society for Pharmacology and Experimental Therapeutics*, **54**, 459-462.

Shiah, S-.G., Chuang, S-.E. and Kuo, M-.L. (2001) Involvement of Asp-Glu-Val-Asp-directed, caspase-mediated mitogen-activated protein kinase kinase 1 cleavage, c-Jun N-terminal kinase activation, and subsequent Bcl-2 phosphorylation for paclitaxel-induced apoptosis in HL-60 cells. *Molecular Pharmacology*, **59**, 254-262.

Shieh S.Y., Ikeda, M., Taya, Y. and Prives, C. (1997) DNA damage-induced phosphorylation of p53 alleviates inhibition of Mdm2. *Cell*, **91**, 325-334.

Shimizu, S., Narita, M. and Tsujimoto, Y. (1999) Bcl-2 family proteins regulate the release of apoptogenic cytochrome *c* by the mitochondrial channel VDAC. *Nature*, **399**, 483-487.

Shire, D., Carillon, C., Kaghad, M., Calandra, B., Rinaldi-Carmona, M., Le Fur, G., Caput, D. and Ferrara, P. (1995) An amino-terminal variant of the central cannabinoid receptor resulting from alternative splicing. *The Journal of Biological Chemistry*, **270**, 3726-3731.

Shivachar, A.C., Martin, B.R. and Ellis, E.F. (1996) Anandamide- and delta9-tetrahydrocannabinol-evoked arachidonic acid mobilization and blockade by SR141716A [N-(Piperidin-1-yl)-5-(4-chlorophenyl)-1-(2,4-dichlorophenyl)-4 - methyl-1H-pyrazole-3-carboximide hydrochloride]. *Biochemical Pharmacology*, **51(5)**, 669-676.

Shohami, E., Gallily, R., Mechoulam, R., Bass, R. and Ben-Hur, T. (1997) Cytokine production in the brain following closed head injury: dexanabinol (HU-211) is a novel TNF-alpha inhibitor and an effective neuroprotectant. *Journal of Neuroimmunology*, **72**, 169-177.

Showalter, V.M., Compton, D.R., Martin, B.R. and Abood, M.E. (1996) Evaluation of binding in a transfected cell line expressing a peripheral cannabinoid receptor (CB2): identification of cannabinoid receptor subtype selective ligands. *Journal of Pharmacology and Experimental Therapeutics*, **278**, 989-999.

Siliciano, J. D., Canman, C. E., Taya, Y., Sakaguchi, K., Appella, E. and Kastan, M. B. (1997) DNA damage induces phosphorylation of the amino terminus of p53. *Genes Development,* **11**, 3471-3481.

Sim, L.J., Hampson, R.E., Deadwyler, S.A. and Childers, S.R. (1996) Effects of chronic treatment with Δ^9-tatrahydrocannabinol on cannabinoid-stimulated [^{35}S]GTPγS autoradiography in rat brain. *The Journal of Neuroscience*, **16(24)**, 8057-8066.

Sims, J.L., Berger, S.J. and Berger, N.A. (1983) Poly(ADP-ribose) Polymerase inhibitors preserve nicotinamide adenine dinucleotide and adenosine 5'-triphosphate pools in DNA-damaged cells: mechanism of stimulation of unscheduled DNA synthesis. *Biochemistry*, **22**, 5188-5194.

Sinor, A.D., Irvin, S.M. and Greenberg, D.A. (2000) Endocannabinoids protect cerebral cortical neurons from *in vitro* ischemia in rats. *Neuroscience Letters,* **278**, 157-160.

Slee, E. A., Harte, M. T., Kluck, R. M., Wolf, B. B., Casiano, C. A., Newmeyer, D. D., Wang, H. G., Reed, J. C., Nicholson, D. W., Alnemri, E. S., Green, D. R. and Martin, S. J. (1999) Ordering the cytochrome c-initiated caspase cascade: hierarchical activation of caspases-2, -3, -6, -7, -8, and -10 in a caspase-9-dependent manner. *Journal of Cell Biology,* **144,** 281-292.

Slipetz, D.M., O'Neill, G.P., Favreau, L., Dufresne, C., Gallant, M., Gareau, Y., Guay, D., Labelle, M. and Metters, K.M. (1995) Activation of the human peripheral cannabinoid receptor results in inhibition of adenylyl cyclase. *Molecular Pharmacology*, **48**, 352-361.

Soderstrom, K., Leid, M., Moore, F.L. and Murray, T.F. (2000) Behavioural, pharmacological, and molecular characterisation of an amphibian cannabinoid receptor. *Journal of Neurochemistry*, **75**, 413-423.

Spear, L.P., Kirstein, C.L. and Frambes, N.A. (1989) Cocaine effects on the developing central motor system: behavioural, psychopharmacological and neurochemical studies. *Annual New York Academy of Science*, **562**, 290.

Spooren, W.P. and Hengerer, B. (2000) DNA laddering and caspase 3-like activity in the spinal cord of a mouse model of familial amyotrophic lateral sclerosis. *Cellular Molecular Biology*, **46(1)**, 63-69.

Stella, N., Schweitzer, P. and Piomelli, D. (1997) A second endogenous cannabinoid that modulates long-term potentiation. *Nature,* **388**, 773-778.

Stiglick, A. and Kalant, H. (1985) Residual effects of chronic cannabis treatment on behaviour in mature rats. *Psychopharmacology*, **85**, 436-439.

Streissguth, A.P. (1983) Alcohol and pregnancy: an overview and an update. *Substance and Alcohol Actions and Misuse*, **4**, 149-173.

Sugden, P. H. and Clerk, A. (1997) Regulation of the ERK Subgroup of MAP Kinase Cascades Through G Protein-Coupled Receptors. *Cell Signalling,* **9**, 337-351.

Sugiura, T., Kondo, S., Sukagawa, A., Tonegawa, T., Nakane, S., Yamashita, A., Ishima, Y. and Waku, K. (1996) Transacylase-mediated and phosphodiesterase-mediated synthesis of *N*-arachidonoylethanolamine, an endogenous cannabinoid receptor ligand, in rat brain microsomes. Comparison with synthesis from free arachidonic acid and ethanolamine. *European Journal of Biochemistry*, **240**, 53-62.

Sugiura, T., Kondo, S., Kishimoto, S., Miyashita, T., Nakane, S., Kodaka, T., Suhara, Y., Takayama, H. and Waku, K. (2000) Evidence that 2-Arachidonoylglycerol but not *N*-Palmitoylethanolamine or anandamide is the physiological ligand for the cannabinoid CB_2 receptor. *The Journal of Biological Chemistry*, **275(1)**, 605-616.

Susin, S.A., Zamzami, N., Castedo, M., Hirsch, T., Marchetti, P., Macho, A., Daugas, E., Geuskens, M. and Kroemer, G. (1996) Bcl-2 inhibits the mitochondrial release of an apoptotic protease. *Journal of Experimental Medicine,* **184**, 1331-1341.

Swaab, D.F. and Mirmiran, M. (1984) Possible mechanisms inderlying the teratogenic effects of medicines on the developing brain. In: Neurobehavioural Teratology. Elsevier, pp. 55.

Szöke, É., Czéch, G. Szolcsányl, J. and Seress, L. (2002) Neonatal anandamide treatment results in prolonged mitochondrial damage in the vanilloid receptor type-1-immunoreactive B-type neurons of the rat trigeminal nerve. *Neuroscience*, **115**, 805-814.

Tennes, K., Avitable, N., Blackard, C., Boyles, C., Hassoun, B., Holmes, L. and Kreye, M. (1985) Prenatal and postnatal exposure in the human. In: Current research on the consequences of maternal drug abuse, National Institute on drug abuse research monograph no. 59, US Department of Health and Human Services, Rockville. pp. 48-60.

Tewari M, Q. L., O'Rourke K, Desnoyers S, Zeng Z, Beidler DR, Poirier GG, Salvesen GS, Dixit V.M. (1995) Yama/CPP32 beta, a mammalian homolog of CED-3, is a CrmA-inhibitable protease that cleaves the death substrate poly(ADP-ribose) polymerase. *Cell,* **81**, 801-809.

Tournier, C., Hess, P., Yang, D.D., Xu, J., Turner, T.K., Nimual, A., Bar-Sagi, D., Jones, S.N., Flavell, R.A. and Davis, R.J. (2000) Requirement of JNK for stress-induced activation of the cytochrome *c*-mediated death pathway. *Science,* **288**, 870-873.

Tramer, M.R., Carroll, D., Campbell, F.A., Reynolds, D.J., Moore, R.A. and McQuay, H.J. (2001) Cannabinoids for control of chemotherapy induced nausea and vomiting: quantitative systematic review. *British Medical Journal*, **323**, 16-21.

Tsou, K., Brown, S., Sanudo-Pena, M.C., Mackie, K. and Walker J.M. (1998) Immunohistochemical distribution of cannabinoid CB_1 receptors in the rat central nervous system. *Neuroscience,* **83(2)**, 393-411.

Turk, B., Dolenc, I., Lenarcic, B., Krizaj, I., Turk, V., Bieth, J. G. and Bjork, I. (2000) Acidic pH as a physiological regulator of human cathepsin L activity. *European Journal of Biochemistry,* **259**, 926-932.

Turkanis, S.A., Partlow, L.M. and Karler, R. (1991) Delta-9-Tetrahydrocannabinol depresses inward sodium current in mouse neuroblastoma cells. *Neuropharmacology,* **30(1)**, 73-77.

Twitchell, W., Brown, S. and Mackie, K. (1997) Cannabinoids inhibit N- and P/Q-type calcium channels in cultured rat hippocampal neurons. *Journal of Neurophysiology,* **78**, 43-50.

Valijent, E., Pages, C., Rogard, M., Besson, M-.J., Maldonado, R. and Caboche, J. (2001) Δ9-tetrahydrocannabinol-induced MAPK/ERK and Elk-1 activation *in vivo* depends on dopaminergic transmission. *European Journal of Neuroscience*, **14**, 342-352.

Valk, P., Verbarkel, S., Vankan, Y., Hol, S., Mancham, S., Ploemacher, R., Mayen, A., Lowenberg, B. and Delwel, R. (1997) Anandamide, a natural ligand for the peripheral cannabinoid receptor is a novel synergistic growth factor for hematopoietic cells. *Blood*, **90**, 1448-1457.

Van Der Stelt, M., Veldeheis, W.B., Bar, P.R., Veldink, G.A., Vliegenthart, J.F.G. and Nicolay, K. (2001) Neuroprotection by Δ^9-Tetrahydrocannabinol, the main active compound in marijuana, against ouabain-induced *in vivo* excitotoxicity. *Journal of Neuroscience,* **21(17)**, 6475-6479.

Velasco, G., Galve-Roperh, I., Sánchez, C., Blázquez, C. and Guzmán, M. (2004) Hypothesis: cannabinoid therapy for the treatment of gliomas? *Neuropharmacology*, **47**, 315-323.

Venters, H.D., Dantzer, R. and Kelley, K.W. (2000) Tumour necrosis factor-alpha induces neuronal death by silencing survival signals generated by the type I insulin-like growth factor receptor. *Annual NY Academy of Science*, **917**, 210-220.

Vereker, E., Campbell, V., Roche, E., McEntee, E. and Lynch, M. A. (2000) Lipopolysaccharide inhibits long-term potentiation in the rat dentate gyrus by activating caspase-1. *The Journal of Biological Chemistry,* **275**, 26252-26258.

Virdee, K., Bannister, A. J., Hunt, S. P. and Tolkovsky, A. M. (1997) Comparison between the timing of JNK activation, c-Jun phosphorylation, and onset of death commitment in sympathetic neurones. *Journal of Neurochemistry,* **69**, 550-561.

Wallach, D., Varfolomeev, E. E., Malinin, N. L., Goltsev, Y. V., Kovalenko, A. V. and Boldin, M. P. (1999) Tumor necrosis factor receptor and Fas signalling mechanisms. *Annual Review Immunology,* **17**, 331-367.

Wang, J. and Friedman, E. (2000) Downregulation of p53 by sustained JNK activation during apoptosis. *Molecular Carcinogenicity*, **29**, 179-188.

Wang, K. K. W. (2000) Calpain and Caspase: Can you tell the difference. *Trends in Neuroscience,* **23**, 20-26.

Wenger, T., Toth, B.E., Juaneda, C., Leonardelli, J. and Tramu, G. (1999) The effects of cannabinoids on the regulation of reproduction. *Life Sciences*, **65(6/7)**, 695-701.

Wheeler, D.B., Randall, A. and Tsien, T.W. (1994) Roles of N-type and Q-type Ca^{2+} channels in supporting hippocampal synaptic tranmission. *Science*, **264**, 107-111.

Whitmarsh, A. J. and Davis, R. J. (1995) Transcripition factor AP-1 regulation of mitogen-activated protein kinase signal transduction pathways. *Journal of Molecular Medicine*, **74**, 589-607.

Williams, G. T. and Smith, C. A. (1993) Molecular regulation of apoptosis: genetic controls on cell death. *Cell,* **74**, 777-779.

Wilson, R.I. and Nicoll, R.A. (2001) Endogenous cannabinoids mediate retrograde signaling a hippocampal synapses. *Nature*, **410**, 588-592.

Wolter, K.G., Hsu, Y-.T., Smith, C.L., Nechustan, A., Xi, X-.G. and Youle, R.J. (1997) Movement of Bax from the cytosol to mitochondria during apoptosis. *The Journal of Cell Biology,* **139(5)**, 1281-1292.

Wood, D.E., Thomas, A., Devi, L.A., Berman, Y., Beavis, R.C., Reed, J.C. and Newcomb, E.W. (1998) Bax cleavage is mediated by calpain during drug-induced apoptosis. *Oncogene*, **17**, 1069-1078.

Wood, D.E. and Newcomb, E.W. (2000) Cleavage of Bax enhances its cell death function. *Experimental Cell Research*, **256(2)**, 375-382.

Xia, Z., Dickens, M., Raingeaud, J., Davis, R. J. and Greenberg, M. E. (1995) Opposing effects of ERK and JNK-p38 MAP kinases on apoptosis. *Science,* **270**, 1326-1333.

Xiang, H., Hochman, D. W., Saya, H., Fujiwara, T., Schwartzkroin, P. A. and Morrison, R. S. (1996) Evidence for p53-mediated modulation of neuronal viability. *Journal of Neuroscience,* **16**, 6753-6765.

Xu, X., Raber, J., Yang, D., Su, B. and Mucke, L. (1997) Dynamic regulation of c-Jun N-terminal kinase activity in mouse brain by environmental stimuli. *Proceedings of the National Academy of Sciences USA,* **94**, 12655-12660.

Yamamoto, K., Ichijo, I.L. and Korsmeyer, S.J. (1999) Bcl-2 is phosphorylated and inactivated by an ASK1/Jun N-terminal protein kinase pathway normally activated at G(2)/M. *Molecular and Cellular Biology*, **19**, 8469-8478.

Yang, D. D., Kuan, C. Y., Whitmarsh, A. J., Rincon, M., Zheng, T. S., Davis, R. J., Rakic, P. and Flavell, R. A. (1997) Absence of excitotoxicity-induced apoptosis in the hippocampus of mice lacking the Jnk3 gene. *Nature,* **389**, 865-870.

Yin, T., Sandhu, G., Wolfgang, C. D., Burrier, A., Webb, R. L., Rigel, D. F., Hai, T. and Whelan, J. (1997) Tissue-specific pattern of stress kinase activation in ischemic/reperfused heart and kidney. *The Journal of Biological Chemistry,* **272**, 19943-19950.

Yin, X-.M., Oltvai, Z.N. and Korsmeyer, S.J. (1994) BH1 and BH2 domains of Bcl-2 are required for inhibition of apoptosis and heterodimerization with Bax. *Nature*, **369**, 321-323.

Yuan, J.Y. and Horvitz, H.R. (1990) The Caenorhabditis genes ced-3 and ced-4 act cell autonomously to cause programmed cell death. *Developmental Biology*, **138**, 33-41.

Yuan, X. M., Li, W., Dalen, H., Lotem, J., Kama, R., Sachs, L. and Brunk, U. T. (2002) Lysosomal destabilization in p53-induced apoptosis. *Proceedings of the National Acadamey of Sciences USA,* **99**, 6286-6291.

Zamzami, N., Susin, S.A., Marchetti, P., Hirsch, T., Gomez-Monterrey, I., Castedo, M. and Kroemer, G. (1996) Mitochondrial control of nuclear apoptosis. *Journal of Experimental Medicine,* **183**, 1533-1544.

Zhou, D. and Song, Z.H. (2001) CB1 cannabinoid receptor-mediated neurite remodeling in mouse neuroblastoma N1E-115 cells. *Journal of Neuroscience Research*, **65(4)**, 346-353.

Zhu, J. and Chen, X. (2000) MCG10, a novel p53 target gene that encodes a KH domain RNA-binding protein, is capable of inducing apoptosis and cell cycle arrest in G(2)-M. *Molecular Cell Biology*, **20(15)**, 5602-5618.

Zhu, W., Freidman, H. and Klein T.W. (1998a) Δ^9-Tetrahydrocannabinol induces apoptosis in macrophages and lymphocytes: involvement of Bcl-2 and caspase-1. *Journal of Pharmacology and Experimental Therapeutics,* **286**, 1103-1109.

Zhu, W., Newton, C., Daaka, Y., Freidman, H. and Klein T.W. (1998b) Δ^9-Tetrahydrocannabinol enhances the secretion of Interleukin 1 from endotoxin-stimulated macrophages. *The Journal of Pharmacology and Experimental Therapeutics*, **270(3)**, 1334-1339.

Zong, W.X., Li, C., Hatzivassiliou, G., Lindsten, T., Yu, Q.C., Yuan, J. and Thompson, C.B. (2003) Bax and Bak can localize to the endoplasmic reticulum to initiate apoptosis. *Journal of Cell Biology*, **162(1)**, 59-69.

Zoratti, M. and Szabo, I. (1995) The mitochondrial permeability transition. *Biochimica et Biophysica Acta.*, **1241**, 1139-176.

Zörnig, M., Hueber, A., Baum, W. and Evan, G. (2001) Apoptosis regulators and their role in tumorigenesis. *Biochimica et Biophysica Acta,* **1551,** F1-37.

Zou, H., Henzel, W.J., Liu, X., Lutschg, A. and Wang, X. (1997) Apaf-1, a human protein homologous C. elegans CED-4, participates in cytochrome *c*-dependent activation of caspase-3. *Cell,* **90**, 405-413.

IX Appendix II - Solutions

Cell Culture Solutions

70% EtOH (100ml)

70ml EtOH

30ml H_2O

PBS

Na_2HPO_4 (80mM)

NaH_2PO_4 (20mM)

NaCl (100mM)

Poly-L-lysine

1mg poly-L-lysine/25ml PBS

Trypsin Solution

0.3mg trypsin/ml PBS

Trypsin Inhibitor Solution

0.1mg trypsin inhibitor/ml PBS

DNase (0.2mg/ml PBS)

$MgSO_4$ (0.1M)/ml PBS

Supplemented Neurobasal Medium (day 1)

Heat inactivated horse serum (10%; 10ml)

Penicillin/Streptomycin (100U/ml; 1ml)

Glutamax (2mM; 1ml)

B27 anti-oxidant (1%; 1ml)/100ml Neurobasal Medium

Antimitotic Neurobasal Medium (day 4)

Heat inactivated horse serum (10%; 10ml)

Penicillin/Streptomycin 100U/ml (1ml)

Glutamax 2mM (1ml)

ARA-C (0.5mg/ml; 1ml)

Neurobasal Medium (100ml)

Replacement Neurobasal Medium (day 5)

Heat inactivated horse serum (10%; 10ml)

Penicillin/Streptomycin (100U/ml; 1ml)

Glutamax (2mM; 1ml)

Neurobasal Medium (100ml)

Cell Harvesting Solutions

Lysis Buffer, pH 7.4 (Harvesting of total culture protein)

HEPES (25mM)

$MgCl_2$ (5mM)

EDTA (5mM)

DTT (5mM)

PMSF (2mM)

Leupeptin (10μg/ml)

Aprotinin (10μg/ml)

Pepstatin (10μg/ml)

Lysis Buffer, pH 7.4 (Harvesting of total cortical slice protein)

HEPES (20mM)

KCl (10mM)

$MgCl_2$ (1.5mM)

EGTA (1mM)

EDTA (1mM)

Dithiothreitol (1mM)

PMSF (0.1mM)

Leupeptin (2μg/ml)

Aprotinin (2μg/ml)

Sucrose (200mM)

Permeabilisation Buffer, pH 7.2 (Harvesting cytosolic culture extracts)

Sucrose (250mM)

KCl (70mM)

NaCl (137mM)

Na_2HPO_4 (4.5mM)

KH_2PO_4 (1.4mM)

PMSF (0.1mM)

Leupeptin (10μg/ml)

Aprotinin (2μg/ml)

Digitonin (200μg/ml)

Mitochondrial Lysis Buffer, pH 7.4 (Harvesting mitochondrial culture extracts)

Tris Base (50mM)

NaCl (150mM)

EGTA (2mM)

Triton-X (0.2%)

Igepal P-40 (0.3%)

PMSF (0.1mM)

Leupeptin (10μg/ml)

Aprotinin (2μg/ml)

DNA Laddering Solutions

Lysis Buffer, pH 8 (Harvesting of DNA)

Tris-HCl (25mM)

EDTA (5mM)

NaCl (100mM)

SDS (0.5%)

Proteinase K (100μg/ml)

TE Buffer, pH 8

Tris-HCl (10mM)

EDTA (5mM)

Ribonuclease A (50μg/ml)

Tris Borate EDTA (TBE) Buffer, pH 8

Tris Base (0.08M)

Boric Acid (40μM)

EDTA (1mM)

Loading Buffer

EDTA (100mM)

SDS (0.1%)

Bromophenol Blue (0.05%)

Ficoll 400 (20%)

SDS-PAGE Solutions

Phosphate buffered saline-Tween 20 (PBS-Tween), pH 7.4

Na_2HPO_4 (80mM)

NaH_2PO_4 (20mM)

NaCl (100mM)

Tween 20 (0.1%)

Tris buffered saline-Tween 20 (TBS-Tween), pH 7.4

Tris-HCl (20mM)

NaCl (150mM)

Tween 20 (0.1%)

Sample buffer, pH 7.4

Tris-HCl (150mM)

Glycerol (10%)

SDS (10%)

β-Mercaptoethanol (5%)

Bromophenol Blue (0.05%)

Stacking gel (4%, pH 6.8)

Acrylamide/bis-acrylamide (30% stock, 13% (v/v), dH_2O 60% (v/v), Tris-HCl (0.05M, 25% (v/v))

SDS (10% w/v stock, 1% (v/v))

APS (10% w/v stock, 0.5% (v/v))

TEMED 0.5% (v/v)

Separating gel (10%, pH 8.8)

Acrylamide/bis-acrylamide (30% stock, 33% (v/v)), dH_2O, 40% (v/v), Tris-HCl, (0.05M, 25% (v/v))

SDS (10% w/v stock, 1% (v/v))

APS (10% w/v stock, 0.5% (v/v))

TEMED 0.05% (v/v)

Separating gel (12%, pH 8.8)

Acrylamide/bis-acrylamide (30% stock, 40% (v/v)), dH_2O, 33% (v/v), Tris-HCl, (0.05M, 25% (v/v)

SDS (10% w/v stock, 1% (v/v))

APS (10% w/v stock, 0.5% (v/v))

TEMED 0.05% (v/v)

Electrode running buffer

Tris Base (25mM)

Glycine (200mM)

SDS (0.1%)

Transfer buffer, pH 8.3

Tris base (25mM)

Glycine (192mM)

Methanol (20%)

SDS (0.05%)

PCR Gel Electrophoresis Solutions

Tris Borate EDTA (TBE) Buffer, pH 8.3

Tris base (0.08M)

Boric Acid (0.04M)

EDTA (1mM)

RNA Seperating Agarose Gel (1 %, pH 8.3)

Agarose (1%)

TBE Buffer (100ml)

PCR Products Seperating Agarose Gel (1.5 %, pH 8.3)

Agarose (1.5%)

TBE Buffer (100ml)

Fluorogenic Assay Solutions

Lysis Buffer, pH 7.4

HEPES (25mM)

$MgCl_2$ (5mM)

Dithiothreitol (5mM)

EDTA (5mM)

PMSF (2mM)

Leupeptin (10μg/ml)

Pepstatin (10μg/ml)

Aprotinin (10μg/ml)

Incubation Buffer, pH 7.4

HEPES (50mM)

Dithiothreitol (10mM)

Glycerol (20%)

In vivo Experimental Solutions

Krebs, pH 7.4

NaCl (136mM)

KCl (2.54mM)

KH_2PO_4 (1.18mM)

$MgSO_4$ (1.18mM)

$NaHCO_3$ (16mM)

Glucose (10 mM)

Subbing Solution

Gelatine (0.5%)

Chrome Alum (0.05%)

X Appendix II - Suppliers

AGB Scientific Ltd., Dublin Industrial Estate, Dublin 11, Ireland.

ALEXIS Corporation LTD., P.O. Box 6757, Bingham, Nottingham, NG13 8LS, UK.

Amersham plc, Amersham Place, Little Chalfont, Buckinghamshire, HP79NA, UK.

Astec-Microflow Systems, 2180 Andrea Lane, Fort Myers, FL33912, USA.

B.Braun Melsungen AG, Carl-Braun Srtaβe 1, D-34212 Melsungen, Germany.

Bachem Ltd., PO Box 260, 17 Westside Industrial Estate, Jackson Street, St. Helens, Meyerside WA9 3AJ, UK.

BD Biosciences Pharmingen, 10975 Torreyana Road, San Diego, CA 921121, USA.

BDH Laboratory Supplies, Poole, Dorset, BH151TD, UK.

Becton Dickinson Labware Europe, Becton Dickinson France S.A., 1 rue Aristide Berges, BP4, 38800 Le Pont De Claix, France.

Biognostik GmbH., Gerhard-Gerdes-Str.19, 37079 Göttingen, Germany.

Biometra GmbH, Rudolph-Wissell Straβe 30, D-37079 Gottingen, Germany.

Bio-Rad Laboratories GmbH., Heidemannstrasse 164, D-80939 Munich, Germany.

Biosource International, 542 Flynn Road, Camarillo, California USA 93012, USA.

Calbiochem International, Merck KGaA, Frankfurter Str. 250, D-64293 Darmstadt, Germany.

Cell Signalling Technology, INC, 166B Cummings Center, Beverly, MA 01915, USA.

CN BIOSCIENCES Ltd., Boulevard Industrial Park, Padge Road, Beeston, Nottingham, NG9 2JR, UK.

Dako Corporation, 6392 Via Road, Carpinteria, CA93013, USA.

FUJIFILM Medical Systems USA, Inc. Headquarters: 419 West Avenue Stamford, CT 06902, USA.

Greiner Bio-One GmbH, Bad Haller Strasse 32, 4550 Kremsmuenster, Austria.

Improvision Software, Viscount Centre II, University of Warwick Science Park, Millburn Hill Road, Coventry , CV4 7HS, UK.

InVitrogen Ltd., Inchinnan Business Park, 3 Fountain Drive, Paisley PA49RF, UK.

Jencons Scientific Ltd., Cherrycourt Way Industrial Estate, Stanbridge Road, Lancashire, WN8 9SP. UK.

Medical Supply Company Ltd., Damastown, Mulhuddart, Dublin 15, Ireland.

Millipore Ireland B.V. Tullagreen Carrigtwohill, Co.Cork, Ireland.

Molecular Probes Europe BV, PoortGebouw, Rijnsburgerweg 10, 2333 AA Leiden, The Netherlands.

Nikon Instech Co., Ltd. Parale Mitsui Bldg., 8, Higashida-cho, Kawasaki-ku, Kawasaki, Kanagawa 210-0005, Japan.

Pall Corporation, 600 South Wagner Road, Ann Arbour, MI48103-9019 USA.

Pierce Biotechnology, 3747 N.Meridian Rd, P.O. Box 117, Rockford, IL61105, USA.

Promega Sciences, 2800 Woods Hollow Road Madison WI 5371, USA.

Roche Diagnostics Ltd., Bell Lane, Lewes, East Sussex, BN7 1LG, UK.

Sarstedt Ltd., Sinnottstown Lane, Drinagh, Wexford, Ireland.

Sartorius AG Ltd., 94-108 Weender Landstraβe, D-37075 Goettingen, Germany.

Scanalytics Inc. 8550 Lee Highway, Suite 400, Fairfax, VA 22031, USA.

Sigma-Aldrich Company Ltd., The Old Brickyard, New Road, Gillingham, Dorset, SP84XT, UK.

Tocris Cookson Ltd., Northpoint Fourth Way, Avonmouth, Bristol BS11 8TA. UK.

Vector Laboratories Inc., Burlingame, CA94010, USA.

Whatman International Ltd., Whatman House, St. Leonard's Road, 20/20 Maidstone, Kent, ME16OLS, UK.

XI Publications

Downer, E.J., Fogarty, M.P. and Campbell, V. A. (2003) Tetrahydrocannabinol-induced neurotoxicity depends on CB_1 receptor-mediated c-Jun N-terminal kinase activation in cultured cortical neurons. *British Journal of Pharmacology,* **140**, 547-57.

Fogarty, M.P., **Downer, E.J.,** and Campbell, V. A. (2003) A role for c-Jun N-terminal kinase 1 (JNK1), but not JNK2, in the β-amyloid-mediated stabilization of protein p53 and induction of the apoptotic cascade in cultured cortical neurons. *Biochemical Journal,* **371**, 789-798.

Downer, E., Boland, B., Fogarty, M., and Campbell, V. (2001) Δ^9-Tetrahydrocannabinol induces the apoptotic pathway in cultured cortical neurones via activation of the CB_1 receptor. *Neuroreport*, **12(18)**, 3973-78.

Downer, E.J., and Campbell, V.A. (2004) The apoptotic actions of tetrahydrocannabinol in the rat cortex vary with post-natal development. *American Society for Neuroscience Abstracts*, (in press).

Downer, E.J., Murphy, Á. and Campbell, V.A. (2004) Tetrahydrocannabinol induction of rat cortical neuronal apoptosis *in vitro* is reliant on p53 induction. *Journal of Anatomy,* (in press).

Redmond, I., **Downer, E.J.**, and Campbell, V. A. (2003) The effect of post-natal development on Tetrahydrocannabinol-induced activation of the apoptotic cascade in the rat cortex. *Journal of Physiology,* **551P**, PC29.

Downer, E., and Campbell, V. (2002) Tetrahydrocannabinol induces apoptosis in cortical neurons. *American Society for Neuroscience Abstracts,* **28**, 892.

Fogarty, M.P., **Downer, E.J.** and Campbell, V.A. (2002) Aβ mediated neurotoxicity through the stress activated protein kinase JNK. *American Society for Neuroscience Abstracts,* **28**, 688.

British Journal of Pharmacology (2003) 140, 547–557 © 2003 Nature Publishing Group All rights reserved 0007–1188/03 $25.00
www.nature.com/bjp

Tetrahydrocannabinol-induced neurotoxicity depends on CB_1 receptor-mediated c-Jun N-terminal kinase activation in cultured cortical neurons

[1]Eric J. Downer, [1]Marie P. Fogarty & *,[1]Veronica A. Campbell

[1]Department of Physiology, Trinity College, Trinity College Institute of Neuroscience, Dublin 2, Ireland

1 Δ^9-Tetrahydrocannabinol (THC), the main psychoactive ingredient of marijuana, induces apoptosis in cultured cortical neurons. THC exerts its apoptotic effects in cortical neurons by binding to the CB_1 cannabinoid receptor. The CB_1 receptor has been shown to couple to the stress-activated protein kinase, c-Jun N-terminal kinase (JNK). However, the involvement of specific JNK isoforms in the neurotoxic properties of THC remains to be established.

2 The present study involved treatment of rat cultured cortical neurons with THC (0.005–50 μM), and combinations of THC with the CB_1 receptor antagonist, AM 251 (10 μM) and pertussis toxin (PTX; 200 ng ml^{-1}). Antisense oligonucleotides (AS) were used to deplete neurons of JNK1 and JNK2 in order to elucidate their respective roles in THC signalling.

3 Here we report that THC induces the activation of JNK *via* the CB_1 receptor and its associated G-protein, $G_{i/o}$. Treatment of cultured cortical neurons with THC resulted in a differential timeframe of activation of the JNK1 and JNK2 isoforms.

4 Use of specific JNK1 and JNK2 AS identified activation of caspase-3 and DNA fragmentation as downstream consequences of JNK1 and JNK2 activation.

5 The results from this study demonstrate that activation of the CB_1 receptor induces JNK and caspase-3 activation, an increase in Bax expression and DNA fragmentation. The data demonstrate that the activation of both JNK1 and JNK2 isoforms is central to the THC-induced activation of the apoptotic pathway in cortical neurons.
British Journal of Pharmacology (2003) **140,** 547–557. doi:10.1038/sj.bjp.0705464

Keywords: Δ^9-Tetrahydrocannabinol; antisense; c-Jun N-terminal kinase; apoptosis; caspase-3; bax

Abbreviations: AS, antisense oligonucleotides; JNK, c-Jun N-terminal kinase; MAPK, mitogen-activated protein kinase; SC, scrambled control oligonucleotides; THC, Δ^9-tetrahydrocannabinol; TUNEL, terminal deoxynucleotidyltransferase-mediated biotinylated UTP nick end labelling

Introduction

Δ^9-Tetrahydrocannabinol (THC), the predominant psychoactive ingredient in preparations of marijuana (*Cannabis saliva*), exerts a broad spectrum of central effects, such as alterations in cognition (Howlett, 1990) and impairment of short-term memory consolidation (Abood & Martin, 1992). THC exerts these effects by binding to G-protein-coupled receptors (Howlett, 1995). While two different subtypes of cannabinoid receptor have been characterised from mammalian tissues, CB_1 (Matsuda *et al.*, 1990) and CB_2 (Munro *et al.*, 1993), the CB_1 receptor is associated with brain regions responsible for mediating the psychoactive effects of THC, such as the cortex and hippocampus (Twitchell *et al.*, 1997; Tsou *et al.*, 1998).

At a cellular level, THC has been shown to modulate a number of neuronal functions, including ion channel activity (Turkanis *et al.*, 1991; Mackie *et al.*, 1995; Twitchell *et al.*, 1997) and neurotransmitter release (Shen *et al.*, 1996; Gessa *et al.*, 1998; Jentsch *et al.*, 1998), and there is increasing evidence suggesting a role for THC in the regulation of neuronal viability. THC has a toxic effect on cultured hippocampal neurons (Chan *et al.*, 1998), glioma cells (Sanchez *et al.*, 1998) and cortical neurons (Campbell, 2001), and inhibits glioma cell growth *in vivo* (Galve-Roperh *et al.*, 2000). In contrast, there is also evidence that THC and other cannabinoids act as neuroprotectants in certain systems. Cannabinoid receptor agonists are neuroprotective in excitotoxic cell death *in vivo* (Panikashvili *et al.*, 2001; van der Stelt *et al.*, 2001) and *in vitro* (Shen & Thayer, 1998; Abood *et al.*, 2001), which is dependent on CB_1 receptor activation. Furthermore, cannabinoids have been shown to protect cultured neurons against glutamate-induced toxicity (Hampson *et al.*, 1998) and *in vitro* hypoxia and glucose deprivation (Nagayama *et al.*, 1999). However, the precise role of the cannabinoid receptors in regulating neuronal viability is poorly understood, although some of the *in vitro* protective effects of cannabinoids (Hampson *et al.*, 1998; Nagayama *et al.*, 1999) are receptor-independent while the neurotoxic effects of THC on cortical (Campbell, 2001) and hippocampal (Chan *et al.*, 1998) cultures are blocked by CB_1 receptor antagonists.

We have recently reported that THC activates the caspase-3 cell death pathway in cultured cortical neurons, resulting in

*Author for correspondence; E-mail: vacmpbll@tcd.ie

DNA fragmentation and programmed cell death (Campbell, 2001). Furthermore, we have shown that the activation of the central CB_1 cannabinoid receptor is vital in the execution of this cell death cascade (Downer *et al.*, 2001). It has been established that the CB_1 receptor couples to several signal transduction pathways (Dill & Howlett, 1988; Bouaboula *et al.*, 1995; Bouaboula *et al.*, 1996; Sanchez *et al.*, 1998; Gomez del Pulgar *et al.*, 2000; Derkinderen *et al.*, 2001) including the stress-activated protein kinase pathway (Rueda *et al.*, 2000). While there is growing evidence that the c-Jun N-terminal kinase (JNK) pathway is central to cell death in the nervous system (Mielke & Herdegen, 2000), the role of JNK in the CB_1 receptor-dependent induction of neuronal apoptosis remains to be established. The present work was therefore undertaken to examine the nature of the link between the CB_1 receptor, activation of JNK and downstream apoptotic consequences in cultured cortical neurons. Furthermore, three JNK isoforms, JNK1, JNK2 and JNK3, have been identified in the mammalian brain (Gupta *et al.*, 1996), and current commercially available JNK inhibitors are unable to distinguish between JNK1-, JNK2- and JNK3-mediated effects. We therefore treated neurons with specific antisense oligonucleotides (AS) that target rat JNK1 or JNK2 mRNA in order to investigate the upstream roles of these JNK isoforms in the THC-induced activation of caspase-3 and subsequent DNA fragmentation.

Methods

Culture of cortical neurons

Primary cortical neurons were prepared from 1-day-old Wistar rats and maintained in neurobasal medium (Gibco BRL, Paisley, U.K.). Rats were decapitated, the cerebral cortices dissected and the meninges removed. The cortices were incubated in phosphate-buffered saline (PBS) with trypsin ($0.25\,\mu g\,ml^{-1}$) for 25 min at 37°C. The cortical tissue was then triturated ($\times 5$) in PBS containing soyabean trypsin inhibitor ($0.2\,\mu g\,ml^{-1}$) and DNAse ($0.2\,mg\,ml^{-1}$) and gently filtered through a sterile mesh filter ($40\,\mu m$). The suspension was centrifuged at $2000 \times g$ for 3 min at 20°C and the pellet resuspended in warm neurobasal medium, supplemented with heat-inactivated horse serum (10%), penicillin ($100\,U\,ml^{-1}$), streptomycin ($100\,U\,ml^{-1}$) and glutamax (2 mM). Suspended cells were plated at a density of 0.25×10^6 cells on circular 10 mm diameter coverslips, coated with poly-L-lysine ($60\,\mu g\,ml^{-1}$), and incubated in a humidified atmosphere containing 5% CO_2:95% air at 37°C for 2 h prior to being flooded with prewarmed neurobasal medium. After 48 h, $5\,ng\,ml^{-1}$ cytosine-arabino-furanoside was added to the culture medium to suppress the proliferation of non-neuronal cells and maintain the purity of the cortical neuronal culture. This ensures that microglia and astrocyte contamination is less than 5% in culture preparations. Medium was exchanged for fresh medium every 3 days and cells were grown in culture for up to 14 days.

Oligonucleotide treatment

JNK antisense (AS) and scrambled control (SC) phosphorothioated oligonucleotides were synthesized by Biognostik (Gottingen, Germany). The sequences used were according to previously published work (Hreniuk *et al.*, 2001) and are complementary to the mRNA encoding rat JNK1 and JNK2 protein: JNK1 AS, 5′-CTCATGATGGCAAGCAATTA-3′; JNK1 SC, 5′-ACTACTACACTAGACTAC-3′; JNK2 AS, 5′-GCTCAGTGGACATGGATGAG-3′ and JNK2 SC, 5′-GGACTACTACACTAGACTAC-3′. Neurons were maintained in supplemented media in the presence of the oligonucleotides for 48 h prior to treatment with THC. *N*-[1-(2,3-dioleoyloxy)propyl]-*N*,*N*,*N*-trimethylammonium/dioleoylphosphatidylethanolamine (DOTMA/DOPE $5\,\mu g\,ml^{-1}$; Life Technologies, Paisley, U.K.) was incorporated into serum-free media for the first 4 h of oligonucleotide treatment to ensure sufficient oligonucleotide uptake. Downregulation of JNK1 and JNK2 protein expression was achieved by using JNK1 AS and JNK2 AS at a final concentration of $2\,\mu M$.

Terminal deoxynucleotidyltransferase-mediated biotinylated UTP nick end labelling (TUNEL)

Apoptotic cell death was determined in cultures using TUNEL staining according to the manufacturer's instructions (Dead-End Colorimetric Apoptosis Detection System; Promega Corporation, Madison, MD, U.S.A.). Following treatment with THC ($5\,\mu M$) for 3 h, cells were fixed with paraformaldehyde (4%) for 30 min at room temperature. Neurons were permeabilised with Triton X-100 (0.2%) and Proteinase K (0.2%) and biotinylated nucleotide was incorporated at the 3′-OH DNA ends using the enzyme terminal deoxynucleotidyl transferase (TdT). Endogenous peroxidases were blocked using 0.3% H_2O_2, and horseradish-peroxidase-labelled streptavidin was bound to the biotinylated nucleotides. Apoptotic cells (TUNEL-positive) were detected using diaminobenzidine, a stable chromagen that stains the apoptotic nuclei of TUNEL-positive cells dark brown. After mounting coverslips on slides, the neurons were viewed under light microscopy at $\times 100$ magnification. Cells displaying apoptotic nuclei were counted and expressed as a percentage of the total number of cells examined (400–500 cells coverslip^{-1}).

Western blot analysis

Cortical neurons were harvested in lysis buffer (25 mM HEPES, 5 mM $MgCl_2$, 5 mM dithiothreitol, 5 mM EDTA, 2 mM PMSF, $5\,\mu g\,ml^{-1}$ leupeptin, $5\,\mu g\,ml^{-1}$ pepstatin, $5\,\mu g\,ml^{-1}$ aprotinin, pH 7.4) and homogenised on ice. Lysates were then centrifuged ($13{,}000 \times g$ for 15 min at 4°C) and the supernatant containing the cytosolic fraction was prepared for SDS–polyacrylamide gel electrophoresis. The cytosolic fraction was diluted to $50\,\mu g\,ml^{-1}$ protein concentration with sodium dodecyl sulphate (SDS) sample buffer (150 mM Tris-HCl pH 7.4, 10% $w\,v^{-1}$ glycerol, 4% $w\,v^{-1}$ SDS, 5% $v\,v^{-1}$ β-mercaptoethanol, 0.002% $w\,v^{-1}$ bromophenol blue) and samples heated to 100°C for 5 min. Samples were separated by electrophoresis on 10 and 12% polyacrylamide minigels and cytosolic proteins were transferred from the gel onto nitrocellulose membrane (Sigma, U.K.). The blots were blocked with 2% BSA for 1 h at 37°C and then incubated with the primary antibody overnight at 4°C. The blots were washed thoroughly with Tris-buffered saline (TBS) containing 0.05% Tween and immunoreactive bands detected using horseradish-peroxidase-conjugated anti-mouse IgG (Sigma, U.K.) or

anti-rabbit IgG (Sigma, U.K.) and an enhanced chemiluminescence (ECL) system (Amersham, U.K.). Primary antibodies used were: monoclonal JNK1 and JNK2 antibodies (Santa Cruz Biotechnology Inc., Santa Cruz, CA, U.S.A.) purified from mouse serum that recognise JNK1 (46 kDa) and JNK2 (54 kDa) protein expression; monoclonal anti-phospho-specific JNK antibody (Santa Cruz Biotechnology Inc., Santa Cruz, CA, U.S.A.) purified from mouse serum that recognises phosphorylated JNK1, JNK2 and JNK3 isoforms; polyclonal Bax antibody (DAKO Corporation, Carpinteria, CA, U.S.A.) purified from rabbit serum that recognises amino acids 43–61 of human Bax. Molecular weight markers were used to confirm the molecular weight of protein bands. Bandwidths were quantified using densitometric analysis (D-Scan PC software).

Measurement of caspase-3 activity

Cleavage of the fluorogenic caspase-3 substrate (Ac-DEVD-7-amino-4-trifluoromethylcoumarin peptide (AFC); Alexis Corporation, U.S.A.) to its fluorescent product was used as a measure of caspase-3 activity. Following treatment with THC (5 μM) for 2 h, cells were harvested in lysis buffer (25 mM HEPES, 5 mM $MgCl_2$, 5 mM dithiothreitol, 5 mM EDTA, 2 mM PMSF, 10 μg ml^{-1} leupeptin, 10 μg ml^{-1} pepstatin, 10 μg ml^{-1} aprotinin, pH 7.4) and homogenised on ice. Samples of supernatant (50 μl) were incubated with the DEVD peptide (10 μM; 4 μl) or incubation buffer (50 μl; 50 mM HEPES, 10 mM dithiothreitol, 20% w v^{-1} glycerol, pH 7.4) for 1 h at 37°C and the fluorescence assessed (excitation, 400 nm; emission, 505 nm) using a Fluoroscan Ascent FL plate reader (MSC Medical Supply Co. Ltd, U.K.).

Drug treatment

THC was obtained from Sigma-Aldrich Company Ltd (Dorset, U.K.). The drug was initially dissolved in methanol and stored at −20°C as an 80 mM stock solution. For use, the stock drug was diluted to a final concentration of 5 μM in prewarmed culture media and 0.007% methanol was used as vehicle control. The selective CB_1 receptor antagonist AM 251 (Tocris Cookson Ltd, Bristol, U.K.) was stored as a 10 mM stock solution in dimethylsulphoxide (DMSO) and diluted to a final concentration of 10 μM in warm culture media for addition to cultures; 0.0001% DMSO was used as a vehicle control for AM 251. Neurons were preincubated with AM 251 for 30 min before treating with THC. Pertussis toxin (PTX; Sigma, Dorset, U.K.) was reconstituted in PBS and neurons were incubated with 200 ng ml^{-1} PTX for 24 h prior to THC treatment.

Statistical analysis

Data are reported as the mean ± s.e.m. of the number of experiments indicated in every case. Statistical analysis was performed by Student's *t*-tests and a one-way ANOVA. A *post hoc* analysis was made by the Student–Neumann–Keuls test. Our criterion for significance was $P<0.05$. Extreme significance differences were expressed by probability values of $P<0.01$ and $P<0.001$.

Results

THC activates JNK1 and JNK2 isoforms within a differential timeframe

Exposure of cultured cortical neurons to THC (5 μM) resulted in the activation of the JNK protein within the cytosol in a time-dependent manner (Figure 1). Cytosolic expression levels of the phosphorylated (active) forms of JNK1 and JNK2 were measured by Western immunoblot and bandwidths were quantified using densitometry. Interestingly, there was a differential timeframe of activation for JNK1 and JNK2. In terms of the JNK1 time course of activation (Figure 1a), in control cells phospho-JNK1 expression was 7.28 ± 0.80 (arbitrary units; mean bandwidth ± s.e.m.) and this was significantly increased to 13.41 ± 1.63 following treatment with THC for 5 min ($P<0.001$, ANOVA; $n=7$). However, no change in phospho-JNK1 expression was observed at subsequent time points, and phospho-JNK1 expression was in fact significantly reduced to 4.21 ± 0.40 following treatment with THC for 2 h ($P<0.05$, ANOVA, $n=7$; Figure 1a).

In contrast, Figure 1b demonstrates that expression of phospho-JNK2 in control neurons was 21.44 ± 3.89 (arbitrary units; mean bandwidth ± s.e.m.) and this was significantly increased to 38.79 ± 6.25 when neurons were cultured in media containing THC (5 μM) for 2 h ($P<0.001$, ANOVA; $n=7$). At earlier time points, treatment with THC had no effect on phospho-JNK2 expression. A sample immunoblot demonstrating the THC-induced activation of JNK1 at 5 min and JNK2 at 2 h is shown in Figure 1c.

Total JNK1 and JNK2 expression was unaffected by THC (5 μM; sample immunoblots shown). In vehicle-treated cells, JNK1 total protein expression was 46.53 ± 1.15 (arbitrary units; mean bandwidth ± s.e.m.) and exposure of neurons to THC for 5 min had no effect on total JNK1 expression (46.92 ± 2.66, $n=5$; Figure 1d). In neurons treated with vehicle alone for 2 h, mean total JNK2 expression was 56.32 ± 7.31 and this was unaffected by exposure to THC for 2 h (56.26 ± 9.09; $n=5$; Figure 1e). Thus, the increase in expression of phosphorylated JNK1 (Figure 1a) and phosphorylated JNK2 (Figure 1b) is not attributable to a THC-induced increase in total JNK protein expression. Furthermore, in our cell culture model, JNK3 expression was very moderate (Figure 1f), hence the relative contribution of JNK1 and JNK2 to the apoptotic cascade was assessed.

Since we have previously shown that 5 μM is the concentration of THC required to induce maximal neuronal degeneration in a CB_1 receptor-dependent manner (Downer *et al.*, 2001), we performed a dose–response analysis of THC-induced JNK activation. Figure 1(g and h) represents sample immunoblots which demonstrate that treatment of cells with THC (0.005–50 μM) evoked a dose-dependent increase in phospho-JNK1 (Figure 1g) and phospho-JNK2 (Figure 1h) expression at 5 and 120 min, respectively.

AM 251 pretreatment prevents THC-induced JNK activation

To determine whether THC-induced JNK activation was dependent on the CB_1 receptor, we employed the use of the selective CB_1 receptor antagonist AM 251 (10 μM). Figure 2 demonstrates that AM 251 prevented the THC-induced

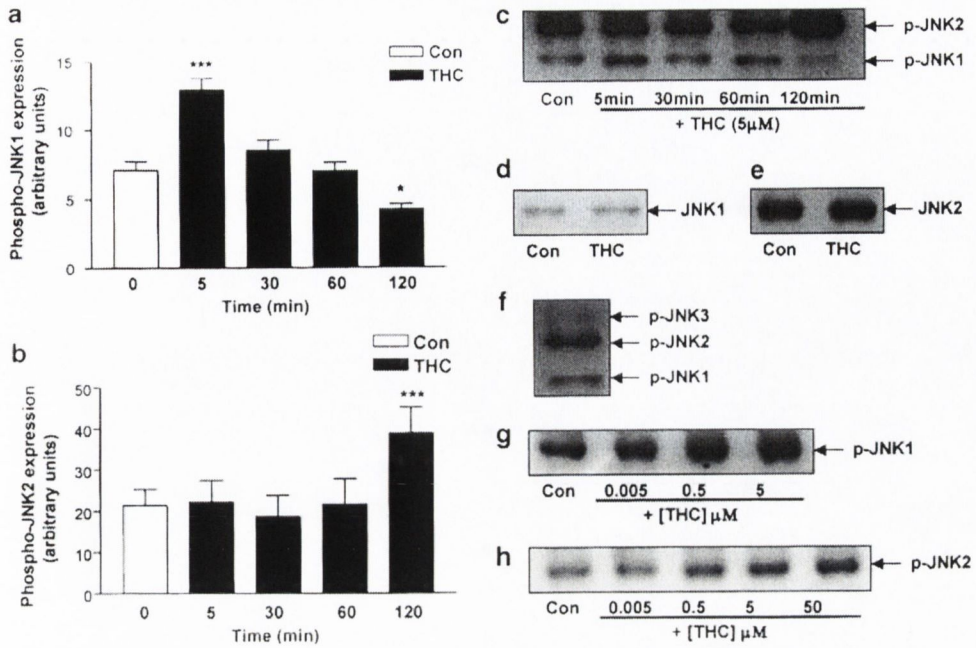

Figure 1 Time course of THC-induced activation of JNK. Cortical neurons were exposed to THC for 5–120 min, then cells were harvested and the cytosolic fractions analysed for the expression levels of the phosphorylated active forms of JNK 1 and JNK2 using Western immunoblot. (a) A significant increase in phospho-JNK1 expression was found following treatment with THC (5 μM) for 5 min. Exposure to THC for 30 and 60 min had no effect on phospho-JNK1 expression. However, treatment with THC for 120 min significantly decreased phospho-JNK1 expression. Results are expressed as mean $\pm$ s.e.m. for seven observations, $^{***}P<0.001$, $^{*}P<0.05$. (b) Phospho-JNK2 expression was significantly increased when neurons were treated with THC (5 μM) for 120 min. Exposure to THC for 5, 30 and 60 min had no effect on phospho-JNK2 expression. Results are expressed as mean $\pm$ s.e.m. for seven observations, $^{***}P<0.001$. (c) A sample Western immunoblot demonstrating the increase in phospho-JNK1 expression at 5 min of THC treatment and the corresponding increase in phospho-JNK2 expression following treatment with THC for 120 min. (d) Neurons were treated with THC (5 μM) for 5 min, then cells were harvested in lysis buffer and the cytosolic fractions analysed for total JNK1 protein expression using Western immunoblot. THC had no effect on JNK1 protein expression at 5 min. Inset: A sample Western immunoblot showing that THC treatment for 5 min had no effect on JNK1 protein expression as compared to vehicle-treated neurons. (e) Cortical neurons were treated with THC (5 μM) for 2 h, then cells were harvested and analysed for total JNK2 protein expression by Western blot analysis. Incubation of cells with THC for 2 h did not affect JNK2 protein expression. Inset: A sample Western immunoblot demonstrating total JNK2 protein expression in vehicle-treated neurons and neurons treated with THC for 2 h. (f) Untreated cortical neurons were harvested and analysed for phosphorylated JNK1, JNK2 and JNK3 expression. JNK3 expression was moderate compared to JNK1/2 expression. (g) A sample Western immunoblot showing that a 5 min treatment with THC increases phospho-JNK1 expression in a dose-dependent manner. Similar results were observed in five separate experiments. (h) A sample Western immunoblot showing that a 120 min treatment with THC increases phospho-JNK2 expression in a dose-dependent manner. Similar results were observed in five separate experiments.

activation of JNK1 and JNK2. Thus, in neurons treated with vehicle for 5 min, phosphorylated JNK1 expression was 44.95 $\pm$ 4.86 (arbitrary units; mean bandwidth $\pm$ s.e.m.) and this was significantly increased following THC treatment (5 μM; 5 min) to 58.67 $\pm$ 3.59 ($P<0.05$, ANOVA, $n=6$; Figure 2a). While pretreatment with AM 251 alone had no effect on phosphorylated JNK1 expression (37.35 $\pm$ 3.43), it prevented the THC-induced increase in phospho-JNK1 expression (38.14 $\pm$ 5.99). Although it has been shown that AM 251 behaves as an inverse agonist (New & Wong, 2003), we were unable to detect any effect of AM 251 on basal JNK activity (Figure 2).

Figure 2b demonstrates that phosphorylated JNK2 expression was significantly increased from 12.83 $\pm$ 0.54 (arbitrary units; mean bandwidth $\pm$ s.e.m.) to 15.72 $\pm$ 0.34 following treatment with THC (5 μM) for 2 h ($P<0.01$, Student's t-test, $n=6$). Exposure to AM 251 (10 μM) alone had no effect on basal phosphorylated JNK2 expression (11.55 $\pm$ 1.75) and it prevented the THC-induced increase in phosphorylated JNK2 expression (12.55 $\pm$ 0.52; Figure 2b). Sample immunoblots demonstrating the activation of JNK1 and JNK2 following THC treatment, and the abolition of these effects in AM 251-treated cells are shown as insets in Figure 2a and b. This result provides evidence of a role for the CB_1 cannabinoid receptor in the THC-induced activation of both JNK1 and JNK2.

PTX abrogates THC-induced JNK1/2 activation

The central CB_1 cannabinoid receptor is coupled to $G_{i/o}$-proteins (Howlett, 1995). The involvement of $G_{i/o}$ in coupling the CB_1 receptor to JNK activation in this system was assessed using PTX (200 ng ml^{-1}). As shown in Figure 3a, PTX pretreatment prior to THC (5 μM) treatment for 5 min (31.92 $\pm$ 5.59 arbitrary units; mean bandwidth $\pm$ s.e.m.) prevented THC-induced JNK1 activation at 5 min (55.98 $\pm$ 4.74; $P<0.05$, ANOVA, $n=5$). Incubation of neurons with methanol vehicle for 5 min (41.44 $\pm$ 2.72) or PTX alone for 24 h (35.06 $\pm$ 3.71) had no effect on JNK1 activity (Figure 3a).

Similarly, Figure 3b demonstrates that phospho-JNK2 expression was significantly increased from 13.90 $\pm$ 0.54 to 22.34 $\pm$ 2.75 (arbitrary units; mean bandwidth $\pm$ s.e.m.) following treatment with THC (5 μM) for 2 h ($P<0.05$, ANOVA, $n=5$). Treatment with PTX (200 ng ml^{-1}) alone had no effect on phosphorylated JNK2 expression (16.05 $\pm$ 1.99), but it

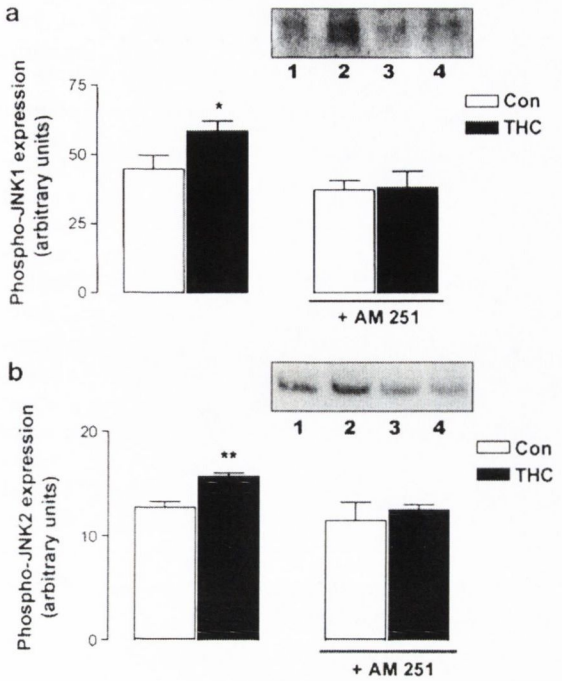

Figure 2 THC-induced activation of JNK is mediated by the CB_1 receptor. (a) Treatment of neurons with THC (5 μM) for 5 min evoked a significant increase in phospho-JNK1 expression. Pre-incubation of cortical neurons with the CB_1 receptor antagonist AM 251 (10 μM) for 30 min abolished the THC-induced increase in phospho-JNK1 expression. Results are expressed as mean $\pm$ s.e.m. for six observations, $^*P<0.05$. Inset: A sample Western immunoblot demonstrating the increase in phospho-JNK1 expression after 5 min of THC treatment (lane 2) compared to control cells (lane 1). While AM 251 had no effect on phospho-JNK1 expression (lane 3), it abolished the ability of THC to increase phospho-JNK1 expression (lane 4). (b) Treatment of neurons with THC (5 μM) for 120 min evoked a significant increase in phospho-JNK2 expression. Pre-incubation of cortical neurons with the CB_1 receptor antagonist AM 251 (10 μM) for 30 min abolished the THC-induced increase in phospho-JNK2 expression. Results are expressed as mean $\pm$ s.e.m. for six observations, $^{**}P<0.01$. Inset: A sample Western immunoblot demonstrating the increase in phospho-JNK2 expression after 5 min of THC treatment (lane 2) compared to control cells (lane 1). While AM 251 had no effect on phospho-JNK2 expression (lane 3), it abolished the ability of THC to increase phospho-JNK2 expression (lane 4).

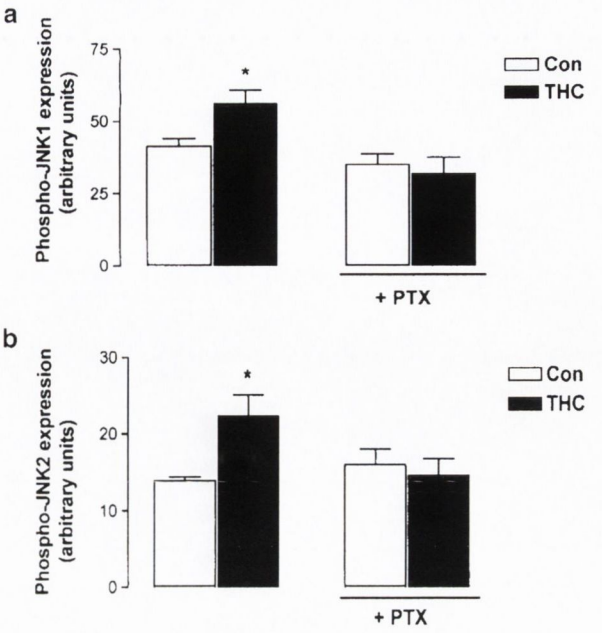

Figure 3 THC-induced JNK activation is mediated by G-protein subtypes $G_{i/o}$. (a) THC (5 μM; 5 min) significantly increased phospho-JNK1 expression and this was prevented by pretreatment with PTX (200 ng ml^{-1}; 24 h). Results are expressed as mean $\pm$ s.e.m. for five observations, $^*P<0.05$. (b) THC (5 μM; 120 min) significantly increased phospho-JNK2 expression and this was prevented by pretreatment with PTX (200 ng ml^{-1}; 24 h). Results are expressed as mean $\pm$ s.e.m. for five observations, $^*P<0.05$.

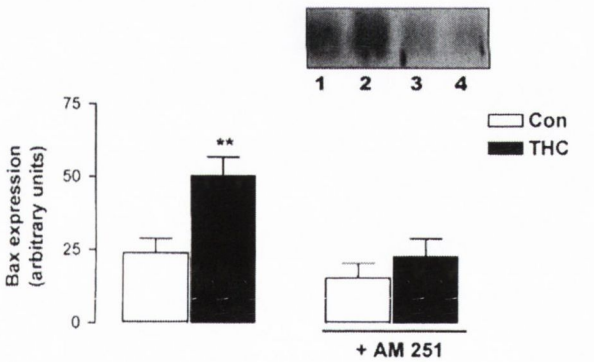

Figure 4 THC increases Bax expression *via* the CB_1 receptor. Neurons were preincubated with AM 251 (10 μM) for 30 min, treated with THC (5 μM) for 2 h and analysed for the expression levels of Bax using Western immunoblotting. THC significantly increased Bax expression and this was abolished by AM 251. Results are expressed as mean $\pm$ s.e.m. for five observations, $^{**}P<0.01$. Inset: A sample Western immunoblot showing that THC increases Bax expression (lane 2) compared to vehicle-treated neurons (lane 1). The stimulatory effect of THC on Bax expression was prevented by AM 251 (lane 4). Exposure of cells to AM 251 alone had no effect on Bax expression (lane 3).

prevented the THC-induced increase in JNK2 activity at 2 h (14.65 $\pm$ 2.12; Figure 3b). These data suggest that the coupling of the CB_1 receptor to G-protein subtypes $G_{i/o}$ facilitates THC-induced JNK1 and JNK2 activation.

AM 251 prevents THC-induced Bax expression

JNK kinases have been linked to neuronal apoptosis by altering the expression of the Bcl family of mitochondrial-associated proteins (Mielke & Herdegen, 2000). In this study, expression levels of the proapoptotic protein Bax were measured by Western immunoblot in cells treated with THC (5 μM) for 2 h and the effect of the CB_1 antagonist AM 251 (10 μM) was assessed. Figure 4 demonstrates that Bax expression in control cells was 23.82 $\pm$ 4.89 (arbitrary units; mean $\pm$ s.e.m.) and this was significantly increased following THC treatment for 2 h to 50.18 $\pm$ 6.43 ($P<0.01$, ANOVA, $n=5$). AM 251 alone had no effect on Bax expression (15.39 $\pm$ 4.96); however, it prevented the THC-induced increase in Bax expression (22.67 $\pm$ 6.01). A sample Western immunoblot demonstrating the CB_1-dependent increase in Bax expression is shown as an inset in Figure 4.

JNK AS downregulates JNK protein expression

Since JNK activation was observed following THC treatment, we employed the use of antisense technology to analyse

whether JNK has an upstream role in the regulation of apoptotic effectors. Cells were exposed to 2 μM of either JNK1 AS or JNK2 AS to downregulate JNK1 and JNK2 protein expression in order to delineate the specific role of each isoform in the cell death pathway. Upon treatment with JNK1 and JNK2 AS, cellular levels of JNK1 and JNK2 protein were markedly reduced (Figure 5a, b). In cells treated with JNK1 SC, JNK1 expression was 19.20 $\pm$ 2.89 (arbitrary units; mean $\pm$ s.e.m.) and this was significantly decreased by 79% when JNK1 AS was incorporated into the media for 48 h ($P<0.05$, Student's t-test, $n=4$; Figure 5a). Similarly, JNK2 AS significantly decreased JNK2 protein expression by 70%, compared to the cells treated with JNK2 SC for 48 h ($P<0.05$, Student's t-test, $n=5$; Figure 5b). The antisense-mediated depletion of JNK1 and JNK2 was specific since JNK2 AS had no effect on JNK1 protein expression (Figure 5a) and, similarly, JNK1 AS had no effect on JNK2 protein expression (Figure 5b). Sample immunoblots demonstrating the antisense-mediated downregulation of JNK1 and JNK2 protein expression are shown as insets in Figure 5a and b.

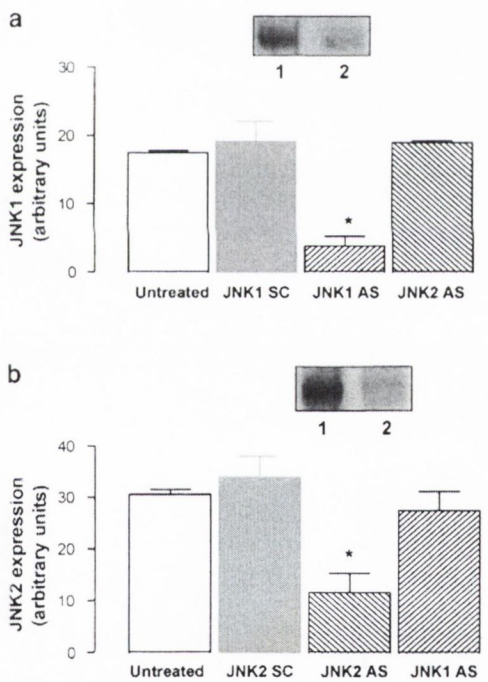

Figure 5 JNK AS effectively reduces JNK protein expression. Neurons were incubated with 2 μM JNK1/JNK2 antisense (AS) or JNK1/JNK2 scrambled control (SC) for 48 h. Cells were harvested in lysis buffer and the total expression of JNK1 and JNK2 protein was examined by Western blot analysis. (a) Treatment with JNK1 AS significantly decreased JNK1 protein expression in comparison to untreated cells and cells treated with JNK1 SC. JNK2 AS had no effect on JNK1 protein expression. Results are expressed as mean $\pm$ s.e.m. for four experiments, $^*P<0.05$. Inset: A sample immunoblot demonstrating that JNK1 AS significantly reduces JNK1 protein expression (lane 2) compared to JNK1 SC-treated neurons (lane 1). (b) JNK2 AS significantly reduced JNK2 protein expression. JNK1 AS had no effect on JNK2 protein expression. Results are expressed as mean $\pm$ s.e.m. for four experiments, $^*P<0.05$. Inset: A sample immunoblot demonstrating the significant reduction in JNK2 protein expression in JNK2 AS-treated neurons (lane 2) compared to JNK2 SC-treated cells (lane 1).

JNK AS prevents THC-induced caspase-3 activation

Apoptotic cell death is typically accompanied by the activation of the cysteine protease caspase-3 (Janicke *et al.*, 1998). Our lab has previously shown the pivotal role of this enzyme in the cell death pathway triggered by THC within the rat cortex (Campbell, 2001; Downer *et al.*, 2001). Here we analysed whether JNK1 or JNK2 is involved in the THC-induced activation of caspase-3. Following downregulation of each of the JNK isoforms using appropriate AS, the role of JNK1 and JNK2 in THC-induced caspase-3 activation was assessed (Figure 6a, b).

The data presented in Figure 6a indicate that treatment with THC (5 μM) for 2 h significantly increased caspase-3 activity from 22.50 $\pm$ 1.67 (mean $\pm$ s.e.m.) to 50.66 $\pm$ 6.86 pmol AFC produced (mg protein)$^{-1}$ min^{-1} ($P<0.05$, ANOVA; $n=8$). In cells treated with JNK1 SC (2 μM) alone for 48 h, caspase-3 activity was comparable to control values (25.09 $\pm$ 5.80 pmol AFC produced (mg protein)$^{-1}$ min^{-1}). Pretreatment with JNK1 AS (2 μM) for 48 h prior to THC treatment prevented the THC-induced increase in caspase-3 activity (31.79 $\pm$ 6.53 pmol AFC produced (mg protein)$^{-1}$ min^{-1}; Figure 6a).

Similarly, Figure 6b demonstrates that a 2 h exposure of cortical neurons to THC (5 μM) significantly increased caspase-3 activity from 22.05 $\pm$ 1.48 (mean $\pm$ s.e.m.) to 63.05 $\pm$ 11.10 pmol AFC produced (mg protein)$^{-1}$ min^{-1} ($P<0.05$, ANOVA, $n=7$). Neurons incubated with JNK2 SC (2 μM) for 48 h showed a level of caspase-3 activity similar

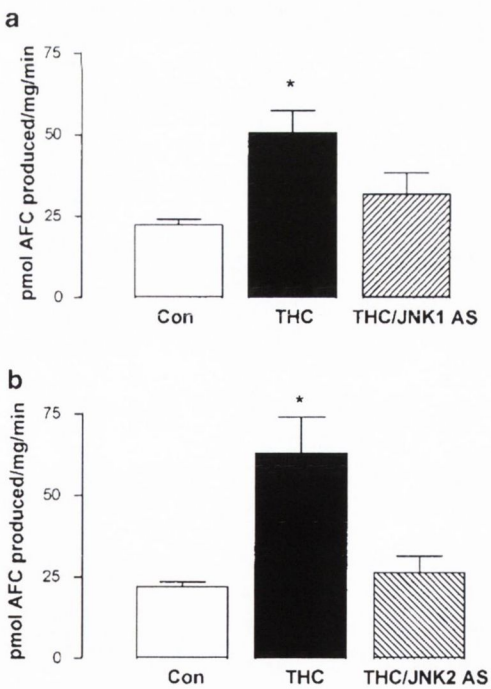

Figure 6 JNK is required for caspase-3 activity in THC-induced apoptosis. (a) Treatment of cortical neurons with THC (5 μM) for 2 h significantly increased caspase-3 activity, as assessed by the cleavage of the fluorogenic DEVD substrate. The stimulatory effect of THC on caspase-3 activity was prevented by pretreatment with JNK1 AS (2 μM; 48 h). Results are expressed as mean $\pm$ s.e.m. for eight observations, $^*P<0.05$. (b) Similarly, pretreatment of cells with JNK2 AS (2 μM; 48 h) prior to THC treatment abolished the stimulatory effect of THC on caspase-3 activity. Results are expressed as mean $\pm$ s.e.m. for seven observations, $^*P<0.05$.

to that measured in vehicle-treated neurons (32.73±8.74 pmol AFC produced (mg protein)$^{-1}$ min^{-1}). Pretreatment with JNK2 AS (2 μM) for 48 h prior to THC treatment prevented the THC-induced increase in caspase-3 activity (26.06±5.20 pmol AFC produced (mg protein)$^{-1}$ (min)$^{-1}$; Figure 6b). These results demonstrate a role for both JNK1 and JNK2 in the THC-induced activation of caspase-3.

JNK AS prevents THC-induced DNA fragmentation

The TUNEL technique was used to demonstrate that the THC-induced DNA fragmentation that we have previously reported (Campbell, 2001) involves JNK1 and JNK2 (Figure 7). In control cells, 19±2% (mean±s.e.m.) of cells displayed fragmented DNA (TUNEL-positive), and this was significantly increased to 50±6% in cells treated with THC (5 μM) for 3 h ($P<0.001$, ANOVA, $n=5$ coverslips; Figure 7a). AS-mediated depletion of JNK1 or JNK2 prevented the THC-induced increase in DNA fragmentation. Thus, exposure of cells to JNK1 AS (2 μM) for 48 h prior to THC treatment prevented the THC-induced increase in TUNEL staining (26±7% TUNEL-positive cells; Figure 7a, b). In contrast, in cells pretreated with JNK1 SC (2 μM), the THC-induced increase in DNA fragmentation was retained (46±6% TUNEL-positive cells, $P<0.001$, ANOVA, $n=5$ coverslips; Figure 7a). Treatment with JNK1 AS (2 μM) alone for 48 h had no effect of the percentage of neurons displaying fragmented DNA (26±6% TUNEL-positive cells.

Similarly, in cells pretreated with JNK2 AS (2 μM) for 48 h before THC (5 μM) treatment, 20±3% of cells were TUNEL-positive (Figure 7a, c). In contrast, cells preincubated with JNK2 SC oligonucleotides (2 μM) for 48 h prior to treatment with THC showed a significant increase in DNA fragmentation (56±3% TUNEL-positive cells, $P<0.001$, ANOVA, $n=5$ coverslips; Figure 7a). Treatment of neurons with JNK2 AS (2 μM) alone for 48 h did not have a neurotoxic effect (20±3% TUNEL-positive cells.

These results demonstrate that depletion of either JNK1 or JNK2 prevents the THC-induced DNA fragmentation. These data are consistent with the caspase-3 result and suggest that both JNK1 and JNK2 are intricately involved in regulating the THC-induced activation of caspase-3 and resultant DNA fragmentation in the apoptotic pathway.

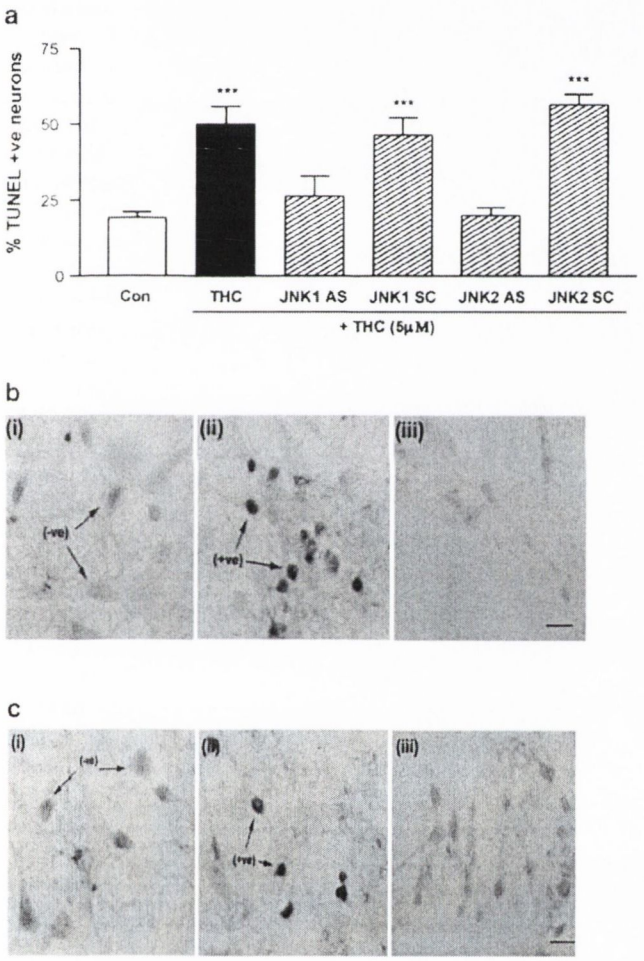

Figure 7 JNK activity is required for THC-induced DNA fragmentation. (a) Exposure of neurons to THC (5 μM) for 3 h significantly increased the percentage of cells with DNA fragmentation. Treatment with JNK1 AS or JNK2 AS (2 μM; 48 h) prior to THC treatment prevented the THC-induced increase in DNA fragmentation. In contrast, in neurons treated with JNK1 SC or JNK2 SC (2 μM; 48 h), THC still evoked a significant increase in DNA fragmentation. Results are expressed as mean±s.e.m. for five observations, ***$P<0.001$. (b) Representative images of (i) control, (ii) THC-treated and (iii) THC/JNK1 AS-treated cortical neurons following TUNEL staining for DNA fragmentation. Arrows indicate TUNEL-negative (−ve) and TUNEL-positive (+ve) cells. Scale bar is 50 μM. (c) Representative images of TUNEL staining of (i) control, (ii) THC-treated and (iii) THC/JNK2 AS-treated cortical neurons. Scale bar is 50 μM.

JNK1 AS pretreatment has no effect on THC-induced JNK2 activity

Since THC was found to increase JNK1 activity (at 5 min) prior to JNK2 activity (at 2 h), we employed the use of antisense technology to analyse whether JNK1 is involved upstream in the regulation of JNK2 activity (Figure 8). Neurons were treated with JNK1 AS (2 μM; 48 h) to down-regulate JNK1 protein expression prior to exposure to THC (5 μM) for 2 h. Treatment of cells with THC for 2 h significantly increased phospho-JNK2 expression from 21.87±2.38 (arbitrary units; mean bandwidth±s.e.m.) to 31.14±2.85 ($P<0.05$, ANOVA, $n=4$). Neurons treated with JNK1 AS alone for 48 h showed a level of JNK2 activity comparable to that found in vehicle-treated neurons (23.99±2.31, $n=4$) and JNK1 AS

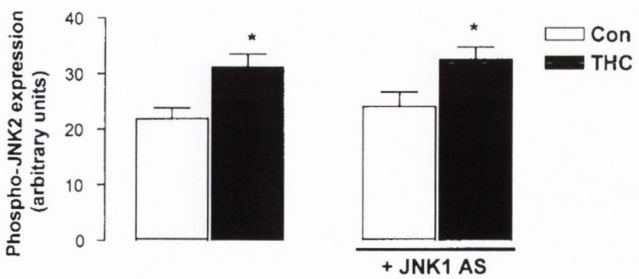

Figure 8 JNK1 is not upstream of JNK2 in THC-induced apoptosis. Neurons were preincubated with JNK1 AS (2 μM) for 48 h, treated with THC (5 μM) for 2 h and analysed for phosphorylated JNK2 expression using Western immunoblot. THC evoked a significant increase in phospho-JNK2 expression. In cells exposed to JNK1 AS, THC was still capable of inducing a significant increase in phospho-JNK2. Results are expressed as mean±s.e.m. for four observations, *$P<0.05$.

failed to prevent the THC-induced increase in phospho-JNK2 expression (32.49 ± 1.90, $P<0.05$, ANOVA, $n=4$). These data suggest that JNK1 does not occupy an upstream role in the regulation of JNK2 activity, despite the differential time course of activation of these JNK isoforms.

Discussion

The aim of this study was to examine the ability of the CB_1 cannabinoid receptor to couple to the JNK signalling pathway, and to assess the role of JNK in THC-induced neurotoxicity in cultured cortical neurons. THC was found to induce the activation of JNK1 and JNK2 within 5 min and 2 h, respectively. The ability of THC to induce activation of both JNK isoforms was blocked by AM 251 and PTX. THC significantly increased Bax expression in an AM 251-sensitive manner. Treatment of cortical neurons with specific AS targeted to rat JNK1 or JNK2 mRNA effectively reduced the protein expression of the respective JNK isoform. AS-mediated reduction of JNK1 and JNK2 protein expression prevented the THC-induced activation of caspase-3 and downstream DNA fragmentation. Data herein suggest that the CB_1 cannabinoid receptor is coupled to JNK in cortical neurons, and that both JNK1 and JNK2 are involved in the regulation of the downstream effectors that are pertinent in the THC-induced apoptotic pathway.

Recently, there has been a growing interest in the proclivity of cannabinoids to control the cell survival/death decision, particularly in neurons. Several studies have revealed that THC can induce neurotoxic effects in a number of cultured cell systems. Specifically, THC has a toxic effect on cultured hippocampal neurons (Chan *et al.*, 1998), cultured cortical neurons (Campbell, 2001) and glioma cells (Sanchez *et al.*, 1998). THC has also been shown to inhibit neuronal cell growth *in vivo* (Galve-Roperh *et al.*, 2000), in addition to its antiproliferative action in neuronal cultures. Furthermore, anandamide, an endogenous ligand of cannabinoid receptors (Devane *et al.*, 1992), induces apoptosis in PC12 cells (Sarker *et al.*, 2003) and lymphocytes (Schwarz *et al.*, 1994). THC-induced apoptosis in hippocampal (Chan *et al.*, 1998) and cortical (Downer *et al.*, 2001) cultures is CB_1 receptor-dependent. Proposed mechanisms of cannabinoid-induced neurotoxicity have included the generation of reactive oxygen species (Chan *et al.*, 1998), activation of the caspase-3 cell death pathway (Campbell, 2001; Downer *et al.*, 2001), sphingomyelin hydrolysis (Sanchez *et al.*, 1998), sustained ceramide accumulation (Galve-Roperh *et al.*, 2000) and activation of the JNK cascade (Sarker *et al.*, 2003).

It should be considered that in contrast to the data supporting cannabinoid-induced neurodegeneration, the bulk of the experimental evidence indicates that cannabinoids may protect neurons from toxic insults. However, it is not clear if this is a CB_1 receptor-dependent process. Nagayama *et al.* (1999) have shown that synthetic cannabinoid receptor agonists decrease hippocampal loss following transient global cerebral ischaemia *via* the CB_1 receptor, and increase cell viability in cerebral cortical cultures subjected to 8 h of hypoxia and glucose deprivation in a CB_1 receptor-independent manner. Cannabinoid receptor agonists are neuroprotective against excitotoxicity *in vivo* (Panikashvili *et al.*, 2001; van der Stelt *et al.*, 2001) and *in vitro* (Shen & Thayer, 1998; Abood *et al.*, 2001), which is prevented by CB_1 antagonists. Furthermore, THC and nonpsychotropic cannabinoids decrease glutamate toxicity in rat cortical neuronal cultures in a receptor-independent process that is not blocked by CB_1 receptor antagonists (Hampson *et al.*, 1998). Overall, it appears that neurotoxic and neuroprotective effects of cannabinoids can be observed, and these differences are likely to depend on a variety of influences, including the nature of the toxic insult, the cell type under study and the particular cannabinoid used.

The cannabinoid CB_1 receptor is distributed mainly in the central nervous system and is localised in brain regions most likely involved in contributing to the psychoactive effects of THC (Twitchell *et al.*, 1997). The rat cortex shows an intense pattern of CB_1 receptor expression, in particular in frontal regions where the CB_1 receptor subtype is found in cortical axons, cell bodies and dendrites (Tsou *et al.*, 1998).

The JNK protein kinases belong to the family of mitogen-activated protein kinases (MAPK) and represent a group of enzymes that are activated by cytokines and environmental stresses (Ip & Davis, 1998). The function of these kinases is to convert extracellular stimuli to intracellular signals that, in turn, control the expression of genes that are essential for many cellular responses, including cell growth and death (Marshall, 1995). These widely distributed kinases are activated by dual phosphorylation on threonine and tyrosine residues by upstream kinases as part of the cellular response to stress (Derkinderen *et al.*, 1999). JNKs are encoded by three different genes *jnk1, jnk2* and *jnk3*, and the products of each gene reveal isoforms with approximate molecular weights of 46 (JNK1), 54 (JNK2) and 57 kDa (JNK3), all of which are found in the mammalian brain (Gupta *et al.*, 1996). Although it is recognised that the JNK3 isoform is distributed throughout the rat cerebral cortex (Carboni *et al.*, 1998), JNK3 protein expression was moderate in our cell culture model, hence the relative contribution of the JNK1 and JNK2 isoforms to the apoptotic process was investigated.

In this study, the time course of THC-induced activation of JNK1 and JNK2 in cultured cortical neurons was assessed. JNK activity was assessed up to the 2 h time point as this is within the timeframe at which we have found significant levels of THC toxicity in cortical neuronal cultures (Campbell, 2001). It was found that THC increases JNK1 and JNK2 activity after 5 min and 2 h of treatment, respectively. Half-maximal stimulation of JNK1 occurred at a lower dose of THC than JNK2, indicating that THC-induced JNK2 activation was more reluctant than JNK1 activation in our cell culture model. It has been established that JNK activation may occur early (Xia *et al.*, 1995) or late (Virdie *et al.*, 1997) in apoptosis, and the finding that THC activates JNK1 and JNK2 within dissimilar timeframes suggests that the JNK isoforms may mediate different signals in cultured cortical neurons. A potential function of JNK may be to initiate programmed cell death (Johnson *et al.*, 1996), and our data demonstrating the early activation of JNK1 (within 5 min), may reflect a role for JNK1 in regulating downstream apoptotic effectors. However, our finding that THC activates JNK2 at 2 h of treatment is consistent with the time point at which maximal neuronal cell death has been previously shown in cortical neurons (Campbell, 2001). It is therefore possible that JNK2 activation may have occurred in response to DNA fragmentation, which is consistent with other studies (Ghahremani *et al.*, 2002).

Furthermore, considering that JNK activity may be regulated by caspase-3 (Ozaki *et al.*, 1999; Hatai *et al.*, 2000), it is possible that JNK2 activity is modulated by caspase-3 in this system. In refute of these hypotheses, antisense-mediated downregulation of JNK2 prevented the THC-induced increase in caspase-3 activation and DNA fragmentation, suggesting that JNK2 is upstream of these components of the apoptotic cascade. It is possible that an early cellular redistribution of JNK2, as opposed to an increase in overall JNK2 activity, may be involved in the apoptotic process. It is of note that although JNK2 activity was increased at 2 h, a concomitant decline in JNK1 activity was observed at this time point. This suggests a functional interaction between JNK1 and JNK2 isoforms and this is supported by evidence that JNK2 negatively regulates JNK1 phosphorylation (Hochedlinger *et al.*, 2002). However, our finding that AS-induced depletion of JNK1 failed to prevent the THC-induced increase in JNK2 activity suggests that JNK1 does not occupy an upstream role in regulating JNK2.

The involvement of JNK cascades in the regulation of cell proliferation *via* G-protein-coupled receptors has been demonstrated (Coso *et al.*, 1996). Our previous studies have demonstrated that the toxic effects of THC involve a PTX-sensitive G-protein (Campbell, 2001). This is consistent with evidence that links the central CB_1 receptor to activation of G-protein subtypes $G_{i/o}$ (Howlett, 1995). To date, the role of G-proteins in neuronal cell death has not been completely clarified since PTX-sensitive G-proteins have been found to exert both proapoptotic (Farkas *et al.*, 1998) and antiapoptotic effects (Jakob & Kreiglsten, 1997). However, data presented here demonstrate that coupling of the CB_1 receptor to PTX-sensitive G-proteins facilitates JNK activation.

JNK has the proclivity to phosphorylate a variety of nuclear and cytoplasmic substrates, some of which are vital for the apoptotic actions of JNK. It has been reported that JNK promotes cell death by promoting cytochrome *c* release from the mitochondria (Tournier *et al.*, 2000). In the nervous system, the proapoptotic mitochondrial-associated protein Bax acts downstream of JNK in regulating the translocation of mitochondrial cytochrome *c* into the cytosol (Kang *et al.*, 1998), and several studies have demonstrated an interaction between JNK and Bax in the cell death cascade (Lei *et al.*, 2002). The apoptotic events that are evoked by THC in cortical neurons include the release of mitochondrial cytochrome *c* into the cytosol following CB_1 receptor activation (Downer *et al.*, 2001), and our finding that THC induces Bax expression following CB_1 activation is a likely mechanism for this event.

Once in the cytosol, cytochrome *c* complexes with a cytosolic factor designated as apoptotic protease activating factor-1 (APAF-1), which in turn triggers the activation of the cysteine protease caspase-3, which contributes to the drastic morphological changes associated with apoptosis by disabling a number of key substrates (Zou *et al.*, 1997). We have previously shown that caspase-3 is central to the apoptotic cascade triggered by THC in cortical neurons (Campbell, 2001; Downer *et al.*, 2001). To elucidate the respective roles of JNK1 and JNK2 in THC-induced caspase-3 activation, we employed antisense technology to downregulate temporarily JNK1 and JNK2 expression. In neurons treated with JNK1 and JNK2 AS, JNK1 and JNK2 protein expression was selectively downregulated. Depletion of JNK1 and JNK2 prevented the THC-induced activation of caspase-3, indicating that both JNK1 and JNK2 isoforms are upstream of caspase-3 in the THC-induced apoptotic cascade.

We have recently shown that THC promotes degeneration of cultured cortical neurons in a time-dependent manner, with a maximal effect occurring 3 h post-treatment (Campbell, 2001). The evidence presented here and by others (Rueda *et al.*, 2000) supports an early interaction between THC and JNK, indicating that JNK activation is an upstream event in the degenerative pathway. The finding that the downregulation of JNK1 and JNK2 using antisense technology effectively blocked THC-induced activation of caspase-3 and downstream DNA fragmentation indicates that both JNK1 and JNK2 are intricately involved in the transduction of THC-induced apoptotic signals. It is of particular note that depletion of either JNK1 or JNK2 isoforms completely abrogated the THC-induced caspase-3 activation and DNA fragmentation. It may be expected that, since THC has the proclivity to couple to both JNK1 and JNK2, depletion of one isoform may result in THC coupling to the remaining isoform to evoke caspase-3 activation and resultant DNA fragmentation. This clearly was not the case and our result may reflect an interaction between JNK1 and JNK2 with respect to the regulation of upstream effectors involved in caspase-3 activation. Indeed, a requirement for both JNK1 and JNK2 has been implicated in the phosphorylation of the p53 tumour suppressor protein (Buschmann *et al.*, 2001), a potential upstream event in the regulation of caspase-3 activity. Furthermore, it has been shown that inhibition of the active forms of both JNK1 and JNK2 prevents cytochrome *c* release from the mitochondria and activation of enzymes upstream of caspase-3 (Bozyczko-Coyne *et al.*, 2001). This study provides evidence of a requirement for both JNK1 and JNK2 in the THC-induced activation of caspase-3 and DNA fragmentation, and may reflect cooperativity between JNK1 and JNK2 in relation to these aspects of the cell death cascade.

To date, little is known about the role of JNK in THC signalling. Rueda *et al.* (2000) have found that JNK1/2 are activated within 5 min of THC treatment and that sustained JNK activation over 3 days of THC insult is required to induce cell death in glioma cells. This suggests that the duration of JNK induction may be the determining factor in the cell death/survival decision. These differences may reflect differential cellular responses of neuronal populations to THC, with cortical neurons being susceptible to early insult of cannabinoid exposure due to the differential activation of the JNK1/2 signalling cascades. We are aware that in the same study of Rueda *et al.* (2000), rat cortical primary neurons were not susceptible to a 3-day exposure to THC, which may reflect the lower dose of THC used in that study. It has recently been found that the endogenous cannabinoid, anandamide, induces apoptosis in PC12, and this is accompanied by the activation of the JNK pathway (Sarker *et al.*, 2003). Furthermore, JNK activity is not affected by THC in hippocampal slices prepared from the adult rat brain (Derkinderen *et al.*, 2001). Thus, the effects of cannabinoids may be dependent on neuronal maturity, with neonatal cultures being susceptible to JNK activation following cannabinoid challenge.

The dose of THC used in the present study to induce the activation of JNK1 and JNK2 was within the concentration range we have previously shown to be neurotoxic to cultured cortical neurons (Campbell, 2001) and is also consistent with the human plasma concentrations of THC (low μM; Chiang & Barnett, 1984). Furthermore, the data demonstrate that THC is toxic for cortical cultures obtained from neonatal rats. Interestingly to date, there is no evidence to suggest that THC is neurotoxic in the adult rat central nervous system (Galve-Roperh *et al.*, 2000). Our findings support the proposal that the apoptotic effects of THC may be operative early during development and may play a modulatory role in neural development (Fernandez-Ruiz *et al.*, 1999). Indeed the consumption of marijuana by women during pregnancy and/or lactation has been shown to affect the neurobehavioural development of their children (Fried, 1995).

In summary, treatment of cortical cultures with THC activates the JNK pathway *via* the CB_1 cannabinoid receptor. An antisense approach revealed that JNK1 and JNK2 are required for the THC-induced activation of caspase-3 and DNA fragmentation in cortical neurons. These findings identify a cannabinoid receptor-dependent transduction pathway associated with THC-induced neurotoxicity.

This study was supported by the Health Research Board Ireland and Enterprise Ireland.

References

ABOOD, M.E. & MARTIN, B.R. (1992). Neurobiology of marijuana abuse. *Trends Pharmacol. Sci.*, **13**, 201–206.

ABOOD, M.E., RIZVI, G., SALLAPUDI, N. & MCALLISTER, S. (2001). Activation of the CB_1 cannabinoid receptor protects cultured mouse spinal neurons against excitotoxicity. *Neurosci. Lett.*, **309**, 197–201.

BOUABOULA, M., POINOT-CHAZEL, C., BOURRIE, B., CANAT, X., CALANDRA, B., RINALDI-CARMONA, M., LE FUR, G. & CASELLAS, P. (1995). Activation of mitogen-activated protein kinases by stimulation of the central cannabinoid receptor CB_1. *Biochem. J.*, **312**, 637–641.

BOUABOULA, M., POINOT-CHAZEL, C., MARCHAND, J., CANAT, X., BOURRIE, B., RINALDI-CARMONA, M., CALANDRA, B., LE FUR, G. & CASELLAS, P. (1996). Signaling pathway associated with stimulation of CB_2 peripheral cannabinoid receptor: involvement of both mitogen-activated protein kinase and induction of Krox-24 expression. *Eur. J. Biochem.*, **237**, 704–711.

BOZYCZKO-COYNE, D., O'KANE, T.M., WU, Z.L., DOBRZANSKI, P., MURTHY, S., VAUGHT, J.L. & SCOTT, R.W. (2001). CEP-1347/KT-7515, an inhibitor of SAPK/JNK pathway activation, promotes survival and blocks multiple events associated with Aβ-induced cortical neuron apoptosis. *J. Neurochem.*, **77**, 849–863.

BUSCHMANN, T., POTAPOVA, O., BAR-SHIRA, A., IVANOV, V.L., FUCHS, S.Y., HENDERSEN, S., FRIED, V.A., MINAMOTO, T., ALARCON-VARGAS, D., PINCUS, M.R., GAARDE, W.A., HOLBROOKE, N.J., SHILOH, Y. & RONAI, Z. (2001). Jun NH_2-terminal kinase phophorylation of p53 on thr-81 is important for p53 stabilization and transcriptional activities in response to stress. *Mol. Cell. Biol.*, **21**, 2743–2754.

CAMPBELL, V.A. (2001). Tetrahydrocannabinol-induced apoptosis in cultured cortical neurones is associated with cytochrome *c* release and caspase-3 activation. *Neuropharmacology*, **40**, 702–709.

CARBONI, L., CARLETTI, R., TACCONI, S., CORTI, C. & FERRAGUTI, F. (1998). Differential expression of SAPK isoforms in the rat brain. An *in situ* hybridisation study in the adult rat brain and during postnatal development. *Mol. Brain Res.*, **60**, 57–68.

CHAN, G.C., HINDS, T.R., IMPEY, S. & STORM, D.R. (1998). Hippocampal neurotoxicity of Δ^9-tetrahydrocannabinol. *J. Neurosci.*, **18**, 5322–5332.

CHIANG, C.W. & BARNETT, G. (1984). Marijuana effect and delta-9-tetrahydrocannabinol plasma level. *Clin. Pharmacol. Ther.*, **36**, 234–238.

COSO, O.A., TERAMOTO, H., SIMONDS, W.F. & GUTKIND, J.S. (1996). Signaling from G protein-coupled receptors to c-Jun kinase involves $\beta\gamma$ subunits of heterotrimeric G proteins acting on a Ras and Rac1-dependent pathway. *J. Biol. Chem.*, **271**, 3963–3966.

DERKINDEREN, P., ENSLEN, H. & GIRAULT, J.-A. (1999). The ERK/MAP-kinases cascade in the nervous system. *Neuroreport*, **10**, R24–R34.

DERKINDEREN, P., LEDENT, C., PARMENTIER, M. & GIRAULT, J.-A. (2001). Cannabinoids activate p38 mitogen-activated protein kinases through CB_1 receptors in hippocampus. *J. Neurochem.*, **77**, 957–960.

DEVANE, W.A., HANUS, L., BREUER, A., PERTWEE, R.G., STEVENSON, L.A., GRIFF, C., GIBSON, D., MANDELBAUM, A., ETINGER, A. & MECHOULAM, R. (1992). Isolation and structure of a brain constituent that binds to the cannabinoid receptor. *Science*, **258**, 1946–1949.

DILL, J.A. & HOWLETT, A.C. (1988). Regulation of adenylate cyclase by chronic exposure to cannabimimetic drugs. *J. Pharmacol. Exp. Ther.*, **244**, 1157–1163.

DOWNER, E., BOLAND, B., FOGARTY, M. & CAMPBELL, V. (2001). Δ^9-Tetrahydrocannabinol induces the apoptotic pathway in cultured cortical neurones via activation of the CB1 receptor. *Neuroreport*, **12**, 3973–3978.

FARKAS, I., BARANYI, L., TAKAHASHI, M., FUKUDA, A., LIPOSITS, Zs., YAMAMOTO, T. & OKADA, H. (1998). A neuronal C5a receptor and an associated apoptotic signal transduction pathway. *J. Physiol.*, **507**, 679–687.

FERNANDEZ-RUIZ, J.J., BERRENDERO, F., HERNANDEZ, M.L., ROMERO, J. & RAMOS, J.A. (1999). Role of endocannabinoids in brain development. *Life Sci.*, **65**, 725–736.

FRIED, P.A. (1995). The Ottawa Prenatal Prospective Study (OPPS): methodological issues and findings – Its easy to throw the baby out with the bath water. *Life Sci.*, **56**, 2159–2168.

GALVE-ROPERH, I., SANCHEZ, C., LUISA CORTES, M., GOMEZ DEL PULGAR, T., IZQUIERDO, M. & GUZMAN, M. (2000). Anti-tumoral action of cannabinoids: involvement of sustained ceramide accumulation and extracellular signal-regulated kinase activation. *Nat. Med.*, **6**, 313–319.

GESSA, G.L., CASU, M.A., CARTA, G. & MASCIA, M.S. (1998). Cannabinoids decrease acetylcholine release in the medial-prefrontal cortex and hippocampus, reversal by SR 141716A. *Eur. J. Pharmacol.*, **355**, 119–124.

GHAHREMANI, M.H., KERAMARIS, E., SHREE, T., XIA, Z., DAVIS, R.J., FLAVELL, R., SLACK, R.S. & PARK, D.S. (2002). Interaction of the c-Jun/JNK pathway and cyclin-dependent kinase in death of embryonic cortical neurones evoked by DNA damage. *J. Biol. Chem.*, **277**, 35586–35596.

GOMEZ DEL PULGAR, T., VELASCO, G. & GUZMAN, M. (2000). The CB_1 cannabinoid receptor is coupled to the activation of protein kinase B/Akt. *Biochem. J.*, **347**, 369–373.

GUPTA, S., BARRETT, T., WHITMARSH, A.J., CAVANAGH, J., SLUSS, H.K., DERIJARD, B. & DAVIS, R.J. (1996). Selective interaction of JNK protein kinase isoforms with transcription factors. *EMBO J.*, **15**, 2760–2770.

HAMPSON, A.J., GRIMALDI, M., AXELROD, J. & WINK, D. (1998). Cannabidiol and (−)Δ^9-tetrahydrocannabinol are neuroprotective antioxidants. *Proc. Natl. Acad. Sci. U.S.A.*, **95**, 8268–8273.

HATAI, T., MATSUZAWAI, A., INOSHITA, S., MOCHHIDA, Y., KURODA, T., SAKAMAKI, K., KUIDA, K., YONEHARA, S., ICHIJO, H. & TAKEDA, K. (2000). Execution of Apoptosis Signal-regulating Kinase 1 (ASK1)-induced apoptosis by mitochondria-dependent caspase activation. *J. Biol. Chem.*, **275**, 26576–26581.

HOCHEDLINGER, K., WAGNER, E.F. & SABAPATHY, K. (2002). Differential effects of JNK1 and JNK2 on signal specific induction of apoptosis. *Oncogene*, **21**, 2441–2445.

HOWLETT, A.C. (1990). Reverse pharmacology of the cannabinoid receptor. *Trends Pharmacol. Sci.*, **11**, 395–397.

HOWLETT, A.C. (1995). Pharmacology of cannabinoid receptors. *Annu. Rev. Pharmacol. Toxicol.*, **35**, 607–634.

HRENIUK, D., GARAY, M., GAARDE, W., MONIA, B.P., MCKAY, R.A. & CIOFFI, C.L. (2001). Inhibition of c-Jun N-terminal kinase 1, but not c-Jun N-terminal kinase 2, suppresses apoptosis induced by ischemia/reoxygenation in rat cardiac myocytes. *Mol. Pharmacol.*, **59**, 867–874.

IP, Y.T. & DAVIS, R.J. (1998). Signal transduction by the c-Jun N-terminal kinase (JNK) – from inflammation to development. *Curr. Opin. Cell Biol.*, **10**, 205–219.

JAKOB, R. & KREIGLSTEN, J. (1997). Influence of flupirtine on a G-protein coupled inwardly rectifying potassium current in hippocampal neurones. *Br. J. Pharmacol.*, **122**, 1333–1338.

JANICKE, R.U., SPRENGART, M.L., WATU, M.R. & PORTER, A.G. (1998). Caspase-3 is required for DNA fragmentation and morphological changes associated with apoptosis. *J. Biol. Chem.*, **273**, 9357–9360.

JENTSCH, J.D., VERRICO, C.D., LE, D. & ROTH, R.H. (1998). Repeated exposure to Δ^9-tetrahydrocannabinol reduces prefrontal cortical dopamine metabolism in the rat. *Neurosci. Lett.*, **246**, 169–172.

JOHNSON, N.L., GARDNER, A.M., DIENER, K.M., LANGE-CARTER, C.A., GLEAVY, J., JARPE, M.B., MINDEN, A., KARIN, M., ZON, L.I. & JOHNSON, G.L. (1996). Signal transduction pathways regulated by mitogen-activated/extracellular response kinase kinase kinase induce cell death. *J. Biol. Chem.*, **271**, 3229–3237.

KANG, C.-D., JANG, J.-H., KIM, K.-W., LEE, H.-J., JEONG, C.-S., KIM, C.-M., KIM, S.-H. & CHUNG, B.-S. (1998). Activation of c-Jun N-terminal kinase/stress-activated protein kinase and the decreased ratio of Bcl-2 to Bax are associated with the auto-oxidized dopamine-induced apoptosis in PC12 cells. *Neurosci. Lett.*, **256**, 37–40.

LEI, K., NIMUAL, A., ZONG, W.X., KENNEDY, N.J., FLAVELL, R.A., THOMPSON, C.B., BAR-SAGI, D. & DAVIS, R.J. (2002). The Bax subfamily of Bcl2-related proteins is essential for apoptotic signal transduction by c-Jun NH(2)-terminal kinase. *Mol. Cell. Biol.*, **22**, 4929–4942.

MACKIE, K., LAI, Y., WESTENBROEK, R. & MITCHELL, R. (1995). Cannabinoids activate an inwardly rectifying potassium conductance and inhibit Q-type currents in AtT20 cells transfected with rat brain cannabinoid receptor. *J. Neurosci.*, **15**, 6552–6561.

MARSHALL, C.J. (1995). Specificity of receptor protein kinase signaling: transient versus sustained extracellular signal-regulated kinase activation. *Cell*, **80**, 179–185.

MATSUDA, L.A., LOIAIT, S.J., BROWNSTEIN, M.J., YOUNG, A.C. & BONNER, T.I. (1990). Structure of a cannabinoid receptor and functional expression of the cloned cDNA. *Nature*, **346**, 561–564.

MIELKE, K. & HERDEGEN, T. (2000). JNK and p38 stress kinases – degenerative effectors of signal-transduction-cascades in the nervous system. *Prog. Neurobiol.*, **61**, 46–60.

MUNRO, S., THOMAS, K.L. & ABU-SHAAR, M. (1993). Molecular characterization of a peripheral receptor for cannabinoids. *Nature*, **365**, 61–65.

NAGAYAMA, T., SINOR, A.D., SIMON, R.P., CHEN, J., GRAHAM, S.H., JIN, K. & GREENBER, D.A. (1999). Cannabinoids and neuroprotection in global and focal cerebral ischemia and in neuronal cultures. *J. Neurosci.*, **19**, 2987–2995.

NEW, D.C. & WONG, Y.H. (2003). BML-190 and AM251 act as inverse agonists at the human cannabinoid CB2 receptor: signalling *via* camp and inositol phosphate. *FEBS Lett.*, **536**, 157–160.

OZAKI, I., TANI, E., IKEMOTO, H., KITAGAWA, H. & FUJIKAWA, H. (1999). Activation of stress-activated protein kinase/c-Jun NH_2-terminal kinase and p38 kinase in calphostin c-induced apoptosis requires caspase-3-like proteases but is dispensable for cell death. *J. Biol. Chem.*, **274**, 5310–5317.

PANIKASHVILI, D., SIMEONIDOU, C., BEN-SHABAT, S., HANUS, L., BREUER, A., MECHOULAM, R. & SHOHAMI, E. (2001). An endogenous cannabinoid (2-AG) is neuroprotective after brain injury. *Nature*, **413**, 527–531.

RUEDA, D., GALVE-ROPERH, I., HARO, A. & GUZMAN, M. (2000). The CB_1 cannabinoid receptor is coupled to the activation of c-Jun N-terminal kinase. *Mol. Pharmacol.*, **58**, 814–820.

SANCHEZ, C., GALVE-ROPERH, I., CANOVA, C., BRACHET, P. & GUZMAN, M. (1998). Δ^9-Tetrahydrocannabinol induces apoptosis in C6 glioma cells. *FEBS Lett.*, **436**, 6–10.

SARKER, K.P., BISWAS, K.K., YAMAKUCHI, M., LEE, K.-Y., HAHIGUCHI, T., KRACHT, M., KITAJIMA, I. & MARUYAMA, I. (2003). ASK1-p38 MAPK/JNK signaling cascade mediates anandamide-induced PC 12 cell death. *J. Neurochem.*, **85**, 50–61.

SCHWARZ, H., BLANCO, F.J. & LOTZ, M. (1994). Anandamide, an endogenous cannabinoid receptor agonist inhibits lymphocytes proliferation and induces apoptosis. *J. Neuroimmunol.*, **55**, 107–115.

SHEN, M., PISER, T.M., SEYBOLD, V.S. & THAYER, S.A. (1996). Cannabinoid receptor agonists inhibit glutamatergic synaptic transmission in rat hippocampal cultures. *J. Neurosci.*, **16**, 4322–4334.

SHEN, M. & THAYER, S.A. (1998). Cannabinoid receptor agonists protect cultured rat hippocampal neurons from excitotoxicity. *Mol. Pharmacol.*, **54**, 459–462.

TOURNIER, C., HESS, P., YANG, D.D., XU, J., TURNER, T.K., NIMUAL, A., BAR-SAGI, D., JONES, S.N., FLAVELL, R.A. & DAVIS, R.J. (2000). Requirement of JNK for stress-induced activation of the cytochrome *c*-mediated death pathway. *Science*, **288**, 870–873.

TSOU, K., BROWN, S., SANUDO-PENA, M.C., MACKIE, K. & WALKER, J.M. (1998). Immunohistochemical distribution of cannabinoid CB_1 receptors in the rat central nervous system. *Neuroscience*, **83**, 393–411.

TURKANIS, S.A., PARTLOW, L.M. & KARLER, R. (1991). Delta-9-tetrahydrocannabinol depresses inward sodium current in mouse neuroblastoma cells. *Neuropharmacology*, **30**, 73–77.

TWITCHELL, W., BROWN, S. & MACKIE, K. (1997). Cannabinoids inhibit N- and P/Q-type calcium channels in cultured rat hippocampal neurons. *J. Neurophysiol.*, **78**, 43–50.

VAN DER STELT, M., VELDHEIS, W.B., BAR, P.R., VELDINK, G.A., VLIEGENTHART, J.F.G. & NICOLAY, K. (2001). Neuroprotection by Δ^9-tetrahydrocannabinol, the main active compound in marijuana, against ouabain-induced *in vivo* excitotoxicity. *J. Neurosci.*, **21**, 6475–6479.

VIRDIE, K., BANNISTER, A.J., HUNT, S.P. & TOLKOVSKL, A.M. (1997). Comparison between the timing of JNK activation, c-Jun phosphorylation, and the onset of death commitment in sympathetic neurones. *J. Neurochem.*, **66**, 550–561.

XIA, Z., DICKENS, M., RAINGEAUD, J., DAVIS, R.J. & GREENBERG, M.E. (1995). Opposing effects of ERK and JNK-p38 MAP kinases on apoptosis. *Science*, **270**, 1326–1331.

ZOU, H., HENZEL, W.J., LIU, X., LUTSCHG, A. & WANG, X. (1997). Apaf-1, a human protein homologous *C. elegans* CED-4, participates in cytochrome *c*-dependent activation of caspase-3. *Cell*, **90**, 405–413.

(Received May 8, 2003
Revised July 10, 2003
Accepted July 21, 2003)

Biochem. J. (2003) **371**, 789–798 (Printed in Great Britain)

A role for c-Jun N-terminal kinase 1 (JNK1), but not JNK2, in the β-amyloid-mediated stabilization of protein p53 and induction of the apoptotic cascade in cultured cortical neurons

Marie P. FOGARTY, Eric J. DOWNER and Veronica CAMPBELL[1]

Department of Physiology, Trinity College Institute of Neuroscience, Trinity College, Dublin 2, Ireland

β-Amyloid (Aβ) peptide has been shown to induce neuronal apoptosis; however, the mechanisms underlying Aβ-induced neuronal cell death remain to be fully elucidated. The stress-activated protein kinase, c-Jun N-terminal kinase (JNK), is activated in response to cellular stress and has been identified as a proximal mediator of cell death. In the present study, expression of active JNK was increased in the nucleus and cytoplasm of Aβ-treated cells. Evaluation of the nature of the JNK isoforms activated by Aβ revealed a transient increase in JNK1 activity that reached its peak at 1 h and a later activation (at 24 h) of JNK2. The tumour suppressor protein, p53, is a substrate for JNK and can serve as a signalling molecule in apoptosis. In cultured cortical neurons, we found that Aβ increased p53 protein expression and phosphorylation of p53 at Ser^{15}. Thus it appears that Aβ increases p53 expression via phosphorylation-mediated stabilization of the protein. Given the lack of availability of a JNK inhibitor that can distinguish between JNK1- and JNK2-mediated effects, we employed antisense technology to deplete cells of JNK1 or JNK2 selectively. Using this strategy, the respective roles of JNK1 and JNK2 on the Aβ-mediated activation of the apoptotic cascade (i.e. p53 stabilization, caspase 3 activation and DNA fragmentation) were examined. The results obtained demonstrate a role for JNK1 in the Aβ-induced stabilization of p53, activation of caspase 3 and DNA fragmentation. In contrast, depletion of JNK2 had no effect on the proclivity of Aβ to activate capase 3 or induce DNA fragmentation. These results demonstrate a significant role for JNK1 in Aβ-mediated induction of the apoptotic cascade in cultured cortical neurons.

Key words: antisense, apoptosis, β-amyloid, c-Jun N-terminal kinase, p53, caspase-3.

INTRODUCTION

Deposition of β-amyloid (Aβ) protein around neurons is a feature of Alzheimer's disease (AD) [1]. Although the 1–42 fibrillar form of Aβ is the most abundant in the AD senile plaque, the 1–40 peptide also has the proclivity to form fibrils and is present in the senile plaque, but to a lesser extent than the 1–42 species [2]. In AD brains, neuropathological hallmarks of apoptosis such as DNA fragmentation have been detected [3] and Aβ is assumed to contribute directly to this pathology by inducing neuronal apoptosis [4]. In support of the hypothesis that Aβ deposition drives the neurodegenerative process, both $Aβ_{1-40}$ and $Aβ_{1-42}$ have been shown to induce neuronal apoptosis *in vitro* [5,6]. There has been a significant interest in identifying the pathways that underlie neuronal responses to Aβ in an attempt to develop novel neuroprotective therapeutic strategies. To date, many signalling pathways have been proposed as mediators of Aβ-induced neuronal apoptosis and these include reactive oxygen species [7], Ca^{2+}-sensitive proteases [8] and cysteine proteases [9]. The stress-activated protein kinase, c-Jun N-terminal kinase (JNK), has been proposed as a mediator of cell death in response to a variety of stimuli such as growth factor deprivation [10], excitotoxicity [11] and oxidative stress [12]. Recent studies [13–15] have also suggested that JNK plays a role in Aβ-mediated effects. In sympathetic neurons and PC12 cells, the 1–42 fragment of Aβ activates JNK and the synthetic JNK inhibitor, CEP-1347, blocks Aβ-mediated neurotoxicity [14]. Three JNK isoforms have been identified, JNK1, JNK2 and JNK3, and these are encoded by independent genes. Since each of these isoforms is expressed in the brain [16], Aβ has the potential to couple with JNK1, JNK2 or JNK3. Thus although the study of Troy et al. [14] provides compelling evidence of a role for JNK in Aβ-mediated neurodegeneration, the synthetic JNK inhibitor used in their study is unable to distinguish between the different JNK isoforms. In the present study, we used antisense technology to determine the respective roles of the JNK isoforms in $Aβ_{1-40}$-mediated neurodegeneration of cultured cortical neurons.

The multifunctional tumour suppressor protein, p53, has been suggested to play a role in the cell death pathway as well as having a role in the regulation of the cell cycle and DNA repair [17]. An increase in p53 expression has been reported in the brain of patients with AD [18] and in transgenic mice that overexpress Aβ [19]. cDNA expression of a dominant-negative p53 mutant [20] and application of a chemical inhibitor of p53 [21] offer protection against Aβ-mediated toxicity. Taken together, these studies provide compelling evidence of a role for p53 in Aβ-mediated neurodegeneration. However, the mechanisms that underlie Aβ-mediated activation of p53 remain to be elucidated. p53 has the proclivity to regulate a variety of functions and this diversity in function arises from the presence of several phosphorylation sites on p53 [22]. Thus phosphorylation on Ser^{15} is associated with the apoptotic effect of p53 [23], whereas phosphorylation at Ser^{392} promotes formation of the p53 tetramer that activates transcription from several cell-cycle-regulating genes in response to DNA damage [24]. The stress-activated protein kinase, p38, has been shown to phosphorylate p53 at Ser^{15} during hypoxic cell

Abbreviations used: Aβ, β-amyloid; AD, Alzheimer's disease; JNK, c-Jun N-terminal kinase; TUNEL, terminal transferase deoxytidyl uridine end-labelling.

[1] To whom correspondence should be addressed (e-mail vacmpbll@tcd.ie).

© 2003 Biochemical Society

death [25]] and chemical stress-induced apoptosis [26]. p53 is also a substrate for JNK [27] and there is evidence for a role for JNK signalling in the regulation of p53 stability and apoptotic capacity [28]. Given that Aβ can couple with the JNK pathway [13,15], the aim of the present study was to evaluate the role of the JNK isoforms, JNK1 and JNK2, in the Aβ-mediated activation of p53 and induction of the apoptotic cascade.

The results from the present study demonstrate a differential time frame of JNK1 and JNK2 activation by Aβ in this system with JNK1 being activated rapidly by Aβ (within minutes), whereas JNK2 activation was delayed by 24 h. Aβ caused an increase in p53 protein expression and phosphorylation of p53 at Ser^{15}. Use of JNK antisense demonstrated that the regulation of p53 by $A\beta_{1-40}$ was mediated via JNK1 as was the Aβ-mediated activation of caspase 3 and DNA fragmentation. These results demonstrate that Aβ has a differential pattern of signalling via the JNK pathway and provide evidence for an interaction between JNK1 and p53 in this system.

EXPERIMENTAL

Culture of cortical neurons

Primary cortical neurons were established from postnatal 1-day-old Wistar rats and maintained in neurobasal medium (Gibco BRL, Paisley, Renfrewshire, Scotland, U.K.). Rats were decapitated and cerebral cortices removed. The dissected cortices were incubated in PBS containing trypsin (0.25 %) for 20 min at 37 °C. The tissue was then triturated (5×) in PBS containing soyabean trypsin inhibitor (0.1 %) and DNase (0.2 mg/ml) and gently filtered through a sterile mesh filter. After centrifugation (2000 *g* for 3 min at 20 °C), the pellet was resuspended in neurobasal medium, supplemented with heat-inactivated horse serum (10 %, v/v), penicillin (100 units/ml), streptomycin (100 units/ml) and glutamax (2 mM). Suspended cells were plated out at a density of 0.25×10^6 cells on circular 10 mm diameter coverslips, coated with 60 μg/ml of poly(L-lysine) and incubated in a humidified atmosphere containing 5 % CO_2/95 % air at 37 °C. After 48 h, 5 ng/ml of cytosine arabinofuranoside was included in the culture medium to prevent proliferation of non-neuronal cells. Culture media were exchanged every 3 days and cells were grown in culture for 12 days before Aβ treatment.

Drug treatment

$A\beta_{1-40}$ (BioSource International, U.K.) was made up as a 1 mM stock solution in PBS and allowed to aggregate for 48 h at 30 °C. For treatment of cortical neurons, Aβ was diluted to a final concentration of 2 μM in prewarmed neurobasal medium. This concentration has been previously used to induce activation of the apoptotic cascade in these cells [8].

Antisense-mediated depletion of JNK1 and JNK2

20-mer phosphorothioate oligonucleotides were purchased from Biognostik (Gottingen, Germany), and the sequences used were complementary with the mRNA encoding rat JNK1 and JNK2 proteins [26]. The sequences used were: JNK1 antisense oligonucleotide, 5′-CTCATGATGGCAAGCAATTA-3′; JNK1 scrambled oligonucleotide, 5′-ACTACTACACTAGACTAC-3′; JNK2 antisense oligonucleotide, 5′-GCTCAGTGGACATGGATGAG-3′; and JNK2 scrambled oligonucleotide, 5′-GGACTACTAC-ACTAGACTAC-3′. Neurons were incubated with 1.2 μM oligonucleotide in serum-free prewarmed neurobasal medium containing 5 μg/ml of *N*-[1-(2,3-dioleoyloxy)propyl]-*N*,*N*,*N*-trimethylammonium/dioleoyl phosphatidylethanolamine (Life Technologies, Paisley, Renfrewshire, Scotland, U.K.). After 4 h, the medium was replaced with supplemented prewarmed neurobasal medium containing 1.2 μM oligonucleotide. The cells were incubated for a further 48 h before treatment with Aβ.

Western-immunoblot analysis of phospho-JNK and phospho-p53 expression

After incubation with Aβ, cortical neurons were harvested in lysis buffer (20 mM Hepes, 10 mM KCl, 1.5 mM $MgCl_2$, 1 mM EGTA, 1 mM EDTA, 1 mM dithiothreitol, 0.1 mM PMSF, 5 μg/ml pepstatin A, 2 μg/ml leupeptin and 2 μg/ml aprotinin; pH 7.4) and left on ice for 20 min. The cells were centrifuged (15 000 *g* for 20 min at 4 °C) and the supernatant was diluted to 50 μg of protein/ml with sample buffer [150 mM Tris/HCl (pH 6.8), 10 % (v/v) glycerol, 4 % (w/v) SDS, 5 % (v/v) 2-mercaptoethanol and 0.002 % (w/v) Bromophenol Blue]. Samples were then heated to 100 °C for 3 min. Proteins (1 μg/lane) were separated by electrophoresis on a 10 % (v/v) polyacrylamide minigel, transferred on to a nitrocellulose membrane and immunoblotted with an anti-active JNK monoclonal antibody (1 : 1000; Santa Cruz Biotechnology, CA, U.S.A.) purified from mouse serum, which recognizes the active forms of JNK1 (p46), JNK2 (p54) and JNK3 (p57) after phosphorylation on Thr^{183} and Tyr^{185}. To monitor expression of non-phosphorylated JNK, the blots were stripped and re-probed with an anti-JNK polyclonal antibody purified from rabbit serum (1 : 1000; Santa Cruz Biotechnology), which recognizes JNK1, JNK2 and JNK3. To monitor p53 phosphorylation, the anti-[phosphoSer^{15}]p53 (1 : 1000; Cell Signaling Technology, Beverly, MA, U.S.A.) and anti-[phosphoSer^{392}]p53 (Biosource International, Nivelles, Belgium) polyclonal antibodies purified from rabbit serum, which recognize p53 phosphorylated on Ser^{15} and Ser^{392} respectively, were used. Expression of the non-phosphorylated form of p53 was established using an anti-p53 polyclonal antibody purified from rabbit serum (Santa Cruz Biotechnology). Immunoreactive bands were detected using the horseradish peroxidase-conjugated anti-mouse IgG (for active JNK) or anti-rabbit IgG (for non-phosphorylated JNK, active p53 and non-phosphorylated p53) and enhanced chemiluminescence. Bandwidths were quantified by densitometry (D-Scan PC software).

p53 mRNA expression

Total RNA was extracted from cortical neurons using TRI Reagent (Sigma–Aldrich). cDNA synthesis was performed on 1 μg of total RNA using oligo(dT) primer according to the manufacturer's instructions (Life Technologies). The RNA was treated with RNase-free DNase I (Life Technologies) at 1 unit/μg of RNA for 15 min at 37 °C. Equal amounts of cDNA were used for PCR amplification for a total of 28 cycles. The cycling conditions were 95 °C for 5 min, followed by cycles of 95 °C for 1 min 15 s, 52 °C for 1 min 15 s and 72 °C for 1 min 30 s. A final extension step was performed at 70 °C for 10 min. Primers were pretested through an increasing number of amplification cycles to obtain reverse transcriptase–PCR products in the exponential range. The PCR products were analysed by electrophoresis on 1.5 % (w/v) agarose gels, visualized by ethidium bromide staining, photographed and quantified using densitometry. Primers used were as follows: rat p53 sense, 5′-GGCCATCTACAAGAAGTCAC-3′ and antisense, 5′-CCAGAAGATTCCCACTGGAG-3′; rat β-actin

© 2003 Biochemical Society

sense, 5′-GAAATCGTGCGTGACATTAAAGAGAAGCT-3′ and antisense, 5′-TCAGGAGGAGCAATGATCTTGA-3′ [30]. The primers generated a p53 PCR product of 317 bp and a β-actin PCR product of 360 bp. To control for any residual genomic DNA contamination, β-actin primers were chosen to span an intron. This meant that any amplification of genomic, rather than cDNA, would result in larger products than those expected. This semi-quantitative technique facilitated estimation of p53 mRNA expression using β-actin as a reference gene. No observable change in β-actin mRNA was observed in any of the treatment conditions.

Terminal transferase deoxytidyl uridine end-labelling (TUNEL)

Apoptotic cell death was assessed using the DeadEnd colorimetric apoptosis detection system (Promega, Madison, WI, U.S.A.). Cells were treated with Aβ for 72 h to evoke maximal DNA fragmentation [8]. Cells were then fixed with paraformaldehyde (4 %, w/v), permeabilized with Triton X-100 (0.1 %) and biotinylated nucleotide was incorporated at 3′-OH DNA ends using the enzyme terminal deoxynucleotidyl transferase. Horseradish peroxidase-labelled streptavidin then bound to the biotinylated nucleotide and this was detected using the peroxidase substrate H_2O_2 and the chromogen diaminobenzidine. Cells were then viewed under light microscopy at ×40 magnification, where the nuclei of TUNEL-positive cells stained brown. Apoptotic cells (TUNEL-positive) were counted and expressed as a percentage of the total number of cells examined. To exclude the possibility that the number of living cells present on the coverslip had an effect on the TUNEL-positive ratio, the same number of cells (approx. 400) was counted for each treatment.

Measurement of caspase 3 activity

Caspase 3 activity was assessed by immunocytochemistry using an anti-active caspase 3 antibody (Promega). Briefly, cells were treated with Aβ for 24 h, fixed with 4 % paraformaldehyde, blocked with 5 % (v/v) goat serum in PBS, incubated with anti-active caspase 3 antibody (1 : 200 dilution, overnight incubation at 4 °C). Immunoreactivity was detected using a biotinylated anti-rabbit IgG antibody and streptavidin conjugated to horseradish peroxidase. Immunoreactive cells were visualized with the chromogen diaminobenzidine, and the number of immunoreactive cells was counted and expressed as a percentage of the total number of cells examined (400–500 cells/coverslip).

Fluorescence immunocytochemistry

Cells were fixed with 4 % paraformaldehyde, permeabilized with 0.1 % Triton X-100 and non-reactive sites were blocked with 5 % goat serum in PBS. To determine the intracellular distribution of active JNK, the cells were incubated overnight with an anti-active JNK antibody (Santa Cruz Biotechnology) purified from mouse serum. To evaluate the efficacy of the antisense oligonucleotides in down-regulating JNK expression, immunolocalization of non-phosphorylated JNK1 and JNK2 was assessed using anti-JNK1 or anti-JNK2 monoclonal antibodies purified from mouse serum antibody (Santa Cruz Biotechnology). Cells were then incubated with anti-mouse IgG conjugated to FITC (Sigma-Aldrich) and viewed by fluorescence microscopy at an excitation of 510 nm.

Statistics

Statistical analysis was performed using ANOVA followed by the *post hoc* Student–Newman–Keuls test and the significance (at the 0.05 level) was indicated. When comparisons were being made between two treatments, a paired Student's t test was performed and $P < 0.05$ or $P < 0.01$ were considered significant.

RESULTS

Aβ activates JNK in cortical neurons

Cortical neurons were exposed to Aβ (2 μM) for 1 and 24 h and JNK activity was examined by fluorescence immunocytochemistry using an antibody that recognizes phosphorylated JNK (Figure 1A). In control conditions phospho-JNK immunoreactivity was detected in some cells, demonstrating a basal level of JNK activation. However, in cells treated with Aβ, a higher intensity of phospho-JNK immunoreactivity was observed in the cytoplasm and nucleus, a distribution which indicates that activated JNK has both cytosolic and nuclear substrates. Potential nuclear substrates of JNK include the transcription factor, c-Jun [16], which has been shown to be responsible for regulating gene expression in response to cellular insults such as Aβ accumulation [15]. The finding that activated JNK also localized in the cytosol may reflect the association of phospho-JNK with cytosolic substrates such as p53 [28].

Time course of Aβ-mediated activation of JNK1 and JNK2

Western-immunoblot analysis was employed to characterize the time course of Aβ-mediated JNK activation and to determine the nature of the JNK isoforms activated by Aβ in lysates prepared from cortical neurons. Aβ evoked a rapid increase in JNK1 activation, as assessed by expression of phosphorylated JNK1 (Figure 1B). Thus at 5 min, the expression of active JNK1 in control cells was 449 ± 36 (mean bandwidth ± S.E.M.; arbitrary units) and this was significantly increased to 541 ± 45 in Aβ-treated cells ($P < 0.05$, Student's paired t test, $n = 6$). Similarly, a significant increase in JNK1 activity was observed after Aβ treatment for 1 and 6 h. At the 1 h time point, JNK1 activity in control cells was 491 ± 12 and this was significantly increased to 593 ± 45 by Aβ ($P < 0.01$, Student's paired t test, $n = 6$). At the 6 h time point, JNK1 activity in control cells was 450 ± 15 and this was significantly increased to 522 ± 20 by Aβ ($P < 0.05$, Student's paired t test, $n = 6$). In contrast, cells treated with Aβ for 18, 24 and 48 h had no observable increase in JNK1 activation. This result demonstrates the temporal nature of the Aβ-mediated activation of JNK1. Although JNK1 activation in response to Aβ occurs rapidly and is sustained for several hours, the activation is decreased by 18 h. A sample immunoblot illustrating the time-dependent activation of JNK1 by Aβ is shown in Figure 1(D). Also shown is an immunoblot demonstrating that total JNK1 protein expression is unaffected by Aβ.

In contrast, a different pattern of JNK2 activation by Aβ was observed. Aβ had no effect on JNK2 activity at the earlier time points of 5 min–18 h; however, JNK2 activity was significantly increased by Aβ at the later time points of 24 and 48 h ($P < 0.05$, Student's t test, $n = 6$; Figure 1C). A sample immunoblot illustrating the time-dependent activation of JNK2 by Aβ is shown in Figure 1(D). Also shown is an immunoblot demonstrating that total JNK2 protein expression is unaffected by Aβ. It is to be noted that significant basal activity of JNK2 is observed in untreated cells; this is consistent with our immunocytochemical results,

© 2003 Biochemical Society

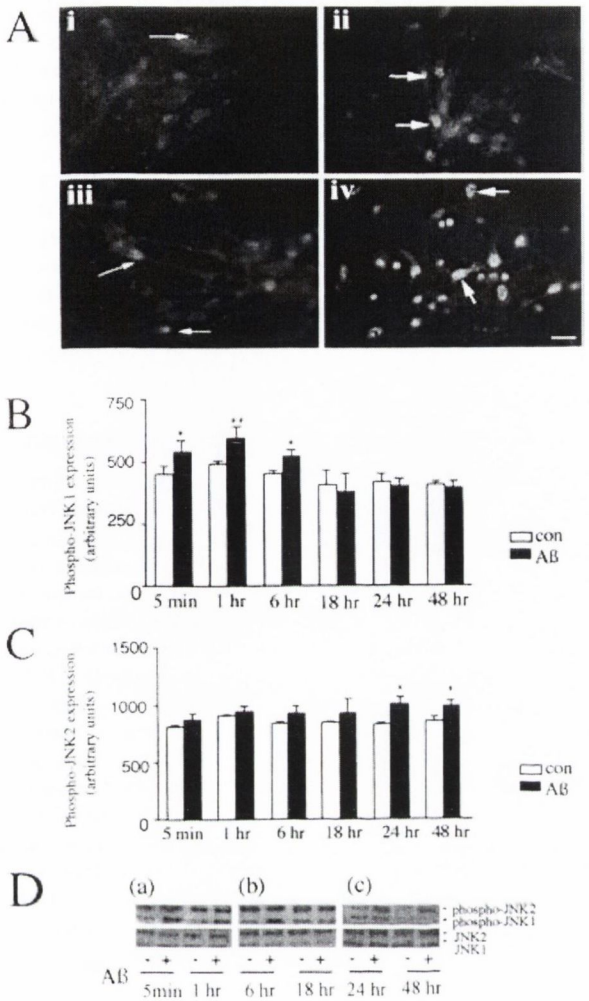

Figure 1 Aβ activates JNK1 and JNK2 within different time frames

(**A**) Cortical neurons were exposed to Aβ (2 μM) for 1 and 24 h and expression of phospho-JNK was monitored by immunofluorescence. In untreated cells (**i**, **iii**) active JNK immunoreactivity is apparent in a subpopulation of cells. In cells exposed to Aβ for 1 h (**ii**) or 24 h (**iv**) more intense phospho-JNK immunostaining is observed in the nucleus and in discrete areas within the cytosol. Arrows indicate cells displaying phospho-JNK immunoreactivity. Scale bar = 20 μm. (**B**) Cells were exposed to Aβ over a range of time points (5 min to 48 h) and phospho-JNK1 expression was monitored by Western-immunoblot analysis. Aβ caused a significant increase in phospho-JNK1 expression at 5 min, 1 and 6 h, but not at subsequent time points. Results are means ± S.E.M. from six independent observations. $^*P < 0.05$, $^{**}P < 0.01$. Statistical analysis was performed using Student's paired *t* test. (**C**) Cells were incubated with Aβ over a range of time points (5 min to 48 h) and phospho-JNK2 expression was monitored by Western-immunoblot analysis. Aβ caused a significant increase in phospho-JNK2 expression at 24 and 48 h, but not at earlier time points. Results are means ± S.E.M. from six independent observations. $^*P < 0.05$. Student's paired *t* test was used for statistical analysis. (**D**) Sample immunoblot demonstrating the Aβ-mediated increase in phospho-JNK1 expression with no concomitant change in expression of phospho-JNK2 or non-phosphorylated forms of JNK1 or JNK2 at (a) 5 min, 1 h, (b) 6 h and (c) 24 and 48 h.

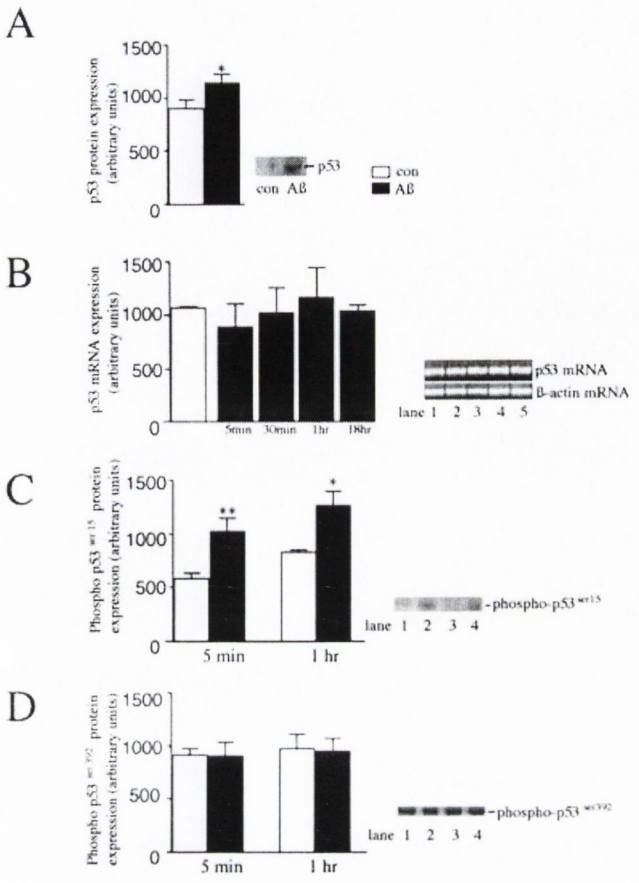

Figure 2 Aβ increases p53 expression and phosphorylation at Ser[15]

(**A**) Cells were exposed to Aβ (2 μM) for 1 h and p53 expression was assessed by Western-immunoblot analysis. Aβ evoked a significant increase in p53 expression. A sample immunoblot demonstrating the Aβ-mediated increase in p53 expression is shown as an inset. Results are means ± S.E.M. from six independent observations. $^*P < 0.05$. Statistical analysis was performed using Student's paired *t* test. (**B**) Cells were treated with Aβ for a range of time points (5 min to 18 h), total RNA was extracted and expression of p53 mRNA was examined by PCR. A representative image of the ethidium bromide-stained gel is shown as an inset. No change in basal (lane 1) p53 mRNA expression was observed after treatment with Aβ for 5 min (lane 2), 30 min (lane 3), 1 h (lane 4) or 18 h (lane 5). Results are means ± S.E.M. from six independent observations. (**C**) After incubation of the cells with Aβ, the expression of p53 phosphorylated on Ser[15] was examined by Western-immunoblot analysis. Aβ caused a significant increase in phosphorylation of p53 at Ser[15] at 5 min and 1 h. A sample immunoblot demonstrating the Aβ-mediated increase in [phosphoSer[15]]p53 is shown as an inset. At 5 min, basal expression of [phosphoSer[15]]p53 (lane 1) is increased by Aβ (lane 2). Similarly, at 1 h, basal expression of [phosphoSer[15]]p53 (lane 3) is increased by Aβ (lane 4). Results are means ± S.E.M. from eight independent observations. $^*P < 0.05$, $^{**}P < 0.01$. Statistical analysis was performed using Student's paired *t* test. (**D**) The effect of Aβ on phosphorylation of p53 at Ser[392] was assessed by Western-immunoblot analysis. Aβ had no effect on the expression of p53 phosphorylated at Ser[392] at 5 min or 1 h. A sample immunoblot demonstrating the lack of effect of Aβ on phosphorylation of p53 at Ser[392] is shown as an inset. At 5 min, basal expression of [phosphoSer[392]]p53 ('phospho-p53[ser392]') (lane 1) is unaffected by Aβ (lane 2). Similarly, at 1 h basal expression of [phosphoSer[15]]p53 ('phospho-p53[ser15]') (lane 3) is unaffected by Aβ (lane 4). Results are means ± S.E.M. from six independent observations.

where phospho-JNK immunoreactivity was detected in some cells in the absence of Aβ. Basal JNK activity also has been observed in other studies [31] and may reflect an endogenous role for JNK2 in regular cell physiology.

Effect of Aβ on p53 mRNA and protein expression

Since p53 is a target for modulation by JNK [27], the effect of Aβ on p53 expression and phosphorylation was examined in the present study (Figure 2). Figure 2(A) demonstrates that Aβ (2 μM, 1 h) evoked a significant 30% increase in p53 protein expression from 905 ± 78 (means ± S.E.M.; arbitrary units) to 1141 ± 88 ($P < 0.01$, Student's paired *t* test, $n = 6$). This increase in p53 expression was not attributable to a transcription event, since Aβ had no modulatory effect on p53 mRNA expression at any of the time points examined (5 and 30 min, 1 and 18 h; Figure 2B). There was no time-dependent

© 2003 Biochemical Society

effect on basal levels of p53 mRNA expression and hence the control data were pooled on the graph for clarity. Since p53 phosphorylation at Ser^{15} can stabilize p53 by preventing ubiquitin-mediated degradation [33], we examined the effect of Aβ on p53 phosphorylation using an antibody that recognizes phospho-Ser^{15} on p53 (Figure 2C). Aβ significantly increased expression of [phosphoSer^{15}]p53 from 587 ± 55 to 1030 ± 116 at 5 min ($P < 0.01$, Student's paired t test, $n = 8$) and from 837 ± 19 to 1265 ± 118 at 1 h ($P < 0.05$, Student's paired t test, $n = 6$). In contrast, Aβ failed to induce phosphorylation of p53 at Ser^{392} at these time points. This result suggests that Aβ increases p53 protein expression by stabilizing the p53 protein via phosphorylation at Ser^{15}.

Depletion of JNK1 and JNK2 by antisense oligonucleotides

To examine the respective roles of JNK1 and JNK2 in the Aβ-mediated modulation of p53 stabilization, antisense technology was employed. We first evaluated the effectiveness of the selected antisense oligonucleotide sequences in down-regulating expression of the JNK1 or JNK2 proteins using immunocytochemistry and Western-immunoblot analysis (Figure 3). Immunocytochemical analysis of JNK1 (Figure 3A, i and ii) and JNK2 (Figure 3A, iii and iv) expression revealed intracellular JNK1 and JNK2 immunoreactivity in control cells that was markedly down-regulated in cells transfected with the respective JNK1 and JNK2 antisense sequences. To quantify the antisense-mediated depletion of the respective JNK isoforms, Western-immunoblot analysis was employed. Figure 3(B) demonstrates that there was no difference in JNK1 expression in untreated cells when compared with cells treated with the scrambled JNK1 control oligonucleotide. However, in cells treated with the antisense JNK1 oligonucleotide for 48 h, JNK1 expression was significantly decreased by 80 % ($P < 0.01$, Student's paired t test; compared with cells treated with JNK1 scrambled oligonucleotide $n = 4$). Figure 3(C) demonstrates an identical result for JNK2. However, in cells treated with the antisense JNK2 oligonucleotide for 48 h, JNK2 expression was also significantly attenuated. Sample immunoblots demonstrating the efficacy of the JNK1 and JNK2 antisense oligonucleotides in down-regulating expression of JNK1 and JNK2 proteins respectively are shown as insets in Figures 3(B) and 3(C). We also verified that the JNK1 antisense had no effect on JNK2 expression (Figure 3D) and that the JNK2 antisense too had no effect on expression of JNK1 (Figure 3E). These results demonstrate that the JNK1 and JNK2 antisense sequences evoke a selective down-regulation in expression of their respective target proteins.

We confirmed that this extent of JNK depletion was sufficient to abrogate Aβ-mediated JNK activation (Figures 3F and 3G). Since the maximal activation of JNK1 and JNK2 occurred after 1 and 24 h treatment with Aβ respectively, the effect of JNK depletion on JNK1 and JNK2 activation was examined at these time points. For JNK1 (Figure 3F) in scrambled oligonucleotide-treated cells, Aβ (2 μM, 1 h) evoked a significant increase in expression of phospho-JNK1 ($P < 0.05$, ANOVA; compared with cells treated with JNK1 scrambled oligonucleotide alone, $n = 6$). However, in JNK1 antisense oligonucleotide-treated cells, the basal expression of activated phospho-JNK1 was 613 ± 39, and 503 ± 57 after incubation with Aβ (2 μM, 1 h, $n = 6$), demonstrating that the JNK1 antisense was effective in reducing the Aβ-mediated stimulation of JNK1 phosphorylation. Figure 3(G) demonstrates that in cells treated with the JNK2 scrambled oligonucleotide, expression of activated phospho-JNK2 was significantly increased by Aβ (2 μM, 24 h; $P < 0.05$, ANOVA; compared with cells

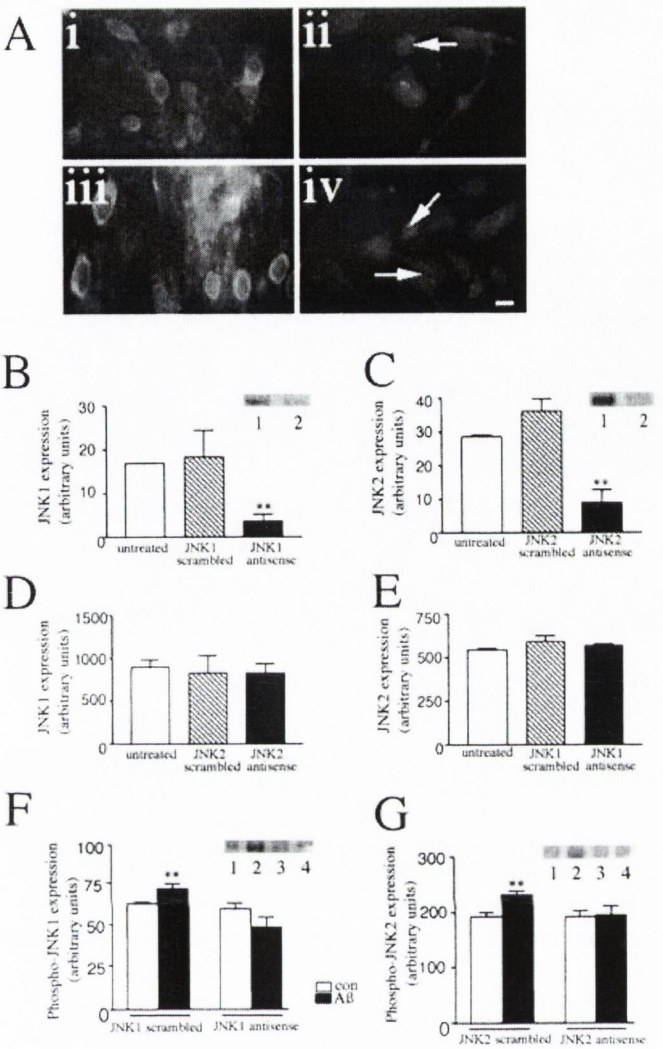

Figure 3 Determination of the efficacy of the JNK antisense sequences in down-regulating JNK1/JNK2 expression

(**A**) Cells were treated with either JNK1 or JNK2 antisense (2 μM) for 48 h and the consequence on JNK1 and JNK2 expression was examined by fluorescence immunocytochemistry using monoclonal JNK1 or JNK2 antibodies. (**i**) In untreated cells, JNK1 expression was localized throughout the cytoplasm with a high level of immunoreactivity at the inner plasma membrane; (**ii**) JNK1 immunostaining was significantly decreased in JNK1 antisense-treated cells; (**iii**) in untreated cells, JNK2 expression was abundant in the cytosol and inner plasma membrane; and (**iv**) JNK2 immunostaining was significantly decreased in JNK2 antisense-treated cells. Cells that have been successfully depleted of JNK are indicated by the arrows. Scale bar = 5 μm. (**B**) Antisense-mediated depletion of JNK1 was quantified by Western-immunoblot analysis. The JNK1 scrambled sequence had no effect on JNK1 expression; however, the JNK1 antisense significantly decreased JNK1 expression by approx. 80 %. A sample immunoblot demonstrating the JNK1 antisense-mediated depletion of JNK1 is shown as an inset. JNK1 is abundant in JNK1 scrambled-treated cells (lane 1) and JNK1 expression is down-regulated in JNK1 antisense-treated cells (lane 2). Results are expressed as means ± S.E.M. from four observations. $^{**}P < 0.01$. Student's paired t test was used for statistical analysis. (**C**) Antisense-mediated depletion of JNK2. The procedure is same as in (**B**). (**D**) Neither JNK2 scrambled nor JNK2 antisense oligonucleotides had any effect on JNK1 expression. Results are expressed as means (arbitrary units) ± S.E.M. from four observations. (**E**) Same as in (**D**), but with JNK2. (**F**) In JNK1 scrambled oligonucleotide-treated cells, Aβ (2 μM, 1 h) retained the ability to stimulate JNK1 activity, as assessed by phospho-JNK1 expression. However, JNK1 antisense abrogated the Aβ-mediated increase in JNK1 activity. Results are expressed as means ± S.E.M. from six observations. $^{**}P < 0.05$. Statistical analysis was performed using ANOVA. (**G**) In JNK2 scrambled oligonucleotide-treated cells, Aβ (2 μM, 24 h) retained the ability to stimulate JNK2 activity, as assessed by phospho-JNK2 expression. However, JNK2 antisense abrogated the Aβ-mediated increase in JNK2 activity. Results are expressed as means ± S.E.M. from six observations, $^{**}P < 0.05$. Statistical analysis was performed using ANOVA.

© 2003 Biochemical Society

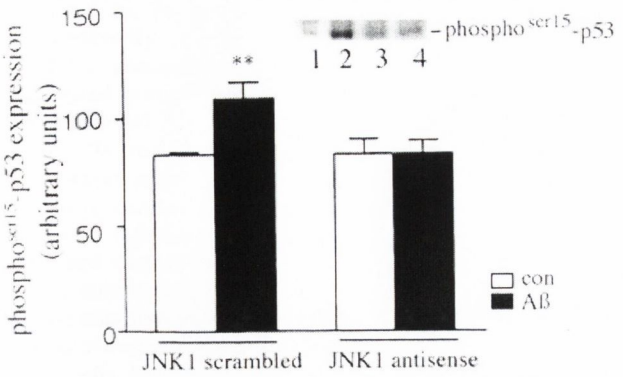

Figure 4 Depletion of JNK1 prevents the Aβ-mediated stimulation of p53 phosphorylation

The consequence of JNK1 depletion on the ability of Aβ to impact on p53 was examined by Western-immunoblot analysis using an antibody that recognizes p53 phosphorylated at Ser[15]. In control scrambled oligonucleotide-treated cells, Aβ (2 μM, 1 h) significantly increased [phosphoSer[392]]p53 expression. In contrast, JNK1 depletion prevented the Aβ-mediated increase in [phosphoSer[15]]p53 expression. Results are the means ± S.E.M. from six independent observations. $^{**}P < 0.05$. Statistical analysis was performed using ANOVA.

treated with JNK2 scrambled oligonucleotide alone, $n = 6$). However, in JNK2 antisense oligonucleotide-treated cells the expression of activated phospho-JNK2 was unaffected by Aβ (2 μM, 24 h, $n = 6$) and this result demonstrates that the JNK2 antisense had the capacity to reduce the Aβ-mediated stimulation of phospho-JNK2.

Having established the efficacy of the JNK1 and JNK2 antisense sequences in depleting expression of their respective target proteins and abrogating the stimulatory effect of Aβ on JNK1 and JNK2 phosphorylation, we used the antisense approach to determine the role of the JNK isoforms in Aβ-mediated activation of p53 and induction of the apoptotic cascade.

JNK1 is involved in Aβ-mediated phosphorylation of p53

Since JNK2 activation by Aβ was only observed at the later time point of 24 h, it seemed unlikely that JNK2 was involved in p53 phosphorylation, since the impact of Aβ on p53 occurred within 60 min. In contrast, Aβ-mediated activation of JNK1 was an earlier event that could potentially be upstream of p53 phosphorylation. Therefore the antisense approach was used to examine the role of JNK1 in the Aβ-mediated phosphorylation of p53 at Ser[15] (Figure 4). After treatment with Aβ (2 μM, 1 h), phospho-p53 expression is significantly increased from 84 ± 1 (means ± S.E.M.; arbitrary units) to 109 ± 8 ($P < 0.05$, ANOVA; compared with control cells, $n = 8$). Although the JNK1 antisense oligonucleotide alone had no effect on p53 phosphorylation, it abolished the stimulatory effect of Aβ on p53 phosphorylation at Ser[15]. A sample immunoblot demonstrating that JNK1 antisense abrogates the Aβ-mediated increase in phospho-p53 expression in shown as an inset in Figure 4.

Thus this result provides evidence of a role for JNK1 in the Aβ-mediated phosphorylation of p53 at Ser[15].

Role of JNK1 and JNK2 in Aβ-mediated activation of apoptotic cascade

A downstream consequence of JNK activation and p53 phosphorylation at Ser[15] is a commitment to the cell death pathway

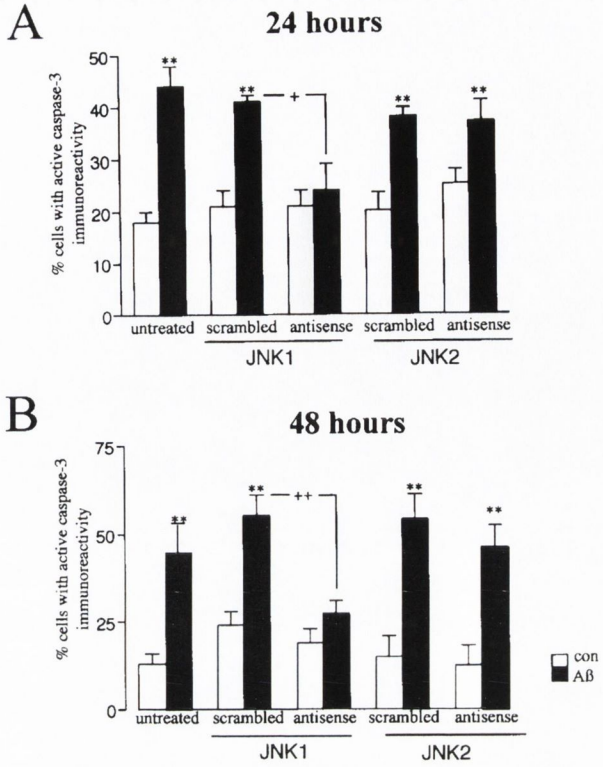

Figure 5 Consequences of JNK1 and JNK2 depletion on Aβ-induced activation on caspase 3 activation

(**A**) The percentage of cells displaying anti-active caspase 3 immunoreactivity was assessed by immunocytochemistry. In cells that had not been treated with oligonucleotide (untreated), Aβ (2 μM, 24 h) significantly increased the percentage of cells displaying active caspase 3 immunostaining by 40 %. In JNK1 scrambled oligonucleotide-treated cells, Aβ also evoked a significant increase in active caspase 3 immunoreactivity. However, this effect was abrogated in JNK1 antisense-treated cells. In contrast, neither the JNK2 scrambled nor the JNK2 antisense oligonucleotide had any effect on the proclivity of Aβ to evoke the increase in active caspase 3 immunoreactivity. Results are the means ± S.E.M. from six independent observations. $^{**}P < 0.05$; $^{+}P < 0.05$. (**B**) The effect of JNK1 and JNK2 depletion on the Aβ-mediated activation of caspase 3 at 48 h was assessed. Other details are the same as in (**A**). $^{**}P < 0.05$; $^{++}P < 0.05$. All statistical analyses were performed using ANOVA.

[17,32]. Since Aβ activates both JNK1 and JNK2 in cortical neurons, the respective roles of JNK1 and JNK2 in coupling Aβ with activation of the apoptotic cascade were examined using the JNK1 and JNK2 antisense oligonucleotides. The components of the apoptotic cascade that were examined in the present study were activation of the caspase 3 and DNA fragmentation.

Caspase 3 activity was examined by immunocytochemistry using an anti-active caspase 3 antibody. Figure 5(A) demonstrates that in untreated cells, the percentage of cells displaying active caspase 3 immunoreactivity was 18 ± 2 % (means ± S.E.M.) and this was significantly increased to 45 ± 4 % after treatment with Aβ for 24 h ($P < 0.05$, ANOVA; compared with untreated cells, $n = 6$ coverslips). After transfection with the JNK1 scrambled oligonucleotide, the Aβ-mediated stimulation of caspase 3 was retained ($P < 0.05$, ANOVA, $n = 6$ coverslips). In contrast, the JNK1 antisense oligonucleotide significantly decreased the Aβ-mediated stimulation of caspase 3 activity ($P < 0.05$, ANOVA; compared with cells treated with Aβ + JNK1 scrambled oligonucleotide, $n = 6$ coverslips). Thus in cells transfected with JNK1 antisense alone, the percentage of cells with active caspase 3 immunostaining was 21 ± 3 % and, in cells treated with Aβ in the presence of JNK1 antisense

© 2003 Biochemical Society

oligonucleotide, 24 ± 4 % of cells displayed active caspase 3 immunoreactivity ($n = 6$ coverslips). This result demonstrates that JNK1 is pertinent in the Aβ-mediated activation of caspase 3 in cultured cortical neurons. In contrast, depletion of JNK2 had no effect on Aβ-mediated activation of caspase 3 at 24 h. Thus in cells treated with JNK2 antisense alone, 25 ± 3 % of cells displayed active caspase 3 immunoreactivity and this was significantly increased to 38 ± 4 % in JNK2-depleted cells treated with Aβ for 24 h ($P < 0.05$, ANOVA; compared with cells treated with JNK2 antisense alone, $n = 6$). Since the Aβ-mediated stimulation of JNK2 was retained after depletion of JNK2, we conclude that JNK2 is not involved in the Aβ-mediated activation of caspase 3 that is found to occur at the 24 h time point.

Since cells had to be incubated with Aβ for 24 h before JNK2 activation was detected, our finding that JNK2 was not involved in the Aβ-mediated activation of caspase 3 at 24 h is not surprising. To determine whether JNK2 was involved in caspase 3 activation at later time points, we repeated the experiment by monitoring the effect of JNK1 and JNK2 antisense on Aβ-mediated activation of caspase 3 at 48 h, a time point that would be downstream of JNK2 activation. Figure 5(B) demonstrates that in untreated cells, the percentage of cells displaying active caspase 3 immunoreactivity was 13 ± 3 % (means ± S.E.M.) and this was significantly increased to 45 ± 8 % after treatment with Aβ for 48 h ($P < 0.05$, ANOVA; compared with untreated cells, $n = 6$ coverslips). After transfection with the JNK1 scrambled oligonucleotide, the Aβ-mediated stimulation of caspase 3 was retained ($P < 0.05$, ANOVA; $n = 6$ coverslips). In contrast, the JNK1 antisense oligonucleotide significantly decreased the Aβ-mediated stimulation of caspase 3 activity ($P < 0.05$, ANOVA; compared with cells treated with Aβ + JNK1 scrambled oligonucleotide, $n = 6$ coverslips). Thus in cells transfected with JNK1 antisense alone, the percentage of cells with active caspase 3 immunostaining was 19 ± 4 % and, in cells treated with Aβ in the presence of JNK1 antisense oligonucleotide, 25 ± 4 % of cells displayed active caspase 3 immunoreactivity ($n = 6$ coverslips). This result demonstrates that JNK1 is pertinent in the Aβ-mediated activation of caspase 3 in cultured cortical neurons at 48 h. In contrast, depletion of JNK2 had no effect on Aβ-mediated activation of caspase 3 at 48 h. Thus in cells treated with JNK2 antisense alone, 13 ± 6 % of cells displayed active caspase 3 immunoreactivity and this was significantly increased to 46 ± 6 % in JNK2-depleted cells treated with Aβ for 48 h ($P < 0.05$, ANOVA; compared with cells treated with JNK2 antisense, $n = 6$). These results demonstrate that JNK1, and not JNK2, is involved in the coupling of Aβ with caspase 3 activation.

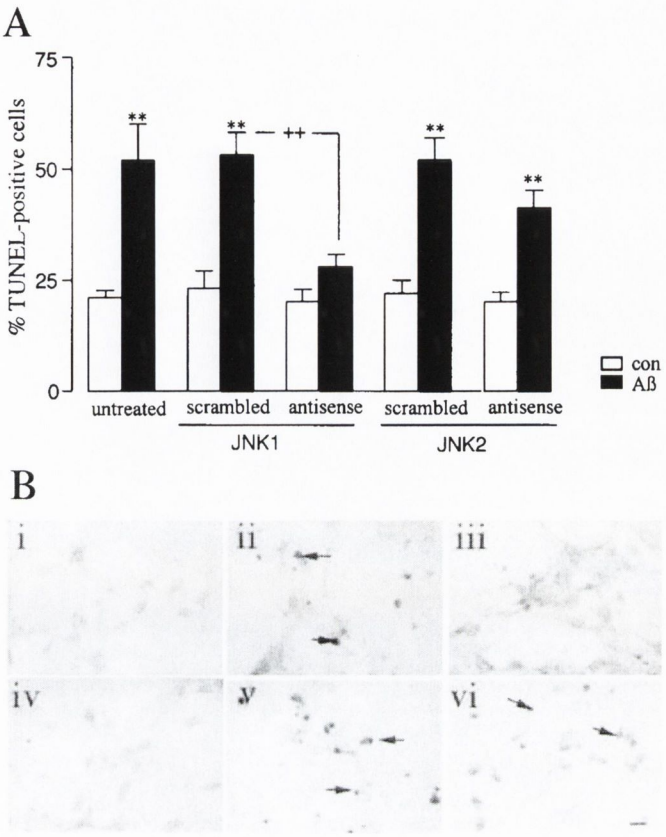

Figure 6 Effect of JNK1 and JNK2 depletion on Aβ-induced DNA fragmentation

(**A**) The effect of JNK1 and JNK2 depletion on the ability of Aβ ('Aß') to induce DNA fragmentation (TUNEL-positive) was assessed. In untreated cells, Aβ significantly increased the percentage of TUNEL-positive cells by 40 %. For JNK1 scrambled oligonucleotide, Aβ also evoked a significant increase in TUNEL-positive cells; however, this effect was significantly decreased in JNK1 antisense-treated cells. Neither the JNK2 scrambled nor the JNK2 antisense oligonucleotides had any effect on the proclivity of Aβ to evoke an increase in active DNA fragmentation. Results are the means ± S.E.M. from six independent observations. $^{**}P < 0.05$; $^{++}P < 0.05$. Statistical analysis was performed using ANOVA. con, control. (**B**) Representative TUNEL staining for cells treated with (i) JNK1 scrambled oligonucleotide, (ii) Aβ + JNK1 scrambled oligonucleotide, (iii) Aβ + JNK1 antisense oligonucleotide, (iv) JNK2 scrambled oligonucleotide, (v) Aβ + JNK2 scrambled oligonucleotide and (vi) Aβ + JNK2 antisense oligonucleotide. Scale bar = 20 μm.

Role of JNK1 and JNK2 in Aβ-mediated DNA fragmentation

One of the later stages in apoptosis is the fragmentation of nuclear DNA. We have previously shown that $A\beta_{1-40}$ has no effect on DNA fragmentation before 48 h, but a maximal 35 % increase in DNA fragmentation is observed after exposure of cortical neurons to $A\beta_{1-40}$ for 72 h [8]; we therefore chose to use that time point in the present study. The effect of Aβ on DNA fragmentation was analysed by TUNEL and the roles of JNK1 and JNK2 in Aβ-mediated DNA fragmentation were assessed after antisense-mediated depletion of the JNK1 and JNK2 isoforms (Figure 6). In untreated cortical neurons, the percentage of cells with fragmented DNA (TUNEL-positive cells) was 21 ± 2 % (means ± S.E.M.) and this was maximally increased to 52 ± 8 % by Aβ (72 h, 2 μM) ($P < 0.05$, ANOVA, $n = 6$ coverslips) as has been previously reported [5]. After transfection with the JNK1 scrambled control oligonucleotide, the Aβ-induced DNA fragmentation was retained ($P < 0.05$, ANOVA, $n = 6$ coverslips). In contrast, the JNK1 antisense oligonucleotide abolished the Aβ-mediated stimulation in DNA fragmentation. Thus in cells transfected with JNK1 antisense oligonucleotide, the percentage of cells with DNA fragmentation was 20 ± 2 % in control cells and 28 ± 3 % in Aβ-treated cells. This result demonstrates that JNK1 is pertinent in the induction of DNA fragmentation by Aβ. Since JNK1 was also found to have a role in the Aβ-mediated activation of caspase 3, a key executioner of apoptosis, the JNK1-dependent DNA fragmentation probably involves caspase 3 as an upstream component of this pathway. To determine the role of JNK2 in Aβ-mediated DNA fragmentation, the cells were transfected with the JNK2 antisense oligonucleotide. Figure 6 demonstrates that after depletion of JNK2, Aβ retained the ability to evoke a significant increase in DNA fragmentation ($P < 0.05$, ANOVA, $n = 6$). Thus JNK1 is the principal isoform involved in

© 2003 Biochemical Society

coupling Aβ with activation of caspase 3 and DNA fragmentation in cortical neurons.

DISCUSSION

The aim of the present study was to examine the roles of JNK1 and JNK2 in Aβ-mediated induction of the apoptotic cascade in cultured cortical neurons. In the absence of a suitable pharmacological inhibitor to distinguish between JNK1- and JNK2-mediated effects, antisense technology was employed to cause a selective down-regulation in expression of JNK1 and JNK2 to examine their respective roles in the apoptotic pathway. Aβ increased phospho-JNK expression in isolated cortical neurons with activated JNK immunoreactivity being localized to discrete regions within the nucleus and cytosol. This pattern of distribution is consistent with the distribution of phospho-JNK in response to other stress stimuli, where nuclear staining may reflect the ability of JNK to regulate transcription of stress-induced genes [33]. The punctate distribution of phospho-JNK that we detect in the cytosol after exposure to Aβ may represent mitochondrial targeting of JNK [34] or association of JNK with cytosolic substrates such as p53 [28]. The results obtained from Western-immunoblot analysis of cell lysates demonstrate a differential temporal activation of JNK1 and JNK2 in cultured cortical neurons. JNK1 was activated rapidly (within 5 min) by Aβ and sustained for several hours. By 18 h, the Aβ-mediated activation of JNK1 had returned to basal levels, demonstrating the temporal effectiveness of this signalling cascade. In contrast, Aβ failed to induce an early activation of JNK2 but JNK2 activity was increased by Aβ at the later time points of 24 and 48 h. The finding that Aβ activates JNK1 and JNK2 within dissimilar time frames suggests that JNK1 and JNK2 may have distinct roles in cellular stress responses to Aβ. Expression of p53 and phosphorylation of p53 at Ser^{15} were increased by Aβ. Phosphorylation of p53 at Ser^{15} has been reported as a proximal event in cellular apoptosis [23] and the ability of Aβ to phosphorylate p53 was abolished in JNK1-depleted cells. The effect of Aβ on downstream apoptotic events, namely caspase 3 activation and DNA fragmentation, was also significantly attenuated after JNK1 antisense treatment. In contrast, depletion of JNK2 had no effect on the ability of Aβ to activate caspase 3 or induce DNA fragmentation.

Our finding that $A\beta_{1-40}$ increases phospho-JNK expression in cortical neurons agrees closely with the effects of other Aβ fragments in neuronal systems. $A\beta_{1-42}$ and $A\beta_{25-35}$ have been reported to increase JNK activity in cortical neurons [13] and $A\beta_{1-42}$ increases JNK phosphorylation in sympathetic neurons and PC12 cells [14]. Although there are similarities in the effects of different Aβ peptides on the JNK pathway, it is to be noted that the time frame for JNK activation varies considerably between different Aβ peptide species. In the present study, we have demonstrated that JNK1 is activated within 5 min of exposure to $A\beta_{1-40}$, whereas the Aβ-mediated activation of JNK2 is not apparent until 24 h. In contrast, $A\beta_{25-35}$ increases JNK1 activity at 4 h, but not at earlier time points [13], and $A\beta_{1-42}$ causes peak activation of both JNK1 and JNK2 within 2–6 h in PC12 cells [14]. It is therefore probable that temporal variations in JNK activation may depend on the nature of the Aβ fragment and cell type.

There has been much interest in the signalling events that underlie Aβ-mediated induction of the apoptotic cascade. The present study and the work of other groups [13,15] provide evidence for Aβ impinging on the JNK signalling pathway. Induction of the apoptotic cascade has been attributed to activation of JNK in several systems [32]. In support of a role for JNK in Aβ-mediated cell death, synthetic inhibitors of JNK protect against Aβ-mediated cell [13], although the exact nature of the JNK isoforms that mediate the Aβ neurodegeneration remains to be established. In the present study, we have successfully employed antisense technology to cause a selective down-regulation in expression of JNK1 and JNK2 proteins. After antisense-mediated down-regulation of JNK1 and JNK2, the ability of Aβ to induce phosphorylation of JNK1 and JNK2 was selectively abolished. However, it was surprising that the antisense-mediated down-regulation in JNK1/2 protein expression was not accompanied by a reduction in basal phospho-JNK expression. This may reflect endogenous activity of the residual JNK that remained after antisense treatment or may be due to an enhanced stability of the phosphorylated form of JNK. Since the selected antisense oligonucleotides blocked Aβ-mediated activation of each of the JNK isoforms, this approach was used to elucidate the respective roles of JNK1 and JNK2 in the Aβ-mediated induction of apoptotic events such as phosphorylation of p53, caspase 3 activation and DNA fragmentation.

Our results demonstrate that $A\beta_{1-40}$ increases p53 expression and phosphorylation of p53 at Ser^{15} in cortical neurons. Aβ had no effect on p53 mRNA expression, although other Aβ fragments (i.e. $A\beta_{31-35}$) have been found to increase p53 mRNA expression within 1–3 h of exposure to Aβ in murine neurons [35]. Thus in the rat cortex, the increase in p53 expression occurs in a transcription-independent manner. p53 has a short half-life, which is prolonged in response to cellular stress [22]. Stress-mediated phosphorylation of p53 at residue 15 disrupts its association with the oncoprotein, Mdm-2, preventing ubiquitin-mediated degradation of p53 and thus stabilizing the p53 protein [36]. The finding that Aβ rapidly phosphorylates p53 at Ser^{15} provides a mechanism for the Aβ-mediated increase in p53 expression. In contrast with the ability of Aβ to phosphorylate p53 at Ser^{15} within 5–60 min, no phosphorylation of the Ser^{392} epitope was observed at this time point. Phosphorylation at Ser^{392} occurs in response to DNA damage [37], but since Aβ does not induce DNA damage until 48–96 h [8], phosphorylation at Ser^{392} would be unlikely to occur within the time frame (5–60 min) used here. Thus phosphorylation of p53 at Ser^{15} is an early event in Aβ signalling that may serve to act as an upstream event in the degenerative pathway. The evidence from the present study and by others [16,21], supports an interaction between Aβ and p53. However, the mechanism of Aβ-induced stabilization of p53 remains to be elucidated. Several mechanisms for p53 stabilization have been proposed and these include caesin kinase [38], DNA-activated kinase [39] and JNK [27,40]. Since we have demonstrated that JNK1 is activated rapidly by Aβ in cortical neurons, we used selective antisense oligonucleotides to down-regulate JNK1 expression to elucidate the role of JNK1 in Aβ-mediated activation of p53. Depletion of JNK1 prevented the Aβ-mediated phosphorylation of p53 at Ser^{15} and this result demonstrates that JNK1 is upstream of p53. In non-neuronal cells, JNK1 has also been shown to bind to and phosphorylate p53 [41], although there is also evidence for activation of p53 in response to DNA damage being upstream of JNK activation [42]. Thus the interrelationship between JNK and p53 signalling probably depends on the type of stress stimulus and status of the cell. JNK2 and JNK3 can also serve as p53 N-terminal Ser^{34} kinases in response to cellular stress [40]. However, since the JNK1 antisense completely abrogated the Aβ-mediated phosphorylation of p53 and Aβ-mediated activation of JNK2 was only detected at the later time points of 24–48 h, which was much later than the time required to stabilize p53, we conclude that JNK2 was not pertinent in the Aβ-mediated activation of p53.

After phosphorylation at Ser^{15}, p53 can contribute to apoptosis by inducing transcription of proapoptotic genes such as *bax*,

© 2003 Biochemical Society

leading to release of mitochondrial cytochrome *c* and activation of caspase 3, a key executioner of apoptosis [23]. Alternatively, p53 may target directly to the mitochondria to induce a transcription-independent apoptotic signal [43]. Thus potential downstream consequences of JNK1-mediated activation of p53 include induction of caspase 3 and the appearance of apoptotic hallmarks such as DNA fragmentation. After depletion of JNK1, the proclivity of Aβ to activate caspase 3 and induce DNA fragmentation was significantly attenuated. JNK2 depletion had no effect on the Aβ-mediated activation of caspase 3 or increase in DNA fragmentation and this suggests that JNK1 is the principal JNK isoform involved in Aβ-mediated activation of the apoptotic cascade. Although Aβ induced caspase 3 cleavage in this system, it is important to note that the role of caspase 3 in Aβ-mediated neurodegeneration remains a matter of debate. In cortical neurons, a caspase 3 inhibitor has been found to protect neurons against some aspects of Aβ-mediated cell death [44], whereas caspase 3 has been found to have no role in Aβ-mediated hippocampal cell death [5]. The role of caspase 3 in Aβ neurodegeneration has therefore been proposed to be brain-region-specific [45]. Our findings that JNK1 and JNK2 have distinct activation profiles and different roles in the Aβ-mediated induction of the apoptotic cascade highlights the complexity of JNK signalling. In ischaemic death, differential roles of JNK1 and JNK2 have also been reported [29] and there is evidence that the profile of JNK activation is dependent on neuronal cell type and the applied stress paradigm [46]. Furthermore, the use of *jnk3* knockout mice has identified a role for JNK3 in Aβ-mediated neurotoxicity [15], whereas in the present study, we found no evidence of JNK3 activation by $A\beta_{1-40}$ (results not shown) and our result suggests a prominent role for JNK1 in Aβ-mediated DNA fragmentation in this system. This lends further support for the idea that the patterns of JNK signalling utilized by Aβ are diverse and may be subject to developmental factors, cell type and animal species. The present study provides evidence for the 1–40 fragment of Aβ coupling with JNK1 upstream of cell death in the cortex and this is relevant since $A\beta_{1-40}$ is detected in the mature senile plaque [2]. However, the nature of the JNK isoform responsible for evoking cell death by $A\beta_{1-42}$, the principal component of the plaque, remains to be resolved.

In conclusion, Aβ induces phosphorylation of JNK1 and JNK2 in cortical neurons with a distinct temporal pattern. Although JNK1 is pertinent in the Aβ-mediated stabilization of p53, activation of caspase 3 and induction of DNA fragmentation, JNK2 is not involved in coupling Aβ with these apoptotic events. An increase in phospho-JNK expression in the AD brain has been reported [47] and our study indicates that JNK1 may contribute to the pathology of the disease by activating p53 and inducing the apoptotic cascade.

This work was supported by the Health Research Board, Ireland.

REFERENCES

1 Miller, D. L., Papayannopoulos, I. A., Styles, J., Bobin, S. A., Lin, Y. Y., Bieman, K. and Iqbal, K. (1993) Peptide composition of the cerebrovascular and senile plaque core amyloid deposits of Alzheimer's disease. Arch. Biochem. Biophys. **301**, 41–52

2 Iwatsubo, T., Odaka, A., Suzuki, N., Mizusawa, H., Nukina, N. and Ihara, Y. (1994) Visualization of Aβ42 and Aβ40 in senile plaques with end-specific β monoclonals: evidence that an initially deposited species is Aβ42. Neuron **13**, 45–53

3 Adamec, E., Vonsattel, J. P. and Nixon, R. A. (1999) DNA strand breaks in Alzheimer's disease. Brain Res. **849**, 67–77

4 Li, Y. P., Bushnell, A. F., Lee, C. M., Perlmutter, L. S. and Wong, S. K. (1996) β-Amyloid induces apoptosis in human-derived neurotypic SH-SY5Y cells. Brain Res. **738**, 196–204

5 Troy, C. M., Rabacchi, S. A., Friedman, W. J., Frappier, T. F., Brown, K. and Shelanski, M. L. (2000) Caspase-2 mediates neuronal cell death induced by β-amyloid. J. Neurosci. **20**, 1386–1392

6 White, A. R., Guirguis, R., Brazier, M. W., Jobling, M. F., Hill, A. F., Beyreuther, K., Barrow, C. J., Master, C. L., Collins, S. J. and Cappai, R. (2001) Sublethal concentration of prion peptide PrP106–126 or the amyloid peptide protein of Alzheimer's disease activates expression of proapoptotic markers in primary cortical neurons. Neurobiol. Dis. **8**, 299–316

7 Suo, Z., Fang, C., Crawford, F. and Mullan, M. (1997) Superoxide free radical and intracellular calcium mediate Aβ(1–42)-induced endothelial toxicity. Brain Res. **762**, 144–152

8 Boland, B. and Campbell, V. (2003) β-Amyloid$_{(1-40)}$-induced apoptosis of cultured cortical neurons involves calpain-mediated cleavage of poly-ADP ribose polymerase. Neurobiol. Aging **24**, 179–186

9 Jordan, J., Galindo, M. F. and Miller, R. J. (1997) Role of calpain and interleukin-1β converting enzyme-like proteases in the β-amyloid-induced death of rat hippocampal neurons in culture. J. Neurochem. **68**, 1612–1621

10 Eilers, A., Whitfield, J., Shah, B., Spadoni, C., Desmond, H. and Ham, J. (2001) Direct inhibition of c-jun N-terminal kinase in sympathetic neurons prevents c-jun promoter activation and NGK-withdrawal-induced death. J. Neurochem. **76**, 439–1454

11 Yang, D. D., Kuan, C. Y., Whitmarsh, A. J., Rincon, M., Zheng, T. S., Davis, R. J., Rakic, P. and Flavel, R. A. (1997) Absence of excitotoxicity-induced apoptosis in the hippocampus of mice lacking the jnk3 gene. Nature (London) **389**, 865–870

12 Yoshizumi, M., Kogame, T., Suzaki, Y., Fujita, Y., Kyaw, M., Kirima, K., Ishizawa, K., Tsuchiya, K., Kagami, S. and Tamaki, T. (2002) Ebselen attenuates oxidative stress-induced apoptosis via the inhibition of the c-jun N-terminal kinase and activator protein-1 signalling pathway in PC12 cells. Br. J. Pharmacol. **136**, 1023–1032

13 Bozcyzko-Coyne, D., O'Kane, T. M., Wu, Z.-L., Dobrzanski, P., Murthy, S., Vaught, J. L. and Scott, R. W. (2001) CEP-1347/KT-7515, an inhibitor of SAPK/JNK pathway activation, promotes survival and blocks multiple events associated with Aβ-induced cortical neuron apoptosis. J. Neurochem. **77**, 849–863

14 Troy, C. M., Rabacchi, S. A., Xu, Z., Maroney, A. C., Connors, T. J., Shelanski, M. L. and Greene, L. A. (2001) β-Amyloid-induced neuronal apoptosis requires c-jun N-terminal kinase activation. J. Neurochem. **77**, 157–164

15 Morishima, Y., Gotoh, Y., Zieg, J., Barrett, T., Takano, H., Flavell, R., Davis, R. J., Shirasaki, Y. and Greenberg, M. E. (2001) β-Amyloid induces neuronal apoptosis via a mechanism that involves the c-jun N-terminal kinase pathway and the induction of the Fas ligand. J. Neurosci. **21**, 7551–7560

16 Gupta, S., Barrett, T., Whitmarsh, A. J., Cavanagh, J., Sluss, H. K., Derijard, B. and Davis, R. J. (1996) Selective interaction of JNK protein kinase isoforms with transcription factors. EMBO J. **15**, 2760–2770

17 Oren, M. (1994) Relationship of p53 in the control of apoptotic cell death. Semin. Cancer Biol. **5**, 221–227

18 Kitamura, Y., Shimohama, S., Kamoshima, W., Matsuoka, Y., Nomura, Y. and Taniguchi, T. (1997) Changes in p53 in the brains of patients with Alzheimer's disease. Biochem. Biophys. Res. Commun. **232**, 418–421

19 LaFerla, F. M., Hall, C. K., Ngo, L. and Jay, G. (1996) Extracellular deposition of β-amyloid upon p53-dependent cell death in transgenic mice. J. Clin. Invest. **98**, 1626–1632

20 Zhang, Y., McLaughlin, R., Goodyer, C. and LeBlanc, A. (2002) Selective cytotoxicity of intracellular β-amyloid peptide 1–42 through p53 and bax in cultured primary human neurons. J. Cell Biol. **156**, 519–529

21 Culmsee, C., Zhu, X., Yu, Q.-S., Chan, S. L., Camandol, S., Guo, Z., Greig, N. H. and Mattson, M. P. (2001) A synthetic inhibitor of p53 protects neurons against death induced by ischemic and excitotoxic insults, and amyloid β-peptide. J. Neurochem. **77**, 220–228

22 Miller, F. D., Pozniak, C. D. and Walsh, G. S. (2000) Neuronal life and death: an essential role for the p53 family. Cell Death Differ. **7**, 880–888

23 Unger, T., Sionov, R. V., Moallem, E., Yee, C. L., Howley, P. M., Oren, M. and Haupt, Y. (1999) Mutation in serines 15 and 20 of human p53 impair its apoptotic activity. Oncogene **18**, 3205–3212

24 Sakaguchi, K., Sakamoto, H., Lewis, M. S., Anderson, C. W., Erickson, J. W., Appella, E. and Xie, D. (1997) Phosphorylation of serine 392 stabilizes the tetramer formation of tumor-suppressor protein p53. Biochemistry **36**, 10117–10124

25 Zhu, Y., Mao, X. O., Sun, Y., Xia, Z. and Greenberg, D. A. (2002) p38 mitogen-activated protein kinase-mediated hypoxic regulation of Mdm2 and p53 in neurons. J. Biol. Chem. **277**, 22909–22914

26 Kwon, Y. W., Ueda, S., Ueno, M., Yodoi, J. and Masutani, H. (2002) Mechanism of p53-dependent apoptosis induced by 3-methylcholanthrene: involvement of p53 phosphorylation and p38 MAPK. J. Biol. Chem. **277**, 1837–1844

27 Adler, V., Pincus, M. R., Minamoto, T., Fuchs, S. Y., Bluth, M. J., Brandt-Rauf, P. W., Friedman, F. K., Robinson, R. C., Chen, J. M., Wang, X. W. et al. (1997) Conformation-dependent phosphorylation of p53. Proc. Natl. Acad. Sci. U.S.A. **94**, 1686–1691

© 2003 Biochemical Society

28 Fuchs, S. Y., Adler, V., Pincus, M. R. and Ronai, Z. (1998) MEKK1/JNK signaling stabilizes and activates p53. Proc. Natl. Acad. Sci. U.S.A. **95**, 10541–10546
29 Hreniuk, D., Garay, M., Gaarde, W., Monia, B. P., McKay, R. A. and Cioffi, C. L. (2001) Inhibition of c-Jun N-terminal kinase 1, but not c-Jun N-terminal kinase 2, suppresses apoptosis induced by ischemia/reoxygenation in rat cardiac myocytes. Mol. Pharmacol. **59**, 867–874
30 Nakajima-Iijima, S., Hamada, H., Reddy, P. and Kakunaga, T. (1985) Molecular structure of the human cytoplasmic β-actin gene: interspecies homology of sequences in the introns. Proc. Natl. Acad. Sci. U.S.A. **82**, 6133–6137
31 Lee, J. K., Park, J., Lee, S. H. and Han, P. L. (1999) Distinct localization of SAPK isoforms in neurons of adult mouse brain implies multiple signaling modes of SAPK pathway. Brain Res. Mol. Brain Res. **70**, 116–124
32 Mielke, K. and Herdegen, T. (2000) JNK and p38 stress kinases – degenerative effectors of signal transduction cascades in the nervous system. Prog. Neurobiol. **61**, 45–60
33 Pena, E., Berciano, M. T., Fernandez, R., Crespo, P. and Lafarga, M. (2000) Stress-induced activation of c-jun N-terminal kinase in sensory ganglion neurons: accumulation in nuclear domains enriched in splicing factors and distribution in perichromatin fibrils. Exp. Cell Res. **256**, 179–191
34 Ito, Y., Mishra, N. C., Yoshida, K., Kharbanda, S., Saxena, S. and Kufe, D. (2001) Mitochondrial targeting of JNK/SAPK in the phorbal ester response of myeloid leukemia cells. Cell Death Differ. **8**, 794–800
35 Yan, X.-Z., Xia, R., Dou, Y., Wang, S.-D., Qiao, Z.-D. and Qiao, J.-T. (2000) Carbachol blocks β-amyloid fragment 31–35-induced apoptosis in cultured cortical neurons. Brain Res. Bull. **51**, 465–470
36 Shieh, S. Y., Ikeda, M., Taya, Y. and Prives, C. (1997) DNA damage-induced phosphorylation of p53 alleviates inhibition by Mdm2. Cell (Cambridge, Mass.) **91**, 325–334
37 Lu, H., Taya, Y., Ikeda, M. and Levine, A. J. (1998) Ultraviolet radiation, but not γ radiation or etoposide-induced DNA damage, results in phosphorylation of the murine p53 protein at serine 389. Proc. Natl. Acad. Sci. U.S.A. **95**, 6399–6402
38 Wang, Y. and Eckhart, W. (1992) Phosphorylation sites in the amino-terminal region of mouse p53. Proc. Natl. Acad. Sci. U.S.A. **89**, 4231–4235
39 Lees-Miller, S. P., Sakaguchi, K., Ullrich, S. J., Appella, E. and Anderson, C. W. (1992) Human DNA-activated protein kinase phosphorylates serines 15 and 37 in the amino-terminal transactivation domain of human p53. Mol. Cell. Biol. **12**, 5041–5049
40 Hu, M. C., Qiu, W. R. and Wang, Y. P. (1997) JNK1, JNK2, and JNK3 are p53 N-terminal serine 34 kinases. Oncogene **15**, 2277–2287
41 Wang, J. and Friedman, E. (2000) Downregulation of p53 by sustained JNK activation during apoptosis. Mol. Carcinog. **29**, 179–188
42 Inamaura, N., Enokido, Y. and Hatanaka, H. (2001) Involvement of c-jun N-terminal kinase and caspase-3-like protease in DNA damage-induced, p53-mediated apoptosis of cultured mouse cerebellar granule neurons. Brain Res. **904**, 270–278
43 Marchenko, N. D., Zaika, A. and Moll, U. M. (2000) Death signal-induced localization of p53 protein to mitochondria. J. Biol. Chem. **275**, 16202–16212
44 Harada, J. and Sugimoto, M. (1999) Activation of caspase-3 in β-amyloid-induced apoptosis of cultured rat cortical neurons. Brain Res. **842**, 311–323
45 Selznick, L. A., Holtzman, D. M., Han, B. H., Gokden, M., Srinivasan, A. N., Johnson, E. M. and Roth, K. A. (1999) *In situ* immunodetection of neuronal caspase-3 activation in Alzheimer's disease. J. Neuropathol. Exp. Neurol. **58**, 1020–1026
46 Mielke, K., Damm, A., Yang, D. D. and Herdegen, T. (2000) Selective expression of JNK isoforms and stress-specific JNK activity in different neuronal cell lines. Mol. Brain Res. **75**, 128–137
47 Zhu, X., Raina, A. K., Rottkamp, C. A., Aliev, G., Perry, G., Boux, H. and Smith, M. A. (2001) Activation and redistribution of c-jun N-terminal kinase/stress-activated protein kinase in degenerating neurons in Alzheimer's disease. J. Neurochem. **76**, 435–441

Received 23 October 2002/16 December 2002; accepted 21 January 2003
Published as BJ Immediate Publication 21 January 2003, DOI 10.1042/BJ20021660

© 2003 Biochemical Society

Δ^9-Tetrahydrocannabinol induces the apoptotic pathway in cultured cortical neurones via activation of the CB_1 receptor

Eric Downer, Barry Boland, Marie Fogarty and Veronica Campbell[CA]

Department of Physiology, Trinity College, Dublin 2, Ireland

[CA]Corresponding Author

Received 6 September 2001; accepted 15 October 2001

Δ^9-Tetrahydrocannabinol, the principal psychoactive component of marijuana, exerts a variety of effects on the CNS, including impaired cognitive function and neurobehavioural deficits. The mechanisms underlying these neuronal responses to tetrahydrocannabinol are unclear but may involve alterations in neuronal viability. Tetrahydrocannabinol has been shown to influence neuronal survival but the role of the cannabinoid receptors in the regulation of neuronal viability has not been fully clarified. In this study we demonstrate that tetrahydrocannabinol promotes the release of cytochrome c, activates caspase-3, promotes cleavage of the DNA repair enzyme poly-ADP ribose polymerase and induces DNA fragmentation in cultured cortical neurones. These effects of tetrahydrocannabinol were completely abrogated by the CB_1 receptor antagonist AM-251. The findings of this study demonstrate that tetrahydrocannabinol induces apoptosis in cortical neurones in a manner involving the CB_1 subtype of cannabinoid receptor. *NeuroReport* 12:3973–3978 © 2001 Lippincott Williams & Wilkins.

Key words: Apoptosis; Cannabinoid receptor; Caspase-3; Poly-ADP-ribose polymerase; Tetrahydrocannabinol

INTRODUCTION

Δ^9-Tetrahydrocannabinol (THC), the principal psychoactive component of marijuana, exerts a variety of effects on the CNS including alterations in cognitive function [1] and impairments in memory formation and retrieval [2]. At a cellular level THC has been found to play a role in the regulation of cell viability. THC induces apoptosis in glioma cells [3], macrophages [4], hippocampal cells [5] and cortical neurones [6]. In contrast, THC also has cytoprotective properties and has been shown to enhance cell survival in the face of oxidative stress [7] and excitotoxicity [8]. The exact mechanisms underlying these contradictory effects of THC on cellular viability are unclear but since THC is a highly lipophilic molecule [9] it has been proposed that THC may utilise receptor-independent mechanisms, such as acting as a reactive oxygen species scavengers [10], to enhance cell survival. In contrast, linkage to the cannabinoid (CB) receptor has been shown to mediate the toxic effects of THC on glioma [3] and hippocampal neurones [5]. While two subytpes of cannabinoid receptor, CB_1 and CB_2, have been identified [11] the CB_1 receptor is pertinent in the central effects of THC [12] and has been localised in several brain regions including the cortex, hippocampus and cerebellum [13]. The CB_1 receptor is coupled to a G-protein [12] and we have recently reported that the detrimental effects of THC on cortical neurones are sensitive to pertussis toxin [6], indicating that G-protein subtypes G_o or G_i have a role in THC-induced neurotoxicity. To investigate whether the induction of cell death by THC proceeded via activation of the CB_1 receptor we examined the effect of the selective CB_1 antagonist AM-251 [14] on THC-induced neurodegeneration of cultured cortical neurones and characterised the role of the CB_1 receptor in the THC-induced activation of several key component of the apoptotic cascade, namely cytochrome c release, caspase-3 activation, poly-ADP-ribose polymerase cleavage and DNA fragmentation.

MATERIALS AND METHODS

Culture of cortical neurones: Primary cortical neurones were established from postnatal 1-day old Wistar rats and maintained in neurobasal medium. Rats were decapitated and cerebral cortices removed. The dissected cortices were incubated in phosphate-buffered saline (PBS) containing trypsin (0.25%) for 20 min at 37°C. The tissue was then triturated (×5) in PBS containing soyabean trypsin inhibitor (0.1%) and DNAse (0.2 mg/ml) and gently filtered through a sterile mesh filter. Following centrifugation at $2000 \times g$ for 3 min at 20°C, the pellet was resuspended in neurobasal medium, supplemented with heat inactivated horse serum (10%), penicillin (100 U/ml), streptomycin (100 U/ml) and glutamax (2 mM). Suspended cells were plated at a density of 0.25×10^6 cells on circular 10 mm diameter coverslips, coated with poly-L-lysine (60 µg/ml), and incubated in a humidified atmosphere containing 5% CO_2:95% air at 37°C. After 48 h 5 ng/ml cytosine-arabino-

furanoside was included in the culture medium to prevent proliferation of nonneuronal cells. Culture media were exchanged every 3 days and cells were grown in culture for up to 14 days.

Drug treatment: THC (Sigma-Aldrich Co. Ltd, Dorset, UK) was stored at −20°C as a 1 mM stock solution in methanol. For treatment of cortical neurones THC was diluted to a final concentration of 5 μM in prewarmed neurobasal medium and 0.01% methanol was used as vehicle. The selective CB_1 receptor antagonist AM 251 (Tocris Cookson Ltd., Bristol, UK) was stored as a 10 mM stock solution in dimethylsuphoxide and diluted to a final concentration of 10 μM in warm culture media; 0.0001% dimethylsulphoxide was used as vehicle control, AM 251 was added to the cultured neurones 30 min prior to incubation with THC. Cells were incubated with THC for 2 h since this was the time-point at which apoptotic changes had previously been observed [6].

TdT-mediated-UTP-end nick labelling (TUNEL): Apoptotic cell death was assessed using the DeadEnd calorimetric apoptosis detection system (Promega Corporation, Madison, USA). Briefly, cells were fixed with paraformaldehyde (4%), permeabilised with Triton-X100 (0.1%), and biotinylated nucleotide was incorporated at 3'-OH DNA ends using the enzyme terminal deoxynucleotidyl transferase (TdT). Horseradish peroxidase-labelled streptavidin then bound to the biotinylated nucleotide and this was detected using the peroxidase substrate H_2O_2 and the chromogen diaminobenzidine. Cells were then viewed under light microscopy at ×100 magnification, where the nuclei of TUNEL positive cells stained brown. Apoptotic cells (TUNEL positive), were counted and expressed as a percentage of the total number of cells examined (400–500 cells/coverslip).

Cytochrome c Western immunoblot: Following incubation with THC (5 μM) ± AM-251 (10 μM), cortical neurones were harvested in lysis buffer (20 mM HEPES, 10 mM KCl, 1.5 mM $MgCl_2$, 1 mM EGTA, 1 mM EDTA, 1 mM dithiothreitol, 0.1 mM PMSF, 5 μg/ml pepstatin A, 2 μg/ml leupeptin, 2 μg/ml aprotinin, pH 7.4) and left on ice for 20 min. Cells were then centrifuged (10 000 × *g* for 10 min at 4°C) and the supernatant containing the cytosolic fraction was prepared for SDS-polyacrylamide gel electrophoresis. The cytosolic fraction was diluted to 50 μg protein/ml with sodium dodecyl sulphate (SDS) sample buffer (150 mM Tris–HCl pH 6.8, 10% v/v glycerol, 4% w/v SDS, 5% v/v β-mercaptoethanol, 0.002% w/v bromophenol blue). Samples were then heated to 100°C for 3 min. Cytosolic proteins (1 μg/lane) were separated by electrophoresis on a 12% polyacrylamide minigel, transferred to nitrocellulose membrane (Satorius, Germany) and immunoblotted with a polyclonal anti-cytochrome c antibody (Santa Cruz Biotechnology Inc, California) purified from rabbit serum. Immunoreactive bands were detected using horseradish peroxidase conjugated anti-rabbit IgG (Sigma, UK) and an enhanced chemiluminescence (ECL) system (Amersham, UK). Mol. wt markers were used to verify the mol. wt of protein bands and purified cytochrome c protein was used for positive identification of protein bands corresponding to cytochrome c. Band widths were quantified using densitometric analysis (D-Scan PC software).

Poly ADP ribose polymerase (PARP) immunocytochemistry: Following treatment of cultured cortical neurones with THC (5 μM) ± AM-251 (10 μM) the cells were fixed in 4% paraformaldehyde, blocked with 5% bovine serum albumin and incubated with an anti-cleavage site specific PARP polyclonal antibody purified from goat serum (BioSource International Inc, UK; 1:50 dilution, 1 h) which specifically recognises the cleaved form of PARP. Immunoreactivity was detected with a biotinylated anti-goat IgG secondary antibody (BioSource International Inc, UK; 1:50 dilution, 1 h incubation) and streptavidin conjugated to horseradish peroxidase (Amersham, UK). Immunoreactive cells were visualised with the chromogen diaminobenzidine. The number of immunoreactive cells were counted and expressed as a percentage of the total number of cells examined (400–500 cells/coverslip).

Measurement of caspase-3 activity: Cleavage of the fluorogenic caspase-3 substrate (DEVD-aminofluorocoumarin (AFC); Alexis Corporation, USA) to its fluorescent product was used as a measure of caspase-3 activity. Cortical neurones were harvested in lysis buffer (25 mM HEPES, 5 mM $MgCl_2$, 5 mM DTT, 5 mM EDTA, 2 mM PMSF, 10 μg/ml leupeptin, 10 μg/ml pepstatin; pH 7.4), subjected to three freeze–thaw cycles and centrifuged at 10 000 r.p.m. for 10 min at 4°C. Samples of supernatant (90 μl) were incubated with the DEVD peptide (500 μM; 10 μl) for 1 h at 30°C. Incubation buffer (900 μl; 100 mM HEPES containing 10 mM DTT; pH 7.4) was added and fluorescence was assessed (excitation, 400 nm; emission, 505 nm).

Caspase-3 activity was also assessed by immunocytochemistry using an anti-active caspase-3 antibody (Promega Corporation, Madison, USA). Briefly, cells were fixed with 4% paraformaldehye, blocked with 5% goat serum in phosphate buffered saline, incubated with anti-active caspase-3 antibody (1:200 dilution, overnight incubation at 4°C). Immunoreactivity was detected using a biotinylated anti-rabbit IgG antibody and streptavidin conjugated to horseradish peroxidase. Immunoreactive cells were visualised with the chromogen diaminobenzidine, the number of immunoreactive cells were counted and expressed as a percentage of the total number of cells examined (400–500 cells/coverslip).

RESULTS

THC-induced DNA-fragmentation is abolished by the CB_1 receptor antagonist AM-251 THC induced a dose-dependent induction of apoptosis in cortical neurones (Fig. 1a). In control cells the percentage of cells displaying DNA fragmentation, as assessed by TUNEL staining was 22 ± 2% (mean ± s.e.m.). The percentage of cells staining TUNEL positive was unaffected by THC at 10 nM (19 ± 4%, $n = 5$). However, treatment of cells with THC at 100 nM, 1 μM, 5 μM and 10 μM for 2 h significantly increased the percentage of cells displaying DNA to 28 ± 2% ($p < 0.05$, Student's *t*-test, $n = 5$), 35 ± 4% ($p < 0.05$, Student's *t*-test, $n = 5$), 49 ± 1% ($p < 0.01$, Student's *t*-test,

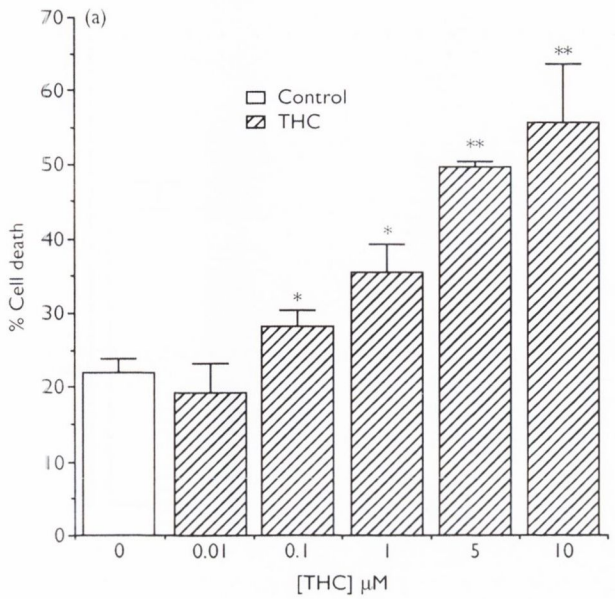

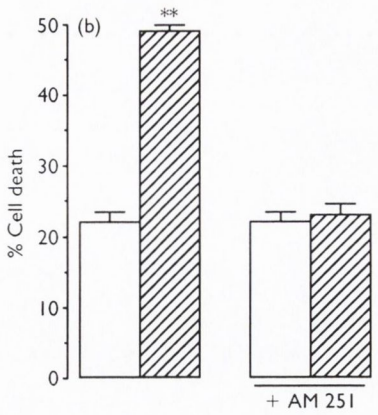

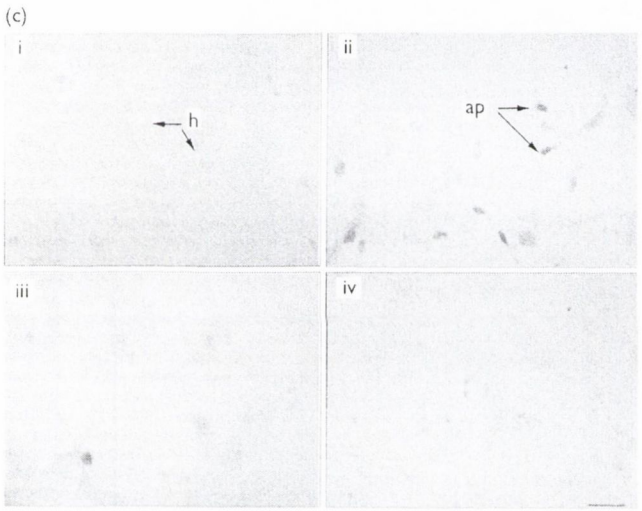

Fig. 1. THC promotes degeneration of cortical neurones via the CB_1 receptor. (**a** Incubation with THC for 2 h induced a dose-dependent increase in DNA fragmentation. Results are expressed as mean ± s.e.m. for 5 observations, $^{*}p < 0.05$; $^{**}p < 0.01$. (**b**) A significant increase in neuronal degeneration was observed following exposure of cortical neurones to THC (5 μM) for 2 h. Preincubation of the cortical neurones with the CB_1 receptor antagonist AM-251 (10 μM) for 30 min abolished the THC-induced increase in TUNEL-positive cells. Results are expressed as mean ± s.e.m. for 5 observations, $^{**}p < 0.01$. (**c**) Representative image of cortical neurones stained with TUNEL. (i) Under control conditions few cells stained positive for DNA fragmentation using TUNEL. (ii) 5 μM THC-treated neurones exhibited a significant increase in TUNEL-positive cells. (iii) Treatment with AM-251 alone had no effect on the number of TUNEL-positive neurones. (iv) Treatment with AM-251 in the presence of THC significantly reduced the number of TUNEL-positive cells. (h, healthy neurones; ap, apoptotic TUNEL-positive neurones). Bar = 25 μm.

$n = 5$) and 55 ± 8% ($p < 0.01$, Student's t-test, $n = 5$), respectively.

Figure 1b demonstrates that the CB_1 receptor antagonist AM-251 blocks THC-induced apoptosis. Treatment of cortical neurones with THC (5 μM) for 2 h significantly increased the percentage of cells displaying DNA fragmentation, as assessed by TUNEL staining, from 22 ± 2% to 49 ± 1% ($p < 0.01$, Student's t-test, $n = 5$). While AM-251 (10 μM) alone had no effect on DNA fragmentation (22 ± 3% TUNEL-positive cells) it prevented the THC-induced increase in DNA fragmentation (24 ± 3% TUNEL-positive cells following treatment with THC in the presence of AM-251).

THC-induced translocation of cytochrome c is abolished by AM-251: An upstream event associated with apoptosis is the translocation of mitochondrial cytochrome c into the cytosol. Cytosolic expression levels of cytochrome c were measured by Western immunoblot and band widths were quantified by densitometry (Fig. 2a). In control cells cytosolic levels of cytochrome c were 22.0 ± 2.06 (arbitrary units) and this was significantly increased to 28.67 ± 2.28 ($p < 0.05$, Student's t-test, $n = 9$) by THC (5 μM). AM-251 (10 μM) alone had no effect on cytosolic cytochrome c expression (mean band width 21.40 ± 1.82) but it prevented the THC-induced increase in cytochrome c expression (mean bind width 21.23 ± 1.75 in cortical neurones treated with THC in the presence of AM-251). A sample immunoblot showing that the THC-induced release of cytochrome c into the cytosol is prevented by AM 251 is shown in Fig. 2a.

AM-251 blocks the THC-induced activation of caspase-3: A consequence of mitochoridrial cytochrome c release is the activation of caspase-3. Figure 2b demonstrates that treatment of cortical neurones with THC (5 μM) for 2 h significantly increased caspase-3 activity, as assessed by the fluorogenic assay, from 13.6 ± 6.0 pmol AFC pro-

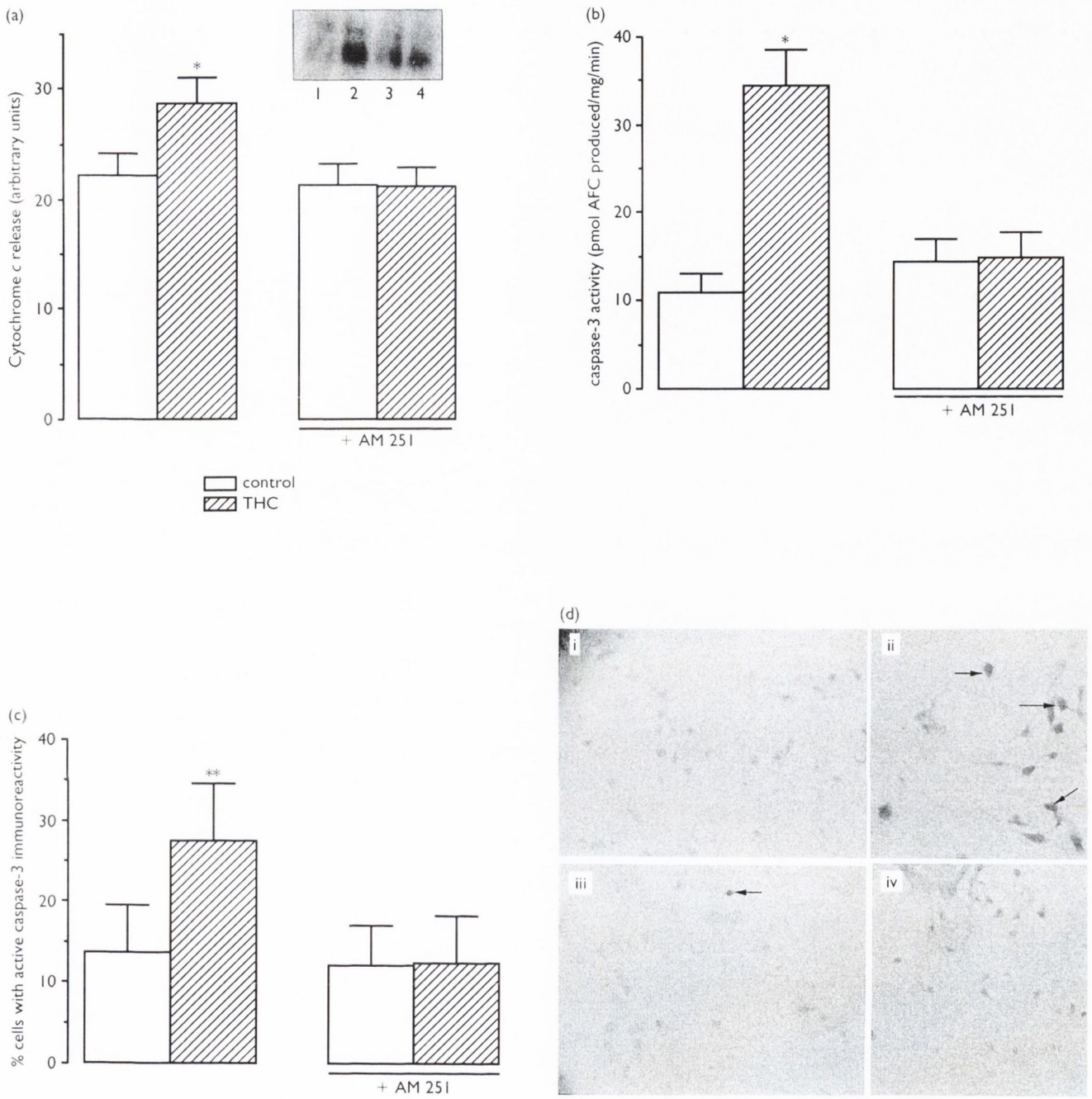

Fig. 2. THC promotes translocation of cytochrome c and activates caspase-3 in a CB_1-receptor-dependent manner A: Cortical neurones were incubated with THC (5 μM), cells were harvested and cytosolic fractions were analysed for cytochrome c expression using western immunoblot. THC significantly increased cytochrome c concentration in the cytosol. While AM-251 treatment had no effect on cytosolic cytochrome c expression, AM-251 inhibited the THC-induced release of mitochondrial cytochrome c. Results are expressed as mean ± s.e.m. of 5 observations, $^{*}p < 0.05$. Inset, a sample Western immunoblot which demonstrates the increase in cytosolic cytochrome c expression in THC-treated cortical neurones (lane 2) compared to control cells (lane 1). While AM-251 had no effect on cytosolic cytochrome c expression (lane 3) it abolished the ability of THC to promote translocation of mitochondrial cytochromic c to the cytoplasm (lane 4). (**b**) caspase-3 activity was assessed by cleavage of the fluorogenic peptide DEVD. Exposure of cells to THC (5 μM) for 2 h significantly increased caspase-3 activity. Pretreatment of the cells with AM-251 abolished the THC-induced increase in caspase-3 activity. Results are expressed as mean ± s.e.m. for 5 observations, $^{*}p < 0.05$. (**c**) The percentage of cells with caspase-3 activity was detected using the anti-active caspase-3 antibody. THC significantly increased the percentage of cortical neurones displaying active caspase-3 immunoreactivity and this was abolished by the CB_1 antagonist AM-251. Results are expressed as mean ± s.e.m. for 7 observations, $^{*}p < 0.05$. (**d**) Representative image of cortical neurones stained with the anti-active caspase-3 antibody. (i) Under control conditions few cells stained positive for active caspase-3 immunoreactivity. (ii) THC-treated neurones exhibited a significant increase in the number of cells displaying active caspase-3 immunoreactivity. (iii) Treatment with AM-251 alone had no effect on the number of cells with active caspase-3. (iv) Treatment with AM-251 in the presence of THC significantly reduced the number of cells displaying cells displaying active caspase-3 immunoreactivity (cells with activated caspase-3 immunoreactivity are indicated by arrows). Bar = 25 μm.

duced/mg protein/min to 27.4 ± 6.30 pmol AFC produced/mg protein/min ($p < 0.05$, Student's t-test, $n = 5$). While AM-251 (10 μM) alone had no effect caspase-3 activity (12.1 ± 4.9 pmol AFC produced/mg protein/min) it prevented the THC-induced increase caspase-3 activity (caspase-3 activity 12.3 ± 6.0 pmol AFC produced/mg protein/min in cortical neurones treated with THC in the presence of AM-251).

An additional method with which to evaluate caspase-3 activity is immunocytochemistry using an anti-active caspase-3 antibody (Fig. 2c). In control cells the percentage of neurones displaying active-caspase-3 immunoreactivity was 11.0 ± 2.2% and this was significantly increased to 34 ± 3.9% ($p < 0.05$, Student's t-test, $n = 7$) by THC (5 μM). AM-251 (10 μM) alone had no effect on active caspase-3 immunoreactivity (14.5 ± 2.7% of neurones displayed active caspase-3 immunoreactivity following AM-251 treatment) but it prevented the THC-induced increase in active caspase-3 immunostaining (14.9 ± 2.8% of cells displayed active caspase-3 immunoreactivity following treatment with THC in combination with AM-251). A photograph of representative anti-active caspase-3 immunostaining for control, THC, AM 251 and THC + AM 251-treated cells is shown in Fig. 2d.

THC-induced PARP cleavage involves the CB_1 receptor: The DNA repair enzyme PARP is a substrate for caspase-3. To determine whether the THC-induced activation of caspase-3 resulted in cleavage of PARP we monitored expression of the 85kDa cleaved form of PARP by immunocytochemistry using a cleavage-site specific anti-PARP antibody (Fig. 3). In vehicle-treated cultures the percentage of neurones displaying immunoreactivity for the 85 kDa form of PARP was 8.4 ± 0.5% and this was significantly increased to 40 ± 3.9% ($p < 0.01$, Student's t-test, $n = 7$) by THC (5 μM). AM-251 (10 μM) alone had no effect on PARP cleavage (8.3 ± 0.8% of neurones displayed immunoreactivity for the 85 kDa form of PARP following AM-251 treatment). However, AM-251 prevented the THC-induced increase in cleaved PARP immunoreactivity (8.1 ± 0.9% of cells displayed immunostaining for the 85 kDa form of PARP following treatment with THC in combination with AM-251). A photograph of representative anti-cleaved PARP immunostaining is shown in Fig. 3b.

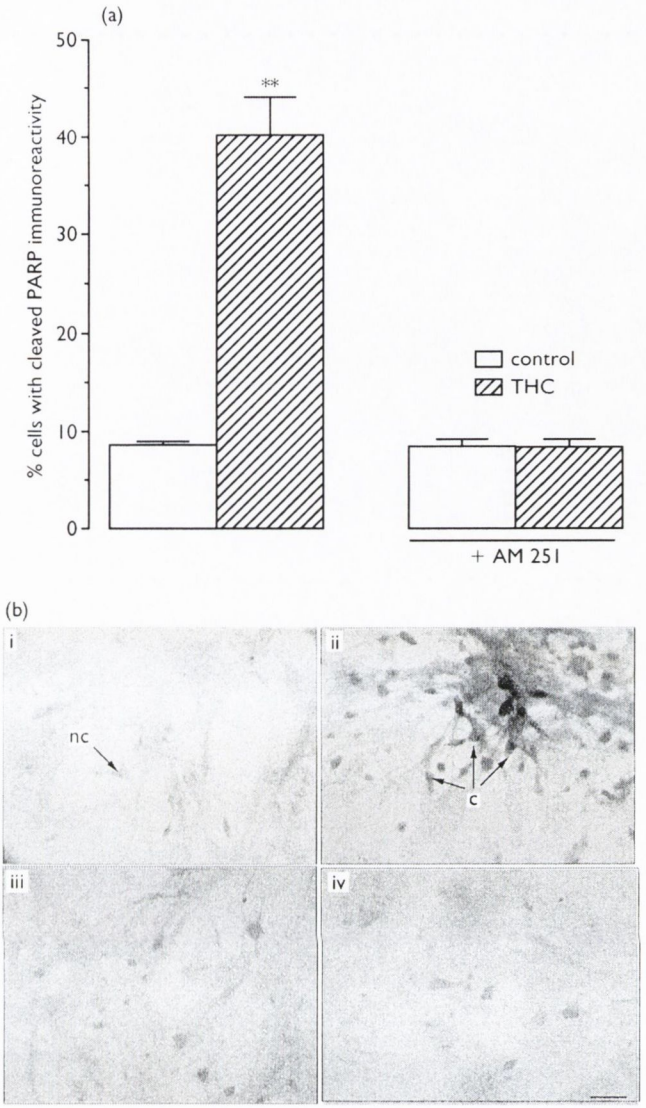

Fig. 3. The THC-induced cleavage of PARP is abolished by AM-251. (**a**) The percentage of cells with PARP cleavage was detected using the anti-cleavage site specific PARP antibody. THC significantly increased the percentage of cortical neurones displaying cleaved PARP immunoreactivity and this was abolished by the CB_1 antagonist AM-251. Results are expressed as mean ± s.e.m. for 7 observations, ** $p < 0.01$. (**b**) Representative image of cortical neurones stained with the anti-cleavage site specific PARP antibody. (i) Under control conditions few cells stained positive for cleaved PARP. (ii) THC-treated neurones exhibited a significant increase in the number of cells displaying cleaved PARP immunoreactivity. (iii) Treatment with AM-251 alone had no effect on the number of cells with cleaved PARP. (iv) Treatment with AM-251 in the presence of THC significantly, reduced the number of cells displaying cells displaying cleaved PARP immunoreactivity (cells with non-cleaved (nc) and cleaved (c) PARP are indicated by arrows). Bar = 25 μm.

DISCUSSION

The aim of this study was to examine whether induction of the apoptotic cascade by THC involved the CB_1 subtype of cannabinoid receptor. The results demonstrate that THC promotes release of mitochondrial cytochrome c into the cytosol, activates the cysteine protease caspase-3, cleaves the DNA-repair enzyme PARP and induces DNA fragmentation in cultured cortical neurones. Each of these events are components of the apoptotic cascade and were Completely blocked by the selective CB_1 receptor antagonist AM 251, demonstrating that THC-induced activation of the cell death pathway is CB_1 receptor-dependent.

Plasma concentrations of THC are in the low micromolar range following consumption of a single marijuana cigarette [16] and THC concentrations in the brain are likely to be comparable given that THC is a lipophilic molecule and will readily cross the blood–brain barrier. The minimal dose of THC which was found to be neurotoxic to cultured cortical neurones was within this concentration range.

Our previous study demonstrated that THC induces neuronal cell death in a manner involving activation of the G-protein subtypes $G_{o/i}$, since the detrimental effects of THC on neuronal viability were blocked by pertussis toxin

[6]. Those results suggested that THC may induce apoptosis in a receptor-dependent manner. However, THC is a lipophilic molecule and it remained a possibility that THC could exert a direct influence on G-proteins in the absence of receptor activation. It has been reported that THC has the proclivity to impact on other signalling mechanisms such as sphingomyelin breakdown [3] and scavenging of reactive oxygen species [7] in a receptor-independent manner.

The role of THC and its associated receptors in the induction of apoptosis is also controversial; THC having been found to possess both pro- and anti-apoptotic properties. THC is neurotoxic to hippocampal neurones [5] and C6 gliomna cells [3] *in vitro* yet it protects neurones from glutamate neurotoxicity [8] and ischemia [15]. The THC-induced degeneration of cultured hippocampal neurones [5] and transformed neural cells *in vivo* [17] was found to involve the CB_1 receptor while induction of apoptosis in C6 glioma cells *in vitro* [3] was receptor-independent. The cyoprotective properties of THC have been attributed to the ability of THC to act as an antioxidant in a receptor-independent manner [7,10]. However, the neuroprotective properties cf cannabimimetic drugs have also been demonstrated to involve CB_1 receptor activation. The results from this study demonstrate that THC induces apoptosis in cultured cortical neurones via a CB_1 receptor-dependent mechanism.

The apoptotic events that are evoked by THC in cortical neurones include the release of mitochondrial cytochrome c into the cytosol. This serves as an initiator of downstream apoptotic events since cytosolic cytochrome c can form a complex with APAF-1 which results in the activation of the cysteine protease caspase-3, a key executor of the cell death pathway [18]. THC was found to increase caspase-3 activity in cortical neurones and induce cleavage of the caspase-3 substrate PARP, demonstrating that the THC-induced cell death proceeds via activation of the caspase-3 branch of the apoptotic cascade. The ability of THC to impact on each of those apoptotic phenomenon was completely abrogated by AM 251 thereby demonstrating that the CB_1 receptor couples THC to these apoptotic signalling events.

The release of cytochrome c is an early event in apoptosis, however, the nature of the link between the CB_1 receptor and cytochrome c release is not fully understood. It is likely that the CB_1 receptor-induced activation of the heterotrimeric G proteins $G_{i/o}$ is involved since we have previously demonstrated that the THC-induced release of cytochrome c is blocked by pertussis toxin [6]. CB_1 receptors can couple to activation of stress-activated protein kinases in a G-protein-dependent manner [19] and these protein kinases regulate the mitochondrial expression of members of the Bcl family of proteins [20]. Given that cytochrome c release is regulated by the mitochondria-associated proteins Bcl and Bax [21] a potential effector for G-protein-mediated modulation includes activation of stress-activated protein kinases and downstream regulation of Bcl and Bax expression at the mitochondrial membrane.

CONCLUSION

THC exerts neurotoxic properties on cultured cortical neurones by promoting the release of cytochrome c, activation of caspase-3 and cleavage of DNA repair enzymes in a CB_1 receptor-dependent manner. The proclivity of cannabinoid receptors to induce apoptosis in neonatal neurones may reflect the role of endogenous cannabinoids in development of the CNS [22] and may also underlie the central nervous system abnormalities that occur in infants exposed to marijuana *in utero* [23].

REFERENCES

1. Reisine T and Brownstein MJ. *Curr Opin Neurobiol* **4 (3)**, 406–412 (1994).
2. Block RI and Ghoneim MM. *Psychopharmacology* **110**, 219–228 (1993).
3. Sanchez C, Galve-Roperh I, Canova C *et al. FEBS Lett* **25**, 6–10 (1998).
4. Zhu W, Freidman H and Klein TW. *J Pharmacol Exp Ther* **286**, 1103–1109 (1998).
5. Chan GC, Hinds TR, Impey S and Storm DR. *J Neurosci* **18**, 5322–5332 (1998).
6. Campbell VA. *Neuropharmacology* **40**, 702–709 (2001).
7. Chen Y and Buck J. *J Pharmacol Exp Ther* **293**, 807–812 (2000).
8. Shen M and Thayer SA. *Mol Pharmacol* **54**, 459–462 (1998).
9. Di Marzo V, Melck D, Bisogno T and De Petrocellis L. *Trends Neurosci* **21**, 521–528 (1998).
10. Hampson AJ, Grimaldi M, Lolic M *et al. Ann NY Acad Sci* **899**, 274–282 (2000).
12. Matsuda LA, Lolait SJ, Brownstein MJ *et al. Nature* **346**, 561–564 (1990).
13. Berrendero F, Garcia L, Hernandez ML *et al. Development* **125**, 3179–3188 (1998).
15. Nagayama T, Sinor AD, Simon RP *et al. J Neurosci* **19**, 2987–2995 (1999).
16. Chiang CW and Barnett G. *Clin Pharmacol Ther* **36**, 234–238 (1984).
17. Galve-Roperh I, Sanchez C, Cortes ML *et al. Nature Med* **6**, 313–319 (2000)
19. Rueda D, Galve-Roperh I, Haro A and Guzman M. *Mol Pharmacol* **58**, 814–820 (2000)
20. Ghatan S, Larner S, Kinoshita Y *et al. J Cell Biol* **150**, 335–347 (2000).
21. Rosse T, Olivier R, Monney L *et al. Nature* **391**, 496–499 (1998).
22. Fernandez-Ruiz JJ, Berrendero F, Hernandez ML *et al. Life Sci* **65**, 725–736 (1999).
23. Fried PA and Watkinson B. *J Dev Behav Pediatr* **11**, 49–58 (1990).